PROGRESS IN BRAIN RESEARCH

VOLUME 97

NATURAL AND ARTIFICIAL CONTROL OF HEARING AND BALANCE

EDITED BY

J.H.J. ALLUM
D.J. ALLUM-MECKLENBURG
F.P. HARRIS
R. PROBST

Division of Experimental Audiology and Neurootology, Department of Otorhinolaryngology, University Hospital, Basel, Switzerland

ELSEVIER
AMSTERDAM – LONDON – NEW YORK – TOKYO
1993

ISBN 0-444-81252-0 (volume)
ISBN 0-444-80104-9 (series)

Elsevier Science Publishers B.V.
P.O. Box 211
1000 AE Amsterdam
The Netherlands

Library of Congress Cataloging-in-Publication Data

Natural and artificial control of hearing and balance / edited by
J.H.J. Allum . . . [et al.].
p. cm. -- (Progress in brain research ; v. 97)
Includes bibliographical references and index.
ISBN 0-444-81252-0 (alk. paper). -- ISBN 0-444-80104-9 (series)
1. Vestibular apparatus--Congresses. 2. Hearing--Congresses.
3. Balance--Congresses. 4. Pfaltz, C. R. (Carl Rudolf)--Congresses.
5. Prosthesis Design--congresses. I. Allum, J. H. J. II. Series
[DNLM: 1. Hearing--physiology--congresses. 2. Cochlea-
-physiology--congresses. 3. Posture--physiology--congresses.
4. Gait--physiology--congresses. W1 PR667J v.97 1993 / WV 272 N285
1993]
QP376.P7 vol. 97
[QP471]
612.8'2 s--dc20
[612.8'5]
DNLM/DLC
for Library of Congress 93-11042
CIP

Printed on acid-free paper

Printed in The Netherlands

List of Contributors

Allum	Prof. J.H.J., Universitäts HNO-Klinik, Petersgraben 4, CH-4031 Basel, Switzerland Tel. +41 61/265 2040 Fax +41 61/265 2750	pp. 331 – 348
Allum-Mecklenburg	Dr. D.J., Universitäts HNO-Klinik, Petersgraben 4, CH-4031 Basel, Switzerland Tel. +41 61/265 2040 Fax +41 61/265 2750	
Ando	Dr. N., Department of Physiology, School of Medicine, Tokyo Medical and Dental University, 1-5-45- Yushima, Bunkyo-ku, Tokyo 113, Japan Tel. +81 3/381 3611 Fax +81 3/5689 0639	pp. 201 – 209
Avan	Dr. P., Biophysics Department, Hôpital Lariboisière, 2, rue Ambroise-Paré, F-75475 Paris Cedex 10, France Tel. +33 1/4995 8108 Fax +33 1/4995 8115	pp. 67 – 75
Bajd	Dr. T., Faculty of Electrical and Computer Engineering, University of Ljubljana, 61001 Ljubljana, Slovenia Tel. +38 61/265 161 Fax +38 61/264 990	pp. 387 – 396
Bélanger	Dr. M., Division of Neuroscience, University of Alberta, Edmonton, Alta. T6G 2S2, Canada Tel. +1 403/492 5749 Fax +1 403/492 1617	pp. 189 – 196
Blamey	Dr. P.J., Human Communication Research Centre, Department of Otolaryngology, University of Melbourne, 384 – 388 Albert Street, East Melbourne, Vic. 3002, Australia Tel. +61 3/665 9551 Fax +61 3/665 9553	pp. 271 – 278
Bögli	Dr. H., Department of Otorhinolaryngology, University Hospital Zürich, Rämistrasse 100, CH-8091, Zürich, Switzerland Tel. +41 1/255 2055 Fax. +41 1/255 4424	pp. 301 – 311
Bonfils	Dr. P., ENT Services, Hospital Boucicaut and Hospital Robert Debré, Paris Cedex, France	pp. 67 – 75
Boom	Prof. H.B.K., Biomedical Engineering Division, Faculty of Electrical Engineering, University of Twente, 7500 AE Enschede, The Netherlands Tel. +31 53/89 27 60 Fax +31 53/32 84 39	pp. 409 – 418
Bouchataoui	Dr. I., U.I.A.-Labo E.N.T., Universiteitsplein 1, B-2610, Wilrijk, Belgium Tel. +32 3/820/2627 Fax +32 3/820 2615	pp. 283 – 289
Cheatham	Dr. M.A., Auditory Physiology Laboratory, Hugh Knowles Center, Frances Searle Building, Northwestern University, Evanston, IL 60208, U.S.A. Tel. +1 708/491 2456 Fax +1 708/491 4975	pp. 13 – 19
de Waele	Dr. C., C.N.R.S., Laboratoire de Physiologie Neurosensorielle, 15, rue de l'Ecole de Medicine, F-75270 Paris Cedex 06, France Fax +33 1 4354 1653	pp. 229 – 243
Dietz	Prof. V. Schweizerisches Paraplegikerzentrum, Klinik Balgrist, Forchstrasse 340, CH-8008 Zürich, Switzerland Tel. +41 1/386 3901.	pp. 181 – 188
Dijkmans	Dr. P., U.I.A.-Labo E.N.T., Universiteitsplein 1, B-2610 Wilrijk, Belgium Tel. +32 3/820 2627 Fax +32 3/820 2615	pp. 283 – 289

Dillier — Dr. N., Department of Otorhinolaryngology, University Hospital Zürich, Rämistrasse 100, CH-8091 Zürich, Switzerland
Tel. +41 1/255 2055
Fax +41 1/255 4424 pp. 301–311

Dooley — Dr. G.J., Human Communication Research Centre, Department of Otolaryngology, University of Melbourne, 384–388 Albert Street, East Melbourne, Vic. 3002, Australia
Tel. +61 3/665 9551
Fax +61 3/665 9553 pp. 271–278

Durfee — Prof. W.K., Massachusetts Institute of Technology, Department of Mechanical Engineering, Room 3-455, 77 Massachusetts Avenue, Cambridge, MA 02139, U.S.A.
Tel. +1 617/253 6237
Fax +1 617/258 6149 pp. 369–381

Edgley — Dr. S., Department of Anatomy,University of Cambridge, Cambridge, United Kingdom pp. 161–171

Ernst — Dr. A., Department of Otolaryngology, University of Tübingen, Silcherstrasse 5, D-7400 Tübingen, Germany
Tel. +49 707/129 3821
Fax +49 707/129 3311 pp. 21–30

Evans — Dr. E.F., University of Keele, Keele, Staffs. ST5 5BG, United Kingdom
Tel. +44 782/621 111
Fax +44 782/613 847 pp. 117–126

Finley — Dr. C.C., Neuroscience Program, Research Triangle Institute, Research Triangle Park, Durham, NC 27709, U.S.A.
Tel. +1 919/541 7424
Fax +1 919/541 6221 pp. 313–321

Futami — Dr. T., Department of Physiology, School of Medicine, Tokyo Medical and Dental University, 1-5-45 Yushima, Bunkyo-ku, Tokyo 113, Japan
Tel. +81 3/381 3611
Fax +81 3/5689 0639 pp. 201–209

Gielen — Prof. C.C.A.M., Department of Medical Physics and Biophysics, University of Nijmegen, Geert Grooteplein noord 21, 6500 HB Nijmegen, The Netherlands
Tel. +31 80/519 222
Fax +31 80/541 435 pp. 153–159

Graf — Dr. W., C.N.R.S., Laboratoire de Physiologie Neurosensorielle, 15, rue de l'Ecole de Medicine, F-75270 Paris Cedex 06, France
Fax +33 1/4354 1653 pp. 229–243

Harris — Dr. F.P., Universitäts HNO-Klinik, Petersgraben 4, CH-4031 Basel, Switzerland
Tel. +41 61/265 2042
Fax +41 61/265 4029 pp. 91–99

Hochmair — Dr. E.S., Institute of Applied Physics and Microelectronics, University of Innsbruck, Technikerstrasse 15, A-6020 Innsbruck, Austria
Tel. +43 512/218 5034
Fax +43 512/218 5032 pp. 291–300

Hochmair-Desoyer — Dr. I.J., Institute of Applied Physics and Microelectronics, University of Innsbruck, Technikerstrasse 15, A-6020 Innsbruck, Austria
Tel. +43 512/218 5034
Fax +43 512/218 5032 pp. 291–300

Honegger — Dr. F., Universitäts HNO-Klinik, Petersgraben 4, CH-4031 Basel, Switzerland
Tel. +41 61/265 2040
Fax +41 61/322 0036 pp. 331–348

Hulliger — Dr. M., Department of Clinical Neurosciences, University of Calgary, Health Sciences Centre, HMRB 106, 3330 Hospital Drive N.W., Calgary, Alta. T2N 4N1, Canada
Tel. +1 403/220 6216
Fax +1 403/283 4740 pp. 173–180

Hutchings — Dr. M.E., University Laboratory of Physiology, Parks Road, Oxford OX1 3PT, United Kingdom
Tel. +44 865/272 475
Fax +44 865/272 469 pp. 127–133

Inglis — Dr. J.T., Department of Physical Therapy, Elborn College, University of Western Ontario, London, Ont. N6G 1H1, Canada pp. 219–228

Jankowska	Dr. E., Department of Physiology, University of Göteborg, S-400 33 Göteborg, Sweden Tel. +46 31/853 508 Fax +46 31/853 512	pp. 161 – 171
Kawasaki	Dr. T., Department of Physiology, School of Medicine, Tokyo Medical and Dental University, 1-5-45 Yushima, Bunkyo-ku, Tokyo 113, Japan Tel. +81 3/381 3611 Fax +81 3/5689 0639	pp. 201 – 209
Khanna	Prof. S.M., Department of Otolaryngology, College of Physicians and Surgeons, Columbia University, 630 West 168th Street, New York, NY 10032, U.S.A. Tel. +1 212/305 3993 Fax +1 212/305 4045	pp. 45 – 51
King	Dr. A.J., University Laboratory of Physiology, Parks Road, Oxford OX1 3PT, United Kingdom Tel. +44 865/272 475 Fax +44 865/272 469	pp. 127 – 133
Kinsbergen	Dr. J., U.I.A.-Labo E.N.T., Universiteitsplein 1, B-2610 Wilrijk, Belgium Tel. +32 3/820 2627 Fax +32 3/820 2615	pp. 283 – 289
Klinke	Prof. Dr. R., Zentrum der Physiologie, Theodor-Stern-Kai 7, D-6000 Frankfurt am Main 70, Germany Tel. +49 69/6301 6976 Fax +49 69/6301 6987	pp. 31 – 43
Kralj	Prof. A., Faculty of Electrical and Computer Engineering, University of Ljubljana, 61001 Ljubljana, Slovenia Tel. +38 61/265 161 Fax +38 61/264 990	pp. 387 – 396
Kuo	Dr. A.D., Mechanical Engineering Department, Stanford University, Stanford, CA 94305, U.S.A. Tel. +1 415/723 9464 Fax +1 415 723 3521	pp. 349 – 358
Lawson	Dr. D.T., Neuroscience Program, Research Triangle Institute, Research Triangle Park, Durham, NC 27709, U.S.A. Tel. +1 919/541 7424 Fax +1 919/541 6221	pp. 313 – 321
Lonsbury-Martin	Prof. B.L., Department of Otolaryngology (D-48), University of Miami Ear Institute, Miami, FL 33101, U.S.A. Tel. +1 305/548 4641 Fax +1 305/547 5552 (326-7610)	pp. 77 – 90
Loth	Dr. D., Biophysics and Nuclear Medicine, Faculty of Medicine Lariboisière, University of Paris 7, Paris Cedex, France	pp. 67 – 75
MacKinnon	Dr. C.D., Department of Kinesiology, University of Waterloo, Waterloo, Ont. N2L 3G1, Canada Tel. +1 519/885 1211 Fax +1 519/746 6776	pp. 359 – 367
Macpherson	Dr. J.M., R.S. Dow N.S.I., 1120 N.W. 20th Avenue, Portland, OR 97209, U.S.A. Fax +1 503 299 7229	pp. 219 – 228
Martin	Dr. G.K., Department of Otolaryngology (D-48), University of Miami Ear Institute, Miami, FL 33101, U.S.A. Tel. +1 305/548 4641 Fax +1 305/547 5552 (326-7610)	pp. 77 – 90
Martin	Dr. R.L., University Laboratory of Physiology, Parks Road, Oxford OX1 3PT, United Kingdom Tel. +44 865/272 475 Fax +44 865/272 469	pp. 127 – 133
McAlpine	Dr. D., University Laboratory of Physiology, Parks Road, Oxford OX1 3PT, United Kingdom, Tel. +44 865/272 475 Fax +44 865/272 469	pp. 127 – 133
Menguy	Dr. C., Biophysics and Nuclear Medicine, Faculty of Medicine Lariboisière, University of Paris 7, Paris Cedex, France	pp. 67 – 75

Moore	Dr. D.R., University Laboratory of Physiology, Parks Road, Oxford OX1 3PT, United Kingdom Tel. +44 865/272 475 Fax +44 865/272 469	pp. 127 – 133
Moorjani	Dr. P.A., MRC Institute of Hearing Research, University of Nottingham, University Park, Nottingham NG7 2RD, United Kingdom Tel. +44 604/223 431 Fax +44 602/423 710	pp. 107 – 115
Mulder	Dr. A.J., Biomedical Engineering Division, Faculty of Electrical Engineering, University of Twente, 7500 AE Enschede, The Netherlands Tel. +31 53/89 27 60 Fax +31 53/32 84 39	pp. 409 – 418
Munih	Dr. M., Faculty of Electrical and Computer Engineering, University of Ljubljana, 61001 Ljubljana, Slovenia Tel. +38 61/265 161 Fax +38 61/264 990	pp. 387 – 396
Offeciers	Dr. E., U.I.A.-Labo E.N.T., Universiteisplein 1, B-2610 Wilrijk, Belgium Tel. +32 3/820 2627 Fax +32 3/820 2615	pp. 283 – 289
Ohl	Dr. F., Institute of Zoology, Technical University Darmstadt, Schnittspahnstrasse 3, D-6100 Darmstadt, Germany	pp. 135 – 143
Ohmori	Prof. H., Department of Physiology, Faculty of Medicine, University of Kyoto, Kyoto, 606-01, Japan Tel. +81 75/753 4351 Fax +81 75/753 4349	pp. 7 – 11
Palmer	Dr. A.R., MRC Institute of Hearing Research, University of Nottingham, University Park, Nottingham NG7 2RD, United Kingdom Tel. +44 604/223 431 Fax +44 602/423 710	pp. 107 – 115
Pearson	Dr. K.G., Division of Neuroscience, University of Alberta, Edmonton, Alta. T6G 2S2, Canada Tel. +1 403/492 5749 Fax +1 403/492 1617	pp. 189 – 196
Peeters	Prof. S., U.I.A.-Labo E.N.T., Universiteitsplein 1, B-2610 Wilrijk, Belgium Tel. +32 3/820 2627 Fax +32 3/820 2615	pp. 283 – 289
Pellionisz	Prof. A.J., NASA Ames Research Center 261-3, Moffett Field, CA 94035-1000, U.S.A. Tel. +1 415/604 4821 Fax +1 415/604 0046	pp. 245 – 256
Popovic	Dr. D.B., Faculty of Electrical Engineering, University of Belgrade, Belgrade, Yugoslavia Correspondence address: The Miami Project to Cure Paralysis, University of Miami School of Medicine, 1600 NW 10th Avenue, R-48, Miami, FL 33136, U.S.A. Tel. +1 305/547 6001/6226 Fax +1 305/548 4427	pp. 397 – 407
Probst	Prof. R., Universitäts HNO-Klinik, Petersgraben 4, CH-4031 Basel, Switzerland Tel. +41 61/265 4105 Fax +41 61/265 4029	pp. 91 – 99
Ramos	Dr. C.F., Biophysics Group, 101 Donner Lab, University of California, Berkeley, CA 94720, U.S.A.	pp. 245 – 256
Ruder	Dr. G.K., Department of Kinesiology, University of Waterloo, Waterloo, Ont. N2L 3G1, Canada Tel. +1 519/885 1211 Fax +1 519/746 6776	pp. 359 – 367
Shannon	Dr. R.V., House Ear Institute, 2100 W. Third Street, Los Angeles, CA 90057, U.S.A. Tel. +1 213/483 4431 Fax +1 213/413 6739	pp. 261 – 269
Scheich	Prof. H., Institut für Neurobiologie, Brennecke-Strasse 6, O-3090 Magdeburg, Germany	pp. 135 – 143

Shinoda	Prof. Dr. Y., Department of Physiology, School of Medicine, Tokyo Medical and Dental University, 1-5-45 Yushima, Bunkyo-ku, Tokyo 113, Japan Tel. +81 3/381 3611 Fax +81 3/5689 0639	pp. 201 – 209
Simonis	Dr. C., Institute of Zoology, Technical University Darmstadt, Schnittspahnstrasse 3, D-6100 Darmstadt, Germany	pp. 135 – 143
Smolders	Dr. J.W.Th., Zentrum der Physiologie, Theodor-Stern-Kai 7, D-6000 Frankfurt am Main 70, Germany Tel. +49 69/6301 6976 Fax +49 69/6301 6987	pp. 31 – 43
Spillmann	Dr. T., Department of Otorhinolaryngology, University Hospital Zürich, Rämistrasse 100, CH-8091 Zürich, Switzerland Tel. +41 1/255 2055 Fax +41 1/255 4424	pp. 301 – 311
Stein	Dr. R.B., Division of Neuroscience, University of Alberta, Edmonton, Alta. T6G 2S2, Canada Tel. +1 403/492 5749 Fax +1 403/492 1617	pp. 189 – 196
Sugiuchi	Dr. Y., Department of Physiology, School of Medicine, Tokyo Medical and Dental University, 1-5-45 Yushima, Bunkyo-ku, Tokyo 113, Japan Tel. +81 3/381 3611 Fax +81 3/5689 0639	pp. 201 – 209
Tax	Dr. A.A.M., Department of Medical Physics and Biophysics, University of Nijmegen, Geert Grooteplein noord 21, 6500 HB Nijmegen, The Netherlands Tel. +31 80/519 222 Fax +31 80/541 435	pp. 153 – 159
Teyssou	Dr. M., Biophysics and Nuclear Medicine, Faculty of Medicine Lariboisière, University of Paris 7, Paris Cedex, France	pp. 67 – 75
Thomas	Dr. H., Institute of Zoology, Technical University Darmstadt, Schnittspahnstrasse 3, D-6100 Darmstadt, Germany	pp. 135 – 143
Tillein	Dr. J., Institute of Zoology, Technical University Darmstadt, Schnittspahnstrasse 3, D-6100 Darmstadt, Germany	pp. 135 – 143
Turk	Dr. R., University of Rehabilitation Institute, University of Ljubljana, 61001 Ljubljana, Slovenia Tel. +38 61/265 161 Fax +38 61/264 990	pp. 387 – 396
van Durme	Dr. M., U.I.A.-Labo E.N.T., Universiteitsplein 1, B-2610 Wilrijk, Belgium Tel. +32 3/820 2727 Fax +32 3/820 2615	283 – 289
van Enis	Dr. P., U.I.A.-Labo E.N.T., Universiteitsplein 1, B-2610 Wilrijk, Belgium Tel. +32 3/820 2627 Fax +32 3/820 2615	pp. 283 – 289
van Netten	Dr. S.M., Department of Biophysics, Laboratory for General Physics, Westersingel 34, 9718 CM Groningen, The Netherlands Tel. +31 50/633 471 Tlx. 77391 ruiso nl	pp. 45 – 51
Vidal	Dr. P.P., C.N.R.S., Laboratoire de Physiologie Neurosensorielle, 15, rue de l'Ecole de Medicine, F-75270 Paris Cedex 06, France Fax +33 1/4354 1653	pp. 229 – 243
Veltink	Dr. P.H., Biomedical Engineering Division, Faculty of Electrical Engineering, University of Twente, 7500 AE Enschede, The Netherlands Tel. +31 53/89 27 60 Fax +31 53/32 84 39	pp. 409 – 418
Wang	Dr. D.H., Department of Physiology and Biophysics, New York University, Medical Center, 550 First Avenue, New York, NY 10016, U.S.A.	pp. 229 – 243
Whitehead	Dr. M.L., Department of Otolaryngology (D-48), University of Miami Ear Institute, Miami, FL 33101, U.S.A. Tel. +1 305/548 4641 Fax +1 305/547 5552 (326-7610)	pp. 77 – 90

Wieman	Dr. C., Department of Kinesiology, University of Waterloo, Waterloo, Ont. N2L 3G1, Canada Tel. +1 519/885 1211 Fax +1 519/746 6776	pp. 359 – 367
Wilson	Dr. B.S., Neuroscience Program, Research Triangle Institute, Research Triangle Park, Durham, NC 27709, U.S.A. Tel. +1 919/541 7424 Fax +1 919/541 6221	pp. 313 – 321
Wilson	Dr. V.J., Rockefeller University, 1230 York Avenue, New York, NY 10021-6399, U.S.A. Tel. +1 212/570 8599 Fax +1 212/570 7974	pp. 211 – 217
Winter	Prof. D.A., Department of Kinesiology, University of Waterloo, Waterloo, Ont. N2L 3G1, Canada Tel. +1 519/885 1211 Fax +1 519/746 6776	pp. 359 – 367
Wit	Dr. H.P., Institute of Audiology, University Hospital, 9700 RB Groningen, The Netherlands Tel. +31 50/612 550 Fax +31 50/696 726	pp. 59 – 65
Yagi	Dr. J., Department of Physiology, School of Medicine, Tokyo Medical and Dental University, 1-5-45 Yushima, Bunkyo-ku, Tokyo 113, Japan Tel. +81 3/381 3611 Fax +81 3/5689 0639	pp. 201 – 209
Yang	Dr. J.F., Division of Neuroscience, University of Alberta, Edmonton, Alta. T6G 2S2, Canada Tel. +1 403/492 5749 Fax +1 403/492 1617	pp. 189 – 196
Zajac	Prof. F.E., Design Division, Mechanical Engineering Department, Stanford University, Stanford, CA 94305-4021, U.S.A. Tel. +1 415/723 9464 Fax +1 415/723 3521	pp. 349 – 358
Zenner	Prof. H.P., Department of Otolaryngology, University of Tübingen, Silcherstrasse 5, D-7400 Tübingen, Germany Tel. +49 707/129 3821 Fax +49 707/129 3311	pp. 21 – 30
Zhao	Dr. W., University of Keele, Keele, Staffs. ST5 5BG, United Kingdom Tel. +44 782/621 111 Fax +44 782/613 847	pp. 117 – 126
Zierhofer	Dr. C., Institute of Applied Physics and Microelectronics, University of Innsbruck, Technikerstrasse 15, A-6020 Innsbruck, Austria Tel. +43 512/218 5034 Fax +43 512/218 5032	pp. 291 – 300

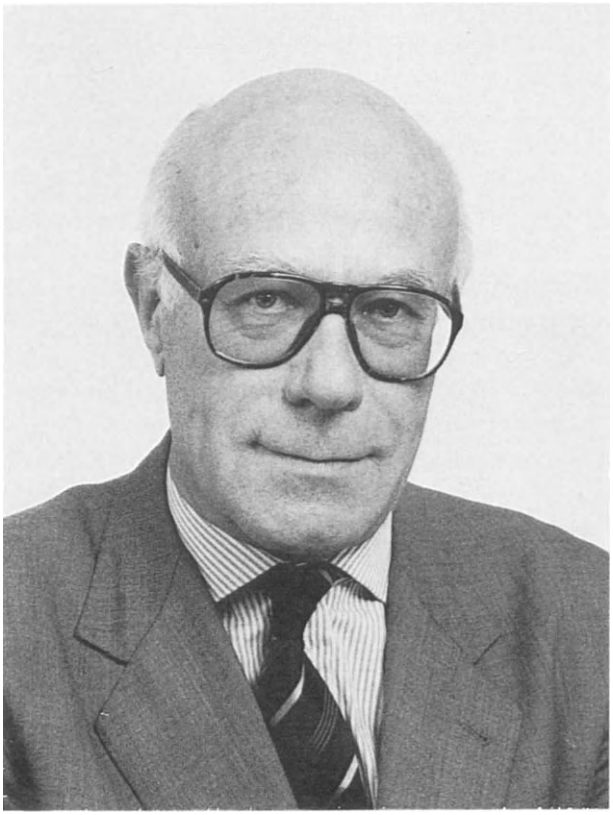

Ad Honorem Professor C.R. Pfaltz

The meeting which formed the basis for this book "Natural and Artificial Control of Hearing and Balance", was held from 4 to 7 September, 1991, in honor of Professor Carl Rudolf Pfaltz. As the organizers of this meeting, it was our pleasure and our challenge to assemble a group of investigators to represent only two segments – hearing and balance – from the diverse professional career of C.R. Pfaltz. This career has been characterized by a desire to unite engineering and biological sciences to advance clinical medicine. We hope to have developed a similar character for this symposium in his honor.

The early years of C. Pfaltz's career, which began with his graduation from the University of Basel in 1948, were marked by experiences in several locations – both geographically and anatomically. His first fellowship at the National Cancer Institute in Villejuif-Paris (Prof. Ch. Oberling) resulted in a series of experimental studies on stomach cancer. His main experimental interest was, however, auditory and vestibular systems, an interest he pursued initially with an MRC Fellowship at the National Hospital for Nervous Diseases at Queen's Square in London. Several research projects with Prof. C.S. Hallpike and his engineering friend Dr. D. Hood, which were subsequently published in *The Journal of Physiology* (Hood and Pfaltz, 1954) and in the *Proceedings of the Royal Society*

(Hallpike and Pfaltz, 1960), formed the basis for his later interest in the auditory and vestibular system and showed him the importance of the interdisciplinary cooperation between the scientist and the clinician. His work at the Hearing and Balance Unit in Queen's Square emphasized to the then young clinician the advantages that the modern electronic components could bring to medical diagnostic techniques. On his return to Basel, he put this idea into practice by developing in the 1960s the first photo-electric eye measuring technique with his neurologist friend Dr. H.R. Richter (Pfaltz and Richter, 1956, 1965; Richter and Pfaltz, 1960; Richter et al., 1966). Until that time, eye movements had been measured with the less accurate electronystagmic techniques developed by another neurologist, Prof. R. Jung, interestingly enough, some few miles away in Freiburg i.Br./Germany. Over time, these techniques have achieved worldwide recognition as one technique to record eye movements accurately, especially when the eye movements themselves can be used to guide equipment, for example, in the guidance of helicopters.

The diverse nature of the research of C. Pfaltz may be realized by scanning his list of over 200 publications. Topics covering basic research and technological advancements in many areas to new operative approaches for middle ear diseases may be found among them. The balance between basic and clinical, vestibular and auditory, peripheral and central nervous system research is evident. However, viewing such a survey is only one of many windows that can be used to understand the impact that C. Pfaltz has had, not only on ENT, but also on the academic community that he served throughout his career.

In 1965, C. Pfaltz was appointed to chair the ORL Department at the university of Basel. Within four years, he had entered the traditional two-year term as Dean of the Medical School. From 1988 to 1990, he was elected Rector of the University. He was not only an able spokesperson for the medical school within the University, but he was also a masterful representative of academic medicine throughout Europe, particularly in Eastern Europe as universities there were allowed to open up to new democratic ideas. Typical of the cooperation he established was that developed between the French, German and Swiss universities lying along the upper Rhine between the Black Forest and Vosges, including Strasbourg, Mulhouse, Freiburg, Karlsruhe and Basel. This was a precursor of emerging international cooperation within the European Community. This cooperation eventually resulted in an agreement under the title EUCOR, The European Confederation of the Universities of the Upper Rhine Region, that was signed (December 13th, 1989) by the Presidents of the seven institutions in the region.

Therefore, Professor Pfaltz's retirement in 1991 followed a distinguished career that was marked by the construction and maintenance of numerous diverse bridges between countries and disciplines. The cartoon on p. xiv is intended to suggest the strength and endurance required to sustain such imaginative efforts – a look at the "faces" there would suggest the pleasure possible from accomplishing such feats. It is through the legacy of mentors such as C. Pfaltz that the historical perspectives of past achievements can be used to further the construction of bridges to future developments. This symposium in his honor represents one such effort.

J.H.J. Allum
F. Harris
C. Akert

References

Hallpike, C.S. and Pfaltz, C.R. (1960) The effects upon vestibular function in the cat of unilateral destruction of the nucleus fastigii. *Proc. R. Soc. Med.*, 53: 1064 – 1067.

Hood, J.D. and Pfaltz, C.R. (1954) Observation upon the effects of repeated stimulation upon rotational and caloric nystagmus. *J. Physiol. (Lond.)*, 124: 130 – 144.

Pfaltz, C.R. and Richter, H.R. (1956) Photoelektrische Nystagmusregistrierung. *Practica ORL*, 118: 263 – 271.

Pfaltz, C.R. and Richter, H.R. (1965) La valeur diagnostique de la réaction vestibulaire galvanique. *Confinia Neurologica*, 25: 203 – 209.

Richter, H.R. and Pfaltz, C.R. (1960) La haute sensibilité en nystagmographie clinique. *Confinia Neurologica*, 20: 393 – 399.

Richter, H.R., Pfaltz, C.R. and Haerri, W. (1966) La rapidité des mouvements oculaires et les conditions d'enregistrement en oculo- et nystagmographie. *Confinia Neurologica*, 28: 300 – 308.

Preface

The work of Professor C.R. Pfaltz has spanned more than 30 years and has included basic research into normal vestibular function, medical diagnosis and treatment of balance and hearing problems, and the clinical application of auditory prostheses. The symposium, "Natural and Artificial Control of Hearing and Balance" was held to honor this career. For this purpose, a group of internationally recognised engineers, basic scientists and clinicians who seek better understanding of how the neurophysiology of the inner ear and related structures of the central nervous system influence hearing and balance were brought together. Our underlying goal was to provide an impetus for the development and enhancement of man-made electrical systems that either produce an artificial sense of hearing or the artificial control of standing and locomotion. This compendium represents the results of this effort.

The reader will find that although mechanisms of balance and hearing have many common elements, it is uncommon to find researchers specifically interested in only one of these disciplines assembled under one thematic roof. An important unifying concept of all sensory systems is that their artificial control can be implemented by taking advantage of the common neural receptivity to electrical stimulation applied externally to the afferent nerve endings of these receptor systems. This factor provides the opportunity to monitor neuro-electrical activity in man and at the same time enhance human function by applying electrical excitation to neurones of dys- or non-functioning motor and sensory systems. Such enhancement of function with artificial neural systems is another common element that emerges in this volume. The papers describe progress in developing prosthetic devices to replace the function of both auditory and balance systems.

In keeping with the format of the symposium, each section in this book begins with a review and critique by the individuals who evaluated the papers at the symposium. At the symposium, each section, in fact, ended with a critical review of a set of 2 – 5 papers. The reviewer provided an overview of the presentations and a critique of their content and design. In this way, the authors were provided the opportunity to respond to questions immediately and then to modify their papers for this volume. Thus, the format of this book approaches a similar format to that of a peer-reviewed journal, except that the interaction between the reviewer and the authors was open and shared with the audience, providing very stimulating discussions.

The first sections cover peripheral (Sections I and II) and central (Section III) aspects of balance and hearing and consider similarities between the two systems that might indicate how similar types of excitatory patterns could be applied through prosthetic devices to afferent nerve fibres. These sections reflect the nature of changes that have occurred in the concepts of auditory processing and vestibular control in recent years.

Predicting and subsequently improving performance following implantation of an auditory prosthesis is dependent upon a clear understanding of peripheral and central transduction of speech signals. The papers in Section I are focused on peripheral processes.

At the most peripheral level, the anatomical and physiological characteristics of hair cells, including their development, recovery following injury and motile properties must be understood. The extent to which hair-cell tuning depends upon coupling to other structures in the inner ear can be appreciated by the comparative study of mechanisms in bird, fish and mammal. Thereby differences between inner and outer hair cell physiology in the mammalian inner ear are revealed. The findings presented here generate questions that must be addressed by auditory physiologists and modelers as they form concepts of sensory transduction.

Since the seminal papers by Kemp in 1978, the study of otoacoustic emissions has been increasing steadily. How otoacoustic emissions can be used to investigate cochlear function, especially related to outer hair cells, is the subject of Section II. Results for spontaneous and evoked otoacoustic emissions and their relation to transduction in both isolated and global regions of the cochlea are included. Also, the distinction between responses produced by high vs. low levels of acoustic stimulation is pointed out. These findings may have important implications for the future development of stimulus schemes for cochlear prostheses. How clinical tests can be devised using the information obtained from ongoing research on otoacoustic emissions is also described.

Section III includes results of investigations into auditory perceptual phenomena that may suggest parameters necessary for central processing of auditory information. Knowledge of the dynamics of complex signals and how the auditory system processes, transforms and transmits speech is fundamental to the development of auditory prostheses. Modification of central auditory processing by such means as altering the peripheral mechanism or conditioning is discussed. Questions raised by the investigators contributing to this section include the effect on learning of through-put and inhibitory responses, whether the role of plasticity in the auditory system can be enhanced through training and how plasticity is altered by early deafness.

Sections IV and V cover physiological aspects of gain control by proprioceptive and vestibular systems during both animal and human stance and gait. The approach considers gain control of proprioceptive reflexes as task-dependent rather than highly variable. The reader will immediately recognise the link between the action of spinal interneurones or the action of fusimotor control on proprioceptive feedback in the cat and the different gating of reflexes during the various human tasks of stance and gait, and wonder how easily artificial control of these neural pathways can be integrated into a prosthetic system for gait control, and how a complete range of limb motions can be artificially achieved.

In healthy and normal subjects, the central nervous system in fact provides a number of solutions to balance problems. Any artificial movement might resolve control of balance by simply copying their action. The papers in Section V deal extensively with the normally functioning concept of transferring a vestibular sensory map to a motor map given that the perceived sensory directions of head movements are entirely different from the pulling directions of muscles holding the head stable in space. These very efficient solutions could usefully be integrated into an artificial system of muscle control. Unfortunately, the current state of engineering for neuroprosthetic control of posture and gait is mainly concerned with resolving problems of stimulation and muscle fatigue.

Section VI reviews psychophysics, speech coding and cochlear implant system design.

The reader will learn that new speech coding strategies emphasize the timing of signals presented to multiple sites along the auditory nerve, that is, emphasize sampling rates, rather than debating the pros and cons of multi- versus single-channel stimulation. Despite their limitations, single-channel devices remain an active part of implant research, however, and the refinement of both single- and multi-electrode devices is discussed along with some performance scores of implanted subjects. Consistent with the papers on coding are investigations of forward and backward masking in implanted patients. Such data about the ability of cochlear implant recipients to deal with discrete timing information provide insight into both the peripheral and central processing of auditory information.

The main thrust of Section VII is to provide the background needed to develop a concept for artificial control of standing and walking in paraplegic man. The answers to questions posed by such control are multi-disciplinary. Indeed, the important questions covered in this section – (1) how should muscle actions be coordinated so that fatigue is eliminated? (2) can spinal reflexes be utilised as part of the muscle control system? and (3) can reflexes of the upper body, such as vestibulo-spinal reflexes, be employed to guide the otherwise flaccid muscles of the lower limbs? – demand a combined approach by neurophysiologists and engineers.

The reader will, we hope, be reminded from the contents of this book that advances in different fields are achieved in different ways. Understanding the process of speech perception has been advanced significantly by cochlear implant engineers as they bypassed auditory transduction processes thereby causing auditory physiologists to reexamine the link between auditory physiology and speech comprehension. Hopefully, understanding can work in both directions. A flow of information on the physiological aspects of proprioceptive and vestibular control of gait might likewise help engineers develop a viable system for its neuroprosthetic control. It was one of the aims of this conference (and this book) to spark such interdisciplinary considerations.

This symposium provided investigators from diverse areas of research a stimulating and intimate atmosphere for scientific exchange. This atmosphere helped set the tone for this meeting, and we hope that this can be appreciated in the contents of this book.

John H.J. Allum
Fran Harris
Dianne Allum-Mecklenburg
Rudolf Probst

Acknowledgements

The generous and most valuable financial support of the following organisations is gratefully acknowledged:

Basel Cantonal Bank, Basel
Boehringer Ingelheim GmbH, Basel
Cochlear AG, Basel
Contact Group for Research (Ciba, Sandoz, Hoffmann-La Roche), Basel
Department of Education, Canton Aargau
Department of Education, Canton Basel-Land
Duplar AG, Bern
Hoechst-Pharma AG, Basel
Ingeno Data AG, Basel
Janssen Pharma AG, Baar
Medi-Lan AG, Fraubrunnen
Swiss Academy of Sciences, Bern
Swiss Life Insurance, Zürich
Swiss National Science Foundation, Bern
Toennies Medical Electronics, Würzberg
University of Basel, Basel

Invaluable secretarial and organisational assistance was provided by Ms. E. Clarke, Ms. W. Brunetti and Ms. D. Shaw.

J.H.J. Allum, D.J. Allum-Mecklenburg, F.P. Harris and R. Probst
Progress in Brain Research, Vol. 97

Overview and critique of Chapters 1 – 5

Hero P. Wit

Institute of Audiology, Groningen, The Netherlands

The five papers discussed below cover a broad range of research in vestibular and auditory receptor physiology. Two papers deal with properties of isolated hair cells, both in birds (Ohmori) and in mammals (Zenner and Ernst). Mammalian hair cell specialization is the subject of the (in vivo) study by Cheatham, while Klinke and Smolders discuss hair cell specialization in birds, and the differences in functioning of mammalian and bird inner ears. The paper by Van Netten and Khanna differs most from the other four. It describes experiments in the lateral line organ of fish that are purely mechanical. The relation of this paper to the other papers is that the sensory cells in the lateral line organ are also hair cells. Together, the five papers give a good impression of the "state of the art" in research of hair cell sensory systems. The papers also generate many questions that should be answered in future experiments because, despite the enormous amount of progress that has been made in the last decade, we are still at the beginning of understanding the functioning of integral hair cell sensory systems.

Ohmori describes some well performed experiments, undertaken to reveal the efferent synapse mechanisms in chick hair cells. Especially through puff application of acetylcholine (ACh), evidence is obtained that ACh may be the neurotransmitter of the efferent synapse onto the hair cell. In speculating on possible functions of the efferent system, the observation of a slow motile response of hair cells elicited by focal application of ACh to the synaptic region of (outer) hair cells (Brownell, 1983) is of interest. These motile responses are observed in mammalian hair cells, while Ohmori studied bird hair cells. This brings up the fundamental question of how different hair cells in different species are. Can we study bird (or turtle, or frog saccular) hair cells to obtain insight in the functioning of the human inner ear? Do hair cells from the lateral line up to the human cochlea only differ in details, or are they essentially different? If hair cells are not essentially different, then why do hearing organs in different species have different properties? Is this a consequence of the number of hair cells, their (tonotopic) arrangement, the micro- and macromechanics of the organ?

This topic is addressed by Klinke and Smolders in investigating and discussing hair cell specialization in birds. These authors come to the conclusion that the functional role of avian short hair cells is different from that of mammalian outer hair cells and that avian tall hair cells cannot be considered to be functionally analogous to mammalian inner hair cells. For the mammalian cochlea, it is generally accepted nowadays that tuning, when measured at the basilar membrane vibration level, is as sharp as tuning at the level of the primary nerve fiber.

Klinke and Smolders state that the situation in pigeons is different: primary afferents are much more sharply tuned than the mechanical vibration of the basilar membrane. The authors propose that processes additional to mechanical membrane tuning (e.g., hair cell properties) are responsible for the final frequency selectivity. But if frequency

selectivity is enhanced by bidirectional transduction (including feedback from the electrical domain to the hydromechanical domain; Weiss (1982)), then it is unlikely that no sharp tuning is observed in the mechanical domain. (The coupling between different stages in the transduction process and its consequences are extensively discussed by Lewis et al. (1985).) Tuning of the avian inner ear is a subject that needs further study.

Tuning of the mammalian inner ear, as reflected in hair cell tuning curves, is the subject of the paper by Cheatham. In vivo studies of hair cell tuning are necessary to obtain insight into the mechanisms for tuning, because tuning of isolated hair cells may differ substantially from tuning of cells in their natural situation. In the natural situation, cells are coupled to their surroundings through hydromechanics (and perhaps also electrically). Furthermore, the efferent neural system may influence the natural situation. Although inner and outer hair cells are believed to have quite different functions in the mammalian cochlea, their electrical properties (in turns two, three and four of the cochlea) do not differ much. Both cell types produce ac and dc receptor potentials in response to sound. There is a difference in response phase at low stimulus frequencies, indicating that the coupling of both types of cell with their surroundings may be different.

If electrical differences between inner and outer hair cells are not essential, what then makes them function differently? Is the most important difference the motor function that outer hair cells can have; and that inner hair cells are thought not to possess? This motor function of mammalian outer hair cells is the subject of the paper by Zenner and Ernst, who state that outer hair cells are proposed to produce mechanical ac and dc responses. The paper gives much information, both on experiments performed in the laboratory of the authors and on work by others. It gives a good survey of what is known about the mechanical properties of outer hair cells; and possible functions for these properties are discussed. An important place is given by the authors to the force that an isolated outer hair cell produces. This force of 14 pN/mV seems large enough to work against the stiffness of the cochlear partition; so it can account for dc displacements. Whether this force also drives the "fast motility" of hair cells is still unknown. To answer this question, the mechanical power that is produced by a hair cell should be measured. (This power is thought to compensate – on a cycle by cycle basis – for friction losses in the organ of Corti.)

Zenner and Ernst mention confirmation in their laboratory of the observation of "dc" movement of outer hair cells upon vibratory stimulation. It is likely that the mechanical demodulation, which is the subject of the paper by Van Netten and Khanna, is related to this property of hair cells. This demodulation may have a key role in transduction in hair cell sensory systems. It may be a quite fundamental property, because the lateral line, in which Van Netten and Khanna have observed the phenomenon, differs in many respects from the highly specialized mammalian cochlea. Mechanical demodulation can be explained by the following subsequent steps: filtering, rectification, integration, and voltage to cell length conversion. All of these steps can be found in mammalian outer hair cells, as can be seen in the papers by Cheatham, and by Zenner and Ernst. But if voltage-to-length conversion is a property of mammalian outer hair cells only, then a different explanation has to be found for Van Netten and Khanna's observation in the lateral line. Furthermore, coding of sensory information by amplitude modulation of a "high" frequency carrier, as proposed by Van Netten and Khanna, implies that a carrier is always present. But where is, for instance, this carrier in the vestibular system, when the stimulus is a low-frequency head motion? So, whether the observed mechanical demodulation is a fundamental property of hair cell sensory systems or just a consequence of the special choice of the stimulus, is a point that needs further study.

However, these five papers on hair cell receptor physiology show without doubt that this field of research is very much alive.

References

Brownell, W.E. (1983) Observations on a motile response in isolated outer hair cells. In: W.R. Webster and L.M. Aitkin (Eds.), *Mechanisms of Hearing,* Monash U. Press, Clayton, Vic., Australia, pp. 5 – 10.

Lewis, E.R., Leverenz, E.L. and Bialek, W.S. (1985) *The Vertebrate Inner Ear,* C.R.C. Press, Boca Raton, FL, pp. 187 – 222.

Weiss, T.F. (1982) Bidirectional transduction in vertebrate hair cells: a mechanism for coupling mechanical and electrical processes. *Hearing Res.,* 7: 353 – 360.

J.H.J. Allum, D.J. Allum-Mecklenburg, F.P. Harris and R. Probst
Progress in Brain Research, Vol. 97

CHAPTER 1

Efferent synapse mechanisms in chick hair cells

Harunori Ohmori

Department of Physiology, Faculty of Medicine, University of Kyoto, Kyoto, 606-01 Japan

Electrical stimulation of the efferent fiber to the hair cell is known to suppress peripheral auditory function. In isolated hair cells from the chick, acetylcholine (ACh) generated membrane hyperpolarization when a puff was applied at concentrations from 1 μM to 5 mM. Ionophoretic application of ACh generated a membrane hyperpolarization with a rapid time course. This is due to the increase of K conductance and is accompanied by the rise of the $[Ca]_i$.

Key words: Hair cell; Mechano-electrical transduction; Adaptation; Efferent synapse; Calcium

Introduction

Hair cells transduce auditory and vestibular information into an electrical signal through the mechanically gated ion channel located in the hair bundle (Hudspeth, 1982; Ohmori, 1988). Mechano-electrical transduction (MET) channels are gated by the angular displacement of the hair bundle and have a unitary conductance of 50 pS (Ohmori, 1985, 1987) or its integer multiples (Crawford et al., 1991). The channel has a broad spectrum of permeable cations; all of the alkaline cations, some organic cations (choline, TMA, TEA) and some divalent cations (Ca, Sr, Ba, Mg, Mn) are permeable; among them, the Ca ion has been found to be the most permeable (Ohmori, 1985).

Ca ions play essential roles in the hair cell. (1) The presence of Ca ions in the extracellular medium is required for the operation of mechano-electrical transduction (Sand, 1975; Hudspeth and Corey, 1977; Ohmori, 1985; Crawford et al. 1991). (2) The adaptation of the MET current is dependent on the extracellular Ca concentration and the membrane potential (Corey and Hudspeth, 1983; Assad et al., 1989; Crawford et al., 1991). The membrane potential probably modifies adaptation through its effects on the influx of Ca ions. (3) Ca ions are the second messengers most likely in the efferent synapse onto the hair cell. Acetylcholine (ACh) has been shown to increase the intracellular Ca concentration ($[Ca]_i$) and to hyperpolarize the hair cell membrane (Shigemoto and Ohmori, 1990). (4) Ca ions must be regulating the release of neurotransmitter from hair cells, but not much is known in this respect (Furukawa and Matsuura, 1978). I will discuss, in this article, roles played by Ca ions in the ACh-induced membrane hyperpolarization, a putative efferent synapse mechanism.

Methods

Experiments were performed on isolated hair cells from the chick. The isolated hair cell was either electrically recorded by using a patch electrode or loaded with fura-2 for fluorescence measurement of $[Ca]_i$. In some experiments, the level of $[Ca]_i$ was step-raised by the photo-activation of a caged Ca compound, Nitr-5. These techniques of cell isolation, electrical recording using a patch electrode, fluorescence measurements of intracellular Ca concentration, and the technique for loading the cell with the caged Ca compound and its photo-

activation were already described elsewhere (Ohmori, 1984, 1985, 1988; Shigemoto and Ohmori, 1990, 1991).

Results and discussion

Acetylcholine as a neurotransmitter of the efferent synapse

Hair cells receive inhibitory efferent innervations. ACh is proposed as the most likely candidate for the neurotransmitter at this efferent synapse (reviewed by Klinke and Galley, 1974; Guth et al., 1976). The activation of some types of muscarinic receptors, which induce membrane hyperpolarization, is reported to facilitate phosphoinositide hydrolysis and then to activate Ca^{2+}-activated K^+ current in glandular cells (Evans and Marty, 1986) and in NG108-15 cells transfected with cDNA or genomic DNA encoding muscarinic ACh receptor (Fukuda et al., 1988). We have reported that in chick hair cells, muscarinic agonists increase the intracellular Ca^{2+} concentration by facilitating Ca^{2+} release from internal store sites (Shigemoto and Ohmori, 1990).

There are clear distinctions between inner and outer hair cells in mammals. Innervation by the efferent fiber is dominant in outer hair cells but is poor in inner hair cells, whereas the afferent fiber innervates mostly the inner hair cell. Differentiation of hair cells is not so clear in birds as in mammals but there are certain distinctions between tall and short hair cells that correspond to the mammalian inner hair cell and the outer hair cell, respectively (Takasaka and Smith, 1971; Tanaka and Smith, 1978).

The tall hair cell is located close to the proximal part of the basilar membrane where nerve fibers lose their myelin coating, and the short hair cell is located at the distal part. Short hair cells receive rich efferent innervations similar to the outer hair cell of the mammalian cochlea. Tall hair cells receive only a poor efferent innervation.

When a puff at a concentration of 100 μM ACh was applied to solitary short hair cells, the membrane potential was hyperpolarized immediately from the resting level of -54 mV to -80 mV (Shigemoto and Ohmori, 1991). The ACh-induced outward current could be generated with a delay of about 10 msec when ACh was applied ionophoretically. Under the current-clamp condition, the membrane was hyperpolarized with a delay of 20 msec (Fig. 1). The ACh-induced current in the tall hair cell is much smaller and is generated with a much longer delay than the current in the short hair cell.

The reversal potential of the ACh-induced current was -80 mV in a 5 mM K extracellular medium when recorded with 155 mM KCl-based intracellular medium. The reversal potential was dependent on $[K]_o$ and was shifted 57 mV per 10-fold change of $[K]_o$. ACh activates a potassium conductance.

The ACh-induced K current was ACh dose-dependent with a K_D of 19 μM and a Hill coefficient of 1.6. The current was blocked by bath-applied 1 μM atropine, and by 100 μM quinine. Quinine is known to block the Ca-activated K channel in the *Aplysia* neuron (Hermann and Gorman, 1981). ACh could induce the K current even in the Ca-free extracellular medium. However, the amplitude of the K current induced by ACh in a Ca-free medium was only 45% of the control, and the second application of ACh in the Ca-free medium reduced the amplitude of the outward current to 35% of the first response in this Ca-free medium.

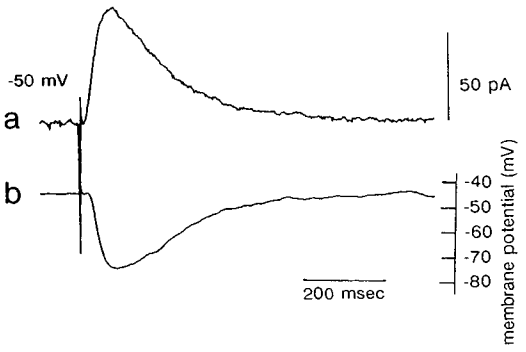

Fig. 1. Time courses of the membrane potential and the current induced by ionophoretically applied ACh. Membrane current (*a*) and potential (*b*) changes were induced by ionophoretic application of ACh (1 M). ACh ejection current was 1 μA and retaining current was 150 nA. (Fig. 9 of Shigemoto and Ohmori, 1991.)

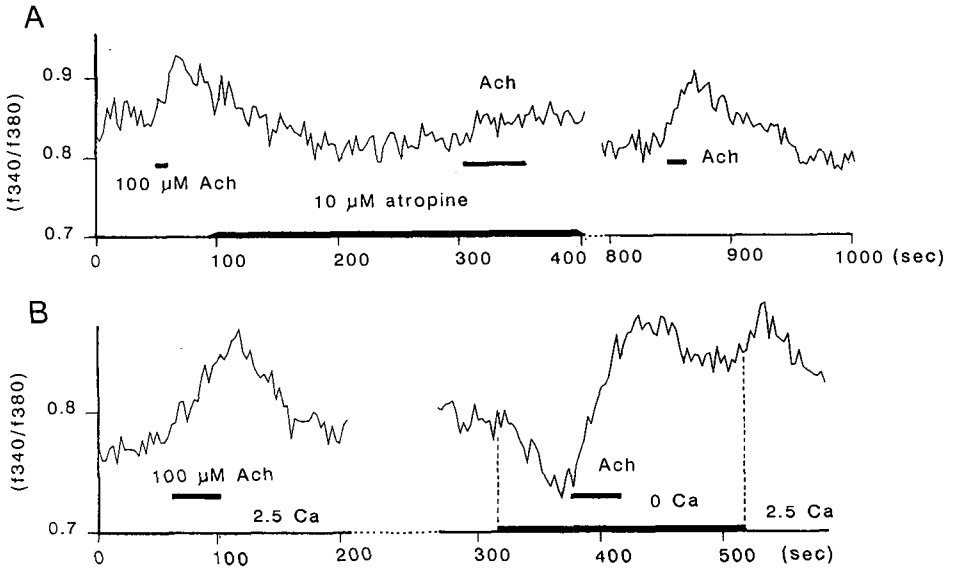

Fig. 2. ACh responses are blocked by atropine and are generated in a Ca-free extracellular medium. *A*. A bath application of 10 μM atropine blocked most of the Ca response generated by 100 μM ACh. The application of atropine is indicated by a bar on the abscissa. The blocking effect was reversible. *B*. Ca response was generated in a Ca-free extracellular medium applied rapidly by the microperfusion method. The flow of Ca-free medium is indicated by a bar on the abscissa. After application of a Ca-free medium, the intracellular Ca concentration is decreased. A flow of 2.5 mM Ca extracellular medium, introduced by suspending the microperfusion of the Ca-free solution, induced a transient rise of intracellular Ca concentration. These two timings are indicated by two vertical broken lines. (Fig. 6 of Shigemoto and Ohmori, 1990.)

When 100 μm ACh was puff-applied to a solitary hair cell, fura-2 fluorescence was changed. The fluorescence which is excited at 340 nm wavelength was increased, and the fluorescence which was excited at 380 nm wavelength was decreased reciprocally after ACh application (Shigemoto and Ohmori, 1990). These changes of fluorescence indicate an increase of the intracellular Ca concentration (Fig. 2).

When 10 μM atropine was bath-applied, the puff application of 100 μM ACh did not induce Ca responses (Fig. 2*A*). The suppression by atropine was reversible. We have not studied detailed dose – response relationships, but atropine seems to be at least one order of magnitude more potent than D-tubocurarine (DTC) as an inhibitor of the ACh-induced intracellular Ca response. DTC suppressed the ACh-induced Ca response only to 33% of the control at a concentration of 1 mM. This might suggest that a cholinergic muscarinic receptor mechanism mediates the ACh-induced rise of the intracellular Ca concentration in the hair cell.

Some type of cholinergic muscarinic receptor is known to facilitate phosphatidylinositol turnover (reviewed by Nathanson, 1987) and generate inositol trisphosphate (IP_3). IP_3 induces release of Ca from intracellular stores (Berridge and Irvine, 1984). We have measured intracellular Ca responses in a Ca, Mg-free extracellular medium. In these experiments, hair cells were bathed in a Ca, Mg-free extracellular medium for at least 5 min before ACh puff application. Only 17 cells out of 133 hair cells tested demonstrated a Ca rise in response to the 100 μM ACh. The time course was similar to that observed in a Ca-containing medium and outlasted the ACh puff, but the response amplitude was small. This small response amplitude and the extremely low incidence of the Ca response (13%) might indicate an influx as the major source of this Ca response. More plausibly, perhaps, the intracellular

Ca reservoir can be small and can deplete quickly in the Ca-free extracellular medium.

When the Ca-free medium was micro-perfused about the hair cells, the fluorescence ratio was decreased indicating a fall of the intracellular Ca concentration. One hundred μM ACh was then puff-applied against hair cells and the intracellular Ca concentration was raised (Fig. 2*B*). This Ca response was similar to the one observed in normal saline and clearly outlasted the ACh puff. At 516 sec, the micro-perfusion of the Ca-free saline was suspended, which introduced 2.5 mM Ca into the extracellular medium and caused a transient rise of the intracellular Ca concentration.

When two identical ACh-puff stimuli were applied in the Ca-free medium, the second Ca response was only 44% of the control obtained when two stimuli were separated by 117 $\pm$ 11 sec (n = 18). Also, it was more suppressed than that in the normal saline where the second Ca response was 90% of the first one when separated by 151 $\pm$ 43 sec (n = 87). The second Ca response in the Ca-free medium was therefore 48% of the second Ca response in the normal medium. This indicates a relatively easy depletion of Ca ions from the intracellular stores and is consistent with the decrease of ACh-induced current amplitudes in the Ca-free medium. These observations support the idea that the ACh-induced K current and the ACh-induced Ca response are closely linked phenomena.

ACh can be the neurotransmitter of the efferent synapse onto the hair cell. It is very likely that ACh activates muscarinic receptors on the hair cell membrane. The activated muscarinic receptors probably activate GTP binding protein. The activated GTP binding protein further activates the metabolic cascade of phospholipase-C and IP_3 leading to the release of Ca^{2+} intracellularly.

The Ca release site in the hair cell is not known. However, the hair cell has a specialized structure underneath the plasma membrane which is called the *sub-surface cistern* (Tanaka and Smith, 1978). This structure could be a candidate of the Ca release site. Probably because of the localization of the muscarinic receptors, subsurface cistern and the Ca-activated K channel in a vicinity close to the efferent synapse, the ACh-induced outward current would be generated with a relatively short delay such as for the case of a second messenger-mediated channel-gating process.

References

Assad, J.A., Hacohen, N. and Corey, D.P. (1989) Voltage dependence of adaptation and active bundle movement in bullfrog saccular hair cells. *Proc. Natl. Acad. Sci. U.S.A.*, 86: 2918 – 2922.

Berridge, M.J. and Irvine, R.F. (1984) Inositol trisphosphate, a novel second messenger in cellular signal transduction. *Nature*, 312: 315 – 321.

Corey, D.P. and Hudspeth, A.J. (1983) Kinetics of the receptor current in bullfrog saccular hair cells. *J. Neurosci.*, 3: 962 – 976.

Crawford, A.C., Evans, M.G. and Fettiplace, R. (1991) The actions of calcium on the mechano-electrical transducer current of turtle hair cells. *J. Physiol. (Lond.)*, 434: 369 – 398.

Evans, M.G. and Marty, A. (1986) Potentiation of muscarinic and alpha-adrenergic response by an analog of guanosine trisphosphate. *Proc. Natl. Acad. Sci. U.S.A.*, 83: 4099 – 4103.

Fukuda, K., Higashida, H., Kubo, T., Maeda, A., Adiba, I., Bujo, H., Mishina, M. and Numa, S. (1988) Selective coupling with K^+ currents of muscarinic acetylcholine receptor sybtypes in NG108-15 cells. *Nature*, 335: 355 – 358.

Furukawa, T. and Matsuura, S. (1978) Adaptive rundown of excitatory post-synaptic potentials at synapses between hair cells and eight nerve fibers in the goldfish. *J. Physiol. (Lond.)*, 276: 193 – 209.

Guth, P.S., Norris, C.H. and Bobbin, R.P. (1976) The pharmacology of transmission in the peripheral auditory system. *Pharmacol. Rev.*, 28: 95 – 125.

Hermann, A. and Gorman, A.L.F. (1981) Quinine blocks the voltage- and calcium-dependent K^+ conductance of *Aplysia* neurons. *Pflügers Arch.*, 389: R23.

Hudspeth, A.J. (1982) Extracellular current flow and the site of transduction by vertebrate hair cells. *J. Neurosci.*, 2: 1 – 10.

Hudspeth, A.J. and Corey, D.P. (1977) Sensitivity, polarity and conductance change in the response of vertebrate hair cells to controlled mechanical stimuli. *Proc. Natl. Acad. Sci. U.S.A.*, 74: 2407 – 2411.

Klinke, R. and Galley, N. (1974) Efferent innervation of vestibular and auditory receptors. *Physiol. Rev.*, 54: 418 – 540.

Nathanson, N.M. (1987) Molecular properties of the muscarinic acetylcholine receptor. *Annu. Rev. Neurosci.*, 10: 195 – 236.

Ohmori, H. (1984) Studies of ionic currents in the isolated vestibular hair cell of the chick. *J. Physiol. (Lond.)*, 350: 561 – 581.

Ohmori, H. (1985) Mechano-electrical transduction currents in

isolated vestibular hair cells of the chick. *J. Physiol. (Lond).*, 359: 189 – 217.

Ohmori, H. (1987) Gating properties of mechano-electrical transducer channel in the dissociated vestibular hair cell of the chick. *J. Physiol. (Lond.)*, 387: 589 – 609.

Ohmori, H. (1988) Mechanical stimulation and fura-2 fluorescence in the hair bundle of dissociated hair cells of the chick. *J. Physiol. (Lond.)*, 399: 115 – 137.

Sand, O. (1975) Effect of different ionic environments on the mechanosensitivity of lateral line organs in the mudpuppy. *J. Comp. Physiol.*, A102: 27 – 42.

Shigemoto, T. and Ohmori, H. (1990) Muscarinic agonists and ATP increase the intracellular Ca^{2+} concentration in chick cochlear hair cells. *J. Physiol. (Lond.)*, 420: 127 – 148.

Shigemoto, T. and Ohmori, H. (1991) Muscarinic receptor hyperpolarizes cochlear hair cells of chick by activating Ca^{2+}-activated K^+ channels. *J. Physiol. (Lond.)*, 442: 669 – 690.

Takasaka, T. and Smith, C.A. (1971) The structure and innervation of the pigeon's basilar papilla. *J. Ultrastruct. Res.*, 35: 20 – 65.

Tanaka, K. and Smith, C.A. (1978) Structure of the chicken's inner ear: SEM and TEM study. *Am. J. Anat.*, 153: 251 – 272.

J.H.J. Allum, D.J. Allum-Mecklenburg, F.P. Harris and R. Probst
Progress in Brain Research, Vol. 97

CHAPTER 2

Cochlear function reflected in mammalian hair cell responses

M.A. Cheatham

Auditory Physiology Laboratory, Hugh Knowles Center, Frances Searle Building, Northwestern University, Evanston, IL 60208, U.S.A.

This report describes response patterns recorded in inner and outer hair cells in the apical three turns of the guinea pig cochlea. Characteristic frequencies (CF) in these regions are approximately 270 Hz in turn four, 1000 Hz in turn three and 4000 Hz in turn two. Although the two receptor types exhibit differences in resting membrane potentials and in response phase at low stimulus frequencies, they both produce ac and dc receptor potentials in response to sound. When measured around CF, both cell types produce a depolarizing dc response at low and moderate levels. This contrasts with results published for basal-turn outer hair cells (Russell and Sellick, 1983; Cody and Russell, 1987) whose responses become asymmetrical only at very high levels.

Key words: Cochlea; Hair cell; Sensory receptors

Introduction

Sensory receptor cells in the mammalian cochlea have fully differentiated into two distinct populations: inner and outer hair cells. Observations have revealed significant anatomical differences which have now been catalogued and form a long list (Lim, 1986). For example, whereas both cell types exhibit a hair bundle, only the tallest row of stereocilia on outer hair cells (OHC) makes firm contact with the overlying tectorial membrane (Kimura, 1966; Hunter-Duvar, 1978). It is also well known (Spoendlin, 1969) that most of the innervating afferent nerve fibers make synaptic contact with inner hair cells (IHC). Thus, information sent to the central nervous system via the auditory nerve reflects, by and large, the output of IHCs. In contrast, neural control from the central nervous system to the periphery is established by incoming efferents that synapse primarily on OHC bodies (Engstrom, 1958; Smith and Sjöstrand, 1961). Axosomatic contacts on IHCs are rare (Smith, 1961; Spoendlin, 1970). In addition, OHCs have been shown to exhibit motility (Brownell et al., 1985; Kachar et al., 1986). This phenomenon is being studied to learn whether changes in cell length may relate to cochlear amplification (Davis, 1983). In other words, OHCs may function as mechanical effectors necessary for the remarkable sensitivity and frequency selectivity of the peripheral auditory system, leaving IHCs as the true sensory receptors (Kim, 1984; also reviewed in Dallos, 1988).

While documentation of the basic functional differences between the two populations of hair cells continues, it is also of interest to study differences that may be expressed longitudinally along the cochlea spiral. For example, while IHC morphology is relatively constant, OHCs change in length by a factor of three to four from base to apex (Brownell et al., 1985; Pujol, 1991). This variation may be

responsible for the increasing inclination of the reticular lamina relative to the basilar membrane (Bohne and Carr, 1979; Lim, 1980). Efferent innervation of OHCs also exhibits significant longitudinal variations as well as changes in neurochemistry (Smith and Sjostrand, 1961; Spoendlin, 1970; Klinke and Galley, 1974; Guth et al., 1976; Warr, 1978; Guinan et al., 1983; Altsculer and Fex, 1986).

In addition, functional differences have been reported in dc receptor potentials (RP) produced by apical (Dallos et al., 1982; Dallos, 1986) versus basal (Russell and Sellick, 1983; Cody and Russell, 1987) OHCs. The dc component is especially important for transmitter release at high frequencies because the ac RP is low-pass filtered by resistances and capacitances in the hair cell's basolateral membrane and by calcium-dependent synaptic processes (Weiss et al., 1974; Russell and Sellick, 1978, 1983; Dallos, 1984, 1985; Palmer and Russell, 1986; Weiss and Rose, 1988; Kidd and Weiss, 1990). It is also well known that tuning curve shape changes dramatically with characteristic frequencies (CF) (Kiang et al., 1965; Evans, 1972; Harris, 1979; Schmiedt, 1989; Ohlemiller and Echteler, 1990). For example, in the 1000 Hz region, tuning curves are V-shaped whereas single units with CFs at 4000 Hz and above exhibit a distinct tip and tail and a greater frequency selectivity. Consequently, this report presents information recorded from both IHCs and OHCs in the apical three turns of the guinea pig cochlea with the purpose of understanding functional differences between the two populations of receptor cells and the longitudinal variations that may be expressed along the cochlea.

Methods

Intracellular recordings of IHCs and OHCs from turns four, three and two are accomplished using a lateral approach to the organ of Corti (OC) (Dallos et al., 1982). The use of young, albino guinea pigs facilitates fenestration of the cochlear bone, which becomes thicker towards the base. Anesthesia is induced and maintained using a combination of sodium pentobarbital and Innovar-Vet. Animals breathe on their own without difficulty.

In a standard track, the recording electrode usually travels approximately 130 μm in the scala media space media space before touching the organ of Corti. Careful distance measures are made to determine the locations at which sensory receptor cells are encountered. In turn two, IHCs are located approximately 135 μm into the organ; OHCs are normally less than 100 μm. After an OHC is recorded, the electrode is advanced to search for the companion IHC and to determine if the track exhibits a normal electrical profile (Dallos, 1985). In turns three and four, the distances traveled are longer. For example, in turn three, IHCs are located approximately 165 μm into the organ; in turn four, approximately 190 μm.

After amplification, responses are low-pass filtered to prevent aliasing. In turns three and four, the filter cut-off frequency is 3000 Hz; in turn two, 6000 Hz. Sampling rate is also increased in turn two and exceeds the Nyquist frequency. Further details can be obtained from previous publications (Dallos, 1985; Cheatham and Dallos, 1989, 1992).

Results and discussion

Inner hair cells in the guinea pig cochlea produce RPs composed of ac and dc components. The ac, which approximates the wave form of the stimulating tone burst, is measured off-line from fast Fourier transforms of averaged response wave forms. The dc component follows the envelope of the stimulus and is measured relative to the baseline in quiet. At low sound levels, hair cell responses are sharply tuned with the largest response produced at the characteristic frequency of the cell. Because frequency selectivity is level-dependent, response patterns at high input levels become low-pass rather than band-pass (Russell and Sellick, 1978; Dallos, 1985).

Frequency response functions from IHCs recorded in turns four, three and two are shown in Fig. 1. These regions roughly correspond to dis-

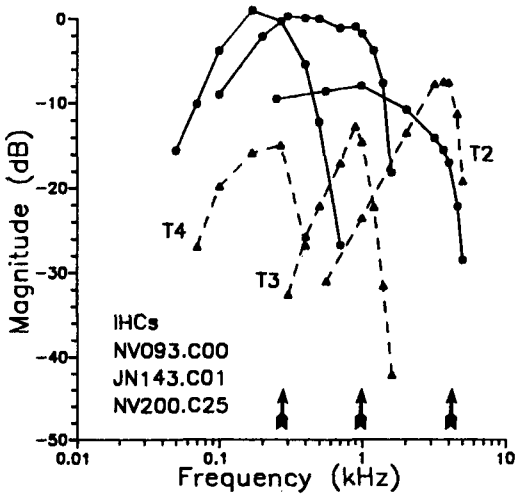

Fig. 1. Inner hair cell frequency-response functions from turns four, three and two (reproduced from Dallos and Cheatham (1992), by copyright permission of the Rockefeller University Press). Stimulus frequency, plotted along the abscissa, is varied to map out the response area of each cell. Arrows designate the CFs of each of the three recording locations. Stimulus level is constant at 50 dB SPL re: 2.0×10^{-5} Pa. The ac RPs are plotted with circles and solid lines; the dc RPs with triangles and dashed lines. Magnitude appears on the ordinate and 0 dB corresponds to 5 mV peak. Membrane potentials of all three cells fall in a range between -28 and -24 mV. The ac responses from turns four and three were plotted using a different format in a previous publication (Dallos, 1986).

tances along the basilar membrane of 17.0, 13.8 and 9.7 mm measured from the base to the middle of the window made in the cochlear bone. The CFs of hair cells at these three locations are approximately 270 Hz, 1000 Hz and 4000 Hz, respectively. These determinations are based on numerous IHC recordings obtained at low levels. Although not obvious from the ac frequency response functions, the dc profiles in Fig. 1 do reflect these estimates.

In Fig. 1, ac RPs are plotted with solid lines and dc responses with dashed lines. Because the range of frequencies that excite cells recorded in turn four is relatively low, their ac responses are not filtered by the basolateral hair cell membrane or the recording electrode. Consequently, there is a similarity between the ac and dc functions, although the dc responses are smaller in magnitude. In contrast, second-turn results, plotted on the right, reveal that the dc RPs produced at CF exceed their ac counterparts. This very likely reflects filtering of the ac RP by the hair cell membrane and by the recording electrode. It is also likely that this higher frequency region of the cochlea is more non-linear than lower frequency recording locations. Because the dc component of the RP is a distortion product, its magnitude is larger towards the base of the cochlea. This

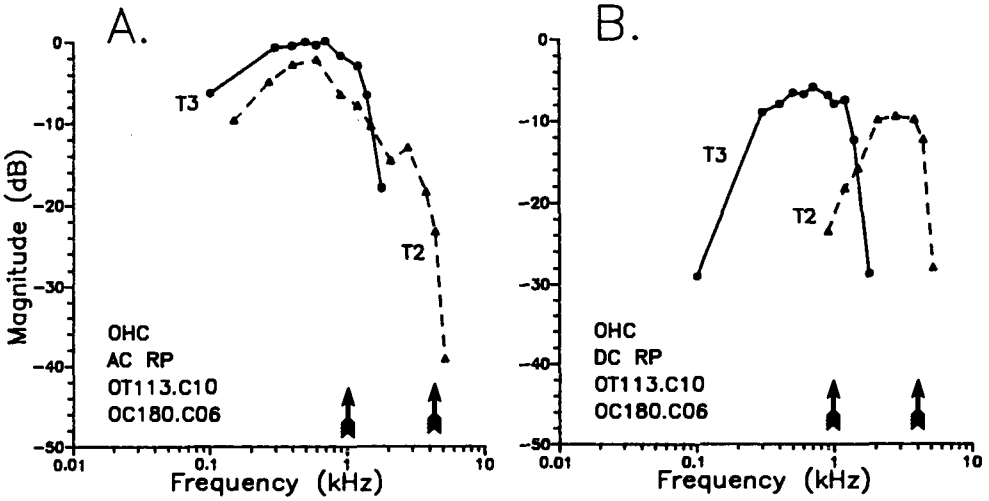

Fig. 2. Frequency-response functions measured at 70 dB SPL for two OHCs in turn three and turn two. Arrows along the abscissa indicate their CFs. The membrane potential of the third (second) turn cell was -75 (-58) mV. Data from turn three have appeared in a slightly different form in another paper (Dallos, 1985). Ac RPs are shown in part *A*; dc RPs in part *B*. The third (second) turn results are plotted with solid (dashed) lines.

increasing degree of non-linearity may have evolved to compensate for the low-pass filtering of the ac RP, which is reflected in the degradation of phase locking at the single unit kevel (Kiang et al., 1965; Harrison and Evans, 1979, Palmer and Russell, 1986). Thus, the dc RP is probably responsible for transmitter release in the basal region of the cochlea (Russell and Sellick, 1978; Schmiedt and Zwislocki, 1978).

Characterization of OHC responses has been more difficult than for IHCs. Presumably, this is because they are less tightly held, are mostly surrounded by fluid and possibly because they are motile. The earliest recordings revealed that in apex and base, OHC resting potentials were different from those observed for IHCs (Dallos et al., 1982; Russell and Sellick, 1983). The latter were generally −40 mV. In other words, IHCs are depolarized relative to surrounding supporting cells. By contrast, OHC resting potentials are roughly −70 mV, which is in line with other cells in the body.

As an example of OHC response patterns, the frequency response functions measured at 70 dB for both ac (part *A*) and dc (part *B*) RPs are plotted in Fig. 2 for turns three and two. The two cells produce similar response patterns although the ac RP (Fig. 2*A*) recorded in the second-turn OHC is filtered to a greater degree by the cell's basolateral membrane than is the response recorded in turn three. Plots of the dc RPs in the right panel demonstrate that OHCs in both of these regions produce depolarizing dc RPs around CF, which has also been reported for OHCs in turn four (Dallos, 1986). It should be emphasized that comparisons between cochlear turns and cell types are intended to be qualitative. Quantitative comparisons are probably premature until more numerous second-turn OHC recordings have been accumulated.

In contrast to Fig. 2, where stimulus frequency was the parameter, input − output functions are plotted in Fig. 3 to compare OHC responses (part *A*) with those measured in the organ of Corti fluid space (part *B*). The stimulus frequency is 3500 Hz. At all levels between 40 and 80 dB SPL, the OHC response is depolarizing and exceeds that recorded

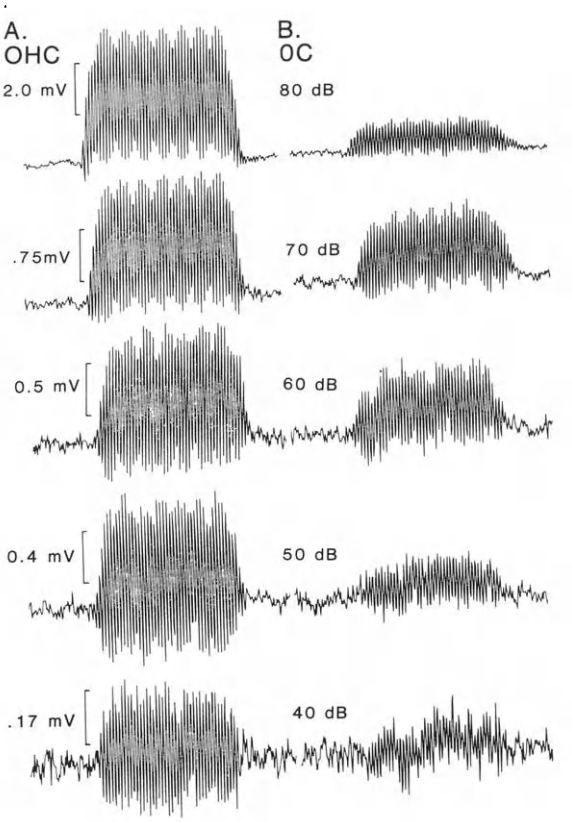

Fig. 3. Response wave forms from an OHC (part *A*) and from the organ of Corti fluid space (part *B*). The stimulus frequency is 3500 Hz. Input sound level is the parameter and varies between 40 and 80 dB SPL. The order of stimulus presentations was as follows: 80, 50, 40, 60 and 70 dB SPL. Both OHC and OC responses are plotted on the same scale to facilitate comparisons. The duration of the tone bursts was 15 msec including the 2.5 msec rise/fall times. The resting potential of the OHC was −82 mV.

extracellularly in the surrounding fluid. The OHC/OC ratio is not constant, which probably reflects a degradation in OHC responsiveness over time. Although the input sound levels are arranged in decreasing order, they were obtained in a randomized sequence.

To compare IHC and OHC responses at one cochlear location, individual response wave forms are displayed in Fig. 4. The stimulus, 3250 Hz, is presented at a level of 80 dB SPL. The figure demonstrates that both cell types produce a sizable response composed of both ac and dc components.

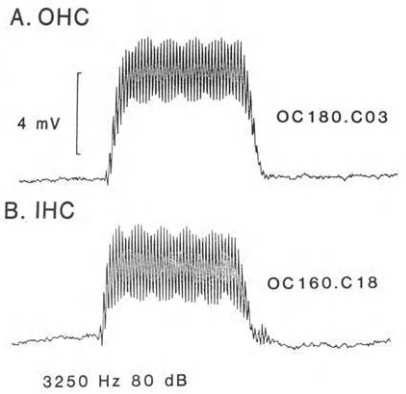

Fig. 4. Response wave forms for an OHC (part *A*) and IHC (part *B*) at 3250 Hz and 80 dB SPL (reproduced from Dallos and Cheatham (1992), by copyright permission of the Rockefeller University Press). The OHC was recorded 55 μm into the OC; the IHC at 130 μm. The OHC resting potential was -58 mV; that for the IHC was -38 mV. Although both cells were from the second turn, they were obtained from different animals.

The latter is depolarizing in both cases and exhibits a similar dynamic pattern in the two cells.

Responses obtained well below CF are presented in Fig. 5. The purpose of this figure is to demonstrate a distinction between the two hair cell populations. These wave forms represent responses to 150 Hz at 80 dB SPL. On the top, the OHC response is compared with that recorded in the OC fluid space adjacent to the cell. The latter is smaller in magnitude than the response recorded intracellularly. Note that OC and OHC responses are in phase. This contrasts with the IHC wave form at the bottom. Here the intracellular ac RP leads the ac response that is measured just outside the cell in the OC. This phase difference between IHCs and OHCs is expressed at all four cochlear locations (Nuttall et al., 1981; Dallos and Santos-Sacchi, 1983; Russell and Sellick, 1983) and confirms that IHC stereocilia are free-standing while the tallest stereocilia of outer hair cells are firmly embedded in the tectorial membrane (Kimura, 1966; Hunter-Duvar, 1978). In other words, at very low frequencies, IHCs are velocity detectors. Above several hundred Hertz, however, both IHCs and OHCs respond to basilar membrane displacement.

It must be emphasized that all IHCs and OHCs recorded using the lateral approach in turns four, three and two produce depolarizing responses when stimulated at and around CF. Although this result is consistent with reports for cultured hair cells in the mouse (Russell et al., 1986; Russell and Richardson, 1987) and with responses from all non-mammalian hair cell systems (Hudspeth and Corey, 1977; Crawford and Fettiplace, 1981; Holton and Weiss, 1983), it differs from in vivo recordings in the base of the guinea pig cochlea (Russell and Sellick, 1983; Cody and Russell, 1987). Outer hair cells with high CFs produce depolarizing RPs only with stimulus levels that are at or above 90 dB SPL. These responses also require several cycles to develop, whereas the dc RPs in basal-turn IHCs are manifest instantaneously as are those exhibited by hair cells in the apex of the cochlea. Because the ac RP is filtered by the hair cell's basolateral membrane, any sensory function for basal-turn OHCs is virtually eliminated.

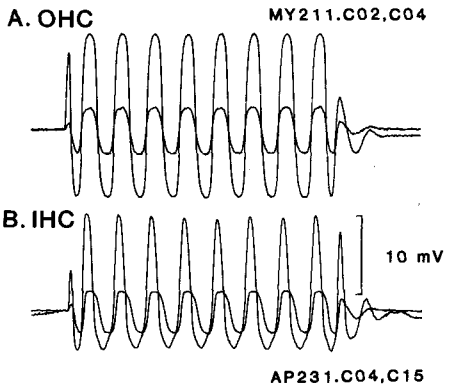

Fig. 5. To demonstrate differences in response phase, wave forms are shown in response to a 150 Hz stimulus at 80 dB SPL (reproduced from Dallos and Cheatham (1992), by copyright permission of the Rockefeller University Press). In part *A*, the OHC (-82 mV resting potential) ac RP is compared with the cochlear microphonic recorded in the OC. The extracellular response is smaller in magnitude than the response recorded in the OHC. In part *B*, the OC response is compared with the response measured in an IHC with a resting potential of -46 mV. The OHC was located 60 μm after contacting the first Hensen cell; the IHC was at 132 μm. These recordings were not made in the same cochlea.

Acknowledgement

This work was supported by NIH Grant DC00089.

References

Altschuler, R.A. and Fex, J. (1986) Efferent neurotransmitters. In: R.A. Altschuler, D.W. Hoffman and R.P. Bobbin (Eds.), *Neurobiology of Hearing*, Raven Press, New York, pp. 323 – 347.

Bohne, B.A. and Carr, C.D. (1979) Location of structurally similar areas in chinchilla cochleas of different lengths. *J. Acoust. Soc. Am.*, 66: 411 – 414.

Brownell, W.E., Bader, C.R., Bertrand, D. and de Ribaupierre, Y. (1985) Evoked mechanical responses of isolated cochlear outer hair cells. *Science*, 227: 194 – 196.

Cheatham, M.A. and Dallos, P. (1989) Two-tone suppression in inner hair cell responses. *Hearing Res.*, 40: 187 – 196.

Cheatham, M.A. and Dallos, P. (1992) Physiological correlates of off-frequency listening. *Hearing Res.*, 59: 39 – 45.

Cody, A.R. and Russell, I.J. (1987) The responses of hair cells in the basal turn of the guinea-pig cochlea to tones. *J. Physiol. (Lond.)*, 383: 554 – 569.

Crawford, A.C. and Fettiplace, R. (1981) Nonlinearities in the responses of turtle hair cells. *J. Physiol. (Lond.)*, 315: 317 – 338.

Dallos, P. (1984) Some electrical circuit properties of the organ of Corti. II. Analysis including reactive elements. *Hearing Res.*, 14: 281 – 291.

Dallos, P. (1985) Response characteristics of mammalian cochlear hair cells. *J. Neurosci.*, 5: 1591 – 1608.

Dallos, P. (1986) Neurobiology of cochlear inner and outer hair cells: intracellular recordings. *Hearing Res.*, 22: 185 – 198.

Dallos, P. (1988) Cochlear neurobiology: some key experiments and concepts of the past two decades. In: G.M. Edelman, W.E. Gall and W.M. Cowan (Eds.), *Auditory Function*, Wiley, New York, pp. 153 – 188.

Dallos, P. and Cheatnam, M.A. (1992) Cochlear hair cell function reflected in intracellular recordings in vivo. In: D.P. Corey and S.D. Roper (Eds.), *Sensory Transduction, Society of General Physiologists Symposium*, Rockefeller University Press, New York, pp. 371 – 393.

Dallos, P. and Santos-Sacchi, J. (1983) AC receptor potentials from hair cells in the low-frequency region of the guinea pig cochlea. In: W.R. Webster and L.M. Aitkin (Eds.), *Mechanisms of Hearing*, Monash University Press, Clayton, Australia, pp. 11 – 16.

Dallos, P., Santos-Sacchi, J. and Flock, A. (1982) Intracellular recordings from cochlear outer hair cells. *Science*, 218: 582 – 584.

Davis, H. (1983) An active process in cochlear mechanics. *Hearing Res.*, 9: 79 – 90.

Engstrom, H. (1958) On the double innervation of the sensory epithelia of the inner ear. *Acta Otolaryngol.*, 49: 109 – 118.

Evans, E.F. (1972) The frequency response and other properties of single fibres in the guinea-pig cochlear nerve. *J. Physiol. (Lond.)*, 226: 263 – 287.

Guinan, J.J., Warr, W.B. and Norris, B.E. (1983) Differential olivocochlear projections from lateral versus medial zones of the superior olivary complex. *J. Comp. Neurol.*, 221: 358 – 370.

Guth, P.S., Norris, C.H. and Bobbin, R.P. (1976) The pharmacology of transmission in the peripheral auditory system. *Pharmacol. Rev.*, 28: 95 – 125.

Harris, D.M. (1979) Action potential suppression, tuning curves and thresholds: comparison with single fiber data. *Hearing Res.*, 1: 133 – 154.

Harrison, R.V. and Evans, E.F. (1979) Some aspects of temporal coding by single cochlear fibers from regions of cochlear hair cell degeneration in the guinea-pig. *Arch. Otol. Rhinol. Laryngol.*, 224: 71 – 78.

Holton, T. and Weiss, T.F. (1983) Receptor potentials of lizard cochlear hair cells with freestanding stereocilia in response to tones. *J. Physiol. (Lond.)*, 345: 205 – 240.

Hudspeth, A.J. and Corey, D.P. (1977) Sensitivity, polarity and conductance changes in the response of vertebrate hair cells to controlled mechanical stimulation. *Proc. Natl. Acad. Sci. U.S.A.*, 74: 2407 – 2411.

Hunter-Duvar, I. (1978) Electron microscopic assessment of the cochlea. *Acta Otolaryngol. (Suppl.) (Stockh.)*, 351: 1 – 44.

Kachar, B., Brownell, W.E., Altschuler, R. and Fex, J. (1986) Electrokinetic shape changes of cochlear outer hair cells. *Nature*, 322: 365 – 368.

Kiang, N.Y-S., Watanabe, T., Thomas, E.C. and Clark, L.F. (1965) *Discharge Patterns of Single Fibers in the Cat's Auditory Nerve*, MIT Press, Cambridge, MA.

Kidd, R.C. and Weiss, T.F. (1990) Mechanisms that degrade timing information in the cochlea. *Hearing Res.*, 49: 181 – 207.

Kim, D.O. (1984) Functional roles of inner- and outer-hair cell subsystems in the cochlea and brainstem. In: C.I. Berlin (Ed.), *Hearing Science: Recent Advances*, College-Hill, San Diego, CA, pp. 241 – 262.

Kimura, R.S. (1966) Hairs of the cochlear sensory cells and their attachment to the tectorial membrane. *Acta Otolaryngol.*, 61: 55 – 72.

Klinke, R. and Galley, N. (1974) Efferent innervation of vestibular and auditory receptors. *Physiol. Rev.*, 54: 315 – 357.

Lim, D.J. (1980) Cochlear anatomy related to cochlear micromechanics: a review. *J. Acoust. Soc. Am.*, 67: 1686 – 1695.

Lim, D.J. (1986) Functional structure of the organ of Corti: a review. *Hearing Res.*, 22: 117 – 146.

Nuttall, A.L., Brown, M.C., Masta, R.I. and Lawrence, M. (1981) Inner hair cell responses to velocity of basilar membrane motion in the guinea pig. *Brain Res.*, 211: 171 – 174.

Ohlemiller, K.K. and Echteler, S.M. (1990) Functional correlates

of characteristic frequency in single cochlear nerve fibers of the Mongolian gerbil. *J. Comp. Physiol. A,* 167: 329 – 338.

Palmer, A.R. and Russell, I.J. (1986) Phase-locking in the cochlear nerve of the guinea-pig and its relation to the receptor potential of inner hair-cells. *Hearing Res.,* 24: 1 – 15.

Pujol, R. (1991) Is the length of OHCs correlated with frequency coding in the cochlea? *Abstr. Assoc. Res. Otolaryngol.,* p. 125.

Russell, I.J. and Richardson, G.P. (1987) The morphology and physiology of hair cells in organotypic cultures of the mouse cochlea. *Hearing Res.,* 31: 9 – 24.

Russell, I.J. and Sellick, P.M. (1978) Intracellular studies of hair cells in the mammalian cochlea. *J. Physiol. (Lond.),* 284: 261 – 290.

Russell, I.J. and Sellick, P.M. (1983) Low-frequency characteristics of intracellularly recorded receptor potentials in guinea-pig cochlea. *J. Physiol. (Lond.),* 338: 179 – 206.

Russell, I.J., Cody, A.R. and Richardson, G.P. (1986) The response of inner and outer hair cells in the basal turn of the guinea-pig cochlea and in the mouse cochlea grown in vitro. *Hearing Res.,* 22: 199 – 216.

Schmiedt, R.A. (1989) Spontaneous rates, thresholds and tuning of auditory nerve fibers in the gerbil: comparisons to cat data. *Hearing Res.,* 42: 23 – 36.

Schmiedt, R.A. and Zwislocki, J.J. (1978) Low frequency neural and cochlear-microphonic tuning curves in the gerbil. *J. Acoust. Soc. Am.,* 64: 502 – 507.

Smith, C.A. (1961) Innervation pattern of the cochlea. The internal hair cell. *Ann. Otol. Rhinol. Laryngol.,* 70: 504 – 527.

Smith, C.A. and Sjöstrand, F.S. (1961) A synaptic structure in the hair cells of the guinea pig cochlea. *J. Ultrastruct. Res.,* 5: 523 – 556.

Spoendlin, H. (1969) Innervation patterns in the organ of Corti in the cat. *Acta Otolaryngol.,* 67: 239 – 254.

Spoendlin, H. (1970) Structural basis of peripheral frequency analysis. In: R. Plomp and G. Smoorenburg (Eds.), *Frequency Analysis and Periodicity Detection in Hearing,* A.W. Sijthoff, Leiden, pp. 2 – 36.

Warr, W.B. (1978) The olivocochlear bundle: its origins and terminations in the cat. In: R.F. Naunton and C. Fernandez (Eds.), *Evoked Electrical Activity in the Auditory Nervous System,* Academic Press, New York, pp. 43 – 63.

Weiss, T.F. and Rose, C. (1988) Stages of degradation of timing information in the cochlea: a comparison of hair-cell and nerve-fiber responses in the alligator lizard. *Hearing Res.,* 33: 167 – 174.

Weiss, T.F., Mulroy, M.J. and Altmann, D.W. (1974) Intracellular responses to acoustic clicks in the inner ear of the alligator lizard. *J. Acoust. Soc. Am.,* 55: 606 – 619.

J.H.J. Allum, D.J. Allum-Mecklenburg, F.P. Harris and R. Probst
Progress in Brain Research, Vol. 97

CHAPTER 3

Sound preprocessing by ac and dc movements of cochlear outer hair cells

H.P. Zenner and A. Ernst

Department of Otolaryngology, University of Tübingen, Germany

In inner and outer hair cells, a sound event results mechano-electrically in a receptor potential from the hair cells by the functioning of apical and lateral K^+-channels. However, after this point, the signal transfer is divided. Inner hair cells (IHC) release an unknown afferent transmitter. By contrast, outer hair cells (OHC) are proposed to produce mechanical ac and dc responses. In our model, the ac components of the sound signal, the carrier frequencies, determine the response of the OHC. Usually, they respond by ac and dc movements. The rapid ac movements of OHC, for which the underlying mechanism is unknown, may respond cycle-by-cycle to and interfere with the carrier frequency of the traveling wave. Near hearing threshold, they could drastically amplify the traveling wave thus contributing to the postulated cochlear amplifier. Active dc movements of the cytoskeleton of the cell body, as well as of the cuticular plate with the sensory hairs, are proposed to respond to millisecond changes of the sound stimulus over time. Such changes could be a modulation of the amplitude (AM), i.e., an increase or decrease of the sound pressure level (SPL), which is reflected in the envelope of the traveling wave. The active mechanical dc response of OHC to the amplitude (AM) and frequency modulation (FM) pattern is then expected to result in dc position changes of the reticular lamina (RL). These should control the operation point of the stereocilia, thus influencing their transfer function and sensitivity. In addition, experimental data suggest that there are modulations of the compliance of the organ of Corti (OC) and changes of its geometry. This dc modulation of micromechanical properties and geometry of the OC by active force generation of OHCs might contribute to automatic gain control, adaptation, TTS, as well as to the homeostasis of the basilar membrane location. In particular, the motile mechanism may protect the vulnerable cochlear partition against high sound pressure levels. Moreover, according to this model, changes of the sound signal with time are expected to be encoded in the actively produced dc movements of the RL. As the signal changes may carry important information (e.g., complex sound signal modulations such as formant transitions in speech), this is extracted and mechanically encoded by the proposed active dc mechanism. It cannot be excluded that the information-carrying dc signal is transferred to inner hair cells contributing to their adequate stimulus. If this is true, then information due to sound signal changes would appear subsequently in the cochlea as active mechanical low-frequency events even at high-carrier frequencies. This would allow the cochlea to adapt parts of its information encoding to the limited frequency of the afferent transmitter release from IHC whose cycle-by-cycle encoding is known to be restricted to low frequencies (phase locking).

Key words: Hair cell; Cochlea; Sensory receptors; Active mechanisms; Otoacoustic emission

Introduction

The cochlea is no longer regarded as a passive mechanical signal analyzer. Active mechanical processes have been suggested that are thought to modulate the oscillations of the basilar membrane (BM) (Rhode, 1971; Zwicker, 1979; LePage and Johnstone, 1980; Kim et al., 1980; Khanna and Leonard, 1982; Sellick et al., 1982). The outer hair cells (OHC) are probably the elements that contribute to this active mechanical control of the BM displacements (Leonard and Khanna, 1984; Brownell

et al., 1985; Zenner et al., 1985a). Cochlear OHC are able to perform two types of active movement in vitro and in situ. These are characterized as reversible, fast ac (Brownell et al., 1985) and reversible, slow dc motility (Zenner et al., 1985b). The ac movements show time constants within the microseconds range, the dc movements are effective within the milliseconds range. This paper summarizes our data and reviews results from the literature to present hypotheses on the possible physiological role of the ac and dc motility of OHC.

According to the cochlear amplifier hypothesis, the ac mechanism (Brownell et al., 1985; Ashmore, 1987; Zenner et al., 1987) responds cycle-by-cycle to the waves of the signal. It seems to explain the biophysical concept of hearing at a low sound pressure level (SPL): mechanical energy is released in a cochlear region basally to the tonotopic point of the test frequency (cochlear amplifier). This leads in turn to an active increase in sensitivity by about 40 dB (Rhode, 1971; Zwicker, 1979; LePage and Johnstone, 1980; Khanna and Leonard, 1982; Sellick et al., 1982).

As a response to changes of SPL or frequency, the dc mechanism supposedly triggers the position of the cochlear partition and the operating point of the stereocilia. Thus, it may influence the sensitivity to low and the protection against high sound pressure levels (Zenner, 1986b,c; LePage, 1987). Moreover, natural sound signals such as human speech are characterized by continuous amplitude and frequency modulations. Formant transitions are an important example of speech waveform modulation and carrier of information (Khanna, this volume). Thus, it cannot be excluded that the active dc response of OHC is an active mechanical encoding strategy of the cochlea to process the information underlying modulations of SPL or frequency. Subsequently, the actively processed information underlying the mechanical dc signal may be transferred to inner hair cells (IHC) for final transduction.

Material and methods

The relevant methods applied in our experiments are extensively described in Zenner et al. (1985a,b, 1987, 1988a, 1989), Zenner (1986b,d, 1988), Gitter and Zenner (1988), Reuter et al. (1988), Reuter and Zenner (1990), Reuter et al. (1991) and Gitter et al. (1992).

Results and discussion

OHC as a potential site of the cochlear amplifier

The most compelling evidence for the genesis of an active mechanical amplification in the cochlea relies on the fact that the amplifier produces a motor force. The cellular substrates for this movement are thought to be the OHC. The basic difference between the characteristics of a travelling wave in a living and in a post-mortem preparation can be attributed to the activity of the OHC. When destroying the OHC selectively in a living organism, the ear does not become deaf, but it loses frequency selectivity and the travelling wave has a broad and unsharp appearance as in the post-mortem ear (Ryan and Dallos, 1975; Dallos and Harris, 1978; Dallos et al., 1980; Liberman and Dodds, 1984).

Kiang et al. (1970) selectively destroyed OHC using kanamycin. This led to a loss of sharp tuning in the single fiber recordings from the cochlear nerve. On the flat part of the tuning curve, positioned at the basal part of the cochlea, the nerve remained preserved (this finding also indicates that the sharp tuning of the eighth nerve is produced by the OHC and not by the nerve itself). It is worth mentioning in this respect that inner ear diseases that produce reduced speech understanding ability (loss of frequency selectivity) primarily begin with a selective destruction of OHC (Meyer zum Gottesberge, 1948; Lehnhardt, 1984).

OHC are anatomically well positioned to modulate the movements of the tectorial membrane (Allen, 1980; Lim, 1980). The number of OHC is triple the number of IHC. At the same time, the OHC are the target of the efferent nerve supply from brain to cochlea (Rasmussen, 1942; Engström, 1958; Smith, 1961; Spoendlin and Gacek, 1963; Spoendlin, 1969).

Manipulations of the crossed olivo-cochlear bun-

dle, about 90% of whose efferent fibers end on OHC, influence the sharp tuning. They lead to a flattened tip of the nerval tuning curves and change the receptor potentials of the IHC (Dallos et al., 1980). This also leads to the conclusion that the tuning curves of the cochlear nerve and of the IHC largely depend on a triggering by the OHC. Therefore the OHC should not only be capable of sound perception, but also should act as peripheral mechanical effector cells (Siegel and Kim, 1982; De Boer, 1983a,b; Flock, 1983; Flock and Strelioff, 1984; Brownell et al., 1985; Zenner et al., 1985a,b, 1988a; Kim, 1986; Zenner, 1986b,c; Ashmore, 1987). From a physiological point of view, this mechanism is called the cochlear amplifier. It is a rule that the smaller the stimulus, the larger the amplification. Subsequently, the resulting signal, actively preprocessed by the motor forces of OHC, is perceived and transduced by IHC and the transduced signal is passed to the cochlear nerve.

Motor forces of OHC. The static mechanical forces that are produced by guinea pig OHC during a contraction have been measured by Gitter et al. (1993). They sucked isolated, viable OHC into capillaries and a defined mechanical load of the cell was used to determine the active force that an OHC needed to overcome an elongating force. An extracellular electrical stimulus of 1 mV was chosen because usually OHC are exposed to a physiological potential difference between the subtectorial (scala media) and Nuel's space (scala tympani), i.e., the electrical fields of cochlear microphonics (CM) and the summating potential (SP). This potential difference is changed at the tip of the OHC during the process of hearing, which produces the CM. When the CM is measured in scala vestibuli and tympani by microelectrodes, it can be measured at the tip of the OHC with a stimulus of approximately 1 mV (Tasaki et al., 1952, 1954). The force of an OHC (third turn) was found to be 14 pN/mV at a compliance of 300 – 400 m/N. Under the assumption of 50 – 60 OHC commonly innervated as a motor unit (LePage, 1987; Plinkert et al., 1990; LePage et al., 1991), a force of 700 pN/mV is produced. The stiffness of the cochlear partition, measured at the basilar membrane with a probe of 25 μm in diameter, is 0.48 N/m corresponding to 480 pN/nm at a distance of 1.6 mm from the stapes (Gummer et al., 1981). Hence, the motor amplitude of 4.5 nm and the force of 700 pN/nm produced by a stimulus of 1 mV in 50 OHC seems to be effective enough to lead to an in situ movement. These results provide a basis for future research to determine the potential work and power of OHC. This will answer the question of whether OHC are able to compensate for the friction of the OC.

Ac Movements of outer hair cells

Ac motility in vitro and in situ. Longitudinal ac movements of the cylindrical cell body of OHC can be electrically induced, as demonstrated by several groups (Brownell et al., 1985; Zenner et al., 1987, 1988a,b; Ashmore, 1987). Their time constant of 240 μsec is within the submillisecond range (Ashmore, 1987; Zenner et al., 1987). A digital subtraction can be used to visualize movements of the cuticular plate in some of the cells, leading to a stereociliary displacement (Zenner et al., 1988a).

The velocity of the electrogenic OHC motility is remarkable (Santos-Sacchi, 1989). The exposure of isolated guinea pig OHC to an ac field induces active longitudinal oscillations up to 30 kHz as shown by photoelectric measurements (Zenner et al., 1987; Gitter and Zenner, 1988, 1993). An intracellular microinjection of an ac current results in a movement with a frequency of up to 10 kHz. Their latency period is only 120 μsec (Ashmore, 1987). A depolarization is followed by a contraction as monitored by video and photoelectrical techniques (Zenner et al., 1985a, 1988b; Ashmore, 1987). A hyperpolarization induces an elongation of the cell body.

An extracellular, electrical ac field induces OHC movements of up to 15 kHz in situ, i.e., within the organ of Corti as visualized by video enhancement and measured by photoelectrical methods (Reuter et al., 1988, 1991; Khanna et al., 1989a,b; Zenner et al., 1989, 1990; Reuter and Zenner, 1990). The motility is limited to that particular region of the organ

of Corti where the OHC are located. Due to their mechanical coupling to OHC, a co-movement of the tunnel of Corti or of the IHC region is seen. A decline of the amplitudes can be observed in vitro and in situ with an increase of motility frequency (Reuter et al., 1991; Gitter and Zenner, 1993). The amplitude of the OHC movement decreases by a minimum of 20 dB/decade above 200 Hz for the extracellular as well as for the intracellular electrical stimulation (Gitter and Zenner, 1993). This corresponds to the electrical corner frequency between 50 Hz and 1.3 kHz as defined by the time constant of 0.13 – 3 msec of the OHC membrane capacity (Dallos, 1985; Santos-Sacchi, 1989). Thus, the loss of amplitude might be due in part to the membrane capacity. One must also consider a hydrodynamic inhibition since it is increased with a rise in velocity. This leads either to a high energy consumption in increasing frequencies of motility or to a reduction in the amplitudes. In both cases, the electromechanical efficiency becomes reduced with increasing frequency.

Unknown mechanism of ac motility. The molecular basis of these fast movements is unknown. They cannot be influenced by dinitrophenol (inhibitor of the cellular energy production), cytochalasine B and phalloidin (they interfere with the actin skeleton of OHC) (Ashmore, 1987; Zenner et al., 1987; Reuter and Zenner, 1990). Hence, actin and myosin can be excluded as underlying molecules and ATP as biochemical energy source. Further controls have shown that another prerequisite for the fast motility is the integrity of the outer cellular membrane consisting of lipid and protein molecules and that the OHC must possess their cylindrical shape (Gitter and Zenner, 1993). A physical process is postulated (Brownell et al., 1985; Kachar et al., 1986; Dallos et al., 1991).

It is a matter of speculation whether these movements are controlled by the receptor potential. The electromechanical efficiency of the receptor potential in isolated OHC has been determined to be 2 μm/V at a resting potential of -70 mV (Santos-Sacchi, 1989). This value seems to be too small (Hudspeth, 1989) for the receptor potential to induce any significant motor effect close to the threshold (Santos-Sacchi, 1989). Electrical fields are possible candidates as the driving signal, which could be demonstrated by Zenner and Gitter (1987) and Reuter and Zenner (1990). In their investigations, non-conducting mannitol solutions were used as the bath for electrically stimulating OHC. In addition, Dallos et al. (1991) also attributed the driving force to an electrical field by investigating OHC sucked into capillaries. Electrical ac fields are produced in vivo by CM and SP around OHC. It might be credible in this respect that the CM trigger a fast ac movement and the SP contribute to the control of a dc movement.

However, it still remains to be elucidated whether the evidenced fast OHC motility actually represents the motor force underlying the active cochlear frequency tuning. In addition, otoacoustic emissions from the cochlea are not limited to mammals. They can also be detected in birds and reptiles, which possess no OHC (Manley et al., 1987; Van Dijk and Wit, 1987; Wit et al., 1989).

Dc movements of outer cells

Active position changes of the cochlear partition. The cochlea is able to change the position of its partition to sound stimuli (LePage, 1987). The cochlea should also be capable of correcting an undesired shift in the cochlear partition resulting from an altered production of endolymph and perilymph (Johnstone et al., 1986). The large dynamic range of hearing is obviously also compressed within the ear by its non-linearity (compression of dynamics). It has to be considered that an increase of the fast (ac) motility of the OHC is linearly correlated to the intensity of the stimulus (Gitter and Zenner, 1991). Hence, this cannot explain the decreasing amplification, i.e., the non-linearity, above 40 dB SPL. At high sound pressure levels, the compression has to be so large that a protective mechanism comes into action. It adapts the cochlea mechanically to prevent a sound-induced injury (adaptation, protection). One possible hypothesis to explain the

above mentioned aspects might be a second mechanism of OHC motility, i.e., the so-called slow motility. Although it has already been experimentally evidenced, its physiological role is still a matter of controversy.

When depolarizing isolated OHC by application of potassium gluconate or a dc current (Zenner et al., 1985a,b, 1988a,b; Zenner, 1986a,b,c,d), slow, reversible contractions and elongations (dc movements) of the cell body linked to a deflection of the cuticular plate and its stereocilia can be reproduced. Their time constants are in the milliseconds range. A change between depolarization and repolarization enables the OHC to pass through several cycles of contraction and elongation. Fura-2 measurements (they display free Ca^{2+}) consequently show an increase of Ca^{2+} during depolarization (Reuter and Zenner, 1990). In another set of experiments, longitudinal movements with a velocity of $3-24$ nm/msec could be induced by an intracellular increase of Ca^{2+} and ATP, leading to a stimulation of the actomyosin network (Flock et al., 1986; Zenner, 1986c, 1988). Shortenings of OHC could also be demonstrated by vibratory stimulation of the cell body (Canlon et al., 1988). A tuning of the slow OHC contraction could be found by stimulation in the low-frequency region (Brundlin et al., 1989).

An experimental increase of the perilymphatic potassium concentration has led to a histologically evidenced contraction of OHC in situ in analogy to the potassium-induced depolarization and contraction of isolated OHC. The length of the IHC remains unchanged. The shortening of the OHC causes a reduced distance between the basilar membrane (BM) and reticular lamina, thus producing a compression of the organ of Corti (Zenner and Gitter, 1989). A sudden increase of the amplitude of electrical stimuli results in an altered position of the reticular lamina towards the scala vestibuli (LePage et al., 1991). LePage observed an acoustically induced shift of the cochlear partition from its mid position. The basilar membrane was shifted towards the vestibular or tympanic scala at higher or lower stimulation frequencies whereas the corresponding point of the BM remained unchanged at frequencies close to the characteristic frequency (CF) (LePage, 1987). In this respect, the BM is shifted towards the scala vestibuli just below the CF and further away from scala tympani. A shift towards the tympanic scala was observed even above the point of the CF.

In case of a link between the OHC-induced shift of the cochlear partition towards tympanic or vestibular scala with a subsequent shift of the TM, one has to expect a dc deflection of the stereocilia of OHC towards the modiolus or laterally. Such a mechanism necessarily influences the transfer function of the stereocilia, which is angle-dependent. Dc deflections of the stereociliary angle out of a mid position into a negative or positive direction lead to a reduced transfer function and, hence, to the sensitivity to vibrations. Vice versa, it can be expected that slow movements of OHC can reverse passively induced displacements of the cochlear partition with a deflection of the stereociliar bundle into the mid position: the passively induced deterioration of the transfer function of the affected hair cells is improved. This means that the mechanism of slow motility is well suited for influencing the operation point of the reticular lamina and, thus, the operation angle of the stereocilia (Zenner, 1986b). The resulting low-frequency changes of hair bundle deflections are to be expected preferably in OHC but not in IHC. It can be assumed therefore that the operation angle, and subsequently the transfer function of the hair bundle of OHC, are changed at the point of a positional change of the cochlear partition whereas the IHC sensitivity is influenced to a lesser extent.

When transferring these ideas to the results of LePage (1987), one notices that only when the BM (and the hair bundle deflection, respectively) is in a mid position, it is sensitive to OHC that are close to the CF. A clear change in position can only be recognized above and below the CF, which must be linked with a deterioration in sensitivity of the vibratory transfer function – predominantly of OHC. The sensitive mid position close to the CF reflects an optimum of amplification because the vibratory transfer function of OHC probably triggers the cochlear amplifier. A positional change below and above the

CF leads to a reduction of amplification. The result would be an optimization of the active travelling wave at the CF and a bilateral inhibition*, as suggested earlier to be a function of the slow motility (Zenner, 1986c). This would support an energy supply for the cochlear amplifier at a certain location. Thus, it cannot be ruled out that this mechanism contributes actively and mechanically to the definition of the location of the fast cochlear amplifier.

Compression of the dynamic range (cochlear attenuator). The elevation of the active travelling wave by the cochlear amplifier is reduced when SPL is increased (largely above 40 dB SPL): the amplification is larger at low than at moderate SPL, i.e., the system is non-linear. The behavior of the fast OHC movements in vitro is non-vulnerable after a challenge and is highly linear with an increase in stimulus. Therefore, these components cannot explain the physiological non-linearity (Gitter and Zenner, 1993). It is credible that an increase in the SPL causes the occurrence of an OHC dc movement (dc component) in addition to the fast (ac component) movement to induce a compressive non-linearity that declines as amplitude increases. It would correspond to an "automatic gain control" (AGC). At the same time, the sensitivity for intensity differences would be decreased, but not to the same extent because of the increase in stimulus intensity. This helps to explain the broader tuning with increases in SPL. The reduced increase of the vibratory amplitude might underly the relative improvement of temporal resolution that occurs at the same time (Dallos, 1988). A linear increase of the vibration amplitude would require such a high velocity and amplitude of the vibrating tissues that it could not be realized within the cochlea. The decreased amplitude, however, would reduce the velocity and improve temporal resolution. This might be of use for speech discrimination at a higher SPL.

Thus, it seems reasonable that the mechanism of the slow OHC motility (dc component) contributes to a compression of the dynamic range by active positioning (Zenner, 1986c) of the cochlear partition and/or by a change in the motility (stiffness, compliance, damping) and geometry of the partition. A dc reduction of the passive displacement ("cochlear attenuator") seems likely to improve the position and, subsequently, the transfer function of the hair bundle, and thus to express more effectively the cochlear ac amplifier. This could contribute to the understanding of speech in higher noise levels. Electrophysiological recordings of OHC of the lower turn (Cody and Russell, 1987) clearly demonstrate that OHC can produce a dc potential only at high SPL or at low frequencies. This corresponds to the idea that it is an OHC requirement to recognize positional changes of the cochlear partition (deviations from the mid position). It cannot be ruled out that the result of this measurement of position is transferred as a nerve signal via the afferent fibers.

Frequency modulation and cochlear amplifier. Observations by Canlon et al. (1988) and Brundin et al. (1989) have shown a frequency-tuned, tonic movement of the hair cell to vibratory stimulation of the OHC body. Our results have confirmed these findings (Reuter and Zenner, in preparation) and could evidence, in addition to ac responses, dc movements of the OHC as responses to changes of the frequency or stimulus intensity. Thus, OHC seem to respond to the stimulus envelope. The ac carrier frequency determines the frequency characteristic of OHC that responds with a dc movement far below the frequency of the stimulus. A high frequency is obviously partly converted into a lower frequency, i.e., a frequency modulation takes place. It cannot be ruled out that the frequency-modulated (down-modulated), mechanical dc signal of OHC represents the basis of an adequate IHC stimulus. The frequency modulation would help to adapt the mechanical signal to the limited frequency of the afferent transmitter release from IHC and of the neural phase locking.

Not all cochlear models require a cycle-by-cycle mode of the cochlear amplifier to account for sharp tuning (Zwicker, 1986a,b). Thus, it cannot be ex-

* Another possible mechanism are antiphasic ac movements.

cluded that the OHC dc response is the cellular basis of the cochlear amplifier. Interestingly, the velocity of the dc OHC movements of 3 – 24 nm/msec (Zenner, 1988) is within the same range as the BM velocity of 30 nm/msec measured by means of the Mössbauer technique with the cochlear amplifier in action (Sellick et al., 1982). Furthermore, in contrast to the electrokinetic ac movements, the ATP-dependent OHC movements are physiologically vulnerable. Moreover, latencies of transiently evoked otoacoustic emissions (TEOAE) are considerably long, which does not exclude a slow-acting non-linearity that possibly responds to the sound signal envelope.

Adaptation, noise protection and TTS. The ear can adapt to a high SPL (Keidel et al., 1961). This is a rather slow process, e.g., the cochlea can adapt to the sound pressure wave of an explosion when the blast wave has reached its maximum beyond 1.5 msec. A sound event that results in injury reaches the maximum pressure in less than 1.5 msec (Pfander, 1975; Becker et al., 1986; Zenner, 1991). The adaptation does not seem to be fast enough in acute noise trauma. An imitation of high SPL by a tonic hair bundle deflection in the frog leads to an adaptation reflected by a progressive decrease of the transduction current. This process has a course that is 1000 times slower than the mechano-electrical transduction. The time constant of a half-saturating stimulus amounts to 30 msec (Eatock et al., 1987). The process of adaptation is dependent upon the endolymphatic Ca^{2+} concentration (Eatock et al., 1987; Assad et al., 1989). The hair bundle becomes less stiff (Howard and Hudspeth, 1987). The underlying mechanism has not yet been experimentally evidenced. The conclusion, after summarizing the few available data, might be that a calcium-dependent, slow mechanical process of adaptation could be involved, as demonstrated in OHC.

The actomyosin-dependent process of motility requires an increase of the free, intracellular Ca^{2+} (Zenner, 1986c, 1988). This correlates nicely to the calcium dependence of the adaptation process (Eatock et al., 1987; Assad et al., 1989). Calcium acts as a second messenger in this process. A second messenger hypothesis fits well to the time course of adaptation, which is rather slow compared to the mechano-electrical transduction. The velocity of the slow hair cell movements is about 3 – 24 nm/msec (Zenner, 1988).

If a slow, active movement of OHC contributes to the adaptation to the SPL, then the following hypothesis can be introduced. A sound-induced displacement of the cochlear partition towards the vestibular scala with a deflection of the stereocilia into the positive direction leads to an unfavorable operation point of the stereocilia. Thus, their sensitivity becomes low and the mechano-electrical transfer function becomes poor. The pronounced deflection is transferred as a massive increase of the transduction current and is followed by a rise of the intracellular calcium. Calcium acts as a second messenger and activates the calmodulin-dependent actomyosin using ATP. As a result, with a radial displacement of the cuticular plate, a lateral movement of the OHC, including their stereocilia, is observed. The linkage of the tips of the stereociliar bundle to the tectorial membrane leads to a rebound of the stereocilia to the negative side. At the same time, the stereociliar bundle comes into a favorable position of deflection where the sensitivity is increased. Thus, the mechano-electrical transfer function is improved. Following this, the signal-to-noise ratio as well as the signal discrimination is improved.

It could be expected that pronounced dc mechanical responses of OHC lead to an increase in the stiffness of the cochlear partition in addition to a change in geometry. The resulting reduced mobility could represent a mechanism of protecting the cochlea from mechanical damage at very high SPL (noise protection). From a certain limit of the OHC movement onwards, one could suggest impaired hearing that would be caused by the changes in the geometry and stiffness of the cochlear partition, thus altering its vibratory capabilities. A preliminary process of this kind could contribute to TTS at high SPL. One possible correlate to slow OHC movements in TTS and noise protection could be the measurable reduction in amplitude of TEOAE after noise exposure.

Otoacoustic emissions are presumably the result of fast movements of OHC (ac motility) whose efficiency is influenced by additional slow OHC movements (dc motility). In turn, this leads to a change in the passive micromechanics of the cochlea and of the active cochlear amplifier.

Homeostasis. A slow mechanism of motility might also be useful for correcting the position of the cochlear partition as a result of minimum physiological changes in perilymph and endolymph production (homeostasis) (Johnstone et al., 1986; Zenner, 1986b,c). It is likely that periodic oscillations in the volume of the newly formed endo- and perilymph occur. The transfer function of the stereocilia would deteriorate, and hearing thresholds would be periodically changed without a correcting mechanism to reposition the partition and the hair bundle of the OHC into the highly sensitive mid position.

Acknowledgements

This study was supported by the Deutsche Forschungsgemeinschaft DFG Ze 149/4 – 4 and SFB Neurobiologie.

References

Allen, J.B. (1980) Cochlear micromechanics: a physical model of transduction. *J. Acoust. Soc. Am.*, 68: 1660 – 1670.

Ashmore, J.F. (1987) A fast motile response in guinea pig outer hair cells; the cellular basis of the cochlear amplifier. *J. Physiol. (Lond.)*, 388: 323 – 347.

Assad, J.A., Hacohen, N. and Corey, D.P. (1989) Voltage dependence of adaption and active bundle movement in bullfrog saccular hair cells. *Proc. Natl. Acad. Sci. U.S.A.*, 86: 2918 – 2922.

Becker, W. Naumann, H.H. and Pfaltz, C.R. (1986) *Hals-Nasen-Ohrenheilkunde*, Thieme, Stuttgart.

Brownell, W.E., Bader, C.R., Bertrand, D. and Ribaupierre, Y. (1985) Evoked mechanical responses of isolated cochlear outer hair cells. *Science*, 227: 194 – 196.

Brundin, L., Flock, A. and Canlon, B. (1989) Sound-induced motility of isolated cochlear outer hair cells is frequency-specific. *Nature*, 342: 814 – 816.

Canlon, B., Brundin, L. and Flock, A. (1988) Acoustic stimulation causes tonotopic alterations in the length of isolated outer hair cells from the guinea pig hearing organ. *Proc. Natl. Acad. Sci. U.S.A.*, 85: 7033 – 7035.

Cody, A.R. and Russell, J.I. (1987) The responses of hair cells in the basal turn of the guinea pig cochlea to tones. *J. Physiol. (Lond.)*, 383: 551 – 569.

Dallos, P. (1985) Response characteristics of mammalian cochlear hair cells. *J. Neurosci.*, 5: 1591 – 1608.

Dallos, P. (1988) Cochlear neurobiology: some key experiments and concepts of the past two decades. In: G.M. Edelman, W.E. Gall and W.M. Cowan (Eds.), *Neurobiological Bases of Hearing*, Wiley, New York, pp. 65 – 84.

Dallos, P. and Harris, D. (1978) Properties of auditory nerve responses in the absence of outer hair cells. *J. Neurophysiol.*, 41: 365 – 368.

Dallos, P., Harris, D.M., Relkin, E. and Cheatham, M.A. (1980) Two-tone supression and intermodulation distortion in the cochlea: effect of outer hair cell lesions. In: G. van den Brink and F.A. Bilsen (Eds.), *Psychophysical, Physiological and Behavioural Studies in Hearing*, Sijthoff and Noordhoff, Rockville, MD, pp. 242 – 249.

Dallos, P., Evans B.N. and Haqllworth, R. (1991) Nature of the motor element in electrokinetic shape changes of cochlear outer hair cells. *Nature*, 350: 1216 – 1218.

De Boer, E. (1983a) No sharpening? A challenge for cochlear mechanics. *J. Acoust. Soc. Am.*, 73: 567 – 573.

De Boer, E. (1983b) On active and passive cochlear models – towards a generalized analysis. *J. Acoust. Soc. Am.*, 73: 574 – 576.

Drenckhahn, D., Kellner, J., Mannherz, H.G., Gröschel-Steward, U., Kendrick-Jones, J. and Scholey, J. (1982) Absence of myosin-like immuno-reactivity in stereocilia of cochlear hair cells. *Nature*, 300: 531 – 532.

Eatock, R.A., Corey, D.P. and Hudspeth, A.J. (1987) Adaption of mechanoelectrical transduction in hair cells of bullfrog's sacculus. *J. Neurosci.*, 7: 2821 – 2836.

Engström, H. (1958) On the double innervation of the sensory epithelia of the inner ear. *Acta Otolaryngol. (Stockh.)*, 49: 109.

Flock, Å. (1983) Hair cells receptors with a motor capacity? In: R. Klinke and R. Hartmann (Eds.), *Hearing – Physiological Bases and Psychophysics*, Springer, Berlin, pp. 2 – 7.

Flock, Å. and Strelioff, D. (1984) Graded and non-linear mechanical properties of sensory hairs in the mammalian hearing organ. *Nature*, 310: 597 – 599.

Flock, Å., Flock, F. and Ulfendahl, M. (1986) Mechanism of movement in outer hair cells and a possible structural basis. *Arch. Otorhinolaryngol.*, 243: 83 – 90.

Gitter, A.H. and Zenner, H.P. (1988) Auditory transduction steps in single inner and outer hair cells. In: H. Duifhuis, J.W. Horst and H.P. Wit (Eds.), *Basic Issues in Hearing; Proceedings of the 8th International Symposium on Hearing*, Academic Press, London, pp. 32 – 41.

Gitter, A.H. and Zenner, H.P. (1993) Electrical field induced outer hair cell motility reaches ultrasound frequencies and

lacks sharp tuning. *Hearing Res.*, in preparation.

Gitter, A.H., Rudert, M. and Zenner, H.P. (1992) Force production by outer hair cells. *Eur. J. Physiol.*, in press.

Gummer, A.W., Johnstone, B.M. and Armstrong, N.J. (1981) Direct measurement of basilar membrane stiffness in the guinea pig. *J. Acoust. Soc. Am.*, 70: 1298 – 1309.

Howard, J. and Hudspeth, A.J. (1987) Mechanical relaxation of the hair bundle mediates adaption in mechanoelectrical transduction by bullfrog's saccular hair cell. *Proc. Natl. Acad. Sci. U.S.A.*, 84: 3064 – 3068.

Hudspeth, A.J. (1989) How the ear's works work. *Nature*, 341: 397 – 404.

Johnstone, B.M., Patuzzi, R. and Yates, G.K. (1986) Basilar membrane measurements and the travelling wave. *Hearing Res.*, 22: 147 – 153.

Kachar, B., Brownell, W.E., Altschuler, R. and Fex, J. (1986) Electrokinetic shape changes of cochlear outer hair cells. *Nature*, 322: 365 – 367.

Keidel, W.D., Keidel, U.O. and Wigand, M.E. (1961) Adaption: loss or gain of sensory intormation. In: W.A. Rosenblith (Ed.), *Sensory Communication*, Wiley, New York, pp. 164 – 192.

Khanna, S.M. and Leonard, D.G.B. (1982) Laser interferometric measurements of basilar membrane vibrations in cats. *Science*, 215: 305 – 306.

Khanna, S.M., Flock, Å. Ulfendahl, M. (1989a) Changes in cellular tuning along the radial axis of the cochlea. *Acta Otolaryngol. (Suppl.) (Stockh.)*, 467: 163 – 173.

Khanna, S.M., Ulfendahl, M. and Flock, Å. (1989b) Modes of cellular vibration in the organ of Corti. *Acta Otolaryngol. (Suppl.) (Stockh.)*, 467: 183 – 188.

Kiang, N.Y.-S., Moxon, E.C. and Levine, R.A. (1970) Auditory-nerve activity in cats with normal and abnormal cochleas. In: G.E.W. Wolstenholme and J. Knight (Eds.), *Sensorial Hearing Loss – Ciba Foundation Symposium*, Churchill, London, pp. 241 – 268.

Kim, D.O. (1986) Active and non-linear cochlear biomechanics and the role of outer-hair-cell subsystems in the mammalian auditory system. *Hearing Res.*, 22: 105 – 114.

Kim, D.O., Molnar, C.E. and Matthews, J.W. (1980) Cochlear mechanics: non-linear behaviour in two-tone responses as reflected in cochlear nerve fibre responses and in ear canal sound pressure. *J. Acoust. Soc. Am.*, 67: 1704 – 1721.

Lehnhardt, E. (1984) Klinik der Innenohrschwerhörigkeiten. *Arch. Otorhinolaryngol. (Suppl.)*, I: 58 – 218.

Leonard, D.G.B. and Khanna, S.M. (1984) Histological evaluation damage in cat cochleas used for measurements of basilar membrane mechanics. *J. Acoust. Soc. Am.*, 75: 515 – 527.

LePage, E.L. (1987) Frequency-dependent self-induced bias of the basilar membrane and its potential for controlling sensitivity and tuning in the mammalian cochlea. *J. Acoust. Soc. Am.*, 82: 1539 – 1545.

LePage, E.W. and Johnstone, M.B. (1980) Non-linear mechanical behaviour of the basilar membrane in the basal turn of the guinea pig cochlea. *Hearing Res.*, 2: 183 – 189.

LePage, E.W., Reuter, G. and Zenner, H.P. (1993) Fiber optic mechanical measurements of summating displacements in guinea pig cochlear explant suggest an adaptive role for the outer hair cells. *Hearing Res.*, in press.

Libermann, M.C. and Dodds, L.W. (1984) Single neuron labeling and chronic cochlear pathology. III. Stereocilia damage and alterations of threshold tuning curves. *Hearing Res.*, 16: 55 – 74.

Lim, D.J. (1980) Cochlear anatomy related to cochlear micromechanic. A review. *J. Acoust. Soc. Am.*, 67: 1686 – 1695.

Manley, G.A., Schulze, M. and Oekingshaus, H. (1987) Otoacoustic emissions in a song bird. *Hearing Res.*, 26: 257 – 266.

Meyer zum Gottesberge, A. (1948) Zur Physiologie der Haarzellen. *Arch. Ohr Nase Kehl Heilk.*, 155: 308.

Pfander, F. (1975) *Das Knalltrauma. Analyse, Vorbeugung, Diagnose, Behandlung, Prognose und Begutachtung*, Springer, Berlin.

Plinkert, P.K., Gitter, A.H., Zimmermann, U., Kirchner, T., Tzartos, S. and Zenner, H.P. (1990) Visualization and functional testing of acetylcholine receptor-like molecules in cochlear outer hair cells. *Hearing Res.*, 44: 25 – 34.

Rasmussen, G.L. (1942) An efferent cochlear bundle. *Anat. Rec.*, 82: 441 – 443.

Reuter, G. and Zenner, H.P. (1990) Active radial and transverse motile responses of outer hair cells in the organ of Corti. *Hearing Res.*, 43: 219 – 230.

Reuter, G., Gitter, A.H. and Zenner, H.P. (1988) In situ motility of outer hair cells. In: C.F. Claussen, M.V. Kirtane and K. Schlitter (Eds.), *Proceedings of the NES; Vertigo, Nausea, Tinnitus and Hypacusia in Metabolic Disorders*, Elsevier Science Publishers, Amsterdam, pp. 201 – 204.

Reuter, G., Gitter, A.H., Thurm, U. and Zenner, H.P. (1992) Photoelectric measurements at high frequencies of outer hair cell induced active radial movements of the reticular lamina. *Hearing Res.*, 60: 236 – 246.

Rhode, W.S. (1971) Observations of the vibration of the basilar membrane in squirrel monkeys using the Mössbauer technique. *J. Acoust. Soc. Am.*, 49: 1218 – 1231.

Ryan, A.F. and Dallos, P. (1975) Effect of absence of cochlear outer hair cells on behavioural auditory threshold. *Nature*, 253: 44.

Santos-Sacchi, J. (1989) Assymetry in voltage-dependent movements of isolated outer hair cells from the organ of Corti. *J. Neurosci.*, 9: 2954 – 2962.

Sellick, P.M., Patuzzi, R. and Johnstone, B.M. (1982) Measurement of basilar membrane motion in the guinea pig using the Mössbauer technique. *J. Acoust. Soc. Am.*, 72: 131 – 141.

Siegel, J. and Kim, D. (1982) Efferent neural control of cochlear mechanics? Olivocochlear bundle stimulation affects cochlear biomechanical nonlinearity. *Hearing Res.*, 6: 171 – 182.

Smith, C.A. (1961) Innervation pattern of the cochlea. *Ann. Otol. Rhinol. Laryngol.*, 70: 504 – 527.

Spoendlin, H. (1969) Innervation patterns in the organ of Corti of the cat. *Acta Otolaryngol. (Stockh.),* 67: 239 – 254.

Spoendlin, H. and Gacek, R. (1963) Electron microscopic studies of the efferent and afferent innervation of the organ of Corti in the cat. *Ann. Otol. Rhinol. Laryngol.,* 72: 660 – 686.

Tasaki, I., Davis, H. and Legouix, J.P. (1952) The space-time pattern of the cochlear microphonics (guinea pig), as recorded by differential electrodes. *J. Acoust. Soc. Am.,* 24: 502 – 519.

Tasaki, I., Davis, H. and Elderedge, D.H. (1954) Exploration of cochlear potentials in guinea pig with a microelectrode. *J. Acoust. Soc. Am.,* 26: 765 – 773.

Van Dijk, P. and Wit, H.P. (1987) Temperature dependence of frog spontaneous otoacoustic emissions. *J. Acoust. Soc. Am.,* 82: 2147 – 2150.

Wit, H.P., Van Dyck, P. and Segenhout, J.M. (1989) In: J.P. Wilson and D.T. Kemp (Eds.), *Cochlear Mechanisms: Structure, Function and Models,* Plenum, New York, pp. 341 – 347.

Zenner, H.P. (1986a) K^+-induced motility and depolarization of cochlear hair cells. Direct evidence for a new pathophysiological mechanism in Menière's disease. *Arch. Otorhinolaryngol.,* 243: 108 – 111.

Zenner, H.P. (1986b) Motile responses in outer hair cells. *Hearing Res.,* 22: 83 – 90.

Zenner, H.P. (1986c) Aktive Bewegungen von Haarzellen: ein neuer Mechanismus beim Hörvorgang. *HNO,* 34: 133 – 138.

Zenner, H.P. (1986d) Molecular structure of hair cells. In: R.A. Altschuler, D.W. Hoffmann and R.P. Bobbin (Eds.), *Neurobiology of Hearing: the Cochlea,* Raven Press, New York, pp. 1 – 21.

Zenner, H.P. (1988) Motility of outer hair cells as an active actin-mediated process. *Acta Otolaryngol. (Stockh.),* 105: 39 – 44.

Zenner, H.P. (1991) Pathophysiologie des auditorischen Systems: In: K. Hierholzer and R.F. Schmidt (Eds.), *Pathophysiologie des Menschen,* VHC Verlagsgesellschaft, Weinheim, 31.1 – 32.16.

Zenner, H.P. and Gitter, A.H. (1987) Die Schallverarbeitung des Ohres. *Physik Unserer Zeit,* 18: 97 – 105.

Zenner, H.P. and Gitter, A.H. (1989) Transduktions- und Motorstörungen cochleärer Haarzellen bei M. Menière und Aminoglycosidschwerhörigkeit. *Laryngol. Rhinol. Otol. (Stuttg.),* 68: 552 – 556.

Zenner, H.P., Gitter, A., Zimmermann, U., Schmitt, U. and Frömter, E. (1985a) Die isolierte, lebende Haarzelle – ein neues Modell zur Untersuchung der Hörfunktion. *Laryngol. Rhinol. Otol. (Stuttg.),* 64: 642 – 648.

Zenner, H.P., Zimmermann, U. and Schmitt, U. (1985b) Reversible contraction of isolated mammalian cochlear hair cells. *Hearing Res.,* 18: 127 – 133.

Zenner, H.P., Zimmermann, U. and Gitter, A.H. (1987) Fast motility of isolated mammalian auditory sensory cells. *Biochem. Biophys. Res. Commun.,* 149: 304 – 308.

Zenner, H.P., Zimmermann, R. and Gitter, A.H. (1988a) Active movements of the cuticular plate induce sensory hair motion in mammalian outer hair cells. *Hearing Res.,* 34: 233 – 240.

Zenner, H.P., Arnold, W. and Gitter, A.H. (1988b) Outer hair cells as fast and slow cochlear amplifiers with a Bidirectional Transduction Cycle. *Acta Otolaryngol. (Stockh.),* 105: 457 – 462.

Zenner, H.P., Reuter, G., Plinkert, P.K., Zimmermann, U. and Gitter, A.H. (1989) Outer hair cells possess acetylcholine receptors and produce motile responses in the organ of Corti. In: J.P. Wilson and D.T. Kemp (Eds.), *Cochlear Mechanisms,* Plenum, New York, pp. 93 – 98.

Zenner, H.P., Reuter, G., Plinkert, P.K. and Gitter, A.H. (1990) Fast and slow motility of outer hair cells in vitro and in situ. In: F. Grandori, G. Cianfrone and D.T. Kemp (Eds.), *Cochlear Mechanisms and Otoacoustic Emissions – Advances in Audiology, Vol. 7,* Karger, Basel, pp. 35 – 41.

Zwicker, E. (1979) A model describing non-linearities in hearing by active processes with saturation at 40 dB. *Biol. Cybern.,* 35: 243 – 250.

Zwicker, E. (1986a) A hardware cochlear nonlinear preprocessing model with active feedback. *J. Acoust. Soc. Am.,* 80: 146 – 153.

Zwicker, E. (1986b) Supression and $(2f_1 - 2f_2)$ difference tones in a nonlinear cochlear preprocessing model with active feedback. *J. Acoust. Soc. Am.,* 80: 163 – 176.

J.H.J. Allum, D.J. Allum-Mecklenburg, F.P. Harris and R. Probst
Progress in Brain Research, Vol. 97

CHAPTER 4

Performance of the avian inner ear

R. Klinke and J.W.Th. Smolders

Zentrum der Physiologie, Frankfurt/Main, Germany

In spite of morphological similarities, the avian inner ear has apparently developed mechanisms of sound transduction that differ from the mammalian solution. This paper is a compilation of the present knowledge.

Key words: Bird; Auditory nerve; Hair cell; Transduction; Endolymphatic potential; Infrasound; Basilar membrane; Tonotopy; Traveling wave; Ototoxic drugs

Introduction

In this paper, the anatomical and physiological properties of the avian inner ear are described with special attention to the transduction processes in the hair cell receptors. It will be demonstrated that not only are vestibular and auditory receptors different, but also that there are striking differences between mammalian and avian hearing mechanisms. These differences apparently force the assumption that there are also differences between mammals and birds in the fundamental steps of hair cell transduction.

Anatomy

Admittedly, at first glance there are obvious anatomical similarities between mammalian and avian (as well as the closely related crocodilian) inner ears. In contrast, all further reptilian, as well as the amphibian and fish auditory organs, differ greatly from the mammal in morphology and function. In birds, as in mammals, there are three scalae (Takasaka and Smith, 1971; von Düring et al., 1985; Manley, 1990) that line the boomerang-shaped papilla basilaris. The length of the papilla is between 2.5 mm (starling) and 11 mm (barn owl) with an average value of 4 mm. The basilar membrane extends between two cartilaginous plates and carries supporting cells and hair cells. The scala media and scala vestibuli are separated by the thick tegmentum vasculosum which is quite different from the mammalian situation. The tegmentum consists of several layers of cells of different types and is thought to produce the potassium-rich endolymphatic fluid and to generate the endolymphatic potential (EP) (Cotanche et al., 1987; Sterkers et al., 1988), which is between +10 and +20 mV, depending upon the species (Cotanche et al., 1987; Vossieck and Klinke, 1990). Thus, the tegmentum seems to be functionally analogous to the mammalian stria vascularis, but biochemical differences obviously exist. These differences concern different ionic mechanisms for the generation of the avian EP. This view is based on the observation that the avian EP is much smaller than that of mammals. It is also insensitive to Furosemide and other loop diuretics (Schermuly et al., 1990), which are known to be ototoxic in mammals and, among other effects, reduce the mammalian EP. Details on other effects of Furosemide will be given in a later section.

On top of the basilar membrane, some 6000 – 11000 sensory hair cells (HCs) are located, depending upon the species. One cross section contains between 10 HCs in the basal and 50 HCs in the apical region of the papilla. The HCs are firmly embedded in supporting cells and, again unlike the mammal, there are no empty spaces in the avian papilla such as the tunnel of Corti or Nuel's space. At least two types of HCs are present, the tall (THCs) and the short (SHCs) hair cells. A morphologically intermediate type of hair cell (ImHC) is described in the transitional zone between the THCs and SHCs. Although this classification is made on anatomical grounds, there are several arguments in support of functional as well as anatomical differences. For example, the innervation pattern of the cells is different (see later), and the equipment of the different cell types with certain ionic channels is cell-specific (Murrow and Fuchs, 1990). Furthermore, in the phylogenetically related crocodiles, which have a very similar inner ear, the separation between the two distinct HC populations is quite clear, and there are no intermediate cell types (von Düring et al., 1974; Leake, 1977; Wever, 1978).

Most of the THCs lie over the superior cartilaginous plate, whereas the ImHCs and the SHCs are located on the free basilar membrane and thus probably experience more of the basilar membrane motion than do the THCs. All HCs carry stereovilli on their free surface. The villi are short in the basal and long in the apical region. Unlike mammalian auditory HCs, a kinocilium is also present. Furthermore, contacts between avian THCs are frequent (Fischer et al., 1991). THCs may communicate through these protuberances. These contacts have never been reported from a mammal nor do they regularly occur in avian SHCs, a further argument for the assumption of at least two different HC classes.

As in the mammal, avian hair cells are covered by a tectorial membrane. In the bird there is, however, no subtectorial space. The ciliary bundles protrude into honeycombed structures in the tectorial membrane. Thus the mode of stimulation of the villi, respectively cilia, may also be different from the mammal (Smith, 1985).

The innervation pattern of the avian papilla basilaris has not yet been sufficiently elaborated. However, it is known that there are both afferent and efferent fibers. All afferent fibers are myelinated, including those to the SHCs. The majority of afferents contact the THCs. THC afferents do not branch and only occasionally innervate two THCs, whereas fibers to the SHCs branch and supply up to 10 hair cells (Rebillard and Pujol, 1983; Whitehead and Morest, 1985; von Düring et al., 1985; L. Schermuly and R. Klinke, unpublished results). The innervation is thus similar to that of the mammal except that mammalian outer hair cell fibers are not myelinated. G.A. Manley (personal communication) reports abneurally located SHCs that do not receive afferent innervation. The efferent innervation is more dense at the SHCs. Also, the supporting cells lateral (abneural) to the SHCs, the hyaline cells, receive an efferent input.

The question of whether or not mammalian inner and outer hair cells (IHCs, OHCs) are equivalent to avian THCs and SHCs, respectively, is entirely unresolved but there are strong arguments against this contention (see later). From the morphological point of view, SHCs are very different from OHCs. Not only is there a difference in shape, but also mammalian OHCs are a highly differentiated type of cell, apparently having specializations for their motor function. In avian SHCs, subsurface cisternae have never been reported, and there is no information as to whether SHCs are endowed with a cortical lattice as are the OHCs (Holley and Ashmore, 1990).

Interestingly, in contrast to mammalian hair cells, avian hair cells can regenerate after destruction by acoustic trauma or by aminoglycosides (Corwin and Cotanche, 1988; Ryals and Rubel, 1988; Ryals and Westbrook, 1990).

Afferent fibers

Neurophysiological data on auditory afferents are available from the pigeon (*Columba livia*), the

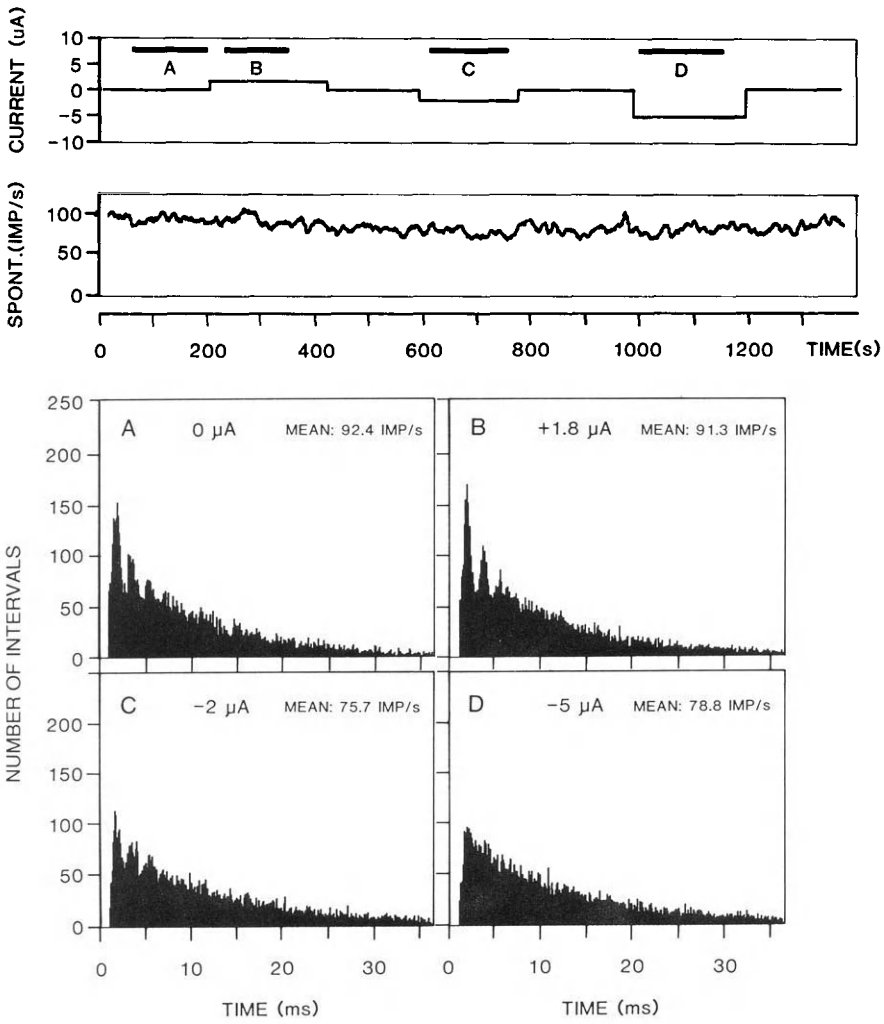

Fig. 1. Spontaneous discharge rate of a pigeon auditory nerve fiber during direct current injection into scale media. Upper trace, current monitor. Positive current results in a more positive endolymphatic potential (EP, mean change about 2 mV/μA). Bars indicate recordings of interval histograms displayed in the lower panels. Next trace, mean spontaneous discharge rate. Lower panels: *A*, control, electrode inserted, no current injected. The peaks in the interval histogram indicate the occurrence of "preferred intervals" during spontaneous firing. *B*, With positive current injection, the preponderance of preferred intervals is increased. *C*, With small negative current, the occurrence of preferred intervals decreases. *D*, With large negative current, preferred intervals disappear and the interval distribution becomes Poisson-like.

starling (*Sturnus vulgaris*), the red-winged black bird (*Agelaius phoeniceus*) and the chicken (*Gallus domesticus*), admittedly hardly representative of song birds. All auditory afferents show an irregular spontaneous discharge rate of between 20 and 200 imp./sec (see Manley, 1990, or Schermuly and Klinke, 1990a, for discussion). Mean spontaneous activities in bird auditory afferents show a monomodal distribution; the peak value of the spontaneous rate is near 90 imp./sec. This is in contrast with mammals and other vertebrates (Liberman, 1978; Smolders and Klinke, 1986) where the distribution is bimodal, i.e., there are populations of low spontaneous and of high spontaneous fibers.

Moreover, in a proportion of the avian fibers, the inter-spike intervals during spontaneous activity are not distributed in a Poisson-like manner as is the case for mammals (see Fig. 1), but certain "preferred intervals" prevail (Manley, 1979). The length of these intervals is related to the frequency to which the fiber is tuned, the characteristic frequency (CF), and their duration is close to 1/CF. It has been the experience in our laboratory that the fibers with preferred intervals always belong to the most sensitive fibers with the highest Q-values found in an individual animal. Preferred intervals have never been reported from mammalian auditory afferents but have been found in many submammalian species. It is presently assumed that the preferred intervals reflect intrinsic properties of the frequency tuning mechanisms of birds and other non-mammalian lower vertebrates*.

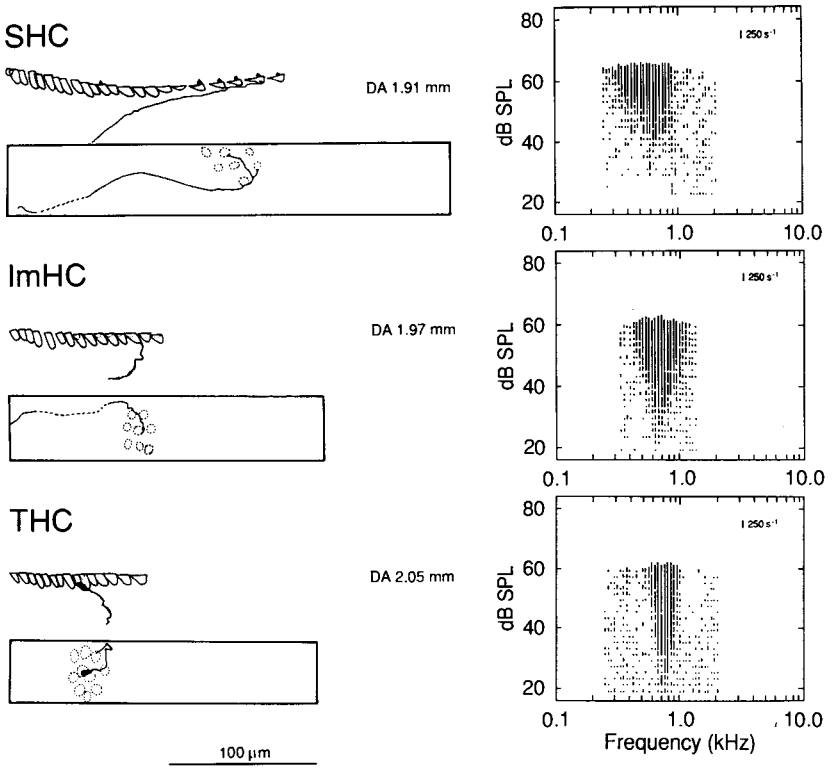

Fig. 2. Responses of three labeled pigeon auditory nerve fibers innervating two short hair cells (SHC), one intermediate hair cell (ImHC) and one tall hair cell (THC), respectively. The fibers originate from comparable longitudinal positions along the basilar membranes (length about 4 mm) of two pigeon ears. DA, distance from the apex. Characteristic frequencies 0.63, 0.71 and 0.75 kHz, mean spontaneous firing rates 80, 62 and 85 imp./sec, respectively. Right hand panels: response areas of the fibers. The length of the vertical bars represents the increase of neural firing rate (above the mean spontaneous firing rate) as a function of the carrier frequency and the sound pressure level re: 20 μPa (dB SPL) of trapezoidally shaped tone burst stimuli of 50 msec duration. A calibration bar is given in the right upper corner of each panel indicating 250 action potentials per second. Left hand panels: transverse section and surface view on the sensory epithelium with the peripheral course and hair cell contacts of each fiber. The neural limbus is on the left hand side. The width of the surface views indicates the total width of the epithelium.

* Note added in proof: recent experimental data from our group have shown that preferred intervals can be provoked in birds as well as in mammals by near-threshold noise and that they are most likely a filter response of sharply tuned and highly sensitive filters to noise (see ARO abstract no. 134, St. Petersburg Beach, FL, 1993).

Most of the afferent fibers from the avian papilla basilaris can be activated by sound in the range from 30 Hz to 6 kHz. Thus, high-frequency hearing is missing in birds, and one may ask the question of whether this could be caused by the functional differences that have been found. The responses are frequency-tuned. Tuning becomes progressively less sharp towards the low-frequency fibers. Thus, the tuning behavior of the avian afferents resembles that of mammals. There is, however, a much larger range of CF thresholds in normally hearing birds than in mammals. Low-frequency tails are not found in the tuning curves of avian fibers, including those with the highest CF. Often the low-frequency slope of the tuning curve is steeper than the high-frequency slope. When fibers responsive to acoustic stimuli are stained (Smolders et al., 1991), it turns out that not only can fibers coming from the THCs or ImHCs be activated by sound, as assumed by Manley et al. (1989), but also that fibers from the SHCs can indeed respond to sound stimuli (Fig. 2). This is in contrast to mammalian OHC-afferents, which are not myelinated and thus are incapable of quick information transfer and which are presumably unresponsive to sound (Robertson, 1984). All mammalian fibers that are responsive to sound have been found to contact IHCs (Liberman, 1982; Liberman and Oliver, 1984). Avian SHC afferents have thresholds that are similar to THC- and ImHC-afferents but the tips of their tuning curves are blunter. This may depend on the innervation pattern, as the respective afferents supply more than one SHC.

Surprisingly, the CF of bird (pigeon) auditory afferents depends on skull temperature (see Fig. 3). With lower temperature, the CF shifts to lower values (Schermuly and Klinke, 1985). Below 30°C, a shift of about one octave/10°C has been determined. This effect of temperature on tuning has also been described for reptiles, e.g., the Tokay gecko (Eatock and Manley, 1981) or the caiman (Smolders and Klinke, 1984) and for amphibians (e.g., Moffat and Capranica, 1976). In contrast, it has not been found in mammals (cat, Klinke and Smolders, 1977; guinea-pig, Gummer and Klinke, 1983) nor does human absolute pitch depend upon body temperature

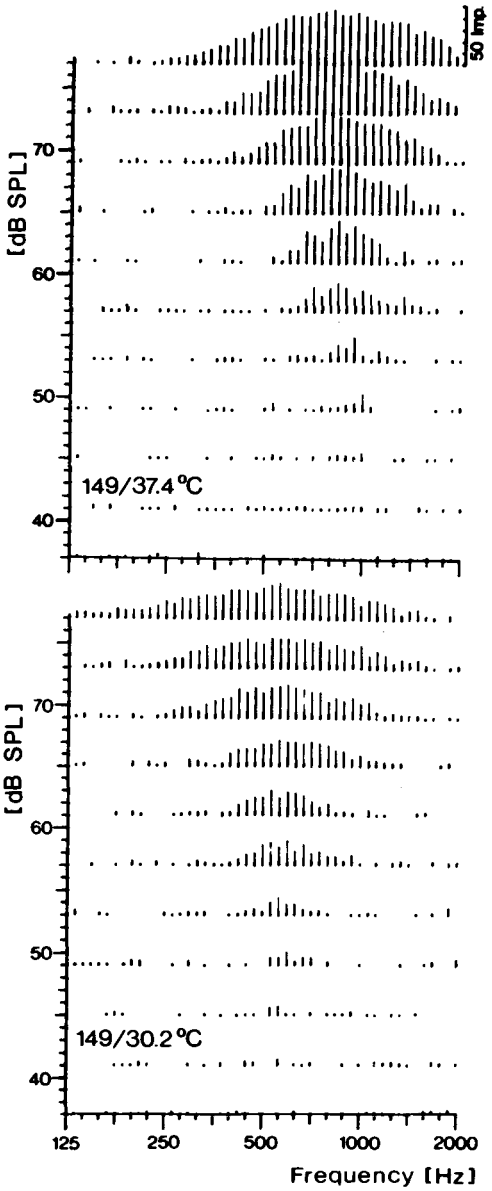

Fig. 3. Responses of the same pigeon primary auditory fiber at two different cochlear temperatures (measured at the round window). Response areas as in Fig. 2. Tone burst duration 100 msec.

(Emde and Klinke, 1977). In mammalian fibers, the decrease of skull temperature leads to a threshold elevation and a loss of sharpness of tuning. This difference is another indication that the fundamental tuning properties in birds and mammals may be

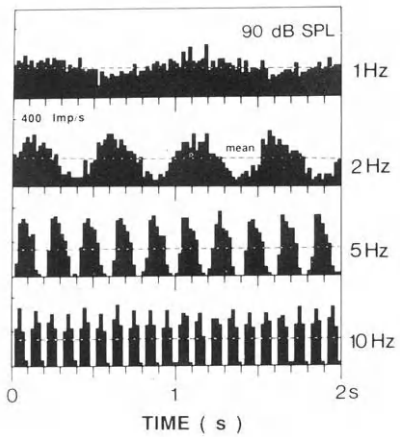

Fig. 4. Peristimulus – time histograms of the discharge rate of a pigeon auditory nerve fiber stimulated with pure tones of 1, 2, 5 and 10 Hz (infrasound) at 90 db SPL. Dashed line, mean firing rate during stimulation (165, 161, 157 and 160 imp./sec). Spontaneous rate 158 imp./sec.

different and argues for the participation of an active process in avian HC transduction.

Finally, among the fibers coming from the pigeon basilar papilla there are some that cannot be activated by acoustic stimuli in the audio-frequency range. These fibers are influenced by infrasound (< 20 Hz) stimuli (Schermuly and Klinke, 1990a). These fibers possess a high spontaneous discharge rate that is modulated by the sound stimulus (see Fig. 4), whereby the mean firing rate remains fairly constant over a wide range of sound intensities. The infrasound fibers are not normally frequency-tuned. If they are, then their tuning is extremely poor. Transitional types to the "ordinary" low-frequency auditory fibers seem to exist. Because the infrasound fibers do not increase their discharge rate during stimulation, a rate threshold, such as determined for ordinary auditory afferents, cannot be defined. However, it is possible to determine a threshold for modulation of the discharge rate (Schermuly and Klinke, 1990a). Modulation thresholds neatly match the behavioral thresholds for pigeon infrasound detection as determined by Kreithen and Quine (1979). The infrasound fibers are therefore likely to be the physiological correlate of pigeon infrasound perception. Horseradish peroxidase staining of these fibers reveals the site of origin: ImHCs and SHCs in the most apical part of the papilla basilaris (Schermuly and Klinke, 1990b).

The modulation of auditory afferents in synchrony with the sound frequency that has been described is not a unique property of infrasound fibers. Almost all avian afferent fibers lock their discharges to a certain phase of the acoustic stimulus, at least up to 4 kHz (Gleich and Narins, 1988; Hill et al., 1989), and in the owl up to 9 kHz (Sullivan and Konishi, 1984). This phase locking of discharges is common to all species that have been studied thus far including mammals (Rose et al., 1967) and lower vertebrates (e.g., caiman, Smolders and Klinke, 1986; bobtail lizard, Manley et al., 1990; frog, Narins and Hillery, 1983). Most importantly, the phase locking occurs at intensities of 10 dB or more below the activation threshold of a fiber. Phase locking can even be found in suppressive side bands of the fibers' response area (tuning curve) where the spontaneous activity of the fiber is reduced by the presence of an acoustic stimulus (Hill et al., 1989). Thus, phase locking is a reflection of hair-cell processes; however, it is not yet clear whether it bears a relation to the preferred intervals in submammalian vertebrates. It seems that the brain can make use of the information contained in the periodicity of the discharges in birds as well as in mammals.

Mechanics

The properties of auditory afferents evidently mirror the processing of acoustic stimuli by the outer and middle ears, by cochlear mechanics, and by the hair cells. The present review must be limited to inner ear processes. However, it should be mentioned that the properties of the system consisting of the tympanic membrane and the columella have been extensively described for the pigeon (Gummer et al., 1989a,b). These results support the hypothesis that the upper frequency limit of hearing is partially determined by the transfer characteristics of the middle ear.

As far as inner ear mechanics are concerned, the existence of preferred intervals and the effects of temperature on avian tuning mechanisms that have been described pose the question of whether a traveling wave does exist along the avian basilar membrane. This question has been addressed by Gummer et al. (1987) using the Mössbauer technique. The authors were able to show that a traveling wave runs along the avian basilar membrane upon acoustic stimulation if the ear is in good physiological condition, as judged from concomitant measurements of the compound action potentials (CAP). If, however, the experimental procedure impairs the ear and leads to a substantial increase in CAP thresholds, then a standing wave pattern is found. As in mammals, the amplitude maxima of the traveling wave tonotopically map frequencies along the basilar membrane (BM), with high frequencies being represented at the basal end (Fig. 5). Thus, the vibration of each location on the basilar membrane is mechanically tuned to a certain frequency. The mechanical tonotopic map coincides with the tonotopic map constructed from the CF of labeled primary auditory fibers as a function of their longitudinal site of innervation along the BM (Fig. 5). If, however, sharpness of mechanical tuning is compared to neuronal tuning, then a major difference becomes obvious: primary afferents are much more sharply tuned than is the mechanical vibration of the BM. The mechanical measurements were made under careful control of the physiological integrity of the cochlea. Under similar conditions, results from mammals reveal virtually identical mechanical and neuronal tuning curves (Sellick et al., 1982; Khanna and Leonard, 1982). Thus it is likely that the difference is not an artefact and that in the bird there are processes in addition to the mechanical basilar membrane tuning, e.g., HC properties, that are responsible for the final frequency selectivity and low thresholds. This view is supported by closer inspection of the off-CF areas of very sensitive neuronal tuning curves. These avian tuning curves seem to be composed of a sharply tuned (narrow) low threshold portion and a less sharply tuned portion in the high-intensity range (Fig. 6). The slopes of this latter segment resemble those of the mechanical tuning curve. Mammalian tuning curves also are composed of two segments, the more sensitive one being susceptible to a number of noxious agents, e.g., sound trauma or intoxication by ototoxic drugs such as the loop diuretic Furosemide (Evans and Klinke, 1982). This drug also alters the mechanical response of the mammalian basilar membrane in such a way that the sensitive portion of the mechanical tuning curve disappears (Ruggero and Rich, 1991). It has thus to be postulated that Furosemide finally impairs the function of the putative cochlear amplifier in the mammalian OHCs. The avian inner ear is not susceptible to loop diuretics and the implications of

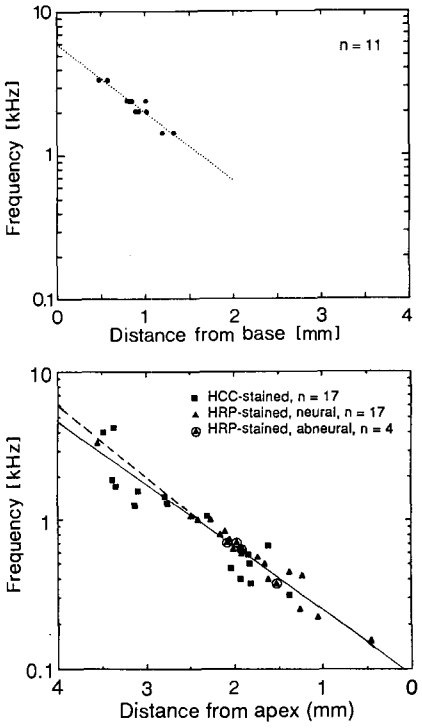

Fig. 5. Upper panel: mechanical tonotopic frequency map of the pigeon basilar membrane measured with the Mössbauer technique. Lower panel: tonotopic frequency map from the characteristic frequency of labeled single auditory nerve fibers of the pigeon as a function of their innervation site on the basilar membrane. Lines are linear regression lines. The dashed line in the lower panel is the regression line through the mechanical data (upper panel) transposed to the coordinates of the neural data. Mechanical and neural regression lines appear to agree well.

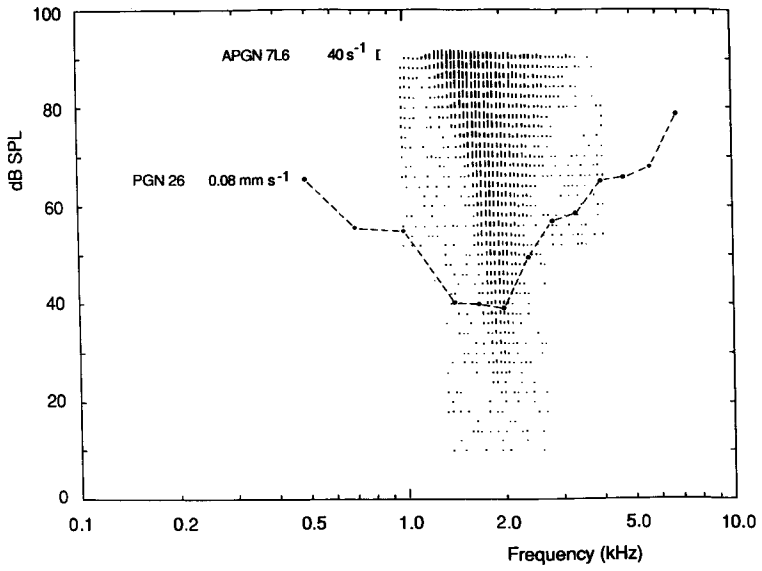

Fig. 6. Mechanical tuning curve in a sensitive healthy ear (animal PGN26, Mössbauer measurement) compared to a neuronal tuning curve of a sensitive single auditory nerve fiber (animal APGN7L6).

this finding for transduction are discussed in the next section.

Transduction

Neither the avian CAP (Wit and Bleeker, 1983; Schermuly et al., 1983) nor the avian EP or single fiber responses (Schermuly et al., 1990) are influenced even by excessive doses of diuretics like Furosemide or ethacrynic acid. Nevertheless, these drugs are potent diuretics in birds as well as in mammals. Thus, another difference between avian and mammalian inner ear mechanisms is evident.

As the proposed mammalian cochlear amplifier is supposed to be based on OHC motility (Brownell, 1985; Zenner et al., 1985; Ashmore, 1987), avian hair cells have also been evaluated for motile responses. Zimmermann et al. (1989) prepared isolated pigeon THCs and SHCs in a manner similar to the preparation for guinea pig OHCs. The cells were kept in a short-term culture and were exposed to an electrical field that is known to produce elongations and contractions of guinea pig OHCs. No indications for motile responses of avian HCs were found. In addition to this negative result, it is hard to conceive how avian HCs could move in situ and in vivo because they are firmly embedded in supporting cells. This is in contrast to mammalian OHCs, which are only loosely held by Deiter's cells and are mainly surrounded by fluid-filled spaces (spaces of Nuel, outer tunnel).

The above findings lead to the hypothesis that the active contribution to frequency tuning in the avian inner ear must be different from the postulated mammalian outer hair cell mechanism. Electrical tuning properties intrinsic to the HCs may be an adequate candidate. Such mechanisms have been proposed for turtle hair cells by Crawford and Fettiplace (1981) on the basis of a ringing response in HC membrane potentials following current injections and direct mechanical stimulation of the hair cell bundles (Crawford and Fettiplace, 1985). Such a ringing response was also described for chick HCs by Fuchs et al. (1988), whereas it has never been found in mammalian HCs. Also, low CF pigeon afferents show a ringing response when a long-lasting

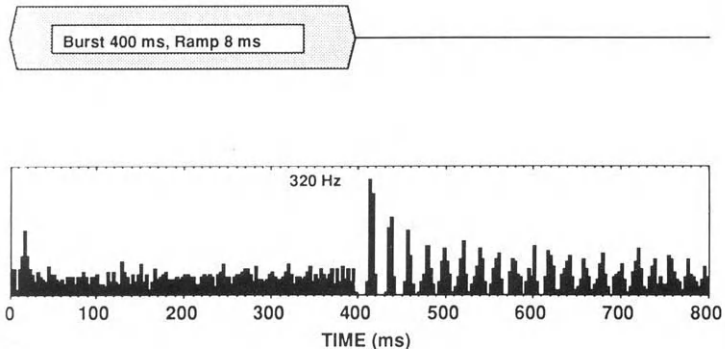

Fig. 7. Ringing response of a pigeon auditory afferent (CF about 50 Hz) to the offset of a 400 msec tone of 320 Hz, which is in the suppressive surround of the tuning curve.

stimulus in the suppressive surround of the tuning curve is switched off (Schermuly et al., 1991, see Fig. 7). So there are good reasons to assume that electrical resonance contributes to the tuning of the avian cochlea. However, the phase responses of primary fibers (Gleich and Narins, 1988) deviate from those expected on the basis of the passive basilar membrane responses (Gummer et al., 1987) and of a second-order resonant hair cell alone. The actual tuning mechanism may therefore involve more complex interactions than a passive basilar membrane motion followed by an independent resonance in the hair cell potential (Lewis, 1987). It should also be mentioned that the preferred intervals in avian spontaneous activity are considered as an indication for a filter mechanism that is unique to the hair cell (see, e.g., Manley, 1990).

If electrical tuning exists, then one must wonder whether or not it can be manipulated. Electrical tuning would possibly depend on the magnitude of the EP and the integrity of certain of the HC's ionic channels. No doubt, the HCs are the transducers proper. Displacement of the stereovilli opens ionic gates that are located on the tips (Hudspeth, 1989) or at the cell apex (Ohmori, 1988) and a transduction current is generated, which is driven by the potential difference between the scala media EP and the interior of the HC. Experimental variation of this potential difference by means of current injections (Vossieck and Klinke, 1990; Vossieck et al., 1991) leaves the mean spontaneous activity unchanged but affects threshold, sharpness of tuning and preferred intervals. The probability of preferred intervals is increased if the EP is increased, and they may completely disappear if the EP is lowered (see Fig. 1). Sound-evoked activity is strongly affected by current injections. Positive currents (making EP more positive) increase the sensitivity of afferent fibers and result in a sharper tuning curve, whereas negative currents lead to an elevation of thresholds and a loss of sharpness of tuning (Fig. 8). The characteristic frequency of the fiber being studied remains the same. The data show that the driving force for the transduction current does influence tuning; however, the mean spontaneous activity is independent of the transduction channel and possibly originates from synaptic noise.

Tuning can likewise be manipulated by channel blockers such as TEA (C.P. Richter and R. Klinke, unpublished results). The introduction of TEA into the scala media leads to a threshold elevation of afferent activity, a loss of sharpness of tuning and a shift of CF to lower frequencies. Partial replacement of endolymphatic K^+ by Na^+ also results in a change of CF (Richter and Klinke, 1991), together with a threshold elevation and a reduction of the Q-value. These data, though preliminary, are in agreement with the assumption of an electrical tuning mechanism in avian HCs. There are, however, also conflicting data. Otoacoustic emissions, first described for humans by Kemp (1978), have also been found in other mammals and are assumed to

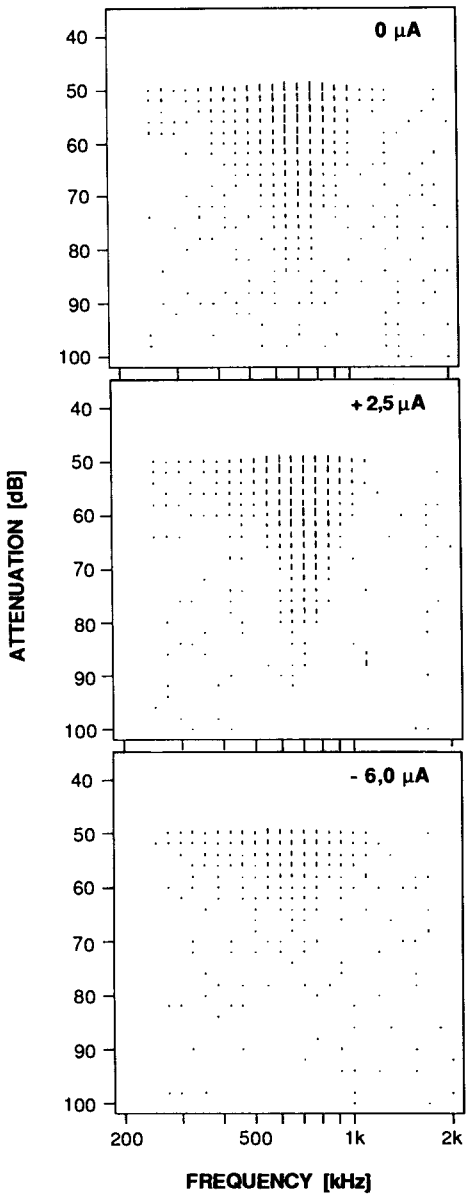

Fig. 8. Response area (as in Fig. 2) of a pigeon auditory nerve fiber during direct current injection into scala media. 0 µA, control, electrode inserted, no current applied. The threshold at the characteristic frequency (0.68 kHz) is at 85 dB attenuation (43 dB SPL). +2.5 µA, positive current injection results in an increase in sensitivity and sharpness of tuning. −6.0 µA, negative current injection results in a large reduction of sensitivity and sharpness of tuning.

result from the postulated OHC amplifier. However, they have also been found in birds (Manley et al., 1987) and crocodiles (Klinke and Smolders, 1984). Because the present authors argue that the division of labour between THCs and SHCs is different from mammalian IHCs and OHCs, the ultimate reason for the generation of otoacoustic emissions must still be clarified.

The above discussion indicates that the functional role of avian SHCs is different from that of mammalian OHCs, and that avian THCs and SHCs are not functionally analogous to mammalian IHCs and OHCs, respectively. However, the findings described do not allow a complete understanding of the underlying functional mechanisms of avian HCs. Several questions remain. For example, why are there so many hair cells in one cross section? Are there gradients in HC properties in longitudinal as well as in transversal directions? What is the real difference between THCs and SHCs, at least in their extreme forms? A few answers can possibly be given. Most likely, the important longitudinal gradient is frequency tonotopy leading finally to the untuned infrasound receptors in the most apical region of the papilla. Transverse gradients have been found in the properties of HC membranes. Murrow and Fuchs (1990) and B.W. Murrow (personal communication) have reported on transverse gradients in equipment with certain ionic channels (i.e., the potassium I_A channel). THCs have few I_A channels. This indicates that the two populations do have different functional roles. Smolders et al. (1992) describe a transversal profile of single fiber threshold and sharpness of tuning (Q_{10dB}) showing that minimal threshold and highest Q_{10dB} are found at about 20% of the basilar membrane width measured from the neural edge. That is to say, sensitivity and frequency selectivity are highest in a region where the THCs are the tallest. However, in the study of Smolders et al. (1992), the number of SHCs encountered is too small to determine gradients within this population of cells. Are there SHCs with different functions? Are the SHCs that are not con-

tacted by afferent fibers, as reported by G.A. Manley (personal communication), a population of HCs that serve an intrinsic function or are these cells just not yet innervated? Although these and other questions cannot be confidently answered at present, the study of avian hearing mechanisms is bound to continue with interesting results.

Acknowledgement

The data from our own laboratory that were reported here were accumulated with support of the Deutsche Forschungsgemeinschaft (SFB 45).

References

Ashmore, J.F. (1987) A fast motile response in guinea pig outer hair cells: the cellular basis of the cochlear amplifier. *J. Physiol. (Lond.)*, 388: 323 – 347.

Brownell, W.E. (1985) Evoked mechanical responses of isolated cochlear outer hair cells. *Science*, 227: 194 – 196.

Corwin, J.T. and Cotanche, D.A. (1988) Regeneration of sensory hair cells after acoustic trauma. *Science*, 240: 1772 – 1774.

Cotanche, D.A., Cotton, C.U., Gatzy, J.T. and Sulik, K.K. (1987) Ultrastructural and electrophysiological maturation of the chick tegmentum vasculosum. *Hear. Res.*, 25: 125 – 139.

Crawford, A.C. and Fettiplace, R. (1981) An electrical tuning mechanism in turtle cochlear hair cells. *J. Physiol. (Lond.)*, 312: 377 – 412.

Crawford, A.C. and Fettiplace, R. (1985) The mechanical properties of ciliary bundles of turtle cochlear hair cells. *J. Physiol. (Lond.)*, 364: 359 – 380.

Eatock, R.A. and Manley, G.A. (1981) Auditory nerve fibre activity in the tokay gecko: II. Temperature effects on tuning. *J. Comp. Physiol. A*, 142: 219 – 226.

Emde, C. and Klinke, R. (1977) Does absolute pitch depend on an internal clock? In: M. Portmann and J.-M. Aran (Eds.), *Les Colloques de l'Institut National de la Santé et de la Recherche Médicale (INSERM), Vol. 68 – Inner Ear Biology*, Editions INSERM, Paris, 145 pp.

Evans, E.F. and Klinke , R. (1982) The effect of intracochlear and systemic furosemide on the properties of single cochlear nerve fibers in the cat. *J. Physiol. (Lond.)*, 331: 409 – 427.

Fischer, F.P., Brix, J., Singer, I. and Miltz, C. (1991) Contacts between hair cells in the avian cochlea. *Hear. Res.*, 53: 281 – 292.

Fuchs, P.A., Nagai, T. and Evans, M.G. (1988) Electrical tuning in hair cells isolated from the chick cochlea. *J. Neurosci.*, 8: 2460 – 2467.

Gleich, O. and Narins, P.M. (1988) The phase response of primary auditory afferents in a songbird (*Sturnus vulgaris L.*). *Hear. Res.*, 32: 81 – 92.

Gummer, A.W. and Klinke, R. (1983) Influence of temperature on tuning of primary-like units in the guinea pig cochlear nucleus. *Hear. Res.*, 12: 367 – 380.

Gummer, A.W., Smolders, J.W.T. and Klinke, R. (1987) Basilar membrane motion in the pigeon measured with the Mössbauer technique. *Hear. Res.*, 29: 63 – 92.

Gummer, A.W., Smolders, J.W.T. and Klinke, R. (1989a) Mechanics of a single-ossicle ear: I. The extra-stapedius of the pigeon. *Hear. Res.*, 39: 1 – 14.

Gummer, A.W., Smolders, J.W.T. and Klinke, R. (1989b) Mechanics of a single-ossicle ear: II. The columella-footplate of the pigeon. *Hear. Res.*, 39: 15 – 26.

Hill, K.G., Stange, G. and Mo, J. (1989) Temporal synchronization in the primary auditory responses in the pigeon. *Hear. Res.*, 39: 63 – 74.

Holley, M.C. and Ashmore, J.F. (1990) Spectrin, actin and the structure of the cortical lattice in mammalian cochlear outer hair cells. *J. Cell Sci.*, 96: 283 – 291.

Hudspeth, A.J. (1989) How the ear's works work. *Nature*, 341: 397 – 404.

Kemp, D.T. (1978) Stimulated acoustic emissions from within the human auditory system. *J. Acoust. Soc. Am.*, 64: 1386 – 1391.

Khanna, S.M. and Leonard, D.B.G. (1982) Basilar membrane tuning in the cat cochlea. *Science*, 215: 305 – 306.

Klinke, R. and Smolders, J. (1977) Effect of temperature shift on tuning properties. In: E.V. Evans and J.P. Wilson (Eds.), *Psychophysics and Physiology of Hearing*, Academic Press, London, pp. 109 – 112.

Klinke, R. and Smolders, J. (1984) Hearing mechanisms in caiman and pigeon. In: L. Bolis, R.D. Keynes and S.H.P. Maddrell (Eds.), *Comparative Physiology of Sensory Systems*, Cambridge Univ. Press, Cambridge, pp. 195 – 211.

Kreithen, M.L. and Quine, D.B. (1979) Infrasound detection by the homing pigeon. *J. Comp. Physiol. A*, 129: 1 – 4.

Leake, P.A. (1977) SEM observations of the cochlear duct in *Caiman crocodilus. Scan. Electron Microsc.*, II: 437 – 444.

Lewis, E.R. (1987) Speculations about noise and the evolution of vertebrate hearing. *Hear. Res., 25*, 83 – 90.

Liberman, M.C. (1978) Auditory-nerve response from cats raised in a low-noise chamber. *J. Acoust. Soc. Am.*, 63: 442 – 455.

Liberman, M.C. (1982) Single-neuron labeling in the cat auditory nerve. *Science*, 216: 1239 – 1241.

Liberman, M.C. and Oliver, M.E. (1984) Morphometry of intracellularly labeled neurons in the auditory nerve: correlations with functional properties. *J. Comp. Neurol.*, 223: 163 – 176.

Manley, G.A. (1979) Preferred intervals in the spontaneous activity of primary auditory neurons. *Naturwissenschaften*, 66: 582 – 584.

Manley, G.A. (1990) *Peripheral Hearing Mechanisms in Reptiles*

and Birds, Springer, Berlin, 288 pp.

Manley, G.A., Schulze, M. and Oeckinghaus, H. (1987) Otoacoustic emissions in a song bird. *Hear. Res.*, 26: 257 – 266.

Manley, G.A., Gleich, O., Kaiser, A. and Brix, J. (1989) Functional differentiation of sensory cells in the avian auditory periphery. *J. Comp. Physiol. A,* 164: 289 – 296.

Manley, G.A., Yates, G.K., Köppl, C. and Johnstone, B.M. (1990) Peripheral auditory processing in the bobtail lizard *Tiliqua rugosa.* IV. Phase locking of auditory-nerve fibers. *J. Comp. Physiol. A,* 167: 129 – 138.

Moffat, A.J.M. and Capranica, R.R. (1976) Effects of temperature on the response properties of auditory nerve fibers in the American toad. *J. Acoust. Soc. Am.*, 60: 80.

Murrow, B.W. and Fuchs, P.A. (1990) Preferential expression of transient current (I_A) by "short" hair cells of the chick's cochlea. *Proc. R. Soc. Lond. (Biol.),* 242: 189 – 195.

Narins, P.M. and Hillery, C.M. (1983) Frequency coding in the inner ear of anuran amphibians. In: R. Klinke and R. Hartmann (Eds.), *Hearing – Physiological Bases and Psychophysics,* Springer, Berlin, pp. 70 – 75.

Ohmori, H. (1988) Mechanical stimulation and Fura-2 fluorescence in the hair bundle of dissociated hair cells of the chick. *J. Physiol. (Lond.),* 399: 115 – 137.

Rebillard, M. and Pujol, R. (1983) Innervation of the chicken basilar papilla during its development. *Acta Otolaryngol. (Stockh.),* 96: 379 – 388.

Richter, C.-P. and Klinke, R. (1991) The effect of high concentration sodium and potassium solutions in the scale media on pigeon primary afferents. In: N. Elsner and H. Penzlin (Eds.), *Synapse-Transmission Modulation,* Thieme, Stuttgart, p. 104.

Robertson, D. (1984) Horseradish peroxidase injection of physiologically characterized afferent and efferent neurones in the guinea pig spiral ganglion. *Hear. Res.*, 15: 113 – 121.

Rose, J.E., Brugge, J.F., Anderson, D.J. and Hind, J.E. (1967) Phase-locked responses to low-frequency tones in single auditory nerve fibers of the squirrel monkey. *J. Neurophysiol.*, 30: 769 – 793.

Ruggero, M.A. and Rich, N.C. (1991) Furosemide alters organ of Corti mechanics: evidence for feedback of outer hair cells upon the basilar membrane. *J. Neurosci.*, 11: 1057 – 1067.

Ryals, B.M. and Rubel, E.W. (1988) Hair cell regeneration after acoustic trauma in adult *Coturnix* quail. *Science,* 240: 1774 – 1775.

Ryals, B.M. and Westbrook, E.W. (1990) Hair cell regeneration in senescent quail. *Hear. Res.*, 50: 87 – 96.

Schermuly, L. and Klinke, R. (1985) Change of characteristic frequency of pigeon primary auditory afferents with temperature. *J. Comp. Physiol. A,* 156: 209 – 211.

Schermuly, L. and Klinke, R. (1990a) Infrasound sensitive neurones in the pigeon cochlear ganglion. *J. Comp. Physiol. A,* 166: 355 – 363.

Schermuly, L. and Klinke, R. (1990b) Origin of infrasound sensitive neurones in the papilla basilaris of the pigeon: a HRP study. *Hear. Res.*, 48: 69 – 78.

Schermuly, L., Göttl, K.-H. and Klinke, R. (1983) Little ototoxic effect of furosemide on the pigeon inner ear. *Hear. Res.*, 10: 279 – 282.

Schermuly, L., Vossieck, T. and Klinke, R. (1990) Furosemide has no effect on endocochlear potential and tuning properties of primary afferent fibres in the pigeon inner ear. *Hear. Res.*, 50: 295 – 298.

Schermuly, L., Vossieck, T. and Klinke, R. (1991) Peri-stimulus suppression and post-stimulus ringing in tuned and untuned fibres of pigeon auditory nerve. In: N. Elsner and H. Penzlin (Eds.), *Synapse-Transmission Modulation,* Thieme, Stuttgart, p. 101.

Sellick, P.M., Patuzzi, R. and Johnstone, B.M. (1982) Measurement of basilar membrane motion in the guinea pig using the Mössbauer technique. *J. Acoust. Soc. Am.*, 72: 131 – 141.

Smith, C.A. (1985) Inner ear. In: A.S. King and J. McLelland (Eds.), *Form and Function in Birds, Vol. 3,* Academic Press, London, pp. 273 – 310.

Smolders, J. and Klinke, R. (1977) Effect of temperature changes on tuning properties of primary auditory fibres in caiman and cat. In: M. Portmann and J.-M. Aran (Eds.), *Les Colloques de l'Institut National de la Santé et de la Recherche Médical (INSERM), Vol. 68 – Inner Ear Biology,* Editions INSERM, Paris, p. 125.

Smolders, J.W.T. and Klinke, R. (1984) Effects of temperature on the properties of primary auditory fibres of the spectacled caiman, *Caiman crocodilus L. J. Comp. Physiol. A,* 155: 19 – 33.

Smolders, J.W.Th. and Klinke, R. (1986) Synchronized responses of primary auditory fibre-populations in *Caiman crocodilus L.* to single tones and clicks. *Hear. Res.*, 24: 89 – 103.

Smolders, J.W.T., Ding, D. and Klinke, R. (1992) Normal tuning curves from primary afferent fibres innervating short and intermediate hair cells in the pigeon ear. In: Y. Cazals, L. Demany and K. Horner (Eds.), *Auditory Physiology and Perception – Advances in Biosciences, Vol. 83,* Pergamon Press, Oxford, 197 – 204.

Sterkers, O., Ferrary, E. and Amiel, C. (1988) Production of inner ear fluids. *Physiol. Rev.*, 68(4): 1083 – 1128.

Sullivan, W.E. and Konishi, M. (1984) Segregation of stimulus phase and intensity coding in the cochlear nucleus of the barn owl. *J. Neurosci.*, 4: 1787 – 1799.

Takasaka, T. and Smith, C.A. (1971) The structure and innervation of the pigeon's basilar papilla. *J. Ultrastruct. Res.*, 35: 20 – 65.

Von Düring, M., Karduck, A. and Richter, H.G. (1974) The fine structure of the inner ear in *Caiman crocodilus. Z. Anat. Entwicklungsgeschichte,* 145: 41 – 65.

Von Düring, M., Andres, K.H. and Simon, K. (1985) The comparative anatomy of the basilar papillae in birds. *Fortschr. Zool.*, 30: 681 – 685.

Vossieck, T. and Klinke, R. (1990) A method for changing the

avian endocochlear potential by current-injection. *Eur. Arch. Otorhinolaryngol.*, 248: 11 – 14.

Vossieck, T., Schermuly, L. and Klinke, R. (1991) The influence of DC-polarization of the endocochlear potential on single fibre activity in the pigeon cochlear nerve. *Hear. Res.*, 56: 93 – 100.

Wever, E.G. (1978) *The Reptile Ear*, Princeton University Press, Princeton, NJ, 1024 pp.

Whitehead, M.C. and Morest, D.K. (1985) The growth of cochlear fibers and the formation of their synaptic endings in the avian inner ear: a study with the electron microscope. *Neuroscience*, 14: 277 – 300.

Wit, H.P. and Bleeker, J.D. (1983) A possible method to study transient effects of ototoxic agents upon the vestibular system. *Arch. Otorhinolaryngol.*, 238: 175 – 178.

Zenner, H.P., Zimmermann, U. and Schmitt, U. (1985) Reversible contraction of isolated mammalian cochlear hair cells. *Hear. Res.*, 18: 127 – 133.

Zimmermann, U., Reuter, G., Gitter, A.H., Zenner, H.P. and Klinke, R. (1989) Isolation and short term culture of pigeon hair cells. In: N. Elsner and W. Singer (Eds.), *Dynamics and Plasticity in Neuronal Systems*, Thieme, Stuttgart, 286 pp.

J.H.J. Allum, D.J. Allum-Mecklenburg, F.P. Harris and R. Probst
Progress in Brain Research, Vol. 97

CHAPTER 5

Mechanical demodulation of hydrodynamic stimuli performed by the lateral line organ

Sietse M. van Netten[1] and Shyam M. Khanna[2]

[1] *Department of Biophysics, University of Groningen, Groningen, The Netherlands and* [2] *Department of Otolaryngology, College of Physicians and Surgeons, Columbia University, New York, NY 10032, U.S.A.*

Tonic displacements of the fish lateral line cupula were observed during stimulation of the organ with amplitude-modulated water motion. The modulation frequency was fixed at 2.4 Hz and the carrier frequency was varied from 25 to 500 Hz. The time waveforms of the cupular displacement at carrier frequencies below 280 Hz and above 470 Hz were essentially amplitude-modulated waves. Between 350 Hz and 410 Hz the magnitude at the modulation frequency increased sharply and the predominant shape of the displacement waveform changed to that of the modulating frequency. The mechanism for extraction of the modulation component may play a key role in the decoding of sensory information.

Key words: Lateral line; Fish; Cupular vibration; Amplitude modulation; Hair cell; Mechanical demodulation

Introduction

Hair cells transduce mechanical vibration into electrical signals in sensory organs of the acousticolateralis system. The mechanics of hair cells is closely related to the transduction properties of mechano-sensory organs, although the precise relationship is still not fully known (for a review see, e.g., Hudspeth, 1989). Measurements on the micromechanics of the stereociliar bundle of hair cells of the bullfrog's sacculus indicate that the mechanical gating of the transduction channels of hair cells is reflected in a non-linear pivoting stiffness of the hair bundle (Howard and Hudspeth, 1988). Spontaneous stereociliar motion has been observed (Crawford and Fettiplace, 1985; Howard and Hudspeth, 1987; Denk and Webb, 1989) as well as bundle movements evoked by electrical stimulation (Assad et al., 1989) or by blockage of the transduction channels (Denk, 1989). These observations suggest that hair cells are not simple passive mechano-detectors.

A specific mechanical property that has been identified only in mammalian outer hair cells is the change of length of the hair cell body in response to electrical (Brownell et al., 1985; Ashmore, 1987) and chemical (Flock et al., 1986; Zenner, 1986) stimuli. Recently, a tonic change of length of the outer hair cell body has also been observed under influence of acoustic stimulation of the cell membrane (Canlon et al., 1988). This response was found to be highly frequency-selective (Brundin et al., 1989). That outer hair cell motility may play an important role in determining the selectivity of the cochlea is supported by the fact that proper outer hair cell functioning is essential to the sharp tuning seen in mechanical responses (Khanna and Leonard, 1986; Ruggero and Rich, 1991) and in auditory nerve fiber responses of the inner ear (Liberman and Dodds, 1984).

Most of the present knowledge on hair cell mechanics has been obtained from studies on isolated hair cell preparations or isolated organs. It has been shown recently that the micromechanics of the hair bundles influences the dynamic behavior of the

tectorial structure (cupula) in the lateral line organ in vivo (van Netten and Kroese, 1987, 1989; van Netten, 1991). In the lateral line organ, the base of the cupula is mechanically attached to the bundles of the hair cells. Therefore, measurements of the motion of a tectorial structure like the cupula in the intact neuromast of the lateral line organ may be used to probe hair bundle micromechanics under in vivo conditions.

In the present study, the mechanical responses of the cupula were measured interferometrically. The cupula shows tonic (low frequency) displacements at the modulation frequency in response to amplitude-modulated vibrations of the canal fluid, in addition to the expected modulated response at the carrier frequency. These results suggest the existence of a demodulating mechanism present at the mechanical level of the lateral line organ.

Methods

African knife-fish *(Xenomystus nigri)* used in these experiments were anesthetized by intraperitoneal injection (24 mg/kg body weight) of Saffan (Glaxo) (Oswald, 1978). The supraorbital canal organ was exposed by carefully removing the overlying skin using an operating microscope. For interferometric measurements of cupular motion, fish were placed in a test chamber containing an oxygenated modified fish Ringer solution (e.g., Kelly and van Netten, 1991), and respired artificially by a flow of this medium. Head and body clamps fixed the position of the fish rigidly. The clamps in turn were attached to the X, Y, Z micro-positioning system and a two-axis goniometer rotation system. This allowed the position of the fish to be changed along the X, Y and Z directions and its angle to be adjusted around each of two perpendicular axes. A more detailed description of the mechanical system is given by Khanna et al. (1989). During the experiments, neuromasts in the canal were observed with a reflected light optical sectioning microscope (Koester, 1980; Koester et al., 1989), equipped with a 20 × objective lens (Olympus), adapted for water immersion with a custom dipping cone. The effective numerical aperture of the combination is 0.5 and has a working distance of 4 mm. A circular aperture with a watertight seal in the side of the test chamber provided the access for the objective lens.

To excite the cupula, local fluid motion was produced under near-field conditions by a piezoelectrically driven glass sphere (ϕ = 0.8 mm) placed in the canal at a distance of about 4 mm from the cupula. The direction of vibration of the sphere was parallel to the longitudinal axis of the canal (see Fig. 1), in which the hair cells have their maximum sensitivity (Flock, 1971). The electrical signals used to drive the glass sphere were digitally synthesized and converted to analog waveform with an Ariel DSP 16-bit digital-to-analog converter and a low-pass filter (Lund and Khanna, 1989). Sinusoidally amplitude-modulated signals were used with carrier frequencies ranging from 25 Hz to about 500 Hz. The modulation frequency (2.4 Hz), the depth of modulation (100%) and the carrier amplitude were kept constant.

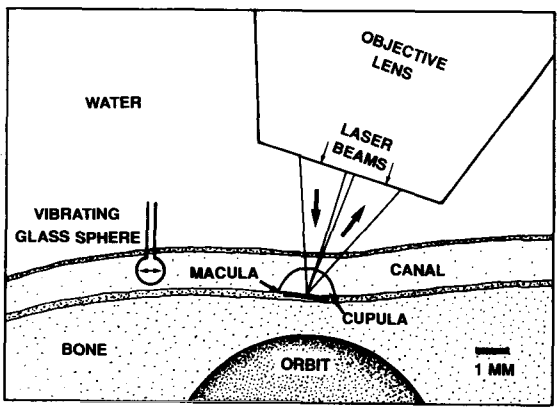

Fig. 1. Basic arrangement for stimulus application and vibratory response measurement of the cupula in the supraorbital canal of a living fish under water. A glass sphere is driven along the length of the canal to produce water motion that stimulates the cupula under near field conditions. The resulting cupular vibration is measured with the laser beam of a heterodyne interferometer which is focused on the cupula through one side of the water immersion objective lens. The region of measurement overlies the sensory hair cells in the macula. Light from this region is reflected through the opposing side of the objective lens to the photodetector. The direction of visualization and vibration measurement was inclined at an angle of about 70° with respect to the plane of the macula.

A heterodyne interferometer (Willemin et al., 1988, 1989) was used to measure velocity of the cupula along the optical viewing axis, which was at an angle of about 70° with respect to the plane of the macula (e.g., van Netten and Khanna, 1993).

Locations for vibration measurements were selected in the cupula close to the tips of the hair bundles, by focusing the laser beam of the interferometer on small, reflective regions inside the transparent cupular matrix (van Netten and Khanna, 1991). Morphological details of these regions and their relationship to the cupula and the hair cells have been discussed elsewhere (Kelly and van Netten, 1991).

Vibratory responses measured with the interferometer were low-pass filtered (cut-off frequency 2500 Hz) and sampled at a rate of 5 kg samples per second with an Ariel DSP 16-bit analog-to-digital converter. The samples were averaged 20 times in a 4096 bin response buffer (0.82 sec each, for a total duration of 16.4 sec). To avoid transients in the response, recording started only after a sufficient delay with respect to the onset of the stimulus. For averaging to be equally effective both for the modulating and the carrier frequency, their values were chosen so that an integral number of cycles of each frequency fitted the response buffer exactly.

The interferometer measures velocity. Therefore, the averaged velocity time waveforms were integrated to obtain displacement responses. To remove possible instrumental dc offsets in the measured velocity signal, which would result in a linearly increasing or decreasing displacement bias, a constant velocity was subtracted from all the bins of the stored velocity response to obtain a zero velocity average over the record length. This procedure forces the last bin of the calculated displacement response to be equal to the first bin.

For inspecting the spectral contents of the displacement responses, FFTs were calculated.

Results

The vibration amplitude of the cupula in response to amplitude-modulated water motion in the canal is shown in Fig. 2 at six carrier frequencies: 278 Hz, 307 Hz, 351 Hz, 410 Hz, 439 Hz and 468 Hz. The sinusoidal modulation frequency was fixed (2.4 Hz). In Fig. 2*a*, the modulation signal used has been added for comparison (upper trace). The displacement time function at each carrier frequency is shown for an 820 msec duration of the stimulus, which corresponds to two modulation cycles. Individual cycles of the carrier wave cannot be seen due to the time scale used for plotting. The response

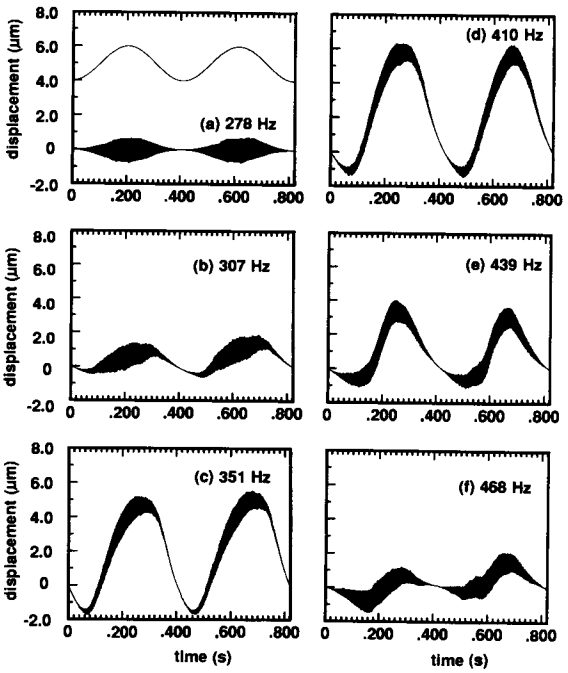

Fig. 2. Vibration amplitude of the cupula as a function of time in response to an amplitude-modulated water motion in the canal. The modulation frequency was maintained constant at 2.4 Hz. The modulation signal is shown for comparison in Fig. 2*a*. Response is shown at six carrier frequencies: (*a*) 278 Hz, (*b*) 307 Hz, (*c*) 351 (Hz), (*d*) 410 Hz, (*e*) 439 Hz and (*f*) 468 Hz. The individual cycles of the carrier wave cannot be seen in these figures due to the time scale used for the plotting. The cupular response is a modulated wave at frequencies below 278 Hz and above 468 Hz, in phase with the modulating wave. The modulation component at 2.4 Hz in the cupular response rises sharply between these frequencies and reaches a maximum at 410 Hz. This response is phase-shifted with respect to the modulating wave. Since the modulating signal is not present in the input, it has been recovered by a demodulation process.

envelope seen in Fig. 2*a* at a carrier frequency of 278 Hz (lower trace) is essentially an amplitude-modulated wave. The shape of the response begins to change dramatically as the carrier frequency is increased. At 307 Hz (Fig. 2*b*), it appears that an out-of-phase signal at the modulating frequency (tonic displacement) has been added to the response shape shown in Fig. 2*a*. The magnitude of this component at the modulation frequency increases with increase in carrier frequency, reaching a maximum at 410 Hz (Fig. 2*d*), where its amplitude is about six times larger than that of the amplitude-modulated carrier wave. The amplitude of the modulation component in the response decreases with further increase in carrier frequency at 439 Hz (Fig. 2*e*) and 468 Hz (Fig. 2*f*). Usually the tonic response starts with a

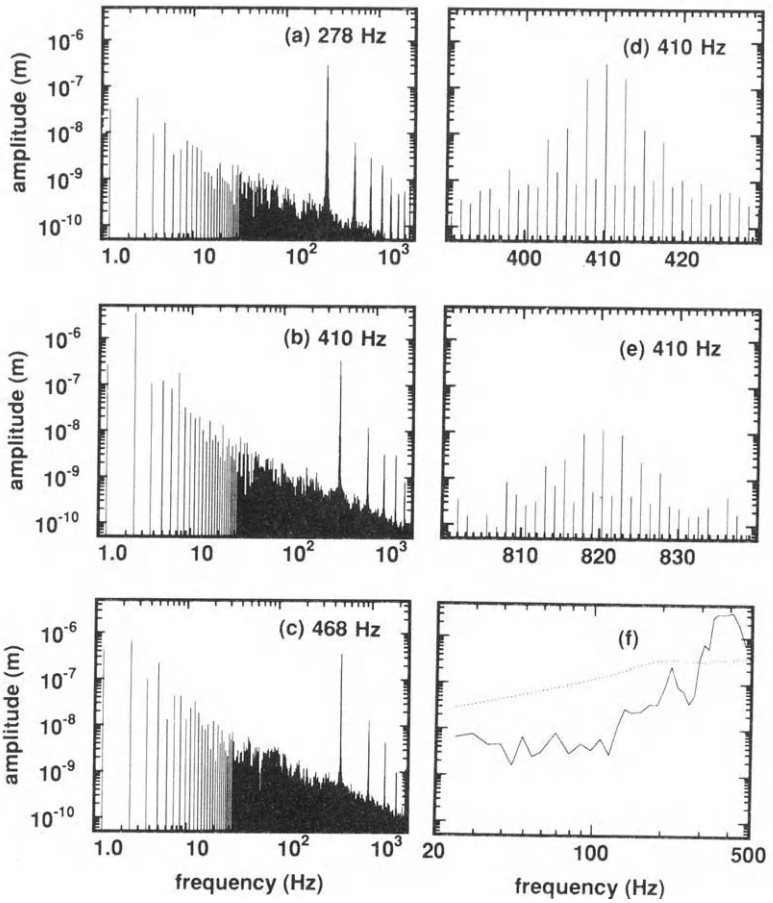

Fig. 3. Spectral components of the cupular response ($a-e$) and tuning curves (f). Fourier transforms of the time functions (Fig. 2) are shown at three carrier frequencies: (*a*) 278 Hz, (*b*) 410 Hz and (*c*) 468 Hz. The response consists of a group of spectral components at (i) the modulating frequency f_m (2.4 Hz), and its harmonics nf_m; (ii) the carrier frequency f_c and its sidebands $f_c \pm nf_m$ ($n = 1, 2 \ldots$); and (iii) multiples of the carrier frequency plus side bands $mf_c \pm nf_m$ ($m = 2, 3 \ldots; n = 1, 2 \ldots$). The spectral component at 2.4 Hz rises clearly above the noise floor at 410 Hz (*b*). The sidebands cannot be seen clearly in the above figures, therefore portions of Fig. 3*b* are enlarged in Figs. 3*d* and 3*e*, showing details of the spectrum around 410 Hz and 820 Hz, respectively. Note the linear frequency scale. The sidebands are separated from each other by $\pm nf_m$. The noise floor decreases with increasing frequency. Fig. 3*f* shows cupular displacement amplitude as a function of the carrier frequency in response to amplitude-modulated water motion. Vibration amplitude at the modulation frequency of 2.4 Hz (solid curve) as well as the carrier (dotted curve) are given. Above 125 Hz, the magnitude of the modulation component increases with frequency and exceeds the response at the carrier frequency between 300 and 500 Hz.

negative displacement (i.e., a displacement component away from the objective lens), while reversing its direction before the modulated carrier reaches its maximum. In some experiments, however, it was observed that the phase behavior of the modulation component may vary with carrier frequency.

The spectra corresponding to the time waveforms at 278 Hz, 410 Hz and 468 Hz are shown in Figs. 3*a-c*. The amplitude of the noise decreases with increasing frequency, roughly as 1/f. Rising above the noise floor are several groups of spectral components. The first group consists of the modulating frequency (2.4 Hz), and its harmonics (4.8 Hz, 7.2 Hz). The second group consists of the carrier frequency (Fig. 3*a*, 278 Hz; Fig. 3*b*, 410 Hz; and Fig. 3*c*, 468 Hz) and its sidebands. The third, fourth and fifth groups consist of multiples of the carrier frequency (e.g., Fig. 3*a*, 2 × 278 Hz, 3 × 278 Hz, 4 × 278 Hz . . .) and their sidebands. The amplitude of the component at the carrier frequency remains essentially unchanged from 278 Hz to 468 Hz, but the amplitude of the component at the modulating frequency changes by a factor of six within this frequency range. The amplitude of the modulating frequency component is therefore sharply frequency-dependent. Details of the sidebands around the carrier and its harmonics cannot be seen in Figs. 3*a-c* due to the frequency scale used, and enlargements of Fig. 3*b* are therefore provided in Figs. 3*d* and 3*e*. In Fig. 3*d*, the carrier frequency component (~ 410 Hz) together with it's first three sidebands (± 2.4 Hz, ± 4.8 Hz and ± 7.2 Hz) can be clearly seen above the noise floor. The spectral components around twice the carrier frequency (~ 820 Hz) are shown in Fig. 3*e*. They include the first three pairs of sidebands (± 2.4 Hz, ± 4.8 Hz and ± 7.2 Hz).

Vibration amplitude of the cupula at the modulation frequency (solid line) and at the carrier frequency (dotted line) are plotted in Fig. 3*f* as functions of carrier frequency.

The response at the modulating frequency stays below the noise level up to about 125 Hz and then rises quickly to a peak at 220 Hz, and a higher but broader maximum between 350 and 410 Hz. The amplitude of the second maximum exceeds the amplitude at the carrier frequency by a factor of 10. The dependence of the tonic response on the maximum level of the carrier was not investigated systematically in this study. We observed, however, that for different levels of the (maximum) AM stimulus, the shape of the response of the tonic response changes. We usually found no clear tonic responses when the magnitude of the response at the carrier frequency was less than 100 nm. At these lower levels, the 2.4 Hz component may not be measurable due to the limited sensitivity of the interferometer at low frequencies.

The response amplitude at the carrier frequency (Fig. 3*f*, dotted line) rises slowly with increasing frequency from 25 Hz to about 150 Hz, and has a broad resonance at about 230 Hz. The components at the carrier frequency in the amplitude-modulated wave experiments show a smooth frequency dependence unlike the modulation frequency component.

Discussion

Linearity of the stimulus

When stimulated with amplitude-modulated canal fluid motion, the cupula of the fish lateral line responds non-linearly. In order to ascertain that the non-linear response originates within the neuromast, it is necessary to verify that the stimulus generation system and the fluid motion produced in the canal are linear. To check the linearity of the stimulus generation system, the displacement of the glass sphere was measured with the interferometer. The glass sphere was placed in the lateral line canal at the same location as it was positioned during cupular vibration experiments. Also, the same stimulus generation and response analysis protocols were used. The stimulus generation system was found to be linear (harmonic distortion < -45 dB).

To test whether the water motion produced was linear, a thin glass fiber ($\phi \sim 2\mu$m) was placed in front of the vibrating glass sphere at the same distance from the sphere as the cupula was under normal measuring conditions (4 mm). Because of its flexibility, the tip of the fiber follows the fluid flow. The motion of the tip of the glass fiber was measured

interferometrically. This experiment was repeated at smaller distances to the sphere. No noticeable modulation component was found in the response of the glass fiber's tip.

We conclude, therefore, that the hydrodynamic stimulus acting on the cupula is a pure amplitude-modulated water motion.

Demodulation of the sensory input

A sinusoidal frequency of 2.4 Hz was used to modulate the carrier frequency in our experiments. The spectrum of the resulting stimulus wave therefore consists of a carrier frequency and two sidebands separated from the carrier frequency by ± 2.4 Hz. There are no spectral components present at the modulating frequency or its harmonics. Since the cupular response contains spectral components at the modulating frequency and its harmonics, it is clear that a demodulation of the input wave has taken place within the mechanics of the neuromast.

One of the simplest models of demodulation is a half-wave rectifier (linear detection) (e.g., Russell, 1962). One of the fundamental properties of such a demodulator is that the ratio of the components at the modulation frequency and carrier frequency at the detector output is less than one and does not change with the input carrier level. We found that this ratio in the cupular responses may be greater than one and that it changes with the input carrier levels we have used; a tonic response was not observed at low stimulus levels at which a clear response at the carrier frequency was still present. When the carrier frequency is changed in small increments (Figs. 3*a-c*), the carrier amplitude and its harmonics remain essentially unchanged, while the amplitude of the modulation component changes dramatically. This observation is also not consistent with a simple rectification scheme. This argument remains valid even when sharply tuned bandpass filters are included at the input of the demodulator and low-pass filters are included at its output.

Both observations on the cupular response therefore are inconsistent with a rectification scheme.

Comparison to other organs

In some experiments we observed very large tonic displacements of the cupula up to several micrometers, which could be confirmed by viewing the motion of the cupula with the optical sectioning microscope. Without having more information on the underlying mechanism, it is not clear which process can cause displacement responses of this magnitude. A possible contribution to the tonic cupular responses by the underlying hair cells has to be investigated.

Recently, comparable (tonic) mechanical responses of inner ear structures were measured in an isolated temporal bone preparation of the guinea pig in response to acoustic amplitude-modulated stimuli (Brundin et al., 1991). Similar effects have also been observed in the motion of the basilar membrane in the basal turn of the guinea pig cochlea (LePage, 1989). It is also interesting that the spectrum of the response to amplitude-modulated stimuli, as observed in the lateral line, parallels the spectrum of PST histograms made of the activity of primary auditory nerve fibers of the cat, in response to amplitude-modulated tones applied to the ear (Khanna and Teich, 1989).

The presence of similar demodulation effects occurring in the periphery of different organs of different animals points to a common property of sensory organs processing mechanically coded information. In communication systems, the information is usually contained in the modulating signal and not in the carrier. The need for an efficient demodulation system may therefore be basic and essential for extraction and transmission of information by mechano-sensory systems.

Acknowledgements

This research was supported by a Fellowship of the Royal Netherlands Academy of Arts and Sciences to SvN and by the Emil Capita Foundation.

References

Ashmore, J.F. (1987) A fast motile response in guinea-pig outer hair cells: the cellular basis of the cochlear amplifier. *J. Phys-*

iol. (Lond.), 388: 323 – 347.

Assad, J.A., Hacohen, N. and Corey, D.P. (1989) Voltage dependence of adaptation and active bundle movements in bullfrog saccular hair cells. *Proc. Natl. Acad. Sci. U.S.A.,* 86: 2918 – 2922.

Brownell, W.E., Bader, C.R., Bertrand, D. and de Ribaupierre, Y. (1985) Evoked mechanical responses of isolated cochlear outer hair cells. *Science,* 227: 194 – 196.

Brundin, L., Flock, Å. and Canlon, B. (1989) Sound-induced motility of cochlear outer hair cells is frequency selective. *Nature,* 342: 814 – 816.

Brundin, L., Flock, Å., Khanna, S. and Ulfendahl, M. (1991) Frequency-specific position shift in the guinea pig organ of Corti. *Neurosci. Lett.,* 128: 77 – 80.

Canlon, B., Brundin, L. and Flock, Å. (1988) Acoustic stimulation causes tonotopic alterations in the length of isolated outer hair cells from the guinea pig hearing organ. *Proc. Natl. Acad. Sci. U.S.A.,* 85: 7033 – 7035.

Crawford, A.C. and Fettiplace, R. (1985) The mechanical properties of ciliary bundles of turtle cochlear hair cells. *J. Physiol. (Lond.),* 364: 359 – 379.

Denk, W. (1989) *Biophysical Studies of Mechano-electrical Transduction in Hair Cells,* PhD thesis, Cornell University.

Denk, W. and Webb, W.W. (1989) Simultaneous recording of fluctuations of hair-bundle deflection and intracellular voltage in saccular hair cells. In: J.P. Wilson and D.T. Kemp (Eds.), *Cochlear Mechanisms: Structure, Function and Models,* Plenum, New York, pp. 125 – 133.

Flock, Å. (1971) Sensory transduction in hair cells. In: W.R. Loewenstein (Ed.), *Principles of Receptor Physiology – Handbook of Sensory Physiology, Vol. 4,* Springer, Berlin, pp. 396 – 441.

Flock, Å., Flock B. and Ulfendahl, M. (1986) Mechanisms of movement in outer hair cells and a possible structural basis. *Arch. Otorhinolaryngol.,* 243: 83 – 90.

Howard, J. and Hudspeth, A.J. (1987) Mechanical relaxation of the hair bundle mediates adaptation in mechanoelectrical transduction by the bullfrog's saccular hair cell. *Proc. Natl. Acad. Sci. U.S.A.,* 84: 3063 – 3068.

Howard, J. and Hudspeth, A.J. (1988) Compliance of the hair bundle associated with gating of mechanoelectrical transduction channels in the bullfrog's saccular hair cells. *Neuron,* 1: 189 – 199.

Hudspeth, A.J. (1989) How the ear's works work. *Nature,* 341: 397 – 404.

Kelly, J.P. and van Netten, S.M. (1991) Topography and mechanics of the cupula in the fish lateral line I. Variation of cupular structure and composition in three dimensions. *J. Morphol.,* 207: 23 – 26.

Khanna, S.M. and Leonard, D.G.B. (1986) Relationship between basilar membrane tuning and hair cell condition. *Hear. Res.,* 23: 55 – 70.

Khanna, S.M. and Teich, M.C. (1989) Spectral characteristics of the response of primary auditory nerve fibers to amplitude-modulated signals. *Hear. Res.,* 39: 143 – 158.

Khanna, S.M., Rosskothen, H. and Koester, C.J. (1989) Mechanical design of the measurement and micropositioning systems. *Acta Otolaryngol. (Stockh.) (Suppl.),* 467: 51 – 59.

Koester, C.J. (1980) Scanning mirror microscope with optical sectioning characteristics: applications in ophthalmology. *Appl. Optics,* 19: 1749 – 1757.

Koester, C.J., Khanna, S.M., Rosskothen, H. and Tackaberry, R.B. (1989) Incident light optical microscope for visualization of cellular structures in the inner ear. *Acta Otolaryngol. (Stockh.) (Suppl.),* 467: 27 – 33.

LePage, E.L. (1989) Functional role of the olivo-cochlear bundle: a motor unit control system in the mammalian cochlea. *Hear. Res.,* 38: 177 – 198.

Liberman, M.C. and Dodds, L.W. (1984) Single-neuron labeling and chronic cochlear pathology. III. Stereocilia damage and alterations of threshold tuning curves. *Hear. Res.,* 16: 55 – 74.

Lund D.T. and Khanna, S.M. (1989) A digital system for the generation of acoustic stimuli and the analysis of cellular vibration data. *Acta Otolaryngol. (Stockh.) (Suppl.),* 467: 77 – 89.

Oswald, R.L. (1978) Injection anaesthesia for experimental studies in fish. *Comp. Biochem. Physiol.,* 60: 19 – 26.

Ruggero, M.A. and Rich, N.C. (1991) Furosemide alters organ of Corti mechanics: evidence for feedback of outer hair cells upon the basilar membrane. *J. Neurosci.,* 11: 1057 – 1067.

Russell, G.M. (1962) *Modulation and Coding in Information Systems,* Prentice-Hall, Englewoods Cliffs, NJ.

van Netten, S.M. (1991) Hydrodynamics of the excitation of the cupula in the fish canal lateral line. *J. Acoust. Soc. Am.,* 89: 310 – 319.

van Netten, S.M. and Khanna, S.M. (1991) Nonlinear mechanics of the cupula in the fish canal lateral line. In: *Abstracts of the Fourteenth Midwinter Research Meeting,* Association for Research in Otolaryngology, p. 37.

van Netten, S.M. and Khanna, S.M. (1993) Mechanics of the cupula and hair cells of the canal lateral line organ of *Notopterus chitala.* (Submitted.)

van Netten, S.M. and Kroese, A.B.A. (1987) Laser interferometric measurements on the dynamic behaviour of the cupula in the fish lateral line. *Hear. Res.,* 29: 55 – 61.

van Netten, S.M. and Kroese, A.B.A. (1989) Hair cell mechanics controls the dynamic behaviour of the lateral line cupula. In: J.P. Wilson and D.T. Kemp (Eds.), *Cochlear Mechanisms: Structure, Function and Models,* Plenum, New York, pp. 47 – 55.

Willemin, J.F., Dändliker, R. and Khanna, S.M. (1988) Laser heterodyne interferometer for submicroscopic vibration measurements in the inner ear. *J. Acoust. Soc. Am.,* 83: 787 – 795.

Willemin, J.F., Khanna, S.M. and Dändliker, R. (1989) Heterodyne interferometer for cellular vibration measurements. *Acta Otolaryngol. (Stockh.) (Suppl.),* 467: 35 – 42.

Zenner, H.P. (1986) Motile responses in outer hair cells. *Hear. Res.,* 22: 83 – 90.

J.H.J. Allum, D.J. Allum-Mecklenburg, F.P. Harris and R. Probst
Progress in Brain Research, Vol. 97

Overview and critique of Chapters 6 – 9

H.P. Zenner

Tübingen, Germany

A summary of these four papers suggests that the generators of otoacoustic emissions probably are not isolated but coupled. In addition, the existence of putative multiple generators for otoacoustic emissions (OAE) in general and of separate generators by emission type are discussed. At least two varying generators have to be differentiated in small mammals. The generators of distortion product otoacoustic emissions (DPOAE) stimulated by high levels have to be distinguished from those associated with low-level DPOAE and transitory evoked otoacoustic emissions (TEOAE). However, this high- and low-level DPOAE difference may not hold for human ears. TEOAE can presently be used as a means of screening for hearing loss in babies and small children. They supposedly represent a global response of cochlear micromechanics. Distortion products are frequency-specific and may be more useful for indicating hearing thresholds by frequency.

The paper by H.P. Wit tries to answer the question of whether spontaneous otoacoustic emissions (SOAE) can be related to a single, isolated oscillator. Wit concludes that SOAE can be generated by a single oscillator but that the oscillator cannot occur in isolation. These results are based on SOAE measurements in human subjects, the determination of artificial SOAE in an artificial ear and on investigations with an electronic van der Pol oscillator coupled to neighboring systems (active filters, oscillators) and driven by white noise.

Large amplitude fluctuations were observed for a SOAE at 1.04 kHz. The Lorentzian fitting was limited to the lower slope. The cross correlation function of the 1.04 kHz SOAE and the 1.13 kHz SOAE within the same ear indicated a coupling of both generators. A fluctuation of the amplitudes and an increase in the width of spectral lines could only be achieved in the acute experiment by a coupling of the neighboring oscillators. Hence, Wit concludes that a single, isolated van der Pol oscillator is not an adequate description of the generation of SOAE.

This paper is an elegant study by a physicist who is used to approaching the items in a straightforward manner as is typical in physics. The biologically interested reader would like to discuss with the author whether the oscillators, as postulated, are represented by equal or different structures. How these oscillators look anatomically or biologically from the author's point of view is a decisive question. Which anatomical structures enable the postulated mechanical coupling between the oscillators?

The group of Avan and coworkers attempted to answer the question of whether TEOAE provide local or more global information on the mechanical status of the cochlea. They investigated the correlation between TEOAE amplitude and thresholds and the pure-tone audiogram between 250 and 8000 Hz in 138 patients. A frequent observation was an octave shift between the TEOAE amplitudes and the audiometric data. These findings contradicted the assumption that TEOAE with a particular dominant frequency are completely determined by the characteristics of the tonotopic region of the cochlea with which they are associated. In addition,

their results indicate that the amplitudes and detection thresholds of TEOAE are not frequency-specific and, thus, are non-local parameters. TEOAE are rather dependent on the residual active cochlear function between the site of the characteristic frequency and the stapes footplate. The authors suggest therefore that the TEOAE thresholds provide no information about the local cochlear status, but that they are correlated to the remaining activity along the organ of Corti. This paper is also of biophysical origin, logical and independent. The chain of arguments leading from the results to the discussion is convincing as well as imaginative.

One clinical application: the TEOAE is the screening of hearing loss in newborns and younger children since a global response of the cochlear mechanics is required to produce a response. When it is possible to measure emissions, normal or nearly normal hearing in at least a portion of the audiometric Hz range can be assumed. The absolute amplitudes of TEOAE are inadequate for detecting early injuries caused by ototoxic drugs or noise when an initial value was not determined before the injury. Intra-individual comparisons can be useful clinically.

The paper by Brenda Lonsbury-Martin et al. describes a series of investigations of TEOAE and DPOAE in humans and experimental animals. The authors tried to contribute to the resolution of the problem concerning the expression and generation factors of the emissions. Furthermore, they investigated which type of emission seems to be most important from a clinical point of view.

By measuring children with middle ear effusions the authors showed that the transfer through the middle ear has a large influence on the expression of the otoacoustic emissions. The expression of emissions is more attenuated in the reverse direction than in the other direction.

The authors could provide a number of arguments that favored the idea that there are different types of emission generators. This multi-generator hypothesis is supported by the finding in rabbit that low-level DPOAE (up to 60 dB) are sensitive to the effects of ethacrynic acid, anoxia and gentamycin. High-level DPOAE are insensitive and can be recorded even 21 h after the death. The difference between TEOAE and DPOAE in detecting hearing loss indicates the contribution of various generator mechanisms. TEOAE can only be recorded up to a hearing loss of 30 dB, whereas DPOAE can be measured even when the hearing loss exceeds 30 dB.

The authors discuss their conclusions with respect to the cellular biology and physiology of the cochlea. The authors share the opinion that an energy-dependent micromechanical process of the outer hair cells (OHC) plays a role in the generation of low-level DPOAE. In the case of high-level DPOAE, passive mechanical elements are supported to be of importance, e.g., the stereociliary stiffness, the structural integrity of the OHC as well as the stiffness of the basilar membrane. However, these authors suggest that level differences of f_1 and f_2 are not potentially as important as the presence of other OAE in influencing DPOAE in humans.

Research strategies that elaborate the parameters of evoking stimuli that detect a SNHL with the highest sensitivity are ongoing.

Probst and Harris also put forward the question of whether TEOAE and DPOAE are generated by the same or different mechanisms. They investigated tone-burst and click-evoked TEOAE and DPOAE in humans with normal and pathological hearing. The authors conclude that both emissions are generated and/or transmitted at least in part by different mechanisms. The growth functions between higher and lower frequency DPOAE/TEOAE are distinctly different. The mean amplitude of DPOAE increases as a function of the frequency while it declines in TEOAE. They are in line with Avan et al. in concluding that TEOAE depend on influences of the basilar membrane basal of the relevant CF. This may not be valid for DPOAE. Probst and Harris refer to the species differences in DPOAE as already described by Lonsbury-Martin et al. Salicylates induce a decline in amplitude of TEOAE, but not DPOAE. The latencies of the TEOAE are longer suggesting a slow, non-linear mechanism that possibly reacts to the envelope of

the stimulus. The latency of the distortion products is shorter, which indicates a fast acting, non-linear cycle-by-cycle mechanism. The site of TEOAE generation is to be closely located at or around the area of characteristic frequency (CF) to find an optimum operation point.

Probst and Harris conclude that the two types of emissions are based on either different generators or different retrograde transmission processes of the cochlea. A combination of both processes seems to be possible, too.

The paper is an excellent clinical investigation that shows to what extent functional conclusions can be drawn from data to the cochlea.

Probst and Harris agree with other authors that TEOAE are applicable as a screening procedure in newborns and younger children for identifying a hearing loss of up to 25 – 30 dB HL as an overall response of the cochlea. Because distortion products are more frequency-specific, the determination of hearing thresholds by Hz may be possible in the future.

J.H.J. Allum, D.J. Allum-Mecklenburg, F.P. Harris and R. Probst
Progress in Brain Research, Vol. 97

CHAPTER 6

Amplitude fluctuations of spontaneous otoacoustic emissions caused by internal and externally applied noise sources

H.P. Wit

Institute of Audiology, University Hospital, Groningen, The Netherlands

The simplest description for the generator of a spontaneous otoacoustic emission (SOAE) is that of a single (isolated) limit-cycle oscillator. Evidence is given that this description is too simple. And it is concluded that study of systems of coupled oscillators is needed to obtain more insight in the processes that generate SOAEs. Part of this conclusion is based on the study of properties of coupled electronic Van der Pol oscillators.

Key words: Cochlear mechanics; Van der Pol oscillator; Suppression; Non-linear system

Introduction

Amplitude and frequency of spontaneous otoacoustic emissions (SOAEs) are not perfectly stable but show fluctuations. These fluctuations can be described reasonably well by assuming that a SOAE is generated by a single isolated limit-cycle oscillator driven by noise (Bialek and Wit, 1984; Van Dijk and Wit, 1990). Because of its mathematical "simplicity", the Van der Pol oscillator was chosen to model such a limit-cycle oscillator.

An important parameter for the behavior of the Van der Pol oscillator is the strength of the nonlinear damping term. If this term is small, then the oscillator behaves as an undamped harmonic oscillator, producing a sine wave oscillation. However, if it is large, then oscillation deviates markedly from a sine wave. The damping parameter ϵ can be derived from measurements of fluctuations of the emission amplitude (Van Dijk and Wit, 1990). Such measurements yield small values for ϵ, if it is assumed that the emission generator is driven by wide band noise. The possibility that the generator is driven by narrow band noise does, however, also exist; and is even attractive, because it can explain many of the observed properties of fluctuating emission signals (Van Dijk and Wit, 1990). In the latter case, ϵ cannot be derived from amplitude fluctuations but has to be measured in an independent way. Such measurements were done by Talmadge et al. (1990), by studying release from suppression of a SOAE. In this paper, a different, but related measurement will be described.

It is generally accepted that SOAE generators reside inside the inner ear. It is very likely then that these generators are coupled to adjacent similar systems, behaving as active filters (Wit, 1989) or as oscillators. This is the reason why some authors have started to make models for the inner ear that consist of coupled oscillators (Van den Raadt and Duifhuis, 1990) or active filters (Furst, 1990).

Coupling to neighboring systems has been proven to be present (Wit, 1990) and may also influence amplitude and frequency fluctuations of SOAEs. This paper deals with that possibility. Amplitude fluctuations are measured for a SOAE that is coupled to a

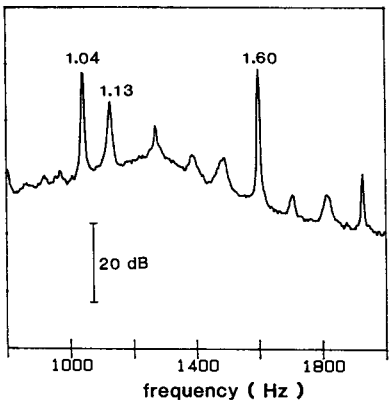

Fig. 1. Long-term (1 min) average spectrum of emission signal from the right ear of subject WK. Frequencies of prominent SOAEs are given in kHz above the spectral peaks.

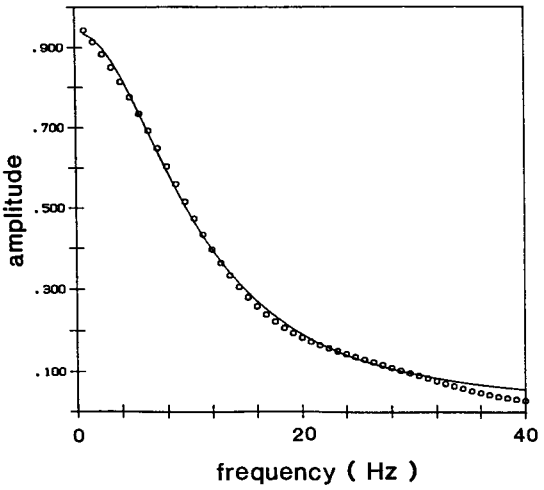

Fig. 2. Measured and smoothed power spectrum (open circles) of envelope of 1.6 kHz emission of subject WK, together with fit to the data points with a Lorentzian (solid line). The (half) width at half maximum of this Lorentzian is 10.0 Hz. The vertical scale has arbitrary units.

neighboring SOAE and for an "isolated" SOAE, and the results are compared.

In order to study the influence of oscillator coupling on amplitude (and frequency) fluctuations, electronic Van der Pol oscillators were built. These oscillators are described, and results obtained with them are given.

Methods and results

Amplitude fluctuations of SOAEs

A long-term (1 min) average spectrum, showing two strong SOAEs for which fluctuations were studied, is shown in Fig. 1. The signal was recorded with a Bruel and Kjaer type 4179 low noise microphone in combination with a Bruel and Kjaer 2660 preamplifier. Procedures for recording and analyses of fluctuations are extensively described elsewhere (Van Dijk and Wit, 1990).

SOAE at 1.60 kHz. The envelope of this SOAE shows fluctuations with low-pass characteristics as shown in Fig. 2. The (half) width of the Lorentzian in this figure is 10.0 Hz. The rms value δA_{rms} for the fluctuation of the amplitude of the SOAE signal was calculated to be: $\delta A_{rms}/A_0 = 0.07$ (A_0 is the average amplitude).

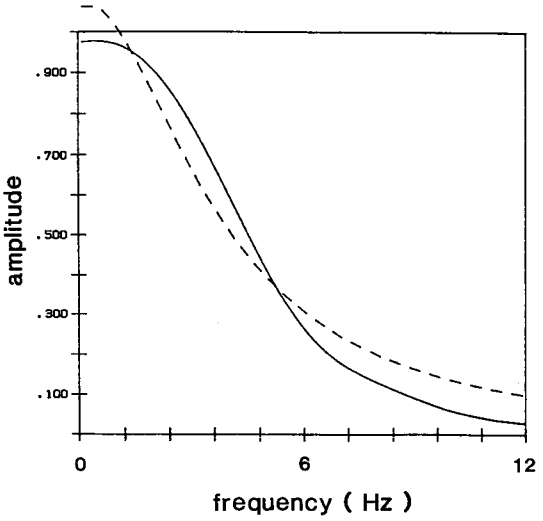

Fig. 3. Measured and smoothed power spectrum (solid line) of envelope of 1.04 kHz emission of subject WK, together with "fit" with a Lorentzian (dashed line). The (half) width at half maximum for the solid line is 5.3 Hz. The vertical scale has arbitrary units.

SOAE at 1.04 kHz. The value for δA_{rms} for this SOAE turned out to be large: $\delta A_{rms}/A_0 = 0.25$. Furthermore, no reasonable fit could be made with a Lorentzian to the SOAE envelope (Fig. 3). The half width of the measured peak in Fig. 3 is 5.3 Hz.

Suppression of 1.6 kHz SOAE

A Van der Pol oscillator can be suppressed by an external tone with a frequency sufficiently far away from the limit cycle frequency of the oscillator (Talmadge et al., 1990). When the amplitude of the suppressing tone is modulated, the amplitude of the oscillator is forced to change also. Talmadge et al. (1990) used square wave modulation to study the relaxation dynamics of SOAEs.

We took a related, but somewhat different, approach: the 1.60 kHz SOAE, shown in Fig. 1, was partly suppressed (4.6 dB below its unsuppressed value) by an externally applied tone of 1.4 kHz. This tone was modulated with 50 Hz low-pass noise (from an HP 3722A noise generator; modulation depth 20%). Correlation between the output signal of the noise generator (= the envelope of the suppressor) and the envelope of the 1.60 kHz SOAE was studied with an Advantest R 9211A two-channel spectrum analyzer. For this purpose, the SOAE was filtered with a Bruel and Kjaer type 1623 tracking filter around 1600 Hz (bandwidth 6%), rectified and

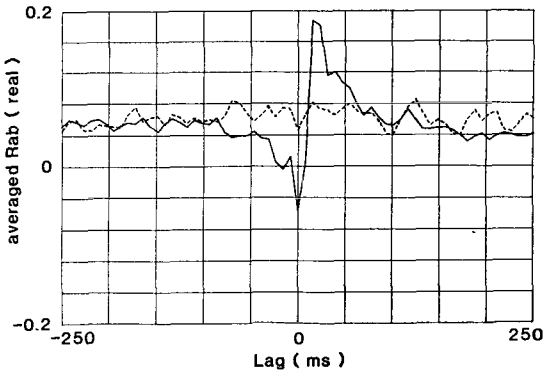

Fig. 4. Cross-correlation function R_{ab} (solid line) for suppressor modulating signal and envelope of 1.6 kHz emission of subject WK, together with the result of a similar measurement in an artificial ear (dashed line). Lag is the time delay between signal *a* (modulator) and signal *b* (emission envelope).

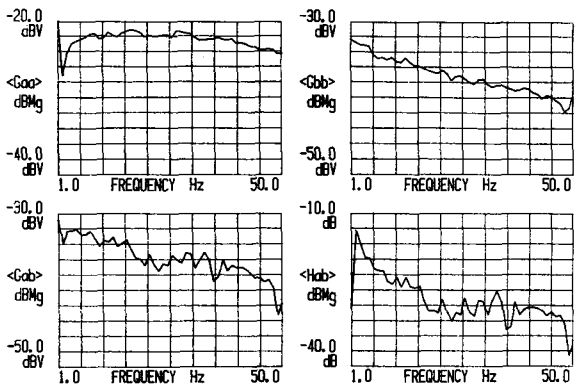

Fig. 5. Results from cross-correlation analysis for suppressor modulating signal (signal *a*) and envelope of 1.6 kHz emission of subject WK (signal *b*). G_{aa}, Averaged power spectrum of signal *a*; G_{bb}, averaged power spectrum of signal *b*. Recording time for *a* and *b*: 200 sec; G_{ab}, averaged cross spectrum (G_{ab}, $S_b \cdot S_a^*$; S_b, Fourier spectrum of signal *b*; S_a^*, complex conjugate of Fourier spectrum of signal *a*); H_{ab}, G_{ab}/G_{aa}.

low-pass filtered (cut-off frequency 50 Hz). The 1.4 kHz component in the microphone signal (generated by the suppressor) was canceled to a large extend by adding the signal from the 1.4 kHz sine wave generator to the microphone signal with proper phase and amplitude.

Fig. 4 gives the cross-correlation function for both envelopes, together with the result of a similar analysis in an artificial ear, in which an "artificial SOAE" of 1.6 kHz was generated for comparison. More information on the correlation between the two signals is given in Fig. 5.

The spectrum analyzer also calculates the impulse response function by inverse Fourier transforming (IFFT) the frequency response function. (The latter function is the ratio of the output Fourier spectrum to the input Fourier spectrum.) The decaying part of the impulse response function, calculated in this way, for the envelope of the 1.60 kHz SOAE is shown in Fig. 6. A computer fit was made to the data points with an exponentially decaying function. The time constant for this function is 34 msec.

Electronic model for Van der Pol-Duffing oscillator

Theory: according to Kirchhoff's first law, the

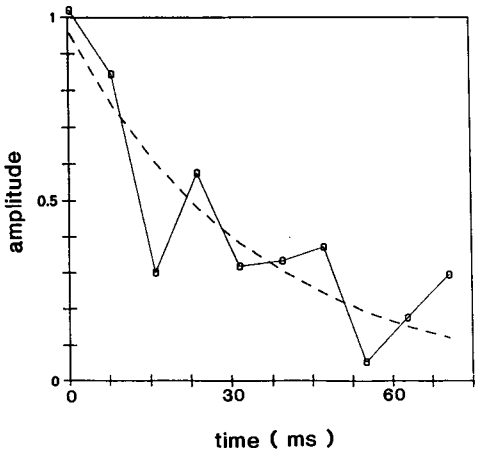

Fig. 6. Decaying part of impulse response obtained from function H_{ab} (Fig. 5) by inverse Fourier transformation (circles), together with fit with exponential function (dashed line), for which the time constant is 34 msec.

sum of currents in Fig. 7 is zero: $i_N + i_C + i_L = 0$. We further assume that the current through the non-linear resistor N can be described by: $i_N = -aV + bV^3$, in which a and b are positive constants. Combining this with the well known relations between current and voltage in C, R and L yields, after some calculation:

$$\ddot{V} + \left(\frac{3bV^2}{C} + \frac{R}{L} - \frac{a}{C}\right)\dot{V} + \frac{1}{LC}(1 + bRV^2)\,V = 0$$

This is the differential equation for a Van der Pol oscillator with non-linear stiffness term (Wit and Van Dijk, 1990).

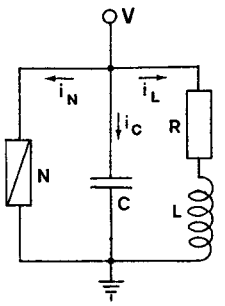

Fig. 7. Schematic of limit-cycle oscillator with non-linear resistance N.

For R = 0, this differential equation reduces to:

$$\ddot{V} + \frac{1}{C}(-a + 3bV^2)\,\dot{V} + \frac{1}{LC}V = 0$$

This is the equation for a Van der Pol oscillator with approximate limit cycle frequency $\omega_0 = (LC)^{-1/2}$ and amplitude $V_0 = 2\left(\frac{a}{3b}\right)^{1/2}$ (Talmadge et al., 1990).

Physical realization of Van der Pol oscillator

As illustrated in Fig. 7, R was taken equal to zero and N was constructed as shown in Fig. 8 (King, 1990). Within a certain range of values of the variable 10k resistor, the circuit behaves as a limit cycle oscillator. By measuring V and V′ simultaneously, the non-linear behavior of N can be studied. A result is given in Fig. 9. Although Fig. 9*b* is not exactly a parabola, the figure shows that the oscillator is a reasonable model for the Van der Pol oscillator. External voltages could be applied to the oscillator through the "external" input (Fig. 8).

In order to study the behavior of coupled oscillators, two oscillators could be coupled through a variable resistor between the "V" outputs.

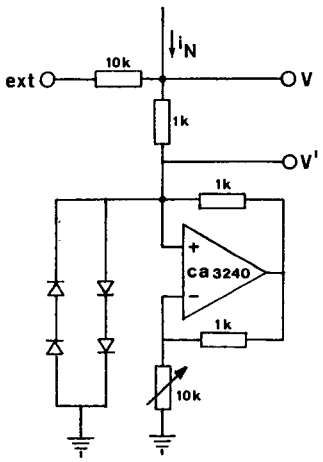

Fig. 8. Schematic of non-linear resistance N (see Fig. 7).

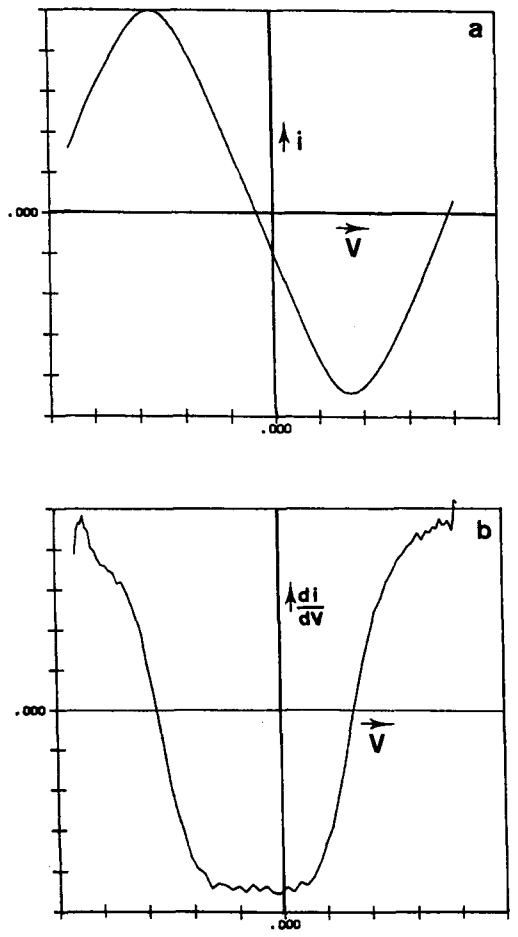

Fig. 9. *a*. Current-voltage characteristics of non-linear resistance N (see Fig. 8). *b*. Differential conductance for N as a function of voltage.

Influence of oscillator coupling on amplitude fluctuations and spectral line width

An electronic Van der Pol oscillator, such as the one described above, with limit cycle frequency $f_0 = 1.2$ kHz, was driven with white noise. This caused the limit cycle amplitude to fluctuate: $A = A_0 + \delta A(t)$.

The δA signal was obtained by rectifying and low-pass filtering the oscillator output signal. An amplitude spectrum of this signal is shown in Fig. 10. The square of it could be fitted well by computer with a Lorentzian with a (half) width of 47 Hz. (This number in itself is not important. It depends on the setting of the variable 10k resistor in the non-linear resistor N but it should be compared to a number that will follow.)

When the oscillator was coupled to a second oscillator (through a resistance of 25 kΩ), its δA increased and amplitude fluctuations occurred more slowly. The second oscillator had a limit cycle frequency of 1.1 kHz and approximately the same amplitude as the first oscillator (when not coupled). It was also driven with white noise that was independent of the noise that drove the first oscillator. In Fig. 10 it is shown that coupling introduces an extra component in the δA signal, giving an increase of $\delta A_{rms}/A_0$ with a factor of 2.3. The square of this extra component could also be fitted well with a Lorentzian of which the (half) width was 6.7 Hz.

The spectral line width of the oscillator increased from 0.36 Hz to 0.67 Hz by coupling it to the second

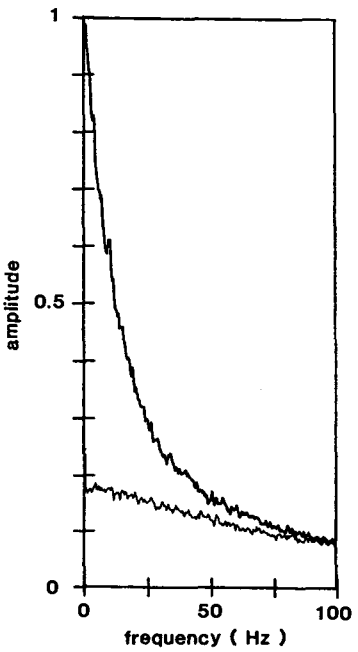

Fig. 10. Amplitude spectrum for envelope of noise-driven electronic Van der Pol oscillator before (thin line, lower curve) and after (thick line, upper curve), coupling to an identical oscillator with different limit-cycle frequency.

oscillator (for measuring method see Wit and Van Dijk, 1990).

Discussion

From the Lorentzian, as shown in Fig. 2, the time constant τ for relaxation of amplitude fluctuations of the SOAE signal can be calculated, using the relation:

$$\tau = \frac{1}{2\pi \cdot \Delta f}$$

in which Δf is the (half) width of the Lorentzian. Because Δf was found to be 10 Hz for the 1.60 kHz SOAE, this gives τ = 16 msec. In order to compare this τ value with that measured for other SOAEs it is convenient to express τ in a number of oscillator cycles: then τ = 26 cycles for the 1.6 kHz SOAE. This number corresponds well with τ values derived from recovery of suppression of SOAEs described by Talmadge et al. (1990). These authors obtained τ = 22 cycles for a 4.30 kHz SOAE and τ = 20 cycles for a 3.45 kHz SOAE.

Many years ago, when studying the fluctuation properties of a rather strong SOAE, we found for this SOAE (at 1.41 kHz) a Δf value of 2.3 Hz. This gives a τ value of 69 msec or 97 cycles (Bialek and Wit, 1984). Some years later, the same SOAE was remeasured by Van Dijk, who found Δf = 3 Hz (subject AS; Van Dijk and Wit, 1990).

The fact that SOAEs seem to require many cycles to recover from amplitude deviations means, in terms of a Van der Pol oscillator description, that the oscillator is "weak". By this we mean the following: in the mathematical description for a Van der Pol oscillator:

$$\ddot{x} + \epsilon (x^2 - 1)\dot{x} + x = 0$$

(this is an oscillator with angular frequency ω = 1 and amplitude A = 2) the amplitude relaxation parameter τ is equal to $(2\pi\epsilon)^{-1}$ cycles. The values, given above for τ for SOAEs mean that ϵ is of the order of 0.01. The consequence of this is that a SOAE behaves as an almost undamped harmonic oscillator ($\ddot{x} + x \approx 0$). In contrast, a Van der Pol oscillator with larger ϵ (e.g., ϵ = 0.1) will behave more "robustly", in the sense that it will return to the limit cycle within a few oscillation cycles after the amplitude deviations. Intuitively, we would think the stronger SOAE's to be the more "robust" ones. (Although larger amplitudes can also be obtained with smaller values for the positive part of the damping term; see Talmadge et al., 1990.) This is in conflict with the very large τ value that we found for the strong 1.41 kHz SOAE of subject AS (corresponding with ϵ = 0.002).

One way to avoid this (supposed) dilemma seems to be the assumption that the noise that causes amplitude fluctuations of SOAEs is not broadband but has a narrow bandwidth equal to the width of the low-pass envelope spectrum (Van Dijk and Wit, 1990). This does explain the small values found for Δf, but it does not explain why similar small Δf values can be derived from the recovery from suppression in the experiment performed by Talmadge et al. (1990). This is preliminarily confirmed by our coherence suppression experiment (Figs. 6–8). From formula (5), given by Talmadge et al. (1990), it can be derived that $\tau_s \approx (a_0/a_s)^2 \cdot \tau_0$; in which τ_0 and a_0 are the time constant and amplitude of the emission in the absence of an external tone, while τ_s and a_s are the corresponding values in the suppressed state. This gives τ_0 = 12 msec (from the measured 4.6 dB amplitude reduction and τ_s = 34 msec), which is in reasonable agreement with the value of 16 msec derived from the Δf measurement.

The results obtained for the 1.04 kHz SOAE described in this paper (Figs. 4 and 5) and the study of the electronic Van der Pol oscillator (Fig. 10) indicate that coupling of a Van der Pol oscillator to (a) neighboring oscillator(s) drastically changes its behavior. Amplitude fluctuations occur more slowly and become larger, and the spectral line width increases. That the 1.04 kHz SOAE is coupled to the neighboring 1.13 kHz SOAE (see Fig. 1) was shown by measurement of the cross-correlation function for the envelopes of the two emission signals (Wit, 1990). Thus, for such "coupled SOAEs", the large

τ (and the broader than predicted spectral peak; Wit and Van Dijk (1990)) can also be explained by assuming that SOAE fluctuations are mainly caused by coupling to neighboring active filters.

It may well be that "isolated" SOAEs, which have no or only weak spectral peaks in their neighborhood, are also influenced by coupling to the environment. This could mean that the single Van der Pol (or a different type of single limit-cycle oscillator) is not a good description for the SOAE generator. This point needs further study.

References

Bialek, W. and Wit, H.P. (1984) Quantum limits to oscillator stability: theory and experiments on acoustic emissions from the human ear. *Physics Lett.*, 104A: 173 – 178.

Furst, M. (1990) Nonlinear transmission line model can predict the statistical properties of spontaneous otoacoustic emissions. In: P. Dallos, C.D. Geisler, J.W. Mathews, M.A. Ruggero and C.R. Steele (Eds.), *The Mechanics and Biophysics of Hearing*, Springer, Berlin pp. 380 – 386.

King, G.P. (1990) Bistable chaos. In: J.P. van der Weele and T.P. Valkering (Eds.), *Nonlinear Dynamics*, University of Twente, Enschede, pp. 11 – 21.

Talmadge, C.L., Long, G.R., Murphy, W.J. and Tubis, A. (1990) Quantitative evaluation of limit-cycle oscillator models of spontaneous otoacoustic emissions. In: P. Dallos, C.D. Geisler, J.W. Mathews, M.A. Ruggero and C.R. Steele (Eds.), *The Mechanics and Biophysics of Hearing*, Springer, Berlin, pp. 235 – 242.

Van den Raadt, M.P.M.G. and Duifhuis, H. (1990) A generalized Van der Pol oscillator cochlea model. In: P. Dallos, C.D. Geisler, J.W. Mathews, M.A. Ruggero and C.R. Steele (Eds.), *The Mechanics and Biophysics of Hearing*, Springer, Berlin, pp. 227 – 234.

Van Dijk, P. and Wit, H.P. (1990) Amplitude and frequency fluctuations of spontaneous otoacoustic emissions. *J. Acoust. Soc. Am.*, 88: 1779 – 1793.

Wit, H.P. (1989) Comment on "A cochlear model for acoustic emissions". *J. Acoust. Soc. Am.*, 85: 2217.

Wit, H.P. (1990) Spontaneous otoacoustic emission generators behave like coupled oscillators. In: P. Dallos, C.D. Geisler, J.W. Mathews, M.A. Ruggero and C.R. Steele (Eds.), *The Mechanisms and Biophysics of Hearing*, Springer, Berlin, pp. 259 – 266.

Wit, H.P. and Van Dijk, P. (1990) Spectral line width of spontaneous otoacoustic emissions. In: F. Grandori, G. Cianfrone and D.T. Kemp (Eds.), *Cochlear Mechanisms and Otoacoustic Emissions*, Karger, Basel, pp. 110 – 116.

J.H.J. Allum, D.J. Allum-Mecklenburg, F.P. Harris and R. Probst
Progress in Brain Research, Vol. 97

CHAPTER 7

Exploration of cochlear function by otoacoustic emissions: relationship to pure-tone audiometry

P. Avan, P. Bonfils[1], D. Loth, M. Teyssou and C. Menguy

Central Service of Biophysics and Nuclear Medicine, Faculty of Medicine Lariboisière, University of Paris, Paris 7 and [1] ENT Services, Hospital Boucicaut and Hospital Robert Debré, Paris, France

The amplitudes, growth functions and detection thresholds of evoked otoacoustic emissions (EOE) were measured in 44 normally hearing subjects and 138 patients with two categories of cochlear dysfunctions: (a) acoustic trauma; and (b) presbycusis. Separate sets of experiments were also performed: (a) detection of stimulus frequency emissions; and (b) click EOE. EOE properties were studied around 2 kHz, 1 kHz and 0.75 kHz (± 0.1 kHz). A partial correlation and multivariate analysis was carried out to investigate the relationships between EOE properties and pure-tone auditory thresholds (from 0.25 to 8 kHz, half-octave steps). For each experiment and each frequency, only one highly significant correlation was found, linearly relating the n kHz EOE threshold with the hearing threshold at 2n kHz: there was a shift of about one octave between EOE amplitudes and audiometric data. This means that EOE thresholds give no direct information about the local cochlear state. A simplified model has been implemented, which assumes that EOE thresholds and amplitudes are proportional to the total number of residual active sites along the organ of Corti, i.e., to the total length of active basilar membrane towards the base of the cochlea. It is shown that this model accounts for the results revealed by the statistical analysis and closely fits the experimental data.

Key words: Cochlear mechanics; Evoked otoacoustic emissions; Stimulus frequency emissions; Audiometry; Acoustic trauma; Presbycusis

Introduction

It is now widely admitted that for the high frequency selectivity of cochlear mechanics to be achieved, normal motile outer hair cells (OHC) are needed. Frequency-selective mechanisms are present in any healthy cochlea and are responsible for its high sensitivity corresponding to normal auditory thresholds. According to the theory of the cochlear amplifier, these mechanisms are highly tuned so that the amplitude of the response to a low-level pure tone is large for only a small number of OHC along a narrow interval on the basilar membrane. Various types of evoked otoacoustic emissions (EOE) are associated with normal electromechanical processes in OHC and are detectable in the outer ear canal (review in Probst et al., 1991). As first proposed by Kemp (1978), they are now widely used as a specific and sensitive non-invasive tool for the diagnosis of cochlear impairment, particularly in the case where no quick objective method is available (e.g., in neonates, Bonfils et al., 1990). The clinical analysis of EOE patterns is binary in most cases, i.e., the presence or absence of a response. Accordingly, subjects are separated into two gross categories, either with normal hearing or with hearing loss $> 20-30$ dB due to OHC impairment. Nevertheless, considering the high frequency selectivity of the underlying mechanisms, the question may be asked whether or not the pattern of the EOE provides reliable information about the local state of the cochlea. The answer might seem obvious in many clinical cases for which some correspondence is found between the shapes of the click-EOE spec-

trum and the pure-tone audiogram (e.g., Kemp et al., 1990). However, it must be kept in mind that the details of how EOE are generated along the cochlea remain unknown. For instance, even the so-called stimulus frequency emissions (SFE), which are elicited by pure tones and should have a simple frequency-specific behavior, appear to originate from contributions along a large fraction of the cochlea (Guinan, 1990).

Several models have been proposed to account for the existence of otoacoustic emissions. Spontaneous emissions are a unique case and are assumed to be produced at frequency f by the activity of a few outer hair cells around the place tuned to f (Gold, 1948; Ruggero et al., 1983; Bialek and Wit, 1984). The situation seems different for other emissions: Gold himself (1988) recalled his early statement that EOE can be generated only because there are inaccuracies in the inner ear system, which result in imperfect cancellation of the contributions of active sites scattered along the cochlea. In some models, changes in the cochlear properties at a place tuned to frequency f are associated with changes in EOE at the same frequency f (e.g., Furst and Lapid, 1988; Zwicker, 1989). A possible interpretation of these results in clinics would be that EOE are fully determined by the local cochlear state. On the contrary, many models, including those quoted above, emphasize that EOE arise from activity distributed along the cochlea (e.g., Wilson, 1980; Strube, 1989), so that there should not be any direct correlation between their properties and purely local cochlear parameters.

The aim of this work was to address these issues by looking for correlations between pure-tone audiometric results and EOE spectral patterns in a large sample of subjects with either normal hearing or various cochlear pathologies. If a "local interpretation" of the previously mentioned models is suitable, then correlations should be found between audiometric threshold and EOE parameters (e.g., amplitude, detection threshold) at the same frequency. Within the framework of global models, the characteristics of an EOE are rather expected to depend on the global residual cochlear function. In the present work, this global function was evaluated by measuring the width of the frequency intervals corresponding to normal or near-normal auditory thresholds.

Materials and methods

Patients and audiometry

Three categories of subjects volunteered for the experiments: 44 were normally hearing young adults, 80 subjects had hearing loss due to presbycusis and 58 had suffered acoustic trauma (due to weapon noise in 82% of cases). In these last two categories, hearing loss was purely of cochlear origin (ascertained from otoscopy, tympanometry, ABR and acoustic reflex studies). Two separate experiments were carried out, E1 for patients with presbycusis and normally hearing subjects, E2 for patients with acoustic trauma. Only the results of one ear per subject were accounted for. In E1, conventional pure-tone audiometry was performed at 0.25, 0.5, 1, 2, 4, 6 and 8 kHz. In E2, additional auditory thresholds at 1.5 and 3 kHz were measured and a Békésy automatic sweep-frequency audiogram was done. This allowed a more precise analysis of auditory losses in these cases where the shape of the audiograms varied much more than those for patients with presbycusis. In addition, for subjects in E2, the widths of two frequency intervals, based upon pure-tone threshold levels, were analyzed from the Békésy audiograms. First, the width of the span of frequencies with thresholds better than 15 dB hearing loss (HL) between 1 and 8 kHz was derived in fractions of an octave. This was designated as Oct_15 (1 kHz). Secondly, a similar analysis was performed for the thresholds better than 30 dB HL: Oct_30 (1 kHz). In the same way, Oct_15 (2 kHz) and Oct_30 (2 kHz) were measured between 2 and 8 kHz. Fig. 1*a* shows a typical example of these measurements. The mean audiograms of subjects are represented in Fig. 1*b*.

Experiment E1: click-evoked otoacoustic emissions

Click-EOE were recorded using a custom-built system (Bonfils et al., 1990). Click-EOE frequency spectra were obtained for stimulus intensities

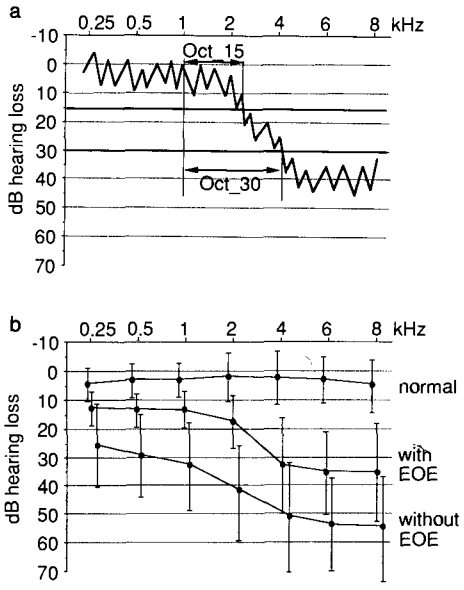

Fig. 1. (*a*) Békésy sweep-frequency audiogram for one subject. Two different limits (i.e., hearing loss of either 15 or 30 dB) were used for evaluating the length of "residual active" cochlea between 1 and 8 kHz. For each choice, the width was measured in octaves (i.e., Oct – 15 and Oct – 30). In this case, Oct – 15 (1 kHz) would be one octave and Oct – 30 (1 kHz) would be two octaves. (*b*) Mean pure-tone audiograms (± 1 S.D.) for the three groups of subjects, i.e., 44 ears with normal hearing and 138 ears with pathology, either with or without detectable EOE.

decreasing in 5 dB steps from 40 dB HL (0 dB HL = average subjective hearing threshold to clicks for normally hearing subjects, i.e., 45 dB peak eq. SPL) to detection threshold of the last visually detectable EOE. Only this last detectable click-EOE was studied. In most cases, the dominant frequency of this response was close to 1 kHz (in 85% of cases, in the range of 0.78 – 1.5 kHz; in 44% of cases, between 0.94 and 1.15 kHz).

Experiment E2: click-evoked and stimulus frequency otoacoustic emissions

Click-EOE were obtained using an ILO88 Otodynamics analyser. The frequency spectra of these EOE were obtained in the same way as for E1, using the linear mode. The detection threshold was measured for the EOE closest to 1 kHz (± 0.1 kHz). All the data files were stored and could be reanalyzed later so that the detection thresholds of the EOE closest to 0.75 and 2 kHz (± 0.1 kHz) could also be measured. This allowed a more complete analysis of EOE patterns than for E1. Stimulus frequency emissions (SFE) were derived from Nyquist plots obtained from a 10 dB SPL pure-tone slowly swept in frequency between 0.7 and 2 kHz (see method in Avan et al., 1991a). The amplitudes of the SFE closest to 0.75 and 1 kHz were measured. (At 2 kHz, the accuracy of measurements was lower, and these SFE were not taken into account.)

In E1 and E2, click-EOE growth functions were plotted and their characteristics were determined. These functions were found to be linear with a slope close to 1 at low click levels, and were non-linear at higher levels. The detection threshold was defined in dB HL as the lowest click intensity eliciting a visually detectable EOE at the chosen frequency (the accuracy of this measurement was 5 dB). The background noise level was kept constant and as low as possible for every patient (i.e., – 30 dB SPL/50 Hz band around 1 kHz). In this way, the detection level of an EOE did not depend on external factors and was characteristic of its behavior in the linear part of its growth function. For 33/80 subjects with presbycusis (41%, group "without EOE" in Fig. 1*b*) and 5/58 (8.6%) subjects with acoustic trauma, there were no detectable click-EOE. The detection thresholds for these subjects was arbitrarily set at 40 dB HL. For E2, SFE measurements directly provided the ratios SFE-amplitude/level of eliciting stimulus. When the amplitudes of SFE and background noise became equal as the level of the eliciting stimulus was decreasing, the SFE detection threshold was defined as the corresponding stimulus level. Then the same analysis as for click EOE was carried out.

Statistical analysis of the data

For every EOE frequency (i.e., 1 kHz in E1, 0.75, 1 and 2 kHz in E2), general correlations between EOE threshold and all pure-tone auditory thresholds were computed. A partial correlation analysis with stepwise regression was then performed. For patients in E2 who had acoustic trauma, a further

analysis was carried out to study the relation of EOE detection threshold to Oct_15 (or Oct_30). All statistical computations were done with BMDP (Dixon et al., 1985) or Statview® statistical packages.

Results

The mean EOE detection threshold at 1 kHz was about 5 dB HL (standard deviation 6 dB) for normally hearing subjects, 16.7 dB HL for the group of subjects with presbycusis, and 14.4 dB HL for the group of subjects with acoustic trauma who had detectable EOE. As described previously by Avan et al. (1991a), general correlation studies demonstrate strong correlations between all possible pairs of pure-tone auditory thresholds, 1 and 2, 2 and 3, 3 and 4, 1 and 4 kHz, etc. In this study, the shape of the audiograms was generally typical of a high-frequency hearing loss, and auditory thresholds were far from being independent variables. Because of this, an analysis that would be restricted to simple correlations or to shape comparisons between EOE patterns and audiograms cannot be considered as valid. Therefore, a partial correlation analysis (stepwise regression) had to be carried out.

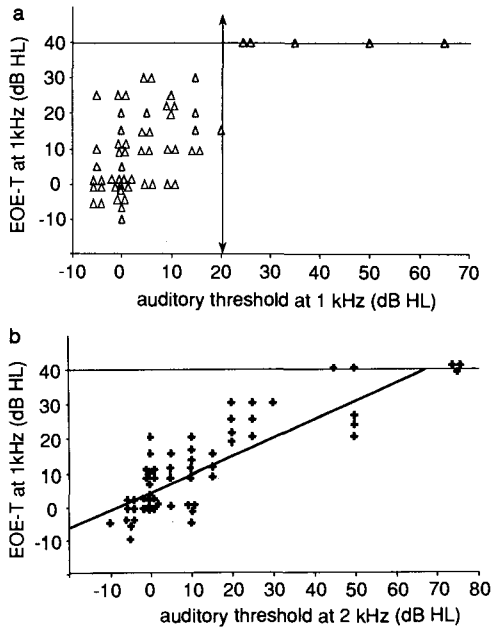

Fig. 2. (*a*) Scatterplot of EOE thresholds (in dB HL) at 1 kHz vs. auditory threshold at the same frequency (58 patients of E2, i.e., with acoustic trauma). The arrow designates the limit of auditory threshold below which 1 kHz EOE are always detectable. (*b*) According to the statistical analysis, only the correlation between 1 kHz EOE threshold and 2 kHz auditory threshold was significant. For five patients without any detectable EOE around 1 kHz, the EOE detection threshold was arbitrarily set at 40 dB HL, which was the highest stimulus used to elicit responses.

In both experiments E1 and E2, the correlation between the 1 kHz EOE threshold and the 1 kHz auditory threshold was not significant (see Fig. 2*a* for E2). The scatterplot of EOE threshold vs. auditory threshold could be separated into two parts (arrow in Fig. 2*a*): for a hearing loss > 20 dB, EOE were never detectable (arbitrary detection threshold fixed at 40 dB HL). For normal or near-normal auditory thresholds (≤ 20 dB HL), EOE thresholds were nearly independent of hearing loss. This confirms that regardless of EOE amplitude, the only relationship between EOE and auditory threshold at a given frequency is binary. Actually, only one significant correlation was found, linearly relating the 1 kHz EOE threshold (1k-EOE-T) and the 2 kHz auditory threshold (2k-T) (see Fig. 2*b*, again for E2):

$$\text{E1 : 1 k-EOE-T} = 0.59 \times \text{2k-T} + 5.5 \text{ (dB HL)}, \quad R^2 = 0.60 \qquad (1)$$

$$\text{E2: 1k-EOE-T} = 0.50 \times \text{2k-T} + 6.7 \text{ (dB HL)}, \quad R^2 = 0.75 \qquad (2)$$

Moreover, similar results were found at 0.75 kHz and 2 kHz for patients in E2:

$$\text{E2: 0.75k-EOE-T} = 0.41 \times \text{1.5k-T} + 9.5 \text{ (dB HL)}, \quad R^2 = 0.65 \qquad (3)$$

$$\text{E2: 2k-EOE-T} = 0.38 \times \text{4k-T} + 11.4 \text{ (dB HL)}, \quad R^2 = 0.51 \qquad (4)$$

These relations were all highly significant ($P < 0.001$). Therefore, there was a large shift between EOE and auditory threshold properties, i.e., more

than 1/2 octave since auditory thresholds were sampled at 1/2-octave intervals. The regressions did not depend on the pathology. Nearly identical regressions were obtained for SFE at 0.75 and 1 kHz (E2).

The data obtained from E2 were re-analyzed using the previously defined variables Oct_15 and Oct_30, measured at 1 and 2 kHz. Considering that EOE thresholds are defined in dB and thus are on a logarithmic scale, the derived variables log[Oct_15] and log[Oct_30] were used. In this way, a linear relationship between EOE-T (in dB) and log[Oct_15] would correspond to a linear relationship between EOE amplitude (in linear units, e.g., Pascal) and Oct_15. Data from subjects without detectable EOE were not taken into account. Thus 53 of 58 cases at 1 kHz and 30 of 58 at 2 kHz were evaluated. A highly significant linear regression was found relating EOE thresholds at 1 and 2 kHz with log[Oct_15(1 kHz)] and log[Oct_15(2 kHz)] (Fig. 3*a*):

$$\text{1k-EOE-T} = -26 \times \log[\text{Oct\_15(1 kHz)}] + 12.7,\ R^2 = 0.68 \quad (5)$$

$$\text{2k-EOE-T} = -19 \times \log[\text{Oct\_15(2 kHz)}] + 19,\ R^2 = 0.50 \quad (6)$$

The slopes of the regression lines corresponded to an increase of about 6 dB of the mean EOE threshold each time the width of the interval corresponding to a normal basal cochlea was divided by two. The relations between EOE-T and log[Oct_30] were less significant and the slope was steeper (e.g., Fig. 3*b* for 1 kHz).

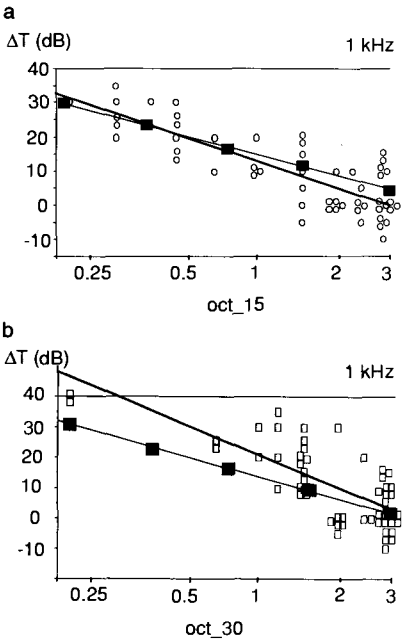

Fig. 3. (*a*) For the patients of E2, the correlation between 1 kHz EOE threshold elevation (ΔT) and width of residual basal cochlea (Oct_15, number of octaves with hearing threshold better than 15 dB HL above 1 kHz) is highly significant and the corresponding linear regression (heavy line) fits the proposed model (thin line, closed squares). The number of data points on this diagram is 53, and the value of Oct_15 was 0 for the five remaining ears without detectable EOE. (*b*) The correlation is not as high when the limit between "active" and "passive" cochlea is set at 30 dB HL (Oct_30).

Discussion

These results suggest that the relationships between EOE detection threshold at a given frequency and the results of tonal audiometry clearly arise from inner ear properties. Because the EOE frequency was fixed in each series of data and every patient had a normal transmission mechanism, the middle ear transfer function did not have to be accounted for and did not play any role in these relationships. In E2, it was always possible to find a detectable EOE at 0.75, 1 and 2 kHz (within 0.1 kHz), except of course when the hearing losses were too great. In E1, the threshold of the EOE was nearly always obtained at a frequency ~ 1 kHz.

The first part of the statistical analysis contradicted the interpretation of local sources for EOE generation, which assumes that EOE properties at a given frequency are fully determined by the cochlear properties at the corresponding place. Several hypotheses may account for this non-local behavior.

First, it is probable that OHC damage at a given place of the cochlea has to be extensive to give rise to significant hearing loss and that increase in audi-

tory threshold is not the most accurate possible measure of cochlear damage (e.g., LePage, 1991). It may be asked whether or not EOE would give a more quantitative evaluation of OHC function than do auditory thresholds and would therefore allow an earlier detection of cochlear dysfunction. Following this hypothesis, no correlation would be expected between EOE and auditory threshold at the same frequency, at least for subjects with a near-normal audiogram. However, the presence of correlations between n kHz-EOE and 2n kHz auditory thresholds, and the relations between EOE thresholds and the total length of residual normal basal cochlea do not substantiate this hypothesis.

These last results rather suggest a second hypothesis, based on the assumption that EOE amplitudes and detection thresholds are not frequency-specific parameters but depend on the function of the whole cochlea between the base and the point with characteristic frequency corresponding to the EOE, i.e., all along the Békésy traveling wave. The apical part of the cochlea cannot contribute to the EOE because it is beyond the cut-off of the traveling wave. An alternative way of stating this hypothesis is to point out that EOE must be generated and then propagated along the basal cochlea before being detected in the ear canal. Even if basal OHC are out of resonance with respect to the frequency of an EOE and cannot efficiently amplify it, their contributions can play an important role in the propagation of the EOE even if the amplitudes of basal OHC responses are small, provided their phases are appropriate.

Many EOE models rely upon such hypotheses. After Gold (1948, 1988), Wilson proposed that EOE arise from imperfect cancellation between responses originating from various places of the organ of Corti (Wilson, 1980; Sutton and Wilson, 1983). EOE might also come from stationary waves along the cochlea due to impedance mismatches (e.g., Kemp, 1986). Inhomogeneities of basilar membrane parameters might give rise to scattering of waves and production of long-delay EOE with a broad spectrum (Manley, 1983; Strube, 1989). (For a detailed review of the numerous models of cochlear mechanics, see Inselberg, 1978, who showed how accounting for the various parameters of the inner ear could deeply influence the resulting models.)

A more complete analysis of these mechanisms was proposed by Zwicker, who used a hardware model in which simulations of various changes in local active mechanisms could be performed (reviewed in Zwicker, 1989). He showed that ripples appear in the amplitude/phase pattern of the traveling wave of a pure tone along the basilar membrane when coupling is introduced between neighboring sections of the model to account for active mechanisms. These ripples are associated with an emission at the oval window. They are strongly enhanced at the evoking frequency when active mechanisms are cut off just at the place tuned to the pure tone. This observation might suggest that EOE properties are influenced by the local cochlear state. However, such models can also be considered from a global point of view. Several authors have proposed that the gain of active mechanisms along the cochlea is not constant but varies in a more or less periodic way (Manley, 1983; Zwicker, 1986; Strube, 1989). Such a lattice of impedance discontinuities may give rise to back-scattering of the wave corresponding to a pure tone. If the wavelength of the excitation (depending on its frequency) is such that all scattered waves are in phase, then the resulting constructive interference would be associated with a strong EOE. This EOE could be considered as resulting from scattering from numerous active sites along the basal cochlea, i.e., one site each time the phase changes by 180° (Zwicker, 1989).

The simplest way of taking these global models into account is to assume that EOE amplitudes are just proportional to the total number of residual active sites along the organ of Corti, i.e., to the total length of active basilar membrane. Every active site is therefore supposed to contribute with the same weight, and such a model can be described as "cochlear democracy".

It is well known that the coding of frequencies along the basilar membrane is logarithmic (reviewed in Dancer, 1988), thus the number of EOE-generating sites per octave should be constant. For instance, let us consider the case of a 1 kHz EOE. There are

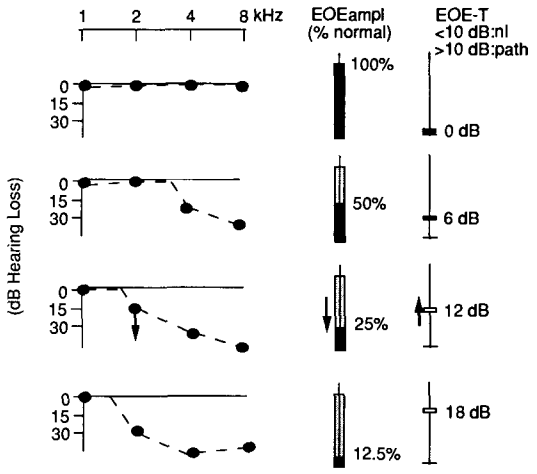

Fig. 4. Relationship between the amplitude of an EOE at 1 kHz (EOE amplitude, linear scale), the detection threshold of this EOE (EOE-T, rightmost bars, dB scale) and the pure-tone audiogram from 1 to 8 kHz (thresholds = closed circles) according to the proposed model applied to several degrees of hearing loss. The development of EOE detection threshold and auditory threshold at 2 kHz is parallel because the change of EOE-T becomes clearly detectable (arrow, rightmost bar) only when the 2 kHz auditory threshold begins to change (leftmost arrow), that is, when the cut-off frequency on the audiogram is just below 2 kHz. This was previously suggested by the multiple regression analysis as illustrated in Fig. 2*b*. Despite this finding, the presence or absence of an EOE at 1 kHz remains correlated with the auditory threshold at 1 kHz.

three normally functioning octaves between 1 and 8 kHz in a normal cochlea, and the resulting EOE amplitude would be normal (100%). Its detection threshold T would also be normal. Now suppose that 50% of the active sites are impaired, so that there is an auditory loss above 3 kHz. The amplitude of the EOE is reduced by 50%, and to make up for that decrease, there must be a 6 dB increase of the evoking stimulus (ΔT = 6 dB). This corresponds exactly to the slope of the plot of EOE threshold vs. log[Oct _ 15] represented in Fig. 3. It should be noticed that, although the cochlear impairment is already large, the increase in detection threshold is nearly negligible because it is of the order of the standard deviation in a normal population. It could be detected only if a record in the same ear was available before its impairment.

If 50% of the remaining active sites again were destroyed, then the EOE amplitude would now be 25% of its initial value, and there would be a 12 dB increase in EOE threshold, which is now noticeable. In correlation, the 2 kHz auditory threshold would begin to increase. Fig. 4 illustrates the parallel evolution of the 1 kHz EOE and the 2 kHz auditory threshold (indicated by the arrows). The full computation derived from the model gives the following result:

$$\Delta T\ (\text{dB}) = 20 \times \log\ [\log\ (fc/f_0)/(\log\ 8/f_0)] \quad (7)$$

where f_0 (in kHz) is the EOE frequency and fc is the highest frequency with a normal auditory threshold. It is easy to check that the slope of the curve representing ΔT vs. fc sharply changes when fc = 4 kHz for a 2 kHz EOE, or when fc = 2 kHz for a 1 kHz EOE, or when fc = 1.5 kHz for a 0.75 kHz EOE.

Therefore, the most straightforward interpretation of EOE threshold variations is based on their dependence versus Oct _ 15. Correlations between EOE and auditory thresholds are only indirect. However, clear results can be drawn from this last study because many audiograms corresponding to sensorineural hearing loss have similar shapes with progressive involvement of the lower frequencies. For these audiograms, the correlation between EOE and auditory thresholds at 1 kHz does not exist because this EOE has disappeared when the auditory threshold begins to increase at 1 kHz. The correlations between 1 kHz EOE threshold and 3, 4, 6 or 8 kHz auditory thresholds do not exist because this EOE is not significantly altered as long as the auditory threshold at 2 kHz remains normal. Only the 2 kHz auditory threshold really "influences" the amplitude of EOE at 1 kHz because the evolution of the two is parallel. However, it must be emphasized that, even in this global model illustrated in Fig. 4, a clear relation does exist between presence or absence of an EOE at frequency f (regardless of its detection threshold) and auditory threshold at f. This is not in contradiction with several clinical studies (Kemp et al., 1990).

Hence, the model proposed here of "cochlear democracy" accounts very well for the results disclosed by both types of statistical analyses. The second analysis, which is based on Fig. 3, also clearly shows that the limit between the active and impaired "passive" cochlea corresponds to a 15 dB rather than a 30 dB HL hearing loss.

Evoked otoacoustic emissions appear to arise from phenomena that are widely distributed along the basilar membrane. Even if EOE are locally generated, in relation to the state and probably the motility of OHC, they need a good basal cochlear state to propagate back to the oval window. Recent work performed on tone-burst evoked emissions in the guinea pig has described similar results when measuring EOE amplitude changes after acoustic overstimulation (Avan et al., 1991b); the amplitude changes of an emission actually depend on the amount of TTS along the whole basal cochlea. One clinical application of EOE that is now widely used is for infant screening (e.g., Bonfils et al., 1990). Because EOE detection gives a global evaluation of the active cochlear mechanisms, this application seems fully justified. In contrast, for early screening of noise-induced hearing loss, some EOE characteristics, such as their amplitude and detection threshold, are only sensitive to cochlear alterations that are already large, which would not allow a follow-up of the early stages of cochlear dysfunction.[1]

Acknowledgements

Work supported by the French "Ministère de l'Environnement", Grant 89090, Sretie-, the "Fonds d'étude du corps médical des hôpitaux de Paris" and the "Fondation de France". The authors would also like to thank Dr. F. Harris and Dr. R. Probst (University ORL clinic, Basel) for several discussions and editorial suggestions.

[1] For long-term monitoring of the action of ototoxic drugs, the situation is different in theory because EOE records can be obtained before treatment. Click EOE and SFE are generally not detectable at 8 kHz, but their lower frequency components (4 kHz for instance) should be sensitive to early hearing losses above 8 kHz. However, the sensitivity of high-frequency audiometry is expected to be higher even in such a case (e.g., Dreschler et al., 1985).

References

Avan, P., Bonfils, P., Loth, D., Narcy, P. and Trotoux, J. (1991a) Quantitative assessment of human cochlear function by evoked otoacoustic emissions. *Hear. Res.*, 52: 99 – 112.

Avan, P., Loth, D., Menguy, C. and Teyssou, M. (1991b) Frequency dependence of changes in guinea-pig cochlear emissions after acoustic overstimulation. *J. Acoustique*, 4: 91 – 94.

Bialek, W. and Wit, H.P. (1984) Quantum limits to oscillator stability: theory and experiments on acoustic emissions from the human ear. *Physics Lett.*, 104A: 173 – 178.

Bonfils, P., Dumont, A., Marie, P., François, M. and Narcy, P. (1990) Evoked otoacoustic emissions in newborn hearing screening. *Laryngoscope*, 100: 186 – 189.

Dancer, A. (1988) Biomécanique de l'audition. In: *Physiologie de la Cochlée*, INSERM, Paris, pp. 27 – 73.

Dixon, W.J., Brown, M.B., Engelman, L., Frane, J.W., Jennrich, R.I. and Toporek, J.D. (1985) *BMDP Statistical Software*, Berkeley University of California Press, Berkeley, CA.

Dreschler, W.A. , van der Hulst, R.J., Tange, R.A. and Urbanus, N.A. (1985) The role of high-frequency audiometry in early detection of ototoxicity. *Audiology*, 24: 387 – 395.

Furst, M. and Lapid, M. (1988) A cochlear model for acoustic emissions. *J. Acoust. Soc. Am.*, 84: 222 – 229.

Gold, T. (1948) Hearing II. The physical basis of the action of the cochlea. *Proc. R. Soc. Lond. (Biol.)*, 135: 492 – 498.

Gold, T. (1988) Historical background to the proposal, 40 years ago, of an active model for cochlear frequency analysis. In: J.P. Wilson and D.T. Kemp (Eds.), *Cochlear Mechanisms, Structures, Functions and Models*, Plenum, New York, London, pp. 299 – 305.

Guinan Jr., J.J. (1990) Changes in stimulus frequency otoacoustic emissions produced by two-tone suppression and efferent stimulation in cats. In: P. Dallos, C.D. Geisler, J.W. Matthews and C.R. Steele (Eds.), *Mechanics and Biophysics of Hearing*, Springer, Berlin, pp. 170 – 177.

Inselberg, A. (1978) Cochlear dynamics: the evolution of a mathematical model. *SIAM Rev.*, 20: 301 – 351.

Kemp, D.T. (1978) Stimulated acoustic emissions from within the human auditory system. *J. Acoust. Soc. Am.*, 64: 1386 – 1391.

Kemp, D.T. (1986) Otoacoustic emissions, travelling waves and cochlear mechanics. *Hear. Res.*, 22: 95 – 104.

Kemp, D.T., Ryan, S. and Bray, P. (1990) A guide to the effective use of otoacoustic emissions. *Ear Hear.*, 11: 93 – 105.

LePage, E.L. (1991) Hysteresis in cochlear mechanics and a model for variability in noise-induced hearing loss. In: A. Dancer, D. Henderson, R.J. Salvi and R.P. Hamernik (Eds.), *Fourth International Conference on the Effects of Noise on*

the Auditory System, Beaune, Mosby Year Book, St-Louis, MO, pp. 106 – 115.

Manley, G. (1983) Frequency spacing of acoustic emissions: a possible explanation. In: W.R. Webster and L.M. Aitkin (Eds.), *Mechanisms of Hearing,* Monash University Press, Clayton, Vic., pp. 36 – 39.

Probst, R., Lonsbury-Martin, B.L. and Martin, G.K. (1991) A review of otoacoustic emissions. *J. Acoust. Soc. Am.*, 89: 2027 – 2067.

Ruggero, M.A., Rich, N.C. and Freyman, R. (1983) Spontaneous and impulsively evoked otoacoustic emissions: indications of cochlear pathology. *Hear. Res.,* 10: 283 – 300.

Strube, H.W. (1989) Evoked otoacoustic emissions as cochlear Bragg reflections. *Hear. Res.,* 38: 35 – 46.

Sutton, G.J. and Wilson, J.P. (1983) Modelling cochlear echoes: the influence of irregularities in frequency mapping on summed cochlear activity. In: E. de Boer and M.A. Viergever (Eds.), *Mechanisms of Hearing,* Delft University Press, Delft, pp. 83 – 90.

Wilson, J.P. (1980) Model of cochlear function and acoustic re-emission. In: G. van den Brink and F.A. Bilsen (Eds.), *Psychophysical, Physiological and Behavioural Studies in Hearing,* Delft University Press, Delft, pp. 72 – 73.

Zwicker, E. (1986) A hardware cochlear nonlinear preprocessing model with active feedback. *J. Acoust. Soc. Am.,* 80: 154 – 162.

Zwicker, E. (1989) Otoacoustic emissions and cochlear travelling waves. In: J.P. Wilson and D.T. Kemp (Eds.), *Cochlear Mechanisms, Structures, Function and Models,* Plenum, New York, London, pp. 359 – 366.

J.H.J. Allum, D.J. Allum-Mecklenburg, F.P. Harris and R. Probst
Progress in Brain Research, Vol. 97

CHAPTER 8

Distortion-product otoacoustic emissions in normal and impaired ears: insight into generation processes

Brenda L. Lonsbury-Martin, Martin L. Whitehead and Glen K. Martin

Department of Otolaryngology, University of Miami Ear Institute, Miami, FL 33101, U.S.A.,

Otoacoustic emissions can be used to study cochlear function in an objective, non-invasive and rapid manner. These and other desirable features of emissions have inspired a significant amount of investigation into the practicalities of utilizing evoked emissions as clinical tests of hearing. Variables which affect the measurement of emissions can be sorted into two major categories consisting of factors affecting either emission generation or expression. The present report consolidates and summarizes recent findings of a series of experiments in our laboratory which address both the generation and expression of transiently evoked and distortion-product otoacoustic emissions. Because these two emission types have the greatest promise of becoming clinically useful, a complete understanding of the factors responsible for their measured properties is particularly important.

Key words: Transiently evoked otoacoustic emissions; Distortion-product otoacoustic emissions; Middle ear dysfunction; Acoustic reflex; Ethacrynic acid; Gentamicin; Lethal anoxia; Aspirin

Introduction

Since their discovery by Kemp (1978) over a decade ago, the potential role of otoacoustic emissions (OAEs) as an objective diagnostic tool in the clinical examination of hearing has been supported by the findings of numerous studies. After the initial investigations which described the basic features of a variety of OAEs in humans (Kemp, 1978, 1979; Kemp and Chum, 1980), further basic work in a wide range of laboratory animals was aimed at increasing our understanding of the generation of OAEs in experimental models of impaired hearing conditions. Knowledge about the properties of OAEs measured in noise-damaged (e.g., Zurek et al., 1982), ototoxic (e.g., Anderson, 1980), hydropic (e.g., Martin et al., 1989), and hypoxic (e.g., Zwicker and Manley, 1981) and anoxic (e.g., Kim et al., 1980) animals further supported the notion that emissions would be useful as objective indicators of the functional status of the organ of Corti's outer hair cells (OHCs), which are the most prevalent and vulnerable sensory cells of the cochlea.

Based on this initial knowledge of OAEs, an increasing number of reports have focused on systematically describing the effects of known otopathologies on the different kinds of emissions exhibited by the human ear. From such information, it is becoming increasingly clear that two types of evoked emissions, the transiently evoked (TEOAE) and the distortion-product otoacoustic emissions (DPOAEs), are the most promising clinically. Also apparent from the increasing amounts of data on human and animal emissions is the recognition that the ability to measure OAEs depends on the contributions of several classes of variables. These crucial sets of contributing factors can be generally described as those related either to the generation of OAEs within the cochlea, or to the final expression of emissions in the external ear canal. Theoretically,

it would be ideal if each variable known to modify the measured properties of emissions could be simply classified into one of these two categories. However, previous findings indicate that assigning these influences to such unequivocal classes is not always justifiable. For example, it is well-recognized that the ability to measure OAEs is considerably affected by such innate biases as gender and age. Thus, determining whether the observation that more women exhibit spontaneous otoacoustic emissions (SOAEs) than do men (Bilger et al., 1990), or that the amplitudes of DPOAEs are larger in younger than in older individuals (e.g., Lonsbury-Martin et al., 1991a) is dependent only on generation or expression processes, is irresolvable based on our current understanding of the fundamental bases of emissions.

However, other variables can be more clearly distinguished as affecting either the generation or expression of OAEs. For example, it is well-recognized that the expression of emissions is influenced by the functional capability of accessory structures, such as the middle ear ossicles or tympanic membrane, to transmit the emitted responses from the cochlea to the outer ear canal. Other factors, such as those governing the production of emissions, obviously conform more clearly to the generation category. Of particular interest with respect to this class of variables are issues concerning the fundamental mechanisms which produce OAEs at the subcellular level, whether these processes are similar in humans and animals, and the proportion of OAE amplitude attributable to active (OHC or micromechanical) versus passive (basilar membrane or macromechanical) generators.

The major purpose of this report is to review results from on-going work in our laboratory which are relevant to furthering our understanding of the variables which influence the measurement of OAEs. To illustrate the significance of the contributions made by conduction factors on the magnitude of OAEs, the effects of middle ear effusion in children and activation of the acoustic reflex in rabbits will be described. Of the research strategies that are available for investigating the underlying generators of OAEs, one approach involves defining the restrictions that systematic variations in stimulus parameters impose upon emission amplitude. Using this strategy, findings are presently accumulating which support the notion that human and animal DPOAEs exhibit distinct features from one another. These results suggest that this emission may have one or more sources of generation within the cochlea. Another method involves manipulating the chemical environment of the cochlea by using ototoxic agents known to diminish cochlear function reversibly or irreversibly to determine the organ of Corti elements which contribute to the production of emissions. Based on this experimental strategy, initial results support the notion that some aspects of TEOAE and DPOAE generator properties are unique to each emission type. Further evidence suggests that the production of DPOAEs, in particular, may be more complex than can be explained on the basis of a simple separation of contributing processes into either active or passive generators.

Methods

The findings presented below have resulted from an ongoing program of research. The aim of this research has been to study the fundamental features of OAEs so that techniques established in experimental settings can be adapted for clinical tests of cochlear function. For the data presented below, the test protocols differed somewhat for either humans or experimental animals; however, several features of the studies were similar. First, although monkeys were always studied while lightly anesthetized, both human and rabbit subjects were examined while awake, unless noted otherwise. Secondly, for DPOAEs, which were tested in both primate species and rabbits, two measurement forms were utilized. One involved a series of amplitude/growth or input/output (I/O) functions, which describe DPOAE amplitudes at discrete frequencies as a function of progressive increases in stimulus level. The other, referred to as the DPOAE "audiogram," plots emission amplitudes in response to

equilevel ($L_1 = L_2$) primaries at a fixed level of stimulation as a function of stimulus frequency. Finally, all emission types in monkeys and humans were measured using identical techniques.

Subjects

Animal subjects were either adolescent (3-months old), pigmented, female rabbits of the New Zealand strain, or were female macaque (*Macaca nemestrina*) monkeys ranging in age from 7 to 15 years. Both species were obtained from commercial suppliers. Human subjects were either children exhibiting some form of hearing impairment, who were seen as patients in an otolaryngology clinic situated in a typical academic setting, or were normally hearing adults, who were recruited according to routine institutional guidelines.

Otoacoustic emissions testing

For measuring DPOAEs, a personal microcomputer-based system (Macintosh IIci) controlled both the stimulus generation and response detection instrumentation. Stimuli typically consisted of two equilevel pure-tone signals at f_1 and f_2 (f_2/f_1 = 1.21 (human/monkey); 1.25 (rabbit)) presented concurrently to the external ear canal. The DPOAE findings are presented with respect to the geometric mean of the primary tones (i.e., $(f_1 \times f_2)^{1/2}$), because previous experimental work in humans and animals has established that this cochlear place is the major generation site for $2f_1$-f_2 emissions (Brown and Kemp, 1984; Martin et al., 1987).

Distortion-product "audiograms" were constructed from emissions obtained in 10 steps per octave (human/monkey), or at 200 Hz intervals (rabbit), from 0.7 to 8 (human/monkey) or from 1 to 16 kHz (rabbit), at three stimulus levels (human/monkey: 65, 75, 85 dB SPL; rabbit: 45, 55, 65 dB SPL). The I/O functions, obtained at a number of discrete frequencies (human/monkey: 1, 2, 3, 4, 6, 8 kHz; rabbit: at half-octave intervals between 1 and 16 kHz), were elicited by varying the levels of the primary stimuli in 5 dB steps, decreasing from 85 to 25 dB SPL (human/monkey), or from 75 dB SPL to the level of the recording system's noise floor (rabbit). An emission was considered to be detectable if its amplitude was > 3 dB above the level of the corresponding noise floor, measured simultaneously at a frequency 50 Hz above that of the DPOAE. Calibration of the acoustic system and speculum/microphone assembly was accomplished according to the substitution procedures described by Lonsbury-Martin et al. (1987) for rabbits and by Harris et al. (1989) for humans. The TEOAEs were measured in both humans and monkeys using a commercial system (Otodynamics Ltd., ILO88) operated in the default (non-linear click) mode (Bray and Kemp, 1987). The human and non-human primates were also screened for SOAEs using previously described techniques (Martin et al., 1985; Lonsbury-Martin et al., 1990).

General experimental protocol

For both normally hearing human subjects and patients, otoacoustic emissions were examined as described above following a routine audiologic assessment of pure tone (air and bone) thresholds, speech-understanding capability, tympanometry and acoustic reflex thresholds. In addition, some normally hearing human subjects, along with some rabbits, were tested using varying f_1 and f_2 levels ($L_1 \neq L_2$).

For the drug-injection experiments in anesthetized rabbits and monkeys, a given experimental session began with the acquisition of baseline measures for all recordable emissions. For monkeys, if these determinations were within the previously established normal limits of their individual TEOAEs and DPOAEs, then sodium salicylate (100 mg/kg) was administered subcutaneously in a single dose, and post-injection emissions were measured at regular intervals over a $4-5$ h period. Results from other experiments in these animals involving comparable injections of saline or the recording of emissions over similar time periods were utilized as "control" data.

For rabbits, if the pre-injection DPOAE "audiograms" and growth functions corresponded to the laboratory's normative data on rabbits, then a baseline I/O measure was obtained at 5.656 kHz, which

is a typically sensitive frequency. By varying primary tone levels between 45 and 75 dB SPL, in 5 dB steps, the effects of ototoxins or anoxia on DPOAEs dominated by low- (for example, those evoked with 45 or 55 dB SPL primary tones) and high-level (those elicited with 75 dB SPL primaries) sources (Whithead et al., 1990) were determined. Following baseline measures, either ethacrynic acid (40 mg/kg), or a lethal dose of sodium pentobarbital (50 mg/kg) was injected intravenously, and the DPOAE I/O at 5.656 kHz was systematically monitored for a minimum of 140 min. A subset of rabbits receiving ethacrynic acid were pre-treated with a single dose of gentamicin (100 mg/kg) administered 2 h prior to the injection of the loop diuretic.

Results

The problems encountered in obtaining responses from ears exhibiting active or chronic infection clearly illustrate the importance of conduction-related factors in measuring OAEs. In Fig. 1, the adverse effects of recurrent bouts of fluid accumulation on both hearing (filled circles) and emissions (TEOAEs (8/16/90); DPOAEs (filled squares)) are shown for the right ear of a 7-year-old girl. For this ear, the clinical audiogram denotes a mild hearing loss with an irregular configuration which was associated with excessive negative pressure in the middle ear (i.e., a type-C tympanogram), and acoustic reflex thresholds > 105 dB hearing level (HL). It is

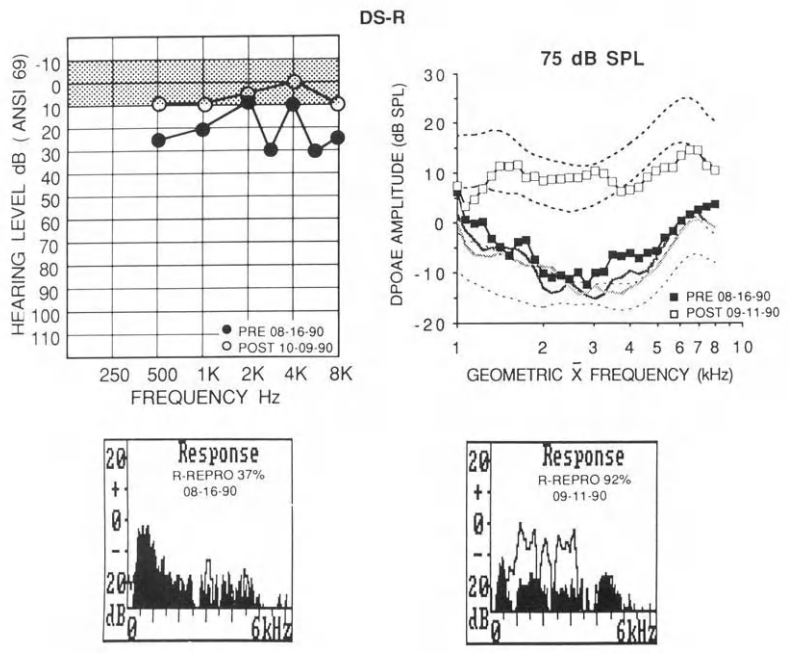

Fig. 1. Hearing levels and evoked OAEs in the right ear of a 7-year-old girl who was tested before (filled symbols) and after (open symbols) surgery, which included a myringotomy and insertion of ventilating tubes, to correct middle ear dysfunction. Both the pre-surgical TEOAEs (response 8-16-90), in which only the background noise in the ear canal is present (shaded region of spectrum), and DPOAEs (filled squares in plot at top right following the noise floor (dark line)) were immeasurable. However, the post-surgical (9-11-90) responses (tympanostomy tubes in place) were improved in that TEOAEs (unshaded area of spectrum) were relatively normal (i.e., the "Repro" (92%) or repeatability value of two separately determined averages was above the average (90%) for children of this age), and the DPOAEs (open squares) were essentially within low-normal limits. The DPOAE amplitudes are compared to the average levels (dotted lines: ± 1 S.D. of emission (top) and noise-floor (bottom) amplitudes) of responses determined from ears of a group of normally hearing children of similar age. For a more complete explanation of the TEOAE plots, see Kemp and Ryan (1991).

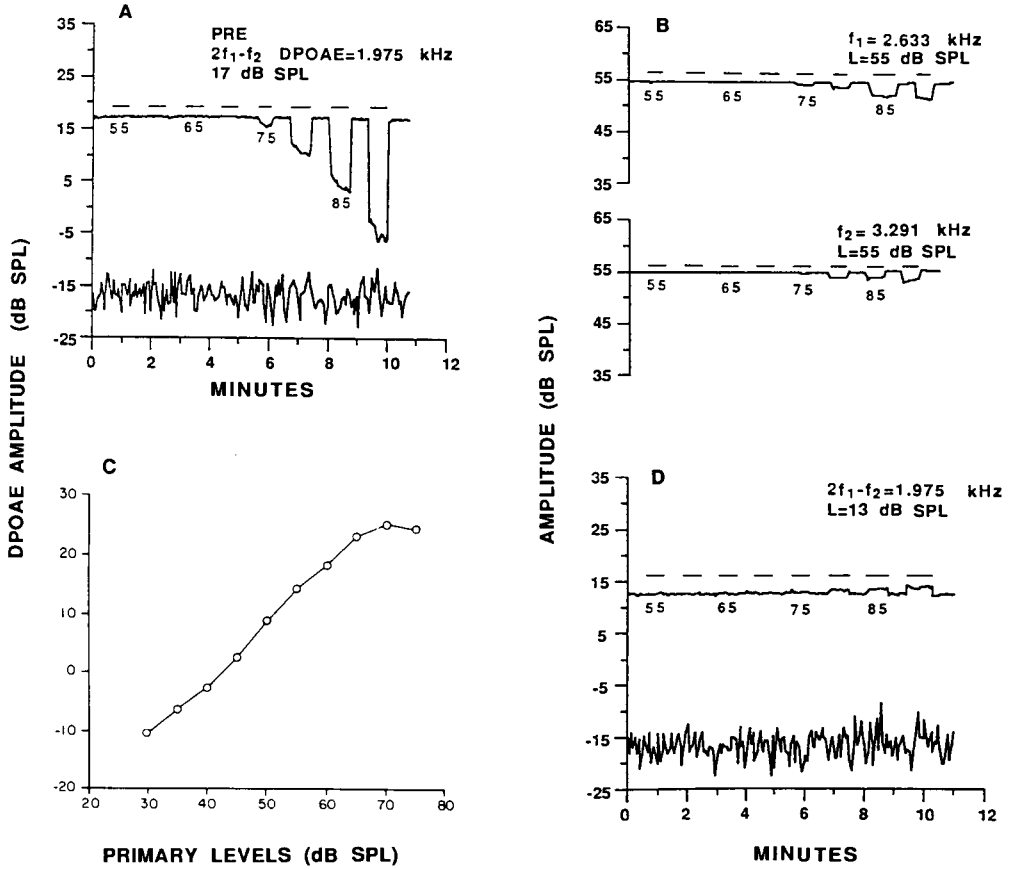

Fig. 2. Effects of a fixed 4 kHz contralateral reflex-eliciting tone on ear canal sound pressure for a 1.975 kHz DPOAE, the f_1 and f_2 primary tones, and a tone at the DPOAE frequency. In each panel, the trace represents the sound pressure level measured in the ear canal, and the horizontal bars above represent contralateral stimulus presentation. The contralateral stimulus was increased from 55 to 90 dB SPL, in 5 dB steps; numbers below the traces indicate contralateral stimulus level. *A*. DPOAE was 17 dB SPL when elicited by $L_1 = L_2 = 55$ dB SPL in the absence of the contralateral tone. *B*. 2.633 kHz (f_1) and 3.291 kHz (f_2) levels. In *A* and *B*, both primaries were presented during the measurement of either the primary or the DPOAE. Both the primaries and the DPOAE decreased in level upon contralateral reflex activation, but to different extents. *C*. DPOAE I/O function at 1.975 kHz showing that about a 20 dB attenuation of the primaries from 55 to 35 dB SPL would be necessary to reduce the DPOAE amplitude by about 22 dB. *D*. Level of a single external tone (1.975 kHz) set to the DPOAE frequency at a similar ear canal sound pressure level as the DPOAE but in the absence of the primaries, and, thus, of the DPOAE. At this frequency, elicitation of the reflex with the contralateral stimulus produced a slight increase in the ear canal sound pressure of the tone. The lower traces in *A* and *D* are the noise floor of the measurement system. Control experiments demonstrated that acoustic cross-over to the test ear was not responsible for the observed changes.

clear from the amplitude spectrum of the TEOAE shown below that no response was elicited from the affected ear. The DPOAE "audiogram" shows that these emissions were also absent in that they essentially tracked the levels of the corresponding noise floor (light stippled line). These findings illustrate the usual observation that a mild hearing dysfunction caused by an inflammation of middle ear tissues disproportionately affects the measurement of emitted responses (Owens et al., 1992).

The remaining data of Fig. 1 illustrate the effects of surgical intervention on hearing and on emission recordability. These results were obtained about 7 weeks after myringotomy and tympanic ventilation

procedures had been performed, which significantly improved the mechanical aspects of the middle ear's transmission system. At the time (9/11/90) when behavioral hearing had fully recovered from the influence of the inflammation (open circles), emission levels for both the TEOAEs and DPOAEs (open squares) were essentially normal.

Other findings in experimental animals also illustrate the possibility that the dependence of emissions on the middle ear's conduction system may be more critical for reverse than for normal forward transmission of signals (Whitehead et al., 1991a). The plot in Fig. 2*A* displays the effects of the acoustic reflex, evoked with a 4 kHz contralateral stimulus, on the sound pressure level of a 1.975 kHz DPOAE measured in a rabbit ear canal. It is clear from these data that when the reflex was fully activated in response to the 90 dB SPL contralateral stimulus, DPOAE amplitude decreased about 22 dB, from 17 to −5 dB SPL. The records in Fig. 2*B*, illustrating the related influence of the contralateral tone on the ear canal levels of f_1 (top) and f_2 (bottom), reveal that the fully activated reflex decreased the levels of the primaries by only a few dB. In combination with other results reporting evidence for an attenuation of forward sound transmission by the rabbit acoustic reflex of only a few dB (Borg, 1971), the present findings suggest that emission expression through the middle ear in the reverse direction undergoes considerably more attenuation by the reflex than does normal inward sound transmission. From the response/growth function of Fig. 2*C*, it is evident that to reduce the DPOAE by a similar 20 dB amount, the equivalent reduction in primary tone levels would have to be about 25 dB. Consequently, the influence of the acoustic reflex on DPOAE amplitude appears to be greater than would be expected from the singular actions of a simple attenuation process. Finally, in Fig. 2*D*, the effects of the reflex on a pure tone stimulus, fixed at the same frequency and at a similar level in the ear canal as the DPOAE, in the absence of the emission, are displayed. From this tracing, it is clear that the level of the tonal stimulus was increased slightly during contralateral reflex activation.

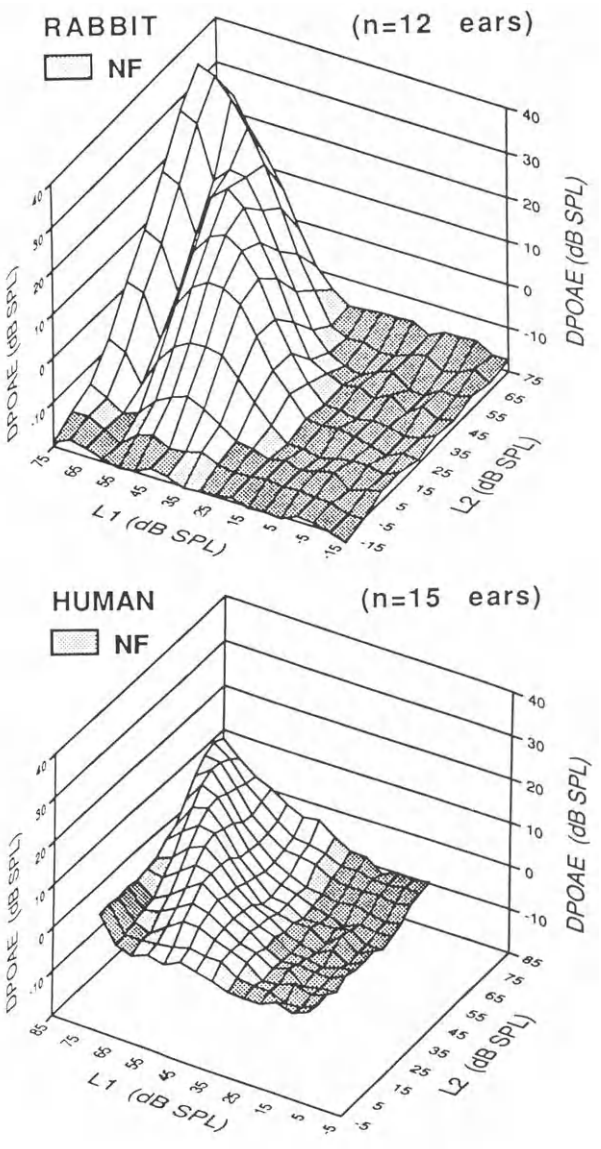

Fig. 3. Three-dimensional plots illustrating average I/O functions collected at the 2 kHz DPOAE by systematically decreasing L_1 in 5 dB steps, from 75 to −15 dB SPL in rabbits (top) and from 85 to 20 dB SPL in humans (bottom), with L_2 fixed from 85 to −15 dB SPL, in 10 dB steps (f_2/f_1 = 1.25). In both species, DPOAEs were detectable for lower levels of L_2 than of L_1. As stimulus levels decreased, maximum DPOAE amplitudes were obtained with L_2 increasingly smaller than L_1. Note that in rabbits, but not in humans, DPOAEs appear to be divided into a low-level "hump" region, and a high-level "background" region, with the boundary occurring at ~ 60 dB SPL. Shaded region represents the noise floor (NF).

Other studies have addressed the issue of whether $2f_1$-f_2 DPOAEs are produced by more than one generator source (Whitehead et al., 1991b). These experiments began by defining the "existence" regions of the DPOAE in normal ears by separately and systematically varying specific stimulus features, such as the primary level difference (L_1-L_2). The three-dimensional plots of Fig. 3 illustrate average I/O functions collected for the 2 kHz DPOAE by decreasing L_1 in 5 dB steps, from 75 to −15 dB SPL, in 12 rabbits ears (top), and from 85 to 20 dB SPL in 15 human ears (bottom), with L_2 fixed at levels from 85 to −15 dB SPL, in 10 dB steps. In both species, DPOAEs were detectable for lower levels of L_2 than of L_1. As stimulus levels decreased, maximum DPOAE amplitudes were obtained with L_2 increasingly smaller than L_1. In rabbits, but not in humans, DPOAEs appeared to be divided clearly into a low-level "hump" region and a high-level "background" region, with the boundary occurring at about 60 dB SPL. Together, these data show important quantitative and qualitative differences in the parametric behavior of the $2f_1$-f_2 DPOAE in rabbits and humans and suggest dissimilarities in their underlying emission generators.

Related findings on the differential physiological vulnerability of the $2f_1$-f_2 DPOAEs elicited by low- and high-level stimuli are also consistent with the notion that, in rabbits, the acoustic-disortion products arise from multiple sources (Whitehead et al., 1992). In these studies, 5.656 kHz DPOAEs were evoked by stimuli varying from 45 to 75 dB SPL and were measured in different rabbits over time, for three experimental conditions. The plots of Fig. 4 display changes in low- (55 dB SPL) and high-level (75 dB SPL) DPOAEs following an acute injection of either ethacrynic acid (*A*) or a combination of gentamicin and ethacrynic acid (*B*), or during anoxia leading to death (*C*). Although not illustrated here for reasons of clarity, DPOAEs evoked by less intense 45 dB SPL primaries, assumed to be generated by "active" micromechanical generators (Whitehead et al., 1990), were completely abolished either temporarily (ethacrynic acid), or permanently (gentamicin/ethacrynic acid, anoxia) by all experimental conditions. This occurred within a few minutes of either drug injection or the induction of anoxia.

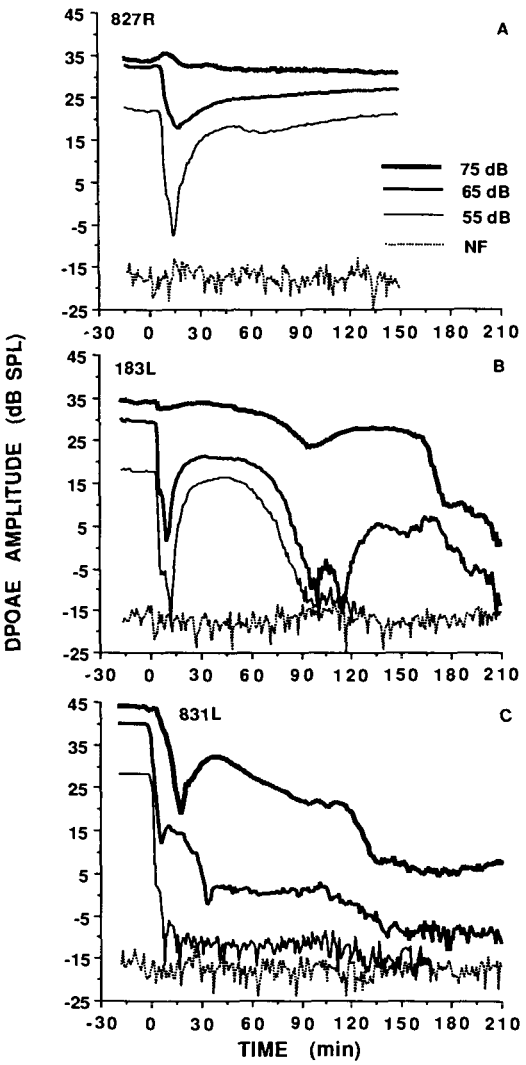

Fig. 4. The amplitudes of 5.656 kHz DPOAEs that were evoked by three primary tone levels (55, 65, 75 dB SPL) as a function of time post-injection in the ears of different rabbits. *A*. DPOAE amplitude before and after the injection of ethacrynic acid. *B*. Emission amplitude in response to an injection of ethacrynic acid in a rabbit which had received gentamicin 2 h earlier. *C*. DPOAE amplitude before and after a lethal dose of sodium pentobarbital. Dotted line along abscissa: noise floor (NF).

The data plotted in Fig. 4*A* illustrate that other low-level DPOAEs, elicited by 55 dB SPL stimuli,

were reduced rapidly and substantially within about 15 min post-injection, and recovered almost completely over the remainder of the monitoring period. At the same time, this dosage of ethacrynic acid had little or no effect on high-level DPOAEs evoked by 75 dB SPL primaries. From these results, it is clear that $2f_1$-f_2 DPOAEs evoked by lower level primaries demonstrated greater vulnerability to ethacrynic acid administration than did those evoked by higher level tones. From the trajectories of the curves of Fig. 4*B*, it is evident that the combined treatment with gentamicin and ethacrynic acid, which would be expected to produce widespread hair cell damage, eliminated low-level DPOEAs evoked by 55 dB SPL primaries, and greatly reduced or abolished moderate- (65 dB SPL) to high-level (75 dB SPL) emissions by the end of the monitoring period. Such an erratic, but steady decline in emission amplitudes was never observed for rabbits receiving only an injection of ethacrynic acid.

The plot in Fig. 4*C* illustrates that low-level DPOAEs were effectively abolished by anoxia which was induced by a lethal overdose of an anesthetic agent, whereas emissions evoked by high-level stimuli were affected in a more complex manner. After the initial decline in amplitude, various degrees of recovery were observed for DPOAEs elicited by moderate- to high-level primaries. Then, following the point of maximum recovery, these emissions gradually declined over the remainder of the recording period. Periodic monitoring in some ears at later times indicated that the moderate- and high-level emissions evoked by stimuli $>$ 60 dB SPL continued to decrease slowly such that by 6 – 8 h post-mortem, DPOAEs were only detectable in response to primaries that were $\geq$ 70 dB SPL. These residual DPOAEs, which were still present at measurement times of up to 21 h post-mortem, were unaffected by long-term ($>$ 30 min), intense ($>$ 125 dB SPL) pure tone exposures, thus implying that they were not of OHC origin. Such findings support the notion that low- and high-level DPOAEs arise from discrete cochlear sources, with the low-level component based upon the actions of an energy-dependent, micromechanical process. However, the proposed strict origin of high-level DPOAEs in the passive macromechanics of the cochlear partition may not be entirely accurate if a third, residual component exists which is resistant to the early effects of the autolytic post-mortem processes, and which probably arises from the cochlea's true passive distortion activity.

A final line of evidence for the multigenerator hypothesis comes from the presence of notable notches in the DPOAE I/O function. The three-dimensional plot of DPOAE-growth functions shown in Fig. 5*A* was acquired from a single rabbit ear by varying $L_1 = L_2$ in 2 dB steps, at 50 Hz intervals, from 3.8 to 4.8 kHz. Inspection of these curves reveals that near the 4.5 kHz region, moderate reversals or notches occurred in the growth functions around the 60 dB SPL primary levels. The results of remeasuring the growth functions of three of these frequencies, denoted by the bold lines in Fig. 5*A*, with a lock-in amplifier, in order to provide both amplitude and phase information, are shown in Fig. 5*B*. The resulting amplitude curves at top were similar to those illustrated in Fig. 5*A*, which were measured with a dynamic signal analyzer. For all three frequencies, the phase plots below indicate that there was relatively little phase change over the linear part of the growth function with increases in the level of the primaries up to about 50 dB SPL. In contrast, for the frequencies displaying either sharp (4.5 kHz) or shallow notches (4.65 kHz) in their amplitude functions, an associated phase lag and reversal were observed. Similar results were determined in other ears tested, and at other frequencies. These findings suggest that notches in rabbit DPOAE growth functions result from a phase cancellation of two approximately equal amplitude components (Whitehead et al., 1990).

In contrast, similar notches observed in the growth functions of normally hearing humans appear to result from the confounding influences of other types of emissions rather than from multiple sources of emission generation (Lonsbury-Martin et al., 1990). In fact, it is noteworthy that in our experience of measuring DPOAE growth curves in

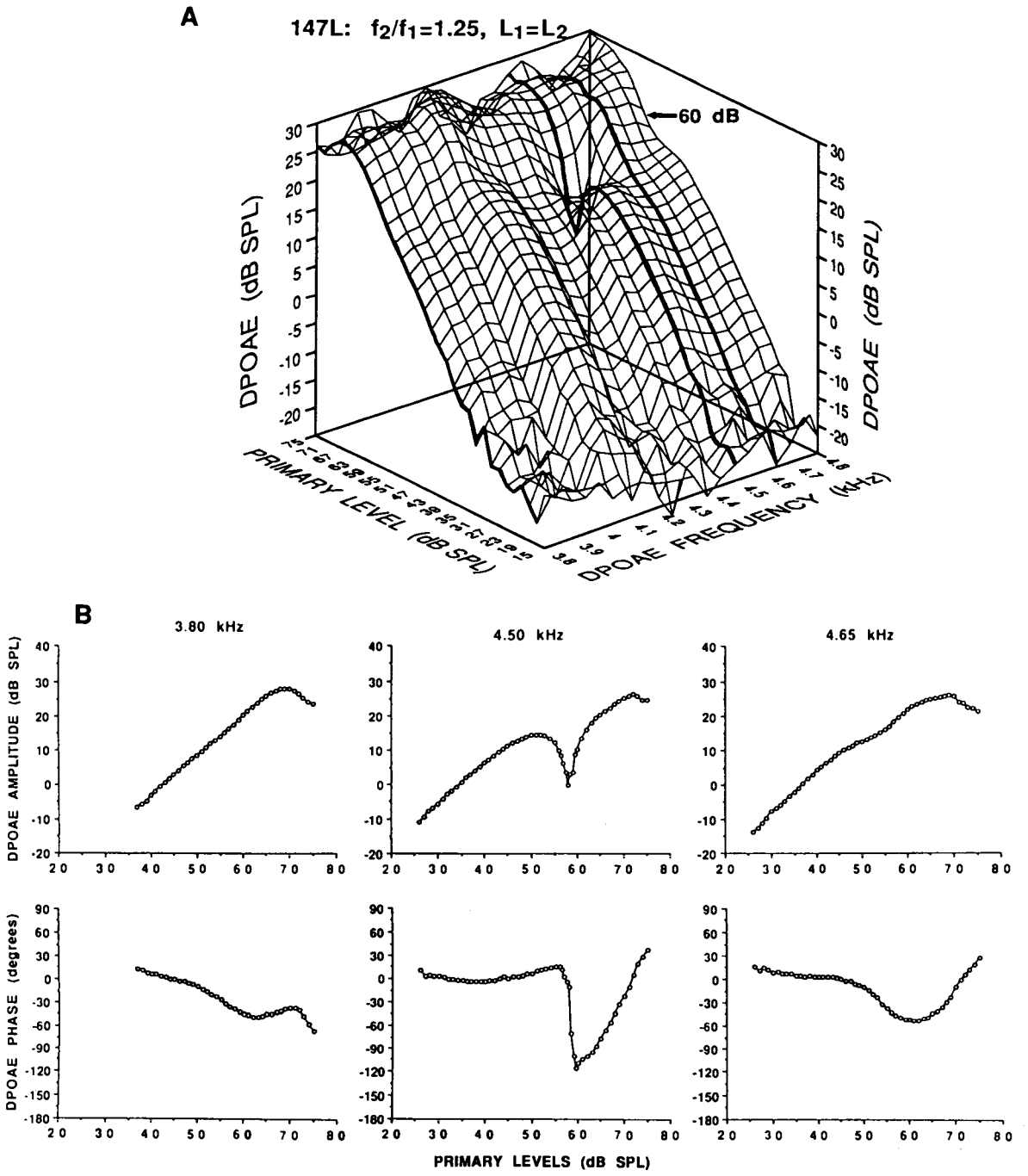

Fig. 5. DPOAE growth functions measured using two separate procedures. *A*. High-resolution (50 Hz intervals) growth functions for DPOAEs (f_2/f_1 = 1.25) from 3.8 to 4.8 kHz measured with a dynamic analyzer for the left ear of rabbit no. 147. L_1 = L_2 was varied in 2 dB steps. *B*. Growth functions from *A* above (in "bold" at 3.8, 4.5 and 4.65 kHz) were remeasured with greater resolution using a lock-in amplifier. Note the similar amplitudes and the positions of the inflections on the I/O curves with respect to the primary level (*x*) axis. In the lower portion of *B*, the phase of the DPOAE (lag is negative) is plotted. The phase of all three plots was arbitrarily set to zero at L_1 = L_2 = 45 dB SPL.

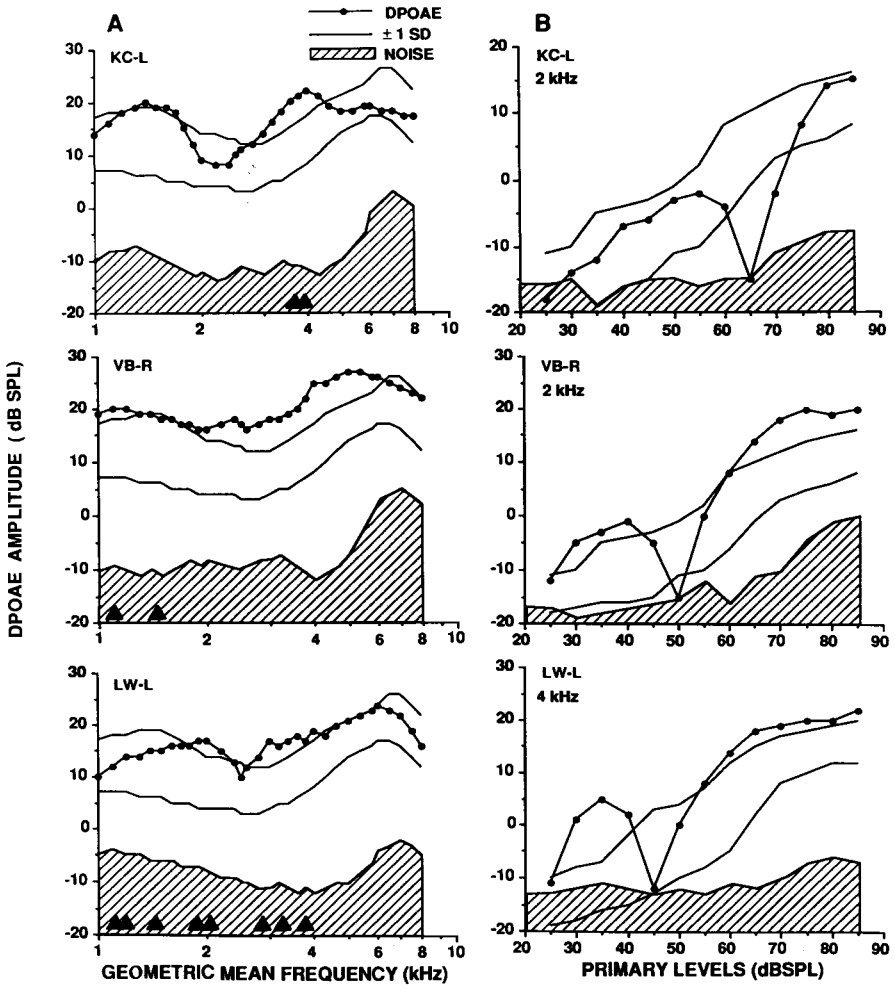

Fig. 6. Typical DPOAEs for three normally hearing subjects with multiple SOAEs. *A*. Conventional 75 dB SPL DPOAE "audiograms." Note the emission levels, which were generally "high" normal, i.e., ≥ + 1 S.D. of the mean levels measured in the ears of normally hearing, young adult subjects. Although outside the measurement range of the DPOAEs, KC and VB had additional SOAEs at frequencies < 1 kHz. *B*. I/O functions for the same individuals, which were selected to illustrate the different positions of "notches," or sharp inversions in the response/growth pattern, with increasing levels of the primaries. Solid triangles: SOAE frequencies; stripes: noise floor; thin lines: ± 1 S.D. of average emission amplitudes for normally hearing, young adult subjects.

hundreds of individuals, only those ears with measurable SOAEs or strong TEOAE peaks have demonstrated the complex notch features which are commonly observed in rabbit I/Os elicited by moderate-level primaries. The plots of Fig. 6 illustrate the effects of multiple SOAEs on the pattern of DPOAE growth for several subjects. These particular examples were selected to illustrate the greater range of the reversal points in the amplitude functions with respect to the level of the primary tones in human ears in comparison to results from small mammals such as rabbits. Thus, in contrast to the stable relationship of notches in the I/Os related to the primary tone levels in rabbit ears, which primarily occur at ~ 60 dB SPL, the notches in I/Os obtained from human ears develop over a much greater extent of the stimulus level dimension. That is, in human ears, they can appear at any level between

about 40 and 80 dB SPL. Thus, the peculiar properties of I/O notches observed from human ears imply that the notches are produced by idiosyncratic interactions of other emission types, such as SOAEs, with DPOAEs, rather than from a systematic interplay of high- and low-level DPOAE generators.

Other work aimed at investigating the possibility that the distinct emission types may be generated by different aspects of the bidirectional, stimulus transduction process utilized the reversible ototoxin, aspirin. Specific experiments in monkeys (n = 5) compared the effects of sodium salicylate

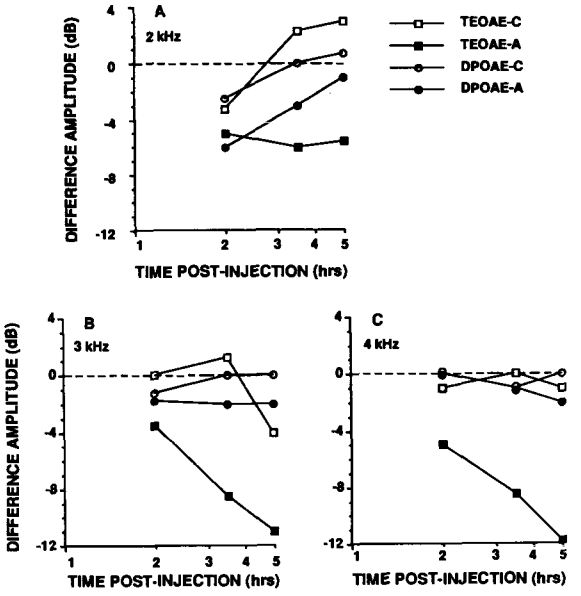

Fig. 7. Average (n = 5 monkeys) amplitude difference functions for TEOAEs (squares) and DPOAEs (circles) as a function of time post-injection of saline (open) or aspirin (solid), for the frequency regions of 2, 3 and 4 kHz shown in panels *A*, *B* and *C*, respectively. The dotted line parallel to the abscissa at "0 dB" represents the anticipated trajectory of the data curves if no differences in emission amplitude occurred between the pre- and post-injection conditions. Note the effects of anesthesia and anesthesia/aspirin on the low-frequency emissions at 2 kHz. However, at the higher frequencies, aspirin caused a substantial reduction in TEOAE amplitudes without significant changes in DPOAEs. Data points for the DPOAE-control condition (open circles) at 4 kHz were identical to DPOAE-aspirin (solid circles) values, at 2 – 3 h post-injection and are partially hidden by the latter symbols. Average plasma salicylate concentration at 5 h post-injection: 16 mg%.

injections on TEOAEs and DPOAEs to those associated with comparable administrations of physiological saline, or simply with the passage of experimental time, during each of four test periods at 0, 2, 3.5 and 5 h post-injection (Lonsbury-Martin et al., 1991b). The amplitude difference plots of Fig. 7, calculated by subtracting "pre-" from "post-injection" amplitudes, compare mean changes in DPOAEs (circles), at 2, 3 and 4 kHz, to the amplitudes of TEOAEs (squares). The comparison was made of the major spectral peaks from the TEOAE data that corresponded to the DPOAE frequencies, for both control (open symbols) and aspirin (filled symbols) conditions. Note that under control conditions, both emissions showed changes of about ± 3 – 4 dB over time. Additionally, whereas both TEOAEs and DPOAEs within the lowest frequency region of 2 kHz decreased during the control and post-aspirin injection periods, TEOAEs in the higher regions of 3 and 4 kHz were affected substantially more than were the DPOAEs following aspirin administration. The results of other experiments aimed at examining the status of the middle ear during aspirin/anesthesia or control/anesthesia conditions by monitoring the ear canal level of a low-frequency probe tone showed that at frequencies < 3 kHz, emission amplitudes varied inversely with tone level. These findings suggest that middle ear influences often confounded the amplitude changes in the low-frequency emissions during both control and aspirin conditions. In contrast, at frequencies ≥ 3 kHz, aspirin reliably reduced TEOAEs, whereas DPOAEs were much less affected. This outcome is consistent with the notion that some aspects of the generation process for acoustic distortion products may be unique from those producing transient emissions.

Discussion

The role of OAEs in the assessment of cochlear function is rapidly changing from that of a research tool to that of an integral component of the routine examination of hearing. The purpose of the present report was to review some of the considerations that

affect the measurement of OAEs, and which must be recognized and/or resolved to permit accurate interpretation of emission properties in clinical situations.

Evidence clearly indicates that the detailed study of expression factors as they influence OAE measures must assume an important role in future research. Animal findings suggest that changes in middle ear transmission by activation of the acoustic reflex attenuates DPOAEs considerably more than might be expected on the basis of the associated changes in the magnitude of the emission-evoking stimuli. However, within our present technical capabilities, it would be difficult to determine the reflex-modified stimulus magnitudes directly within the cochlea and subsequently to predict the expected reduction in emission amplitude.

In human studies of the effects of middle ear effusions on OAEs, many cases have been measured in which there are dramatic reductions in emission amplitudes without measurable changes in associated pure tone thresholds. Such observations strongly imply that the amplitudes of the eliciting tones reaching the cochlea are relatively unchanged by the middle ear factors, whereas processes involved in conducting emissions in the reverse manner, to the ear canal, are drastically affected. Thus, subtle middle ear effects must be ruled out before OAE amplitudes can be interpreted as providing meaningful estimates of the functional status of OHCs. Even more confusing in appreciating the influence of transmission-related factors on OAEs are the observations for several sporadic cases in which the amplitudes of TEOAEs were relatively unaffected by middle ear pathology, whereas DPOAE amplitudes were significantly reduced. Such findings cannot be simply explained by the magnitude of sensory cell loss, because it is well-established that TEOAEs are substantially more affected by lower amounts of hearing loss than are DPOAEs. That is, TEOAEs are typically absent when pure tone thresholds are ~ 30 dB HL, whereas DPOAEs, although somewhat reduced in amplitude, are still easily measured under these impaired conditions. Thus, it appears that in some instances, subtle, as yet undefined alterations to the middle ear can differentially influence the reverse transmission of the various types of emissions. Conditions which cause such effects clearly need to be appreciated before straightforward clinical interpretations of OAEs can be achieved.

Another important issue for the eventual understanding of OAE characteristics concerns their source of generation, which is particularly important for DPOAEs. Clearly, in small laboratory mammals, there appear to be multiple sources of DPOAE origination. Several generator sources have been revealed by a number of experimental strategies. These include the systematic manipulation of the parametric features of the stimulus paradigm used to evoke emissions, detailed investigations of notches in the DPOAE growth functions, and chemical poisoning of the cochlea. As a whole, the results of these maneuvers disclose that at least two sources are involved in the generation of DPOAEs. One source dominates DPOAE production in response to high-level primary tones. The other source is associated with lower stimulus levels and with physiological vulnerability and appears to be quite dependent on cochlear energy supplies. Thus, low-level DPOAEs may closely track transduction currents and cochlear microphonic responses, whereas higher level DPOAEs may reflect the physical integrity of the organ of Corti and basilar membrane properties.

The findings of the animal studies also raise an important clinical question concerning the levels of the evoking stimuli which will detect sensorineural hearing loss most sensitively. Whereas in rabbits there appear to be two distinct DPOAE generator sources which relate to the levels of the primaries, initial work in our laboratory has been unsuccessful in clearly identifying two such sources in humans. Rather than there being a preferred stimulus level for eliciting DPOAEs optimally in humans, preliminary observations suggest that the presence of other emission types and their interaction with DPOAEs may be of greater significance for interpreting the meaningfulness of human findings. Clearly, more studies are needed to achieve a definitive answer to

this important question concerning the most appropriate levels of stimulation for evaluating cochlear function in patients.

Because the amplitudes of DPOAEs are considerably larger in animals, it is possible that a two-level process is easily measured in animal subjects, whereas it is more difficult in human ears. If the human ear also possesses several level-dependent generators, then it would appear that the stimulus levels required to reveal their existence would be near the distortion-limiting capacity of current instrumentation. There are many examples of patients with sensorineural hearing loss in which the attempt to elicit DPOAEs with 75 dB SPL primary tones failed. Therefore, if a high-level generator process exists in humans, it must be elicited by stimulus levels above 75 dB SPL.

Parametric studies of the influence of L_1-L_2 on DPOAE amplitudes are not only relevant to the two generator source issue, but also reveal that for each set of primary tones, there is an optimal level difference between f_1 and f_2 which is needed to produce the largest DPOAE. This finding clearly has clinical implications in that it will be important to determine the influence of such level difference phenomena on the ability of DPOAEs to detect defects in OHC function. It is conceivable that selective modification of the L_1-L_2 variable will significantly alter the sensitivity of the DPOAE examination.

A final consideration for future research efforts concerns understanding the sites involved in the presumed bidirectional stimulus transduction processes, which are responsible for the generation of the various types of emissions. In its simplest form, current thinking assumes that sound stimulation leads to bending of the OHC stereocilia, which in turn results in current flow through the tips of the stereocilia and into the hair cells. It is further assumed that such current flow causes the OHC to contract, thus resulting in an enhancement of the motion of the basilar membrane. Knowledge concerning how OAEs arise from this process is just now beginning to be acquired. Studies with aspirin suggest that this ototoxic compound can dramatically reduce TEOAEs, whereas DPOAEs remain relatively unaffected. Aspirin applied to OHCs in vitro has been shown to block the motile properties of these cells (Shehata et al., 1991). If these findings are substantiated in other laboratories, then it seems possible that the different OAEs may reflect several distinct stages of the transduction process to varying degrees. Thus, TEOAEs may rely primarily on the cycle-by-cycle motile properties of the OHC, whereas DPOAEs may arise from the more mechanically based aspects of cochlear transduction related to stereocilia features such as stiffness or ion channel patency, the structural integrity of OHCs, and the physical properties of the basilar membrane. Such issues are presently the active focus of basic research and will contribute further to our knowledge of the factors affecting emission generation and expression. However, it is believed that these subtle refinements will not affect the continued development of techniques for applying OAE findings to the diagnosis of cochlear and, perhaps, middle ear disease.

Acknowledgements

The research supporting the work reported here was funded in part by the Public Health Service (DC00313, DC00613, ES03500), and the Deafness Research Foundation. The authors thank B.B. Stagner, Marcy J. McCoy, D.J. Murray, M.E. Knapp and D.L. Himes, for technical assistance.

References

Anderson, S.D. (1980) Some ECMR properties in relation to other signals from the auditory periphery. *Hear. Res.*, 2: 273–296.

Bilger, R.C., Matthies, M.L., Hammel, D.R. and Demorest, M.E. (1990) Genetic implications of gender differences in the prevalence of spontaneous otoacoustic emissions. *J. Speech Hear. Res.*, 33: 418–432.

Borg, E. (1971) Regulation of middle ear sound transmission in the nonanesthetized rabbit. *Acta Physiol. Scand.*, 86: 175–190.

Bray, P. and Kemp, D.T. (1987) An advanced cochlear echo technique suitable for infant screening. *Br. J. Audiol.*, 21: 191–204.

Brown, A.M. and Kemp, D.T. (1984) Suppressibility of the $2f_1$-

f_2 stimulated acoustic emissions in gerbil and man. *Hear. Res.*, 13: 29 – 37.

Harris, F.P., Lonsbury-Martin, B.L., Stagner, B.B., Coats, A.C. and Martin, G.K. (1989) Acoustic distortion products in humans: systematic changes in amplitude as a function of f_2/f_1 ratio. *J. Acoust. Soc. Am.*, 85: 220 – 222.

Kemp, D.T. (1978) Stimulated acoustic emissions from within the human auditory system. *J. Acoust. Soc. Am.*, 64: 1386 – 1391.

Kemp, D.T. (1979) Evidence of mechanical nonlinearity and frequency selective wave amplification in the cochlea. *Arch. Otorhinolaryngol.*, 224: 37 – 45.

Kemp, D.T. and Chum, R. (1980) Properties of the generator of stimulated acoustic emissions. *Hear Res.*, 2: 213 – 232.

Kemp, D.T. and Ryan, S. (1991) Otoacoustic emission tests in neonatal screening programmes. *Acta Otolaryngol. (Stockh.) (Suppl.)*, 482: 73 – 84.

Kim, D.O., Molnar, C.E. and Matthews, J.W. (1980) Cochlear mechanics: nonlinear behavior in two-tone responses as reflected in cochlear-nerve-fiber responses and in ear-canal sound pressure. *J. Acoust. Soc. Am.*, 67: 1704 – 1721.

Lonsbury-Martin, B.L., Martin, G.K., Probst, R. and Coats, A.C. (1987) Acoustic distortion products in rabbits. I. Basic features and physiological vulnerability. *Hear. Res.*, 28: 173 – 189.

Lonsbury-Martin, B.L., Harris, F.P., Stagner, B.B., Hawkins, M.D. and Martin, G.K. (1990) Distortion-product emissions in humans: II. Relations to stimulated and spontaneous emissions and acoustic immittance in normally hearing subjects. *Ann. Otol. Rhinol. Laryngol. (Suppl.)*, 236: 14 – 28.

Lonsbury-Martin, B.L., Cutler, W.M. and Martin, G.K. (1991a) Evidence for the influence of aging on distortion-product otoacoustic emissions in humans. *J. Acoust. Soc. Am.*, 89: 1749 – 1759.

Lonsbury-Martin, B.L., Whitehead, M.L., Henley, C.M. and Martin, G.K. (1991b) Differential effects of sodium salicylate on the distinct classes of otoacoustic emissions in rabbit and in monkey. *Assoc. Res. Otolaryngol. Abstr.*, 14: 67.

Martin, G.K., Lonsbury-Martin, B.L., Probst, R. and Coats, A.C. (1985) Spontaneous otoacoustic emissions in the nonhuman primate: a survey. *Hear. Res.*, 20: 91 – 95.

Martin, G.K., Probst, R., Scheinin, S.A., Coats, A.C. and Lonsbury-Martin, B.L. (1987) Acoustic distortion products in rabbits. II. Sites of origin revealed by suppression and pure-tone exposures. *Hear. Res.*, 28: 191 – 208.

Martin, G.K., Stagner, B.B., Coats, A.C. and Lonsbury-Martin, B.L. (1989) Endolymphatic hydrops in rabbits: behavioral thresholds, acoustic distortion products, and cochlear pathology. In: J.B. Nadol (Ed.), *Second International Symposium on Meniere's Disease, Pathogenesis, Pathophysiology, Diagnosis and Treatment*, Kugler and Ghedini, Berkeley, CA, pp. 205 – 219.

Owens, J.J., Lonsbury-Martin, B.L. and Martin, G.K. (1992) Distortion-product emission measures in children with acquired hearing loss. *Sem. Hear.*, 13: 53 – 66.

Shehata, W.E., Brownell, W.E. and Dieler, R. (1991) Effects of salicylates on shape, electromotility, and membrane characteristics of isolated outer hair cells from guinea pig cochlea. *Acta Otolaryngol. (Stockh.)*, 111: 707 – 718.

Whitehead, M.L., Lonsbury-Martin, B.L. and Martin, G.K. (1990) Actively and passively generated acoustic distortion at $2f_1$-f_2 in rabbits. In: P. Dallos, C.D. Geisler, J.W. Matthews, M.A. Ruggero and C.R. Steele (Eds.), *Mechanics and Biophysics of Hearing*, Springer, New York, pp. 243 – 250.

Whitehead, M.L., Martin, G.K. and Lonsbury-Martin, B.L. (1991a) Effects of the crossed acoustic reflex on distortion-product otoacoustic emissions in awake rabbits. *Hear. Res.*, 51: 55 – 72.

Whitehead, M.L., McCoy, M.J., Lonsbury-Martin, B.L. and Martin, G.K. (1991b) Acoustic distortion at $2f_1$-f_2 in human and rabbits ears. *Assoc. Res. Otolaryngol. Abstr.*, 14: 67.

Whitehead, M.L., Lonsbury-Martin, B.L. and Martin, G.K. (1992) Evidence for two discrete sources of $2f_1$-f_2 distortion-product otoacoustic emission in rabbit: II. Differential physiological vulnerability. *J. Acoust. Soc. Am.*, 92: 2662 – 2682.

Zurek, P.M., Clark, W.W. and Kim, D.O. (1982) The behavior of acoustic-distortion products in the ear canals of chinchillas with normal or damaged ears. *J. Acoust. Soc. Am.*, 72: 774 – 780.

Zwicker, E. and Manley, G. (1981) Acoustical responses and suppression-period patterns in guinea pigs. *Hear. Res.*, 4: 43 – 52.

J.H.J. Allum, D.J. Allum-Mecklenburg, F.P. Harris and R. Probst
Progress in Brain Research, Vol. 97

CHAPTER 9

A comparison of transiently evoked and distortion-product otoacoustic emissions in humans

Rudolf Probst and Frances P. Harris

HNO-Universitätsklinik, Basel, Switzerland

The measurement of transiently evoked otoacoustic emissions (TEOAEs) can identify a hearing loss exceeding 25 – 30 dB HL with high sensitivity. However, further quantification of the hearing loss is not possible, and the frequency specificity of TEOAEs has been questioned. Distortion-product otoacoustic emission (DPOAE) measurements are being developed for clinical use in the hope that they will be more frequency-specific than are TEOAEs. We have compared TEOAEs and DPOAEs in both normally hearing and hearing-impaired subjects with the purpose of learning more about the frequency specificity of these two types of emissions. In a first investigation, toneburst-evoked OAEs were compared to DPOAEs stimulated at 1, 2 and 4 kHz in ten ears without spontaneous otoacoustic emissions of ten normally hearing subjects. Input/output (I/O) functions of DPOAEs at frequency regions of 1 and 2 kHz were characterized by roll-overs and irregularities that were not present in either DPOAE I/O functions at 4 kHz or in TEOAE I/O functions at 1, 2 and 4 kHz. Mean slopes of the I/O functions increased with increasing frequency for DPOAEs and decreased for TEOAEs. In a second investigation, click-evoked OAEs and DPOAEs (stimulated by pure tones in the frequency range of 0.75 – 6 kHz) were measured in 42 ears of 21 normally hearing subjects and 128 ears of 64 subjects with varying degrees of sensorineural hearing loss. Results from both investigations revealed that the amplitude ratio between DPOAEs and TEOAEs changed systematically with frequency. DPOAE amplitudes became larger with increasing frequency and TEOAE amplitudes became smaller. It can be concluded from these findings that TEOAEs and DPOAEs are either generated, transmitted, or influenced differentially during the measurement procedure in the higher frequency regions. The findings are consistent with an influence of the basal portions of the basilar membrane on TEOAEs that may not be present for DPOAEs.

Key words: Comparison of otoacoustic emissions; Distortion-product otoacoustic emission; Transiently evoked otoacoustic emission; Cochlear non-linearity

Introduction

Transiently evoked otoacoustic emissions (TEOAEs) and distortion-product otoacoustic emissions (DPOAEs) result from a normal or near normal cochlear system (Mountain, 1980; Brownell, 1990). An intact function of outer hair cells (OHC) seems to be essential and damage to OHCs affects the generation of both emissions (Horner et al., 1985).

A number of properties and characteristics of TEOAEs are clearly different from DPOAEs (for review, see Probst et al., 1991). It is still unclear to what extent these two emission types are generated by the same or by different processes. The most conspicuous differences include different prevalences and amplitudes in different species and different effects of salycilates upon the two emission types in the same ear.

The association of OAEs to an intact function of OHCs has prompted the proposal that the measurement of emissions can be used as an objective test for determining hearing and for monitoring the status of the cochlea (Kemp et al., 1986; Probst et al., 1986; Martin et al., 1990). Until recently, TEOAEs have been used more routinely than have DPOAEs

in this capacity. One reason for this may be the commercial availability of the instrumentation. This trend may change with the introduction of commercially available instrumentation for measuring DPOAEs and as more research is presented that identifies the clinical usefulness of the technique. Thus, it is becoming increasingly important to understand the relation of the two types of emission to each other and to OHC damage that may or may not produce threshold changes. We have compared the characteristics of TEOAEs and DPOAEs in human subjects in two investigations.

Methods

Investigation I

Toneburst-evoked and distortion-product OAEs were measured in one ear of ten normally hearing subjects, eight men and two women ranging in age from 18 to 29 years (M = 23 years). All subjects had normal otoscopic inspection, hearing thresholds < 15 dB hearing loss (HL) from 0.25 to 8 kHz (including 0.75, 1.5, 3 and 6 kHz), normal results of immittance audiometry, and no spontaneous otoacoustic emissions (SOAEs) in the test ear. Additionally, subjects were screened for the presence of broad-spectrum TEOAEs using click stimuli. The sample consisted of three right and seven left ears. All ears had TEOAEs containing a distribution of energy from approximately 0.7 to 4.5 kHz. This range encompassed the frequency span of the toneburst measurements.

Emissions were elicited with stimuli in the frequency regions of 1, 2 and 4 kHz. For DPOAEs, the geometric mean of two continuous pure tones, f_1 and f_2, was at one of the three frequencies. A frequency separation ratio of f_2/f_1 = 1.22 was selected as being optimal for the generation of $2f_1$-f_2 across frequency based upon the parametric study of Harris et al. (1989). Stimuli were equal in level and were decreased in 5 dB steps from 65 to 25 dB SPL (or until no DPOAE above the system's noise floor was observed in the spectrum). For TEOAEs, cosine-windowed tonebursts presented at a 20 msec rate were used as stimuli. They ranged in level from approximately 36 to 84 dB average peak intensity level in the ear canal and were presented in increasing 6 dB steps.

The instrumentation used for both DPOAE and TEOAE measures has been described in detail elsewhere (Harris and Probst, 1990). Briefly, DPOAEs were measured with a probe, consisting of an ER-10 microphone and two ER-2 earphones. Stimuli at f_1 and f_2 were generated by separate channels of an HP 3326A frequency synthesizer and were mixed acoustically in the ear canal. The ear canal sound pressure was detected by the microphone, and the output was led to an ER-72 preamplifier followed by a custom-built low-noise high-pass amplifier filter with a cut-off frequency of 400 Hz that provided 20 dB of amplification. Following amplification, eight fast Fourier transforms of the output were sampled by the signal analyzer. Analysis bandwidths were 1.5 Hz for the 1 kHz condition and 1.875 Hz for the 2 and 4 kHz conditions. The level of $2f_1$-f_2 and of the noise floor at a representative adjacent frequency were recorded manually.

All tests for TEOAEs were performed with an ILO88 Otodynamic analyser (Otodynamics Ltd.) controlled by a Compaq portable III computer. One of the three tonebursts was presented at a gain setting on the instrument of −30 dB (approximately 36 dB SPL) and 256 samples of the ear canal sound pressure were averaged in the 20 msec post-stimulus time. Averaged responses were bandpass-filtered and stored for later analysis. Filter bandwidths varied by center frequency, corresponding to the toneburst frequencies, and ranged from approximately 0.8 kHz for the 1 kHz condition to 3 kHz for the 4 kHz condition. The selected stimulus was then increased in consecutive 6 dB steps until averaged responses were obtained for nine levels. This procedure was repeated for the two remaining frequencies.

Investigation II

DPOAE growth functions and click-evoked OAEs for both ears were measured in 21 young adult subjects with normal hearing and in 64 patients with sensorineural hearing loss. The instrumentation

used for the measurement of both of these emissions was identical to that described for Investigation I; however, the stimuli were different. DPOAEs were measured with the geometric mean of f_1 and f_2 at 0.75, 1, 1.5, 2, 3, 4 and 6 kHz. The frequency ratio of f_2/f_1 was 1.22 and L_2 was 6 dB below L_1. Stimuli were presented at levels (L) from L_1 = 70 to L_1 = 25 dB SPL in decreasing 5 dB steps. All measurements were under computer control (Macintosh IIx).

Stimuli for generating TEOAEs were 80 μsec rectangular pulses presented at a rate of 20 msec presented using the "non-linear" software option of the ILO88 Otodynamics analyser. The spectrum of the click stimulus was relatively flat and included energy across the frequency range of the analysis window from approximately 0.6 to 4.5 kHz. Above 4.5 kHz, there was a 125 dB/octave roll-off in the frequency response of the system. The frequency-response characteristics of the system are compensated for automatically by the software of the ILO88. Responses were sampled in a 20 msec window post-stimulus time and were stored after 260 averages were performed.

Results from the two investigations were analyzed separately. Statistical analyses were performed using Statview II on a Macintosh IIx computer.

Results

Results from the first investigation revealed differences in the growth functions of DPOAEs and

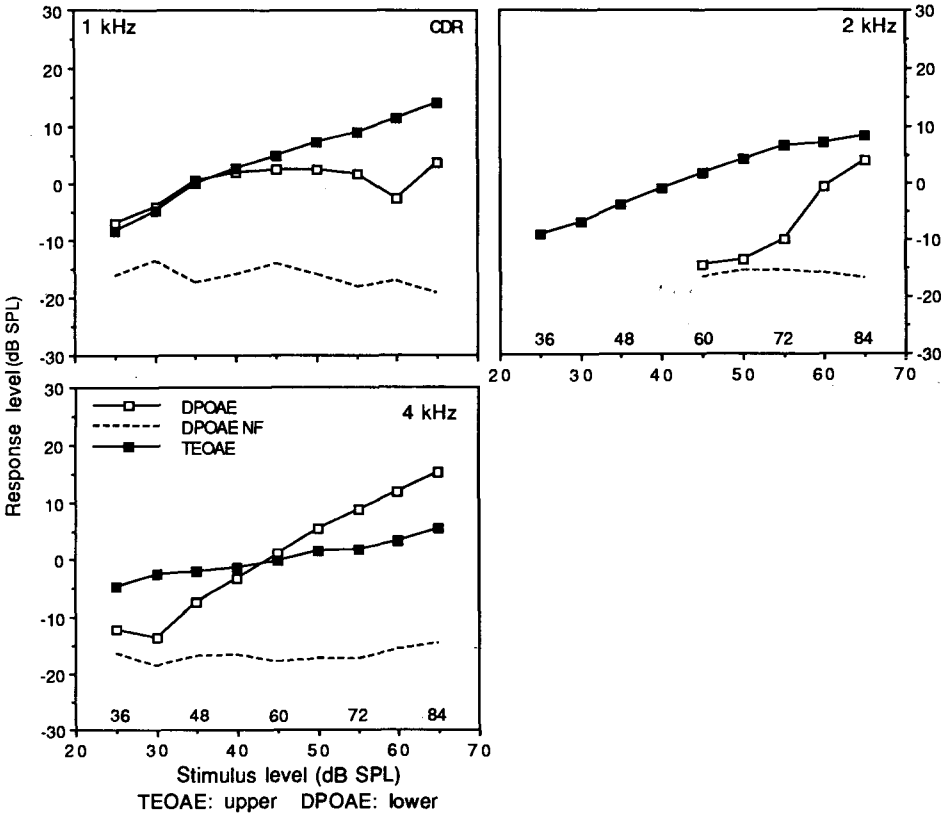

Fig. 1. Growth functions of DPOAEs ($L_1 = L_2$, f_2/f_1 = 1.22) and TEOAEs generated using tonebursts at 1, 2 and 4 kHz for the right ear (R) of subject CD. DPOAE functions are characterized by saturation, roll-over and dips that are not present in the TEOAE growth functions. Slopes of the growth functions of DPOAEs increase as a function of frequency, whereas TEOAE growth functions decrease or change only slightly. NF, noise floor.

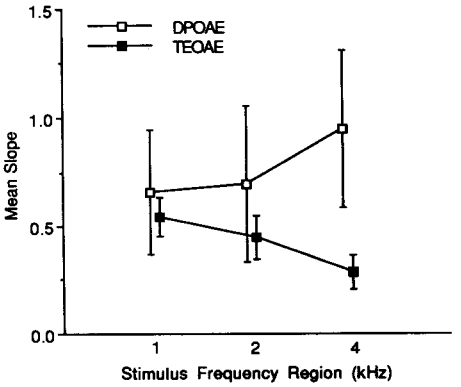

Fig. 2. Mean slopes (± 1 S.D.) of DPOAE and TEOAE growth functions for stimuli at 1, 2 and 4 kHz. Across frequency, mean slopes increased for DPOAE functions and decreased for TEOAE functions.

TEOAEs. The results for one subject are presented in Fig. 1, to illustrate the nature of these differences. The DPOAE growth functions were characterized by dips and roll-overs that were not present in the growth functions of TEOAEs. These non-uniformities were more prevalent in the 1 and 2 kHz regions than in the 4 kHz region. Furthermore, the rate of growth of the responses varied by emission type and by frequency. This is further evident when examining the mean values for the slopes of the growth functions, which are illustrated in Fig. 2. As stimulus frequency region increased, DPOAE growth functions became steeper (M = 0.66, 0.69 and 0.95 for 1, 2 and 4 kHz), whereas the slopes of the TEOAE growth functions decreased (M = 0.54, 0.45 and 0.28 for 1, 2 and 4 kHz). Across emission types, results were significantly different ($P < 0.01$) at 4 kHz. Within emission types, only the TEOAE slopes at 4 kHz differed significantly from the slopes at the other two frequencies.

The maximum levels of DPOAEs obtained with stimuli from 50 to 65 dB SPL were compared with the levels of TEOAEs for higher level stimuli for the sample of ten ears in the first investigation. As illustrated in Fig. 3, the levels for each of the three frequencies were correlated; the 1 and 2 kHz correlations were higher (r = 0.83 and r = 0.89, respectively) than the 4 kHz correlation (r = 0.61). Although reductions in the absolute amplitude of the 4 kHz toneburst-evoked responses might be expected because of the poor high-frequency response of the ILO88 system, affectation of the growth of the responses would not be expected.

Results from the second investigation were compared for selected frequency regions and for overall response level. These comparisons are illustrated in Fig. 4. DPOAE response levels obtained for L_1 = 70, L_2 = 64 dB SPL were averaged and compared with the energy in the spectrum of the TEOAEs obtained with click stimuli at 86 dB SPL. For the comparisons, the energy in a 400 Hz wide band corresponding to three frequency regions was taken from the spectrum of the click-evoked

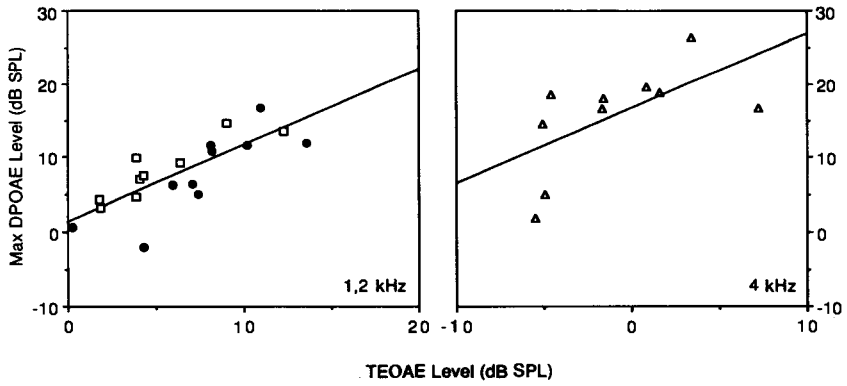

Fig. 3. Comparison of maximum levels of DPOAE and TEOAE responses for 1, 2 and 4 kHz stimuli (1k, dots; 2k, open squares; 4k, triangles). Correlations were higher for the 1 and 2 kHz results than for the 4 kHz results.

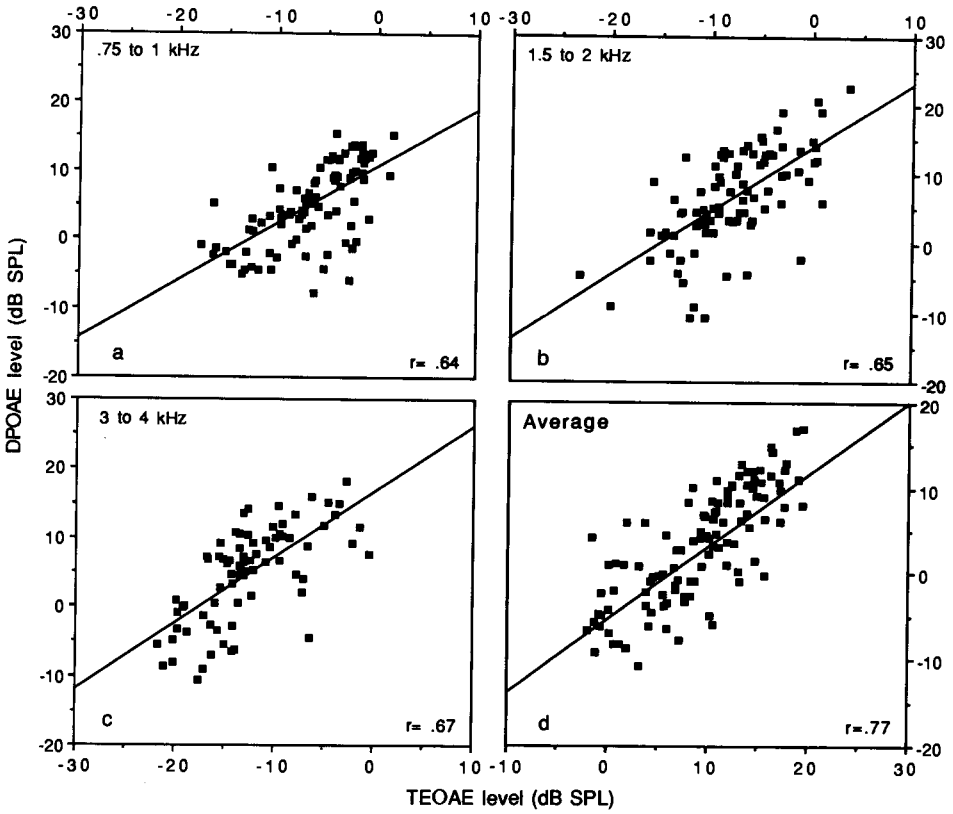

Fig. 4. Correlation of DPOAE level with TEOAE level by frequency for 170 ears with a broad range of pure tone threshold levels. Panel (*a*): 0.75, 1 kHz; panel (*b*): 1.5, 2 kHz; panel (*c*): 3, 4 kHz; panel (*d*): averaged DPOAE response level (0.75 – 4 kHz) with overall power of the TEOAE. Note that the axis values for panel (*d*) differ from those in the other three panels.

reponse. Panels (*a*) through (*c*) (Fig. 4) illustrate results for the lower (0.75, 1 kHz), mid (1.5, 2 kHz) and higher (3, 4 kHz) frequency ranges, respectively. The results in panel (*d*) represent the overall click-evoked response level compared with the averaged DPOAE responses for the six individual frequency regions. Results from both the normally hearing and the hearing-impaired ears are included (n = 170). The highest correlation (r = 0.77) was obtained for the overall click-evoked response level and the averaged DPOAE responses from 0.75 to 4 kHz.

The slopes of the regression lines in panels (*a*) to (*c*) increase systematically from 0.83 × at 1 kHz to 0.95 × at 4 kHz, indicating a stable or increasing amplitude of DPOAEs with increasing stimulus frequency together with a decreasing amplitude of click-evoked responses from 1 to 4 kHz. Therefore, the finding of smaller amplitudes at 4 kHz for TEOAEs obtained using tonebursts in the ten ears of Investigation I is corroborated by the results of Investigation II, which were obtained using clicks and slightly different methods.

Discussion

These studies have compared TEOAEs and DPOAEs in the same ears of normally and pathologically hearing subjects with the aim of learning more about the similarities and differences of these two types of emission. Inferences concerning the generation processes, the frequency specificity, and

the clinical applications of TEOAEs and DPOAEs can be made from such comparisons.

Our results indicate that TEOAE and DPOAE amplitudes are correlated to some extent in the same ear (Figs. 3 and 4). A large amount of interindividual variability is known for all types of OAEs, and this has not been accounted for completely. For example, spontaneous OAEs are present in only about 40% of normally hearing human ears and can be detected only exceptionally in non-primate ears (for review, see Probst et al., 1991). Normally hearing ears with spontaneous OAEs demonstrate larger amplitudes and generally broader overall spectra of TEOAEs than do ears without spontaneous emissions, even when the ears are audiologically comparable (Probst et al., 1986). The concept of a set of ears with OAEs that are relatively easy to measure may be considered from a functional perspective. So-called "active" ears may provide more information about cochlear non-linear mechanisms in combination with outer and middle ear mechanics, which includes the microphone probe as part of the transmission line. Alternatively, these ears may use higher gains for cochlear amplification than do ears with OAEs that have relatively small amplitudes. Possibly, the specific arrangement of OHCs along the basilar membrane (BM) may also contribute to interindividual differences (Probst, 1990). Whatever the reason for these relatively large interindividual differences, the significant correlations between TEOAE and DPOAE amplitudes within the examined frequency range of 1 – 4 kHz indicate that "active" ears have TEOAEs and DPOAEs that are both relatively high in amplitude. To a first approximation, it is thus likely that TEOAEs and DPOAEs are derived from some common process. However, it remains to be demonstrated if this correlation is an effect of a better "window" to the cochlea, in the form of a more effective transmission line, or if some common generation process is more active in some ears and in some frequency regions than in others.

In spite of the significant correlation between TEOAE and DPOAE amplitudes, clear differences between these two types of emission were identified. These included differences in absolute amplitudes and in growth functions between lower and higher frequency regions. Overall, the growth functions of DPOAEs were steeper and had more non-uniformities than did those of TEOAEs (Figs. 1 and 2). It has been demonstrated previously that non-uniform DPOAE growth functions are even more common when L_1 is greater in amplitude than L_2 (Harris and Probst, 1990). The most obvious differences between the growth functions were present as a function of increasing frequency of the stimuli. The shallower slopes of low-frequency TEOAE growth functions became even shallower at higher frequencies. In contrast, the slopes of the DPOAE growth functions, which were not significantly steeper than those of the TEOAE functions at 1 and 2 kHz, became significantly steeper at 4 kHz. With increasing frequency of the stimuli, growth of DPOAEs increased, whereas growth of TEOAEs decreased. Similar trends were evident when amplitudes of the responses obtained with relatively high stimulus levels were compared (Fig. 4). Whereas the amplitudes of TEOAEs were clearly smaller at 4 kHz than at either 1 or 2 kHz, the amplitudes of DPOAEs were about the same or slightly higher at 4 kHz than at either 1 or 2 kHz. Although technical factors may have contributed in part to the differences in TEOAE amplitudes across frequency for click stimuli, the stimulus levels for the tonebursts were held relatively constant across frequency. Up to approximately 4.5 kHz, the system's response is relatively flat. Analogous to the previous discussion of interindividual differences, the differences in DPOAE and TEOAE growth functions and amplitudes could be the result either of different processes in retrograde transmission or in cochlear generation. A combination of both transmission and generation differences is also conceivable.

Examination of TEOAE thresholds in ears with high-frequency hearing loss led Avan et al. (1991) to conclude that TEOAEs were not a local phenomenon of the stimulated site of the BM. They considered amplitudes and thresholds of TEOAEs to be dependent upon the state of the entire BM from the stimulated site towards the cochlear base. Loss of

the number of active elements over half of the BM from the stimulated site basalward would reduce the amplitude of TEOAEs by half. According to the model proposed by Avan et al. (this volume), TEOAEs are either a reflection of global cochlear activity or their propagation back to the stapes is dependent upon an active contribution of the BM. Our finding of smaller amplitudes of TEOAEs with increasing frequency is consistent with such a model in that TEOAEs generated by higher frequencies, rather than lower frequencies, would have a shorter portion of the BM either to generate them or to contribute to their backward propagation.

If the assumption of a basal BM contribution to TEOAEs is correct, then it follows that the absence of amplitude decreases for high-frequency DPOAEs implies a fundamentally different mechanism of either generation or propagation of the two emissions. The retrograde traveling wave of TEOAEs is propagated by a BM not occupied by other stimuli and the active mechanism can be assumed to be at its most effective operating point. In contrast, the DPOAE at $2f_1$-f_2 is generated apically to the place of maximal BM displacement during stimulation, and it is transported to the stapes through this stimulated BM region. This may partially explain the occurrence of non-uniformities in the growth functions of DPOAEs and the relative amplitudes of the emissions. The active elements would be saturated in at least some regions of the BM and could not contribute to the backward propagation of the emission. Our findings are consistent with such an explanation. A difference in the properties of the retrograde propagation could explain the amplitude differences between TEOAEs and DPOAEs relative to frequency.

Whether only the retrograde propagation mechanisms along the BM are different for the two emission types or whether the generation mechanisms themselves are different cannot be answered by our investigations. Some evidence in the literature suggests differences in the generation process itself. One such indication is a clear difference in the properties of DPOAEs from different species (Probst, 1990). Laboratory animals, such as rabbits (Lonsbury-Martin et al., 1987) or rodents (Brown and Gaskill, 1990) with regular patterns of OHCs along the BM, show considerably larger DPOAEs than do primates (Martin et al., 1988) or humans (Probst and Hauser, 1990) with OHC patterns that are much less regular. In contrast, TEOAEs are much larger in amplitude in humans than in small laboratory animals, where they may be difficult to detect.

An additional indication of different generation processes between TEOAEs and DPOAEs is the finding of a differential influence of salicylates on the two types of emission in humans (Wier et al., 1988) and primates (Martin et al., 1988).

Kemp (1988) suggested a division between slow-acting cochlear non-linearities, which respond to the envelope of the stimulus, and fast-acting non-linearities, which respond cycle by cycle. The long latencies found in human TEOAEs indicate that they are generated predominantly by a slow-acting non-linearity. Absolute latency of DPOAEs is difficult to measure, but group latencies can be defined by phase measurements. Phase measurements by Kemp (1986) indicated that the latency of DPOAEs depends on stimulus parameters. Short group latencies occur with relatively large f_2/f_1 ratios, and it can be assumed that DPOAEs are at least partially generated by a fast-acting non-linearity.

In summary, variations across species, in drug responses and in latencies argue for some differences in generation processes of TEOAEs and DPOAEs. Even if this is the case, our finding of a significant correlation of TEOAE and DPOAE amplitudes makes it probable that these different generation processes share some common properties. The question then becomes, is one technique better than another for clinical purposes of screening or monitoring cochlear function? Both measurements have certain limitations. Intersubject variability in human ears with normal functional hearing sensitivity is relatively large in both measurements, and it may make interpretation of findings difficult. In particular, the accuracy with which the magnitude of hearing loss by frequency can be predicted using DPOAEs or TEOAEs appears to have limita-

tions. In addition, the frequency ranges of both measurements, when obtained using current techniques, have shortcomings. The high-frequency response for the most widely used system of measuring TEOAEs is limited to 4 kHz and the separation of low-frequency DPOAEs (below 1 kHz) from background noise must be improved. As technology improves, simplicity of measurement is becoming less of an issue than it has been formerly.

A critical point in selecting one measurement over the other may be the frequency specificity of the two types of emission. Our own results (Probst et al., 1987) and those of Avan et al. (1991) question the frequency specificity of TEOAEs and suggest that they are a response of a relatively large section of the BM. Numerous investigations have determined that TEOAEs are absent when overall auditory sensitivity exceeds approximately 25 – 30 dB HL (Probst et al., 1991). Because of this, click-evoked OAEs are a very effective technique as a screening procedure for the identification of hearing loss, especially in neonates and small children.

The findings of this study are consistent with the possibility that DPOAEs are more frequency-specific than are TEOAEs. The steady-state condition of the stimulation by continuous pure tones and the high probability that only a limited region of the BM is contributing to the fast-acting non-linearity producing DPOAEs support this notion. However, only further physiological and clinical investigations will definitively resolve this question.

Most likely, both TEOAE and DPOAE measures will be important in evaluating the auditory system's response to transient or to steady-state stimuli, depending upon the particular clinical question that is being asked. It is already clear that OAE measurements are an important contribution to clinical auditory evaluation.

Acknowledgements

This work was supported by a grant to R. Probst from the Swiss National Foundation (Proj. Nr. 32-25514.88).

References

Avan, P., Bonfils, P., Loth, D., Trotoux, J. and Narcy, P. (1991) Quantitative assessment of human cochlear function by evoked otoacoustic emissions. *Hear. Res.*, 52: 99 – 112.

Brown, A. and Gaskill, S. (1990) Measurement of acoustic distortion reveals underlying similarities between human and rodent mechanical responses. *J. Acoust. Soc. Am.*, 88: 840 – 849.

Brownell, W.E. (1990) Outer hair cell electromotility and otoacoustic emissions. *Ear Hear.*, 11: 82 – 92.

Harris, F.P. and Probst, R. (1990) Growth function of tone burst and distortion-product otoacoustic emissions in humans. In: P. Dallos, C.D. Geisler, J.W. Matthews, M.A. Ruggero and C.R. Steele (Eds.), *The Mechanics and Biophysics of Hearing*, Springer, Berlin, pp. 178 – 185.

Harris, F.P., Lonsbury-Martin, B.L., Stagner, B.B., Coats, A.C. and Martin, G.K. (1989) Acoustic distortion products in humans: systematic changes in amplitude as a function of f1/f2 ratio. *J. Acoust. Soc. Am.*, 85: 220 – 229.

Horner, K.C., Lenoir, M. and Bock, G.R. (1985) Distortion product otoacoustic emissions in hearing-impaired mutant mice. *J. Acoust. Soc. Am.*, 78: 1603 – 1611.

Kemp, D.T. (1986) Otoacoustic emissions, travelling waves and cochlear mechanisms. *Hear. Res.*, 22: 95 – 104.

Kemp, D.T. (1988) Developments in cochlear mechanics and techniques for noninvasive evaluation. In: D.G. Stephens (Ed.), *Measurements in Hearing and Balance*, Karger, Basel, pp. 27 – 45.

Kemp, D.T., Bray, P., Alexander, L. and Brown, A.M. (1986) Acoustic emission cochleography – practical aspects. *Scand. Audiol. (Suppl.)*, 15: 71 – 96.

Lonsbury-Martin, B.L., Martin, G.K., Probst, R. and Coats, A.C. (1987) Acoustic distortion products in rabbit ear canal. I. Basic features and physiological vulnerability. *Hear. Res.*, 28: 173 – 189.

Martin, G.K., Lonsbury-Martin, B.L., Probst, R. and Coats, A.C. (1988) Spontaneous otoacoustic emissions in a nonhuman primate: I. Basic features and relations to other emissions. *Hear. Res.*, 33: 49 – 68.

Martin, G.K., Ohlms, L.A., Franklin, D.J., Harris, F.P. and Lonsbury-Martin, B.L. (1990) Distortion product emissions in humans. III. Influence of sensorineural hearing loss. *Ann. Otol. Rhinol. Laryngol. (Suppl.)*, 236: 29 – 44.

Mountain, D.C. (1980) Changes in endolymphatic potential and crossed olivocochlear bundle stimulation alters cochlear mechanics. *Science*, 210: 71 – 72.

Probst, R. (1990) Otoacoustic emissions: an overview. In: C.R. Pfaltz (Ed.), *New Aspects of Cochlear Mechanics and Inner Ear Pathophysiology*, Karger, Basel, pp. 1 – 91.

Probst, R. and Hauser, R. (1990) Distortion product otoacoustic emissions in normal and hearing-impaired ears. *Am. J.*

Otolaryngol., 11: 236 – 243.

Probst R., Coats, A.C., Martin, G.K. and Lonsbury-Martin, B.L. (1986) Spontaneous, click- and toneburst-evoked otoacoustic emissions from normal ears. *Hear. Res.*, 21: 261 – 275.

Probst, R., Lonsbury-Martin, B.L. and Martin, G.K. (1991) A review of otoacoustic emissions. *J.Acoust. Soc. Am.*, 89: 2027 – 2067.

Wier, C.C., Pasanen, E.G. and McFadden, D. (1988) Partial dissociation of spontaneous otoacoustic emissions and distortion products during aspirin in humans. *J. Acoust. Soc. Am.*, 84: 230 – 237.

J.H.J. Allum, D.J. Allum-Mecklenburg, F.P. Harris and R. Probst
Progress in Brain Research, Vol. 97

Overview and critique of Chapters 10 – 13

M.A. Cheatham

Evanston, IL 60208, U.S.A.

Of the papers in this section on central auditory physiology, the contribution by Scheich et al. is most closely related to the theme of this meeting on Natural and Artificial Control of Hearing and Balance. Their introduction acknowledges dissatisfaction with the average improvement across all cochlear implant patients and with the inability to accurately specify the prognosis for any given individual candidate prior to implantation. In this regard, the authors suggest that plasticity exhibited in the central auditory pathway may be a critical factor in post-operative performance. Thus, the possibility exists that auditory training may play an important role in rehabilitation if cortical plasticity is maintained following deafness. The study of learning-induced plasticity reported by Scheich et al. is an attempt to expand understanding in this area of research.

The purpose of these preliminary gerbil experiments was to determine the degree to which aversive conditioning changes cortical frequency representation. If the latter represents a specific effect, then changes in frequency response characteristics should be restricted to the conditioned stimulus and its adjacent frequencies. In other words, learning-induced changes should be restricted to the stimulus frequency whose significance is acquired during conditioning (Weinberger and Diamond, 1988). This suggests that results from control experiments are necessary to rule out the possibility that changes produced by conditioning do not simply reflect a general increase in excitability. Consequently, it is unfortunate that blurring in the frequency representation demonstrated for the differential conditioning paradigm (Scheich et al., Fig. 5) prevented an analysis of spatial shifts in 2-deoxyglucose labeling for trained versus control groups. These results are especially important before we can know if associative learning influences the representation of frequency in auditory cortex. While the long-term payoff of this scientific approach could be dramatic, its clinical impact awaits further experimental results.

The paper by Moore et al. addresses the degree to which plasticity is expressed in adults versus neonates. In these experiments, neonatal cochlear ablation induces degeneration in ventral cochlear nucleus (CN) on the operated side as well as an altered connectivity to the inferior colliculus (IC) on the non-operated side. Since the IC provides an obligatory synapse in the ascending auditory pathway, recordings here are well placed to reflect differences between the brain-stems of animals raised with only one cochlea versus those with two.

Results from ablated ferrets verify earlier reports for gerbil (Nordeen et al., 1983; Kitzies and Semple, 1985) and demonstrate that single units recorded in the central nucleus of the IC on the unoperated side have lower thresholds, higher discharge rates, larger dynamic ranges and shorter latencies when compared to responses recorded in animals with two cochleae.

Additional recordings from superior colliculus (SC) on the operated side demonstrated broader spatial receptive fields but only at moderate levels. This is consistent with an earlier report in guinea pig

by Palmer and King (1985) who suggested that this effect reflects the removal of inhibitory ipsilateral inputs. The degree to which enhanced excitability observed in the contralateral IC relates to changes produced in spatial receptive fields measured in the ipsilateral SC remains to be determined. However, an anatomical basis for this idea does exist in that the central nucleus of IC projects to both the dorsal cortex and the external cortex of IC (Coleman and Clerici, 1987). The latter regions are also known to innervate superior colliculus (Edwards et al., 1979). Since the ferret has an extremely long postnatal period of development, it may be an ideal animal for studying the maturation of neural connections necessary to establish spatial maps in the auditory system and the importance of binaural interactions to the organization of the central auditory pathway.

Because knowledge obtained at lower levels in the auditory system is undoubtedly important to our understanding of the physiology of higher-order stations, it is useful to characterize input to the central nervous system. Since auditory nerve responses to single and two-tone inputs have been thoroughly documented, Palmer and Moorjani concentrate on how more complex signals are represented. This provides an important first step in the study of central mechanisms which underlie the perception of speech. One of the motivations behind this research is the observation that listeners are able to selectively attend to one speaker in the presence of a competing message. Since an important clue to selective listening is the difference in fundamental frequency or voice pitch between two speakers, Palmer and Moorjani were interested to learn how this acoustic feature is represented in the timing of neural discharges and to what extent this representation is affected by cochlear hearing loss.

By presenting synthetic vowels in pairs, concurrently and monaurally, Palmer (1990) showed that the temporal aspects of neural discharges in normal guinea pigs contain sufficient information for the identification of fundamental frequency and for the segregation of constituents in the two vowels. However, in pathological animals single units have elevated thresholds and broader tuning curves. In addition, these units frequently exhibit modulation only at the lower of the two fundamental frequencies of the double vowel, thereby removing one of the cues for identification. This may relate to synchrony suppression (Young and Sachs, 1979) in which strong, low-frequency components in the spectrum dominate a unit's response, effectively masking responses to weaker components. Since tuning curves in pathological animals are broader than normal, low-frequency energy can "capture" the response and decrease synchrony. If these changes described for pathological animals also characterize hearing loss in man, they will ultimately result in vowel confusions as Palmer and Moorjani point out.

The final paper in this section contributes to our understanding of neural circuitry within CN which represents an obligatory synapse for all auditory nerve fibers. Studies in dorsal CN were undertaken by Evans and Zhao to determine whether different cell types respond selectively to GABA and glycine and which aspects of the inhibitory response are mediated by each neurotransmitter. Since cells in this region have complex response patterns, dorsal CN is thought to exhibit a high level of synaptic integration. The GABA system was investigated using bicuculline (BIC) which antagonizes the $GABA_A$ receptor and baclofen (BAF) which is a $GABA_B$ agonist. Strychnine (STR) was used to block the effects produced by glycine.

Based on responses produced by Type IV cells, which may be associated with giant and/or fusiform cells, application of STR produced a release from inhibition. This was demonstrated in Type IV cells whose non-monotonic rate-intensity functions become monotonic during application of the glycine antagonist. This confirms a previous report by Caspary et al. (1987). If this sustained inhibition observed in Type IV cells is related to inputs from Type II interneurons as suggested by Young et al. (1988), then the Evans and Zhao results imply that Type II cells use glycine as a transmitter.

Although the Evans and Zhao results are generally consistent with Caspary et al.'s previous findings, the changes presented in Fig. 2 from Evans and

Zhao for a Type IV cell differ from the Caspary et al. (1987) report. The latter states that this blocker of the $GABA_A$ receptor does not influence cells with non-monotonic rate-level functions. Perhaps resolution of these inconsistencies will be revealed in further investigations. It would also be beneficial if response properties were collected during recovery periods to demonstrate reversibility of these pharmacological effects. Certainly these results from in vivo experiments, coupled with those using the slice preparation (Rhode et al., 1983), should provide a basis for understanding neural processing in dorsal cochlear nucleus.

References

Caspary, D.M., Pazara, K.E., Kossl, M. and Faingold, C.L. (1987) Strychnine alters the fusiform cell output from the dorsal cochlear nucleus. *Brain Res.*, 417: 217 – 282.

Coleman, J.R. and Clerici, W.J. (1987) Sources of projections to subdivisions of the inferior colliculus in the rat. *J. Comp. Neurol.*, 262: 215 – 226.

Edwards, S.B., Ginsburgh, C.L., Henkel, C.K. and Stein, B.E. (1979) Sources of subcortical projections to the superior colliculus in the cat. *J. Comp. Neurol.*, 184: 309 – 330.

Kitzies, L.M. and Semple, M.N. (1985) Single-unit responses in the inferior colliculus: effects of neonatal unilateral cochlear ablation. *J. Neurophysiol.*, 53: 1483 – 1500.

Nordeen, K.W., Killackey, H.P. and Kitzies, L.M. (1983) Ascending projections to the inferior colliculus following unilateral cochlear ablation in the neonatal gerbil, *Meriones unguiculatus. J. Comp. Neurol.*, 214: 144 – 153.

Palmer, A.R. (1990) The representation of the spectra and fundamental frequencies of steady-state single- and double-vowels in the temporal discharge patterns of guinea pig cochlea nerve fibers. *J. Acoust. Soc. Am.*, 88: 1412 – 1426.

Palmer, A.R. and King, A.J. (1985) A monaural space map in the guinea-pig superior colliculus. *Hear. Res.*, 17: 267 – 280.

Rhode, W.S., Smith, P.H. and Oertel, D. (1983) Physiological response properties of cells labelled with horseradish peroxidase in cat dorsal cochlear nucleus. *J. Comp. Neurol.*, 213: 427 – 447.

Weinberger, N.M. and Diamond, D.M. (1988) Dynamic modulation of the auditory system by associative learning. In: G.M. Edelman, W.E. Gall and M.W. Cowan (Eds.), *Auditory Function: Neurobiological Bases of Hearing,* Wiley, New York.

Young, E.D. and Sachs, M.B. (1979) Representation of steady-state vowels in the temporal aspects of the discharge patterns of populations of auditory nerve fibers. *J. Acoust. Soc. Am.*, 66: 1381 – 1403.

Young, E.D., Shofner, W.P., White, J.A., Robert, J-M. and Voigt, H.F. (1988) Response properties of cochlear nucleus neurons in relationship to physiological mechanisms. In: G.M. Edelman, W.E. Gall and W.M. Cowan (Eds.), *Auditory Function: Neurobiological Bases of Hearing,* Wiley, New York, pp. 277 – 312.

J.H.J. Allum, D.J. Allum-Mecklenburg, F.P. Harris and R. Probst
Progress in Brain Research, Vol. 97

CHAPTER 10

Responses to speech signals in the normal and pathological peripheral auditory system

A.R. Palmer and P.A. Moorjani

MRC Institute of Hearing Research, University Park, Nottingham NG7 2RD, U.K.

The responses to single (/a/ and /i/) and double vowel (/a,i/) stimuli of normal guinea pig cochlear nerve fibres are compared with those from animals with a cochlear hearing loss. When the threshold losses are sufficient to exclude the higher harmonics of the /i/, the temporal representation of the second and higher formants is lost. Smaller threshold elevations allow a representation of the second formant when the vowel /i/ is presented alone. However, under double vowel stimulation wider auditory filters allow the capture of the synchrony of high characteristic frequency fibres by lower frequencies thereby losing the higher formants of the /i/ and also much of the information about its fundamental frequency.

Key words: Peripheral auditory system; Hearing loss; Speech signals; Guinea pig

Introduction

The voice of a competing speaker represents a particularly difficult interfering noise in speech perception, even for normal hearing subjects, because the target voice and the background have similar acoustic characteristics. A cochlear hearing impairment exacerbates these difficulties. When a difference in the fundamental frequency (F0) is introduced between members of a pair of voiced vowels, normal listeners often hear two separable voices and their identification performance improves (Scheffers, 1983; Assmann and Summerfield, 1990). We have previously shown that, in normal animals, the fundamental frequencies and the spectra of the constituents of double vowels are well represented in the temporal aspects of the discharge of cochlear nerve fibres (Palmer, 1988, 1990). In the present study, to gain some insight into the nature of the difficulty in attending to a single speaker caused by a cochlear hearing loss, we compare the responses to single and double vowels of cochlear nerve fibres from the normal control animals of our previous study with those from guinea pigs treated with kanamycin. Kanamycin treatment results in destruction of outer hair cells in the cochlea and changes in those cells that remain (see for example, Dallos and Harris, 1978; Harrison and Evans, 1979a; Hackney et al., 1990). The functional effects of these sequelae have been well documented and appear similar to those of other insults to the cochlea (see Patuzzi et al., 1989, for a review) in producing elevation of the minimum threshold of cochlear nerve fibres and a loss of their sharp tuning. Broadening of the auditory filter and increase in threshold are characteristic of hearing loss of cochlear origin in humans (see Moore, 1987, for review).

Methods

Anaesthesia and preparation

Pigmented guinea pigs of 200 g initial weight were given a daily subcutaneous injection of 400 mg/kg kanamycin for ten days. The animals received no kanamycin injection for a period of at least seven days following the last injection. The minimum de-

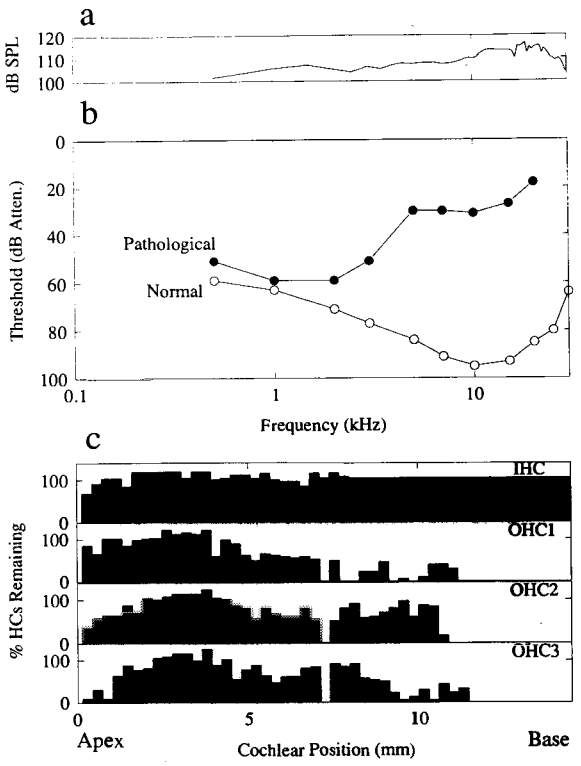

Fig. 1. (*a*) The maximum output level (i.e., at 0 dB attenuation) of the sound system in dB SPL for the normal animal for which the CAP thresholds are shown in Fig. 1*b*. This curve is typical of those measured in all animals in the study. (*b*) Thresholds of the CAP for a normal and a pathological guinea pig. (*c*) Percent of inner hair cells (IHC) and outer hair cells (OHC1 – 3) remaining in the cochlea of the guinea pig for which the CAP audiogram is shown in Fig. 1*b*.

lay we used before the recording experiment was nine days and the maximum was 35 days. We have compared the pathology across three different groups of animals which were used at different delays after the final injection: 9 – 15 days, 15 – 20 days and 20 – 35 days. The range of threshold elevation was broadly similar in each group. This is consistent with the wide variation found by Hackney et al. (1990) after long survival times. It is conceivable that with some of the survival times which we used, the pathology may not have completely stabilized, but it seems unlikely that this would materially affect the conclusions drawn. The pathology resulting from the pharmacological insult was assessed by: (i) the cochlear action potential (CAP) threshold as a function of the frequency (Fig. 1*b*) of a short tone burst (10 msec duration, 0.2 msec rise/fall); (ii) surface preparations of the cochlea (Fig. 1*c*); and (iii) the threshold (Fig. 2) and response areas of single auditory nerve fibres (Fig. 3). As can be seen in Fig. 2, the threshold loss was variable across animals from 20 to 60 dB at any frequency below about 5 kHz.

A total of 21 kanamycin-treated animals were used. The responses to the vowel stimuli of a further 21 normal animals, which have been extensively reported elsewhere (Palmer, 1990), served as comparison control data. Animals were anaesthetized with a neuroleptic technique (0.06 mg atropine sulphate, 30 mg/kg sodium pentabarbitone, 4 mg/kg droperidol, 1 mg/kg phenoperidine). Supplementary doses of sodium pentabarbitone and phenoperidine were administered as required. The animals were tracheotomized and a core temperature was maintained at 37°C.

Full details of the preparation may be found in Palmer et al. (1986). Briefly, recordings were made

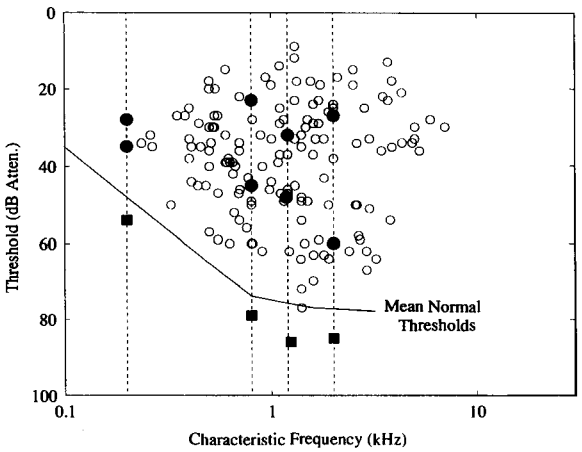

Fig. 2. Thresholds at the best frequency of the fibres recorded from animals treated with kanamycin. The vertical lines are positioned at the harmonic closest to each of the first two formants of the constituents of the double vowel. The filled symbols show the best frequency and threshold of the fibres whose responses are shown in Figs. 4 and 5. The squares indicate data from normal animals.

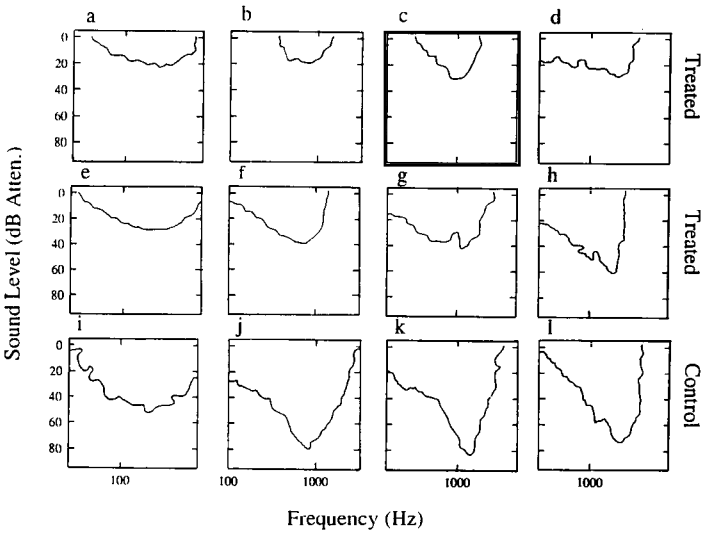

Fig. 3. Response areas of 12 fibres from normal and pathological cochleas demonstrating the range of threshold loss and increase in width of tuning. The response was first determined to a single presentation of a series of tone bursts (5 msec rise/fall, 50 msec duration, 5/sec) covering a five octave range of frequency in 1/10 octave steps and a 90 dB range of level in 5 dB steps. The lines are equal response contour lines calculated objectively.

using 2.7 M KCl-filled micropipettes introduced under direct vision into the cochlear nerve via a posterior craniotomy. The CAP was recorded using a round window electrode and its threshold was estimated by audio-visual criteria.

Following the completion of recordings, animals were decapitated and their cochleas were rapidly removed, placed in 2.5% gluteraldehyde and perfused through the oval and round windows. The cochleas were post-fixed in 1% osmium tetroxide, washed, brought up to 70% alcohol and then dissected for surface preparation.

Stimulation and recording

The vowel sounds /a/ (F0 100 Hz) and /i/ (F0 125 Hz) were produced using a software cascade synthesizer (Klatt, 1980). The double vowel /a(100),i(125)/ was produced by summing the digital waveforms of the single vowels (see fig. 2 of Palmer, 1990, for the double vowel spectrum). The three speech stimuli were presented at a range of sound levels, but all data shown in this paper were obtained with /a/ at 83 dB SPL, /i/ at 77 dB SPL and /a(100),i(125)/ at 85 dB SPL. The frequencies of the first two formants of the vowels were 270 Hz and 2290 Hz for the /i/ and 730 Hz and 1090 Hz for the /a/. The vowels were output from a computer at a 10 kHz sampling rate via an antialiasing filter (set to produce 20 dB of attentuation at 5 kHz, the Nyquist frequency) into a Bruel and Kjaer (4134) 12.7 mm condenser driver and monitored a few millimetres from the tympanic membrane using a second 12.7 mm condenser microphone via a calibrated 1 mm probe tube. Sound levels in this paper are expressed in dB SPL (i.e., r.m.s. pressure levels in dB re 20 mPa). A typical sound system calibration showing the level at maximum output is shown in Fig. 1*a*.

Bursts of wideband noise were used as search stimuli, and the characteristic frequency (CF) and minimum threshold of each fibre were determined using audio-visual criteria. Bursts of the vowel sounds were then presented (500 msec duration at 1/sec) until either 100 presentations were completed or 5000 spikes had been collected. During presentation of the vowels, times of occurrence of neural discharges were measured to 10 μsec accuracy using the computer.

The number of discharges synchronized to the components of the vowels was assessed by Fourier analysis of period histograms locked to the 40 msec period of the double vowel. The distribution, within the ensemble of nerve fibres, of phase-locking to the harmonic components of the vowel stimuli was assessed by computing the average localized synchronized rate (ALSR) function (following Young and Sachs, 1979) in which the average is taken of the discharge synchronized to each component among nerve fibres tuned (± 0.5 octaves) to that component. In principle, it is possible to generate ALSR functions without any matched filtering (Palmer 1990), but this results in inclusion of irrelevant rectifier distortion products. There is ample evidence for shifts in best frequency with threshold elevation in a range of pathologies, but the magnitude of this shift at low best frequencies is unspecified. Thus, we have used a relatively wide frequency interval to minimize inaccuracies involved in the determination of the best frequency of pathological tuning curves.

Results

Responses of single fibres

Fig. 2 shows the minimum thresholds (open and closed circles) from all single fibres in the 21 animals treated with kanamycin. Within each single animal the distribution of thresholds was limited to 20 – 30 dB at any frequency. The vertical dashed lines show frequencies close to the first and second formants of the constituents of the double vowel. The actual frequencies of the dashed lines are 0.2 kHz, 0.8 kHz, 1.2 kHz and 2.0 kHz. The filled symbols on these lines show the thresholds of the twelve fibres for which we illustrate the responses in Figs. 3 and 4; the circles are from treated animals and the squares from normal animals. Fig. 3 shows the response areas of fibres both from normal guinea pigs (*i* – *l*, bottom row) and from guinea pigs with raised thresholds as a result of kanamycin treatment (*a* – *h*). The fibres from the pathological cochleas have been selected to show an intermediate (*e* – *h*)

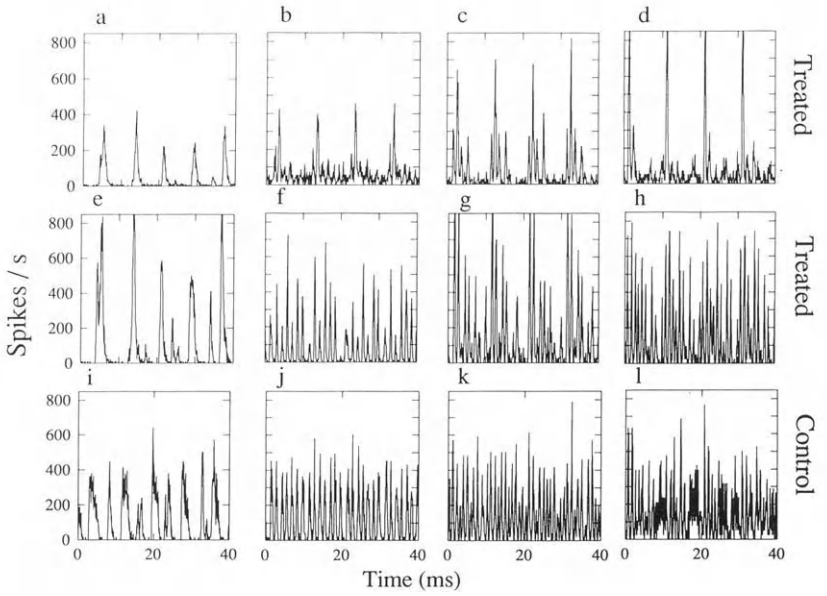

Fig. 4. Period histograms of the responses to the double vowel /a(100),i(125)/ at 85 dB SPL from the same 12 fibres for which response areas are shown in Fig. 3. Binwidth = 78 μsec.

and a severe degree of threshold loss (*a* – *d*). In common with all previous studies of kanamycin intoxication (e.g., Dallos and Harris, 1978; Harrison and Evans, 1979a), we show a loss of the low-threshold sharply tuned tip of the response area. Fig. 4 shows the responses of the same twelve fibres to the double vowel /a(100),i(125)/ in the form of period histograms locked to the period of the double vowel (40 msec). The normal fibres (Fig. 4*i* – *l*) tend to respond to an intense harmonic near a formant peak (this result has been extensively documented; Young and Sachs, 1979; Sinex and Geisler, 1983; Delgutte and Kiang, 1984; Palmer et al., 1986; Palmer, 1990). This is particularly evident in the Fourier spectra of the period histograms (not shown here), but can also be deduced by counting the number of peaks occurring in one period. For example, the fibre in Fig. 4*i* has a CF of 200 Hz and shows ten peaks per 40 msec indicating a strong response to 250 Hz which is the frequency of the harmonic closest to the F1 of the /i/. A similar analysis of the other three histograms from the control fibres reveals a response to an harmonic near a formant of one of the constituents of the double vowel. With increasing threshold elevation and loss of sharp tuning there is a progressive increase in the modulation of the response at the 10 msec period of the F0 of the /a/ (100 Hz) accompanied by a shift in the responsiveness away from the higher frequency components. This is especially evident in the right column, where the fibre in Fig. 4*d* fires preferentially at 10 msec intervals rather than at shorter intervals corresponding to the formant frequency. Even for the lowest CF fibres this tendency is still evident; ascending the left column the response shifts from a domination by 250 Hz (the first formant of /i/) to domination by 125 Hz (F0 of /i/).

Responses of populations of fibres

The modulations in the period histograms (see Fig. 4*b*) provide a potential cue for F0. The distribution, across the population of fibres, of the relative strength of the modulation (quantified as the synchronization index which is calculated as the amplitude of the Fourier component at the F0 divided by the mean discharge rate, which is the zero frequency Fourier component) to each of the F0s of the constituents of the double vowel, is shown separately for normal and kanamycin-treated animals in Fig. 5. In normal animals (Fig. 5*a,b*), different frequency

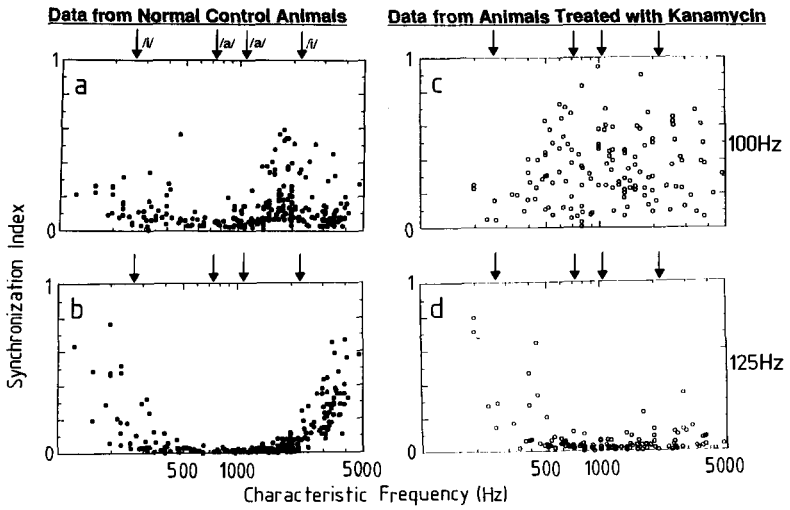

Fig. 5. (*a*) The magnitude (estimated as the synchronization index; the Fourier component at F0 normalized by the magnitude of the zero frequency Fourier component) and distribution of the modulation of normal fibre discharges to the F0 of the constituent vowel /a/. (*b*) The magnitude and distribution of the modulation of normal fibre discharges to the F0 of the constituent vowel /i/. (*c*) and (*d*) are the analogous plots for the pathological fibres.

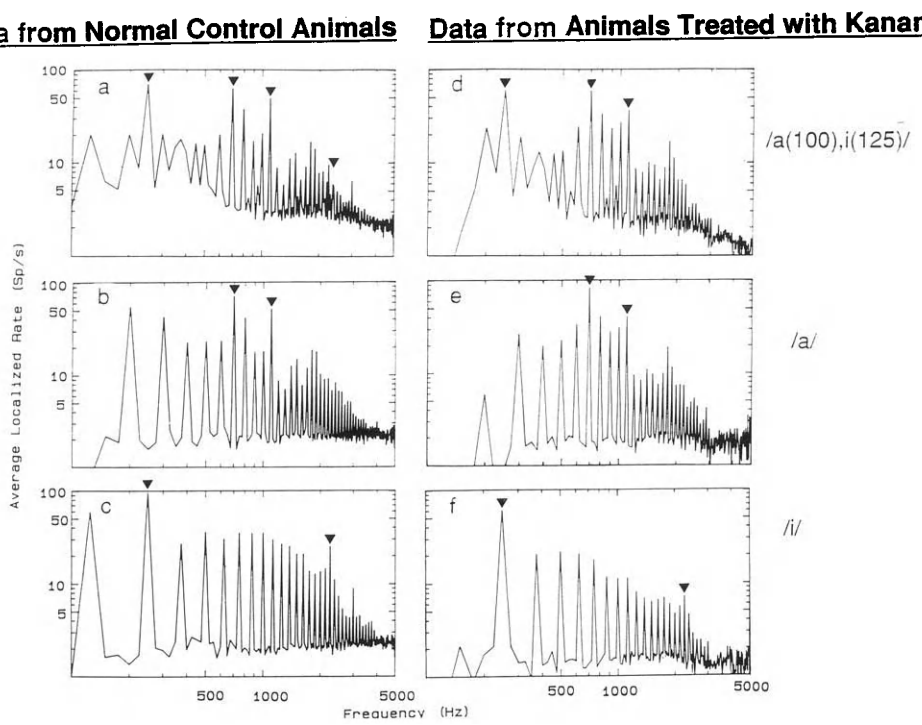

Fig. 6. Average localized synchronized rate (ALSR) functions (after Young and Sachs, 1979) of the responses of normal cochlear nerve fibres to (*a*) the double vowel /a(100),i(125)/, (*b*) the single vowel /a/ and (*c*) the single vowel /i/. (*d*), (*e*) and (*f*) are analogous plots for the population of pathological nerve fibres. The inverted triangles show the harmonics closest to the first two formants of the single vowels and of the constituents of the double vowel.

regions of the population respond to either 100 Hz (at low frequency or between the second formants of the vowels) or 125 Hz (at low frequency or above the second formant of /i/). In the pathological fibres (Fig. 5*c,d*), the modulation to 100 Hz is evident throughout the frequency range except at the lowest frequencies which is the only region showing modulation to 125 Hz. (The arrows in this figure show the frequencies of the first two formants of the constituent vowels, the middle ones are the /a/.)

Fig. 6 shows ALSR functions which summarize the distribution of synchrony to the components of the /a/ (Fig. 6*b,e*), the /i/ (Fig. 6*c,f*) and the double vowel (Fig. 6*a,d*) within the populations of nerve fibres from normal and pathological cochleas. In Fig. 6*a* – *c* synchronized responses can be seen to the harmonics of /i/ and /a/ with larger responses at harmonics nearest the formants which are arrowed. Fig. 6*d* – *f* shows the same analyses for the fibres from kanamycin-treated animals. The fibre responses to the double vowel in Fig. 4 and the population response in Fig. 6*d* show a reduced representation of harmonics of the /i/. In particular, the responses to the higher harmonics of the /i/ are no longer visible in the population response to the double vowel and have been replaced to harmonics of the /a/. The single-vowel population responses are quite similar to those from normal animals, particularly for the vowel /a/. However, the magnitude of the phase-locking to each of the harmonics of the /i/ in quiet is smaller in the pathological than in the normal population. This is because the majority of the fibre responses which contributed to the averages in the pathological population were from fibres stimulated close to their (elevated) thresholds. The pathological population response resembles the normal response qualitatively, particularly in respect of the more prominent responses to harmonics close to the

first and second formants (compared to the responses to other adjacent harmonics). The reason for the well-defined peak at the second formant in the pathological population is the inclusion of fibres with thresholds quite close to those of normal fibres with CFs in the region of the higher formants (see Fig. 2).

Fig. 7 shows a cepstral analysis (Bogert et al., 1963; Miller and Sachs, 1984; Palmer, 1990; a form of non-linear autocorrelation which exposes periodic components) of the population response to the double vowels. For the normal population (Fig. 7*a*) this gives a clear indication of the two F0 frequencies in the peaks at the appropriate time delays (8 and 10 msec). In contrast, as a result of the preponderance of responses to harmonics of the /a/, the cepstrum for the kanamycin data (Fig. 7*b*) shows little indication of the 125 Hz F0 (at the 8 msec position).

Finally, Fig. 8 shows the segregation of the responses to the constituent vowels by sampling the population responses in Fig. 6*a,d* twice, once at the harmonics of the F0 of /a/ (100 Hz) and separately at the harmonics of the F0 of /i/. The dashed lines show the population responses to the single constituent vowels when presented alone. The dots show shared harmonics. The segregated responses in Fig. 8*a,b* at the formant frequencies are remarkably like those obtained to the single vowel alone. The lower magnitude of the phase-locking to the harmonics of the /i/ situated between the first and second formants (in Fig. 8*b*) reflects synchrony suppression of the fibres in this region as a result of their domination by harmonics of the /a/ (see Young and Sachs, 1979). Ignoring the fact that informant concerning the F0 of the /i/ has been severely degraded in the pathological fibres (see Fig. 7), a similar segregation by twice sampling the data in Fig. 6*d* is shown in Fig. 8*c,d*. The second formant of the /i/ is completely absent from the segregated population response in Fig. 8*d*. This is despite the fact that the second formant is visible in the population response to the /i/ alone. The loss is not, therefore, simply a case of the second formant not having enough amplitude to enter the response areas of the pathological fibres (which have a raised threshold). In pooling the data from the pathological cochleas no attempt has been made to ensure a homogeneous threshold elevation and responses from near-normal cochleas have been included. If only fibres with threshold losses at best frequency exceeding 30 dB are used to compute the population response, the peak at the second formant of /i/ disappears even when the vowel is presented in quiet. Under these circumstances, the loss of information about the second formant

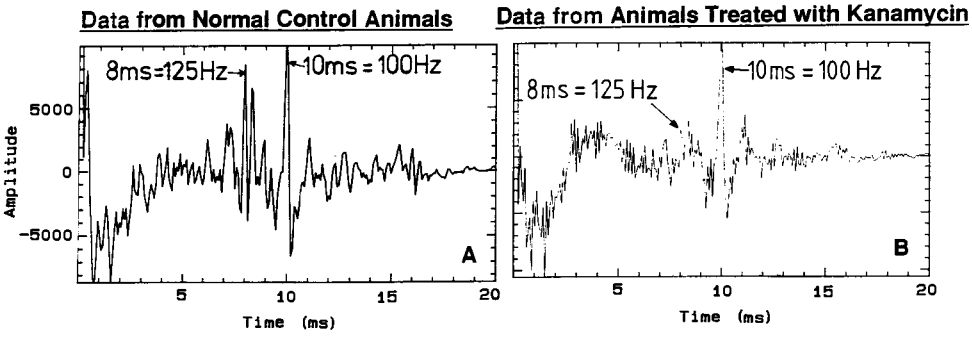

Fig. 7. Cepstra of the population responses to the double vowel from normal (left panel) and pathological fibres (right panel). Cepstra are a form of non-linear autocorrelation function which emphasize periodic components of frequency spectra and which are obtained by taking the inverse Fourier transform of the power spectrum of the curves shown in (*a*) and (*d*). The peaks in the left panel clearly indicate the presence of both the 100 and 125 Hz harmonic series whereas evidence of the 125 Hz series is absent from the right panel.

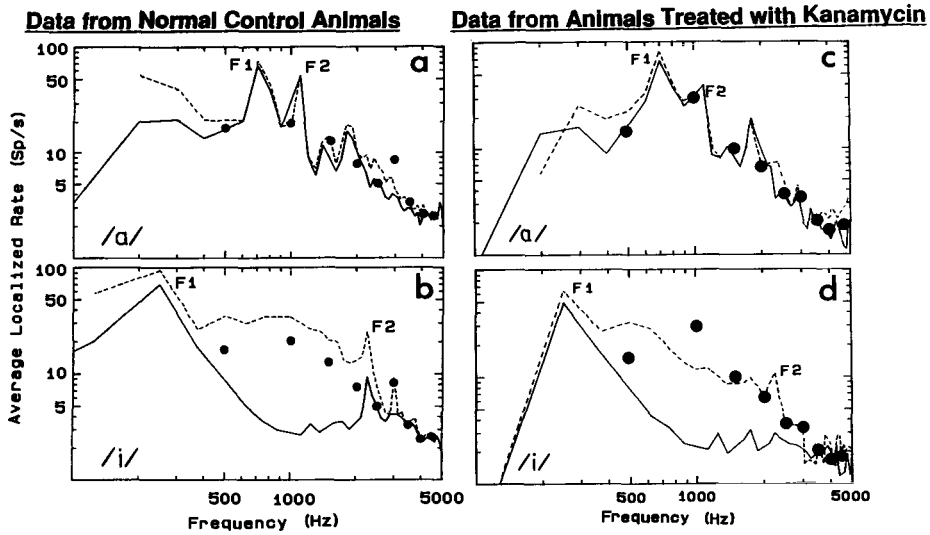

Fig. 8. ALSR functions sampled only at the harmonics of either 100 Hz (*a,c*) or 125 Hz (*b,d*) for the normal fibres (*a,b*) and the pathological fibres (*c,d*). The dashed lines show the functions obtained when the single vowels /a/ (*a,c*) or /i/ (*b,d*) were presented alone. The solid lines are derived by sampling the ALSR function to the double vowel /a(100),i(125)/ separately at the harmonics of each constituent.

merely reflects inadequate energy activating fibres at the F2 frequency as a result of the threshold elevation.

Discussion

Insults to the cochlea which result in a sensorineural hearing loss produce a threshold elevation and a broadening of the psychophysical and physiologically measured filter functions. The threshold loss alone would result in high-frequency components of speech sounds not being heard. However, the results which are described here suggest that even for less severe threshold losses, the representation of high-frequency components may be disrupted in the presence of interfering sounds. There is some dispute as to the degree of disruption of the timing of impulses as a result of kanamycin treatment (cf. Harrison and Evans, 1979b; Woolfe et al., 1981), but there is no doubt that, in the present study, the remaining phase-locking was sufficient for a temporal/place representation of the spectrum of the single vowels (including the second formant of /i/). When the two vowels were simultaneously presented, the phase-locking to harmonics of the /a/ dominated the activity in the region of the F2 of the /i/. The effective level of a tone only needs to be about 20 dB higher than a second tone for it to dominate the phase-locked output of a cochlear nerve fibre completely, and tones lower in frequency more readily dominate the discharge (Brugge et al., 1969). No doubt the threshold elevation in the region of the F2 of /i/ and the broadening of tuning both contributed to this effect by increasing the effective level of the components of /a/ passing through the cochlear nerve fibre filters.

We do not know if the temporal/place code is important for speech perception nor if a mild hearing loss results in the specific kinds of interference between speech sounds shown here. However, if this were the case, we should be able to make some predictions of the additional difficulties which would result. For example, since the first formant of /i/ in isolation is heard as /u/, impaired subjects who identify the single vowel /i/ correctly, should hear the same vowel as an /u/ when another vowel such as /a/ is simultaneously present.

Acknowledgements

We wish to thank Drs. A.Q. Summerfield and I.M. Winter for critical reading of this manuscript.

References

Assmann, P.A. and Summerfield, A.Q. (1990) Modeling the perception of concurrent vowels: vowels with different fundamental frequencies. *J. Acoust. Soc. Am.*, 88: 680 – 697.

Bogert, B.P., Healy, M.J.R. and Tukey, J.W. (1963) The frequency analysis of time series for echoes: cepstrum, pseudocovariance, cross-cepstrum and saphe cracking. In: M. Rosenblatt (Ed.), *Proceedings of Symposium on Time Series Analysis,* Wiley, New York, pp. 209 – 243.

Brugge, J.F., Anderson, D.J., Hind, J.E. and Rose, J.E. (1969) Time structure of discharges in single nerve fibers of the squirrel monkey in response to complex periodic sounds. *J. Neurophysiol.*, 32: 386 – 401.

Dallos, P. and Harris, D. (1978) Properties of auditory nerve responses in absence of outer hair cells. *J. Neurophysiol.*, 41: 365 – 383.

Delgutte, B. and Kiang, N.Y.S. (1984) Speech coding in the auditory nerve: I. Vowel-like sounds. *J. Acoust. Soc. Am.*, 75: 866 – 878.

Hackney, C.M., Furness, D.N. and Steyger, P.S. (1990) Structural abnormalities in inner hair cells following kanamycin-induced outer hair cell loss. In: P. Dallos, C.D. Geisler, J.W. Matthews, M.A. Ruggero and C.R. Steele (Eds.), *The Mechanics and Biophysics of Hearing,* Springer, Berlin, pp. 10 – 17.

Harrison, R.V. and Evans, E.F. (1979a) Cochlear fibre responses in guinea pigs with well defined cochlear lesions. *Scand. Audiol. (Suppl.),* 9: 83 – 92.

Harrison, R.V. and Evans, E.F. (1979b) Some aspects of temporal coding by single fibres from regions of cochlear hair cell degeneration in the guinea pig. *Arch. Otol. Rhinol. Laryngol.*, 224: 71 – 78.

Klatt, D.H. (1980) Software for a cascade/parallel formant synthesizer. *J. Acoust. Soc. Am.*, 67: 971 – 995.

Miller, M.I. and Sachs, M.B. (1984) Representation of voice pitch in the discharge patterns of auditory nerve fibres. *Hear. Res.*, 14: 257 – 279.

Moore, B.C.J. (1987) Psychophysics of normal and impaired hearing. *Br. Med. Bull.*, 43: 887 – 908.

Palmer, A.R. (1988) The representation of concurrent vowels in the temporal discharge patterns of auditory nerve fibres. In: H. Duifhuis, J.W. Horst and H.P. Wit (Eds.), *Basic Issues in Hearing,* Academic Press, London, pp. 244 – 251.

Palmer, A.R. (1990) The representation of the spectra and fundamental frequencies of steady-state single- and double-vowel sounds in the temporal discharge patterns of guinea pig cochlear-nerve fibres. *J. Acoust. Soc. Am.*, 88: 1412 – 1426.

Palmer, A.R., Winter, I.M. and Darwin, C.J. (1986) The representation of steady-state vowel sounds in the temporal discharge patterns of the guinea pig cochlear nerve and primary-like cochlear nucleus neurons. *J. Acoust. Soc. Am.*, 79: 100 – 113.

Patuzzi, R.B., Yates, G.K. and Johnstone, B.M. (1989) Outer hair cell receptor current and sensorineural hearing loss. *Hear. Res.*, 42: 47 – 72.

Scheffers, M.T.M. (1983) *Sifting Vowels: Auditory Pitch Analysis and Vowel Segregation,* Doctoral Thesis, University of Groningen.

Sinex, D.G. and Geisler, C.D. (1983) Responses of auditory nerve fibres to consonant-vowel syllables. *J. Acoust. Soc. Am.*, 73: 602 – 615.

Woolfe, N.K., Ryan, A.F. and Bone, R.C. (1981) Neural phase-locking properties in the absence of cochlear outer hair cells. *Hear. Res.*, 4: 335 – 346.

Young, E.D. and Sachs, M.B. (1979) Representation of steady-state vowels in the temporal aspects of the discharge patterns of populations of auditory nerve fibres. *J. Acoust. Soc. Am.*, 66: 1381 – 1403.

J.H.J. Allum, D.J. Allum-Mecklenburg, F.P. Harris and R. Probst
Progress in Brain Research, Vol. 97

CHAPTER 11

Varieties of inhibition in the processing and control of processing in the mammalian cochlear nucleus

E.F. Evans and W. Zhao

Department of Communication and Neuroscience, University of Keele, Keele, Staffs., ST5 5BG, U.K.

Seven-barrel micropipettes were used to apply drugs microiontophoretically to single units in the dorsal cochlear nucleus (DCN) in chloralose-anaesthetised guinea-pigs. While both agonists and antagonists of putative neurotransmitters in the cochlear nucleus have been investigated in these experiments, the main thrust has been to explore the influence of specific antagonists on cells' spectral and temporal properties, thus elucidating the effects of naturally occurring inhibitory transmitters. At least five types of inhibition appear to be pharmacologically/physiologically separable: (1) Stimulus-evoked tonic "lateral/sideband" inhibition: glycinergic; (blocked by strychnine); responsible for the lateral inhibition of dorsal cochlear nucleus (DCN) type III and IV cells. Strychnine has its predominant effect on sustained (lateral) inhibition compared with the more transient forms of inhibition. Subtraction of receptive field maps enables us to visualise the extent of the inhibitory receptive field. It extends virtually throughout the unit's response field for both these classes but is generally, especially in type IV cells, maximal at the characteristic frequency (CF). This type of inhibition will primarily be responsible for enhancing spectral contrasts in the way that, in the visual system, surround inhibition enhances visual contrast. Furthermore, lateral inhibitory sidebands can "bias" the "working point" of a cell's response so that the dynamic range of effective stimuli and response can be extended. (2) "Background" tonic inhibition: $GABA_A$ergic; (blocked by bicuculline). Blocking this inhibition generally results in an increase in the background (i.e., spontaneous) activity. This inhibition is probably responsible for adjusting excitatory-inhibitory contrasts in both spectral and temporal domains. (3) Stimulus-related off-inhibition appears to be neither glycinergic nor $GABA_A$ergic. Blocking these receptors actually enhances off-inhibition. Nicotinic cholinergic blockers may have a small effect on off-inhibition, but so far we have not been able to block it entirely. This off-inhibition is important for enhancing temporal contrast. This inhibition must, therefore, be mediated by other transmitters, yet undetermined, or by a local feedback circuit or, less likely, be a membrane-based after-effect of stimulation. (4) Pre-synaptic inhibition, mediated by $GABA_B$ receptors presumed to act on primary afferent terminals, thus controlling afferent input to DCN principal cells. (5) Short-latency contralateral inhibition, mediated by glycine.

Key words: Hearing; Auditory pathway; Cochlear nucleus; Neuropharmacology; Glycine; GABA; Cholinergic; Inhibition; Contralateral

Introduction

The cochlear nucleus (CN) is the first stage in the auditory pathway at which inhibition (mediated synaptically in response to single stimuli) is encountered. It is now well recognised that the units of the dorsal division of the cochlear nucleus (DCN) exhibit most of the inhibitory effects encountered in the cochlear nucleus (Evans and Nelson, 1973a).

In the present work, an automated receptive field mapping paradigm (Evans, 1974, 1979b) has been exploited, together with neuropharmacological techniques adapted from the pioneering methods of Caspary (e.g., Caspary et al., 1979) to attempt to dissect out different varieties of inhibition in the dorsal cochlear nucleus of the chloralose anaesthetised guinea-pig. Chloralose has been used as the maintenance anaesthesia following surgery under

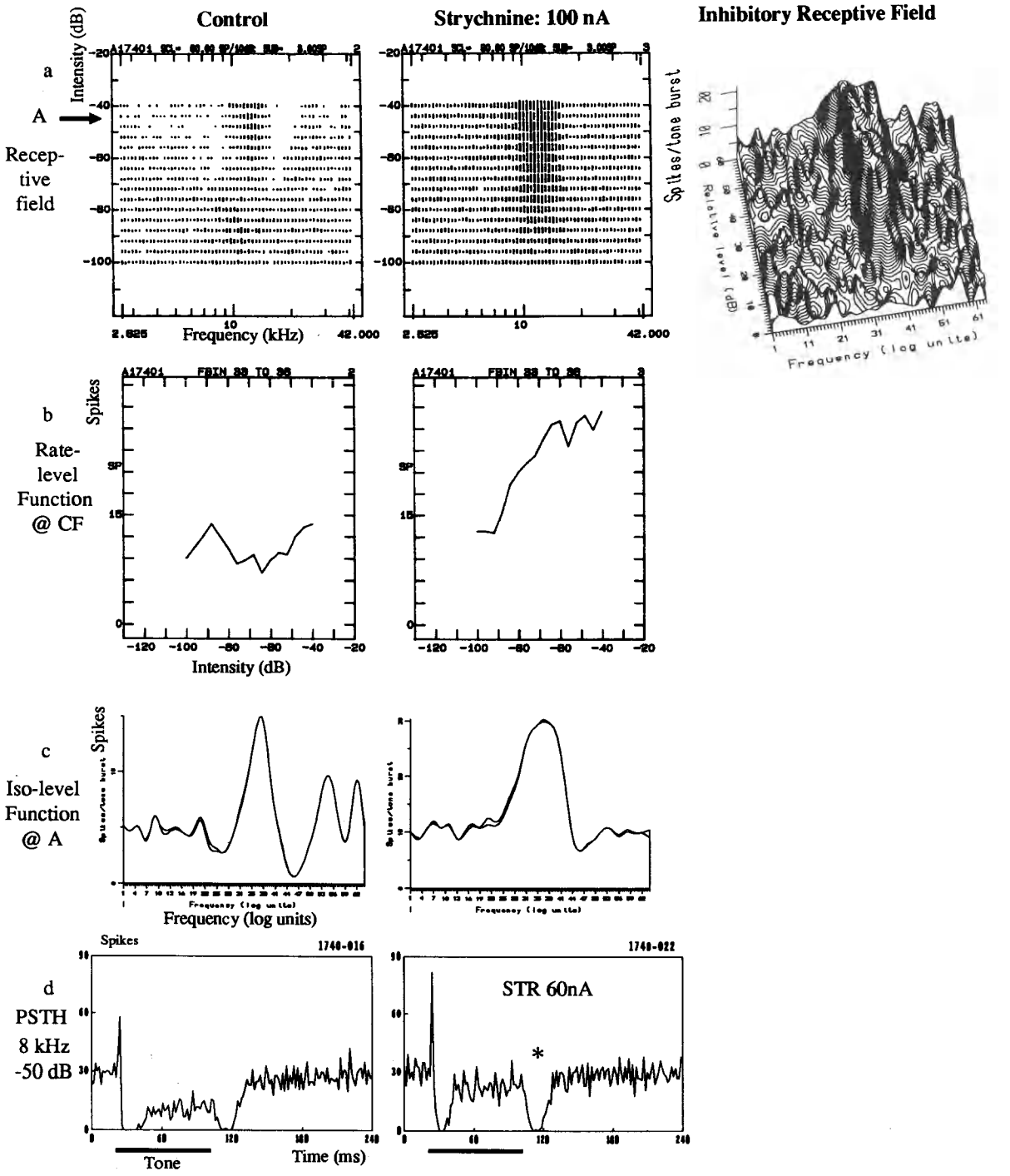

Fig. 1. Effect of strychnine on (*a*) receptive field, (*b*) rate-level function, (*c*) iso-level function, and (*d*) peristimulus time histograms of a type IV cell in DCN. Row (*a*): receptive field maps, before (left), and during (middle) application of strychnine; (right) 3D-contour map of the strychnine-blocked inhibition, obtained by subtracting the control receptive field map from that under strychnine. Row (*b*):

neuroleptanaesthesia (Evans, 1979a,b), because its actions, at least in the cat (Evans and Nelson, 1973a) had least effect on inhibition in the cochlear nucleus, and it provides a highly stable anaesthetic regime in the guinea-pig.

For neuropharmacological dissection of putative inhibitory transmitters, we have studied the effects of iontophoretic application of the specific antagonists of the transmitters, besides those of the agonists themselves and the interactions between agonists and antagonists. This review of our work, however, will concentrate on the results obtained with the antagonists alone so as to elucidate the effects of naturally occurring inhibition. This avoids drawing conclusions potentially based on non-specific effects of the iontophoretic application of the agonists themselves. To this end, we have adapted and extended the techniques of Caspary (e.g., Caspary et al., 1979) as described in more detail in Zhao and Evans (1990, 1991) and Evans and Zhao (1993a,b).

Methods

Briefly, extracellular recordings were made by 7-barrel micropipettes in guinea-pigs anaesthetised with neuroleptanaesthesia for surgery (Evans, 1979a) and maintained by alpha-chloralose (40 mg/kg) given every 2 h or so. The central barrel of the 7-barrelled micro-electrode is NaCl-filled for recording; two barrels are used respectively for current balancing (NaCl) and for localisation of the electrode position (Fast Green). The remaining four barrels contained four agonists or antagonists drawn from: GABA, bicuculline (antagonist to $GABA_A$ receptors), Baclofen (agonist of $GABA_B$ receptors), glycine, strychnine (antagonist to glycine receptors), acetylcholine, atropine (antagonist to muscarinic cholinergic receptors), curarine (antagonist to nicotinic cholinergic receptors). The responses of cochlear nucleus cells recorded extracellularly were collected to pure-tone stimuli of generally 80 msec duration presented four times per second. The tones were presented in a pseudo-random sequence of frequencies and intensities so that a range of 60 dB and typically three octaves was covered evenly in about 4 min of data collection (Evans, 1974, 1979b). The resolution in the intensity domain was typically 4 dB; in the frequency dimension: 1/64 of three octaves. Concurrently, the number of spikes evoked by the cell during the tone burst was counted and plotted (as in Fig. 1*a*) as the length of a vertical bar, the centre of which indicates the respective tone frequency and intensity. Sections can be cut through the receptive field maps: vertically to produce rate-level functions (as in Fig. 1*b*), and horizontally (as in Fig. 1*c*, where the stimulus intensity is marked as A in Fig. 1*a*) to produce iso-level functions. Separately, peristimulus time histograms (PSTH) were collected at on-characteristic (best) frequency (on-CF) and at off-CF frequencies using typically 80 msec tones (see Fig. 1*d*). All tones were shaped with 5 msec linear rise and fall times. In all cases, data were collected before, during and following administration of the antagonist to ensure that the drug effects were fully reversible. One advantage of the automated receptive field mapping paradigm is that by subtracting the control receptive field map (e.g., Fig. 1*a*, left panel) from the receptive field map obtained by blocking the inhibition with the specific antagonist (Fig. 1*a*, middle panel), a receptive field map of the inhibition is obtained (Fig. 1*a*, right-hand panel, plotted as a 3D-contour map; see Evans and Zhao, 1993a,b).

---

rate-level functions obtained at CF (12 kHz), from the receptive field maps of row (*a*). Note conversion by strychnine of non-monotonic rate-level function (control) into a steep monotonic function (right). Row (*c*) shows iso-level functions taken at 52 dB above threshold (−44 dB), indicated by the arrow A in (*a*). Note extensive inhibitory sidebands in control case (left), surrounding narrowed excitatory response region, and removed by the strychnine blockade (right) with widening of the excitatory area and reduction in response contrast. Row (*d*) shows peristimulus time histograms of the cell at 8 kHz, i.e., in the inhibitory sideband below CF. Note strychnine blockade of the *sustained* inhibition only, leaving unaffected the transient inhibition at the onset of the stimulus, and off-inhibition (indicated by asterisk).

"Lateral/sideband" type inhibition

The classical tone-evoked inhibition of the dorsal cochlear nucleus is exemplified in the receptive field map of a type IV cell in Fig. 1*a*, left-hand panel.

We have now shown this inhibition to be glycinergic (Zhao and Evans, 1990; Evans and Zhao, 1993a,b): it can be completely blocked by strychnine (antagonist to glycine receptors), e.g., Fig. 1*a*, centre panel. Here, the receptive field is converted into an excitatory response area, similar to that of a cochlear nerve fibre in shape, but about 2.5 times wider (see below). Subtracting the control receptive field from that in which the glycinergic input is blocked gives, in the right-hand panel of Fig. 1*a*, the glycinergic inhibitory receptive field, shown as a 3D-contour plot. This shows the important result that while the inhibition may appear to be predominantly "lateral" or "sideband", in reality it extends throughout the receptive field and is strongest at the excitatory CF. The previous iontophoretic experiments of Caspary et al. (1987) with strychnine blockade have revealed the existence of glycinergic inhibition at CF. We have now shown that glycinergic inhibition extends beyond the CF region to account for the inhibitory sidebands also.

In experiments reported elsewhere (Zhao and Evans, 1992), we have shown that the excitatory response areas of type IV cells under strychnine blockade are about 2.5 times wider than those of corresponding cochlear nerve fibres from the data of Evans et al. (1992). Thus, the convergent input from at least three cochlear nerve fibres, on average, must be involved in determining the excitatory input to a type IV cell in the dorsal cochlear nucleus of the guinea-pig. Likewise, comparing the bandwidth of the type IV DCN inhibitory receptive fields 10 dB above threshold with the excitatory bandwidth of cochlear nerve fibres of similar CF, the receptive field was found to be some four times larger (Zhao and Evans, 1992). This implies that at least four cochlear nerve fibres, on average, converge upon the interneurones responsible for the inhibitory receptive field. It needs to be emphasized that these type IV cells were found predominantly in the central region of the DCN and probably represent giant cells.

In row (*d*) of Fig. 1 are shown peristimulus time histograms in response to tone bursts at 8 kHz (i.e., in the lower inhibitory sideband). These show that the glycinergic inhibition, blocked by strychnine, is sustained. The transient onset inhibition (and off-inhibition: see later) is not so readily blocked.

The rate-level functions (Fig. 1, row *b*) show that the strychnine blockade converts the non-monotonic rate-level function characteristic of type IV cells into a monotonic rate-level function (right panel). It also shows an increase in the slope of the rate-level function. Similar effects have previously been reported by Caspary et al. (1987). For units with relatively monotonic rate-level functions (e.g., type I and type II cells in the DCN), the effects of strychnine blockade are comparable: the slope of the rate-level function is increased and also the discharge range (i.e., the range of discharge rates between threshold and saturation; Zhao and Evans, 1991).

Row (*c*) shows the effect of strychnine blockade on the iso-level rate function, i.e., a horizontal section through the receptive field map, 4 dB below the maximum level (-44 dB, shown by the arrow at A in row *a*). The left-hand iso-level function shows the strong inhibitory sidebands on either side of a narrow excitatory response area. During strychnine blockade of the inhibition (right-hand iso-level function, corresponding to the centre panel of Fig. 1*a*), the lower inhibitory sideband is completely blocked while the high-frequency inhibitory sideband is almost completely blocked. The loss of this inhibition reveals the true width of the excitatory response, being substantially wider than in the control case, as has been noted above. It also reveals how the spectral contrast (i.e., the ratio of discharge rate between the excitatory centre of the receptive field and the surrounding frequencies) is dependent upon the inhibitory sidebands. "Lateral" or "sideband" inhibition therefore serves to enhance spectral contrast.

Background/tonic inhibition

We have shown the existence of a tonic "background" inhibition on most of the cell types in the DCN, which inhibition is $GABA_A$-ergic and, therefore, is blocked by bicuculline (Zhao and Evans, 1990; Evans and Zhao, 1993a,b). An example of this, for a type IV cell, is shown in Fig. 2. The upper

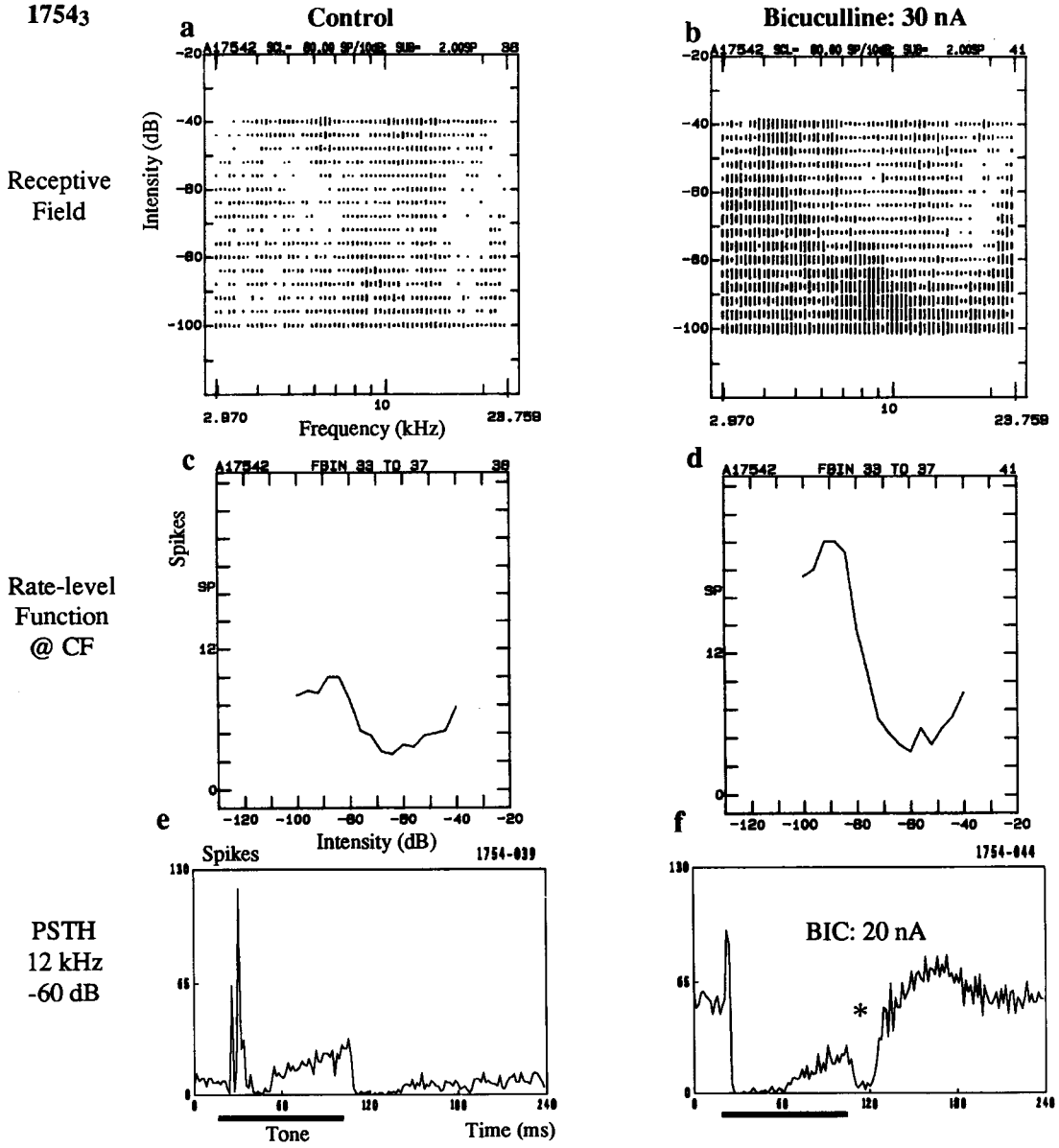

Fig. 2. Effect of iontophoretically applied bicuculline on receptive field of a type IV DCN cell. (*a*), (*b*): Receptive field maps showing increase in spontaneous activity under bicuculline blockade, revealing and enhancing a wide field of inhibition (*b*). (*c*), (*d*): Rate-level function showing enhancement of the non-monotonic function under bicuculline blockade (*d*). (*e*), (*f*): Peristimulus time histogram at CF (12 kHz). Note increase in spontaneous activity under bicuculline blockade (*f*), revealing and enhancing transient and sustained inhibition and converting excitation at CF to net inhibition, leaving intact off-inhibition (indicated by asterisk).

row shows the receptive field maps characteristic of a type IV cell (*a*) before, and (*b*) during bicuculline blockade. The receptive field map (*b*) shows how the bicuculline blockade has increased the background spontaneous activity, without affecting, and even enhancing the inhibitory receptive field.

We have some evidence that this inhibitory blockade by bicuculline does not produce a non-specific increase regardless of stimulus frequency and intensity. Using our subtraction technique (see above; Evans and Zhao, 1993a,b) to compute the effect of the transmitter, its overall inhibitory effect is found to be interrupted at frequencies and intensities corresponding to the excitatory response area, in at least type I cells. Surprisingly, part of this region shows actual excitation. This could occur by a disinhibitory process involving $GABA_A$ action on a glycinergic inhibitory pathway, by interaction between $GABA_A$ and excitatory amino acid systems or, less likely, by a non-specific effect of iontophoretic current on the cell.

The second row in Fig. 2 shows some of the effects of bicuculline blockade of the background inhibition on the rate-level functions. The effects are opposite to those from strychnine. The non-monotonicity of the rate-level function is enhanced. In studies of other types of DCN cells (Zhao and Evans, 1991; Evans and Zhao, 1993a,b), the slopes of the rate-level functions are decreased by application of bicuculline. In several cases, the reduction in slope is accompanied by a reduction in the driven firing rate, thus representing a decrease in the gain of the cell response.

In the lower row in Fig. 2, the peristimulus time histograms of the type IV cell show the enhancement of the spontaneous activity (*f*). This reveals a sustained inhibition during the tone, compared with the mild excitatory response (*e*) in the control and recovery conditions, respectively.

Off-inhibition

This is the inhibition following the end of a stimulus, examples of which are shown in Fig. 1*d* and Fig. 2*f*, also marked by the asterisk in both figures. Neither strychnine nor bicuculline had any effect on this off-inhibition, except that the latter served to enhance it by increasing the background activity. Nor is the off-inhibition sensitive to blockers of muscarinic cholinergic receptors (atropine) (see Zhao and Evans, 1991; Evans and Zhao, 1993a,b). However, we have some preliminary evidence of some effects of nicotinic receptor blockers. During the application of curarine, there is a marked reduction, but not complete blockade, of the off-inhibition. Unfortunately, the curarine also increases somewhat the spontaneous activity. Nevertheless, the degree of off-inhibition seems much less than might be accounted for by the increase in spontaneous activity alone, but this does need to be confirmed.

The question arises of course whether the off-inhibition is a synaptic phenomenon rather than simply a membrane-based phenomenon. That the latter is unlikely to be the case, has been argued by Evans and Nelson (1973a), who presented evidence that the bandwidth of the off-inhibition was more closely related to that of the on-inhibition than to that of the on-excitation. That the off-inhibition can occur without preceding excitation is also shown by the asterix in Figs. 1*d* and 2*f*, again inconsistent with a wholly membrane-determined origin of the off-inhibition.

Pre-synaptic inhibition

Fig. 3 shows an example of the island of excitation in the CF region of a type IV DCN cell, almost entirely blocked by the application of Baclofen (right panel), an agonist of $GABA_B$, thought to be a pre-synaptic inhibitory transmitter.

Similar, although not identical, effects have been reported by Caspary et al. (1984). In particular, in at least one of our cases (shown in Fig. 3), Baclofen could block excitatory input virtually completely, without effect on the spontaneous activity.

Contralateral inhibition

We have shown (Evans and Zhao, 1993b) that stimulation of the contralateral ear evokes an inhibi-

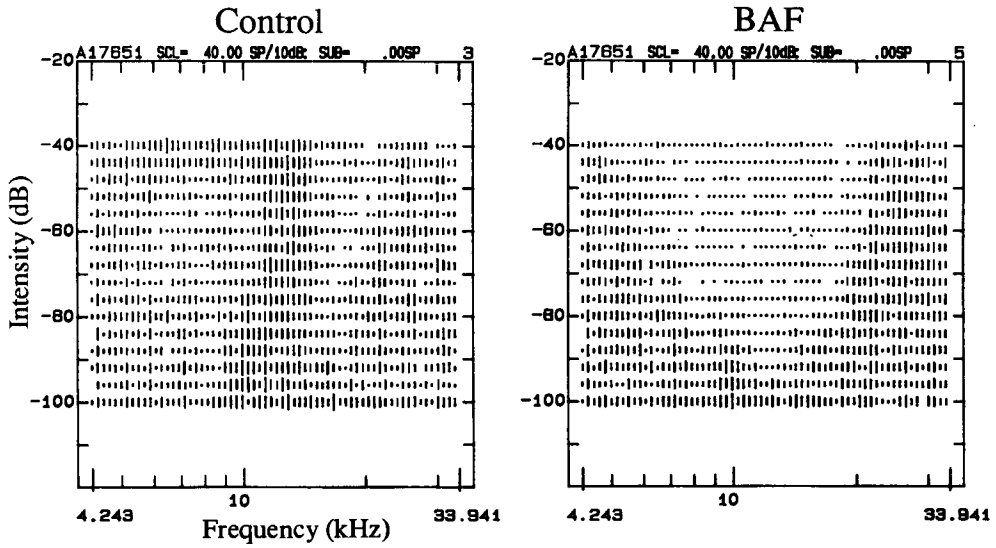

Fig. 3. Effect of $GABA_B$ agonist, Baclofen, on a type IV cell in DCN. Control receptive field map (left) shows mixture of extensive inhibition and central excitatory patches in the type IV receptive field. Right panel shows the disappearance of the excitatory input under Baclofen (30 nA). Note that Baclofen blocked the excitatory response in the receptive field with little effect on the spontaneous activity.

tory receptive field at or just above (in frequency) the ipsilateral excitatory receptive field. Fig. 4*a* shows this in a type III unit under stimulation from the ipsilateral ear (left column) and the contralateral ear (right column). Stimulation of the contralateral ear evoked an inhibitory field at the CF of the ipsilateral excitatory field with, most importantly, a similar threshold to the ipsilateral responses (thus eliminating the possibility of involvement of contralateral acoustic (bone-conducted) cross-talk).

The latency of this contralateral inhibition is short, being about 5 msec greater than ipsilateral excitation (Fig. 4*b*). In other words, it is in the region of 10 msec from stimulus onset. Fig. 4*c,d* shows evidence in another cell that this contralateral inhibition is glycinergic. Fig. 4*c* shows the receptive field maps of ipsilateral (left) and contralateral (right) stimulation. The peristimulus time histograms in (*d*) show the blockade, by strychnine, of the contralateral inhibition.

Conclusions

(1) The glycinergic system responsible for the "lateral/sideband" inhibition in dorsal cochlear nucleus units is frequency-specific and is responsible for the non-monotonic rate-level function. It is also necessary for the enhancement of spectral contrasts, and narrows the response area. It is presumably also responsible for the phenomenon described by Palmer and Evans (1982) in which maskers, surrounding a narrow-band signal and falling in the inhibitory side-bands, can "bias" the working point of a DCN cell, thus extending enormously its dynamic range.

This tone-related sustained inhibition is presumably mediated by the specific inhibitory pathway ending on the basal dendrites of giant cells, probably derived from the activity of the glycinergic vertical cells (e.g., Osen et al., 1990), with additional input from the ventro-tubercular tract arising from the VCN (Evans and Nelson, 1973b; Young et al., 1988).

(2) The $GABA_A$-ergic system, on the other hand, appears to be responsible for a "non-specific" inhibition of background (spontaneous) activity except in the region of the receptive field occupied by the excitation (for type I cells at least) and/or surround

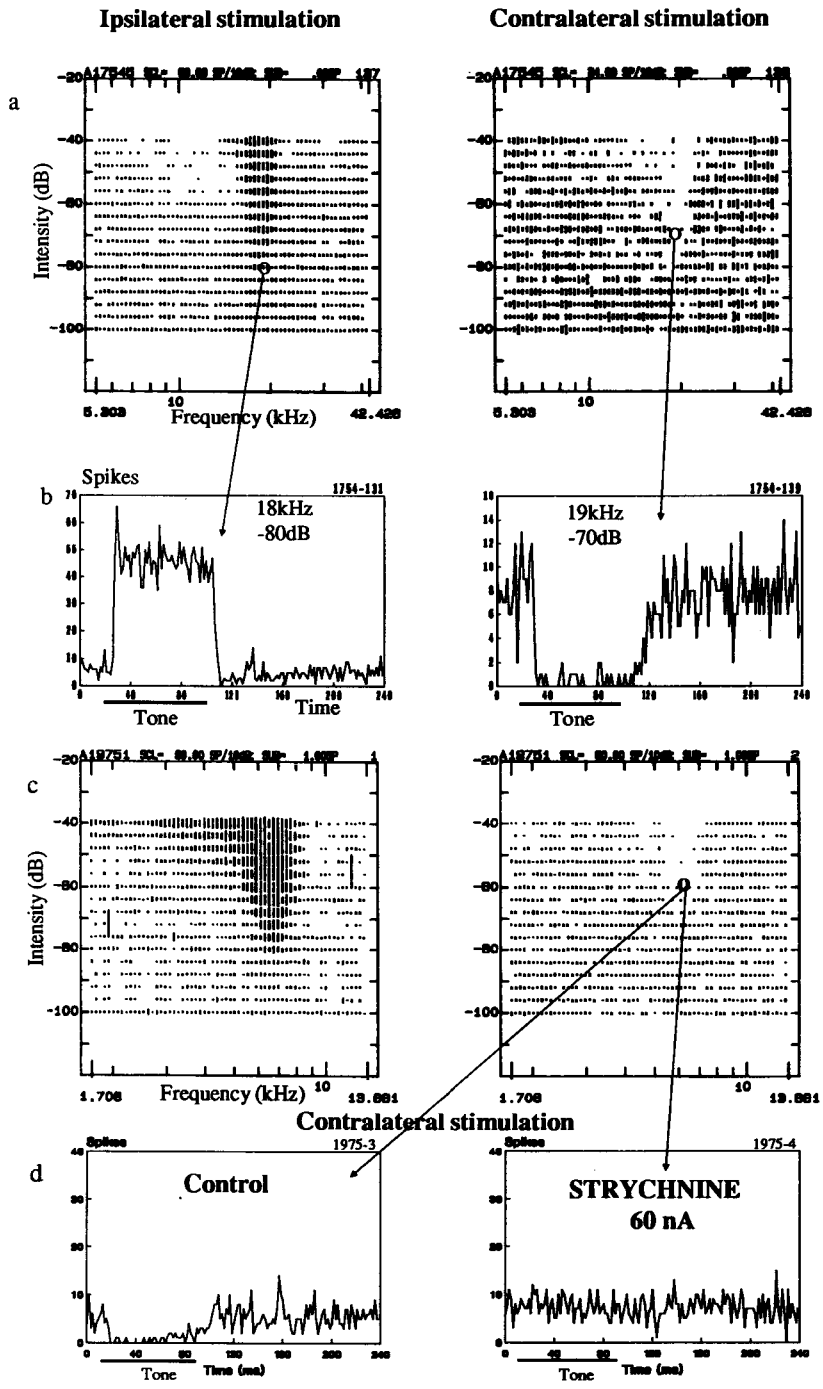

Fig. 4. Contralateral inhibition. (*a*): Receptive field maps of a type III cell, obtained with ipsilateral tone stimulation (left) and contralateral stimulation (right). (*b*): Peristimulus time histograms indicating the ipsilateral excitation and contralateral inhibition obtained with similar tone stimulus parameters (marked by the circles in *a*). (*c*): Receptive field maps of a type I cell, obtained with ipsilateral tone stimulation (left) and contralateral stimulation (right). (*d*): Peristimulus time histograms of contralateral stimulation at the frequency and intensity marked by the circle in (*c*), showing blockade of the contralateral inhibition by 60 nA strychnine.

inhibition (for type II, III and IV cells). It thus can serve to enhance spectral contrast by reducing background spontaneous activity, and by increasing the gain of the cell's response. It is important to emphasize that the apparent adjustment of the "background" tonic inhibitory influence by the $GABA_A$-ergic system does not affect the glycinergic stimulus-evoked inhibitory system; rather it serves to enhance or even reveal it.

It seems likely that the $GABA_A$-ergic effects are mediated by the less stimulus-specific input (from the descending pathways?) via the granule cell-parallel fibre system on to the apical dendrites of the pyramidal/fusiform and giant cells by way of the stellate and/or cartwheel cells (e.g., Osen et al., 1990). However, the more specific effects described above in the region of the excitatory response and lateral inhibitory response regions can only easily be explained if there is a $GABA_A$-ergic inhibitory input onto stimulus-specific glycinergic cells that in turn inhibit the cells from which recordings were made.

(3) Since off-inhibition enhances the contrast between the difference in discharge rate corresponding to stimulus "on" to stimulus "off", off-inhibition is presumably responsible for enhancement of temporal contrast (Evans, 1985).

(4) Presynaptic inhibition. The effects of Baclofen are presumably related to the action of presynaptic $GABA_B$ terminals on the primary afferent dendrites on the type IV cells, therefore regulating the degree of their afferent input.

(5) Contralateral inhibition. The latency of the contralateral inhibition is much shorter than the latencies given in the earliest reports of contralateral inhibition (e.g., 30 – 60 msec; reviewed by Klinke et al., 1970), but is similar to that found by Mast (1970), i.e., 8 – 25 msec. This would be consistent with input from the commissural cells in the contralateral VCN (e.g., Cant and Gaston, 1982; Osen et al., 1990). That this inhibition is glycinergic was suggested on anatomical grounds by Wenthold et al. (1987) and Osen et al. (1990).

Thus, the combined use of our automated receptive field mapping technique and iontophoretic application of a variety of pharmacological putative inhibitory antagonists has allowed us to dissect out at least five types of inhibition in the DCN. To these we can presumably add onset (transient) inhibition, as yet not characterized pharmacologically.

Adjustment of these separable systems confers on the auditory system the potential of exquisitely fine control of information processing, particularly spectral and temporal contrast enhancement, in the cochlear nucleus.

Acknowledgements

Supported in part by the Medical Research Council and by the Wellcome Trust.

References

Cant, N.B. and Gaston, K.C. (1982) Pathways connecting the right and left cochlear nuclei. *J. Comp. Neurol.*, 212: 313 – 326.

Caspary, D.M., Havey, D.C. and Faingold, C.L. (1979) Effects of microiontophoretically applied glycine and GABA on neuronal response patterns in the cochlear nuclei. *Brain Res.*, 172: 179 – 185.

Caspary, D.M., Rybak, L.P. and Faingold, C.L. (1984) Baclofen reduces tone-evoked activity of cochlear nucleus neurons. *Hear. Res.*, 13: 113 – 122.

Caspary, D.M., Pazara, K.E., Kossl, M. and Faingold, C.L. (1987) Strychnine alters the fusiform cell output from the dorsal cochlear nucleus. *Brain Res.*, 417: 273 – 282.

Evans, E.F. (1974) Auditory frequency selectivity and the cochlear nerve. In: E. Zwicker and E. Terhardt (Eds.), *Facts and Models in Hearing*, Springer, Heidelberg, pp. 118 – 129.

Evans, E.F. (1979a) Neuroleptanaesthesia for the guinea pig: an ideal anaesthetic procedure for long-term physiological studies of the cochlea. *Arch. Otolaryngol.*, 105: 185 – 186.

Evans, E.F. (1979b) Single unit studies of the mammalian auditory nerve. In: H.A. Beagley (Ed.), *Auditory Investigations: the Scientific and Technological Basis*, Oxford University Press, Oxford, pp. 324 – 367.

Evans, E.F. (1985) Aspects of the neuronal coding of time in the mammalian peripheral auditory system relevant to temporal resolution. In: A. Michelsen (Ed.), *Time Resolution in Auditory Systems: 11th Danavox Symposium*, Springer, Berlin, Heidelberg, New York, pp. 74 – 95.

Evans, E.F. and Nelson, P.G. (1973a) The responses of single neurones in the cochlear nucleus of the cat as a function of their location and the anaesthetic state. *Exp. Brain Res.*, 17: 402 – 427.

Evans, E.F. and Nelson, P.G. (1973b) On the functional relationship between the dorsal and ventral divisions of the cochlear nucleus of the cat. *Exp. Brain Res.*, 17: 428 – 442.

Evans, E.F. and Zhao, W. (1993a) Inhibition in the dorsal cochlear nucleus: pharmacological dissection, varieties, nature and possible functions. In: W.A. Ainsworth (Ed.), *Cochlear Nucleus: Structure and Function in Relation to Modelling – Advances in Speech Hearing and Language Processing, Vol. 3*, in press.

Evans, E.F. and Zhao, W. (1993b) Neuropharmacological and neurophysiologial dissection of inhibition in the mammalian dorsal cochlear nucleus. In: M. Merchan and J.M. Juiz (Eds.), *The Mammalian Cochlear Nuclei: Organization and Function*, Plenum, New York, pp. 253 – 266.

Evans, E.F., Pratt, S.R., Spenner, H. and Cooper, N.P. (1992) Comparisons of physiological and behavioural properties: auditory frequency selectivity. In: Y. Cazals, K. Horner and L. Demany (Eds.), *Advances in the Biosciences, Vol. 3*, Pergamon, Oxford, pp. 159 – 169.

Klinke, R., Boerger, G. and Gruber, J. (1970) The influence of the frequency relation in dichotic stimulation upon the cochlear nucleus activity. In: R. Plomp and G.F. Smoorenburg (Eds.), *Frequency Analysis and Periodicity Detection in Hearing*, Sijthoff, Leiden, pp. 161 – 165.

Mast, T.E. (1970) Binaural interaction and contralateral inhibition in dorsal cochlear nucleus of the chinchilla. *J. Neurophysiol.*, 33: 108 – 115.

Osen, K.K., Ottersen, O.P. and Storm-Mathisen, J. (1990) Colocalization of glycine-like and GABA-like immunoreactivities: a semiquantitative study of individual neurons in the dorsal cochlear nucleus of cat. In: O.P. Ottersen and J. Storm-Mathisen (Eds.), *Glycine Neurotransmission*, Wiley, New York, Chichester, pp. 417 – 451.

Palmer, A.R. and Evans, E.F. (1982) Intensity coding in the auditory periphery of the cat: responses of cochlear nerve and cochlear nucleus neurons to signals in the presence of Bandstop masking noise. *Hear. Res.*, 7: 305 – 323.

Wenthold, R.J. (1987) Evidence for a glycinergic pathway connecting the two cochlear nuclei: an immunocytochemical localization of the postsynaptic receptor. *Brain Res.*, 415: 183 – 187.

Young, E.D., Shofner, W.P., White, J.A., Robert, J.M. and Voigt, H.F. (1988) Response Properties of Cochlear Nucleus Neurones in Relationship to Physiological Mechanisms. *Annual Symposium of The Neurosciences Institute*, Wiley, New York, pp. 277 – 312.

Zhao, W. and Evans, E.F. (1990) Pharmacological (microiontophoretic) investigation of receptive-field and temporal properties of units in the cochlear nucleus. *Br. J. Audiol.*, 24: 193.

Zhao, W. and Evans, E.F. (1991) Dorsal cochlear nucleus units: neuropharmacological effects on dynamic range and off-inhibition. *Br. J. Audiol.*, 25: 53 – 54.

Zhao, W. and Evans, E.F. (1992) Bandwidths of excitatory and inhibitory receptive fields in the dorsal cochlear nucleus. *Br. J. Audiol.*, 26: 179 – 180.

J.H.J. Allum, D.J. Allum-Mecklenburg, F.P. Harris and R. Probst
Progress in Brain Research, Vol. 97

CHAPTER 12

Functional consequences of neonatal unilateral cochlear removal

David R. Moore, Andrew J. King, David McAlpine, Russell L. Martin and Mary E. Hutchings

University Laboratory of Physiology, Parks Road, Oxford OX1 3PT, U.K.

The physiological consequences of unilateral cochlear removal in infancy were assessed by recording the responses of neurones in the ferret inferior colliculus and superior colliculus to acoustic stimulation of the intact ear. Animals were lesioned between postnatal days P5 and P40 and survived for at least a year prior to recording. In the inferior colliculus ipsilateral to the intact ear, neurones had lower thresholds and wider dynamic ranges following earlier (P5) than following later (P40, adult) cochlear removal. In the superior colliculus contralateral to the intact ear, neurones had broader spatial tuning in response to high-level, free-field stimulation following cochlear removal at P25, than had neurones in normal, unlesioned adults. The neural map of auditory space was also disrupted in the lesioned animals. However, at low stimulus levels the auditory space map was unaffected by the cochlear removal. These results show a developmental sensitive period for the effects of unilateral cochlear removal on the responses of ferret inferior colliculus neurones, and a level-dependent effect of cochlear removal on the responses of superior colliculus neurones.

Key words: Hearing; Audition; Binaural; Physiology; Midbrain; Ferret; Maps

Introduction

The development and maintenance of neurones depends on the connections they make with their targets and the input they receive. Throughout the nervous system this dependence is particularly pronounced early in life, from the time the first connections are formed until, in some systems, adulthood is reached. Early deafness has been shown to produce many changes in the cellular and molecular biology of individual auditory neurones (see Rubel et al., 1990) and in the connections made between neurones (see Moore, 1991a). However, the implications of these changes for hearing, in cases of subtotal deafness, have received relatively little attention. This is clearly an issue of great importance, since most forms of neonatal hearing loss are incomplete, fluctuating, asymmetric between the ears, and potentially treatable.

Our research has focused on the effects of unilateral cochlear removal, a form of hearing loss that is radical and reproducible, and that leaves one ear intact for functional and control studies. Neonatal cochlear removal has both generative and degenerative anatomical consequences. It leads to an increase in the number and distribution of brainstem projections deriving from the intact ear (Rubel et al., 1981; Nordeen et al., 1983; Moore and Kitzes, 1985; Moore and Kowalchuk, 1988), and to a decrease in neurone number and size in the cochlear nucleus (CN; Born and Rubel, 1985; Moore, 1990a) on the lesioned side and superior olivary complex (SOC) nuclei on both sides of the brain (Moore, 1990b). Physiologically, cochlear removal produces

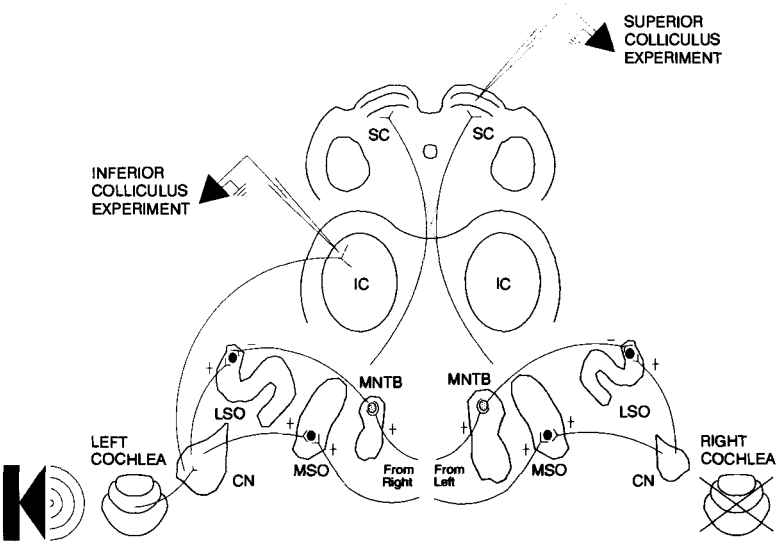

Fig. 1. Summary of the physiological experiments on the IC and SC, showing sites of cochlear removal, acoustic stimulation and recording. Some nuclei (right CN, right LSO, left MNTB) are reduced in size to represent the degenerative effects of neonatal, right cochlear removal. All of the ascending auditory projections from the CN that are shown have been found to be changed by cochlear removal. Projections from the ventral IC to the SC are bilateral. Abbreviations: CN, cochlear nucleus; IC, inferior colliculus; LSO, lateral superior olive; MNTB, medial nucleus of the trapezoid body; MSO, medial superior olive; SC, superior colliculus.

an increase in responsiveness of neurones in the inferior colliculus (IC; Kitzes, 1984; Kitzes and Semple, 1985) and primary auditory cortex (AI; Reale et al., 1987) on the side of the intact ear to acoustic stimulation of that ear (Fig. 1). In this paper, we report on the developmental time course for physiological changes in the IC and we explore the effects of early cochlear removal on another aspect of auditory system function, the representation of sound location in the superior colliculus (SC; King and Hutchings, 1987).

Methods

General

Ferrets were born and reared in the laboratory animal house. Removal of the right cochlea was performed under steroid anaesthesia ("Saffan"; 0.5 – 2 ml/kg) on postnatal days P5, P25 or P40 as described previously (Moore and Kowalchuk, 1988). Animals were reared to adulthood (1 – 2 years) and prepared for acute physiological recording from the IC (Moore et al., 1983) or SC (King and Hutchings, 1987). Briefly, the animals were barbiturate-anaesthetized, supported in a frame that left the head unobstructed and, for the SC experiments, paralysed with gallamine and artificially respired. Acoustic stimuli were delivered to the left ear either through a sealed headphone incorporating a probe microphone (IC experiments), or via a loudspeaker mounted on a hoop at a distance of 0.58 m from the head (SC experiments). Tungsten-in-glass microelectrodes were advanced through a craniotomy into the brain until single neural units were isolated. At the conclusion of the experiment, the animals were perfused with fixative. The midbrain and the right temporal bone were sectioned and stained to confirm the placement of the electrode tracks and the totality of the cochlear removal.

IC experiments

In "normal" control animals the right cochlea was removed during the surgical preparation for recording. Recordings were made in the central nucleus of the left IC (ICC; Fig. 1). Pure-tone stimuli (300 msec duration, presented at 0.9 Hz)

were used to produce frequency-threshold (tuning) curves. The stimulus was then set at the unit's best frequency, and rate-level (intensity) functions were obtained at 5 or 10 dB resolution. Off-line analysis was used to determine the threshold, discharge type (onset, sustained) and dynamic range of each unit. Comparisons between groups were made using either an analysis of variance with planned comparisons between individual means or a χ^2 test (Snodgrass, 1977).

SC experiments

Cochlear removals were performed only on P25 ferrets. Recordings were made in the right SC (Fig. 1). Broad-band noises (100 msec, presented at 0.6 Hz) were used to determine the threshold of deep-layer units for the stimulus position previously found to be most effective in producing visual responses in the superficial SC layers of the same electrode penetration (see King and Hutchings, 1987). Spatial receptive fields were measured using stimulus levels of 10 (± 5) dB and 30 (± 5) dB above this threshold and at azimuthal (i.e., horizontal) positions separated by 20° around the animal's head.

Results

IC experiments

Recordings were obtained from 349 units that were excited by auditory stimulation of the ipsilateral ear (Fig. 1). Many other units that were acoustically unresponsive or exclusively inhibited by high-frequency ipsilateral stimulation were also isolated in each group. In normal animals, about 2/3 of the excited units responded only at the onset (within 50 msec) of the tone stimulus (Fig. 2*A*). Almost all the rest responded throughout the stimulus ("sustained"). A similar distribution of discharge patterns was obtained for animals receiving cochlear removal at P25 and P40. For animals lesioned at P5, the ratio of onset to sustained units was about 1:1. A non-parametric statistical comparison of the data in Fig. 2*A* showed that this difference was not significant ($\chi^2 = 4.7$, $df = 3$, $0.2 > P > 0.1$).

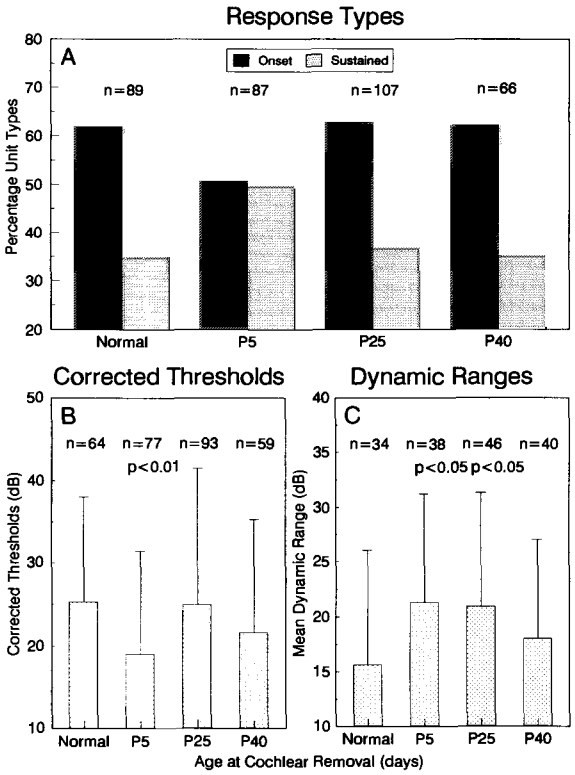

Fig. 2. Results of IC experiments. *A*. Percentage of units classified as onset or sustained. *B*. Mean thresholds (± 1 S.D.), normalized to the neural audiogram for the ferret (see text). *C*. Mean dynamic ranges of units with saturating intensity functions.

Thresholds of the excited units varied with frequency and between treatment groups. In order to control for frequency-related variation, we corrected the threshold for each unit by expressing it relative to the envelope of the most sensitive thresholds obtained to contralateral stimulation in an earlier study of the normal ferret ICC (Moore et al., 1983). The results (Fig. 2*B*) showed that thresholds were lower in the P5 group than in the normal group (N vs. P5: $F_{1,289} = 7.2$, $P < 0.01$). Neither of the other lesioned groups differed significantly from the normals.

Dynamic ranges were calculated by subtracting the stimulus level at 10% of the maximum response level from that at 90% of the maximum response level on each unit's intensity function. Units that did not saturate within the intensity range studied

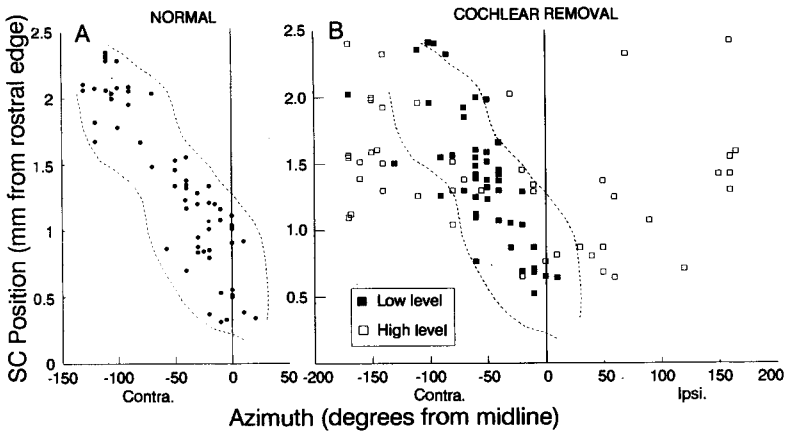

Fig. 3. Results of SC experiments. Relation between SC recording site, expressed in millimetres from the rostral edge of the nucleus, and the azimuthal position from which the stimulus evoked the maximum spike count for each unit. *A*. Normal animal data. Data points represent a mixture of high (> 20 dB re. threshold) and low (< 10 dB re. threshold) level stimulation. *B*. Data from animals receiving a unilateral cochlear removal at P25. Low- and high-level stimuli were as defined in *A*. The dashed lines in each part of the figure are the envelope of the normal data.

(usually up to 90 dB SPL) and units having highly irregular intensity functions were excluded from this analysis. The results for the remaining (saturating and non-monotonic) units are shown in Fig. 2*C*. Both the P5 ($F_{1,154} = 6.2$, $P < 0.05$) and the P25 ($F_{1,154} = 5.8$, $P < 0.05$) groups had significantly broader dynamic ranges than the normals. The P40 group did not differ from the normals.

SC experiments

Recordings were obtained from 52 units in the right SC of adult animals that had the right cochlea removed at P25. Control data from 64 units in the right SC of normal adult ferrets were available from another study (King and Hutchings, 1987). The relation between the SC recording position and best stimulus azimuth in the "normal" group is shown in Fig. 3*A*. The neural map of azimuth extended from just ipsilateral to the midline (+20°), through the contralateral, frontal field (0° to −90°) and into the contralateral, rear quadrant (to −130°). A close relation was found between recording position and best azimuth, and this relation was maintained across a wide range of stimulus levels.

The SC representation of azimuth in animals receiving a unilateral cochlear removal at P25 depended on stimulus level. Near threshold ("low level" in Fig. 3*B*) spatial representation closely followed that observed in normals, as shown by the dashed line envelope of the normal data plotted in both parts of Fig. 3. However, at stimulus levels 25−35 dB above threshold, the spatial receptive fields of most neurones broadened and the best spatial positions occupied the entire available sound field (+170° to −170°). Best positions were not organised topographically or correlated with cell location in the SC.

Discussion

Unilateral cochlear removal in infancy was shown to change the responses of IC neurones ipsilateral to the intact ear to acoustic stimulation of that ear. The changes were relatively subtle and dependent on the age of the animal at the time of the removal. For the SC, the results following unilateral cochlear removal at P25 were similar to those reported by Palmer and King (1985) following unilateral cochlear removal in adult guinea pigs. A normal map of auditory space was evident at near threshold levels

in both cases, but there was no topographic order in the distribution of best positions at suprathreshold levels.

Previous physiological studies of the effects of cochlear removal in infancy have been limited to a single age point during the first postnatal week. In gerbils, Kitzes (1984) showed that the proportion of recording sites in the IC that were excited by stimulation of the ipsilateral, intact ear increased from 42% to 86% following cochlear removal at P2. For single units, response thresholds were lower, peak discharge levels were higher, response patterns were more sustained, and response latencies were shorter in the neonatally lesioned animals (Kitzes and Semple, 1985). Qualitatively, we found the same results in our P5 lesioned ferrets and, by the dynamic range index, in our P25 lesioned ferrets. However, the changes in our experiments were quantitatively small.

One possible explanation for the differences between the gerbil and ferret data is that, although both species are altricial, the gerbil is less developed at P2 than the ferret is at P5 and, consequently, the gerbil brain was more dependent on normal afferent input at the time of cochlear removal. It is therefore interesting to contrast both these species with the cat, a relatively precocious carnivore. Reale and his colleagues (1987) have shown that, following unilateral cochlear removal between P0 and P3, cat AI ipsilateral to the intact ear is changed qualitatively in the same ways as the gerbil and ferret IC. Quantitatively, their results more closely resembled the gerbil than the ferret. Both the cat and the gerbil studies suggested a close similarity between the ipsilateral responses in the lesioned animals and normal contralateral responses. In the ferret, contralaterally evoked excitatory responses (Moore et al., 1983, and unpublished data) are more common and much stronger than ipsilaterally evoked responses, even after cochlear removal at P5.

It is difficult to reconcile these observations, since the neurological development of a P0 – P3 cat is comparable to that of a P25 ferret (Linden et al., 1981; Moore, 1991b). Perhaps AI, like visual cortical areas (see Sherman and Spear, 1982), is more physiologically vulnerable to sensory deprivation and unilateral deafferentation than are sub-cortical areas. Alternatively, different species may simply have different auditory system developmental sensitive periods or susceptibility to hearing loss, despite their similarity on other measures of neural development and plasticity.

Whatever the reason(s) for the quantitative differences between ferrets, gerbils and cats, the qualitative similarities in neural response to cochlear removal suggest that radical unilateral hearing loss in any mammalian species may increase sensitivity to sounds presented to the normal ear. It is, however, necessary to view these results from a different perspective. The higher levels of the mammalian auditory system, including the IC and AI, are normally much more strongly influenced by contralateral stimulation (Glendenning and Masterton, 1983; Heffner and Heffner, 1990) than by ipsilateral stimulation. There is presently only scant evidence concerning the influence of the intact ear on contralateral brain structures following early unilateral removal; Reale and colleagues (1987) found a small increase in the mean threshold of AI neurones contralateral to the intact ear. In their anatomical study, Nordeen and her colleagues (1983) found a significant decrease in the number of neurones projecting from the CN on the intact side to the contralateral IC. This finding contrasted with the significant increase in the size of the ipsilateral projection. Thus, it may be that the contralateral influence of the intact ear declines in parallel with the increased ipsilateral influence. Given the greater role of contralateral pathways in normal hearing (Jenkins and Masterton, 1982; Heffner and Heffner, 1990), these data suggest that sensitivity to sounds presented to the intact ear may be poorer than normal. We are presently investigating these possibilities by obtaining behavioural audiograms in cochlear ablated ferrets (Martin et al., 1991).

Although the SC map of auditory space was similarly affected by cochlear removal in the P25 ferret as in the adult guinea pig (Palmer and King, 1985), there was a difference between the results of the two experiments. SC responses became very broadly

tuned to sound azimuth at high sound levels following acute cochlear removal in adult guinea pigs. While many auditory responses were also broadly tuned in our study, others exhibited spatial response profiles that were sharply tuned, albeit to abnormal positions. Whether this difference reflects a developmentally related change in sensitivity to cochlear removal, the different survival times following the removal, or a genuine species difference remains to be determined. Suprathreshold spatial tuning in the SC is based on binaural localization cues (Palmer and King, 1985; Middlebrooks, 1988). These cues will be unavailable following unilateral cochlear removal, so any developmental change in sensitivity must reflect a change in neural responses to the spectral cues to sound position provided by the outer ear (Carlile, 1990).

The ferret SC receives most of its ascending auditory input from regions ventral to the ipsilateral ICC, primarily lateral, dorsal and rostral to the dorsal nucleus of the lateral lemniscus (Fig. 1; A.J. King and D.R. Moore, unpublished data). Evidence from the cat suggests that those regions receive their predominant input either from the ICC (Aitkin et al., 1981) or in parallel with projections to the ICC (Aitkin, 1986). An increase in the dynamic range of neurones in the left IC (Fig. 2*C*) following removal of the right cochlea at P25 might, therefore, be reflected in an increase in suprathreshold response levels in the left SC. The influence of the left IC on the right SC may be either indirect, via the commissural projection from one SC to the other (Behan, 1985), or direct, since the SC receives a small input from the contralateral, ventral IC. In either case, the physiological relation between changes in auditory brain-stem activity and changes in the fidelity of spatial representation in the SC have yet to be determined.

Acknowledgements

This research was supported by grants from the Medical Research Council, the Lister Institute, and the Wellcome Trust. RLM is a C.J. Martin Fellow of the Australian National Health and Medical Research Council.

References

Aitkin, LM. (1986) *The Auditory Midbrain,* Humana Press, Clifton, NJ, 246 pp.

Aitkin, L.M., Kenyon, C.E. and Philpott, P. (1981) The representation of the auditory and somatosensory systems in the external nucleus of the cat inferior colliculus. *J. Comp. Neurol.,* 196: 25 – 40.

Behan, M. (1985) An EM-autoradiographic and EM-HRP study of the commissural projection of the superior colliculus in the cat. *J. Comp. Neurol.,* 234: 105 – 116.

Born, D.E. and Rubel, E.W. (1985) Afferent influences on brain stem auditory nuclei of the chicken: neuron number and size following cochlea removal. *J. Comp. Neurol.,* 231: 435 – 445.

Carlile, S. (1990) The auditory periphery of the ferret, II: the spectral transformations of the external ear and their implications for sound localization. *J. Acoust. Soc. Am.,* 88: 2196 – 2204.

Glendenning, K.K. and Masterton, R.B. (1983) Acoustic chiasm: efferent projections of the lateral superior olive. *J. Neurosci.,* 8: 1521 – 1537.

Heffner, H.E. and Heffner, R.S. (1990) Effect of bilateral auditory cortex lesions on absolute thresholds in Japanese macaques. *J. Neurophysiol.,* 64: 191 – 205.

Jenkins, W.M. and Masterton, R.B. (1982) Sound localization: effects of unilateral lesions in central auditory system. *J. Neurophysiol.,* 47: 987 – 1016.

King, A.J. and Hutchings, M.E. (1987) Spatial response properties of acoustically responsive neurons in the superior colliculus of the ferret: a map of auditory space. *J. Neurophysiol.,* 57: 596 – 624.

Kitzes, L.M. (1984) Some physiological consequences of neonatal cochlear destruction in the inferior colliculus of the gerbil. *Brain Res.,* 306: 171 – 178.

Kitzes, LM. and Semple, M.N. (1985) Single-unit responses in the inferior colliculus: effects of neonatal unilateral cochlear ablation. *J. Neurophysiol.,* 53: 1483 – 1500.

Linden, D.C., Guillery, R.W. and Cucchiaro, J. (1981) The dorsal lateral geniculate nucleus of the normal ferret and its postnatal development. *J. Comp. Neurol.,* 203: 189 – 211.

Martin, R.L., Hine, J.E. and Moore, D.R. (1991) Hearing in ferrets with unilateral cochlear removal. *Soc. Neurosci. Abstr.,* 17: 232.

Middlebrooks, J.C. (1988) Auditory mechanisms underlying a neural code for space in the cat's superior colliculus. In: G.M. Edelman, W.E. Gall and W.M. Cowan (Eds.), *Auditory Function,* Wiley, New York, pp. 431 – 456.

Moore, D.R. (1990a) Auditory brainstem of the ferret: early cessation of developmental sensitivity of neurons in the cochlear nucleus to removal of the cochlea. *J. Comp. Neurol.,* 302:

810 – 823.

Moore, D.R. (1990b) Excitatory but not inhibitory synapses prevent transneuronal degeneration following deafferentation in the developing ferret auditory system. *Neurosci. Lett. (Suppl.)*, 38, S71.

Moore, D.R. (1991a) Hearing loss and auditory brainstem development. In: M. Hanson (Ed.), *The Fetal and Neonatal Brainstem*, Cambridge University Press, pp. 161 – 184.

Moore, D.R. (1991b) Development and plasticity of hearing in the ferret. In: R.A. Altschuler, D.W. Hoffman, R.P. Bobbin and B.M. Clopton (Eds.), *The Neurobiology of Hearing: Central Auditory System*, Raven Press, New York, pp. 461 – 476.

Moore, D.R. and Kitzes, L.M. (1985) Projections from the cochlear nucleus to the inferior colliculus in normal and neonatally cochlea-ablated gerbils. *J. Comp. Neurol.*, 240: 180 – 195.

Moore, D.R. and Kowalchuk, N.E. (1988) Auditory brainstem of the ferret: effects of unilateral cochlear lesions on cochlear nucleus volume and projections to the inferior colliculus. *J. Comp. Neurol.*, 272: 503 – 515.

Moore, D.R., Semple, M.N. and Addison, P.D. (1983) Some acoustic properties of neurones in the ferret inferior colliculus. *Brain Res.*, 269: 69 – 82.

Nordeen, K.W., Killackey, H.P. and Kitzes, L.M. (1983) Ascending projections to the inferior colliculus following unilateral cochlear ablation in the neonatal gerbil, *Meriones unguiculatus. J. Comp. Neurol.*, 214: 144 – 153.

Palmer, A.R. and King, A.J. (1985) A monaural space map in the guinea-pig superior colliculus. *Hear. Res.*, 17: 267 – 280.

Reale, R.A., Brugge, J.F. and Chan, J.C.K. (1987) Maps of auditory cortex in cats reared after unilateral cochlear ablation in the neonatal period. *Dev. Brain Res.*, 34: 281 – 290.

Rubel, E.W., Smith, Z.D.J. and Steward, O. (1981) Sprouting in the avian brainstem auditory pathway: dependence on dendritic integrity. *J. Comp. Neurol.*, 202: 397 – 414.

Rubel, E.W., Hyson, R.L. and Durham, D. (1990) Afferent regulation of neurons in the brain stem auditory system. *J. Neurobiol.*, 21: 169 – 196.

Sherman, S.M. and Spear, P.D. (1982) Organization of visual pathways in normal and visually deprived cats. *Physiol. Rev.* 62: 738 – 855.

Snodgrass, J.G. (1977) *The Numbers Game*, Oxford University Press, Oxford, 466 pp.

J.H.J. Allum, D.J. Allum-Mecklenburg, F.P. Harris and R. Probst
Progress in Brain Research, Vol. 97

CHAPTER 13

Functional organization and learning-related plasticity in auditory cortex of the Mongolian gerbil

H. Scheich, C. Simonis, F. Ohl, J. Tillein and H. Thomas

Institute of Zoology, Technical University Darmstadt, 6100 Darmstadt, Germany

Key words: Auditory cortex; Neuronal plasticity; Tone-bursts; 2-Deoxyglucose; Gerbil

Introduction

There is recent progress in cochlea implant technology, identification of suitable patients for implants, and postoperative training programs, all with a remarkable benefit for hearing and speech communication of some formerly deaf patients (Fraysse and Cochard, 1989). Nevertheless, the average improvement across all implanted patients and, consequently, the prognosis before an implant is not yet satisfactory. There is the possibility that plasticity in the central auditory system of deaf patients is a critical factor which determines the final postoperative level of hearing and speech perceptability in each case. Only limited information is available about mechanisms of plasticity in auditory cortex (Weinberger and Diamond, 1987; McMullen and Glaser, 1988; Diamond and Weinberger, 1989; Robertson and Irvine, 1989; Edeline et al., 1990; Weinberger, 1990), in contrast to a host of studies of visual cortex plasticity (see Singer, 1987). Knowledge is sufficient neither in terms of sensitive phases for auditory cortex organization during development, nor in the adult system of learning-induced plasticity, nor of compensatory plasticity after peripheral lesions. Without specific animal studies, it seems hopeless to determine which of these alternatives are relevant for patients after various periods of deafness, i.e., for implant prognosis.

The Mongolian gerbil (*Meriones unguiculatus*) has recently become a mammalian model for the study of auditory mechanisms. The foremost reasons for the growing interest in gerbil audition are: (1) the unusual, almost human-like, low-frequency hearing specialization (Finck and Sofouglu, 1966; Ryan, 1976), which is reflected by expansion of the low-frequency representations in auditory structures (Ryan et al., 1982; Steffen et al., 1988); among other factors, this favors speech-related studies in that species; (2) the enlarged middle ear cavities which permit a direct experimental access to the turns of the cochlea; and (3) the fact that (1) and (2) are found in a small, easily bred laboratory animal. The following report reflects an initial attempt to study one aspect of auditory cortical plasticity in this promising animal model, namely adult auditory learning. Data are suitable as a baseline for studies of the other two types of plasticity.

Basic functional organization of auditory cortex: electrophysiology

As there were no previous studies, the tonotopic organization of gerbil primary auditory cortex (AI) and surrounding fields was analyzed in our laboratory using standard microelectrode mapping techniques (Tillein, 1988; Thomas, 1989; Scheich, 1991a,b). Multiple tangential dorsoventral elec-

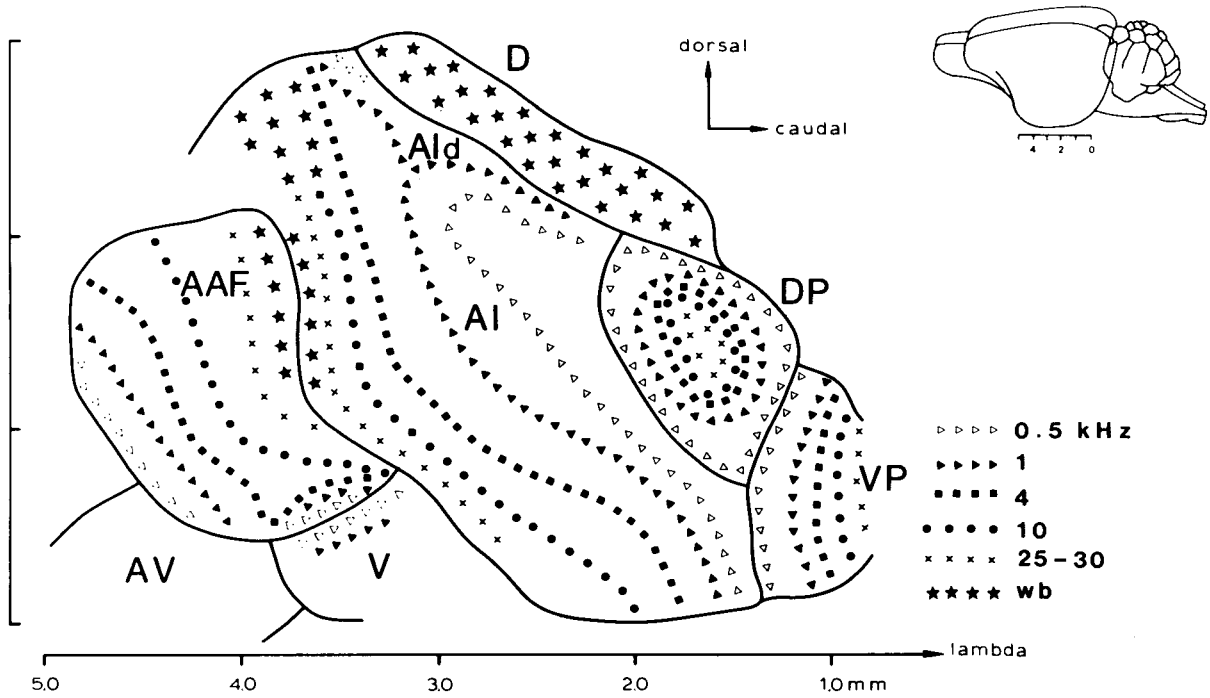

Fig. 1. Summary map of tonotopic organization of multiple fields in the left auditory cortex of the Mongolian gerbil. Approximate course and distances of isofrequency contours schematized from data obtained in best frequency (BF) unit mapping experiments. Areas marked with asterisks contain wide-band units responding with little variation to frequencies between 1 and 30 kHz (with permission from Scheich, 1991b).

trode tracks were made in each animal under light anesthesia. Electrodes remained in granular and supragranular layers and recording positions had a distance of 100 μm. Single and multi-unit activity were analyzed using 250 msec tone bursts (0.1 – 45.0 kHz, 70 dB SPL). On-responses were integrated for up to ten repetitions and the best frequency (BF) determined in the frequency response histogram. The tonotopic (i.e., the BF-related) organization of AI covers the described hearing range of gerbils (Fig. 1). High BFs were represented rostrally and low frequencies caudally, in terms of isofrequency contours, with a roughly dorsoventral orientation.

There are additional tonotopic maps adjacent to AI. Rostral to AI a smaller field with a complete tonotopic gradient, but reversed to the one in AI, was mapped (mirror image representation) and termed anterior auditory field (AAF). BFs in a range from 0.1 to 43.0 kHz were found in AI and AAF. Representation of lower BFs up to 8 kHz had higher spatial resolution. Unit responses obtained in AI as well as in AAF were strong with usually narrow tuning and short latencies.

Caudal to AI two additional small tonotopically organized fields, a dorsoposterior field (DP) and a ventroposterior field (VP) were identified. In both fields, low BFs were located rostrally adjacent to the low-frequency representation in AI. High-frequency representations were found caudally in VP. In DP, BFs were concentrically organized with high BFs located in the center. Responses to tone bursts within DP and VP were relatively weak with longer latencies and broader tuning compared to AI and AAF.

Penetrations dorsocaudal to AI revealed an area of broadly tuned neurons without tonotopic organization, interpreted as a secondary belt region (field D). In the transition area between AI and D,

responses were similar to those found in the low-frequency range of AI and AAF but without a straightforward tonotopy (AId). Ventral to the high-frequency border between AAF and AI, a rapid decrease to low BFs leads to the assumption of an additional auditory field termed ventral field V. Responses were similar to those of DP and VP. The location of AI and AAF appeared to be within koniocortex in Nissl-stained sections, while the remaining fields lay outside.

Basic functional organization of auditory cortex: deoxyglucose labeling

Gerbil auditory cortex fields were also mapped tonotopically using the radioactive 2-deoxyglucose (2DG) technique (Sokoloff et al., 1977). Narrow-band, frequency-modulated (FM) tone bursts and pairs of alternating pure-tone bursts (both at about 75 dB SPL, 2/sec) served as stimuli. Details of the methods used for gerbils are found in Scheich (1991a) and Caird et al. (1991). In short, adult awake gerbils in a small cage were exposed to the acoustic stimuli for 90 min in an anechoic chamber after an i.p. injection of 18 μCi ^{14}C-2-fluoro-2-deoxyglucose. Serial horizontal sections of the brains were exposed to Kodak NMB X-ray film for two weeks. Topological measurements of labeled frequency band laminae were made using reconstructions of the hemispheres from enlarged prints (magnification, $\times$ 7.5). 2DG uptake chiefly correlates with the energy requirements of the membrane sodium pump (Mata et al., 1980), and thus reflects ongoing electrical activity. It has been shown that peak metabolic activity corresponds to the location of units with the corresponding BF in electrophysiological and 2DG combination experiments in the same animal (Theurich et al., 1984).

The primary field (AI) and the rostrally adjacent smaller field (AAF) showed prominent frequency-specific dorsoventral stripes of labeling with a variable width ($\sim$ 200 μm) extending radially across the cortical layers and tangentially in roughly dorsoventral direction (frequency band laminae, FB laminae) (see Fig. 2). FB laminae in AI and AAF shifted as a function of stimulus frequency relative to each other. FB laminae also shifted with respect to a landmark in the lateral hippocampus which was found to form a reliable and independent spatial reference across individual brains. Quantitative densimetric spatial analysis of the FB laminae locations, obtained with different frequencies, revealed mirror-

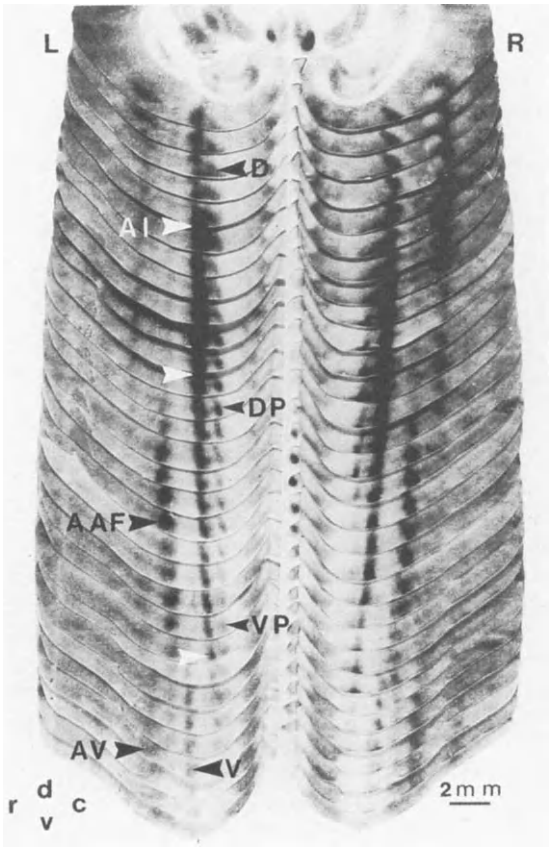

Fig. 2. Reconstruction of 2-deoxyglucose labeled auditory cortical fields in the gerbil. Serial horizontal section autoradiographs of left (L) and right (R) hemispheres after 2/sec stimulation with 1 and 2 kHz alternating tones. The 1 and 2 kHz frequency band laminae in each of the different fields are fused to one particularly dark band. Using small frequency "jumps" of one octave increases the contrast of the banding patterns, which facilitates identification of the fields. The spacing of the sections exaggerates the dorsoventral extent of auditory cortex but allows one to follow the radial extent of labeling through the cortical depth in each section. Note spatial correspondence of the two data sets by comparing left hemisphere of this figure with the electrophysiological map in Fig. 1.

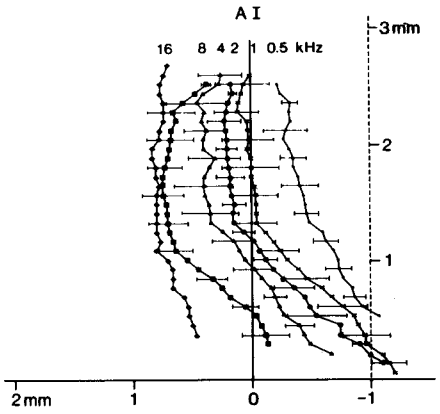

Fig. 3. Average tonotopic map of gerbil AI obtained from 2-deoxyglucose labeling experiments with different frequencies. The peak labeling in each AI frequency band lamina obtained with the different tone frequencies was referred to the rostrocaudal position of a reliable landmark in the brain (anterior tip of the hippocampus = 0 on the coordinate scale) and averaged for different cases and the two hemispheres. Ordinate scale corresponds to relative dorsoventral extent of AI labeling on the surface of the hemisphere. Note relatively small (± 200 μm) standard deviation of the dorsal aspect of the 1 kHz contour from the hippocampus reference (x = 0). For comparison with electrophysiological map of AI, see Fig. 1.

imaged tonotopic maps of AI and AAF, as in the electrophysiological study. In AI, the progression from low- to high-frequencies was from caudal to rostral and in AAF the gradient was reversed leading to a common high-frequency border of the two fields.

In the AI map the spatial resolution for frequencies below 8 kHz (speech range) showed similar octave intervals (~ 200 μm/octave) and was better for frequencies below 1 kHz. AI showed generally higher spatial resolution for frequencies as well as longer isofrequency contours than AAF. Differential metabolic 2DG responses to the described stimuli in conjunction with the electrophysiological data allowed one to distinguish in addition a ventral (V), an anterior ventral (AV), a dorsoposterior (DP), a ventral posterior (VP) and a dorsal field (D).

The 2DG patterns provided standard tonotopic maps of AI and AAF averaged across many individuals and, in addition, topological data of all fields in conjunction with reliable landmarks of gerbil auditory cortex (Fig. 3). Functional 2DG labeling cannot replace an electrophysiological approach due to missing temporal resolution. However, the technique allows comprehensive collection of robust data sets of representation (i.e., of the geometry of evoked auditory activity patterns) in cortical fields. Therefore, the technique also appeared to be suitable to study learning-induced activity. Prominent learning-induced changes of 2DG uptake have previously been shown in the auditory and limbic system of rats using a classical aversive conditioning paradigm (Gonzalez-Lima and Scheich, 1984, 1986a,b). The use of the 2DG technique for learning studies appears to be favorable for a number of reasons including the fact that 2DG accumulation occurs predominantly in presynaptic terminals and with dendrites reflecting primarily circumsynaptic electrical activity (Heil and Scheich, 1986).

Learning-induced changes of 2-deoxyglucose uptake

The following learning studies in gerbil auditory cortex were designed to test whether aversive conditioning changes the frequency representation in fields AI and AAF (Simonis and Scheich, in preparation). Animals in a first experiment were injected with 2DG prior to classical conditioning using a 1 kHz slightly frequency-modulated tone burst (10 sec, 75 dB SPL) as conditioned stimulus (CS), followed by a foot-shock as unconditioned stimulus (US). During a 2DG session of 40 min 100 pairs of stimuli were presented with pseudo-randomized pauses.

Quantitative topological analysis of labeling in autoradiographs was performed using an image processor. Densimetric values of pixels were averaged across the radial and dorsoventral extent of FB laminae with a resolution of about 10 μm which resulted in distributions with relative peaks. The peak-to-peak distance between the labeled frequency band laminae in AI and AAF was significantly larger in the paired animals with respect to unpaired controls with the same stimuli. This cor-

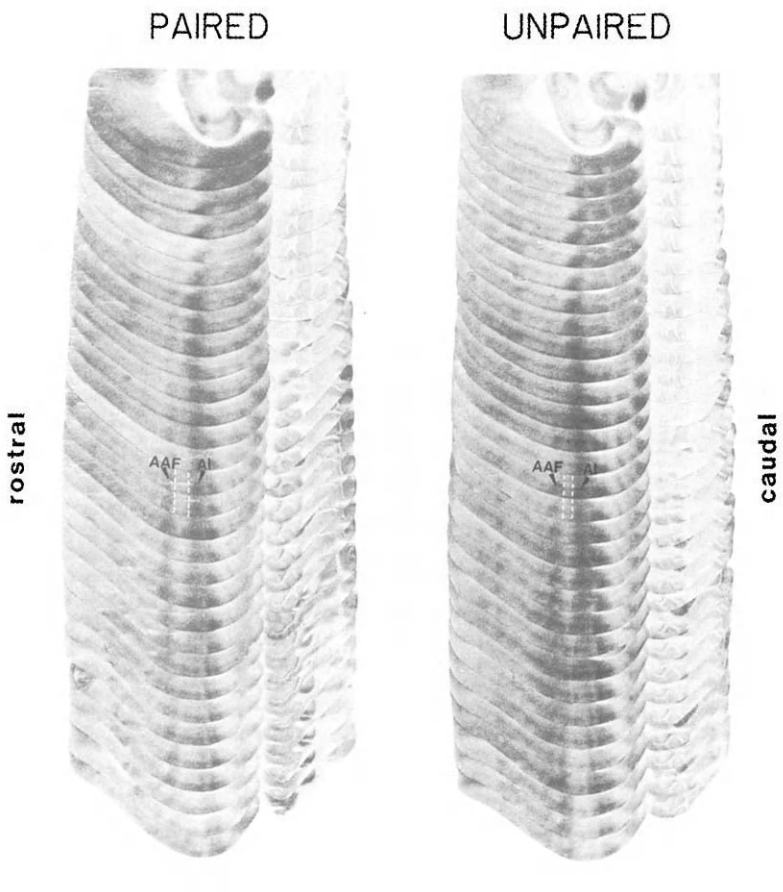

Fig. 4. 2-Deoxyglucose labeling of gerbil auditory cortex during aversive classical conditioning on 1 kHz tone bursts (100 stimuli in 40 min). In comparison to paired presentation of tones and foot-shocks in the conditioned animals the controls received the same number of the two stimuli during the 2DG session but in an unpaired (random) fashion. The most conspicuous difference between the two groups of animals is the change in the distance between the two labeled 1 kHz frequency band laminae in AI and AAF which is larger in the conditioned cases. Thus, classical conditioning shifts tonotopic representation toward lower frequencies.

responds to the visual impression of a larger separation of the two bands as shown in the montage of Fig. 4. Peak shifts were in the range of 100 – 200 μm. In a tonotopic frame of reference of the two mirror-imaged fields AI and AAF, an increased peak distance of labeling would correspond to a shift of maximum activity towards lower frequencies.

In a second experiment, animals were trained in a shuttle box to avoid the shock after a 1 kHz tone. In the following 2DG session (recall session) the animals received only occasional shocks when they made mistakes. The peak-to-peak distance between AI and AAF frequency band laminae was the same in this avoidance conditioned group compared to controls which were previously habituated to only the tones in the shuttle box and received no shocks. However, the total width of the labeled frequency band laminae in AI and AAF in the avoidance conditioned group was significantly larger than in the controls.

The spatial changes of stimulus representations revealed by these two studies suggest that the populations of neurons which are maximally activated during associative learning and during recalling

learned information are partially different, and are also partially different from the population maximally activated by the meaningless tones.

To show that these effects are frequency-specific and not due to some general increase of cortical excitability by any frequency, animals were trained with a differential conditioning paradigm (Fig. 5). The two frequencies (CS+ = 1 kHz and CS− = 10 kHz) were presented randomly and the animals had to respond to the CS+ by avoiding a foot-shock, whereas the CS− was not paired with a shock. For a second group the foot-shock was paired with 10 kHz. In a subsequent 2DG session, the two experimental groups and a control group were exposed to 1 and 10 kHz (Fig. 5). A naive control group was stimulated with 1 and 10 kHz without shocks. In both experimental groups, i.e., after training, we found in the 2DG session a relatively

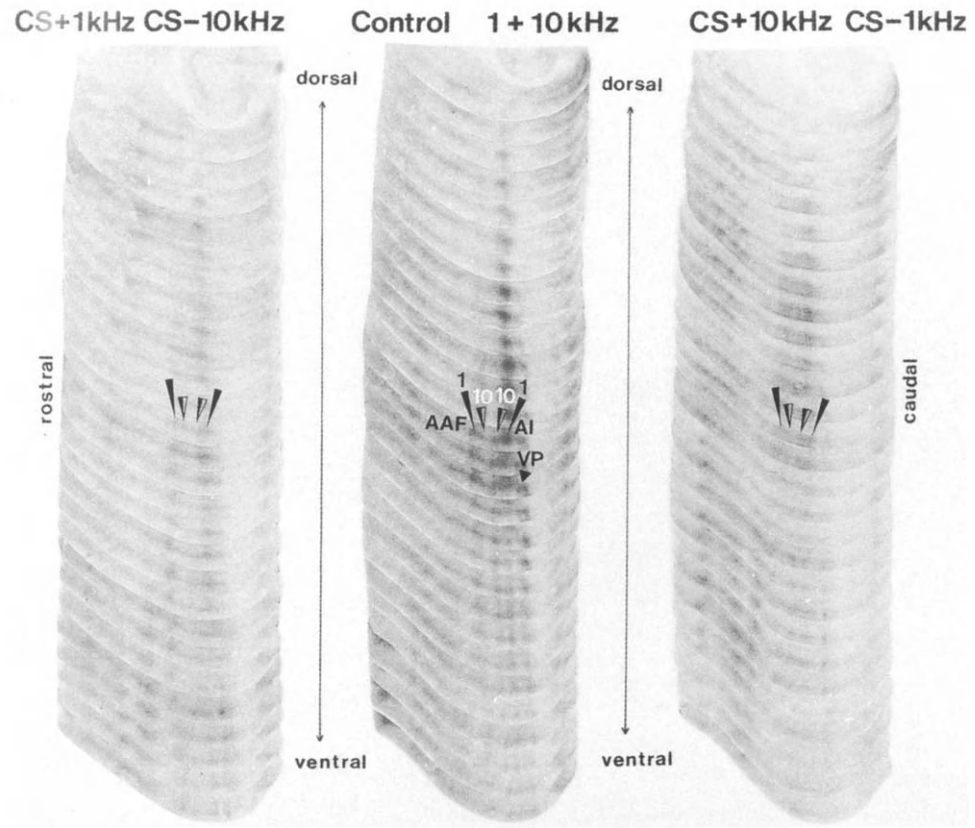

Fig. 5. 2-Deoxyglucose labeling of gerbil auditory cortex after conditioned differential frequency responses. One group of animals (left) was previously trained to avoid a foot-shock upon presentation of a 1 kHz, slightly frequency-modulated tone burst (CS+) and not to jump upon presentation of 10 kHz tone bursts (CS−, no foot-shock). In another group (right) the paradigm was reversed. During the 2DG session (75 tone stimuli in 45 min) the trained animals rarely made a mistake and thus received few foot-shocks. A naive control group (middle) was stimulated with the same number of 1 and 10 kHz tones without foot-shocks in the same random fashion as the experimental groups. In this group, the 1 kHz and 10 kHz frequency band laminae are separable in AI and, at higher magnification, also in AAF, and have about equal labeling intensity. In the CS+ 1 kHz group labeling at 10 kHz in AI and AAF is reduced almost to background levels. Note the clear area between the two 1 kHz frequency band laminae (small arrowheads). In the CS+ 10 kHz group, there is more activity in the 10 kHz frequency band laminae compared to the CS+ 1 kHz cases, but the 1 kHz frequency band laminae have retained some activity. These differences in the two conditioned groups suggest that differential meaning of two frequencies are reflected in the tonotopic 2DG labeling but that 1 and 10 kHz are not equivalent in producing differential 2DG effects.

more intense and broader CS+ representation, while the representation of CS− was relatively depressed. Due to some blur of frequency representation in the two trained groups in comparison to the control group (see Fig. 5), spatial shifts of labeling could not be analyzed.

The results together lead to the following preliminary conclusions: tone conditioning appears to produce primarily spatial changes of activity patterns in fields of auditory cortex and differential tone conditioning also produces differential changes of activity levels. Spatial changes are not simply expansions of the conditioned frequency representation but shifts in one or the other direction across the tonotopic gradient. Thus, spatial representation of frequencies in cortical tonotopic maps does not seem to be rigid but can be influenced to some degree by learning. The spatial shifts are relatively large (100 – 200 μm). With respect to tonotopic labeling in AI of control animals (see Fig. 3), i.e., 200 μm for one octave in the 1 kHz range, the learning-induced shifts of peak labeling reach 0.5 octaves. This is under the assumption that AI and AAF both contribute to the measured shifts. If only one field would undergo changes the shift of representation would be larger.

Electrophysiological changes after classical conditioning

A parallel approach to learning was taken in awake chronically prepared gerbils (head mount and chamber implanted) with single and multi-unit recordings in primary auditory cortex (chamber technique) before and after classical conditioning (Ohl, 1991). Gerbils with painless cranial fixation sat quietly in a housing tube for many recording sessions and tolerated mild electrocutaneous stimulation at the tail as an unconditioned stimulus (US). The frequency receptive field (FRF) of each unit was analyzed before conditioning with approximately 70 dB SPL free-field stimulation at the contralateral ear. Then, one frequency was paired between 50 and 100 times with the US which produced occasional tail flicks. Subsequently, the FRF was analyzed again.

As a typical non-frequency-specific effect, both spontaneous and evoked spike rate of units dropped after conditioning. If the BF of a given unit was used as a conditioned stimulus (CS) frequency no remarkable influences were seen on the overall shape of the FRF. Specific and reliable changes of FRF configuration occurred with CS frequencies located on the slopes of FRFs. It was not the response to the CS nor to the BF, however, which increased but responses to frequencies adjacent to the CS. Responses to the CS remained the same or decreased. This is shown for a unit in Fig. 6 which had a BF at 100 Hz and was conditioned with 1000 Hz. BF and CS responses remained essentially the same after conditioning but two side-peaks at 600 Hz and 1200 Hz appeared. A number of units showed more complicated conditioned FRFs with a relative drop of response at the CS and asymmetric or multiple side peaks of relatively increased responses.

Although a decisive mechanistic interpretation is still a matter of debate, preliminary network modeling of laterally interacting units (by F.O. in our group) suggests lateral inhibition conveyed by Hebbian-like synapses to underly the observed frequency-specific plastic effects. In any case, it seems clear that the changes are not due to individual properties of any given conditioned neuron but rather to a cooperative effect in a larger network, either cortical or subcortical. Thus, the frequency-specific conditioning effect does not depend on the individual tuning characteristics of a neuron but rather on the conditioning frequency. In other words, retuning of a neuron is not simply proportional to the unconditioned frequency responses in the FRF. More specifically, there is no response change or a slight depression of response to the conditioned frequency itself. Thus, the influence on frequencies adjacent to the CS must involve other, presumably, neighboring connected neurons driven by the CS.

The electrophysiological results are suitable to explain heuristically the 2DG results of conditioning, and both together provide some insight in how learning changes cortical representation of sounds.

Obviously, frequency conditioning does not alter the tuning of those units with a BF corresponding to the CS very much, i.e., these units appear to remain in the ensemble of conditioned neurons. Instead, tonotopically neighboring units are incorporated into the conditioned ensemble to a varying degree. As there is also a general unspecific decrease of activity of all units during conditioning, the incorporation effect would not necessarily result in a simple increase of labeling and widening of a labeled frequency band lamina but rather to complex spatial shifts of the distribution of labeling. The fine pattern of such redistributions of activity in large neuronal ensembles may depend on the type of conditioning and on context variables as suggested by the 2DG results. It is appealing to speculate that the meaning of sounds is stored by such cooperative effects which shift the weight of activity within and beyond the limits of previously responsive neuronal ensembles.

Discussion

Our gerbil results on learning-induced retuning of neurons are in line with results in other mammalian auditory cortices (Diamond and Weinberger, 1989; Edeline et al., 1990). In conjunction with the 2DG data, however, single unit plasticity is put on a different scale, namely that large changes of spatial representation of sounds occur in tonotopic maps. That tonotopic organization is not rigid, neither during development (King and Moore, 1991), nor after partial cochlear lesions (Robertson and Irvine, 1989), appears somewhat less surprising than similar effects as a result of simple conditioning. As the observed shifts of maximum activation across the tonotopic gradient are in the range of octave intervals and are found along the extent of FB laminae (several millimeters), very large numbers of neurons must be involved in forming new functional ensembles. How this conflicts with the spectral processing of other sounds remains to be determined. In principle, a strategy of large, but not completely overlapping, representations of spectrally similar sounds could be the way cortex is solving this problem, if an additional requirement is fulfilled. There should be a relatively wide meshwork of non-plastic and rigidly responding neurons which guarantee tonotopic fidelity. Many neurons within the meshwork could then be flexibly involved to shape the representation of sounds with different meaning.

What can possibly be learned from these results for making cochlear implants more successful? Learning in the normal animal is capable of functionally reorganizing even tonotopic gradients in auditory cortex. Therefore, it seems obvious that more elaborate auditory training should have a fundamental role in the rehabilitation process, if only a fraction of the cortical plasticity potential is maintained after extended periods of deafness. Furthermore, tonotopic organization fundamentally involves most neurons in multiple maps of auditory cortex, probably all capable of learning-induced changes. Therefore, spectral aspects of sounds produced by implants should be more in the focus of interest as they may be vehicles of re-learning.

References

Caird, D., Scheich, H. and Klinke, K. (1991) Functional organization of auditory cortical fields in the Mongolian gerbil (*Meriones unguiculatus*). Binaural 2-deoxyglucose patterns. *J. Comp. Physiol., A,* 168: 13–26.

Diamond, D.M. and Weinberger, N.M. (1989) Role of context in the expression of learning-induced plasticity of single neurons in auditory cortex. *Behav. Neurosci.,* 103: 471–494.

Edeline, J.-M., Massioui, N.-E. and Dutrieux, G. (1990) Frequency-specific cellular changes in the auditory system during acquisition and reversal of discrimative conditioning. *Psychobiology,* 18: 382–393.

Fink, A. and Sofouglu, M. (1966) Auditory sensitivity in the Mongolian gerbil (*Meriones unguiculatus*). *J. Aud. Res.,* 6: 313–319.

Fraysse, B. and Cochard, N. (Eds.) (1989) *Cochlear Implant: Acquisitions and Controversies – Symposion on Cochlear Implants,* Presses Paragraphic, Toulouse.

Gonzalez-Lima, F. and Scheich, H. (1984) Neural substrates for tone-conditioned bradycardia demonstrated with 2-deoxyglucose. I. Activation of auditory nuclei. *Behav. Brain Res.,* 14: 213–233.

Gonzalez-Lima, F. and Scheich, H. (1986a) Neural substrates for tone-conditioned bradycardia demonstrated with 2-deoxyglucose. II. Auditory cortex plasticity. *Behav. Brain Res.,* 20: 281–293.

Gonzalez-Lima, F. and Scheich, H. (1986b) Classical conditioning of tone-signaled bradycardia modifies 2-deoxyglucose uptake patterns in cortex, thalamus, habenula, caudate-putamen and hippocampal formation. *Brain Res.*, 363: 239 – 256.

Heil, P. and Scheich, H. (1986) Effect of unilateral and bilateral cochlea removal on 2-deoxyglucose patterns in the chick auditory system. *J. Comp. Neurol.*, 252: 279 – 301.

King, A.J. and Moore, D.R. (1991) Plasticity of auditory maps in the brain. *Trends Neurosci.*, 14: 31 – 37.

Mata, M., Fink, D.J., Grainer, H., Smith, C.B., Davidson, J., Savaki, H., Schwartz, W.J. and Sokoloff, L. (1980) Activity-dependent energy metabolism in rat pituitary primarily reflects sodium pump activity. *J. Neurochem.*, 34: 213 – 215.

McMullen, N.T. and Glaser, E.M. (1988) Auditory cortical responses to neonatal deafening: pyramidal neuron spine loss without changes in growth or orientation. *Exp. Brain Res.*, 72: 195 – 200.

Ohl, F. (1991) Elektrophysiologische Korrelate plastischer Prozesse im auditorischen Cortex der Mongolischen Wüstenrennmaus (*Meriones unguiculatus*). Diplomarbeit, Technische Hochschule, Darmstadt.

Robertson, D. and Irvine, D.R.F. (1989) Plasticity of frequency organization in auditory cortex of guinea pigs with partial unilateral deafness. *J. Comp. Neurol.*, 282: 456 – 471.

Ryan, A. (1976) Hearing sensitivity in the Mongolian gerbil (*Meriones unguiculatus*). *J. Acoust. Soc. Am.*, 59: 1222 – 1226.

Ryan, A., Woolf, N.K. and Sharp, R.R. (1982) Tonotopic organization in the central auditory pathway of the Mongolian gerbil: a 2-deoxyglucose study. *J. Comp. Neurol.*, 207: 369 – 380.

Scheich, H. (1991a) Representational geometries of telencephalic auditory maps in birds and mammals. In: B.L. Finlay, G. Innocenti and H. Scheich (Eds.), *The Neocortex, Ontogeny and Phylogeny,* NATO Series, New York, pp. 119 – 136.

Scheich, H. (1991b) Auditory cortex: comparative aspects of maps and plasticity. *Curr. Opin. Neurobiol.*, 1: 236 – 247.

Singer, W., Gray, C.M., Engel, A.K., König, P., Artola, A. and Bröcker, W. (1991) Formation of cortical cell assemblies. In: P.J. Sejnowski and C.F. Stevens (Eds.), *Cold Spring Harbour Symposium on Quantitative Biology, Vol. LV,* Cold Spring Harbour Press, NY, pp. 939 – 952.

Sokoloff, L., Reivich, H., Kennedy, C., Des Rosiers, M.H., Patlak, C.S., Pettigrew, K.D., Sakurada, O. and Shinohara, N. (1977) The [^{14}C]deoxyglucose method for the measurement of local cerebral glucose utilization. Theory, procedure and normal values in the conscious and anesthetized albino rat. *J. Neurochem.*, 28: 897 – 916.

Steffen, H., Simonis, C., Thomas, H., Tillein, J. and Scheich, H. (1988) Multiple fields, their architectonics and connections in the Mongolian gerbil. In: J. Syka and R.B. Masterton (Eds.), *Auditory Pathway – Structures and Function,* Plenum, New York, pp. 223 – 228.

Theurich, M., Müller, C.M. and Scheich, H. (1984) 2-Deoxyglucose accumulation parallels extracellularly recorded spike activity in the avian auditory neostriatum. *Brain Res.*, 322: 157 – 161.

Thomas, H. (1989) Funktionelle und anatomische Organisation des auditorischen Cortex beim Gerbil (*Meriones unguiculatus*). Dissertation, Technische Hochschule, Darmstadt.

Tillein, J. (1988) Tonotopie im auditorischen Cortex der Mongolischen Wüstenrennmaus (*Meriones unguiculatus*). Diplomarbeit, Technische Hochschule, Darmstadt.

Weinberger, N.M. and Diamond, D.M. (1987) Physiological plasticity in auditory cortex: rapid induction by learning. *Prog. Neurobiol.*, 29: 1 – 55.

Weinberger, N.M. and Diamond, D.M. (1990) Retuning of auditory cortex: a preliminary model. *Concepts Neurosci.*, 1: 91 – 132.

J.H.J. Allum, D.J. Allum-Mecklenburg, F.P. Harris and R. Probst
Progress in Brain Research, Vol. 97

Overview and critique of Chapters 14 – 18

J. Duysens

Nijmegen, The Netherlands

In recent years it has become increasingly clear that it is misleading to describe the activity of motoneurones or interneurones as resulting from the input from a single source such as a descending command, or a proprioceptive, or exteroceptive reflex pathway. Instead, it is important to understand this activity in the context of the motor task to be executed. This is true for automated movements, such as those that occur during postural corrections and locomotion, as well as for voluntary movements.

Task-dependency during the latter type of movements was investigated by Tax and Gielen in an elegant series of experiments on single motor unit recruitment in elbow muscles during force and movement tasks. The force threshold of their units was found to depend both on the direction of the torque (e.g., supination, flexion) and on type of task (force or movement). Their conclusions about the existence of task-related subpopulations of motoneurones can be seen as parallelling similar views, based on studies of leg muscles ("task groups", Loeb, 1985). Nevertheless, some limitations in the experimental design suggest caution in the interpretation of the data. The force threshold, defined by Tax and Gielen, was measured at the elbow joint, not at the muscles involved. Hence, the relative torque contribution of the different muscles in force and movement tasks can only be estimated quite indirectly. It would therefore be of interest, either to include surface EMG recordings as extra estimators of force, or to extend these experiments to studies on animals, in which muscle force can be measured directly (Loeb et al., 1980).

A second salient feature of the paper by Tax and Gielen concerns the shift in the initial firing rate at recruitment in force as opposed to movement tasks. Although this shift is relatively small (e.g., a transition in firing rate from 10 to 12 Hz), the result is consistent and has far-reaching consequences, since it suggests that even the intrinsic properties of motoneurones can be adapted to the requirements of different tasks. The authors interpret their data mainly in the context of the effects of monoamines on the membrane properties of motoneurones (Conway et al., 1988), but some alternative hypotheses should be considered as well. The force and voluntary movement tasks, used by Tax and Gielen, almost certainly led to different fusimotor sets (Prochazka et al., 1985), or more generally, to changes in sensory contexts, which may have affected the motoneurones differentially. In addition, the conclusion about the specific effects of force commands (involving monoaminergic pathways) should be evaluated in the context of a possible role of force feedback on motoneurones as well. Other factors, such as for example different rates of depolarization of the motoneurones in the various tasks, could theoretically also have contributed to the observed shift in initial firing rate.

During the automated movements of locomotion, task-dependency emerges in the form of changes in gain of various reflexes. Summarizing an impressive set of experiments, Stein, Yang, Bélanger and Pearson describe how the gain of H-reflexes decreases as one changes from standing to walking and running. So far, this "task-dependent

gating" has only been fully documented for H-reflexes in soleus. However, to establish whether a general decrease in gain occurs in proprioceptive reflexes under these locomotor conditions, it would be of interest to know more about the gain changes in other muscles as well. Soleus is a slow "postural" muscle and one can therefore not easily extrapolate these results to other fast muscles. This problem is also present for the phase dependency of the responses. Stein et al. showed that the gain of both H-reflexes and tendon reflexes in soleus increases during the stance phase of walking. In contrast, for quadriceps Dietz et al. (1990a,b) found a decrease for both types of reflexes under the same circumstances. Another unresolved issue is the functional interpretation of the reduced gain in soleus H-reflexes just after footfall. Is this related to the landing of the foot in an attempt to preserve the normally occurring yield in that phase? Dyhre-Poulsen et al. (1991) showed that the soleus H-reflex was small at touchdown when landing from a downward jump, but large at touchdown while hopping. Hence the gain of the soleus H-reflex seems more a function of the post-landing requirements than of the landing itself.

Stein described a similar difficulty in interpretation arising for the phase-dependent modulation and reversal of the cutaneous reflexes. According to Yang and Stein (1990), the meaning of the modulation and reversal of tibialis anterior responses with medium latency lies in the adjustment of corrective responses to external perturbations during the step cycle ("stumbling corrective responses", Forssberg, 1979). However, during swing, the changes in joint angles correlated with these cutaneous reflexes are small, and do not resemble the behavioral corrections to mechanical perturbations. Therefore, one should consider the alternative interpretation that the medium latency responses represent an exaggeration of activity in reflex pathways which are continuously used during the step cycle, even when no correction is needed. Movement induces increased firing in afferents from the skin, even if the latter is not in direct contact with external surfaces (Loeb et al., 1977; Hulliger et al., 1979). Skin stretch is often overlooked as a source of movement feedback. Lundberg et al. (1987) suggested that such afferent activity from the skin is combined with sensory signals from muscle receptors in reflex pathways which are continuously used to assist movement. For example, the facilitation of reflexes in flexor muscles, such as tibialis anterior, in late stance and early swing should perhaps not be seen as corrective responses but rather as an exaggeration of activity in so-called FRA pathways which assist in the generation of flexion movements at the onset of swing.

Whatever the correct interpretation of the gating data may be, it is of great interest that phase-dependent modulation is now being investigated clinically. The finding, reported by Stein, that patients with spasticity often show a considerable loss in phase-dependent modulation of H-reflexes, indicates that there is a possible link between gait abnormalities and defective gating mechanisms in spinal reflexes.

In his paper, Hulliger also reviews some clinical data. The ataxia, resulting from pyridoxine intoxication, is attributed mostly to a loss of proprioceptive feedback. At present, however, it is uncertain how much cutaneous afferent input contributes to these ataxia's. Nevertheless, Hulliger is probably right when he points out that some of the observed deficits may be due to long-term effects. He argues that Ia feedback may be used to optimize motor programs. This could occur against a background of high dynamic fusimotor drive, for which Hulliger and his colleagues obtained convincing evidence, using an elegant method to reconstruct fusimotor activation profiles during movements. Although this method has its limitations (the reconstruction is made with one or two gamma fibers, while in reality up to 12 gamma fibers can affect the signals from a spindle afferent), there is no reason to doubt some of the predictions concerning the presence of high dynamic gamma drive during difficult tasks, such as beam walking. Interestingly, in humans the H-reflexes in such tasks are smaller than during normal walking (Llewellyn et al., 1990), which would imply that, paradoxically, a high dynamic fusimotor gain

may go hand in hand with a low reflex gain. Could it be useful to control a high sensitivity of the peripheral receptor while centrally we already have the ability to control the gain of these incoming signals? Hulliger answers with a clear no. He believes that artificial control of gait does not require peripheral gain control. However, the results of the beam walking, mentioned above, may undermine his conclusion. In such difficult tasks, it may be advantageous to be able to have both peripheral and central gain control. For example, it may be useful to have a high peripheral sensitivity to be able to make fast corrective movements, based on projections to higher motor centers, while at the same time reducing the stiffness of the parent muscles by lowering the gain in segmental reflex pathways. It may be argued that the same goal can be achieved by having a different gain control at the segmental and supraspinal level. However, this would require that the sensor always operates at its most sensitive level. This is a severe limitation since the sensor then saturates when large changes in length have to be signaled. The big advantage of peripheral gain control (not only for spindles but also for other sensors such as retinal rods during dark adaptation) is that the full dynamic range of the afferent elements can be used to measure over different ranges of stimulus intensities. Is it wise to disregard this elegant design principle at this early stage of thinking about artificial control of gait?

The contribution of Dietz also addresses task-dependent gating of responses but the emphasis is on postural responses to natural stimuli, such as translational movements of the supporting surface. Through a series of imaginative experiments, he was able to demonstrate that the amplitude of these bilaterally occurring responses increased in situations where destabilization was most pronounced. It is argued that the position of the body's center of gravity in relation to the support surface is the controlled variable. Furthermore, Dietz suggests that the modulation of the amplitude of the responses is caused by interactions with activity from load-detecting receptors from extensor muscles. This certainly is a very intriguing proposition, requiring further discussion. In motor control, the emphasis has been too long on length feedback and it is only recently that the need for force-regulating mechanisms has been fully recognized (Taylor and Gottlich, 1985). Whether one has to control precisely the force needed to grasp an egg between fingers or whether one has to adjust corrective postural responses as a function of body loading (e.g., constant changes in length, induced by platform perturbations under water in the Dietz' experiments), feedback from load detectors is essential.

In Dietz' opinion, the latter feedback is primarily used to modulate the responses, which are presumed to originate from the activation of group II afferents. The question remains, however, whether loading or unloading of muscles could not have been the direct cause of some of the observed responses rather than the modulating factor. Certainly, Dietz showed a close correlation between response amplitude and changes in ankle angle. However, the experiments did not permit the measurement of the loading of the different muscles involved and it is quite possible that the observed responses were well related to these (unmeasured) force changes as well as to the variations in muscle length. During locomotion of thalamic cats, it has been shown that loading of extensors prevents the initiation of the flexor burst, needed for the onset of swing (Pearson and Duysens, 1976; Duysens and Pearson, 1980). This effect could be traced to activation of Ib afferents from these extensors. In this situation, the unloading of extensors is thus a prerequisite for the activation of flexors. These findings have recently been confirmed in a preparation with fictive locomotion (Conway et al., 1987).

Whether the load receptors act directly or indirectly, it will be a challenge for further research to identify the receptors themselves. Ib afferents are the prime candidates of the "extensor load detectors", mentioned by Dietz. This is a very sensible proposition, since it is known from the work of Houk and Henneman (1967) that these receptors are best recruited by active contraction of the parent muscles and that they could function as load detectors (for recent review, see Jami, 1992). Mechano-

receptors of the foot could play this role as well, but Dietz argues that these are not likely to contribute, since anesthesia of the skin has little effect on the postural responses. However, there may be redundancy in the afferent systems signaling load and hence, substitution of one system by the other is quite possible in such cases. In support of this redundancy idea is the observation that Ib and cutaneous afferents converge on common interneurones (Lundberg et al., 1977). This implies that information about changes in load, as detected by cutaneous mechanoreceptors from the foot and by extensor Golgi tendon organs, is combined in the spinal cord (see also Taylor and Gottlich, 1985; Schomburg, 1990).

It is at the level of the spinal cord that Dietz argues postural responses are generated. This is certainly the most likely possibility in view of the relatively short latency of the responses and in view of the evidence that the responses are due to activation of group II rather than of group I afferents (Dietz et al., 1985). Nevertheless, for tibialis anterior responses to electrical stimulation of the sural nerve, Burke et al. (1991) and Meinck et al. (1985) claimed that responses with a latency of respectively 90 and 80 msec could, in principle, arise from a transcortical loop. One should keep in mind, however, that long latencies do not necessarily imply long loops and that responses to mechanical stimulation have longer latencies than those to electrical shocks. To settle this issue, experiments with magnetic stimulation of the cortex may be helpful, as they have been in providing evidence for a cortical involvement for the long-latency stretch reflex of the human thumb (Capaday et al., 1991). The possibility of the release of a brain-stem "triggered response", such as the spinobulbospinal (SBS) reflex, cannot be ruled out either. For the gastrocnemius response a SBS reflex is unlikely because of the dependence of the amplitude of the responses on propioceptive feedback. However, as pointed out by Dietz, the tibialis anterior response amplitude and latency to forward perturbation was about equal on both sides, even following unilateral displacement. This would be consistent with the release of a common brain-stem "program". Dietz' argument (Dietz et al., 1990a,b) for a spinal rather than a supraspinal "program" is partly based on the observation that adaptations in interlimb coordination survive spinal transections in cats. However, the interlimb coordination, referred to in these animal experiments, is related to phase shifts of stepping movements, which are out of phase, while the presently described coordination involves "in phase" coordination. Moreover, although evidence for a spinal central pattern generator (CPG) is abundant for the cat, similar convincing evidence is not available for humans.

In the cat, the first detailed description of the operation of the CPG came from Jankowska and colleagues (Jankowska et al., 1967). Since these pioneering studies, she has continued to explore spinal circuitry and her contribution in this book summarizes some of the most recent data from this excellent work. Jankowska and Edgley report on three types of spinal interneurones, involved in the control of posture and locomotion. Especially exciting is the discovery of the excitatory group II interneurones, since these are the only group of identified last-order interneurones able to activate motoneurones. The description of these premotor elements has raised hope that we can soon start to unravel the details of the spinal locomotor CPG. However, although most of the evidence available supports the notion that these neurones play a part in locomotion (in particular "fictive" locomotion), the question remains whether they are part of the CPG. None of the six neurones of this type, described by Edgley et al. (1988), showed DOPA-induced long-lasting discharges in phase with activity from flexors or extensors, as has been found in the initial DOPA studies (Jankowska et al., 1967). Instead, DOPA selectively depressed these neurones as well as all other types of group II interneurones in the intermediate zone and in the ventral horn.

Jankowska and Edgley also argue for a role of the group II interneurones in phase-dependent reflex reversals. A discussion about the neural substrate for this type of reversal is particularly welcome in view of the recent demonstrations of such reversals in humans (see contribution of Stein et al.). The

main argument of Jankowska for a role in phase switching is that these group II interneurones receive potent input from hip muscles and that it has been shown that hip position is important for reflex reversals. Clearly, it would be of great interest to have recordings from these interneurones in behaving animals but the technical difficulties for this type of experiment have yet to be solved. More feasible, for the time being, would be experiments to determine whether the proposed phase-switching neurones are sensitive to extensor unloading, since it has been shown that this is an essential feature for the transition from stance to swing (see above).

In the final part of their paper, Jankowska and Edgley present a summary of the data on commissural interneurones. Since group II afferents are able to activate some of these neurones, it is tempting to speculate that these commissural interneurones may play a role in bilaterally occurring responses to unilateral perturbations, such as those described by Dietz. In relation with the latter work, it would also have been quite interesting to have a review of the Goteborg work on "Ib inhibitory interneurones", but this was omitted because these neurones have yet to be shown to be active during either fictive locomotion or postural reactions of the cat.

With respect to these "Ib interneurones", it is worth noting that this terminology is being gradually abandoned because of the proven convergence from other types of afferents on these interneurones (Lundberg et al., 1977; Powers and Binder, 1985), and the question then arises whether similar difficulties will not emerge with the "group II interneurone" terminology, currently used by Jankowska and colleagues. Certainly, the main input to these neurones is from group II interneurones in the reduced preparations used, but there is also extensive convergence from other afferents and it is not known in which pathways these interneurones operate predominantly in the intact animal. Hence, one should keep in mind the restrictions, inherent to any classification of this type, in order to avoid that these terms become a straightjacket to our thinking about the functioning of spinal circuitry (for more details see, for example, the recent discussion about the Flexor Reflex Afferents terminology in Schomburg, 1990).

References

Burke, D., Dickson, H.G. and Skuse, N.F. (1991) Task-dependent changes in the responses to low-threshold cutaneous afferent volleys in the human lower limb. *J. Physiol. (Lond.)*, 432: 445–458.

Capaday, C., Forget, R., Fraser, R. and Lamarre, Y. (1991) Evidence for a contribution of the motor cortex to the long-latency stretch reflex of the human thumb. *J. Physiol. (Lond.)*, 440: 243–255.

Conway, B.A., Hultborn, H. and Kiehn, O. (1987) Proprioceptive input resets central locomotor rhythm in the spinal cat. *Exp. Brain Res.*, 68: 643–656.

Conway, B.A., Hultborn, H., Kiehn, O. and Mintz, I. (1988) Plateau potentials in alpha-motoneurones induced by intravenous injection of L-dopa and clonidine in the spinal cat. *J. Physiol. (Lond.)*, 405: 369–384.

Dietz, V., Quintern, J. and Berger, W. (1985) Afferent control of human stance and gait: evidence for blocking of group I afferents during gait. *Exp. Brain Res.*, 61: 153–163.

Dietz, V., Horstmann, G.A. and Berger, W. (1989) Interlimb coordination of leg-muscle activation during perturbation of stance in humans. *J. Neurophysiol.*, 62: 680–693.

Dietz, V., Discher, M., Faist, M. and Trippel, M. (1990a) Amplitude modulation of the human quadriceps tendon jerk reflex during gait. *Exp. Brain Res.*, 82: 211–213.

Dietz, V., Faist, M. and Pierrot-Deseilligny, E. (1990b) Amplitude modulation of the quadriceps H-reflex in the human during the early phase of gait. *Exp. Brain Res.*, 79: 221–224.

Duysens, J. and Pearson, K.G. (1980) Inhibition of flexor burst generation by loading ankle extensor muscles in walking cats. *Brain Res.*, 187: 321–332.

Dyhre-Poulsen, P., Simonsen, E.B. and Voigt, M. (1991) Dynamic control of muscle stiffness and H reflex modulation during hopping and jumping in man. *J. Physiol. (Lond.)*, 437: 287–304.

Edgley, S.A., Jankowska, E. and Shefchyk, S. (1988) Evidence that mid-lumbar neurones in reflex pathways from group II afferents are involved in locomotion in the cat. *J. Physiol. (Lond.)*, 403: 57–71.

Forssberg, H. (1979) Stumbling corrective reaction: a phase-dependent compensatory reaction during locomotion. *J. Neurophysiol.*, 42: 936–953.

Houk, J.C. and Henneman, E. (1967) Responses of Golgi tendon organs to active contraction of the soleus muscle of the cat. *J. Neurophysiol.*, 30: 466–481.

Hulliger, M., Nordh, E., Thelin, A.E. and Vallbo, A.B. (1979) The responses of afferent fibres from the glabrous skin of the hand during voluntary finger movements in man. *J. Physiol.*

(Lond.), 291: 233 – 249.

Jami, L. (1992) Golgi tendon organs in mammilian skeletal muscle: functional properties and central actions. *Physiol. Rev.*, 72: 623 – 666.

Jankowska, E., Jukes, M.G.M., Lund, S. and Lundberg, A. (1967) The effect of DOPA on the spinal cord. 6. Half-centre organization of interneurones transmitting effects from the flexor reflex afferents. *Acta Physiol. Scand.*, 70: 389 – 402.

Llewellyn, M., Yang, J.F. and Prochazka, A. (1990) Human H-reflexes are smaller in difficult beam walking than in normal treadmill walking. *Exp. Brain Res.*, 83: 22 – 28.

Loeb, G.E. (1985) Motoneurone task groups: coping with kinematic heterogeneity. *J. Exp. Biol.*, 115: 137 – 146.

Loeb, G.E., Bak, M.J. and Duysens, J. (1977) Long-term unit recording from somatosensory neurons in the spinal ganglia of the freely walking cat. *Science*, 197: 1192 – 1194.

Loeb, G.E., Walmsley, B. and Duysens, J. (1980) Obtaining proprioceptive information from natural limbs: implantable transducers vs. somatosensory neuronrecordings. In: M.R. Neuman, D.G. Fleming, P.W. Cheung and W.H. Ko (Eds.), *Physical Sensors for Biomedical Applications*, CRC Press, Baton Rouge, FL, pp. 135 – 149.

Lundberg, A., Malmgren, K. and Schomburg, E.D. (1977) Cutaneous facilitation of transmission in reflex pathways from Ib afferents to motoneurones. *J. Physiol. (Lond.)*, 265: 763 – 780.

Lundberg, A., Malmgren, K. and Schomburg, E.D. (1987) Reflex pathways from group II muscle afferents. 3. Secondary spindle afferents and the FRA; a new hypothesis. *Exp. Brain Res.*, 65: 294 – 306.

Meinck, H.M., Benecke, R. and Conrad, B. (1985) Cutaneomuscular control mechanisms in health and disease: possible implications on spasticity. In: A. Struppler and A. Weindl (Eds.), *Electromyography and Evoked Potentials*, Springer, Berlin-Heidelberg, pp. 75 – 83.

Pearson, K.G. and Duysens, J. (1976) Function of segmental reflexes in the control of stepping in cockroaches and cats. In: R.E. Herman, S. Grillner, D. Stuart and P. Stein (Eds.), *Neural Control in Locomotion*, Plenum, New York.

Powers, R.K. and Binder, M.D. (1985) Distribution of ologosynaptic group I input to the cat medical gastrocnemius motoneuron pool. *J. Neurophysiol.*, 53: 497.

Prochazka, A., Hulliger, M., Zangger, P. and Appenteng, K. (1985) Fusomotor set: new evidence for α-independent control of gamma-motoneurones during movement in the awake cat. *Brain Res.*, 339: 136 – 140.

Schomburg, E.D. (1990) Spinal sensorimotor systems and their supraspinal control. *Neurosci. Res.*, 7: 265 – 340.

Taylor, A. and Gottlich, S. (1985) Convergence of several sensory modalities in motor control. In: W.J. Barnes and M.H. Gladden (Eds.), *Feedback and Motor Control in Invertebrates and Vertebrates*, Croom Helm, London, pp. 77 – 93.

Yang, J.F. and Stein, R.B. (1990) Phase-dependent reflex reversal in human leg muscles during walking. *J. Neurophysiol.*, 63: 1109 – 1117.

J.H.J. Allum, D.J. Allum-Mecklenburg, F.P. Harris and R. Probst
Progress in Brain Research, Vol. 97

CHAPTER 14

New aspects of human muscle coordination as revealed by motor-unit studies

A.A.M. Tax and C.C.A.M. Gielen

Department of Medical Physics and Biophysics, University of Nijmegen, The Netherlands

Increasing evidence has become available against the view that individual muscles should be regarded as functional units in the control of force by the motor apparatus. The relative contribution of various motoneurone pools (belonging to a single muscle) to muscle force appears to depend on the direction of torque exerted by the corresponding limb. This clearly indicates the presence of more than one control or activation parameter for the total motoneurone pool of a single muscle. Windhorst et al. (1989) have even proposed a combined sensory and neuromuscular partitioning, such that segmental control mechanisms are based on subdivisions of motoneurone pool – muscle complexes. Size-related recruitment occurs within these subdivisions rather than in the motoneurone pool as a whole. Moreover, motoneurones can operate in various modes (different relative contributions of the recruitment mechanism and the firing frequency mechanism to muscle force) related either to movement or to force. This indicates that muscle coordination is organised differently in force tasks and in movement tasks. These properties of motoneurone activation mentioned above are difficult to incorporate in existing models on sensorimotor organisation. Some of these discrepancies will be reviewed in order to highlight future directions for modelling.

Key words: Muscle; Motor units; Movement coordination; Human arm movements

Introduction

The control of posture and movement is one of the important functions of the central nervous system (CNS). Both from an architectural (Kuypers, 1985) and a functional (Bernstein, 1967; Schmidt, 1978; Brooks, 1986; Denier van der Gon, 1988) point of view the motor system is generally assumed to be built up in parallel but hierarchically organized stages. At the highest level an internal representation of the outer world, the body and the limbs is constructed on the basis of experience and actual sensory information. At this level perception, cognition, motivation and attention play an important role with regard to the decisions to act and to the planning of movements (Pew, 1984). At a lower level the resulting signals are thought to be transformed into motor programmes. Then the suitable muscles are selected and eventually, at the lowest (spinal) level, their motoneurone pools are activated. The CNS centres can only perform appropriately if they receive a continuous stream of afferent (sensory) information. Therefore, "one often uses the term sensorimotor system to connote the totality of afferent and efferent functions participating in muscular activity" (Schmidt, 1978).

Investigation of the sensorimotor system in humans is hampered by the fact that the motor centres are inaccessible to direct measurement. However, muscle-fibre activity recorded by means of intramuscular fine-wire electrodes reflects the activity of its parent motoneurone in the spinal cord. In this way motoneurone activity in the spinal cord can be measured indirectly. The motoneurone can be activated by (direct) projections originating from higher centres and/or by sensory projections that may be

influenced by the fusimotor system (γ-activation). In other words, "the motor unit serves as the final common pathway for motor integration at the cellular level" (Houk and Rymer, 1981). Therefore, measurements of motor-unit activity alone do not allow conclusions to be drawn about important issues relating to motoneuronal control, such as α-γ linkage (Granit, 1955) or independent α-γ control (Prochazka et al., 1985). Nevertheless, motor-unit studies can provide detailed information on the important question of muscle coordination. As two examples of this we will describe, in more detail, the different coordination of elbow flexor muscles in force and movement tasks and, in short, the non-homogeneous activation of muscles acting around the elbow joint. These results will be discussed in light of current models on muscle coordination in various motor tasks.

Motor-unit studies

Motor-unit activity of elbow flexor muscles in force and movement tasks

Recruitment and firing frequency behaviour of motor units in the m. biceps, m. brachialis and m. brachioradialis have been investigated in three different conditions (Tax et al., 1989, 1990a,b). Condition I: isometric flexion contractions in which the exerted torque at the wrist is slowly increased. In this experiment the upper arm is 80° abducted and supported under the elbow joint. The angle between the forearm and the upper arm is fixed at 100° (the reference position; 180° corresponds to full extension of the forearm). Condition II: small *voluntary* movements near the reference position while the subject is exerting a constant or increasing torque in flexion direction. Condition III: the subject is instructed to exert increasing flexion torques while movements are imposed by a torque motor. The movements in conditions II and III can be either in flexion or in extension direction. The velocity of the movements is constant and very small (2 – 15°/sec angular velocity in the elbow joint). Motor-unit activity in the various elbow flexor muscles is compared, near the reference position, in conditions I, III (both a force task) and II (movement task).

The recruitment threshold of motor units in m. biceps brachii is found to be considerably lower for voluntary flexion and extension movements (condition II) than for isometric contractions (condition I), even at velocities as low as 2°/sec. For velocities greater than 2°/sec the recruitment thresholds appear to depend weakly on the velocity of the movement. The slight decrease in recruitment threshold for increasing velocities agrees rather well with the effect of the force-velocity relation. Contrary to the results in m. biceps brachii the recruitment threshold of the motor units in m. brachialis and m. brachioradialis is found to be considerably higher for voluntary flexion and extension movements than for isometric contractions. The amount of decrease (biceps) and increase (brachialis, brachioradialis) is proportional to the isometric recruitment threshold (see Fig. 1). This means that within one population of motor units the recruitment order is generally the same during isometric contractions and slow voluntary movements. For all three elbow

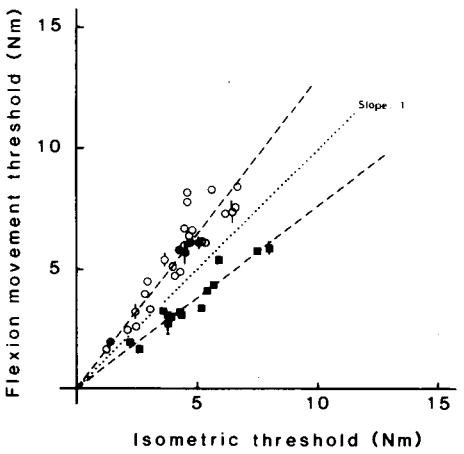

Fig. 1. Joint recruitment data of m. biceps (filled squares), m. brachialis (open circles) and m. brachioradialis (filled circles). For each investigated motor unit the estimated recruitment threshold for slow voluntary flexion movements is plotted against the average isometric recruitment threshold. A slope equal to one would indicate that the recruitment behaviour is similar in both types of task. (Used by permission from Tax et al., 1990b.)

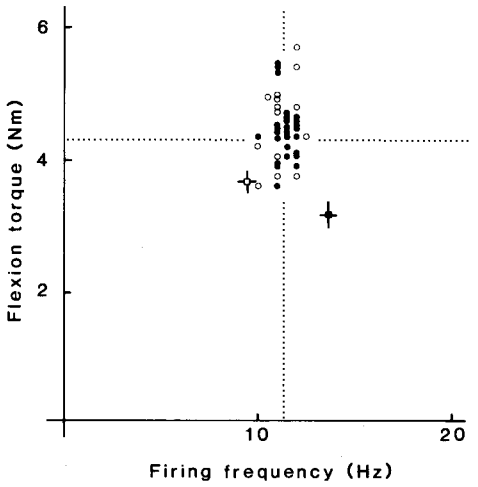

Fig. 2. Data obtained from one typical biceps motor unit. Combinations of flexion recruitment threshold and initial firing frequency during the first second after recruitment for contractions during imposed movements in flexion (filled circles) and extension (open circles) direction. In addition, the average recruitment threshold and the average initial firing frequency for *voluntary* flexion (filled square) and extension (open square) movements are plotted, together with the estimated errors. The point of intersection of the two dotted lines indicates the average recruitment threshold and the average initial firing frequency for isometric contractions. (Used by permission from Tax et al., 1990a.)

flexor muscles the initial firing frequency of the motor units depends on the direction of movement: at recruitment the motor units start firing with a higher firing frequency during voluntary flexion movements and a lower firing frequency during voluntary extension movements than during isometric contractions (see, for instance, Fig. 2).

Two main conclusions are drawn from these results. First of all, the similar recruitment order within each flexor muscle for isometric contractions and for both voluntary flexion and extension movements indicates a homogeneous activation of the motoneurone pools in these conditions. However, the firing frequency at recruitment of the motoneurones can be adjusted rather independently: the motoneurones seem to possess several different "modi operandi" related to the required task. This means that the relative contribution of the two force-grading mechanisms, i.e., the recruitment of motor units and the modulation of their firing frequency, is task-dependent. Secondly, the relative activation of the three synergistic elbow flexor muscles is different for isometric contractions and slow voluntary movements (against a constant and an increasing load). The relative contribution to the total exerted flexion torque in the elbow is estimated to increase to approximately 48% for biceps and to decrease to approximately 45% for brachialis and brachioradialis during slow voluntary movements in comparison with the relative contribution of 36% and 57%, respectively, during isometric contractions. It has been argued that these differences have to be ascribed mainly to the different recruitment behaviour of the three elbow flexor muscles in the two tasks.

In both force tasks, i.e., the isometric flexion contractions (condition I) and the flexion contractions during imposed movements (condition III), the recruitment levels and the firing frequency behaviour of the motor units of all three muscles have been found to be similar (see Fig. 2). However, these motor-unit characteristics are quite different in slow movement tasks (condition II), as is described in the previous paragraph. Thus, a specific recruitment and firing frequency behaviour is not related to the presence or absence of movement itself, but rather to the instruction to the subject. This implies that the remarkably different motor-unit behaviour in force and movement tasks cannot be caused by differences in afferent signals without concomitant changes in the central activation of the α and/or γ motoneurone pools. A simple redistribution of central activity among the same efferent nerve bundles that project onto the α and/or γ motoneurone pools of the elbow flexor muscles cannot account for both the different recruitment and firing frequency behaviour during voluntary movements. A possible explanation might be that primarily intrinsic spinal mechanisms are controlled by supra-spinal input such that both the excitability and the firing frequency of the motoneurones can be adjusted (Conway et al., 1988). It is concluded that the *central* activation of the α and/or γ motoneurone pools of the three elbow flexor muscles is remarkably different

for force tasks and slow (voluntary) movement tasks, even if the same torques are exerted and/or the same movements are made.

Non-homogeneous activation of human arm muscles

The recruitment behaviour of motor units belonging to muscles acting around the elbow joint has been studied as a function of *isometric* torque in flexion/extension and supination/pronation direction (ter Haar Romeny et al., 1984; van Zuylen et al., 1988; Denier van der Gon et al., 1991). For the m. biceps brachii (caput longum) three different groups of motor units have been distinguished by virtue of their recruitment behaviour. For the first group of motor units the recruitment threshold only depends on the amount of exerted flexion torque. This group is never active during for instance contractions in supination direction only. The recruitment threshold of the second group only depends on the amount of supination torque (and is never active for purely flexion torques). Finally, the recruitment threshold of the third group depends on a linear combination of supination and flexion torques. So, depending on the task (isometric flexion or supination) different groups of motor units may be active by a different amount. Due to this inhomogeneous activation, the recruitment order within a muscle is not fixed, but is task-dependent. Within a subpopulation of motor units in the muscle there is a fixed recruitment order. It has been shown that subpopulations of motor units, each with a different recruitment behaviour, exist in almost all arm muscles (van Zuylen et al., 1988; Jongen, 1989). Therefore, individual muscles cannot be considered as functional units in the control of the motor apparatus.

Muscle models

Equilibrium point hypothesis

The so-called λ-model (Feldman, 1986; Feldman et al., 1990) is a nice example of how both central and afferent signals can be thought to participate in muscular activity. It will be sufficient to discuss it here in its simplest form. Starting point for this model is an empirical finding. Consider a subject that is counteracting a particular load at a particular elbow angle. The instruction "not to intervene voluntarily to forearm deflections when the load is removed" is thought to fixate the central drive to the sensorimotor system during the (step-by-step) unloading. This results in a force-length curve at a (presumably) constant central drive. This is called an invariant characteristic (IC). It is important to note that, as a consequence of the tonic stretch reflex, muscle activity is not a constant in this experiment. The IC has therefore a dual (central-reflex) nature. By changing the initial conditions (different combinations of elbow torque and elbow angle) a set of IC's can be found. This led Feldman to the idea that muscle together with reflex and central control mechanisms behaves like a non-linear spring, the zero length of which is the controllable parameter (λ, which is set by the central drive). For one pair of agonist/antagonist muscles acting around a single joint this can be expressed in the general mathematical form:

$$F = f(x - \lambda)$$

in which F is the exerted force, x the muscle length, and f the form of the IC that determines the stiffness of the sensorimotor system. This stiffness is thought to be built up by a contribution of both intrinsic muscle stiffness and a combined length feedback by muscle spindles and force feedback by Golgi tendon organs (Houk and Rymer, 1981). Central commands to the α- and/or γ-motoneurones are supposed to specify the zero length (λ) and therefore a particular IC. The sensorimotor system will be in equilibrium if F is exactly counteracting the actual load. This corresponds to a unique point (the equilibrium point, EP) on the particular IC. This EP specifies muscle activity, force and length as a consequence of the interaction between the muscle and the load. In general, the λ-model gives a unique solution (EP) for both *voluntary* (setting the parameter λ and thus choosing a particular IC) and *involuntary* (changing x or changing the load) motor processes. A change in the parameter λ will lead on the one

hand to a force change in isometric conditions and on the other hand to a movement in isotonic conditions. This means that, as far as the model is concerned, force and voluntary movement are controlled by *one single mechanism.* This conclusion holds for all models that are based on an equilibrium point hypothesis (e.g., Bizzi, 1980; Hogan, 1985).

However, the experimental results described above (see p. 155) definitely contradict this view. The existence of task-dependent muscle coordination and task-dependent "modi operandi" of the motoneurones has far-reaching consequences for views on the control of posture and movement. Muscle coordination seems to be organised on the basis of different principles for force tasks and (slow) movement tasks. These principles are not yet understood.

The spring-like property of the effector system, as described previously, is consistently found in all neuromuscular systems ranging from single functionally isolated muscles to sets of several synergistic and antagonistic muscles operating to control joint rotations or even whole arm movements. This indicates that the λ-model may be extended to describe the coordination of different muscles acting around one or more joints (Feldman et al., 1990). However, the model is quite empirical and does not give specific predictions for the relative activations of various synergistic muscles that act across a joint.

Muscle coordination

One of the main problems concerning the coordination of muscle activation for movements or torques in a particular direction is that, for some motor tasks, the number of muscles acting across one or more joints is (thought to be) larger than strictly necessary. This gives rise to the possibility that a torque or movement in a particular direction can be realized by a large variety of different muscle activation patterns. Despite this redundancy, a unique activation pattern of muscles is generally observed in various subjects. The rationale by which the muscles act at any instant is not readily apparent. In the past a number of theories on muscle coordination have been put forward. These theories can be divided into two classes.

In the first class of theories it is hypothesized that the CNS, in order to solve the problem of redundancy, optimises some cost function (e.g., Yeo, 1976; Crowninshield and Brand, 1981; Dul et al., 1984a,b; Herzog 1986). Such a cost function should be non-linear because linear criteria inherently predict discrete muscle action (orderly recruitment of muscles!) instead of synergistic action (Dul et al., 1984a). However, the non-linear (often non-physiological) criteria used, although providing a solution to the problem of redundancy, do in general not agree with experimental findings (van Zuylen et al., 1988). Another contribution may come from (biomechanical) considerations pointing at a different role for mono- and bi-articular muscles. First, Hogan (1985) has proposed that bi-articular muscles are necessary in order to regulate the end-point stiffness of a particular limb. Secondly, van Ingen Schenau (1989) has defined a concept of minimising negative work delivered by muscles. This concept deals with the fact that a particular combination of movement displacement and exerted force of a limb may require that a mono-articular muscle is activated while lengthening. In such a situation the muscle dissipates work rather than contributing to the work done by the limb. Since the work delivered by the limb is equal to the sum of work delivered by all muscles, a negative work production by one muscle has to be compensated by an increased amount of work by another muscle. In minimising this dissipation of work a special role is attributed to the bi-articular muscles in multi-joint movements. This model predicts (qualitatively) a different coordination of mono- and bi-articular muscles in force and movement tasks in agreement with those described above (see p. 155) and data of Gielen et al. (1990). However, it cannot account for the different "modi operandi" of the motoneurones.

The second class of theories is based upon the idea that the organisation of the sensorimotor system is fundamentally a result of transforming sensory per-

ception into motor action. This idea is first elaborated explicitly by means of the controversial "tensor" analysis (Pellionisz and Llinas, 1982; for an application, see Gielen and van Zuylen, 1986). Later, other researchers suggested that the solution to the redundancy problem in muscle coordination should be found in the correlation between the muscle spindle signals of the various muscles. For instance, Jongen et al. (1989) have proposed that the CNS would use a minimal but sufficient set of principle activation vectors, which were determined by a matching of efferent (to the muscles) and afferent (from the muscle spindles) signals. And quite recently, the relevance of neural networks to the coordination of neuromuscular systems has been investigated (Denier van der Gon et al., 1990).

An implicit assumption in all muscle models discussed is that the muscles are homogeneously activated. In the case of a combined sensory and neuromuscular partitioning (Windhorst et al., 1989) *parts* of muscles may be seen as separate units, presumably with size-related recruitment within those subpopulations, and a different behaviour may come to the fore if these parts have on average different mechanical advantages. In this light, Loeb (1985) has proposed the concept of task groups as a functional compartmentalization of the motor apparatus. However, it remains unclear how the models mentioned above should account for all the different subpopulations that are found in human arm muscles (Denier van der Gon et al., 1991).

Acknowledgements

We gratefully acknowledge financial support by the Dutch Foundation for Biophysics (NWO), the ESPRIT BRA project MUCOM (no. 3149) and the UOP from the Medical Faculty of the University of Nijmegen. Part of this work has been carried out at the department of Medical and Physiological Physics, University of Utrecht, The Netherlands.

References

Bernstein, N. (1967) *The Coordination and Regulation of Movements,* Pergamon Press, London.

Bizzi, E. (1980) Central and peripheral mechanisms in motor control. In: G.E. Stelmach and J. Requin (Eds.), *Tutorial in Motor Behavior,* North-Holland, Amsterdam, pp. 131 – 144.

Brooks, V.B. (1986) *The Neural Basis of Motor Control,* Oxford University Press, New York.

Conway, B.A., Hultborn, H., Kiehn, O. and Mintz, I. (1988) Plateau potentials in α-motoneurones induced by intravenous injection of L-DOPA and clonidine in the spinal cat. *J. Physiol. (Lond.),* 405: 369 – 384.

Crowninshield, R.D. and Brand, R.A. (1981) A physiologically based criterion of muscle force prediction in locomotion. *J. Biomech.,* 14: 793 – 801.

Denier van der Gon, J.J. (1988) Motor control: aspects of its organisation, control signals and properties. In: W. Wallinga, H.B.K. Boom and J. de Vries (Eds.), *Electrophysiological Kinesiology,* Elsevier Science Publishers BV (Biomedical Division), Amsterdam, pp. 9 – 17.

Denier van der Gon, J.J., Coolen, A.C.C., Erkelens, C.J. and Jonker, H.J. (1990) Self-organizing neural mechanisms possibly responsible for muscle coordination. In: J.M. Winters and S.L.-Y. Woo (Eds.), *Multiple Muscle Systems,* Springer, New York, pp. 335 – 342.

Denier van der Gon, J.J., Tax, A.A.M., Gielen, C.C.A.M. and Erkelens, C.J. (1991) Synergism in the control of force and movement of the forearm. *Rev. Physiol. Biochem. Pharmacol.,* 118: 97 – 124.

Dul, J., Townsend, M.A., Shiavi, R. and Johnson, G.E. (1984a) Muscular synergism, I. On criteria for load sharing between synergistic muscles. *J. Biomech.,* 17: 663 – 673.

Dul, J., Johnson, G.E., Shiavi, R. and Townsend, M.A. (1984b) Muscular synergism, II. A minimum-fatigue criterion for load sharing between synergistic muscles. *J. Biomech.,* 17: 675 – 684.

Feldman, A.G. (1986) Once more on the equilibrium-point hypothesis (λ-model) for motor control. *J. Motor Behav.,* 18: 17 – 54.

Feldman, A.G., Adamovich, S.V., Ostry, D.J. and Flanagan, J.R. (1990) The origins of electromyograms – explanations based on the equilibrium point hypothesis. In: J.M. Winters and S.L.-Y. Woo (Eds.), *Multiple Muscle Systems,* Springer, New York, pp. 195 – 213.

Gielen, C.C.A.M. and van Zuylen, E.J. (1986) Coordination of forearm muscles during flexion and supination: application of the tensor analysis approach. *Neuroscience,* 17: 527 – 539.

Gielen, C.C.A.M., van Ingen Schenau, G., Tax, A.A.M. and Theeuwen, M. (1990) The activation of mono- and bi-articular muscles in multi-joint movements. In: J.M. Winters and S.L.-Y. Woo (Eds.), *Multiple Muscle Systems,* Springer, New York, pp. 302 – 311.

Granit, R. (1955) *Receptors and Sensory Perception,* Yale University Press, New Haven, CT.

Herzog, W. (1986) Muscle force predictions using a non-linear optimal design. *J. Neurosci. Methods,* 17: 196.

Hogan, N. (1985) The mechanics of multi-joint posture and

movement control. *Biol. Cybern.*, 52: 315 – 331.

Houk, J.C. and Rymer, W.Z. (1981) Neural control of muscle length and tension. In: J.M. Brookhart and V.B. Mountcastle (Eds.), *Handbook of Physiology (The Nervous System, Motor Control)*, Am. Physiol. Soc., Bethesda, MD, pp. 257 – 323.

Jongen, H.A.H. (1989) Theories and experiments on muscle coordination during isometric contractions, PhD. Thesis, University of Utrecht.

Jongen, H.A.H., Denier van der Gon, J.J. and Gielen, C.C.A.M. (1989) Activation of human arm muscles during flexion/extension and supination/pronation tasks: a theory on muscle coordination. *Biol. Cybern.*, 61: 1 – 9.

Kuypers, H.G.J.M. (1985) The anatomical and functional organization of the motor system. In: M. Swash and C. Kennard (Eds.), *The Scientific Basis of Clinical Neurology*, Churchill Livingston, Edinburgh.

Loeb, G.E. (1985) Motorneurone task groups: coping with kinematic heterogeneity. *J. Exp. Biol.*, 115: 137 – 146.

Pellionisz, A. and Llinas, R. (1982) Space-time representation in the brain. The cerebellum as a predictive space-time metric tensor. *Neuroscience*, 7: 2949 – 2970.

Pew, R.W. (1984) A distributed processing view of human motor control. In: W. Prinz and A.F. Sanders (Eds.), *Cognition and Motor Processes*, Springer, Berlin.

Prochazka, A., Hulliger, M., Zangger, P. and Appenteng, K. (1985) "Fusimotor set": new evidence for α-independent control of γ-motoneurones during movement in awake cat. *Brain Res.*, 339: 136 – 140.

Schmidt, R.F. (1978) Motor systems. In: R.F. Schmidt (Ed.), *Fundamentals of Neurophysiology*, Springer, New York, pp. 158 – 204.

Tax, A.A.M., Denier van der Gon, J.J., Gielen, C.C.A.M. and van den Tempel, C.M.M. (1989) Differences in the activation of m. biceps brachii in the control of slow isotonic movements and isometric contractions. *Exp. Brain Res.*, 76: 55 – 63.

Tax, A.A.M., Denier van der Gon, J.J., Gielen, C.C.A.M. and Kleyne, M. (1990a) Differences in central control of m. biceps brachii in movements tasks and force tasks. *Exp. Brain Res.*, 79: 138 – 142.

Tax, A.A.M., Denier van der Gon, J.J. and Erkelens, C.J. (1990b) Differences in coordination of elbow flexor muscles in force tasks and in movement tasks. *Exp. Brain Res.*, 81: 567 – 572.

ter Haar Romeny, B.M., Denier van der Gon, J.J. and Gielen, C.C.A.M. (1984) Relation of the location of a motor unit in human biceps muscle and its critical firing levels for different tasks. *Exp. Neurol.*, 85: 631 – 650.

van Ingen Schenau, G.J. (1989) From rotation to translation: constraints on multi-joint movements and the unique action of bi-articular muscles. *Human Movement Sci.*, 8: 301 – 337.

van Zuylen, E.J., Gielen, C.C.A.M. and Denier van der Gon, J.J. (1988) Coordination and inhomogeneous activation of human arm muscles during isometric torques. *J. Neurophysiol.*, 60: 1523 – 1548.

Windhorst, U., Hamm, T.M. and Stuart, D.G. (1989) On the function of muscle and reflex partitioning. *Behav. Brain Sci.*, 12: 629 – 681.

Yeo, B.P. (1976) Investigations concerning the principle of minimal total muscle force. *J. Biomech.*, 9: 413 – 416.

J.H.J. Allum, D.J. Allum-Mecklenburg, F.P. Harris and R. Probst
Progress in Brain Research, Vol. 97

CHAPTER 15

Interactions between pathways controlling posture and gait at the level of spinal interneurones in the cat

E. Jankowska[1] and S. Edgley[2]

[1] *Department of Physiology, University of Göteborg, Göteborg, Sweden, and* [2] *Department of Anatomy, University of Cambridge, Cambridge, U.K.*

The properties of three interneuronal populations controlling posture and locomotion are briefly reviewed. These are interneurones mediating reciprocal inhibition of antagonistic muscles and interneurones in pathways from secondary muscle spindle afferents to ipsilateral and contralateral motoneurones, respectively. It will be shown that these interneurones subserve a variety of movements, with functionally specialized subpopulations being selected under different conditions. Mechanisms for gating the activity of these neurones appear to be specific for each of them but to act in concert. Interneurones which are active during locomotion and postural reactions are distributed over many segments of the spinal cord and over several of Rexed's laminae, both in the intermediate zone and in the ventral horn (Berkinblit et al., 1978; Bayev et al., 1979; Schor et al., 1986; Yates et al., 1989). The location of neurones discharging during neck and labyrinthine reflexes is illustrated in Fig. 1*A* and *B* but indications that neurones with an even wider distribution contribute to locomotion, scratching and the related postural reactions have been provided by neuronal markers which preferentially label active neurones (WGA-HRP; see Noga et al., 1987) or neurones with active genetic transcription (c-*fos*; I. Barajon, personal communication; Dai et al., 1991). Such a wide distribution indicates a high degree of non-homogeneity, since neurones of different functional types are usually located in different laminae. It has been demonstrated that some of these neurones may be particularly important for setting up the rhythm of muscle contractions specific for different gaits or scratching, as part of their "pattern generators" (see, e.g., Grillner, 1981). Other neurones may be primarily involved in initiation of these movements or in postural adjustments combined with them. A considerable proportion of neurones mediating these movements are nevertheless likely to be used not in one particular type of movement but in a variety of movements, and contribute to postural reactions and locomotion as well as to various segmental reflexes and centrally initiated movements; they are likely to operate as last order (premotor) interneurones of several spinal pathways to motoneurones. One of the indications that this is the case is the overlap between the areas of location of interneurones active during postural reactions, locomotion, or scratching and the areas of location of premotor interneurones (Fig. 1*C,D*). The latter were labelled by loading motoneurones with WGA-HRP and by its subsequent retrograde transneuronal transport (see Harrison et al., 1986). This review will deal with only three representatives of such premotor interneurones and will be limited to those which are most directly activated by receptors signalling postural disturbances and/or are active during fictive locomotion.

Key words: Spinal interneurones; Locomotion; Posture

Interneurones mediating reciprocal inhibition (Ia inhibitory interneurones)

Ia inhibitory interneurones are used to adjust the degree of contraction of muscles acting in opposite directions at hinge joints. They exert, for instance, a stronger inhibition of motoneurones of antagonists when only one muscle group is to be active, than during co-contractions of agonists and antagonists (Hultborn et al., 1971a,b; J.B. Nielsen, personal communication). Also, their activity and the degree of the inhibition they exert, is therefore adjusted as a part of the preprogramming of various movements. Their actions are weakened primarily via Renshaw cells which have them under a strong inhibitory control (Hultborn et al., 1971a,b; see also

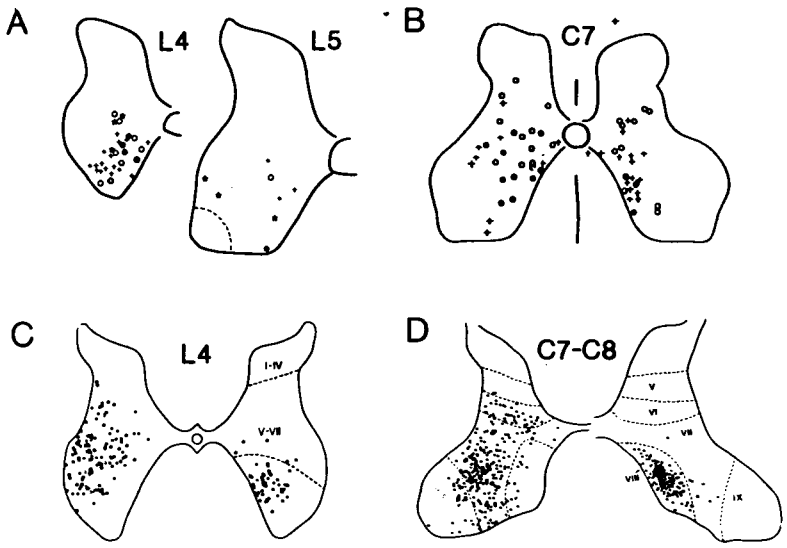

Fig. 1. *A* and *B*, distribution of neurones responding to neck rotation and to vestibular tilt, respectively. Responses of all neurones in *A* were modulated during neck rotation; those with input from group I and II afferents are indicated by stars and circles. Of neurones marked in *B*, those responding at a short latency to vestibular tilt are indicated by filled circles; neurones to the left and to the right were recorded from preparations with intact labyrinths or from canal-plugged preparations, respectively. *C* and *D*, premotor neurones labelled by retrograde transneuronal transport of WGA-HRP from semitendinosus and deltoid muscle nerves in the indicated segments. (Modified from fig. 7 of Yates et al., 1989) (*A*), fig. 3 of Schor et al., 1986 (*B*), fig. 3 of Jankowska and Skoog, 1986 (*C*) and fig. 2 of Alstermark and Kümmel, 1986 (*D*) with permission.)

Hultborn and Lundberg, 1972; Fu et al., 1978) while a variety of neuronal systems converging upon them may enhance their activity (for references, see Jankowska, 1992). Ia inhibitory interneurones and their actions are easily identifiable by their recurrent inhibition, because no other interneurones of spinal segmental pathways have been found to be inhibited by Renshaw cells (Hultborn et al., 1971a). It could therefore be established with confidence that Ia inhibitory interneurones are activated in conjunction with a number of segmental reflexes, locomotor, postural and centrally initiated reactions.

A contribution of Ia inhibitory interneurones to locomotion has been revealed in two ways. One was by demonstrating that they are rhythmically active during fictive locomotion (when movements are prevented by muscle paralysis; Feldman and Orlovsky, 1975; Pratt and Jordan, 1987; Cabelguen, 1988). In the absence of movements their rhythmic activity cannot be induced by peripheral afferents and must be evoked by intrinsic spinal networks or by supraspinal neurones. Discharges of Ia inhibitory interneurones induced under these conditions coincide with those phases of the step cycle during which their target motoneurones ought to be inhibited. The second kind of evidence goes beyond mere coincidence, showing that the major part of the inhibition of motoneurones evoked during fictive locomotion is evoked via these interneurones. The evidence consists of showing that this inhibition is practically abolished by activation of Renshaw cells by stimulation of a ventral root (Fu et al., 1975). The disinhibition of motoneurones following ventral root stimulation is illustrated in Fig. 2*A* where the arrow indicates the time of the stimulus application during an IPSP induced by a neuronal system operating during fictive locomotion.

Ia inhibitory interneurones also have been shown to contribute to tonic neck reflexes. They are tonically active in preparations which display such reflexes and their activity is then modulated by neck rotation (Yamagata et al., 1991). Individual inter-

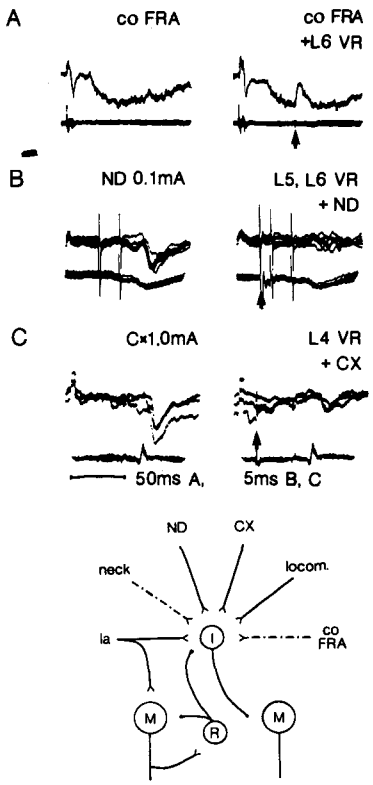

Fig. 2. Examples of the contribution of Ia inhibitory interneurones to the inhibition of three PBST motoneurones: during locomotor-like activity (*A*), and during actions mediated by vestibulo-spinal (*B*) and cortico-spinal (*C*) tract neurones. Control responses are to the left. Responses following activation of Renshaw cells by stimulation of ventral roots (arrows) are to the right. Strong depression of IPSPs evoked from contralateral flexion reflex afferents (co FRA, in the cat), from Deiters nucleus (ND, in the cat), and from motor cortex (CX, in the baboon) by Renshaw cells indicates that they were evoked mainly (or exclusively) by Ia inhibitory interneurones. (Modified from fig. 2 of Fu et al., 1975 (*A*), fig. 1 of Hultborn and Udo, 1972a (*B*) and fig. 1 of Jankowska et al., 1976 (*C*).) The diagram summarizes interactions occurring at the level of Ia inhibitory interneurones mentioned in the text. Continuous and dashed lines indicate direct and indirect connections, respectively. I, Ia inhibitory interneurone; R, Renshaw cell; M, motoneurone.

neurones have, in addition, been found to respond to neck movements with different vector orientations. Different subpopulations of Ia inhibitory interneurones may thus be used in variants of the neck reflexes. The modulation appears to be particularly strong for interneurones with Ia input from the knee and hip extensors quadriceps, and much weaker for interneurones with Ia input from ankle and toe extensors.

No reports have so far been published on the behaviour of Ia inhibitory interneurones during reflexes evoked from the labyrinths. However, there are two other indications for their contribution to these reflexes. The first is that Ia inhibitory interneurones have strong input from the lateral vestibular nucleus and that their actions on motoneurones are strongly facilitated by vestibulospinal tract neurones (Grillner and Hongo, 1972; Hultborn and Udo, 1972a,b; Hultborn et al., 1976). The depression of disynaptic IPSPs evoked from the lateral vestibular nucleus in motoneurones by activation of Renshaw cells (Hultborn and Udo, 1972a) provides, in addition, evidence that Ia inhibitory interneurones play a major role in mediating these IPSPs. The potency of the depression of the IPSPs in Fig. 2*B* suggests in fact that vestibulospinal tract neurones may inhibit motoneurones primarily via Ia inhibitory interneurones. However, this may only be the case of the inhibition of flexor (in particular knee and hip flexor) motoneurones since separate interneurones appear to be used to mediate inhibitory actions of group Ia afferents and vestibulospinal neurones on ankle flexor and on any extensor motoneurones (Grillner and Hongo, 1972; ten Bruggencate and Lundberg, 1974; Hultborn et al., 1976).

Involvement of Ia inhibitory interneurones in other postural reflexes is indicated by their strong activation during crossed extension reflexes (ten Bruggencate and Lundberg, 1974; Hultborn et al., 1976). Again this is not the case for all Ia inhibitory interneurones. Those involved mediate primarily inhibition of knee and hip flexors.

Cortico- and rubro-spinal tract neurones are likely to use Ia inhibitory interneurones during voluntary movements since these interneurones are effectively excited by them. This has been demonstrated both in the cat (Lundberg and Voorhoeve, 1972; Hultborn et al., 1976; Illert and Tanaka, 1976) and in primates (Jankowska et al., 1976). Ia inhibitory interneurones appear to make a particularly strong contribution to the inhibition evoked by

cortico-spinal neurones in primates in which IPSPs evoked by cortico-spinal neurones are evoked disynaptically, while the most direct pathway in the cat appears to be trisynaptic. IPSPs evoked in primates are also more effectively depressed by Renshaw cells. An example of such a depression is shown in Fig. 2*C*.

Considering that none of these movements would be likely to be evoked in isolation, the stimuli which induce them must interact to govern the activity of Ia inhibitory interneurones, as summarized in the diagram in Fig. 2. These interneurones must thus be nodal points of the coordination of locomotor, postural and centrally initiated movements at a premotoneuronal level.

Interneurones in disynaptic reflex pathways from group II muscle afferents (group II interneurones)

Interneurones in pathways from group II muscle afferents are used to coordinate activity of a greater variety of muscles than Ia inhibitory interneurones since they affect the activity of muscles at several joints in a limb. This is true for interneurones in polysynaptic as well as disynaptic pathways from these afferents. Interneurones interposed in disynaptic pathways have been found to be particularly numerous in midlumbar segments and to include both excitatory and inhibitory interneurones which directly synapse upon motoneurones (Edgley and Jankowska, 1987; Cavallari et al., 1987). There are also indications that the midlumbar interneurones might serve a somewhat different function than interneurones in caudal lumbar segments since the two subpopulations are preferentially activated by group II afferents of different muscles (of quadriceps, gracilis, sartorius, and pretibial flexors, or of triceps surae, plantaris and hamstring; see Edgley and Jankowska, 1987). However, only very few observations have so far been made on caudal lumbar group II interneurones and only the midlumbar ones will be discussed here.

Some of the midlumbar interneurones appear to contribute to the synaptic drive to motoneurones during locomotion since they are rhythmically active during fictive locomotion (Shefchyk et al., 1990) and are readily activated by stimuli applied within the mesencephalic locomotor region (Edgley et al., 1988). An example of disynaptic EPSPs evoked from the latter region is shown in Fig. 3*A*. However, not all of the group II interneurones behave in this way. Furthermore, since only Ia inhibitory interneurones appear to inhibit motoneurones during fictive locomotion, only excitatory group II

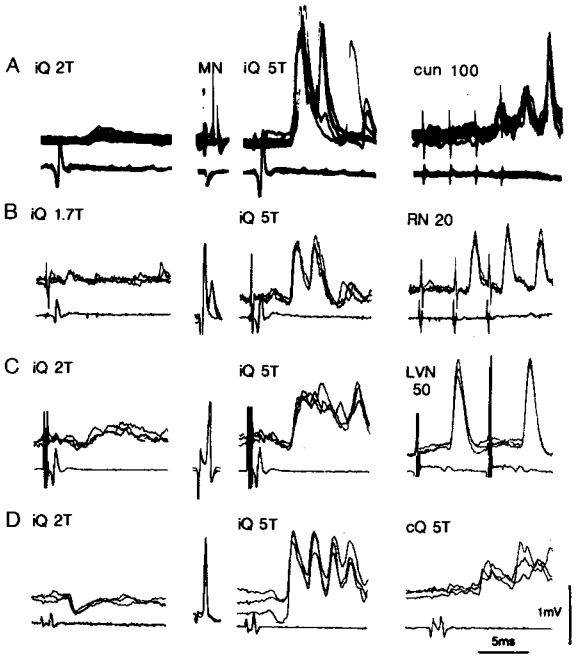

Fig. 3. Examples of peripheral and descending input to midlumbar interneurones involved in locomotion and postural reflexes. *A, B, C* and *D*, records from four midlumbar interneurones with monosynaptic input from group II muscle afferents (in the middle column) and without (*A,C*) or only minimal (*B,D*) input from group I afferents (in the left column). Records in the right column illustrate disynaptic EPSPs evoked from the mesencephalic locomotor region (cun, nucl. cuneiformis), monosynaptic EPSPs from the contralateral red nucleus (RN) and the ipsilateral lateral vestibular nucleus (LVN) and di- or trisynaptic EPSPs from contralateral group II afferents, respectively. All the interneurones were located in the intermediate zone of the L4 or L5 segments and were antidromically activated from the motor nuclei (MN) in the L7 segment, as indicated in the left column. (Modified from fig. 3 of Edgley et al., 1988 (*A*), from unpublished material of Davies and Edgley (*B,C*) and from fig. 2 of Bajwa et al., 1992 (*D*).) Stimulus intensities are in multiples of threshold (T) for group I afferents in the quadriceps (Q) nerve and in μA for cun, RN and LVN.

interneurones would be expected to act. Both the excitatory and the inhibitory group II interneurones might, on the other hand, be used during actual locomotion to assist the transition from the stance to the swing phase of the step- and/or phase-dependent reflex reversal. At least, their input conforms to that required of interneurones used for these purposes (see Grillner, 1981; Edgley and Jankowska, 1987).

Strong involvement of group II interneurones in the labyrinthine and neck reflexes is indicated by studies of Brink et al. (1984, 1985), Suzuki et al. (1985, 1986) and Yates et al. (1988, 1989). The results of these studies show that a considerable proportion of lumbar interneurones activated by tilt or rotation of the neck are located in laminae VI and VII of the midlumbar segments, in the same laminae and in the same segments as the population of group II interneurones described by Edgley and Jankowska (1987). Some of these were activated by group II afferents in the same muscle nerves and were, in addition, found to project to motor nuclei (Yates et al., 1988, 1989). In agreement with this, a considerable proportion of group II interneurones appears to be activated by vestibulo-spinal tract fibres (Davies and Edgley, 1993) and, as illustrated in Fig. 3*C*, the coupling between them is monosynaptic.

Most of group II interneurones could also be used as last order interneurones in crossed reflex actions, since the majority of them are powerfully influenced by contralateral group II afferents (Bajwa et al., 1991, and unpublished observations). The latencies of EPSPs evoked in them are indicative of a disynaptic coupling; an example of such EPSPs is shown in Fig. 3*D*.

The organization and the properties of the population of group II interneurones is still under investigation. The available evidence shows, nevertheless, that it includes several highly functionally specialized subpopulations which are recruited under different circumstances. Of these the excitatory interneurones synapsing on motoneurones are, as already mentioned, more likely to be activated during fictive locomotion than the inhibitory ones. Different subpopulations of these interneurones respond to head rotation in different directions (Brink et al., 1984; 1985; Suzuki et al., 1986; Yates et al., 1989) and would, therefore, be activated during different movements. Thus, it is not surprising that only some subpopulations of group II interneurones are affected by descending tract neurones. They may be monosynaptically contacted not only by vestibulospinal neurones, but also by reticulo-, cortico- and rubro-spinal neurones (Davies and Edgley, in preparation). An example of monosynaptic EPSPs evoked from the red nucleus is shown in Fig. 3*B*. However, only some descending tract neurones have been found to converge on the same interneurones, for example reticulo- and vestibulo-spinal neurones or cortico- and rubro-spinal neurones. They would thus not interact with all of the other peripheral or intraspinal sources of input.

The descending inhibitory control of these neurones appears to be less differentiated. This is particularly true for the control exerted by descending monoaminergic neurones, since activity of any group II interneurones in the intermediate zone of midlumbar segments has been found to be depressed by noradrenaline and of those in the dorsal horn by serotonin (Bras et al., 1990). However, subsets of the involved monoaminergic neurones (those in locus coeruleus, subcoeruleus or Kölliker-Fuse nuclei, or in various raphe nuclei, see Noga et al., 1992) might control specific subpopulations of group II neurones. It may, therefore, be relevant for the control of transmission to group II interneurones that subsets of cells in locus coeruleus and subcoeruleus are differently affected by labyrinthine and neck receptors (Barnes et al., 1989; Manzoni et al., 1989; Pompeiano et al., 1990).

The specificity of the monoaminergic control of group II interneurones is also indicated by the fact that it is restricted to one kind of input: that from group II muscle afferents (Bras et al., 1989b,1990; Noga et al., 1992). This is illustrated in Fig. 4 on population EPSPs evoked in midlumbar segments (*A* and *B*) and on PSPs evoked in motoneurones (*C*). The early and the later components of these potentials were evoked by group I and group II afferents

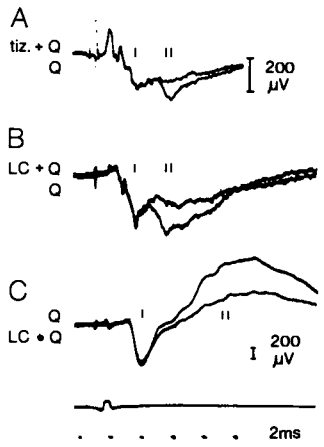

Fig. 4. *A*. Effects of locally applied tizanidine (tiz), an α_2 NA agonist, on two components of a monosynaptic population EPSP (extracellular field potential) evoked in midlumbar interneurones from group I and II afferents, as indicated. Superimposed averaged records before (larger) and during (smaller) application of the drug. (Modified from fig. 2 of Bras et al., 1990.) *B* and *C*. Effects of stimuli applied in the locus coeruleus on group I and group II components of a similar population EPSP (*B*) and on PSPs evoked in a posterior biceps-semitendinosus motoneurone (*C*) by stimulation of the quadriceps nerve with stimuli maximal for both group I and group II afferents. Superimposed averaged records as in *A*. (From Jankowska, Riddell, Skoog and Noga, in preparation).

of quadriceps (Q), as indicated. The figure shows that only the group II components were depressed after a local application of an α_2 NA agonist, tizanidine (tiz.) and after conditioning stimuli applied in one of the nuclei of origin of the descending monoaminergic neurones, the locus coeruleus (LC).

Observations illustrated in Fig. 4*A* suggest furthermore that when the descending noradrenergic control is out of order, group II interneurones may be responsible for the pathologically exaggerated stretch, flexion and postural reflexes associated with spasticity. In agreement with such a suggestion, a drug, tizanidine, which is highly effective in reducing spasticity in hemiplegia, tetraplegia, multiple sclerosis and spastic paresis (see, e.g., Bes et al., 1988), has apparently no effect on reflex actions of other afferents, except nociceptors (e.g., Davies and Johnston, 1984; Bras et al., 1989b, 1990).

Commissural interneurones in crossed reflex pathways from group II afferents

Commissural neurones are used to coordinate activity of muscles on both sides of the body. Those with group II input have been found in midlumbar segments, in laminae V – VII (Bras et al., 1989a) and in lamina VIII (Jankowska and Noga, 1990). However, commissural neurones operating as last order interneurones are located primarily in lamina VIII, both in the lumbosacral and cervical enlargements (Harrison et al., 1986; Alstermark and Kümmel, 1986). As illustrated in Fig. 1*C* and *D*, they appear thus to constitute a separate interneuronal population from the last order ipsilaterally projecting interneurones which are located primarily in laminae VI and VII. There are nevertheless indications that the ipsilaterally and contralaterally projecting interneurones with group II input operate in concert. As illustrated in Fig. 3, they are often excited by group II afferents of the same nerves (Edgley and Jankowska, 1987; Jankowska and Noga, 1990; Arya et al., 1991), although excitation by contralateral group II afferents is evoked only indirectly, is less effective and often requires more than one stimulus. The two interneuronal populations may also be co-excited by the same descending tract fibres, especially the vestibulo- and reticulospinal. This is indicated by the similarities in the descending input to lamina VII and lamina VIII neurones (Kozhanov and Shapovalov, 1977; Davies and Edgley, 1992). The distribution of neurones activated during labyrinthine and tonic neck reflexes within both lamina VII and lamina VIII (Brink et al., 1985; Suzuki et al., 1986; Yates et al., 1988, 1989; cf. Fig. 1.*A,B* and Fig. 1*C,D*) leads to the same conclusion. It is also in keeping with the demonstration that vestibulo-spinal tract neurones terminate in both these laminae (especially those terminating outside motor nuclei; Shinoda et al., 1986).

Interneurones of the two populations may also excite each other. The ipsilaterally acting group II interneurones might contact the commissural interneurones via their axon collaterals in lamina VIII

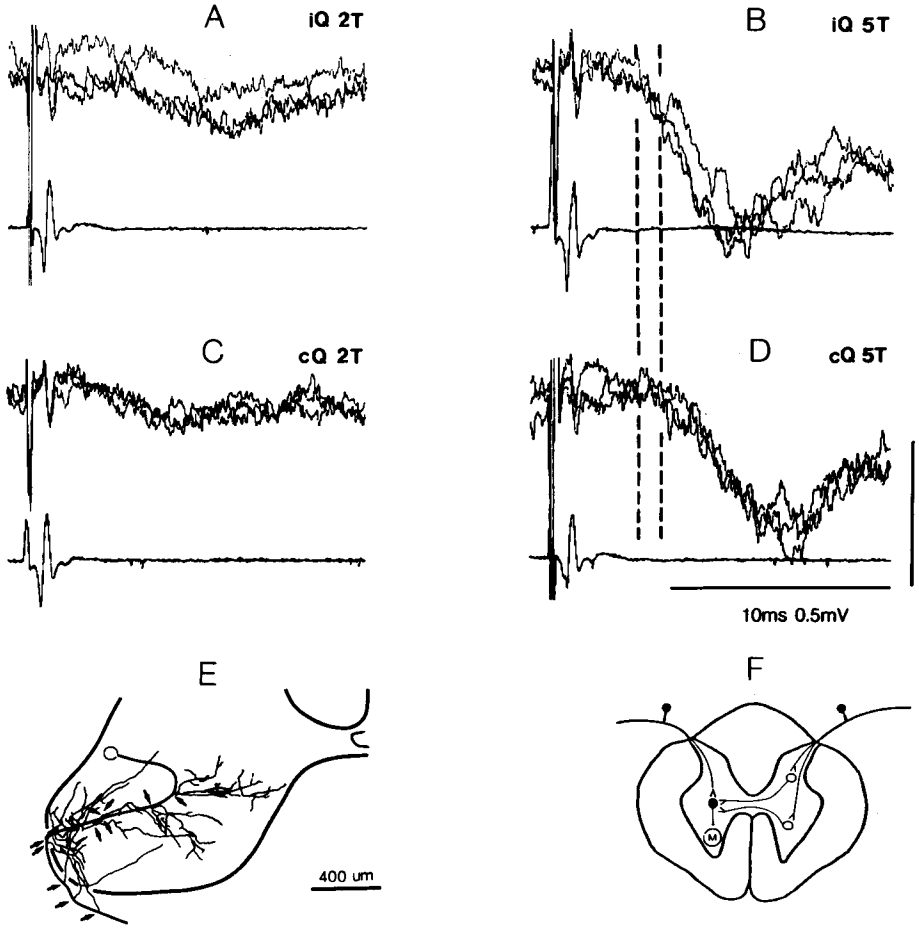

Fig. 5. Comparison of PSPs evoked in a gastrocnemius motoneurone from group II afferents in the ipsilateral and the contralateral quadriceps nerve. The stimulus intensity was maximal for group I afferents and at threshold for group II afferents for records in *A* and *C* while it was maximal for group II afferents in *B* and *D*. Dashed lines indicate the onset of the IPSPs. (Modified from fig. 1 of Arya et al., 1991, and unpublished data.) *E*. An example of terminal axonal branching of one of the ipsilaterally projecting midlumbar group II interneurones in the L5 segment. (Modified from fig. 6 of Bras et al., 1989a.) *F*. Diagram of the likely coupling in the pathways mediating the IPSPs. o and •, Excitatory and inhibitory interneurones respectively; M, motoneurone in a more caudal segment.

(Bras et al., 1989a), with an example shown in Fig. 5*E*. Axonal projections of lamina VIII neurones have not yet been established. However, either these neurones, or dorsal horn interneurones with crossed projections (Bras et al., 1989a) will be needed to mediate actions of contralateral group II afferents, separately or together, upon group II interneurones and be interposed between group II afferents and contralateral motoneurones as hypothesized in Fig. 5*F*. Fig. 5*D* shows that at least inhibition of motoneurones is evoked at short latency, which is not much longer than the latency of IPSPs evoked from ipsilateral group II afferents (Fig. 5*B*); it may thus involve only one additional interneurone in its pathway.

Crossed actions of group II afferents are strongly dependent on the experimental conditions in that inhibition of all kinds of contralateral motoneurones is evoked when the spinal cord is intact while actions conforming to the pattern of the crossed extension

reflex are evoked after spinal transection (Arya et al., 1991). The question of which descending pathways are responsible for the state dependence of these group II actions is under investigation, but given the profound effects of monoamines on ipsilaterally projecting neurones and their likely linkage to crossed reflexes, an involvement of noradrenergic pathways must be a strong possibility. The pattern of crossed extension would seem appropriate to locomotion with an alternating gate. If the system of midlumbar interneurones is involved in switching from stance to swing in the step cycle, its operation should simultaneously promote contralateral stance (i.e., activation of extensors and inhibition of flexors). The significance of the generalized inhibition seen with the spinal cord intact is less clear but it may reflect a pattern suitable for in-phase movements or postural control during standing. A possible contribution of commissural group II interneurones to locomotion has not yet been directly investigated. Preliminary observations show, however, that these neurones may be as effectively activated by stimuli applied in the mesencephalic locomotor region (Jankowska and Noga, 1990) as the ipsilaterally projecting group II interneurones.

Concluding remarks

Individual neurones of all of the interneuronal populations discussed above may have somewhat different target motoneurones and will contribute to different motor synergies. They may thus be selectively activated to maintain the correct posture whenever task-dependent motor synergies are to be selected, as postulated by Macpherson (1988). Predominant input from proximal muscles to all midlumbar interneurones which are involved in locomotion and in labyrinthine, neck and crossed extension reflexes is well suited for postural corrections in quadrupedal stance since such corrections involve activation of lower limb muscles in a proximal to distal sequence, both in cats and in humans (Macpherson et al., 1989). They would thus undoubtedly depend on input from the quadriceps and other proximal muscles and joints. Input to group II interneurones from the flexor digitorum longus and pretibial flexors as well as from the quadriceps (Edgley and Jankowska, 1987; Jankowska and Noga, 1990) would, furthermore, subserve strong synergies of thigh and foot muscles during postural perturbations (Rushmer et al., 1983). In contrast, interneurones with group II input from ankle extensors might be more important for postural adjustments in the bipedal stance of humans (in distal to proximal sequence, Macpherson et al., 1989) in which changes at the ankle joint and the stretch of triceps surae are essential (see, e.g., Nashner, 1976; Dietz et al., 1987, 1989). Since perturbations involving changes in one ankle joint are followed by changes in muscle activity of both limbs, and since crossed reflex actions of group I afferents are very weak, these adjustments would be most likely mediated by neurones with group II input (see also Berger et al., 1984).

Gating of activity of Ia inhibitory interneurones and of group II interneurones involves different specific mechanisms. It is achieved primarily via Renshaw cells for the former and via monoaminergic descending tract neurones for the latter. However, in both labyrinthine and neck reflexes the two gating systems appear to operate together. As shown by D'Ascanio et al. (1985), cells in locus coeruleus adjust the gain of responses in both these reflexes and a considerable proportion of cells in locus coeruleus is affected by labyrinthine as well as by neck receptors, often in a reciprocal manner (Manzoni et al., 1989; Pompeiano et al., 1990). They might thus enhance the out-of-phase modulation of the activity of group II interneurones during labyrinthine and neck reflexes (Wilson et al., 1984). They might also correlate activity of these neurones with the activity of Ia inhibitory interneurones via Renshaw cells. Ia inhibitory interneurones are not affected by stimuli applied in locus coeruleus and Fig. 4 shows that Ia reciprocal IPSPs are not depressed by them (Jankowska, Riddell, Skoog and Noga, in preparation). However, their activity will be modified by changes in activity of Renshaw cells

which are secondary to changes in the activity of neurones in the locus coeruleus (Pompeiano, 1988).

References

Alstermark, B. and Kümmel, H. (1986) Transneuronal labelling of neurones projecting to forelimb motoneurones in cats performing different movements. *Brain Res.*, 376: 387 – 391.

Arya, W.A., Bajwa, S. and Edgley, S.A. (1991) Crossed reflex actions from group II muscle afferents in the lumbar spinal cord of the anaesthetized cat. *J. Physiol. (Lond.)*, 444: 117 – 131.

Bajwa, S., Edgley, S.A. and Harrison, P.J. (1992) Crossed actions on group II-activated interneurones in the midlumbar segments of the cat spinal cord. *J. Physiol. (Lond.)*, 455: 202 – 217.

Barnes, C.D., Manzoni, D., Pompeiano, O., Stampacchia, G. and d'Ascanio, P. (1989) Responses of locus coeruleus and subcoeruleus neurons to sinusoidal neck rotation in decerebrate cat. *Neuroscience*, 31: 371 – 392.

Bayev, K.V., Dekhtyarenko, A.M., Zavadskaya, T.V. and Kostyuk, P.G. (1979) Activity of lumbar interneurons during fictitious locomotion in thalamic cats. *Neirofizyologija*, 11: 329 – 338.

Berger, W., Dietz, V. and Quintern, J. (1984) Corrective reactions to stumbling in man: neuronal co-ordination of bilateral leg muscle activity during gait. *J. Physiol. (Lond.)*, 357: 109 – 125.

Berkinblit, M.B., Deliagina, T.G., Feldman, A.G., Gelfand, I.M. and Orlovsky, G.N. (1978) Generation of scratching. I. Activity of spinal interneurones during scratching. *J. Neurophysiol.*, 41: 1040 – 1057.

Bes, A., Eysette, M., Pierrot-Deseilligny, E., Rohmer, F. and Warter, J.M. (1988) A multi-centre double-blind trial of tizanidine, a new antispastic agent, in spasticity associated with hemiplegia. *Curr. Med. Res. Opin.*, 10: 709 – 718.

Bras, H., Cavallari, P., Jankowska, E. and Kubin, L. (1989a) Morphology of midlumbar interneurones relaying information from group II muscle afferents in the cat spinal cord. *J. Comp. Neurol.*, 290: 1 – 15.

Bras, H., Cavallari, P., Jankowska, E. and McCrea, D. (1989b) Comparison of effects of monoamines on transmission in spinal pathways from group I and II afferents in the cat. *Exp. Brain Res.*, 76: 27 – 37.

Bras, H., Jankowska, E., Noga, B. and Skoog, B. (1990) Comparison of effects of various types of NA and 5-HT agonists on transmission from group II muscle afferents in the cat. *Eur. J. Neurosci.*, 2: 1029 – 1039.

Brink, E.E., Suzuki, I., Timerick, S.J.B. and Wilson, V.J. (1984) Directional sensitivity of neurons in the lumbar spinal cord to neck rotation. *Brain Res.*, 323: 172 – 175.

Brink, E.E., Suzuki, I., Timerick, S.J.B. and Wilson, V.J. (1985) Tonic neck reflex of the decrebrate cat: a role for propriospinal neurons. *J. Neurophysiol.*, 54: 978 – 987.

Cabelguen, J.-M. (1988) Activity of interneurones mediating Ia reciprocal inhibition of PBSt and RF motoneurones during fictive locomotion in the thalamic cat. *Eur. J. Neurosci. (Suppl.) – Abstracts of the 11th Annual Meeting, European Neuroscience Association*, p. 266.

Cavallari, P., Edgley, S.A. and Jankowska, E. (1987) Postsynaptic actions of midlumbar interneurones on motoneurones of hindlimb muscles in the cat. *J. Physiol. (Lond.)*, 389: 675 – 690.

Dai, X., Douglas, J.R., Nagy, B.R., Noga, B.R. and Jordan, L.M. (1991) Localization of spinal neurons activated during treadmill locomotion using the c-*fos* immunohistochemical method. *Soc. Neurosci. Abstr.*, 16: 889.

D'Ascanio, P., Bettini, E. and Pompeiano, O. (1985) Tonic inhibitory influences of locus coeruleus on the response gain of limb extensors to sinusoidal labyrinth and neck stimulations. *Arch. Ital. Biol.*, 123: 69 – 100.

Davies, H.E. and Edgley, S.A. (1992) Supraspinal inputs to midlumbar short-propriospinal neurones in the cat spinal cord. *J. Physiol. (Lond.)*, in press.

Davies, J. and Johnston, S.E. (1984) Selective anti-nociceptive effects of tizanidine (DS 103-282), a centrally acting muscle relaxant, on dorsal horn neurones in the feline spinal cord. *Br. J. Pharmacol.*, 82: 409 – 421.

Dietz, V., Quintern, J. and Sillem, M. (1987) Stumbling reactions in man: significance of proprioceptive and preprogrammed mechanisms. *J. Physiol. (Lond.)*, 386: 149 – 163.

Dietz, V., Horstmann, G.A. and Berger, W. (1989) Interlimb coordination of leg-muscle activation during perturbation of stance in humans. *J. Neurophysiol.*, 62: 680 – 693.

Edgley, S.A. and Jankowska, E. (1987) An interneuronal relay for group I and II muscle afferents in the midlumbar segments of the cat spinal cord. *J. Physiol. (Lond.)*, 389: 675 – 690.

Edgley, S.A., Jankowska, E. and Shefchyk, S. (1988) Evidence that interneurones in reflex pathways from group II afferents are involved in locomotion in the cat. *J. Physiol. (Lond.)*, 403: 57 – 73.

Feldman, A.G. and Orlovsky, G.N. (1975) Activity of interneurons mediating reciprocal Ia inhibition during locomotion. *Brain Res.*, 84: 181 – 194.

Fu, T.-C., Jankowska, E. and Lundberg, A. (1975) Reciprocal Ia inhibition during the late reflexes evoked from the flexor reflex afferents after DOPA. *Brain Res.*, 85: 99 – 102.

Fu, T.-C., Hultborn, H., Larsson, R. and Lundberg, A. (1978) Reciprocal inhibition during the tonic reflex in the decerebrate cat. *J. Physiol. (Lond.)*, 284: 345 – 369.

Grillner, S. (1981) Control of locomotion in bipeds, tetrapods and fish. In: V.B. Brooks (Ed.), *Handbook of Physiology – The Nervous System, Vol. II. Motor Control, Part 2*, William and Wilkins, Baltimore, MD, pp. 1179 – 1236.

Grillner, S. and Hongo, T. (1972) Vestibulospinal effects on motoneurones and interneurones in the lumbosacral cord.

Prog. Brain Res., 37: 243 – 262.

Harrison, P.J., Jankowska, E. and Zytnicki, D. (1986) Lamina VIII interneurones interposed in crossed reflex pathways in the cat. *J. Physiol. (Lond.)*, 371: 147 – 166.

Hultborn, H. and Lundberg, A. (1972) Reciprocal inhibition during the stretch reflex. *Acta Physiol. Scand.*, 85: 136 – 138.

Hultborn, H. and Udo, M. (1972a) Convergence in the reciprocal Ia inhibitory pathway of excitation from descending pathways and inhibition from motor axon collaterals. *Acta Physiol. Scand.*, 84: 95 – 108.

Hultborn, H. and Udo, M. (1972b) Recurrent depression from motor axon collaterals of descending inhibitory effects in motorneurones. *Acta Physiol. Scand.*, 85: 44 – 57.

Hultborn, H., Jankowska, E. and Lindström, S. (1971a) Recurrent inhibition from motor axon collaterals of transmission in the Ia inhibitory pathway to motoneurones. *J. Physiol. (Lond.)*, 215: 591 – 612.

Hultborn, H., Jankowska, E. and Lindström, S. (1971b) Recurrent inhibition of interneurones monosynaptically activated from group Ia afferents. *J. Physiol. (Lond.)*, 215: 613 – 636.

Hultborn, H., Illert, M. and Santini, M. (1976) Convergence on interneurones mediating the reciprocal Ia inhibition of motoneurones. III. Effects from supraspinal pathways. *Acta Physiol. Scand.*, 96: 368 – 391.

Illert, M. and Tanaka, R. (1976) Transmission of corticospinal IPSPs to cat forelimb motoneurones via high cervical propriospinal neurones and Ia inhibitory interneurones. *Brain Res.*, 103: 143 – 146.

Jankowska, E. (1985) Further indications for enhancement of retrograde transneuronal transport of WGA-HRP by synaptic activity. *Brain Res.*, 341: 403 – 408.

Jankowska, E. (1992) Interneuronal relay in spinal pathways from proprioceptors. *Prog. Neurobiol.*, 38: 335 – 378.

Jankowska, E. and Noga, B.R. (1990) Contralaterally projecting lamina VIII interneurones in middle lumbar segments in the cat. *Brain Res.*, 535: 327 – 330.

Jankowska, E. and Skoog, B. (1986) Labelling of midlumbar neurones projecting to cat hindlimb motoneurones by transneuronal transport of a horseradish peroxidase conjugate. *Neurosci. Lett.*, 71: 163 – 168.

Jankowska, E., Padel, Y. and Tanaka, R. (1976) Disynaptic inhibition of spinal motoneurones from the motor cortex in the monkey. *J. Physiol. (Lond.)*, 258: 467 – 487.

Kozhanov, V.M. and Shapovalov, A.I. (1977) Synaptic organization of supraspinal control over propriospinal ventral horn interneurons in cat and monkey spinal cord. *Neirofiziologija*, 9: 177 – 184.

Lundberg, A. (1979) Multisensory control of spinal reflex pathways. *Prog. Brain Res.*, 50: 11 – 28.

Lundberg, A. and Voorhoeve, P. (1962) Effects from the pyramidal tract on spinal reflex. *Acta Physiol. Scand.*, 56: 201 – 219.

Lundberg, A., Malmgren, K. and Schomburg, E.D. (1987) Reflex pathways from group II muscle afferents. 1. Distribution and linkage of reflex actions to alpha-motoneurones. *Exp. Brain Res.*, 65: 271 – 281.

Macpherson, J.M. (1988) Strategies that simplify the control of the quadrupedal stance. II. Electromyographic activity. *J. Neurophysiol.*, 60: 218 – 231.

Macpherson, J.M., Horak, F.B., Dunbar, D.C. and Dow, R.S. (1989) Stance dependence of automatic postural adjustments in humans. *Exp. Brain Res.*, 78: 557 – 566.

Manzoni, D., Pompeiano, O., Barnes, C.D., Stampacchia, G. and D'Ascanio, P. (1989) Convergence and interaction of neck and macular vestibular inputs on locus coeruleus and subcoeruleus neurons. *Pflügers Arch. Eur. J. Physiol.*, 413: 580 – 598.

Nashner, L.M. (1976) Adapting reflexes controlling the human posture. *Exp. Brain Res.*, 26: 59 – 72.

Noga, B.R., Shefchyk, S.J. and Jordan, L.M. (1987) Localization of last order spinal interneurons participating in the production of locomotion in the cat. *Soc. Neurosci. Abstr.*, 13: 826.

Noga, B.R., Bras, H. and Jankowska, E. (1992) Transmission from group II muscle afferents is depressed by stimulation of locus coeruleus/subcoeruleus, Kölliker-Fuse and raphe nuclei in the cat. *Exp. Brain Res.*, 88: 502 – 516.

Pompeiano, O. (1988) The role of Renshaw cells in the dynamic control of posture during vestibulospinal reflexes. *Prog. Brain Res.*, 76: 83 – 95.

Pompeiano, O., Manzoni, D., Barnes, C.D., Stampacchia, G. and D'Ascanio, P. (1990) Responses of locus coeruleus neurons to sinusoidal stimulation of labyrinth receptors. *Neuroscience*, 35: 227 – 248.

Pratt, C.A. and Jordan, L.M. (1987) Ia inhibitory interneurons and Renshaw cells as contributors to the spinal mechanisms of fictive locomotion. *J. Neurophysiol.*, 57: 56 – 71.

Rossignol, S. and Gauthier, L. (1980) An analysis of mechanism controlling the reversal of crossed spinal reflexes. *Brain Res.*, 182: 31 – 45.

Rushmer, D.S., Russell, C.J. and Macpherson, J. (1983) Automatic postural responses in the cat: responses to headward and tailward translation. *Exp. Brain Res.*, 50: 45 – 61.

Schor, R.H., Suzuki, I., Timerick, S.J.B. and Wilson, V.J. (1986) Responses of interneurons in the cat cervical cord to vestibular tilt stimulation. *J. Neurophysiol.*, 56: 1147 – 1156.

Shefchyk, S., McCrea, D., Kriellaars, P., Fortier, P. and Jordan, L. (1990) Activity of interneurons within the L4 spinal segment of the cat during brain-stem evoked fictive locomotion. *Exp. Brain Res.*, 80: 290 – 295.

Shinoda, Y., Ohagaki, T. and Futami, T. (1986) The morphology of single lateral vestibulospinal tract axons in the lower cervical spinal cord of the cat. *J. Comp. Neurol.*, 249: 226 – 241.

Suzuki, I., Timerick, S.J.B. and Wilson, V.J. (1985) Body position with respect to the head or body position in space is coded by lumbar interneurons. *J. Neurophysiol.*, 54: 123 – 133.

Suzuki, I., Park, B.R. and Wilson, V.J. (1986) Directional sensi-

tivity of, and neck afferent input to, cervical and lumbar interneurons modulated by neck rotation. *Brain Res.*, 267: 356 – 359.

ten Bruggencate, G. and Lundberg, A. (1974) Facilitatory interaction in transmission to motoneurones from vestibulospinal fibres and contralateral primary afferents. *Exp. Brain Res.*, 19: 248 – 270.

Wilson, V.J., Ezure, K. and Timerick, S.J.B. (1984) Tonic neck reflex of the decerebrate cat: response of spinal interneurones to natural stimulation of neck and vestibular receptors. *J. Neurophysiol.*, 51: 567 – 577.

Yamagata, Y., Yates, B.J. and Wilson, V.J. (1991) Participation of Ia reciprocal inhibitory neurons in the spinal circuitry of the tonic neck reflex. *Exp. Brain Res.*, 84: 461 – 464.

Yates, B.J., Kasper, E.E., Brink, E.E. and Wilson, V.J. (1988) Peripheral output to L4 neurons whose activity is modulated by neck rotation. *Brain Res.*, 449: 377 – 380.

Yates, B.J., Kasper, J. and Wilson, V.J. (1989) Effects of muscle and cutaneous hindlimb afferents on L4 neurons whose activity is modulated by neck rotation. *Exp. Brain Res.*, 77: 48 – 56.

J.H.J. Allum, D.J. Allum-Mecklenburg, F.P. Harris and R. Probst
Progress in Brain Research, Vol. 97

CHAPTER 16

Fusimotor control of proprioceptive feedback during locomotion and balancing: can simple lessons be learned for artificial control of gait?

M. Hulliger

Department of Clinical Neurosciences, University of Calgary, Calgary, Canada T2N 4N1

The possibilities for central control of primary spindle afferents through fusimotor efferents for gain control in motor control mechanisms are briefly reviewed. While the existence of separate pathways for independent control of static and dynamic γ-motoneurones is well established, it proved more difficult to demonstrate that gain control of spindle feedback, attributable to alterations in static and dynamic fusimotor drive, indeed took place in voluntary movements. However, earlier qualitative indications, that Ia sensitivity (and hence the balance of static over dynamic drive) was adjusted differently in different motor tasks, have recently been confirmed in experimental simulation studies, in which the fusimotor activation profiles, that were required to reproduce chronically recorded spindle Ia discharge patterns, were reconstructed. These studies indicated that Ia sensitivity and dynamic γ-drive were low in routine movements (walking), but that they could be dramatically increased in motor tasks which were either difficult or unfamiliar (landing from falls, balancing on narrow walk beams, adjustment to imposed disturbances). This suggested that sensitization of spindle feedback could play a significant role in motor adaptation. In line with this, studies in patients with large fibre sensory (including proprioceptive) neuropathies indicated that long-term motor deficits (affecting motor adaptation and learning) could be at least as serious as short-term motor dysfunction (due to loss of reflex control). It is suggested that spindle Ia feedback may play a dual role: in addition to its contribution to short-term reflex control of posture and movement, it may also be used for optimization or maintenance of motor programs, especially if its gain is increased by significant dynamic fusimotor drive. For artificial control of gait the peripheral gain control provided by the fusimotor system need hardly be imitated, since "central" gain control circuits can easily come up with the same performance. Yet parallel central processing of one and the same signal in multiple modes, conceivably with different gains, may be desirable. For moment-to-moment control of gait there may be a need for servo-like short-term control. In addition, there may also be a need for long-term processing of peripheral feedback signals, in order to construct long-term estimates of kinematic movement parameters to monitor any gradual deviation from target performance. Fast digital signal processors can now be used to compute real-time running averages of analogue signals, and these could be used to optimize activation patterns continually.

Key words: Proprioceptors; Gait; Sensory neuropathies; Muscle spindles

Introduction

Among mechanoreceptors muscle spindles are unique in that they receive efferent innervation, which is mediated by static and dynamic fusimotor neurones, which in mammals are mostly γ-motoneurones. Unlike other proprioceptors, they are therefore under direct control by the central nervous system. Functionally, there are many facets to the phenomenon of fusimotor excitation of muscle spindle afferents, and their role in motor control indeed need not be restricted to a single function (Matthews, 1981). However, one particular aspect of fusimotor action has attracted special interest, ever since static and dynamic γ-motoneurones were first distinguished (Matthews, 1962): their ability to ad-

just the sensitivity of primary (Ia) spindle afferents (to length variations of the parent muscle) over a wide operating range. Static fusimotor action mostly reduces Ia sensitivity to imposed movements, often very significantly, while dynamic action tends to increase sensitivity quite dramatically, unless movements are very small (Goodwin et al., 1975; Hulliger et al., 1977a). Thus, in combining activation of static and dynamic efferents, the CNS can regulate the sensitivity (or gain) of proprioceptive feedback from spindle afferents over a significant range, the precise value of sensitivity depending on the balance between static and dynamic fusimotor output (Hulliger et al., 1977b).

The requirement for such feedback gain regulation was that static and dynamic γ-motoneurones would have to be controlled independently by the CNS, to permit adjustment of spindle Ia sensitivity between the two extremes, as determined by pure γ_S or pure γ_D action. Feasibility in principle of such sensory gain control was readily confirmed in acute experiments. In reduced preparations a number of areas or descending motor pathways have been identified, from which upon electrical stimulation either static or dynamic fusimotor neurones were activated, either predominantly or selectively (for reviews, see Matthews, 1972; Hulliger, 1984). Of particular interest for the present considerations are the findings that largely or exclusively dynamic fusimotor effects could be elicited from circumscribed mesencephalic and diencephalic structures, the MesADC region of Appelberg (1981) and his colleagues, another juxta-rubral region (rostral to the red nucleus) described by Taylor et al. (1992), and the habenulo-interpeduncular system of Taylor and Donga (1989).

However, functional interpretation of observations based on electrical activation of CNS structures in anaesthetized or otherwise reduced preparations has its well-recognized limitations. On the one hand, possibilities may be overestimated, since massive unphysiological stimulation may excite systems, which under normal conditions are never recruited to the same extent. Conversely, other possibilities may be overlooked, since polysynaptic central pathways may be suppressed by anaesthesia or due to an altered state of responsiveness following central lesions (like decerebration).

The question of feedback gain regulation by selective control of static and dynamic fusimotor efferents therefore had to be addressed in recordings during voluntary motor performance, either in freely moving animals or in human subjects. In the seventies, with the advent of human microneurography and chronic single unit recording techniques for laboratory animals, answers could be expected relatively quickly. However, it soon became apparent that the matter would not be resolved immediately, since recordings from small γ-motoneurones proved to be difficult. Indeed up to the present time, for good technical reasons, direct recordings from fully identified γ-efferents have not been achieved (for technical details, see Prochazka and Hulliger, 1983). Therefore the issue had to be addressed more indirectly by relying on quantitative evaluation of recordings from spindle afferents, which technically were less demanding, in order to deduce underlying fusimotor recruitment strategies. The conclusions regarding γ-efferent activation patterns are of course less certain because they are indirect. For the present consideration of the extent of spindle feedback gain control this limitation is less serious, because variations of afferent sensitivity can still be measured, even though the fusimotor activation patterns responsible can only be estimated.

Estimation of fusimotor activity

The findings reviewed below were obtained using an experimental simulation method, in order to estimate the fusimotor activation patterns which, together with the length variations in the parent muscle, determined spindle primary afferent discharge patterns during a variety of movements performed by chronically implanted freely moving animals (Hulliger and Prochazka, 1983; Hulliger et al., 1987, 1989). These simulations were carried out in separate, anaesthetized cats, where chronically recorded movements were reproduced as passively imposed whole muscle length variations. While

recording from Ia afferents (which were selected to match the passive stretch response characteristics of the chronically recorded unit), functionally single static and dynamic fusimotor efferents were activated either individually or in combination, using a range of different activation patterns. These activation patterns were either pre-determined, when explicit concepts of fusimotor strategies were tested (Hulliger and Prochazka, 1983), or they were progressively altered, using an iterative optimization procedure, until simulated Ia responses matched chronically recorded target responses (Hulliger et al., 1987, 1989). In either case, when chronic target responses were adequately matched, the successful γ-activation patterns were taken as estimates of the fusimotor discharge profiles, that had determined the chronically recorded afferent response.

For several reasons, the above simulation method can only provide approximate estimates of fusimotor activation profiles. The most serious reservations arise, first, from the question of uniqueness of solution and, second, from the question to what extent mechanical events and, in particular, local length variations during active muscle contraction are adequately imitated by imposing passive movements, even if whole muscle length variations are identical.

Clearly, strictly unique solutions could not be obtained when reconstructing fusimotor discharge patterns from chronic afferent recordings, especially in those cases where target responses were likely determined by combined static and dynamic fusimotor drive, and where therefore optimization of activation patterns in two independent efferent channels had to be allowed. However, as pointed out elsewhere (Hulliger et al., 1989), in cases of powerful fusimotor drive the characteristic features of static or dynamic action (large dynamic stretch response transients in the case of γ_D, high-rate maintained firing during rapid shortening for γ_S) often proved sufficiently discriminative to impose boundary conditions for reconstruction of fusimotor activation profiles, which in turn limited the range of choices. In these situations the problem of non-uniqueness was more quantitative than qualitative, relating to the question of precise levels of drive, rather than whether fusimotor action of one type or other was present or not.

Muscle length has ceased to be a simple variable, and from the present simulation studies it is not entirely clear, which facets of muscle length are most significant, and which simplifications are permissible, when attempting to describe or reproduce the length variations of natural movements. Based on ultrasound transit-time measurements with implanted piezo-electric crystals, Hoffer and colleagues (Hoffer et al., 1989) have described dramatic discrepancies between whole muscle length variations and local muscle fibre length changes during normal locomotion. In the extreme, muscle fibre length could decrease, while whole muscle length still was allowed to increase, and vice versa. This observation has since been confirmed in acute experiments, where the medial gastrocnemius muscle was activated using distributed stimulation of ventral root filaments (Weytjens and Hoffer, 1991). These observations clearly deserved attention since muscle fibre length variation, although not identical, can probably be taken as a scaled approximation of muscle spindle length changes during active movements. From this point of view, the above simulations should aim at reproducing local fibre length, rather than global muscle length variations. However, technically this would not be straightforward, since the local vs. global length discrepancy appears to vary with muscle topography (Hoffer et al., 1992), suggesting that afferent recordings would regularly have to be supplemented by topographically correct local length recordings.

In spite of the sometimes dramatic differences between presumed spindle length and whole muscle length, for simulation studies the problem may again be more quantitative than qualitative. Even before the era of local fibre length recordings it was evident that the substitution (in simulations) of passively imposed movements for actively generated movements required justification. Control experiments with distributed stimulation of non-fusimotor ventral root filaments (to reproduce also the

active force modulation during normal locomotion) had revealed remarkably small loading and unloading effects on afferent responses to simultaneously imposed movements when at the same time fusimotor efferents were also activated (Appenteng et al., 1983). When the matter was re-investigated more carefully, using a length compensation technique, the estimates of global vs. local length discrepancy again were considerably smaller than those obtained with the ultrasound method (Elek et al., 1990). These studies led to the conclusion that the omission of active force simulation during simulation of length and fusimotor activation profiles, would produce only minor, quantitative rather than qualitative, errors in the estimates of fusimotor activation patterns. However, size and incidence of errors in the estimates of fusimotor drive remain to be determined more systematically.

Flexible fusimotor control in freely moving animals

From about 1975 onwards, reports on spindle afferent recordings during a variety of movements (both in freely moving animals and in reduced preparations) had emphasized various degrees of dissociation of α-, γ_S- and γ_D-activation patterns (reviewed in Prochazka, 1981, 1989; Hulliger, 1984, 1987). However, these conclusions were mostly based on purely qualitative deductions from afferent discharge patterns and not further supported by experimental tests. Yet the general conclusion, that Ia sensitivity (and hence the balance between static and dynamic fusimotor drive) was adjusted differently in different motor tasks, has more recently been confirmed in experimental simulation studies. The main findings were:

First, routine locomotion in freely moving cats was characterized by relatively low Ia discharge rates. Simulations suggested that this was due to the presence of relatively low-rate static fusimotor activity which, in addition, was largely tonic and clearly unrelated to the rhythmic activation pattern of α-motoneurones, as seen in EMG recordings (Prochazka et al., 1985; Hulliger et al., 1985). Further, while the resolution of the simulation technique did not permit to entirely rule out the presence of dynamic drive, any activation of dynamic efferents was at best very modest, since additional low-rate (20/sec) activation of single dynamic γ-motoneurones consistently failed to yield better, and mostly led to less satisfactory, matches of chronic target responses by experimentally simulated responses (Hulliger et al., 1986).

Second, imposed limb movements, which were resisted by the animal, regularly were accompanied by very pronounced levels of dynamic fusimotor drive, while static fusimotor activation was reduced or entirely switched off (Hulliger et al., 1985; Prochazka et al., 1985). Dynamic activation patterns were often tonic, and appreciable levels of drive tended to be maintained over several cycles of imposed movement. Yet at the beginning of imposed movement sequences episodes of gradual build-up of γ_D activation rates were also documented.

Third, during episodes of rapid paw shake movements dynamic fusimotor efferents were selectively activated and elicited powerful sensitization of spindle Ia afferents to the rapid oscillatory stretches. Simulation analysis demonstrated that dynamic drive was set to high levels during the rapid movement episodes, and reset to insignificant values during intercalated periods of rest (Prochazka et al., 1989). Similarly, when animals prepared for the impact of landing on a support surface, Ia afferents were strongly sensitized due to predominant or selective dynamic fusimotor activation, and simulation analysis revealed comparable waxing and waning γ_D discharge profiles, with setting during preparation, followed by resetting upon landing (Hulliger et al., 1989).

Fourth, when cats were about to lose balance while walking on a narrow beam, corrective reactions were accompanied by a significant transient increase of dynamic drive, which again strongly sensitized extensor muscle Ia afferents to the stretches associated with crouching movements. However, in this paradigm dynamic efferents were not activated exclusively, since the γ_D transient occurred against

a background of largely tonic γ_S firing (Hulliger et al., 1989).

These findings provided further evidence for flexibility and a considerable degree of selectivity of central activation of fusimotor neurones, in particular of dynamic γ-efferents. They also were compatible with the notion that predominant and powerful activation of dynamic efferents might be related to unfamiliarity or even novelty of motor tasks. However, it still cannot be ruled out that the degree of difficulty or other behavioural factors could be alternative or cooperative determinants of powerful γ_D activation. Yet if novelty were involved, this would suggest that sensitization of spindle feedback could also play a significant role in motor adaptation and certain forms of motor learning.

The puzzle of apparent fusimotor silence in man

At present, the above observations from cat studies cannot as yet be generalized, for instance, to make inferences on the role of proprioceptive feedback in motor control mechanisms in man. Microneurographic recordings in man so far have consistently revealed spindle afferent firing rates which are much lower than those seen in cat and monkey (for details, see Prochazka and Hulliger, 1983; Hulliger, 1984; Gandevia and Burke, 1992), with increases of discharge rates during active, compared with passive movements, which rarely exceeded 20–30 impulses/sec. Qualitatively, based on these observations, the conclusion seems inevitable, that in the motor paradigms, which so far have been explored with microneurographic techniques in human subjects, fusimotor activation has at best been rather modest. Yet this remains to be corroborated quantitatively, perhaps in simulation studies along the lines above, or in direct recordings from unambiguously identified γ-motoneurones.

The observation of apparently only weak fusimotor action in man was surprising, since human spindles seem not to be any different from other mammalian spindles. If anything, they are more richly supplied with fusimotor fibres, suggesting that powerful fusimotor activation should be possible (see Hulliger, 1984). The recent demonstration of only minimal alterations of fusimotor drive (inferred from afferent recordings) in motor adaptation and matching tasks (Al-Falahe and Vallbo, 1988; Vallbo and Al-Falahe, 1990) only adds to the puzzle, since in cat very powerful dynamic fusimotor activation was found in adaptive motor behaviour (see above). Moreover, the microneurographic evidence of low-key performance of the human fusimotor system is not made any less enigmatic by the observations in patients (see below), that apparently selective large fibre sensory neuropathies, which lead to major proprioceptive deficits, indeed go hand in hand with significant loss of motor function.

However, before any notion of fusimotor and spindle feedback insignificance in man can be accepted, a much wider range of motor paradigms still has to be explored in human subjects. The motor tasks, which so far have been used for proprioceptive afferent recordings in man, often were isometric contractions, and/or entailed only relatively small forces and limited movement ranges and speeds, hardly comparable to the parameter ranges covered in animal running, jumping, landing or paw-shaking.

Motor deficits after selective deafferentation

Until quite recently, mostly unimpressive motor deficits were found in surgically deafferented animals (e.g., Goodwin and Luschei, 1974; Taub, 1976 (review); Sanes et al., 1985). Then, however, several reports on more selective large-fibre sensory neuropathies (mostly in man, without loss of voluntary strength, either due to pyridoxine intoxication, or to other insults of unknown etiology) described significant motor disabilities. These were either fairly restricted, limiting the ability to learn new or difficult motor tasks (Rothwell et al., 1982) and to correct inappropriate movements (Sanes et al., 1985), or they were generalized, resulting in disturbed gait and gross ataxia (e.g., Schaumburg et al., 1983; Windebank et al., 1985).

These deficits were mostly attributed to loss of

feedback from large-fibre proprioceptive afferents, including muscle spindle afferents. In the case of pyridoxine intoxication the purely sensory nature of the primary insult has convincingly been demonstrated in animal studies, since degenerative lesions have been found in large first-order sensory, but not in motor fibres (Hoover and Carlton, 1981; Windebank et al., 1985). However, whilst seemingly quite plausible in this general formulation, the details of interpretation are far from obvious. At least three different mechanisms could contribute to motor disability after proprioceptive loss: first, short-term deficiencies due to absence of feedback for ongoing regulation of movement; second, long-term disorganization of interneuronal or relay nuclei circuitry, following terminal degeneration and sprouting; and third, long-term disorganization or degradation of motor programs, due to absence of intermittent updating and maintenance on the basis of sensory feedback information (with "motor program" merely referring to the CNS' ability to generate well-orchestrated motor output).

While firm conclusions would still be premature, there is nevertheless circumstantial evidence to argue that not all of the above motor deficits can be attributed to short-term loss of ongoing, reflex-type regulation of movement. In early stages of subacute (low-dose) intoxication sensory fibre deficits are manifest without, or before, the manifestation of motor deficits (Xu et al., 1989). This would be difficult to reconcile with loss of short-term reflex function being solely responsible for all forms of motor dysfunction described above, since motor deficits should then develop in parallel with sensory deficits. However, the reported absence of motor disability was based on crude clinical assessment of motor behaviour of experimental animals and clearly requires more careful quantification of motor function.

In spite of such reservations, the hypothesis may be formulated that in the motor syndrome, which results from large-fibre sensory neuropathy, long-term motor deficits (affecting motor adaptation and learning) could be at least as serious as short-term motor dysfunction (arising from loss of proprioceptive reflex control), and that spindle Ia feedback may play a dual role: in addition to its contribution to short-term reflex control of posture and movement, it may also be relied on for optimization or maintenance of motor programs, especially when it is sensitized by augmented dynamic fusimotor drive.

Implications for artificial control of gait?

Considering the observations reviewed above, any recommendations for the design of artificial gait controllers can at best be very tentative, since current understanding even of the peripheral motor control mechanisms of biological controllers is so obviously limited, and many of the above conclusions are still speculative.

For artificial control of gait there is hardly a need for sensitivity control of peripheral transducers, i.e., there is no compelling reason, why length gauges or goniometers should be equipped with the equivalent of fusimotor innervation, since feedback gain control can probably be achieved by "central" control circuits just as effectively. Yet central gain control of length and, more generally, of kinematic feedback signals may be desirable to provide adaptive capabilities. For instance, it may be beneficial to use feedback from the periphery in dual mode, for parallel control strategies, operating with different "central" gains. For subtle moment-to-moment control of gait there is a need for servo-like short-term control. For this, moderate gains may be indicated, simply to avoid instability and oscillation. In addition, there may also be a need for long-term adjustment of "central" commands, e.g., when stimulation of muscle is complicated by fatigue. High gain processing of peripheral feedback may then be necessary to construct long-term estimates of movement parameters (e.g., kinematic profiles) to monitor any gradual deviation from target performance. Fast digital signal processors can now be used to compute, in real time, running averages of analogue signal patterns, and these could be used to optimize activation patterns continuously. However, single optimization strategies are unlikely to give stable

performance. For instance, when long-term drift of performance is due to muscle fatigue, different adjustments are indicated than when it arises from external mechanical conditions (variations in load or gait surface properties). Decision-making strategies will then have to be developed, using a wider range of feedback sources (conceivably including torque or force, in addition to kinematic feedback signals) or consultation of the subject, or both.

Lessons for artificial control of gait can probably be learned from motor systems physiology, but they are unlikely to be simple.

Acknowledgements

This work was supported by grants form the Alberta Herritage Foundation for Medical Research and the Canadian Medical Research Council.

References

Al-Falahe, N.A. and Vallbo, Å.B. (1988) Role of the human fusimotor system in a motor adaptation task. *J. Physiol. (Lond.),* 401: 77 – 95.

Appelberg, B. (1981) Selective central control of dynamic gamma motoneurones utilized for the functional classification of gamma cells. In: A. Taylor and A. Prochazka (Eds.), *Muscle Receptors and Movement,* Macmillan, London, pp. 97 – 108.

Appenteng, K., Hulliger, M., Prochazka, A. and Zangger, P. (1983) Distributed α- and γ-stimulation in anaesthetized cats during simulation of normal movements: matching of spindle afferent discharge patterns to deduce fusimotor action. *J. Physiol. (Lond.),* 339: 10P.

Elek, J., Prochazka, A., Hulliger, M. and Vincent, S. (1990) In-series compliance of gastrocnemius muscle in cat step cycle: do spindles signal origin-to-insertion length? *J. Physiol. (Lond.),* 429: 237 – 258.

Gandevia, S.C. and Burke, D. (1992) Does the nervous system depend on kinaesthetic information to control natural limb movements? *Behav. Brain Sci.,* in press.

Goodwin, G.M. and Luschei, E.S. (1974) Effects of destroying spindle afferents from jaw muscles on mastication in monkeys. *J. Neurophysiol.,* 37: 967 – 981.

Goodwin, G.M., Hulliger, M. and Matthews, P.B.C. (1975) The effects of fusimotor stimulation during small amplitude stretching on the frequency-response of the primary ending of the mammalian muscle spindle. *J. Physiol. (Lond.),* 253: 175 – 206.

Hoffer, J.A., Caputi, A.A., Pose, I.E. and Griffiths, R.I. (1989) Roles of muscle activity and load on the relationship between muscle spindle length and whole muscle length in the freely walking cat. *Progr. Brain Res.,* 80: 75 – 85.

Hoffer, J.A., Caputi, A.A. and Pose, I.E. (1992) Activity of muscle proprioceptors in cat posture and locomotion: relation to EMG, tendon force, and the movement of fibres and aponeurotic segments. *IBRO Symposium Series,* Pergamon Press, London, in press.

Hoover, D.M. and Carlton, W.W. (1981) The subacute neurotoxicity of excess pyridoxine HCl and clioquinol (5-chloro-7-iodo-8-hydroxyquinoline) in beagle dogs. II. Pathology. *Vet. Pathol.,* 18: 757 – 768.

Hulliger, M. (1984) The mammalian muscle spindle and its central control. *Rev. Physiol. Biochem. Pharmacol.,* 101: 1 – 110.

Hulliger, M. (1987) The role of muscle spindle receptors and fusimotor neurones in the control of movement. In: R.J. Ellingson, N.M.F. Murray and A.M. Halliday (Eds.), *The London Symposia (EEG Suppl., 39),* Elsevier, Amsterdam, pp. 58 – 66.

Hulliger, M. and Prochazka, A. (1983) A new stimulation method to deduce fusimotor activity from afferent discharge recorded in freely moving cats. *J. Neurosci. Methods,* 8: 197 – 204.

Hulliger, M., Matthews, P.B.C. and Noth, J. (1977a) Static and dynamic fusimotor action on the response of Ia fibres to low frequency sinusoidal stretching of widely ranging amplitude. *J. Physiol. (Lond.),* 267: 811 – 838.

Hulliger, M., Matthews, P.B.C. and Noth, J. (1977b) Effects of combining static and dynamic fusimotor stimulation on the response of the muscle spindle primary ending to sinusoidal stretching. *J. Physiol. (Lond.),* 267: 839 – 856.

Hulliger, M., Zangger, P., Prochazka, A. and Appenteng, K. (1985) Fusimotor "set" vs. α-γ linkage in voluntary movement in cats. In: A. Struppler and A. Weindl (Eds.), *Electromyography and Evoked Potentials – Advances in Applied Neurological Sciences, Vol. 1,* Springer, Heidelberg, pp. 56 – 63.

Hulliger, M., Prochazka A. and Zangger, P. (1986) Fusimotor activity in freely moving cats. Tests of concepts derived from reduced preparations. In: S. Grillner, P.S.G. Stein, D.G. Stuart, H. Forssberg and R.M. Herman (Eds.), *Neurobiology of Vertebrate Locomotion,* Macmillan, London, pp. 593 – 605.

Hulliger, M., Horber, F., Medved, A. and Prochazka, A. (1987) An experimental simulation method for iterative and interactive reconstruction of unknown (fusimotor) inputs contributing to known (spindle afferent) responses. *J. Neurosci. Methods,* 21: 225 – 238.

Hulliger, M., Dürmüller, N., Prochazka, A. and Trend, P. (1989) Flexible fusimotor control of muscle spindle feedback during a variety of natural movements. *Prog. Brain Res.,* 80: 87 – 101.

Matthews, P.B.C. (1962) The differentiation of two types of fusimotor fibre by their effects on the dynamic response of muscle spindle primary endings. *Q. J. Exp. Physiol.,* 47: 324 – 333.

Matthews, P.B.C. (1972) *Mammalian Muscle Receptors and their Central Actions,* Arnold, London, 630 pp.

Matthews, P.B.C. (1981) Muscle spindles: their messages and their fusimotor supply. In: J.M. Brookhart, V.B. Mountcastle and V.B. Brooks (Eds.), *Handbook of Physiology – The Nervous System, Vol. II, Motor Control, Part 1,* American Physiological Society, Bethesda, MD, pp. 189 – 228.

Prochazka, A. (1981) Muscle spindle function during normal movement. *Int. Rev. Physiol.,* 25: 47 – 90.

Prochazka, A. (1984) Chronic techniques for studying neurophysiology of movement in cats. In: R. Lemon (Ed.), *Methods of Neuronal Recording in Conscious Animals – Ibro Handbook Series, Methods in the Neurosciences, Vol. 4,* Wiley, Chichester, pp. 113 – 128.

Prochazka, A. (1989) Sensorimotor gain control: a basic strategy of motor systems? *Prog. Neurobiol.,* 33: 281 – 307.

Prochazka, A. and Hulliger, M. (1983) Muscle afferent function and its significance for motor control mechanisms during voluntary movements in cat, monkey, and man. In: J.E. Desmedt (Ed.), *Motor Control Mechanisms in Health and Disease – Advances in Neurology, Vol. 39,* pp. 93 – 132.

Prochazka, A., Hulliger, M., Zangger, P. and Appenteng, K. (1985) "Fusimotor set": new evidence of α-independent control of γ-motoneurones during movement in the awake cat. *Brain Res.,* 339: 136 – 140.

Prochazka, A., Hulliger, M., Trend, P., LLewellyn, M. and Dürmüller, N. (1989) Muscle afferent contribution to control of paw shakes in normal cats. *J. Neurophysiol.,* 61: 550 – 562.

Rothwell, J.C., Traub, M.M., Day, B.L., Obeso, J.A., Thomas, P.K. and Marsden, C.D. (1982) Manual motor performance in a deafferented man. *Brain,* 105: 515 – 542.

Sanes, J.N., Mauritz, K.-H., Dalakas, M.C. and Evarts, E.V. (1985) Motor control in humans with large-fiber sensory neuropathy. *Hum. Neurobiol.,* 4: 101 – 114.

Schaumburg, H., Kaplan, J., Windebank, A., Vick, N., Rasmus, S., Pleasure, D. and Brown, M.J. (1983) Sensory neuropathy from pyridoxine abuse. A new megavitamin syndrome. *N. Engl. J. Med.,* 309: 445 – 448.

Taub, E. (1976) Movement in nonhuman primates deprived of somatosensory feedback. *Exercise Sports Sci. Rev.,* 4: 335 – 374.

Taylor, A. and Donga, R. (1989) Central mechanisms of selective fusimotor control. *Progr. Brain Res.,* 80: 27 – 35.

Taylor, A., Donga, R. and Jüch, P.J.W. (1992) Fusimotor effects of midbrain stimulation on jaw muscle spindles of the anaesthetized cat. *Exp. Brain Res.,* in press.

Vallbo, Å.B. and Al-Falahe, N.A. (1990) Human muscle spindle response in a motor learning task. *J. Physiol. (Lond.),* 421: 553 – 568.

Weytjens, J.L.F. and Hoffer, J.A. (1991) Forces generated by cat medial gastrocnemius motor units during simulated walking. *Soc. Neurosci. Abstr.,* 17: 648.

Windebank, A.J., Low, P.A., Blexrud, M.D., Schmelzer, J.D. and Schaumburg, H.H. (1985) Pyridoxine neuropathy in rats: specific degeneration of sensory axons. *Neurology,* 35: 1617 – 1622.

Xu, Y., Sladky, J.T. and Brown, M.J. (1989) Dose-dependent expression of neuronopathy after experimental pyridoxine intoxication. *Neurology,* 39: 1077 – 1082.

J.H.J. Allum, D.J. Allum-Mecklenburg, F.P. Harris and R. Probst
Progress in Brain Research, Vol. 97

CHAPTER 17

Gating of reflexes in ankle muscles during human stance and gait

V. Dietz

Paraplegic Centre, University Hospital Balgrist, Zurich, Zwitserland

Holding the body's centre of gravity steady represents the crucial variable for the stabilization of posture in upright stance in man. Results from two experimental approaches suggest that force-dependent receptors are required, in addition to the well-known systems involved in sway stabilization, for equilibrium control. One approach concerns bilateral leg muscle activation during stance. Unilateral or bilateral leg displacements were induced while subjects stood on a treadmill with split belts. A unilateral displacement induced a bilateral EMG response. During bilateral displacements the EMG activity was linearly summed or subtracted, depending on whether the legs were displaced in the same or opposite directions. Both legs acted in a cooperative manner: each limb affected the strength of muscle activation and the time-space behaviour of the other. This interlimb coordination is suggested to be mediated by spinal interneuronal circuits, which are themselves under supraspinal (e.g., cerebellar) control. The other approach concerns the modulation of postural reflexes under simulated "microgravity" in water immersion. An approximately linear relationship was found between contact forces and impulse-directed EMG response amplitudes in the leg muscles. Out of water loading of the subjects resulted in no further increase of the response amplitude. It was concluded that the function of proprioceptive reflexes involved in the stabilization of posture depends on the presence of contact forces opposing gravity. Extensor load receptors are thought to signal changes of the projection of body's centre of mass with respect to the feet. The interaction of the afferent input from these receptors with the other systems involved in postural control is not yet fully understood.

Key words: Bilateral leg muscle coordination; Muscle activity; Motor control; Human posture; Spinal stretch reflex; Muscle receptor; Leg displacement; Centre of gravity; Water immersion

Introduction

The regulation of human posture and locomotion is based on the finely tuned coordination of muscle activation between the two legs. Although the control of bilateral leg muscle activation and movement usually takes place at a subconscious level, voluntary interaction with these mechanisms can occur. The potential for independent voluntary control of the movements of a single leg, as well as the more usual automatically coordinated movements of both legs, requires adequate neuronal mechanisms to achieve a task-directed coupling of bilateral leg muscle activation. In the spinal cat it has been shown that differences in treadmill speeds between the two sides of the body can produce some adjustments to the speed of each limb (Forssberg et al., 1976; Grillner, 1981), indicating that the spinal cord contains networks responsible for each limb that can be connected in a variety of ways (Grillner, 1981). Similar observations have been noted for infant walking (Thelen et al., 1987).

The control of bilateral leg muscle activation during stance and gait is directed to keep the body's centre of gravity over the feet. From a simple mechanical viewpoint, the aim of all of the known postural control mechanisms is to hold the body's centre of gravity constant within a certain range. For

stability, the projection of the centre of gravity must meet the support surface within the area of the feet, in order to prevent falling. From these considerations, several questions arise: which mechanism senses that the centre of gravity projects within the required range? What known receptor systems could provide this information and, if such receptor system exists, how does it interact with the known postural control mechanisms?

Several different mechanisms for the control and stabilization of human posture against destabilizing impulses have been discussed in the literature during recent years. Among these the influence of proprioceptive (Diener et al., 1984; Dietz et al., 1979, 1987), visual (Berthoz et al., 1979) and vestibular (Allum and Pfaltz, 1985; Keshner et al., 1987) inputs has been demonstrated by various experimental approaches. Recent experimental results (Dietz et al., 1989b; Gollhofer et al., 1989) indicate that other mechanisms might be involved in postural stabilization. Here, an alternative posture control mechanism is postulated which is sensitive to the position of the centre of gravity with respect to the feet.

Reflex modulation and interlimb coordination

When an obstacle is spotted appropriate avoidance movements of the relevant leg are voluntarily initiated. These movements are accompanied by an automatic, supportive activation of the other leg. This potential for independent voluntary control of the movements of a single leg, in addition to the more usual automatic coordination of the movements of both legs, requires that adequate neuronal mechanisms exist to achieve task-directed coupling of bilateral leg muscle activation.

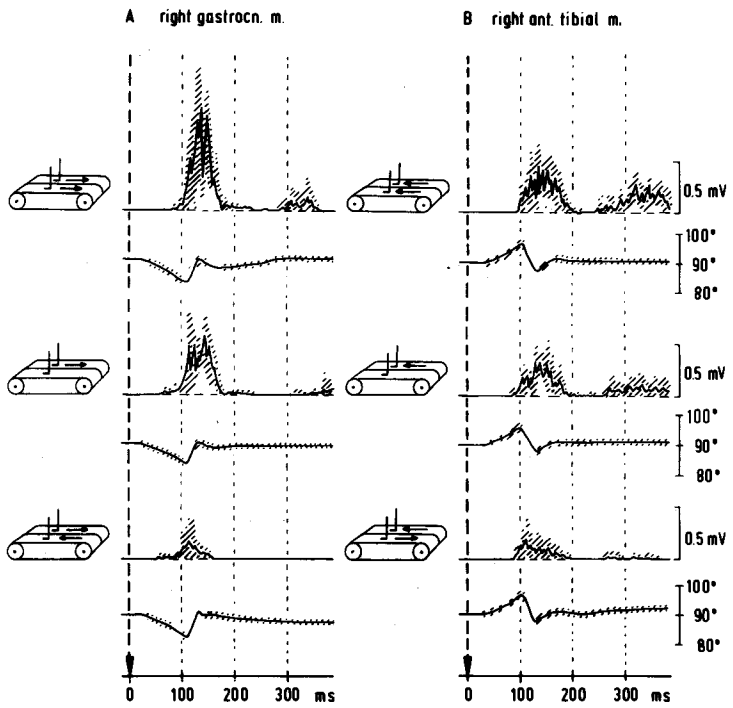

Fig. 1. Mean values (with S.D.) of the rectified and averaged (n = 10) gastrocnemius (A) and tibialis anterior (B) response of the right leg, together with the movement at the right ankle joint, after backward (A) and forward (B) directed acceleration of the treadmill in one subject. Top to bottom: bilateral, unilateral and opposing perturbations. Arrow indicates the onset of displacement at the ankle joint. (From Dietz et al., 1989a.)

Unilateral leg displacements during stance, balancing and gait evoke a *bilateral* response pattern, with a similar onset latency on both sides (shortest onset latencies during balancing: about 55 msec (Dietz and Berger, 1982, 1984)). Nevertheless, the contralateral leg muscles are not activated after a unilateral displacement during stance or balancing when the legs are not supporting the upper body (Dietz and Berger, 1984), i.e., we assume that a "postural program" is active (Horak and Nashner, 1986). During stance, bilateral leg flexor or extensor activity is induced, whereas during gait, the bilateral pattern is dependent on the phase of the gait cycle (Berger et al., 1984; Dietz et al., 1984, 1986). Furthermore, obstruction of the swing phase of gait, which does not, in itself, apply stretch to a leg muscle, is also followed by a functional bilateral leg muscle activation pattern (Dietz et al., 1986).

Further information about the organisation and functional significance of the interlimb coordination of leg muscle activity in the control of bipedal stance was obtained when perturbations were applied during stance on a treadmill with split belts (Dietz et al., 1989a). Unidirectional bilateral perturbations are followed by larger EMG responses in both legs. For a given acceleration rate, the EMG amplitude in one leg is about equal to the sum of the EMG amplitudes of both the displaced and non-displaced leg obtained during unilateral displacement. A subtraction effect is obtained when the legs are simultaneously displaced in opposite directions: EMG responses in both legs are significantly smaller than those obtained after unilateral displacement (Fig. 1). Consequently, in addition to the synergies of distal and proximal leg muscles (Horak and Nashner, 1986; for review, see Nashner, 1986), a bilateral co-activation of muscles also occurs. During bilateral displacements, the activity induced by relative movement of the respective contralateral leg is enhanced or suppressed, depending on whether the legs are displaced in the same or in opposite directions (Dietz et al., 1989a).

From a functional point of view, this interlimb coordination is necessary in order to keep the body's centre of gravity over the feet: the bilateral activation seen during unilateral displacements produces rapid, automatic co-contraction of the non-displaced leg, providing a more stable base from which to compensate for the perturbation (Fig. 2). During bilateral perturbation, the destabilisation of body equilibrium is greater than during unilateral perturbation. The mutual enhancement of the response amplitude allows a more effective contractile force to compensate for the perturbation. A displacement of the legs in opposite directions causes the body's centre of gravity to fall between the legs. Thus, a reduced level of compensatory responses is needed to regain body equilibrium in this condition.

This interlimb coordination is thought to be based on a central mechanism and, in view of the short latencies of the bilateral responses, mediated at a spinal level. A cerebellar contribution to interlimb coordination, via reticulospinal neurons, has been suggested both in the cat (Ito, 1984) and in man (Bonnet et al., 1976). Nevertheless, in the spinal cat, differences in treadmill speed between the two sides of the body can produce some adjustments to the speed of each limb (Forssberg and Grillner, 1973; Forssberg et al., 1976; Grillner, 1981), indicating that the spinal cord contains networks responsible for each limb, which can be connected in a variety of ways (Grillner, 1981). Similar observations have been made during stepping of seven-month-old infants on a split-belt treadmill (Thelen et al., 1987): when the belts run with different speeds, both legs act in a cooperative manner, each limb affecting the time-space behaviour of the other.

It may be assumed that a close interaction exists between the spinal interneuronal circuits responsible for interlimb coordination and the peripheral afferent input. This interaction is presumably observed when displacements of different velocity are induced unilaterally. Reflex responses in synergistic muscles of both legs are graded according to the size of the proprioceptive input from the primarily displaced joint (Berger et al., 1987; Dietz et al., 1989a). We postulate that the spinal coordination is under supraspinal control, because the bilateral EMG pattern is disrupted in patients with spasticity (Berger and Dietz, 1984).

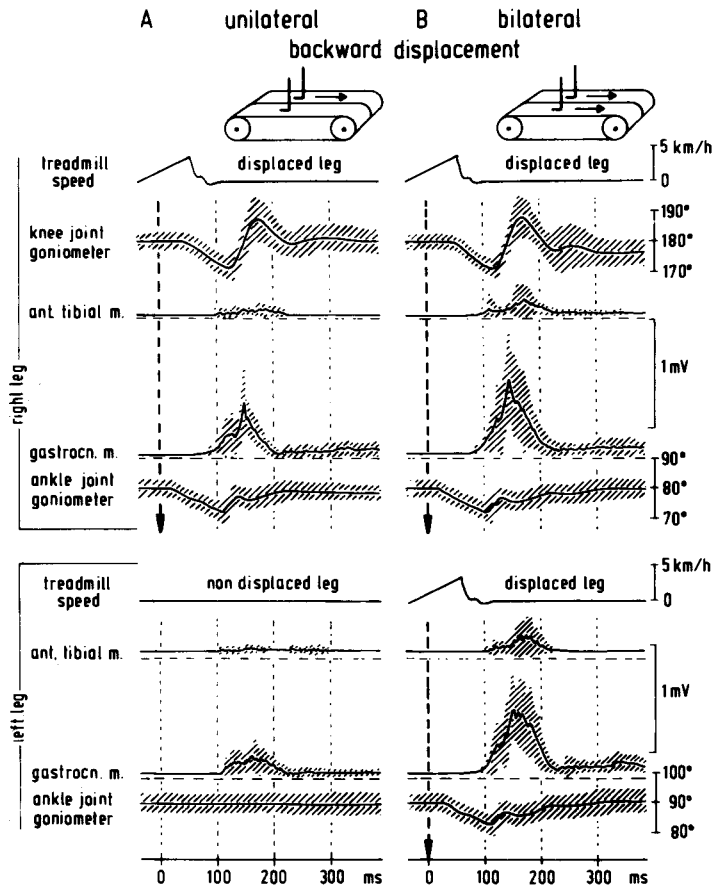

Fig. 2. Mean values (with S.D.) of the rectified and averaged (n = 10) bilateral EMG responses of the legs, together with the corresponding joint movements, after a unilateral (*A*) and bilateral (*B*) backward-directed acceleration of the treadmill in 32 subjects. Arrow indicates the onset of displacement at the ankle joint. (From Dietz et al., 1989a.)

Influence of gravity on postural reflexes

Most investigations of stance and gait have led to the conclusion that the EMG adjustments observed in a particular condition can be related to the demands of equilibrium control. Keeping the body's centre of mass over the feet represents, therefore, an important variable controlled by neuronal mechanisms. This suggestion is highlighted by observations that, depending on the conditions of stance, muscle stretch does not necessarily result in a compensatory stretch reflex response, but instead in an antagonistic muscle activation (Hansen et al., 1988; Gollhofer et al., 1989). Furthermore, the amplitude of a "stretch" reflex response is dependent on whether the legs are displaced in the same or in opposite directions (Dietz et al., 1989a). But how is the position of the body's centre of mass relative to the feet signaled to the CNS? This question has received little attention in most investigations of postural control. We are just beginning to appreciate the influence that gravity has on motor and sensory behaviour such as the perception of motion. We postulate that for an appropriate gain control of postural reflexes, apart from the thoroughly investigated muscle proprioceptive inputs, additional peripheral information is required which should be "gravity"-dependent.

Investigations of postural reactions in weightlessness experienced during space flights have indicated that, while the timing of the response pattern following displacement of the feet is preserved, EMG responses are greatly reduced in amplitude (Clément et al., 1984, 1985; Young et al., 1986; Koslovskaya et al., 1988). In addition, the otolith-modulated muscle response sensitivity is low after in-flight adaptation, with an associated decrease in awareness of direction and magnitude of motion (Reschke et al., 1984). The consequence of these changes for postural control is a reduced weighting of gravity-based signals in favour of visual and tactile cues (Young et al., 1986).

To further investigate the receptors involved in signaling changes in the position of the body's centre of mass with respect to the support surface, the buoyancy of the body in a water-filled pool has been used to simulate some of the effects of weightlessness (Dietz et al., 1989b) (Fig. 3). Compared to postural reactions studied during space flights, such an experimental approach has the advantage of leaving the effect of gravity on vestibular receptor function unaltered yet still permits a manipulation of body weight. If a "gravity" or strictly speaking, relative weight dependence of the compensatory EMG responses exists, then manipulating body weight should affect the responses to destabilizing platform impulses.

During immersion there exists a close relationship (for the gastrocnemius $r = 0.63$, $P < 0.0001$; for the tibialis anterior $r = 0.82$, $P < 0.0001$) between actual body weight and the magnitude of the EMG responses following both backward and forward displacement (Fig. 4). As during space flights (Clément et al., 1985), the postural pattern is qualitatively preserved. Out of water, however, no significant correlation exists between loading of the subjects and the EMG responses. This saturation of the response out of water might represent a natural limi-

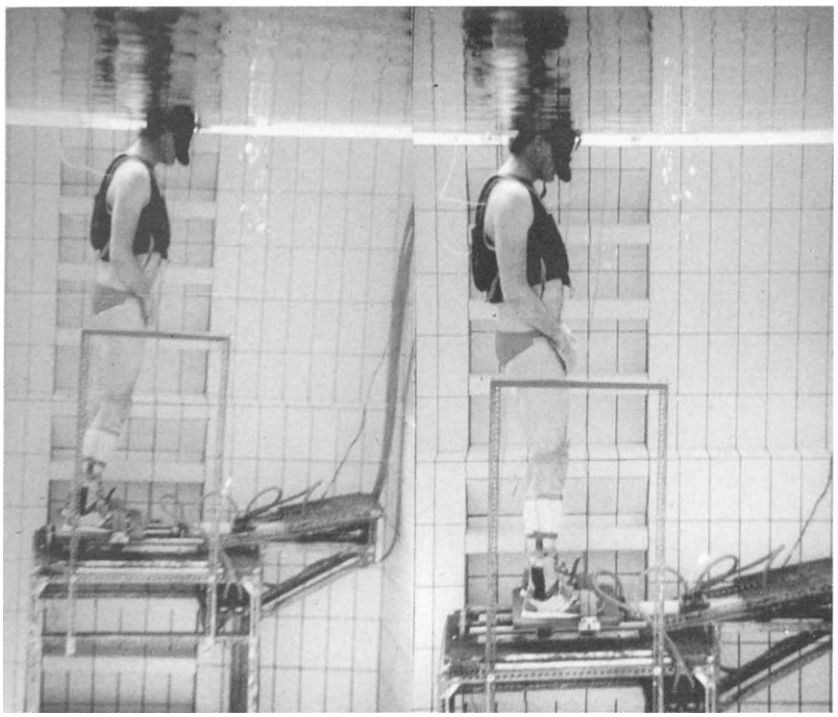

Fig. 3. Equipment, showing the platform used to induce backward and forward displacements under water.

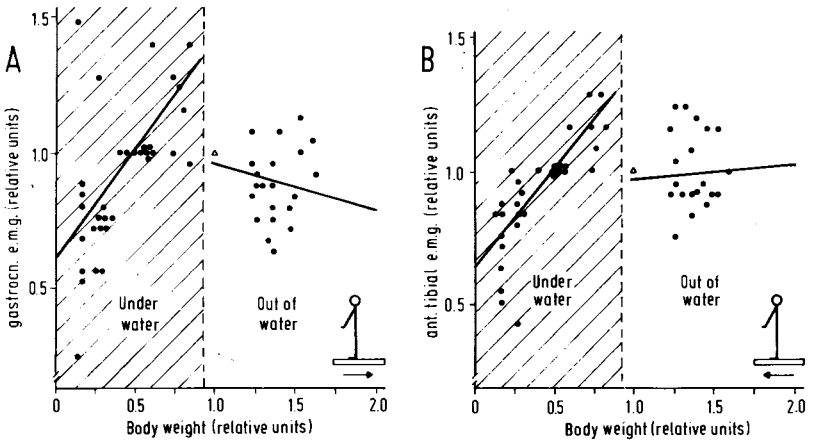

Fig. 4. Correlative functions between body weight (abscissa) and integrated EMG responses (ordinate) following backward (*A*, gastrocnemius m.) and forward (*B*, tibialis anterior m.) displacement. The data of ten subjects were normalized with respect to the integrated EMG activity and the body weight to displacements induced unloaded out of water and are displayed as scatter diagrams and regression lines for both conditions. (From Dietz et al., 1989b.)

tation of muscle activation, in order to prevent possible injury (i.e., rupture) of the musculo-skeletal system (Dietz et al., 1989b).

From the observations obtained in the immersion experiments, there is some evidence that the function of reflexes known to be involved in the stabilization of human posture (e.g., muscle proprioceptive and vestibulo-spinal reflexes) depends on the activity of receptors within the body which indicate the deviations of the body's centre of mass from a certain neutral position (cf. Mittelstaedt, 1964; Clément and Rezette, 1985). In addition, such receptor signals may be important for the selection of appropriate "synergies", i.e., of the centrally programmed pattern (cf. Hasan and Stuart, 1988). The latter point is exemplified by the difference in patterns between translational and rotational ankle perturbations (Hansen et al., 1988; Gollhofer et al., 1989). There is, in addition, some new evidence that limb geometry represents an essential parameter for the control of the centre of gravity during quadrupedal stance (Lacquaniti et al., 1990).

In order to achieve gain modulation of postural reflexes and selection of appropriate patterns, the following mechanisms may be considered: (1) the strength of background activity in the leg muscles might change with the body weight during stance, leading to a gain modulation of the postural reflexes. The results of the immersion study make this rather unlikely, as the amount of EMG activity in the leg muscles preceding the compensatory EMG responses did not systematically change with the loading, and the level of voluntary leg muscle activity did not visibly affect the compensatory responses (Dietz et al., 1989b); (2) pressure receptors on the sole of the foot might signal the actual forces exerted on the supporting surface. This would fit with the suggestion that stimulation of cutaneous mechanoreceptors is responsible for variations of the initial burst of EMG activity in the agonist muscle during the response to perturbation in animals and man (Seguin and Cooke, 1983). This possibility is unlikely because compensatory responses are preserved after ischemic blockade of the skin afferents of the feet (Berger et al., 1984; Diener et al., 1984); and (3) input from pressure receptors distributed over the whole body (within joints and the vertebral column) may converge with other reflex pathways on spinal interneuronal circuits, as has been shown to be the case in the cat (Lundberg et al., 1987).

The latter receptor system may, indeed, be responsible for the effects seen in the immersion experiments. Slowly adapting receptors within the

knee joint, sensitive to externally applied pressure, have been found in the cat (Clark, 1975) and these could supply such information about contact forces. Similarly, knee articular receptors, in man, contribute little to the signaling of joint position, but rather, contribute to deep pressure sensation (Burgess et al., 1982). These receptors may also indicate changes of body weight and changes of the position of the centre of mass with respect to the feet (Horstmann and Dietz, 1990). The function of the otolith system has already been suggested to depend on the presence of contact forces opposing gravity (Roberts, 1973, 1979; Baumgarten, 1987; Dietz et al., 1991). Alternatively, load receptors within the leg extensor muscles may signal changes of the projection of the centre of body's mass (Dietz et al., 1992). Such receptors have been shown to interact with spinal locomotor rhythms in the cat (Conway et al., 1987). Further investigations are necessary to define more precisely the location and distribution of these pressure or load receptors.

Conclusions

Irrespective of the conditions under which stance and gait are investigated the neuronal pattern evoked during a particular task is always directed to hold the body's centre of mass over the base of support. All control mechanisms must, therefore, be considered and discussed in this respect. One consequence is that the selection of afferent input by the central mechanisms must correspond to the actual requirements for body stabilization. Furthermore, neuronal signals of muscle stretch or length alone are insufficient for the control of upright posture. Only a combination of afferent inputs can provide the information needed to control the body equilibrium. Some of these complex interactions between afferent inputs have been partially revealed in the last years: the functions of proprioceptive reflexes and of the otoliths depend on contact forces and/or load receptors within the extensor muscles, which include information about the position of the body's centre of gravity relative to the feet.

References

Allum, J.H.J. and Pfaltz, C.R. (1985) Visual and vestibular contributions to pitch sway stabilization in the ankle muscles of normals and patients with bilateral peripheral vestibular deficits. *Exp. Brain Res.*, 58: 82 – 94.

Baumgarten, R.J. (1987) General remarks on the role of the vestibular system in weightlessness. *Arch. Otorhinolaryngol.*, 244: 135 – 142.

Berger W. and Dietz, V. (1984) Interlimb coordination of posture in patients with spastic paresis. Impaired function of spinal reflexes. *Brain*, 107: 965 – 978.

Berger, W., Dietz, V. and Quintern, J. (1984) Corrective reactions to stumbling in man: neuronal coordination of bilateral leg muscle activity during gait. *J. Physiol. (Lond.)*, 357: 109 – 125.

Berger, W. Dietz, V. and Horstmann, G. (1987) Interlimb coordination in man. *J. Physiol. (Lond.)*, 390: 135P.

Berthoz, A., Lacour, M., Soechting, J.F. and Vidal, P.P. (1979) The role of vision in the control of posture during linear motion. In: R. Granit and O. Pompeiano (Eds.), *Progress in Brain Research – Reflex Control of Posture and Movement, Vol. 50,* Elsevier, Amsterdam, pp. 197 – 209.

Bonnet, M., Gurfinkel, V.S., Lipshits, M.J. and Popov, K.E. (1976) Central programming of lower limb muscular activity in the standing man. *Agressologie* 17: B35 – B42.

Burgess, P.R., Wei, J.Y., Clark, F.J. and Simon, J. (1982) Signaling of kinesthetic information by peripheral sensory receptors. *Annu. Rev. Neurosci.*, 5: 171 – 187.

Clark, F.J. (1975) Information signaled by sensory fibers in medial articular nerve. *J. Neurophysiol.*, 38: 1464 – 1472.

Clément, G. and Rezette, D. (1985) Motor behavior underlying the control of an upside-down vertical posture. *Exp. Brain Res.*, 59: 478 – 484.

Clément, G., Gurfinkel, V.S., Lestienne, F., Lipshits, M.I. and Popov, K.E. (1984) Adaptation of postural control of weightlessness. *Exp. Brain Res.*, 57: 61 – 72.

Clément, G., Gurfinkel, V.S., Lestienne, F., Lipshits, M.I. and Popov, K.E. (1985) Changes of posture during transient perturbations in microgravity. *Aviat. Space Environ. Med.*, 56: 666 – 671.

Conway, B.A., Hultborn, H. and Kiehn, O. (1987) Proprioceptive input resets central locomotor rhythm in the spinal cat. *Exp. Brain Res.*, 68: 643 – 656.

Diener, H.C., Dichgans, J., Guschlbauer, B. and Mau, H. (1984) The significance of proprioception on postural stabilization as assessed by ischemia. *Brain Res.*, 296: 103 – 109.

Dietz, V. and Berger, W. (1982) Spinal coordination of bilateral leg muscle activity during balancing. *Exp. Brain Res.*, 47: 172 – 176.

Dietz, V. and Berger, W. (1984) Inter-limb coordination of posture in patients with spastic paresis: impaired function of spinal reflexes. *Brain*, 107: 965 – 978.

Dietz, V., Schmidtbleicher, D. and Noth, J. (1979) Neuronal mechanisms of human locomotion. *J. Neurophysiol.*, 42: 1212 – 1222.

Dietz, V., Quintern, J. and Berger, W. (1984) Corrective reactions to stumbling in man: functional significance of spinal and transcortical reflexes. *Neurosci. Lett.*, 44: 131 – 135.

Dietz, V., Quintern, J., Boos, G. and Berger, W. (1986) Obstruction of the swing phase during gait: phase-dependent bilateral leg muscle coordination. *Brain Res.*, 384: 166 – 169.

Dietz, V., Quintern, J. and Sillem, M. (1987) Stumbling reactions in man: significance of proprioceptive and preprogrammed mechanisms. *J. Physiol. (Lond.)*, 368: 149 – 163.

Dietz, V., Horstmann, G.A. and Berger, W. (1989a) Interlimb coordination of leg muscle activation during perturbation of stance in humans. *J. Neurophysiol.*, 62: 680 – 693.

Dietz, V., Horstmann, G.A., Trippel, M. and Gollhofer, A. (1989b) Human postural reflexes and gravity – an under water simulation. *Neurosci. Lett.*, 106: 350 – 355.

Dietz, V., Trippel, M., Discher, M. and Horstmann, G.A. (1991) Compensation of human stance perturbations: selection of the appropriate electromyographic pattern. *Neurosci. Lett.*, 126: 71 – 74.

Dietz, V., Gollhofer, A., Kleiber, M. and Trippel, M. (1992) Regulation of bipedal stance: dependency on "load" receptors. *Exp. Brain Res.*, 89: 229 – 231.

Forssberg, H. and Grillner, S. (1973) The locomotion of the acute spinal cat injected with clonidine i.v. *Brain Res.*, 50: 184 – 186.

Forssberg, H., Grillner, S. and Rossignol, S. (1976) Interaction between the two hindlimbs of a spinal cat walking on a split belt. *Proceedings of the Third International Conference on Motor Control, Albena, Bulgaria*, p. 9 (abstract).

Gollhofer, A., Horstmann, G.A., Berger, W. and Dietz, V. (1989) Compensation of translational and rotational perturbations in human posture: stabilization of the centre of gravity. *Neurosci. Lett.*, 105: 73 – 78.

Grillner, S. (1981) Control of locomotion in bipeds, tetrapods, and fish. In: M. Brookhart and V.B. Mountcastle (Eds.), *Handbook of Physiology – The Nervous System. Motor Control, Vol. II, Part 2*, Am. Physiol. Soc., Washington, DC, pp. 1179 – 1235.

Hansen, P.D., Woollacott, M.H. and Debu, B. (1988) Postural responses to changing task conditions. *Exp. Brain Res.*, 73: 627 – 636.

Hasan, Z. and Stuart, D.G. (1988) Animal solutions to problems of movement control: the role of proprioceptors. *Annu. Rev. Neurosci.*, 11: 199 – 123.

Horak, F.B. and Nashner, L.M. (1986) Central programming of postural movements: adaptation to altered support-surface configurations. *J. Neurophysiol.*, 55: 1369 – 1381.

Horstmann, G.A. and Dietz, V. (1990) A basic posture control mechanism: the stabilization of the centre of gravity. *Electroenceph. Clin. Neurophysiol.*, 76: 165 – 176.

Ito, M. (1984) *The Cerebellum and Neural Control*, Raven Press, New York.

Keshner, E.A., Allum, J.H.J. and Pfaltz, C.R. (1987) Postural coactivation and adaptation in the sway stabilizing responses of normals and patients with bilateral vestibular deficit. *Exp. Brain Res.*, 69: 77 – 92.

Koslovskaya, I., Dimitrieva, I., Grigorieva, L., Kirenskaya, A. and Kreidich, Y.U. (1988) Gravitational mechanisms in the motor system. Studies in real and simulated weightlessness. In: V.S. Gurfinkel, M.E. Joffe, J. Massion and J.P. Roll (Eds.), *Stance and Motion. Facts and Concepts*, Plenum, New York, pp. 37 – 48.

Lacquaniti, F., Le Taillanter, M., Lopiano, L. and Maioli, C. (1990) The control of limb geometry in cat posture. *J. Physiol. (Lond.)*, 426: 177 – 192.

Lundberg, A., Malmgren, K. and Schomburg, E.D. (1987) Reflex pathway from group II muscle afferents. 3. Secondary spindle afferents and the FRA: a new hypothesis. *Exp. Brain Res.*, 65: 294 – 306.

Mittelstaedt, H. (1964) Basic control patterns of orientational homeostasis. *Symp. Soc. Exp. Biol.*, 18: 365 – 385.

Nashner, L.M. (1986) Organization of human postural movements during standing and walking. In: S. Grillner, P. Stein, D.G. Stuart, H. Forssberg and R.M. Herman (Eds.), *Wenner-Gren International Symposium Series – Neurobiology of Vertebrate Locomotion, Vol. 45*, Macmillan, London, pp. 637 – 648.

Reschke, M.F., Anderson, D.J. and Homick, J.L. (1984) Vestibulospinal reflexes as a function of microgravity. *Science*, 225: 212 – 214.

Roberts, T.D.M. (1973) Reflex balance. *Nature*, 244: 156 – 158.

Roberts, T.D.M. (1979) Otoliths and uprightness. In: R. Granit and O. Pompeiano (Eds.), *Reflex Control of Posture and Movement – Progress in Brain Research, Vol. 50*, Elsevier, Amsterdam, pp. 493 – 499.

Seguin, J.J. and Cooke, J.D. (1983) The effects of cutaneous mechanoreceptor stimulation on the stretch reflex. *Exp. Brain Res.*, 52: 152 – 154.

Thelen, E., Ulrich, B.D. and Niles, D. (1987) Bilateral coordination in human infants: stepping on a split-belt treadmill. *J. Exp. Psychol. Hum. Percept. Perform.*, 13: 405 – 410.

Young, L.R., Oman, C.M., Watt, D.G., Money, K.E., Lichtenberg, B.K. and Kenyon, R.V. (1986) Canadian vestibular experiments on the spacelab-1 mission: 1. Sensory adaptation to weightlessness and readaptation to one-g: an overview. *Exp. Brain Res.*, 64: 291 – 298.

J.H.J. Allum, D.J. Allum-Mecklenburg, F.P. Harris and R. Probst
Progress in Brain Research, Vol. 97

CHAPTER 18

Modification of reflexes in normal and abnormal movements

R.B. Stein, J.F. Yang, M. Bélanger and K.G. Pearson

Division of Neuroscience, University of Alberta, Edmonton, Canada

The trajectories observed for the limb during human locomotion are determined by a mixture of influences, some arising from neural circuits entirely within the central nervous system and others arising from a variety of sensory receptors. Muscle reflexes are highly modulated during locomotion in an adaptive manner within each phase of the step cycle. Furthermore, the modulation can be modified quickly for different tasks such as standing, walking and running, probably by changes in presynaptic inhibition. This modulation is often lost or severely reduced in patients with spasticity after spinal cord or head injury. In normal subjects cutaneous reflexes can be completely reversed from exciting to inhibiting a muscle during each step cycle, particularly in muscles that normally show two bursts of activity per cycle (e.g., tibialis anterior). In some patients stimulation of a mixed nerve (e.g., common peroneal) can directly produce muscle contraction, generate a reflex response (flexor reflex) and transiently reduce spasticity in antagonist (extensor) muscles. Thus, simple systems employing stimulation can enhance gait to a certain extent in patients with incomplete injuries.

Key words: Locomotion; Reflex; Spinal cord; Spasticity

Introduction

The basic spinal reflexes have been well studied over the last century, but new information continues to emerge concerning the manner in which they adapt the normal pattern of neural activity to varying environmental conditions and fail to adapt this activity in pathological states. This paper reviews some of the recent data and the implications for the replacement of motor function, for example by patterned electrical stimulation after spinal cord injury or stroke.

H-reflexes

The classical tendon jerk arises in large part from the monosynaptic connection of the muscle spindle afferents to the α motoneurons. The electrical analogue of this reflex, known as the H-reflex, can be studied by stimulating muscle nerves, such as the tibial nerve in the popliteal fossa, with surface electrodes (Fig. 1*A*). Movement of the stimulating electrodes may take place during walking for example, but a variety of stimulus levels can be applied. At each phase of the step cycle levels that stimulate approximately the same fraction of motor axons (monitored by the motor or M-wave in the muscle of interest) and so presumably stimulate an approximately constant fraction of muscle spindle afferents are chosen. Further details of the methods can be found elsewhere (Capaday and Stein, 1986).

Under conditions in which the M-wave (recorded over soleus muscle, an ankle extensor) is constant (Fig. 1*B*), a clear modulation of the H-reflex is observed (Fig. 1*C*), more or less in parallel with the activation of this muscle during the step cycle (Fig. 1*D*). Similar results have been found in this and other muscles during walking (Crenna and Frigo, 1987; Brooke et al., 1991; but see Dietz et al., 1990). A simple explanation for the parallel increase might

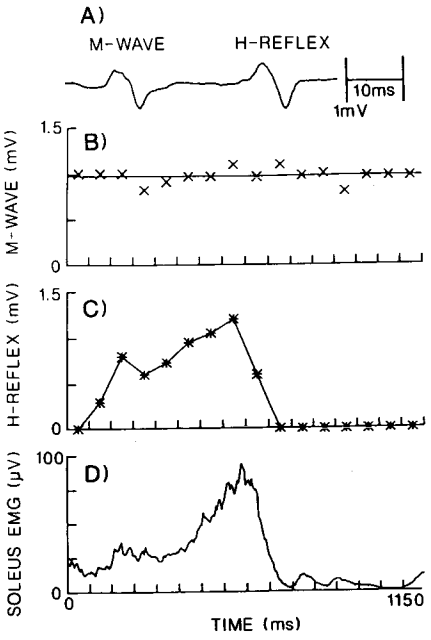

Fig. 1. A stimulus to the tibial nerve *(A)* produces two EMG responses in the soleus muscle, an M-wave from direct excitation of motor axons and an H-reflex from stimulation of the large Ia fibres from muscle spindles. These sensory fibres excite the α motoneurons and produce a reflex response, named after the neurologist Hoffmann who first described it. During walking, when the stimulus is such that the M-wave is fairly constant *(B)*, the H-reflex changes *(C)*, approximately in parallel with the EMG activity in the muscle *(D)*, which was measured after rectification and averaging a number of cycles. Each cycle began when the heel first touched the ground. From Stein and Capaday (1988).

be that more motoneurons are depolarized and hence able to fire later in the stance phase as a result of the stimulus. However, when the same levels of activity are generated tonically during standing, much larger responses are observed, particularly at low levels of activity. Furthermore, with an auditory cue to begin walking, the reflexes can be switched from those appropriate for standing to those appropriate for walking within a reaction time (Edamura et al., 1991). Marked differences are also seen between walking and running, even at a constant speed and/or EMG level (Edamura et al., 1991). These recent results suggest that reflexes can be modulated differently for the requirements of different behaviours, a phenomenon known as "task-dependent reflex modulation". Somewhat different patterns have also been observed during hopping, jumping and cycling (Boorman et al., 1989; Moritani et al., 1990; Dyhre-Poulsen et al., 1991). How many different types of reflex modulation can be observed in various common tasks remains to be seen.

Stretch reflexes

Electrical stimulation is an effective tool to probe central factors controlling reflexes but can not give a quantitative estimate of the muscle activity produced by a given amount of stretch. We therefore devised a method for stretching soleus and the other ankle extensor muscles at various times during the stance phase of locomotion (Yang et al., 1991a). During much of the stance phase the ankle extensors are being stretched, but a pneumatic system was able to provide an extra stretch of 3 – 5° at comparable

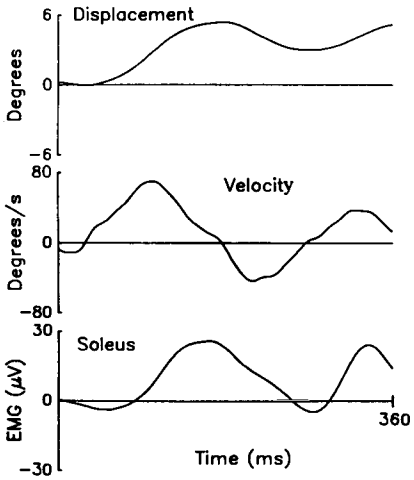

Fig. 2. The displacement and reflex EMG produced by a pneumatic device for flexing the ankle could be determined by comparing control and perturbed steps. By subtracting one from the other the displacement and velocity (obtained by numerical differentiation of the displacement) could be compared with the EMG produced. The EMG followed the velocity closely so that the latency and "reflex gain" of the reflex (as μV of EMG per velocity of stretch in deg/sec) could be estimated. From Yang et al. (1991a).

velocities to that observed during the normal step cycle (see Fig. 2).

The additional stretch induced an extra EMG, and the EMG was closely related in time and amplitude to the velocity of stretch applied. In particular, the EMG followed the time course of velocity with a mean delay of 38 msec in the seven subjects studied, a latency which would be expected for a monosynaptic reflex in human ankle extensor muscles. A measure of the reflex gain could also be obtained by fitting the extra EMG generated as a linear function of the velocity of the stretch (details in Yang et al., 1991a). The gain measured in this way

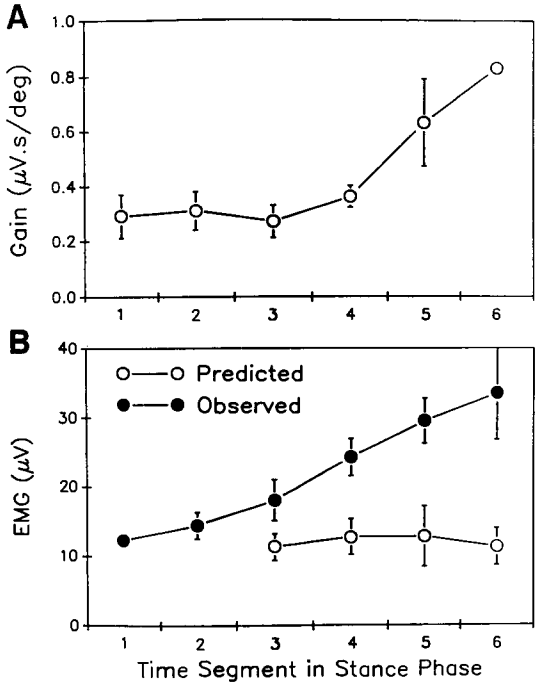

Fig. 3. The reflex gain (calculated as shown in Fig. 2) increases during the stance phase *(A)*. Multiplying this gain by the velocity of ankle dorsiflexion in undisturbed walking provides an estimate *(B)* for the contribution of a velocity-sensitive reflex to the activation of the soleus muscle (open circles) over the period of the stance phase when the muscle is being stretched. The whole step cycle was divided into 16 equal phases starting at heel strike (see Fig. 1) and the period of muscle stretch during stance typically included phases 3 – 6. The solid circles represent the soleus EMG amplitude associated with normal walking, averaged across seven subjects (±1 standard error). From Yang et al. (1991a).

increased steadily during the stance phase (Fig. 3*A*) in much the same way as the H-reflex (Fig. 1). This confirms that the H-reflex is a good measure of the short-latency stretch reflex changes taking place here.

During much of the stance phase of walking the soleus muscle is being stretched as the forward progression of the body flexes the ankle while the foot is flat on the ground. Knowing the velocity of the stretch at a given time and the gain in Fig. 3*A*, we can calculate the EMG (in μV) that would be produced by this velocity in deg/sec. The predicted value is shown as open circles in Fig. 3*B* for comparison with the observed values (closed circles). Note that a substantial part (30 – 60%) of the observed EMG can be accounted for by the stretch reflex. The velocities used in this study were comparable to those normally observed during walking, but the predictions make the assumption that the reflex is linear, which may not be justified (Aldridge and Stein, 1982).

Our results differ somewhat from those of Dietz et al. (1987) who found that the latencies of the responses in gastrocnemius muscle were much longer (65 – 85 msec). They did find earlier (presumably monosynaptic) responses in young children (Berger et al., 1985) and in patients with spastic hemiparesis (Dietz, 1987). However, Dietz' group applied the perturbations early in the stance phase when the reflex gain is low. Also, the perturbations were applied to the treadmill belt, rather than the ankle itself. Finally, the threshold for the monosynaptic stretch may be higher in gastrocnemius than in soleus muscle, which is a classic slow muscle with active stretch reflexes.

Cutaneous reflexes

An even more striking degree of modulation can be observed in reflexes elicited by stimulating nerves that contain wholly or mainly cutaneous afferents, such as the sural nerve or the tibial nerve at the ankle (Yang and Stein, 1990). In Fig. 4 two stimuli separated by 10 msec were applied to the tibial nerve at the ankle and the changes in the ongoing EMG in the

TA muscle were recorded. A complex response was observed consisting of excitation at early (E) middle (M) and later (L) latencies (Fig. 4*B*).

For more detailed examination the responses were averaged at 16 different phases in the step cycle (Fig. 4*A*). At phase 6 during stance, when this muscle was inactive, no reflex was observed. During much of swing (phase 10), when the TA muscle gives a burst of activity to flex the ankle, a strong excitation was observed at the middle latency. The TA muscle gives a second burst late during swing (phase 14), in preparation for heel contact to control the rapid extension of the ankle that would otherwise occur. At this time the middle latency response has changed from excitation to inhibition. A similar reflex reversal was also recorded from other muscles that similarly have two bursts of EMG activity during each step (Yang and Stein, 1990; Duysens et al., 1990). These publications also consider the functional significance of this interesting reflex reversal.

The early response was not observed with purely cutaneous nerves such as the sural nerve and may arise from muscle receptors, since the tibial nerve provides branches that innervate toe muscles. The origin of the latest response is also not known, but is of sufficient latency (> 100 msec) that it may well involve supraspinal connections. Interestingly, neither of these responses showed the reversal found at the middle latency.

Effects of injury

Spinal cord injury, head injury and stroke can all affect the modulation of reflexes described in previous sections. Even when an injury does not completely paralyse the limb, a frequent consequence is "spasticity" which involves exaggerated responses to muscle stretch. Maintained stretching of the ankle extensor muscles, for example, may lead to a continuing oscillation at 5 – 10 Hz which is referred to as "clonus". Fig. 5 shows results from a patient who had suffered a head injury five months earlier.

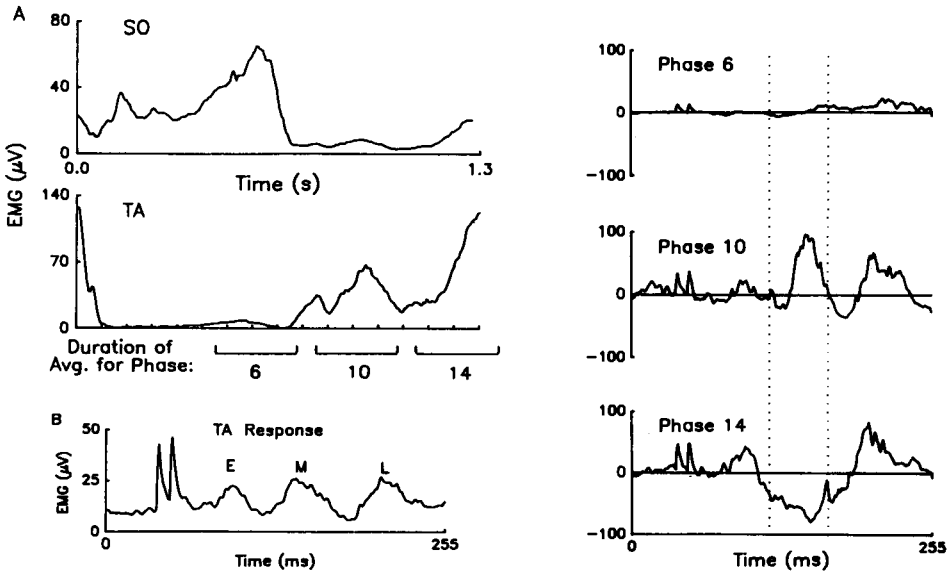

Fig. 4. In contrast to the soleus (SO) muscle, the tibialis anterior (TA) muscle has two bursts of EMG activity in a step cycle, which has been divided into 16 parts for further analysis *(A)*. The rectified and integrated EMG *(B)* produced by two stimuli to the tibial nerve (artifacts) shows an early (E), a middle (M) and a late (L) response. However, no reflex response occurred to stimuli while the TA was inactive during stance (phase 6). When the muscle was active during much of swing (phase 10) a large reflex was observed at the middle latency (after subtracting the EMG that occurred on control cycles). During the second burst (phase 14) an inhibition is observed at middle latencies, even though the excitations at earlier and later latencies were similar. Modified from Yang and Stein (1990).

He made a good recovery, but still had some spasticity and some problems which walking. With levels of stimulation that were comparable to those used in normal subjects much less modulation of the H-reflex was observed (Fig. 5*B*).

However, when the stimulus was lowered to the point that the M-wave was barely detectable, the H-reflex was modulated more normally. Thus, some of the normal reflex modulation during walking was preserved, although the reflex appeared to be so brisk that the response "saturated" with the stimulus levels we conventionally used. Other patients showed little modulation even at the lowest levels of stimulation tested, although the results were quite variable. In a population of 21 patients studied only five patients showed modulation less than 50% of the maximum H-wave value over the whole step cycle (Yang et al., 1991b). Another 11 patients showed modulation between stance and swing, but showed less than 50% modulation within the stance phase. Finally, five patients showed relatively normal modulation (> 50%) within the stance phase.

No significant correlation was observed between the speed at which these patients could walk and the reflex modulation they showed. A patient with very limited ability to walk might have a relatively normal reflex modulation, whereas one with better walking ability might have little reflex modulation. This suggests that different pathways control the alternating pattern of walking and the associated modulation of reflex pathways. Thus, they can be differentially affected in an incomplete spinal cord or head injury.

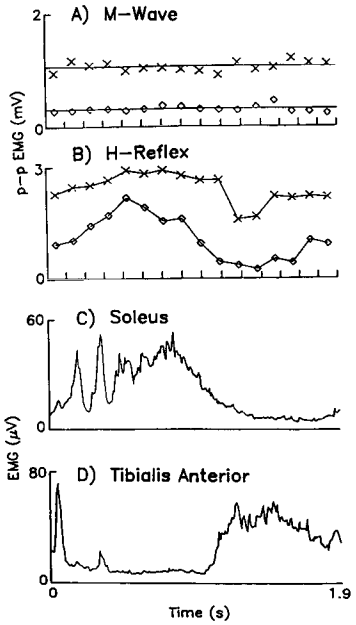

Fig. 5. Two levels of stimulation were used with a head injury patient. With a stimulus that produced about a 1 mV M-wave (× in part *A*) little modulation was seen in the H-reflex *(B)*. However, with a lower stimulus that produced a much smaller M-wave (◇) a clear modulation was observed. The abnormally large reflex may be responsible for the alternating bursts of activity in the soleus *(C)* and tibialis anterior *(D)* muscles shortly after heel contact (further details in the text and Fig. 6). From Stein et al. (1991).

Stretch reflexes and clonus

The large EMG bursts seen early in the step cycle of spastic hemiparetic subjects (e.g., Fig. 5) are consistent with our observations on the large reflexes and reduced modulation of H-reflexes in spastic subjects. Fig. 6 shows the averaged response of one sub-

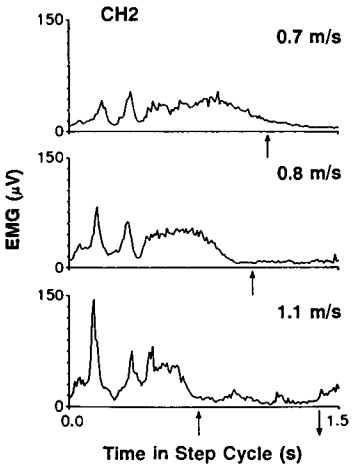

Fig. 6. The EMG bursts in the soleus muscle of the patient in Fig. 5 are velocity-sensitive. Their amplitude increased with increasing walking speeds (in m/sec). Arrows pointing up represent the end of the stance phase whereas the arrow pointing down represents the end of the step cycle in the bottom trace. The step cycle was > 1.5 sec at the two lower speeds. From Yang et al. (1991b).

ject walking at three different speeds on a treadmill. The onset of the traces coincides with heel strike. As soon as the foot is flat on the ground and the ankle begins to flex, a large peak in the soleus EMG is observed, presumably due to an abnormally large stretch reflex. Note that at higher speeds and hence higher velocities of stretch the response is much larger, consistent with the velocity sensitivity of the reflex described above. These responses will transiently slow forward progression; once the ankle flexion resumes a second response occurs. The periodicity of the responses is similar to the clonus observed by stretching these muscles by hand, and in some patients many bursts are observed even in averaged records (Yang et al., 1991b).

Cutaneous reflexes and walking

The effects of injury on the modulation of cutaneous reflexes have not yet been studied although cutaneous reflexes have long been used to replace motor function after injury or stroke. Lieberson et al. (1961) stimulated the common peroneal nerve in patients who were unable to flex the ankle sufficiently during gait to prevent it from dragging on the ground (foot drop). In fact, stimulation of the nerve has at least three actions. Firstly, the direct stimulation of motoneurons to ankle flexor muscles produces dorsiflexion to overcome foot drop, as mentioned above. Secondly, higher levels of stimulation produce a withdrawal reflex that generates flexion at other joints (hip and knee). Note that the flexor or withdrawal reflex only occurs at levels that would be noxious to a person with intact sensation. However, such levels can be routinely used in persons who have lost much or all sensation as a result, for example, of spinal cord injury. The reversal of cutaneous reflexes in a single muscle, described above, only occurs at lower levels of stimulation, although modulation of reflexes still persists with stronger stimuli (Bélanger and Patla, 1984; Crenna and Frigo, 1984).

Finally, the stimulation may transiently block extensor spasticity. Results are shown for one patient in Fig. 7. The common peroneal nerve was stimulated for 1 sec at a level used by this patient to assist locomotion. The H-reflex to soleus muscle was measured at various times relative to the stimulation. A decline in the H-reflex is observed over several hundred milliseconds and it gradually recovers after the period of stimulation with a similar time course.

Note that the common method of treating spasticity is with Baclofen, a drug which is an agonist of the transmitter γ-amino butyric acid (GABA). It acts at

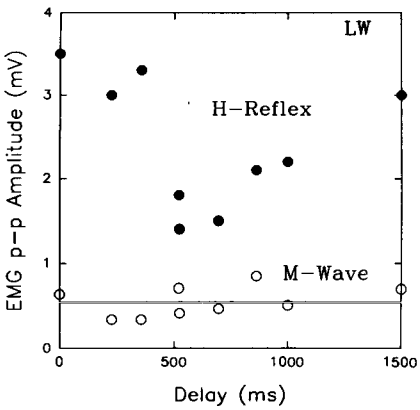

Fig. 7. Time course in the H-reflex (filled circles) before, during and after a 1 sec period of stimulation to the common peroneal nerve at the rate (20 Hz) and amplitude used by this spinal cord-injured patient to generate a step. The M-wave (open circles) remained virtually constant throughout.

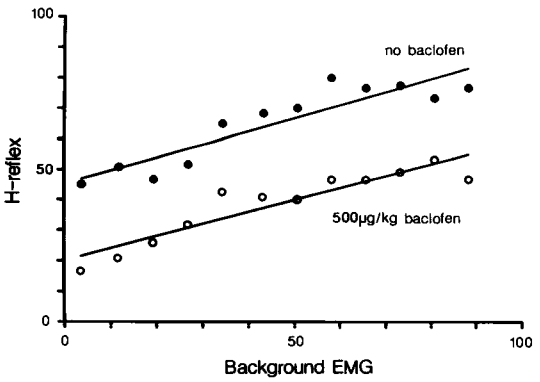

Fig. 8. Effect of the GABA agonist Baclofen on H-reflexes in the soleus muscle of a decerebrate cat. Different levels of EMG activity were generated by stimulating the contralateral common peroneal nerve to elicit a crossed extensor reflex before and after systemical application of the drug at the dose indicated. EMG and reflexes are in arbitrary units.

the $GABA_B$ receptor subtype which is involved in presynaptic inhibition in the spinal cord (Peng and Frank, 1989). Application of Baclofen in a decerebrate cat (Fig. 8) decreases the H-reflex at all levels of EMG activity in the soleus muscle. EMG activity was produced in this preparation by stimulation of the contralateral common peroneal nerve to generate a crossed extensor reflex. Thus, this drug can reduce H-reflexes tonically, but will not of course produce the precise reflex modulation within a step described in earlier sections. Cutaneous stimulation is also well known to produce presynaptic inhibition lasting for 100 – 200 msec (Eccles, 1964) and is presumably responsible, at least in part, for the decline in the H-reflex shown in Fig. 7. Thus, electrical stimulation has the potential to restore reflex modulation, as well as generating muscle contractions in these patients.

Improvement of walking by electrical stimulation

Recently, we have examined a number of patients with incomplete spinal cord injury. All patients could stand but walking was either not possible or was greatly slowed. Fig. 9 shows the effect of stimulating the common peroneal nerve to elicit or augment the swing phase of the step cycle in these patients. With stimulation all could walk, including four patients who were totally unable to do so without stimulation. The gain in speed (4 – 5 m/min) was small and independent of the speed they could produce in the absence of stimulation. This extra speed was obviously most important to those who could not walk at all or only at the very slowest speeds in the absence of stimulation. They tended to be the patients who used the system of stimulation on a regular basis at home.

Why did the stimulation not produce a greater increase in speed? To answer this question we examined the pattern of walking as a function of the duration of the step cycle, as shown in Fig. 10. Although the swing phase was somewhat longer in the patients who walked more slowly, the range (2 – 3 times) was much less than the range in the time to complete a step (more than 10 times). As a result the swing phase, plotted as a percentage of the step cycle, declines from the value of about 40% seen in normal individuals (Winter, 1987) to about 10% in the slowest subjects. Clearly, to make substantial improvements the stance phase, not the swing phase, must be shortened in these patients. Other muscles must be stimulated to produce forward momentum of the body over the limb (e.g., Marsolais and Kobetic, 1987), as well as nerves to modulate reflexes phasically, but the best way to restore functional gait in these patients remains a challenge for the future.

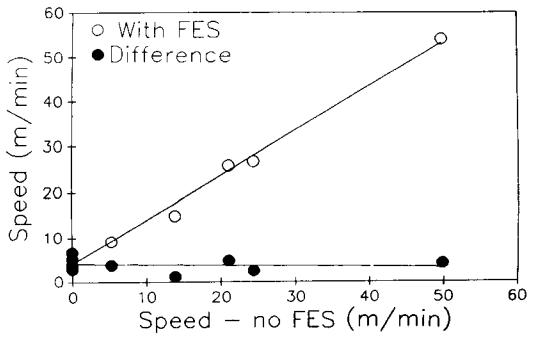

Fig. 9. Effect of stimulation of the common peroneal nerve in a group of patients with incomplete spinal cord injuries on the speed of walking. Note that some patients were unable to walk at all without stimulation (0 m/min) but could walk at 4 – 5 m/min with stimulation. Others could walk at various speeds without stimulation and increased their speed by about the same amount.

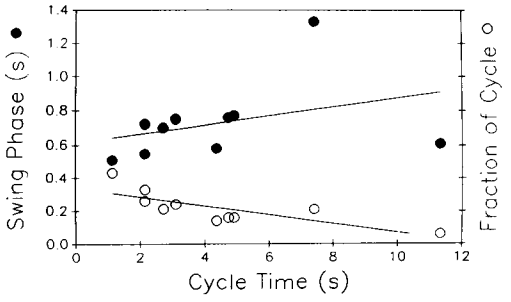

Fig. 10. The duration of the swing phase is plotted as a function of the average time of one step cycle for the same group of patients as in Fig. 9. The fraction of the step cycle occupied by the swing phase is also plotted and this declines from the normal value of 0.4 to a value close to 0.1 for the slowest patients.

Acknowledgements

The original research described in this paper was supported by a grant from the Medical Research Council of Canada. Dr. Bélanger was a fellow of the FRSQ (Québec).

References

Aldridge, J.W. and Stein, R.B. (1982) Nonlinear properties of the stretch reflex studied in the decerebrate cat. *J. Neurophysiol.*, 47: 179 – 192.

Bélanger, M. and Patla, A.E. (1984) Corrective responses to perturbation applied during walking in humans. *Neurosci. Lett.*, 49: 291 – 295.

Berger, W., Quintern, J. and Dietz, V. (1985) Stance and gait perturbations in children: developmental aspects of compensatory mechanisms. *Electroenceph. Clin. Neurophysiol.*, 61: 385 – 395.

Boorman, G.I., Becker, W.J. and Lee, R.G. (1989) Modulation of the H-reflex during stationary cycling in normal humans and patients with spinal spasticity. *Soc. Neurosci. Abstr.*, 15: 691.

Brooke, J.D., Collins, D.F., Boucher, S. and McIlroy, W.E. (1991) Modulation of human short latency reflexes between standing and walking. *Brain Res.*, 548: 172 – 178.

Capaday, C. and Stein, R.B. (1986) Amplitude modulation of the soleus H-reflex in the human during walking and standing. *J. Neurosci.*, 6: 1308 – 1313.

Crenna, P. and Frigo, C. (1984) Evidence of phase-dependent nociceptive reflexes during locomotion in man. *Exp. Neurol.*, 85: 336 – 345.

Crenna, P. and Frigo, C. (1987) Excitability of the soleus H-reflex arc during walking and stepping in man. *Exp. Brain Res.*, 66: 49 – 60.

Dietz, V. (1987) Role of peripheral afferents and spinal reflexes in normal and impaired human locomotion. *Rev. Neurol. (Paris)*, 4: 241 – 254.

Dietz, V., Quintern, J. and Sillem, M. (1987) Stumbling reactions in man: significance of proprioceptive and preprogrammed mechanisms. *J. Physiol. (Lond.)*, 386: 149 – 163.

Dietz, V., Faist, M. and Pierrot-Deseilligny, E. (1990) Amplitude modulation of the quadriceps H-reflex in the human during the early stance phase of gait. *Exp. Brain Res.*, 79: 221 – 224.

Duysens, J., Trippel, M., Horstmann, G.A. and Dietz, V. (1990) Gating and reversal of reflexes in ankle muscles during human walking. *Exp. Brain Res.*, 82: 351 – 358.

Dyhre-Poulsen, P., Simonsen, E.B. and Voigt, M. (1991) Dynamic control of muscle stiffness and H reflex modulation during hopping and jumping in man. *J. Physiol. (Lond.)*, 437: 287 – 304.

Eccles, J.C. (1964) *The Physiology of Synapses*, Springer, Berlin.

Edamura, M., Yang, J.F. and Stein, R.B. (1991) Factors that determine the magnitude and time course of human H-reflexes in locomotion. *J. Neurosci.*, 11: 420 – 427.

Lieberson, W., Holmquest, H.J., Scott, D. and Dow, A. (1961) Functional electrotherapy stimulation of the peroneal nerve synchronized with the swing phase of the gait of hemiplegic patients. *Arch. Phys. Med.*, 42: 101 – 105.

Marsolais, E.B. and Kobetic, R. (1987) Functional electrical stimulation for walking in paraplegia. *J. Bone Joint Surg.*, 69A: 728 – 733.

Moritani, T., Oddsson, L. and Thorstensson, A. (1990) Differences in modulation of the gastrocnemius and soleus H reflexes during hopping in man. *Acta Physiol. Scand.*, 138: 575 – 576.

Peng, Y. and Frank, E. (1989) Activation of $GABA_B$ receptors causes presynaptic inhibition at synapses between muscles spindle afferents and motoneurons in the spinal cord of bullfrogs. *J. Neurosci.*, 9: 1502 – 1515.

Stein, R.B. and Capaday, C. (1988) The modulation of human reflexes during functional motor tasks. *Trends Neurosci.*, 11: 328 – 332.

Stein, R.B., Yang, J.F., Edamura, M. and Capaday, C. (1991) Reflex modulation during normal and pathological human locomotion. In: M. Shimamura (Ed.), *The Neurobiological Basis of Human Locomotion*, Japan Scientific Societies Press and Springer Verlag, Tokyo and Berlin, pp. 335 – 346.

Winter, D.A. (1987) *The Biomechanics and Motor Control of Human Gait*, University of Waterloo Press, Waterloo, Canada.

Yang, J.F. and Stein, R.B. (1990) Phase-dependent reflex reversal in human leg muscles during walking. *J. Neurophysiol.*, 63: 1109 – 1117.

Yang, J.F., Stein, R.B. and James, K.B. (1991a) Contribution of peripheral afferents to the activation of the soleus muscle during walking in humans. *Exp. Brain Res.*, 87: 679 – 687.

Yang, J.F., Fung, J., Edamura, M., Blunt, R., Stein, R.B. and Barbeau, H. (1991b) H-reflex modulation during walking in spastic paretic subjects. *Can. J. Neurol. Sci.*, 18: 443 – 452.

J.H.J. Allum, D.J. Allum-Mecklenburg, F.P. Harris and R. Probst
Progress in Brain Research, Vol. 97

Overview and critique of Chapters 19 – 23

R.B. Stein

University of Alberta, Edmonton, Canada

Throughout the papers on the topic of vestibular control of posture, a consistent theme can be discerned, namely the importance of geometrical aspects in the vestibular control of posture. This may not be surprising since the vestibular system has long been known to be organized to obtain information about the movement of the head in several dimensions, as well as its relation to the vertical (gravity vector). This information must be transformed to signals appropriate for the control of body posture, but the nature of this transform has only attracted much attention in the last decade. Geometric aspects have also featured prominently in recent work on the motor cortex (e.g., Georgopoulos, 1991), the spinal cord (e.g., Bizzi et al., 1991) and eye movements (e.g., Hepp et al., 1988). Indeed, since organisms function in a world of geometric objects, our movements must be matched to these objects. However, it is only in recent years that the understanding of the neural substrate has advanced sufficiently and the computational power has become available to test these ideas rigorously.

The neck muscles are particularly complex (e.g., Abrahams and Richmond, 1988), but clearly vital to the task of linking head position to body posture. The paper by Shinoda et al. describes the linkage between ampullary nerves and four of the more than 30 neck muscles. The pattern of excitatory and inhibitory connections recorded intracellularly from motoneurons is more complex than previously thought. Nonetheless, some straightforward rules are presented in the discussion of this study, both about the pattern of synaptic events and the responses to external perturbations.

Wilson is more concerned with the relative contribution of vestibulospinal and reticulospinal tracts as substrates for vestibulospinal reflexes. He points out the importance of reticulospinal neurons in vertical vestibulocollic reflexes, as compared to the reflexes in the horizontal plane. One of the interesting facts to emerge is the distributed nature of the processing, involving the vestibular organs, pontomedullary reticulospinal neurons and the convergence of inputs within the neck itself.

Macpherson and Inglis approach the problem of postural control from the opposite viewpoint, because postural mechanisms have been studied in Macpherson's laboratory for a number of years in intact cats. The platform on which the cats stand can be perturbed in eight different directions and the response characterized in terms of the force vector and EMG pattern. After bilateral labyrinthectomy, the animals changed their standing pattern somewhat for several days, but were able to respond appropriately, although overreacting to horizontal displacements. Thus, they conclude that vestibular information is not required for the selection or the triggering of appropriate postural responses to translation, a conclusion that will no doubt be questioned and re-examined in the years to come.

Vidal and colleagues have also studied postural control in the whole animal after centrifugation, the parameters of which can apparently be adjusted to selectively lesion parts of the guinea-pig vestibular system. They note that the cervical vertical column of many animals is normally oriented so that the

utricular macula is brought approximately into the horizontal plane with respect to the earth's gravitational field. Also, the range of motion in the head-neck system is sufficiently constrained to limit the number of degrees of freedom and simplify the computational problem of gaze stabilization, for example. The nervous system doesn't have to control separately all the 30 plus muscles of the neck mentioned above! Indeed, they suggest that the behavioral deficits they observe are consistent with the projection pattern of monosynaptic contacts from second-order vestibular neurons to the spinal cord. This raises the question, as yet unanswered, of whether the later, polysynaptic potentials recorded by Shinoda et al. are of functional significance.

The final paper in this set by Pellionisz and Ramos describes theoretical attempts to model the geometrical transformations necessary to convert neural signals observed in the vestibular system to those produced for control of posture. The idea is that the complex transformation from a covariant to a contravariant representation according to the "tensor theory" of Pellionisz can be carried out by neural nets, although these nets will not be of the back-propagation variety popularized by Hopfield (1982) and utilized for a variety of purposes in the last decade. The need for theoretical work sufficiently sophisticated to be able to cope with the immense volume of experimental data is impossible to deny. The final form of this synthesis remains elusive, but this series of papers provides a good overview of the current "state of the art".

References

Abrahams, V.C and Richmond, F.J. (1988) Specialization of sensorimotor organization in the neck muscle system. *Prog. Brain Res.*, 76: 125 – 135.

Bizzi, E., Mussa-Ivaldi, A. and Giszter, S. (1991) Computations underlying the execution of movement: a biological perspective. *Science,* 253: 287 – 291.

Georgopoulos, A.P. (1991) Higher order motor control. *Annu. Rev. Neurosci.*, 14: 361 – 377.

Hepp, K., Vilis, T. and Henn, V. (1988) On the generation of rapid eye movements in three dimensions. *Ann. N.Y. Acad. Sci.*, 545: 140 – 153.

Hopfield, J. (1982) Neuronal networks and physical systems with emergent collective computational abilities. *Proc. Natl. Acad. Sci. U.S.A.*, 79: 2554 – 2558.

J.H.J. Allum, D.J. Allum-Mecklenburg, F.P. Harris and R. Probst
Progress in Brain Research, Vol. 97

CHAPTER 19

Synaptic organization of the vestibulo-collic pathways from six semicircular canals to motoneurons of different neck muscles

Y. Shinoda, Y. Sugiuchi, T. Futami, N. Ando, T. Kawasaki and J. Yagi

Department of Physiology, School of Medicine, Tokyo Medical and Dental University, 1-5-45, Bunkyo-ku, Yshima, Tokyo, Japan

The pattern of inputs from six semicircular canals to neck motoneurons was investigated by stimulating six ampullary nerves electrically and recording intracellular potentials from motoneurons of the rectus capitis dorsalis (RD), the complexus (COMP) and the obliquus capitis caudalis (OCA) muscles at the upper cervical cord of the cat. RD and COMP motoneurons received disynaptic excitation from bilateral anterior and contralateral horizontal ampullary nerves and disynaptic inhibition from bilateral posterior and ipsilateral horizontal ampullary nerves. OCA motoneurons received excitation from ipsilateral vertical and contralateral horizontal ampullary nerves and inhibition from contralateral vertical and ipsilateral horizontal ampullary nerves. Ipsilateral disynaptic inhibitory postsynaptic potentials and contralateral disynaptic excitatory postsynaptic potentials to these motoneurons were mediated by the medial longitudinal fasciculus (MLF) and the other postsynaptic potentials by the extra-MLF pathways. The results indicated that motoneurons of a neck muscle have its own characteristic pattern of inputs from six semicircular canals.

Key words: Semicircular canal; Vestibular nucleus; Vestibulospinal neuron; Spinal cord; Motoneuron; Neck; Medial longitudinal fasciculus

Introduction

Stimulation of individual semicircular canals produces canal-specific neck movements (Suzuki and Cohen, 1964). The pattern of connections between different semicircular canals and dorsal neck muscle motoneurons was first investigated by Wilson and Maeda (1974). Their results have shown that dorsal neck motoneurons receive excitation from bilateral anterior and contralateral horizontal canals and inhibition from bilateral posterior and contralateral horizontal canals. It has been assumed that this organized pattern of short-latency postsynaptic potentials (PSPs) is seen for all dorsal neck motoneurons (Wilson and Melvill-Jones, 1979). However, there are more than 30 neck muscles and they should be controlled in a proper spatial combination to induce compensatory head movements in stimulated planes (Ezure and Sasaki, 1978; Schor and Miller, 1981; Baker et al., 1985). Therefore, there must be more than one pattern of connections between six semicircular canals and motoneurons of different neck muscles.

In the following we will summarize the pattern of connections and the pathways between six semicircular canals and motoneurons of three neck muscles at the upper cervical cord in the cat (Sugiuchi et al., 1992a). The experiments were performed in anesthetized cats by analyzing intracellular potentials in motoneurons evoked by electrical stimulation of the ampullary nerves. The results show that there is more than one pattern of connections between six

semicircular canals and dorsal neck motoneurons. Each muscle has its own characteristic pattern of input from six semicircular canals.

Methods

Experiments were performed on ten cats anesthetized with ketamine hydrochloride (Kyowahakko, Tokyo, Japan, 25 mg/kg, i.m.) followed by intravenous injection of α-chloralose (Wakojunyaku, Osaka, Japan, 50 mg/kg). In order to stimulate ampullary nerves, bipolar stimulating electrodes (two fine stainless steel wires glued together) were implanted near the ampullary nerves through small holes made in bony canals as described by Suzuki et al. (1969). The stimulating electrodes were implanted on six ampullary nerves in both labyrinths in each experiment. Final electrode positions were determined by monitoring characteristic eye movements elicited by stimulation of individual ampullary nerves with trains of 35 pulses of 0.2 msec duration at an interval of 2.0 msec from a constant current generator. Thresholds of eye movements were usually 5 – 25 μA and patterns of eye movements generally remained unchanged with three-fold increases in stimulating currents. Muscle nerves to three neck muscles, the complexus (COMP), the obliquus capitis caudalis (OCA), and the rectus capitis dorsalis (RD) muscles at C1 (Sugiuchi and Shinoda, 1992), were dissected for stimulation. Dorsal laminectomy was made at C1 and C2 to record intracellular potentials from neck motoneurons. After implantation of the stimulating electrodes for the ampullary nerves, the animals were immobilized and artificially ventilated. Glass microelectrodes were filled with 3 M KCl and had a resistance of 8 – 15 megohms. Depolarizing or hyperpolarizing currents were passed through the recording electrode to check excitatory postsynaptic potentials (EPSPs) and inhibitory postsynaptic potentials (IPSPs).

In some experiments, lesions were made in the medial longitudinal fasciculus (MLF) to determine the pathways in the brain-stem from the vestibular nuclei to neck motoneurons. The MLF was cut at the level of the obex with a fine blade under visual observation. Lesions were reconstructed histologically on the serial sections of the brain-stem. After each experiment, the positions of the implanted electrodes were examined in relation to target ampullary nerves with an operating microscope.

Results

Properties of postsynaptic potentials elicited by vestibular-nerve stimulation

We recorded from 85 neck motoneurons whose resting potentials generally ranged from −40 to −85 mV. Vestibular inputs from the ipsi- and contralateral side were examined by stimulating the whole vestibular nerves, while recording intracellular potentials from motoneurons of each muscle (Fig. 1). In a COMP motoneuron, large depolarization was evoked from the contralateral side and depolarization followed by hyperpolarization from the ipsilateral side, whereas in an RD and an OCA motoneuron, depolarization followed by hyperpolarization was evoked from the contralateral side and depolarization from the ipsilateral side. As in this example, PSPs induced by stimulation of either the contra- or ipsilateral whole vestibular nerves had complex but characteristic patterns in motoneurons of individual neck muscles. This result suggests that there may be more than one input pattern from six semicircular canals to motoneurons of different neck muscles, or that input strengths from individual semicircular canals are different in motoneurons of different muscles in spite of the same input pattern.

Stimulation of individual ampullary nerves evoked EPSPs and IPSPs in all motoneurons examined (Figs. 2 – 4). The PSPs evoked from a single canal nerve were either depolarization or hyperpolarization, and a depolarization-hyperpolarization sequence evoked by whole vestibular-nerve stimulation was not observed near thresholds. The shape of the PSPs was very simple near threshold, and later peaks with the same polarity appeared with an increase of stimulus intensity. When stimulus intensities were increased to 3 – 4 times

threshold for the PSPs, a depolarization-hyperpolarization sequence was sometimes induced. This was probably due to current spread to adjacent ampullary nerves or otolith nerves. Thresholds of the EPSPs and IPSPs were less than 50 μA, usually 20 – 30 μA. The latency of the EPSPs ranged from 1.1 to 2.8 msec (n = 208) and that of the IPSPs from 1.2 to 3.0 msec (n = 215). Since the latency of intra-axonal spikes recorded from vestibulo-spinal axons at C1 ranged from 0.8 to 1.6 msec (n = 53), most of these earliest PSPs evoked in neck motoneurons were regarded as disynaptic from the primary afferents (Akaike et al., 1973; Shinoda et al., 1988a,b, 1990; Sugiuchi et al., 1992a), but the later PSPs were considered to be trisynaptic. The amplitude of disynaptic EPSPs and IPSPs was 300 μV to 2.5 mV. The amplitude of the peak depolarization ranged from 500 μV to 8 mV and sometimes was large enough to induce action potentials.

Pattern of postsynaptic potentials evoked from six ampullary nerves

(1) Rectus capitis dorsalis motoneurons. The typical pattern of inputs elicited by stimulation of six ampullary nerves in an RD motoneuron is shown in Fig. 2. Stimulation of either the ipsi- or the contralateral anterior ampullary nerve produced EPSPs and stimulation of the posterior ampullary nerve on either side produced IPSPs. Stimulation of the ipsi- and contralateral horizontal ampullary nerves produced IPSPs and EPSPs, respectively. This typical response pattern to separate stimulation of six ampullary nerves was observed in a majority of the RD motoneurons examined. In some RD motoneurons, however, inputs from one or two ampullary nerves were lacking. This lack of input was not due to improper implantation of stimulating electrodes, since large PSPs could be evoked in other motoneurons at lower stimulus intensities in the same preparations.

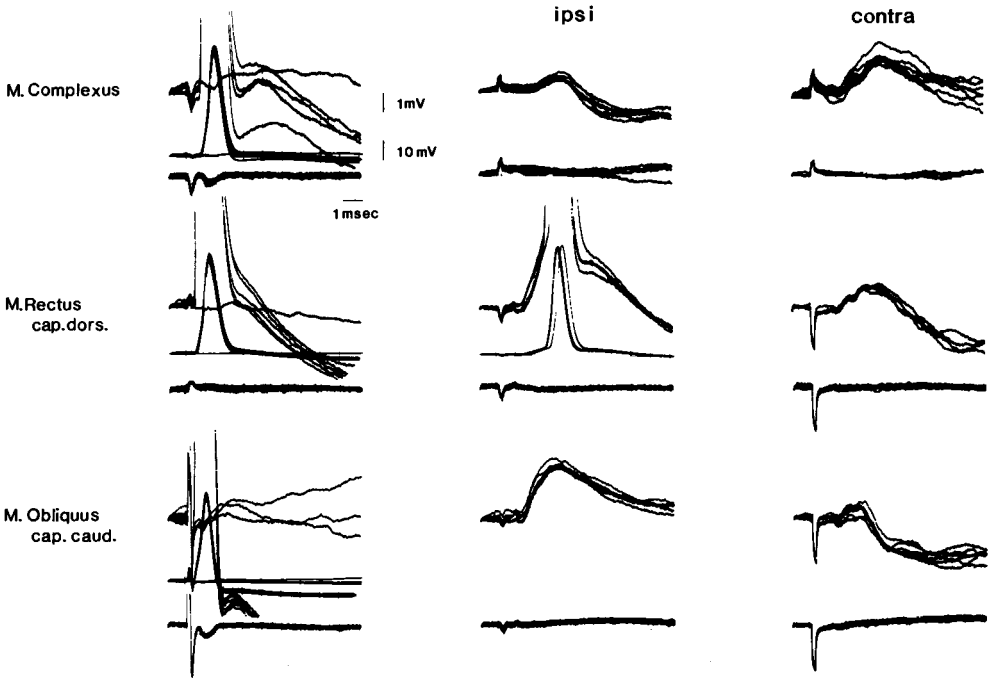

Fig. 1. Vestibular inputs to different neck motoneurons from the ipsilateral and contralateral sides. Left column: identification of neck motoneurons by antidromic activation. Middle and right columns: postsynaptic potentials recorded in the motoneurons following stimulation of the whole vestibular nerve on the ipsilateral (middle column) and contralateral side (right column).

(2) Complexus motoneurons. The typical pattern of inputs to a COMP motoneuron is shown in Fig. 3. Stimulation of the anterior ampullary nerve on either side and the horizontal ampullary nerve on the contralateral side produced disynaptic EPSPs, whereas stimulation of the posterior ampullary nerve on either side and the horizontal ampullary nerve on the ipsilateral side produced disynaptic IPSPs. This input pattern from six semicircular canals was observed in a majority of the COMP motoneurons examined at C1.

(3) Obliquus capitis caudalis motoneurons. The typical input pattern from six semicircular canals to an OCA motoneuron is illustrated in Fig. 4. Stimulation of either the ipsilateral anterior or posterior ampullary nerve produced EPSPs, whereas stimulation of either the contralateral anterior or posterior ampullary nerve produced IPSPs. Stimulation of the contra- and ipsilateral horizontal ampullary nerves produced EPSPs and IPSPs, respectively. This typical pattern was most consistently found in OCA motoneurons at C1.

Evaluation of stimulus spread within the labyrinth

In the results described above, most motoneurons of individual neck muscles had their own typical input pattern from six semicircular canals. The input pattern recorded in motoneurons of a particular muscle by stimulation of six ampullary nerves was consistent from one experiment to another. This evidence provides support for reliability of our implantation technique. There was, however, atypical input from one or two ampullary nerves in some motoneurons for individual muscles. Thus, it was essential to ascertain that the typical pattern was not contaminated by stimulus spread to other nerves in the labyrinth and to determine the origin of the atypical

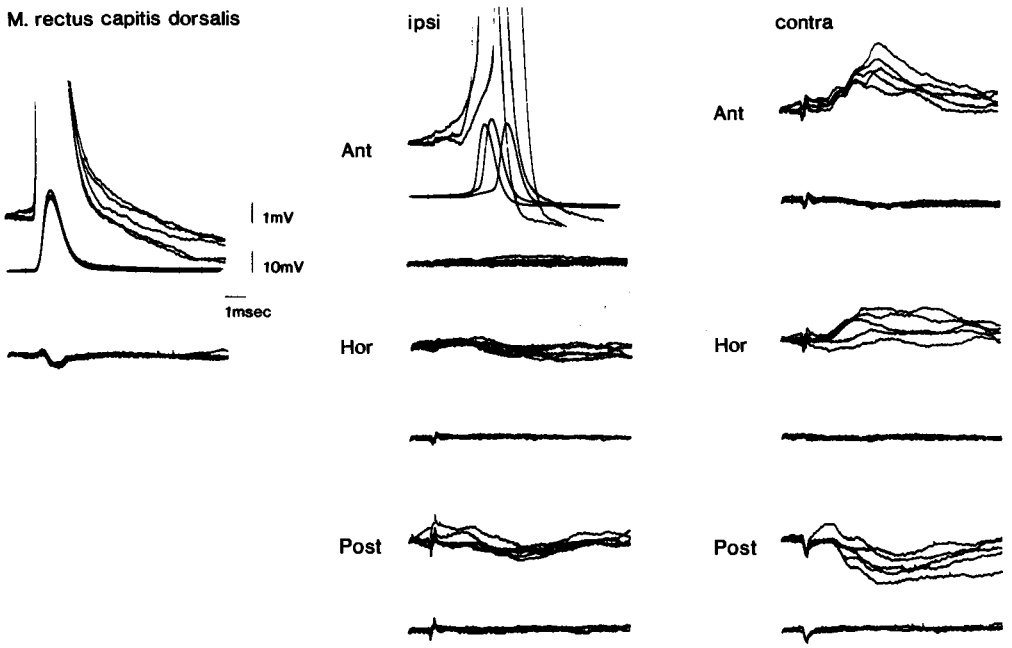

Fig. 2. Typical pattern of inputs from six semicircular canals in an RD motoneuron. Left: antidromic potentials evoked by stimulation of the RD muscle nerve. Middle: postsynaptic potentials evoked by stimulation of the ipsilateral anterior (Ant), horizontal (Hor) and posterior (Post) ampullary nerves. Right: postsynaptic potentials evoked by stimulation of the contralateral anterior, horizontal and posterior ampullary nerves. The upper traces indicate intracellular potentials and the lower traces juxtacellular field potentials in each panel. Upward deflection indicates positivity.

input. Stimulation of each ampullary nerve produces a characteristic eye movement, and stimulus spread to nearby ampullary nerves can be detected by change in the direction of eye movements (Suzuki and Cohen, 1964). At the beginning of the experiments, this condition was always satisfied, but a change in stimulus conditions may have taken place during the experiments. This possibility, however, was negligible. If this change had taken place, the response pattern of motoneurons of a particular muscle to stimulation of six ampullary nerves should have changed systematically in the middle of the experiments. The possible current spread to adjacent vestibular nerves (Kasahara and Uchino, 1974; Wilson et al., 1977) was extensively examined and that possibility was excluded in this series of the experiments. Implanted electrode tip positions in the semicircular canals were carefully checked under a microscope after each experiment and microscopic observation confirmed the proper placements of the stimulating electrodes on the target ampullary nerves, when the typical effects were elicited at low-stimulus intensities.

Pathways from six ampullary nerves to neck motoneurons

To determine the central pathways linking six semicircular canals and neck motoneurons, a lesion was made in the MLF at the medulla and the effect of ampullary nerve stimulation was compared before and after the lesion. Fig. 5 shows the effect of the MLF lesion on the PSPs evoked from six ampullary nerves in COMP motoneurons at C1. Before a lesion, COMP motoneurons usually received disynaptic EPSPs from the bilateral anterior and contralateral horizontal ampullary nerves and disynaptic IPSPs from the ipsilateral horizontal and the bilateral posterior ampullary nerves. After a lesion

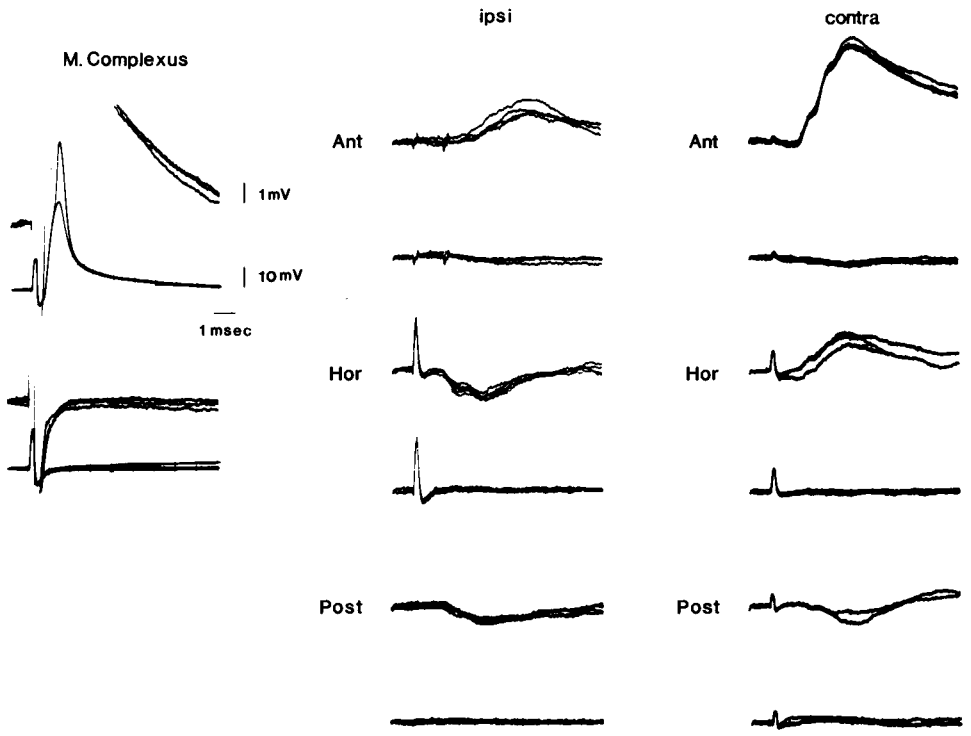

Fig. 3. Typical pattern of inputs from six semicircular canals to a COMP motoneuron at C1. The arrangement of the records and abbreviations are the same as in Fig. 2.

in the MLF ipsilateral to the recording site, the disynaptic IPSPs evoked from the ipsilateral horizontal and posterior ampullary nerves completely disappeared, whereas the EPSPs evoked from the ipsilateral anterior ampullary nerve remained unaffected (Fig. 5*B*). The disynaptic PSPs evoked from three contralateral ampullary nerve disappeared after MLF sectioning (Fig. 5*C*). The lesion in the MLF contralateral to the recording site had no effect on these evoked responses. In some COMP motoneurons (Fig. 5), the longer-latency EPSPs were evoked from the contralateral anterior ampullary nerve after MLF sectioning, suggesting that this remaining connection was more than disynaptic and via the extra-MLF pathway. Usually, the disynaptic PSPs evoked from the three contralateral ampullary nerves were completely abolished in COMP motoneurons after the ipsilateral MLF sectioning, but in some COMP motoneurons, trisynaptic IPSPs evoked from the contralateral posterior ampullary nerve did not disappear.

Similar lesion experiments were performed to determine the pathways from six semicircular canals to RD and OCA motoneurons. In RD motoneurons, interruption of the MLF abolished disynaptic EPSPs and IPSPs evoked from the contralateral ampullary nerves and also disynaptic IPSPs from the ipsilateral horizontal and posterior ampullary nerves, but did not affect disynaptic EPSPs from the ipsilateral anterior ampullary nerve. Therefore, this result indicates that the pathways to RD motoneurons are the same as those to COMP motoneurons. In OCA motoneurons, section of the MLF abolished disynaptic EPSPs evoked from the contralateral horizontal ampullary nerve and disynaptic IPSPs evoked from the contralateral posterior and ipsilateral horizontal ampullary nerves, but did not affect disynaptic EPSPs evoked from the ip-

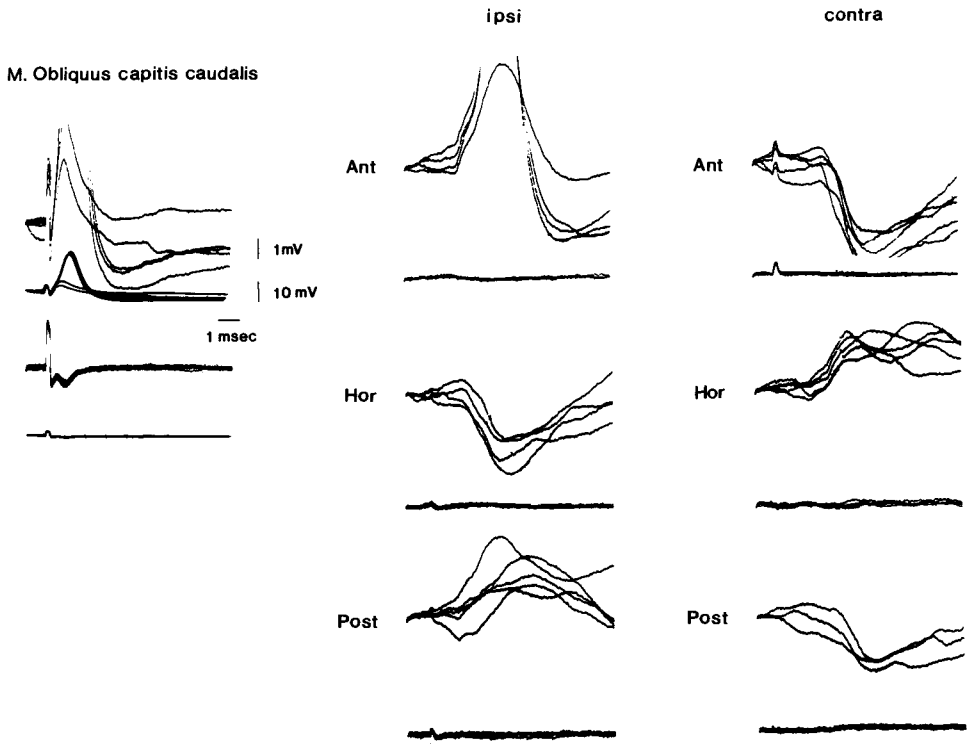

Fig. 4. Typical pattern of inputs from six semicircular canals to an OCA motoneuron at C1.

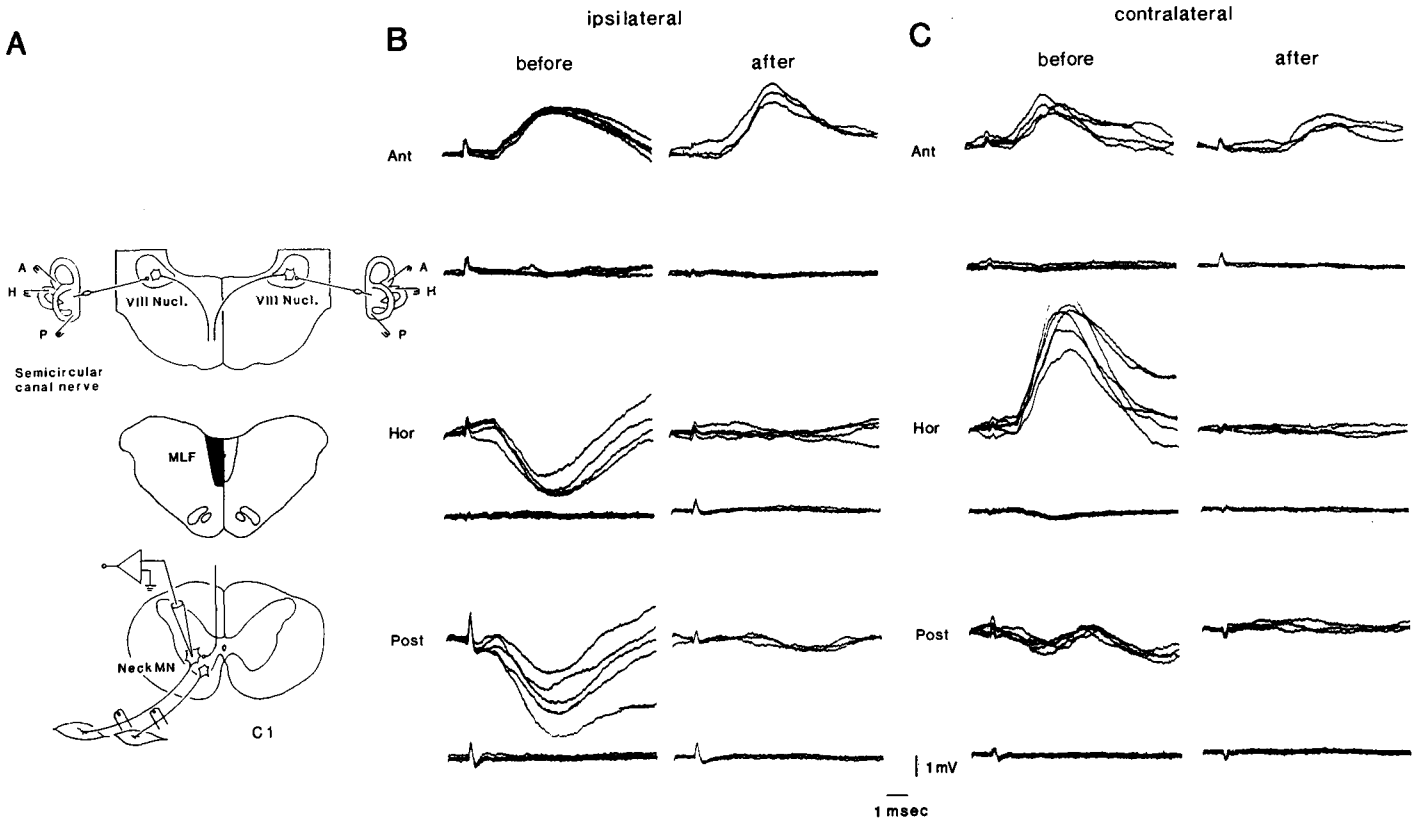

Fig. 5. Effect of sectioning the MLF on postsynaptic potentials evoked from six semicircular canals in COMP motoneurons. The lesion was made in the MLF ipsilateral to the motoneurons at the level of the obex (*A*). *B*. Records before (left column) and after the lesion (right column), showing typical PSPs evoked by stimulation of the three ipsilateral ampullary nerves. *C*. Postsynaptic potentials evoked from the contralateral ampullary nerves before and after the lesion.

silateral anterior and posterior ampullary nerves. Trisynaptic IPSPs evoked from the contralateral anterior and posterior ampullary nerves remained after sectioning the MLF.

Discussion

The present study demonstrated the existence of multiple patterns of input from six semicircular canals to motoneurons of different neck muscles. Motoneurons of each neck muscle had its own characteristic input pattern. One of the general rules of innervation is that neck motoneurons usually receive disynaptic excitatory and inhibitory inputs from all six semicircular canals, although the strength of input from each canal is different. This disynaptic connection supports the morphological findings that secondary vestibulo-spinal axons make direct contact with neck motoneurons (Shinoda et al., 1986, 1988a,b, 1990, 1992a,b). Wilson and Maeda (1974) suggested that a dorsal ramus motoneuron may be influenced by as many as six ampullae. The present study provides the evidence, based on a large number of samples, that virtually all motoneurons of different dorsal neck muscles examined are influenced by six semicircular canals. The pattern of connections between six semicircular canals and motoneurons is very characteristic of each dorsal neck muscle. In RD and COMP motoneurons at C1, stimulation of bilateral anterior and contralateral horizontal canals produced EPSPs and that of bilateral posterior and ipsilateral horizontal canals produced IPSPs (Figs. 2 and 3). This pattern is similar to the pattern for motoneurons of biventer and complexus muscles at C3 reported by Wilson and Maeda (1974). However, the pattern for OCA motoneurons is very different; the motoneurons receive excitation from the ipsilateral vertical canals and inhibition from the contralateral vertical canals (Fig. 4). These results indicate that there are at least two patterns of input from vertical canals for dorsal neck muscle motoneurons. As to the horizontal canal inputs, all motoneurons of three neck muscles examined received excitation from the contralateral side and inhibition from the ipsilateral side and there is only one pattern of input for all dorsal neck motoneurons.

The disynaptic pathways from the contralateral canals to RD, OCA and COMP motoneurons are by way of the MLF ipsilateral to the motoneurons (Fig. 5). Most of these crossed effects are probably conveyed by vestibulo-oculo-collic neurons located either in the medial or the descending vestibular nucleus (Uchino and Hirai, 1984; Isu et al., 1988; Uchino and Isu, 1992). Inhibitory inputs from the ipsilateral semicircular canals to RD, OCA and COMP motoneurons were abolished by interruption of the ipsilateral MLF, but excitatory inputs remained unaffected (Fig. 5). This result is consistent with the finding in biventer and complexus motoneurons (Wilson and Maeda, 1974). The excitatory signals may be conveyed to these motoneurons by vestibulo-collic neurons located in the lateral vestibular nucleus (Uchino and Isu, 1992). Trisynaptic IPSPs from the contralateral ampullary nerves are at least partly mediated by spinal commissural neurons (Sugiuchi et al., 1992b).

It is worthwhile to consider how the pattern of excitatory and inhibitory inputs to neck motoneurons is related to compensatory neck movements for head stabilization in response to external disturbances. When bilateral anterior canals are simultaneously stimulated, the head moves straight up, rotating on the bitemporal axis (Suzuki and Cohen, 1964). The RD and COMP muscles must be involved in this compensatory movement, since the RD and COMP muscles are excited from the bilateral anterior canals and inhibited from the bilateral posterior canals. Accordingly, when the head is rotated downward in the sagittal plane, these muscles are maximally contracted, so that the compensatory head movement to raise the head to the normal position results. When the head is rotated upward, these muscles are maximally inhibited and help neck flexors return the head to the normal position. Head rotation in the frontal plane results in excitation of the anterior and posterior canals on one side. Simultaneous electrical stimulation of the unilateral vertical canals results in the head rotation on the naso-occipital axis to the unstimulated side (Suzuki and

Cohen, 1964). When the head is rotated in the frontal plane, excitation of the anterior and posterior canals on the rotated side results in excitation of the ipsilateral OCA muscle and inhibition of the contralateral OCA muscle. Thus, the OCA muscle must be involved in the compensatory head movement on the naso-occipital axis. Qualitatively, the pattern of inputs from six semicircular canals to motoneurons of each neck muscle can properly explain the direction of the compensatory head movement described above. However, more quantitative information on the input from each semicircular canal to a motoneuron is required in order to characterize the functional involvement of each muscle in compensatory head movement in the same plane as the activated semicircular canal.

Acknowledgements

This study was supported partly by a research grant from the Human Frontier Science Program.

References

Akaike, T., Fanardjian, V.V., Ito, M. and Ohno, T. (1973) Electrophysiological analysis of the vestibulospinal reflex pathway of rabbit. II. Synaptic actions upon spinal neurones. *Exp. Brain Res.*, 17: 497 – 515.

Baker, J., Goldberg, J. and Peterson, B. (1985) Spatial and temporal response properties of the vestibulocollic reflex in decerebrate cats. *J. Neurophysiol.*, 54: 735 – 756.

Ezure, K. and Sasaki, S. (1978) Frequency-response analysis of vestibular-induced neck reflex in cat. I. Characteristics of neural transmission from horizontal semicircular canal to neck motoneurons. *J. Neurophysiol.*, 41: 445 – 458.

Isu, N., Uchino, Y., Nakashima, H., Satoh, S., Ichikawa, T. and Watanabe, S. (1988) Axonal trajectories of posterior canal-activated secondary vestibular neurons and their coactivation of extraocular and neck flexor motoneurons in the cat. *Exp. Brain Res.*, 70: 181 – 191.

Kasahara, M. and Uchino, Y. (1974) Bilateral semicircular inputs to neurons in cat vestibular nuclei. *Exp. Brain Res.*, 20: 285 – 296.

Schor, R.H. and Miller, A.D. (1981) Vestibular reflexes in neck and forelimb muscles evoked by roll tilt. *J. Neurophysiol.*, 46: 167 – 178.

Shinoda, Y., Ohgaki, T. and Futami, T. (1986) The morphology of single lateral vestibulospinal tract axons in the lower cervical cord of the cat. *J. Comp. Neurol.*, 249: 226 – 241.

Shinoda, Y., Ohgaki, T., Futami, T. and Sugiuchi, Y. (1988a) Vestibular projections to the spinal cord: the morphology of single vestibulospinal axons. In: O. Pompeiano and J.H.J. Allum (Eds.), *Vestibulospinal Control of Posture and Movement – Progress in Brain Research, Vol. 76,* Elsevier, Amsterdam, pp. 17 – 27.

Shinoda, Y., Ohgaki, T., Sugiuchi, Y. and Futami, T. (1988b) Structural basis for three-dimensional coding in the vestibulospinal reflex; morphology of single vestibulospinal axons in the cervical cord. *Ann. N.Y. Acad. Sci.*, 545: 216 – 227.

Shinoda, Y., Ohgaki, T., Futami, T. and Sugiuchi, Y. (1990) Comparison of the branching patterns of lateral and medial vestibulospinal tract axons in the cervical spinal cord. In: J.H.J. Allum and M. Hulliger (Eds.), *Afferent Control of Posture and Locomotion – Progress in Brain Research, Vol. 80,* Elsevier, Amsterdam, pp. 137 – 147.

Shinoda, Y., Ohgaki, T., Sugiuchi, Y. and Futami, T. (1992a) The morphology of medial vestibulospinal axons in the upper cervical cord of the cat. *J. Comp. Neurol.*, 316: 151 – 172.

Shinoda, Y., Ohgaki, T., Sugiuchi, Y., Futami, T. and Kakei, S. (1992b) Functional synergies of neck muscles innervated by single medial vestibulospinal axons. *Ann. N.Y. Acad. Sci.*, 656: 507 – 518.

Sugiuchi, Y. and Shinoda, Y. (1992) Organization of the motor nuclei innervating epaxial muscles in the neck and back. In: A. Berthoz, W. Graf and P.P. Vidal (Eds.), *Head-Neck Sensory-Motor System,* Oxford University Press, New York, pp. 235 – 240.

Sugiuchi, Y., Futami, T., Ando, N., Kawasaki, S., Yagi, J. and Shinoda, Y. (1992a) Patterns of connections between six semicircular canals and neck motoneurons. *Ann. N.Y. Acad. Sci.*, 656: 957 – 959.

Sugiuchi, Y., Kakei, S. and Shinoda, Y. (1992b) Spinal commissural neurons mediating vestibular input to neck motoneurons in the cat upper cervical cord. *Neurosci. Lett.*, 145: 221 – 224.

Suzuki, J. and Cohen, B. (1964) Head, eye, body and limb movements from semicircular canal nerves. *Exp. Neurol.*, 10: 393 – 405.

Suzuki, J., Tokumasu, K. and Goto, K. (1969) Eye movements from single utricular nerve stimulation in the cat. *Acta Otolaryngol.*, 68: 350 – 362.

Uchino, Y. and Hirai, H. (1984) Axon collaterals of anterior semicircular canal-activated vestibular neurons and their coactivation of extraocular and neck motoneurons in the cat. *Neurosci. Res.*, 1: 309 – 325.

Uchino, Y. and Isu, N. (1992) Properties of vestibulo-ocular and/or vestibulo-collic neurons in the cat. In: A. Berthoz, W. Graf and P.P. Vidal (Eds.), *Head-Neck Sensory-Motor System,* Oxford University Press, New York, pp. 266 – 272.

Wilson, V.J. and Maeda, M. (1974) Connection between semicircular canals and neck motoneurons in the cat. *J. Neurophysiol.*, 37: 346 – 357.

Wilson, V.J. and Melvill-Jones, G. (1979) *Mammalian Vestibular Physiology,* Plenum, New York.

Wilson, V.J., Gacek, R.R., Maeda, M. and Uchino, Y. (1977) Saccular and utricular input to cat neck motoneurons. *J. Neurophysiol.*, 40: 63 – 73.

J.H.J. Allum, D.J. Allum-Mecklenburg, F.P. Harris and R. Probst
Progress in Brain Research, Vol. 97

CHAPTER 20

Vestibulospinal reflexes and the reticular formation

V.J. Wilson

The Rockefeller University, New York, NY 10021, U.S.A.

While both vestibulospinal and reticulospinal tracts contribute to vestibulospinal reflexes, their respective roles are not fully understood. Previous evidence suggests that reticulospinal fibers make an important contribution to the horizontal vestibulocollic reflex (VCR) of the decerebrate cat. Recent work addresses their contribution to the vertical VCR. On the basis of study of reflex and vestibulocollic neuron dynamics, it appears that processing which is necessary to produce some of the spatial properties of the vertical VCR takes place outside the vestibular nuclei. Recording from pontomedullary reticulospinal neurons receiving vestibular input and projecting to different levels of the spinal cord reveals that almost no cells receive only vertical canal input, while approximately half receive otolith input. As is the case for vestibulocollic neurons, these reticulospinal neurons also lack the properties required to produce all of the VCR's spatial properties. Two conclusions are that in response to stimuli in vertical planes pontomedullary reticulospinal fibers are best suited to contribute to otolith reflexes, and that spatial properties of the VCR depend in part on convergence of inputs within the neck itself.

Key words: Vestibulospinal fibers; Reticulospinal fibers; Spatial transformation; Vestibulocollic reflex

Introduction

It has long been known that the vestibulospinal and reticulospinal tracts both receive vestibular input and are part of the neural substrate of vestibulospinal reflexes, but their relative contribution to these reflexes remains uncertain. Some requirements must be met before this problem can be addressed. First, we need to know the temporal and spatial properties of vestibulospinal reflexes. Second, similar information must be obtained about the vestibular input to vestibulo- and reticulospinal neurons, preferably to neurons whose level of projection in the spinal cord is known. Only then can we begin to assess the contribution that vestibular and reticular neurons make to reflex behavior. In recent years, much data has been gathered about vestibular reflexes evoked by sinusoidal stimuli in horizontal and vertical planes and acting on the neck and forelimbs of the decerebrate cat (reviewed in Wilson and Peterson, 1981; Schor and Miller, 1981; Bilotto et al., 1982; Dutia and Hunter, 1985; Baker et al., 1985; Wilson et al., 1986). Similar stimuli have been used to study vestibulospinal neurons (e.g., Boyle and Pompeiano, 1981; Kasper et al., 1988; Wilson et al., 1990). There has been little investigation of the responses of reticulospinal neurons to natural vestibular stimulation, except for the work of Pompeiano and his colleagues (Manzoni et al., 1983; Pompeiano et al., 1984), who studied responses of these neurons to roll stimuli, and recent experiments in our laboratory (Bolton et al., 1991, 1992). The results of these experiments help clarify the role of reticulospinal fibers in the vestibular reflex acting on the neck (vestibulocollic reflex or VCR).

The vestibulocollic reflex

Studies on the neural substrate of the VCR were initially done on the reflex evoked by sinusoidal

horizontal rotations (reviewed in Wilson and Peterson, 1981; Bilotto et al., 1982). In brief, reflex output to dorsal neck muscles lags input acceleration considerably at low frequencies, bringing the phase of the EMG close to a position signal at, for example, 0.2 Hz. Thus, the integration of the incoming canal input, which is in phase with stimulus velocity, produces a signal appropriate for a reflex compensating for a change in angular head position. At higher frequencies, phase advances and gain increases, and the output approaches an acceleration signal by 3 Hz. The most direct pathway linking the horizontal canal with neck motoneurons is disynaptic, with axons in the medial vestibulospinal tract (MVST) in the medial longitudinal fasciculus (MLF) (Fig. 1; Wilson and Maeda, 1974). This pathway must be part of the neural substrate of the reflex, but what is its contribution to reflex dynamics? Ezure and Sasaki (1978) showed that the dynamics of second-order canal neurons resemble those of canal afferents, and that there is a considerable phase lag between their responses and those of neck muscles. It is hard to see how neurons that respond in this manner can produce the low-frequency, phase-lagging reflex behavior. In fact, interruption of the disynaptic pathway by lesions of the MLF has no obvious effect on the horizontal VCR, not only at low frequencies, but at higher ones as well (Ezure et al., 1978; Bilotto et al., 1982); a decrease in gain is seen only when deeper lesions impinge on the reticular formation. Although higher-order vestibular neurons do show responses with muscle-like dynamics in response to sinusoidal polarization of the horizontal canal nerve, a paradigm in which stimulus spread to utricular afferents is hard to rule out completely (Peterson et al., 1981), the lesion experiments suggest an important role for reticulospinal fibers in the horizontal VCR.

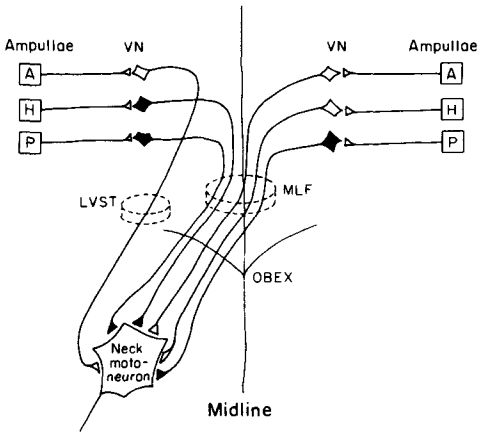

Fig. 1. Diagrams of disynaptic connections between ipsilateral and contralateral semicircular canal ampullae and dorsal neck motoneurons. A, H, P, anterior, horizontal and posterior ampullae, respectively; VN, vestibular nuclei; LVST, lateral vestibulospinal tract; MLF, medial longitudinal fasciculus (from Wilson and Maeda, 1974).

The VCR evoked by stimuli in vertical planes is more complex because it results from activation not only of the vertical canals but also of the otolith organs (Schor and Miller, 1981; Dutia and Hunter, 1985; Baker et al., 1985). Accordingly, dynamics of the reflex are as expected from convergent otolith and canal input: phase is near position and gain flat at low frequencies; above 0.1 Hz gain begins to rise and phase advances, approaching 90° at 2 Hz. Note that the central integrator which transforms a velocity canal input to a position response at low frequencies in the horizontal VCR is not needed for the vertical VCR because of the presence of the otolith input. Spatial properties of the reflex have been studied in detail by Baker et al. (1985), who looked at the responses evoked by sinusoidal stimuli oriented in many different planes. Two aspects of their results are of particular interest. First, at frequencies at which canal input predominates, the response vector orientation of some neck muscles, i.e., the stimulus plane that produces the maximal reflex response, suggests that these muscles receive bilaterally convergent input from symmetric vertical canals, for example from the two anterior canals. Second, muscles often display spatiotemporal convergence (STC behavior), i.e., convergence of inputs with different spatial and temporal properties. Evidence for such behavior is that the muscle's response vector orientation shifts with stimulus frequency; that response phase depends on stimulus orientation; and that at intermediate frequencies (usually 0.1 or 0.2 Hz) it may be impossible to define a vector orientation because all directions of tilt are

equally effective. A likely explanation for STC behavior is convergence of canal and otolith inputs that are not aligned spatially. We can again ask the question: what is the role of vestibulocollic pathways, linking vestibular nuclei to neck, in producing such reflex behavior? As shown in Fig. 1, some of the disynaptic pathways, i.e., the bilateral pathways from the posterior canal and the crossed pathway from the anterior canal, are in the MLF, while the pathway from the ipsilateral anterior canal is in the lateral vestibulospinal tract (LVST). It is well known that there is strong otolith input to the nuclei that give rise to the LVST, but indirect evidence suggests that crossed disynaptic otolith pathways may be in the MVST (Wilson and Melvill Jones, 1979). With the pathways more diverse and less conveniently grouped than is the case with the horizontal VCR, the effects of lesions are more difficult to interpret. Miller et al. (1982) looked at the effect of MVST lesions on the reflex evoked by roll tilt, and observed little change other than some loss of gain, especially at higher stimulus frequencies. With a stimulus limited to roll, Miller and colleagues could not detect any effect of the lesion on spatial properties of the reflex. It would therefore be of interest to test the effect of MLF lesions on response vector orientations of neck muscles.

The responses of vestibulocollic neurons to sinusoidal tilt in vertical planes have been investigated in decerebrate preparations similar to those used for reflex studies (Wilson et al., 1990). Spontaneously active neurons in Deiters' nucleus and the descending vestibular nucleus were identified with antidromic stimulation as terminating in the neck segments. Many of these neurons responded to sinusoidal whole body tilt. Once their response vector orientation was determined using a stimulus combining pitch and roll ("wobble", Schor et al., 1984), sinusoidal stimuli oriented near the response vector and delivered at different frequencies were used to classify the neurons according to the type of vestibular input that they received. On the basis of dynamics, the population was divided into neurons receiving input primarily from vertical canals (44%), otoliths (19%), otolith + canal (12%), or

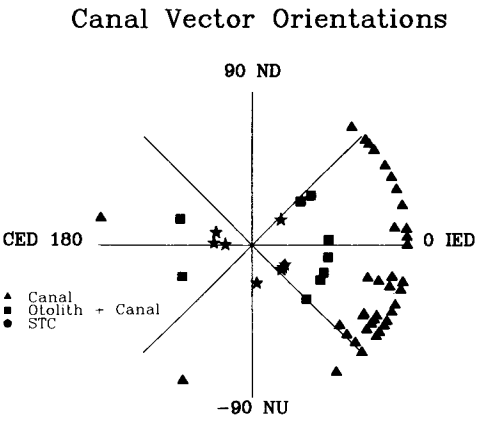

Fig. 2. Response vector orientations of vestibulocollic neurons, determined by the use of wobble stimuli, typically at 0.5 Hz. Neurons of different classes are grouped in concentric circles. Neurons that respond maximally to ipsilateral ear down (IED) roll rotations have vector orientations of 0°, those responding best to contralateral ear down (CED) roll have orientations of 180°. Orientations of 90° and −90° correspond to nose down (ND) and nose up (NU) pitch, respectively (modified from Wilson et al., 1990).

demonstrating STC behavior (10%); 15% could not be classified. While this population of neurons can account for VCR dynamics, it cannot account for all of the reflex's spatial behavior for two reasons. First, the small fraction of STC neurons appears to be insufficient to produce the behavior seen at the reflex level. Second, while many neurons with input from canals (canal only, otolith + canal, STC) received convergent input from more than one canal, and their response vectors were shifted from canal planes, the shift was almost invariably towards roll (Fig. 2): this indicates convergence between the anterior and posterior canals on the same side. Convergence between bilateral anterior or posterior canals, required to produce the response vector orientation seen in some neck muscles, would produce vectors in the pitch quadrants. As can be seen in Fig. 2, such vectors were conspicuously absent. Wilson et al. (1990) studied only neurons terminating in the neck segments and, therefore, excluded from their sample neurons giving a collateral branch to the upper cervical grey matter, then continuing to more caudal levels. Such neurons are un-

likely to have properties very different from those of vestibulocollic neurons, however, because the behavior of the population of Wilson et al. (1990) was essentially the same as that of an unselected sample of vestibular nucleus neurons studied earlier by Kasper et al. (1988).

In summary, the evidence suggests that neurons other than vestibulospinal neurons play an important role in both horizontal and vertical vestibulocollic reflexes, and that some of the processing required to produce these reflexes takes place outside the vestibular nuclei. In addition to the neck segments themselves, a likely locus for such processing is the reticular formation.

Reticulospinal neurons and the vestibulocollic reflex

The lesion studies discussed above demonstrate that the horizontal VCR functions normally after interruption of the disynaptic vestibulocollic pathway in the MVST, and imply that it can be produced by reticulospinal fibers. Unfortunately, little is known so far about the responses of identified reticulospinal fibers to activation of the horizontal canal. Peterson et al. (1981) observed that, when the horizontal canal nerve was stimulated by sinusoidal polarizing current, reticulospinal neurons, like some vestibulospinal neurons, could have muscle-like responses with a phase lag at low frequencies. As already mentioned, it is hard to completely rule out some spread to the utricular nerve with this form of stimulation. Sasaki and Shimazu (1981) noted responses of some reticulospinal neurons to horizontal rotation, but did not study them systematically. Better understanding of the contribution of reticulospinal neurons to the horizontal VCR requires a comprehensive study of the dynamics of their responses to horizontal rotation.

As part of our investigation of the neural basis of the vertical VCR, we have recently studied the responses of pontomedullary reticulospinal neurons to whole body rotations in vertical planes (Bolton et al., 1991, 1992). The neurons, which projected in the lateral and medial reticulospinal tracts, were located medially in n. pontis caudalis and n. gigantocellularis, over a rostrocaudal extent ranging from the facial nerve to the rostral pole of the hypoglossal nucleus. Neurons in these areas make excitatory and inhibitory connections, mono- and polysynaptic, with neck and limb motoneurons (Wilson and Peterson, 1981). The level of the spinal cord to which each neuron projected was identified by antidromic stimulation as being rostral to C5 (neck or N cells), in the cervical enlargement (C cells), in the thoracic cord (T cells), or in the lumbar cord (L cells). Few cells had axons terminating in the neck (13%), in agreement with earlier studies (Peterson et al., 1975; Iwamoto and Sasaki, 1990). However, Iwamoto et al. (1990) have recently shown that reticulospinal neurons projecting as far as the thoracic cord have

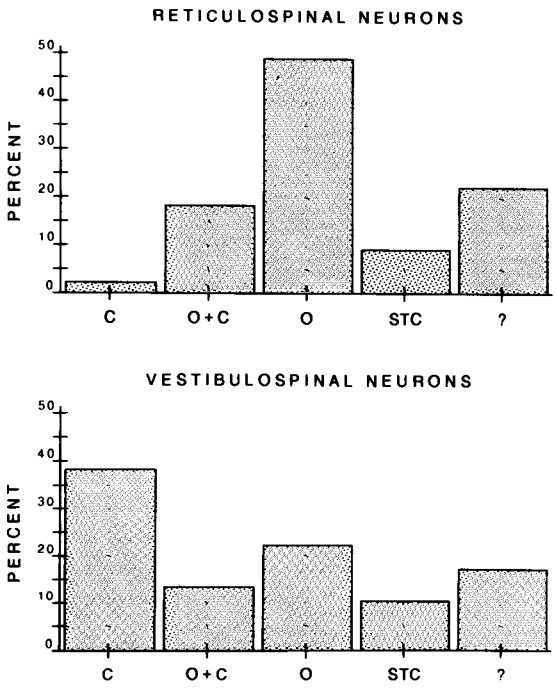

Fig. 3. Distribution of different vestibular response types among reticulospinal and vestibulospinal neurons. The RS population consists of 65 neurons (data from Bolton et al., 1991, 1992). The 113 vestibulospinal neurons include 86 vestibulocollic neurons (from Wilson et al., 1990) and 27 neurons driven antidromically from an electrode at the C4 level (from Kasper et al., 1988).

a high likelihood of sending a collateral to the neck grey matter, and N, C and T cells together make up 49% of our sample. Comparison of the properties of this group of neurons with those of L cells reveals no obvious difference either in spatial tuning or in distribution of inputs from different receptors in the labyrinth; for the rest of this paper I will therefore consider them together as RS neurons.

Sixty-five spontaneously active RS neurons that responded to whole body tilt were studied as in our previous experiments: each neuron's response vector orientation was determined with the wobble stimulus, then dynamics were studied with sinusoidal stimuli aligned with this vector. Although reticular neurons are at least one synapse further away from the input than are vestibular nucleus neurons, the same response types as in vestibular nuclei were found for RS neurons. There was input from vertical canals (2% of the neurons), otoliths (49%), otolith + canal (18%), and there were cells with STC behavior (9%); 22% of the cells could not be classified. Fig. 3, which compares these percentages with those obtained for a population of vestibulospinal neurons, shows a striking difference between them. Whereas neurons receiving only vertical canal input make up the largest component of the vestibulospinal population, such neurons are essentially absent from the RS group. Such absence could be due to extensive convergence within the reticular formation, resulting in a large number of otolith + canal and STC neurons, but this is not the case. The percentage of otolith + canal and STC neurons is similar in the two populations, and there is a very large fraction of RS neurons with only otolith input. Even where present, canal input to RS neurons is weaker than in the vestibular nuclei: at frequencies where canal input becomes dominant, 0.2 and 0.5 Hz, the gain of otolith + canal RS neurons is lower than that of vestibulospinal neurons. On the other hand, the gain of the otolith input to RS neurons is comparable in strength to what is seen in the vestibular nuclei. It should be noted that while looking for RS neurons, we studied 21 neurons that could not be driven antidromically from the spinal cord and presumably projected elsewhere: seven of these neurons (33%) received their input from vertical canals.

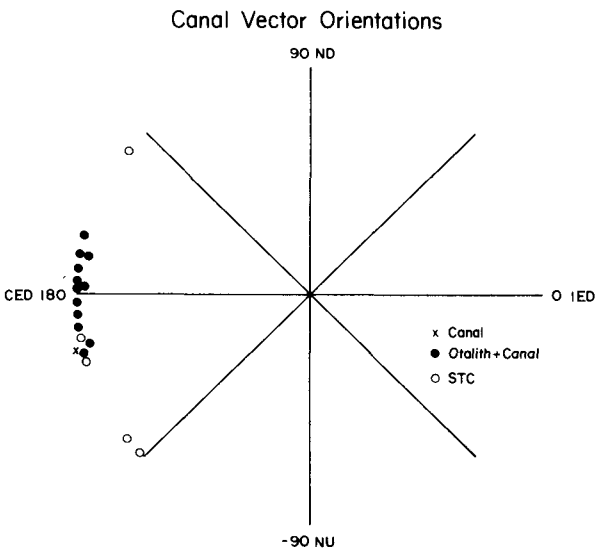

Fig. 4. Response vector orientations of RS neurons, determined by the use of wobble stimuli, typically at 0.5 Hz. Abbreviations as in Fig. 2 (data from Bolton et al., 1991, 1992).

The scarcity of RS neurons with only vertical canal input means that any contribution that RS neurons make to the spatial transformation of canal signals that produces the response vector orientations seen in neck muscles must be made by otolith + canal and STC neurons. Both have convergent otolith and canal input, with the latter presumably dominating at higher frequencies of stimulation. Fig. 4 shows vector orientations, determined at 0.5 Hz, of 18 of these neurons. In contrast to the behavior of vestibular neurons (Fig. 2), all vectors are oriented contralaterally, as was the case for the majority of neurons that Manzoni et al. (1983) classified as receiving otolith or otolith + canal input. More to the point, all but one of the vectors are in the roll quadrants and most are very close to roll.

Although the precise contribution of reticulospinal fibers to the VCR cannot be determined without knowing whether they are excitatory or inhibitory, and what their targets are, several things are clear from these results. First, in the decerebrate cat, ver-

tical canal signals, unlike horizontal canal activity, reach the neck mainly via the vestibulospinal tracts, with little RS contribution. This is consistent with the result of MLF lesions, which would interrupt crossed anterior canal and all posterior canal pathways, leading to the gain decrease at high frequencies observed by Miller et al. (1982). Gain at low freqencies would be less sensitive to such lesions because of the substantial otolith signal carried by RS fibers, many of which are outside the MLF (Petras, 1967). Second, neck muscle response vectors with orientations in the pitch quadrants are no more likely to be generated in the pontomedullary reticular formation than in the vestibular nuclei. The appropriate convergence most likely takes place in the neck, where it has already been shown that bilateral pathways from the anterior and posterior canals converge on the same motoneurons (Fig. 1; Wilson and Maeda, 1974). Third, with a small number of STC neurons in both vestibular nuclei and reticular formation, it appears that convergence in the neck also makes a contribution to reflex STC behavior. Finally, the results suggest that for the vertical VCR the most important contribution of RS fibers is to otolith reflexes. Because RS fibers projecting to all levels of the cord have similar properties, this also applies to their contribution to otolith reflexes acting on the limbs and trunk.

Acknowledgements

Work in the author's laboratory was supported by N.I.H. grants NS02619 and DC00693.

References

Baker, J., Goldberg, J. and Peterson, B. (1985) Spatial and temporal properties of the vestibulocollic reflex in decerebrate cats. *J. Neurophysiol.*, 54: 735–756.

Bilotto, G., Goldberg, J., Peterson, B.W. and Wilson, V.J. (1982) Dynamic properties of vestibular reflexes in the decerebrate cat. *Exp. Brain Res.*, 47: 343–352.

Bolton, P., Goto, T., Schor, R.H., Wilson, V.J., Yamagata, Y. and Yates, B.J. (1991) Reticulospinal neurons and vertical vestibulospinal reflexes. *Soc. Neurosci. Abstr.*, 17: 317.

Bolton, P., Goto, T., Schor, R.H., Wilson, V.J., Yamagata, Y. and Yates, B.J. (1992) Response of pontomedullary reticulospinal neurons to vestibular stimuli in vertical planes, and their role in vertical vestibulospinal reflexes of the decerebrate cat. *J. Neurophysiol.*, 67: 639–647.

Boyle, R. and Pompeiano, O. (1981) Responses of vestibulospinal neurons to neck and macular vestibular inputs in the presence or absence of the paleocerebellum. *Ann. N.Y. Acad. Sci.*, 374: 373–394.

Dutia, M.B. and Hunter, M.J. (1985) The sagittal vestibulocollic reflex and its interaction with neck proprioceptive afferents in the decerebrate cat. *J. Physiol. (Lond.)*, 359: 17–29.

Ezure, K. and Sasaki, S. (1978) Frequency-response analysis of vestibular-induced neck reflex in cat. I. Characteristics of neural transmission from horizontal semicircular canal to neck motoneurons. *J. Neurophysiol.*, 41: 445–458.

Ezure, K., Sasaki, S., Uchino, Y. and Wilson, V.J. (1978) Frequency-response analysis of the vestibular-induced neck reflex in cat. II. Functional significance of cervical afferents and polysynaptic descending pathways. *J. Neurophysiol.*, 41: 459–471.

Iwamoto, Y. and Sasaki, S. (1990) Monosynaptic excitatory connections of reticulospinal neurones in the nucleus reticularis pontis caudalis with dorsal neck motoneurons in the cat. *Exp. Brain Res.*, 80: 277–289.

Iwamoto, Y., Sasaki, S. and Suzuki, I. (1990) Input-output organization of reticulospinal neurones, with special reference to connections with dorsal neck motoneurones in the cat. *Exp. Brain Res.*, 80: 260–276.

Kasper, J., Schor, R.H. and Wilson, V.J. (1988) Response of vestibular neurons to head rotations in vertical planes. I. Response to vestibular stimulation. *J. Neurophysiol.*, 60: 1753–1764.

Manzoni, D., Pompeiano, O., Stampacchia, G. and Srivastava, U.C. (1983) Responses of medullary reticulospinal neurons to sinusoidal stimulation of labyrinth receptors in decerebrate cat. *J. Neurophysiol.*, 50: 1059–1079.

Miller, A.D., Roossin, P.S. and Schor, R.H. (1982) Roll tilt reflexes after vestibulospinal tract lesions. *Exp. Brain Res.*, 48: 107–112.

Peterson, B.W., Fukushima, K., Hirai, N., Schor, R.H. and Wilson, V.J. (1981) Responses of vestibulospinal and reticulospinal neurons to sinusoidal vestibular stimulation. *J. Neurophysiol.*, 43: 1236–1250.

Petras, J.M. (1967) Cortical, tectal and tegmental fiber connections in the spinal cord of the cat. *Brain Res.*, 6: 275–324.

Pompeiano, O., Manzoni, D., Srivastava, U.C. and Stampacchia, G. (1984) Convergence and interaction of neck and macular vestibular inputs on reticulospinal neurons. *Neuroscience*, 12: 111–128.

Sasaki, S. and Shimazu, H. (1981) Reticulovestibular organization participating in generation of horizontal fast eye movement. *Ann. N.Y. Acad. Sci.*, 374: 130–143.

Schor, R.H. and Miller, A.D. (1981) Vestibular reflexes in neck and forelimb muscles evoked by roll tilt. *J. Neurophysiol.*, 46: 167–178.

Schor, R.H., Miller, A.D. and Tomko, D.L. (1984) Responses to head tilt in cat central vestibular neurons. I. Direction of maximum sensitivity. *J. Neurophysiol.,* 51: 136 – 146.

Wilson, V.J. and Maeda, M. (1974) Connections between semicircular canals and neck motoneurons. *J. Neurophysiol.,* 37: 346 – 357.

Wilson, V.J. and Melvill Jones, G. (1979) *Mammalian Vestibular Physiology,* Plenum, New York, 365 pp.

Wilson, V.J. and Peterson, B.W. (1981) Vestibulospinal and reticulospinal systems. In: *Handbook of Physiology – The Nervous System,* Am. Physiol. Soc., Bethesda, MD, pp. 667 – 702.

Wilson, V.J., Schor, R.H., Suzuki, I. and Park, B.R. (1986) Spatial organization of neck and vestibular reflexes acting on the forelimbs of the decerebrate cat. *J. Neurophysiol.,* 55: 514 – 526.

Wilson, V.J., Yamagata, Y., Yates, B.J., Schor, R.H. and Nonaka, S. (1990) Response of vestibular neurons to head rotations in vertical planes. III. Response of vestibulocollic neurons to vestibular and neck stimulation. *J. Neurophysiol.,* 64: 1695 – 1703.

J.H.J. Allum, D.J. Allum-Mecklenburg, F.P. Harris and R. Probst
Progress in Brain Research, Vol. 97

CHAPTER 21

Stance and balance following bilateral labyrinthectomy

Jane M. Macpherson and J. Timothy Inglis[1]

R.S. Dow Neurological Sciences Institute, Good Samaritan Hospital and Medical Center, Portland, OR, U.S.A. and [1]Department of Physical Therapy, Elborn College, University of Western Ontario, London, Canada

Although vestibular input codes head acceleration, it is not clear whether or not this signal is critical for triggering the initial postural response to a perturbation of stance, and for determining the appropriate direction of response. These experiments were designed to examine the contribution of vestibular inputs to the control of balance in the freely standing cat. Four cats were trained to stand quietly on a moveable force platform. The animal's stance was unexpected perturbed by applying a linear ramp-and-hold translation to the support surface in each of eight different directions in the horizontal plane. The characteristics of quiet stance and the response to the perturbations were quantified in terms of the 3-D ground reaction forces under each paw and the EMG activity in selected muscles. The animals were bilaterally labyrinthectomized, and their responses compared before and after lesion. The cats were able to stand stably on the platform within 2 – 3 days of the lesion. During quiet stance, there was no change in the distribution of vertical forces under the paws and no increase in sway area. Horizontal plane forces, which were normally outwardly directed on the diagonals, became more laterally directed and transiently larger in amplitude. The level of tonic EMG activity increased in some extensors and flexors, and decreased in others, compared to control. The responses to platform translation were characterized by normal spatial and temporal patterns and latencies of EMG activity. Furthermore, all cats continued to use the force constraint strategy that is characteristic of the intact animal (Macpherson, 1988a). The only clear deficit in performance was a transient hypermetria, characterized by an over-response to the translation. Although the cats over-responded, they were still able to maintain their balance successfully. The moderate changes in quiet stance and in response to perturbation gradually returned to control values over 8 – 10 days following the lesion. These results suggest that vestibular information is not necessary for triggering appropriate postural responses evoked by support surface translations, nor for selecting the direction of response.

Key words: Posture; Balance; Quadrupedal stance; Vestibular system; Cat; Ground reaction forces; Electromyography

Introduction

Bilateral loss of the vestibular end-organs has profound consequences for motor behavior, especially in the acute phase, but also long-term. Following this lesion, animals exhibit broad-based stance, ataxic gait, uncontrolled pendular head movements, problems with dynamic equilibrium, and impairment in gaze stabilization (Magnus, 1926; Dow, 1938; Carpenter et al., 1959; Money and Scott, 1962; Igarashi et al., 1970; Kasai and Zee, 1978; Lacour and Xerri, 1981; Marchand et al., 1988; Grossman and Leigh, 1990). During the compensation phase, many of these symptoms lessen in severity or disappear, although even after one year of recovery, dynamic equilibrium, locomotion, and the control of head movements are still deficient (Igarashi et al., 1970; Marchand et al., 1988; Thomson et al., 1991). These studies suggest that the vestibular system is critically involved in the control of stance and balance, but that over time, other sensory systems can compensate to some extent for the loss of vestibular inputs.

The specific role of the vestibular system in the selection and triggering of postural responses to perturbations of stance is not fully understood. It has

been suggested that vestibular inputs are most effective for stabilization of low-frequency sway rather than rapid perturbations (Nashner, 1971; Mauritz and Dietz, 1980; Keshner et al., 1987). Initially, Nashner found that the latency of vestibular-evoked EMG responses in the lower limbs (> 180 msec) was too long to account for the postural responses evoked by perturbations of the support surface (postural response latency 70 – 100 msec) (Nashner, 1971, 1973). Subsequent studies have suggested that vestibular stimulation can produce more rapid evoked activity in lower limb muscles, in the range of 50 – 80 msec (Bussel et al., 1980; Allum and Pfaltz, 1985; Fries et al., 1988; Dietz et al., 1988b). Studies of patients with bilateral absence of vestibular function have demonstrated impaired balance in only certain tasks (Bussel et al., 1980; Allum and Pfaltz, 1985; Keshner et al., 1987; Horak et al., 1990; Kleiber et al., 1990), but not in others (Dietz et al., 1988a,b; Horak et al., 1990). Moreover, the amplitude of vestibular-evoked EMG activity in intact subjects appears to be rather small (Dietz et al., 1988b; Shupert et al., 1990). Thus, the particular conditions under which vestibular afferent input is critical for balance have not been fully clarified. This study was designed to evaluate the contribution of vestibular inputs in the cat to the control of quiet stance and to the response to small, slow translations of the support surface in the horizontal plane.

Methods

Four adult female cats (weight range 3 – 4 kg) were trained using positive reinforcement to stand, unrestrained, on a moveable force platform. Once trained, the animals were implanted under general anesthesia and aseptic conditions with chronically indwelling electrodes to monitor the electromyographic (EMG) activity of selected muscles. The equipment, training and surgical procedures have been fully described elsewhere (Macpherson et al., 1987). Balance was assessed quantitatively during periods of quiet stance and during the postural response to small perturbations applied to the support surface. During testing, cats were allowed to stand with their forepaws and hindpaws at their preferred separation. This same stance separation was enforced following the lesion by the placement of the force plates. The perturbation consisted of a ramp-and-hold linear translation of the support surface in each of eight different directions evenly spaced in the horizontal plane. The amplitude of translation was scaled relative to the direction of translation from a minimum of 2.5 cm in the lateral direction to 4.0 cm in the longitudinal direction. The platform achieved a plateau linear velocity of approximately 15 cm/sec for all directions of perturbation. Perturbations were delivered while the animal was standing quietly with the head facing forward. No warning was given as to the time of translation, although several practice trials were given at each new direction in order to obtain well-adapted responses. All trials for a given direction were recorded sequentially and the ordering of directions was done pseudo-randomly.

After control data were collected, the vestibular end-organs of each animal were lesioned bilaterally in one surgery, using the drilling technique of Money and Scott (1962). The completeness of the lesion was evaluated behaviorally by verifying absence of post-rotary nystagmus following whole-body rotation without vision, and absence of righting reactions following drops from the supine position without vision. Only one animal (BO) showed evidence of an incomplete lesion; its righting reactions recovered, although no nystagmus was ever observed. The animals were tested on the platform as soon as they could stand, and were monitored throughout the recovery period for up to five months post-lesion.

Postural responses were quantified in terms of the three-dimensional ground reaction forces under each paw, and the rectified and integrated EMG activity. For quiet stance, forces and EMGs were averaged over 500 msec epochs. Video recordings were made of the animals during data collection and only those epochs in which an animal was standing quietly with its head facing forward were selected for analysis. The responses to translation were ana-

lyzed using a quasi-static approach. The force recorded under each paw was integrated to obtain the change from background force, and that value was divided by the time of integration to give the average change in force. The average change in force was compared before and after lesion for the vertical component (loading and unloading) and the horizontal plane vector (resultant of the longitudinal and lateral forces). Post-lesion EMG latencies, and force and EMG amplitudes were tested for significant differences from control at a probability of $P < 0.05$ using analysis of variance followed by Dunnett's post-hoc test for comparison to a control.

Results

Following labyrinthectomy, the three cats with the complete lesion were severely ataxic and exhibited large, pendular head movements. They lay on their abdomens with limbs outstretched and made no attempt to sit or stand. Lying on a slick surface (linoleum) induced profound instability and whole-body oscillations, even in the prone position. Lying on a textured surface (towel or rubber mat) enabled the animals to maintain stability. By day 2 (two cats) or day 4 (one cat), these animals were able to stand stably and to walk with a broad-based, staggering gait. Falls were frequent and usually associated with voluntary head movements or a change in direction during walking. Rapid recovery of motor function occurred during the first 8 – 10 days followed by a slower improvement over the first month. From the end of the first month to the fifth month post-lesion, there was no noticeable change in motor behavior. The cat with the incomplete lesion was able to walk with a staggering, crouched gait within 5 h of the

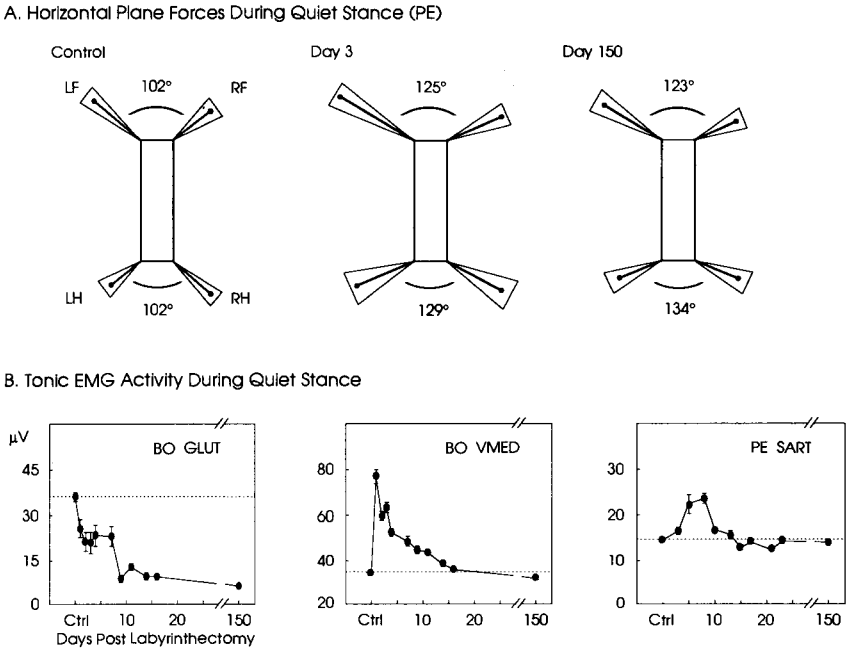

Fig. 1. Changes in quiet stance following bilateral labyrinthectomy. *A*. Average force directions and amplitudes exerted by the limbs in the horizontal plane are represented by the lines projecting from the corners of each rectangle. Triangles surrounding each line represent the S.E.M. Note the lateral bias in the direction of the forces on day 3 and day 150 following the lesion, as demonstrated by the increase in angle between the forelimb forces and between the hindlimb forces. LF, left forelimb; RF, right forelimb; LH, left hindlimb; RH, right hindlimb. *B*. Time course of change in averaged tonic EMG activity for three muscles. The horizontal dotted line in each graph indicates the control level, prior to lesion. Error bars represent S.E.M. PE, cat with complete lesion; BO, cat with incomplete lesion. GLUT, gluteus medius; VMED, vastus medialis; SART, sartorius.

surgery. Head movements were hypermetric with large amplitude oscillations, but not as uncontrolled as for the other cats. More details of the lesioned animals' general motor behavior can be found in Thomson et al. (1991).

Surprisingly, there was no significant change in the quantitative measures of stability during both quiet stance and platform translations, even though the animals' general motor behavior was profoundly affected.

Quiet stance

Following labyrinthectomy, there was no significant change in the four cats in the distribution of vertical forces under the four limbs, as has previously been reported (Marchand and Amblard, 1979). Furthermore, there was no increase in sway area during the 500 msec epochs, as measured by the area of excursion of the center of pressure.

During quiet stance in the intact animal, horizontal plane forces are directed outward along the diagonals (Macpherson, 1988a). Immediately following the lesion, all animals exerted horizontal forces with larger amplitude, and in a more lateral direction (Fig. 1*A*). The horizontal force amplitudes returned to control levels after 8 – 10 days, but the directions remained significantly biased toward the lateral plane for as long as the animals were monitored (five months post-lesion). It should be noted that the change in direction of the horizontal forces is also characteristic of intact animals that are forced to stand with their forepaws and hindpaws closer in the longitudinal plane than their preferred stance.

EMG activity from hindlimb and abdominal muscles was monitored in two cats, PE with a complete lesion and BO with an incomplete lesion. Both animals showed similar patterns in the changes in tonic activity during quiet stance. These changes could not be classified according to muscle groups (i.e., flexors vs. extensors). For example, the hip extensor, gluteus medius, decreased in tonic activity following the lesion, whereas the knee extensor, vastus medialis, and the ankle extensor, soleus, increased in tonic activity (see Fig. 1*B* for examples). Anterior sartorius, a hip flexor/knee extensor, showed a small, transient increase in activity. Semi-

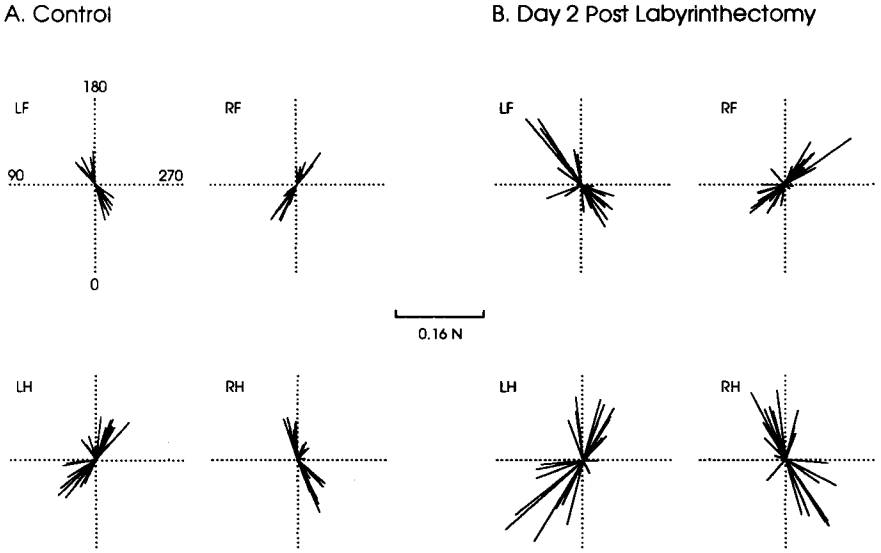

Fig. 2. Active force vectors exerted by each limb in the horizontal plane during response to eight different directions of translation, before (*A*) and 2 days after lesion (*B*). Each vector represents the average change in force during the active response period. Regardless of the direction of translation, each limb exerted an active force in one of only two preferred directions in the horizontal plane, the force constraint strategy. Note that this strategy remained intact immediately following labyrinthectomy, although vector amplitudes were significantly increased. 0°, posterior; 90°, leftward; 180°, anterior; 270°, rightward with respect to the cat. N, Newtons.

tendinosus and gracilis exhibited little tonic activity both before and after lesion. Finally, rectus abdominis, which was not tonically active in the intact animal, showed a significant increase in activity following lesion.

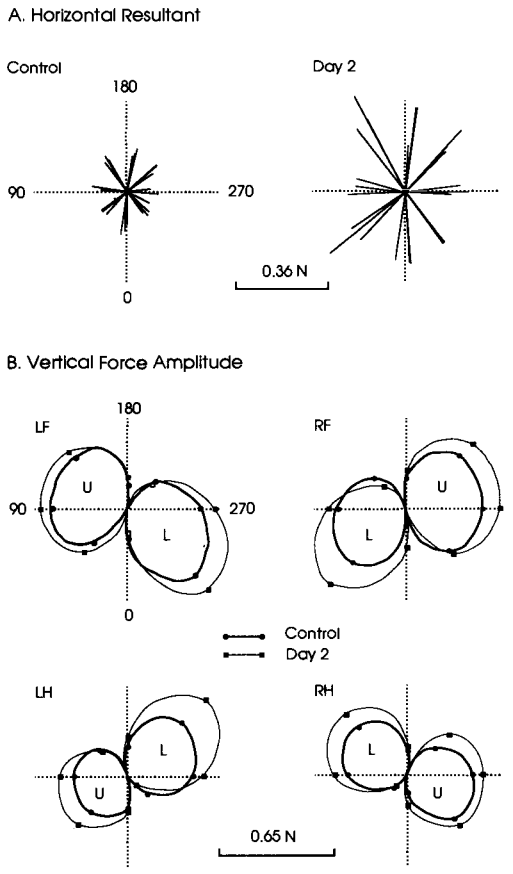

Fig. 3. *A*. Vector sum, or resultant, of the active force vectors exerted by the four paws for each of eight different directions of translation (0°, 45°, etc.). The resultant was opposite to the direction of platform movement. Note that following lesion (day 2) the resultant vectors retained the appropriate directions, but were considerably increased in amplitude (hypermetria). *B*. Polar plots of the average change in vertical force under each limb following translation. The angle is the direction of translation and the radius is the amplitude of the change in vertical force. Each plot shows two petal-shaped regions corresponding to increased vertical force, or loading (L), and decreased vertical force, or unloading (U) of the respective limb. Note the increase in the amplitude of the force response following lesion (light lines, square symbols) compared to control (dark lines, round symbols). Abbreviations as in Fig. 2.

Response to perturbations

We have previously shown that intact cats responded to horizontal translation of the support surface with a strategy termed the force constraint (Macpherson, 1988a): regardless of the direction of translation, the average change in force under each limb is constrained to one of only two preferred directions in the horizontal plane (Fig. 2*A*). In contrast, the amplitude of this force vector is varied as a function of the direction of perturbation. Thus, the resultant of the forces applied by the four limbs is in a direction opposite to platform movement (Fig. 3*A*, control). Following labyrinthectomy, all cats continued to use this force strategy. The only difference from control was an increase in amplitude of the force vectors (Figs. 2*B*, 3*A*, day 2). Similarly, the changes in vertical force were also greater following lesion (Fig. 3*B*). This hypermetria, or over-response to the perturbation, was followed by braking forces to correct for the overshoot. Hypermetria in the postural response was observed only during the initial recovery phase of 8 – 10 days post-lesion. After this time, the force amplitudes returned to control levels and remained there as long as the animals were monitored. All four cats, including the partially lesioned animal BO, showed the same changes in their response to perturbation.

In the intact animal, the force constraint strategy is accompanied by a characteristic spatial pattern of EMG activity (Macpherson, 1988b) evoked at a latency of 40 – 60 msec. Following lesion, there was no statistically significant change in either the pattern or the latency of muscle activation. However, there were changes in the amplitude of activation of some muscles, as illustrated in Fig. 4. The flexors, sartorius, semitendinosus, and rectus abdominis all showed large increases in evoked excitations. The hip extensor, gluteus medius, and the knee extensor, vastus medialis, showed a small increase in excitation amplitude, whereas the ankle extensor, soleus, showed no change in evoked excitations following lesion. However, gluteus medius, vastus medialis, and soleus all showed significantly more inhibition when the limb was unloaded post-lesion (e.g., Fig. 4, response at 45° and 135°). The changes in evoked

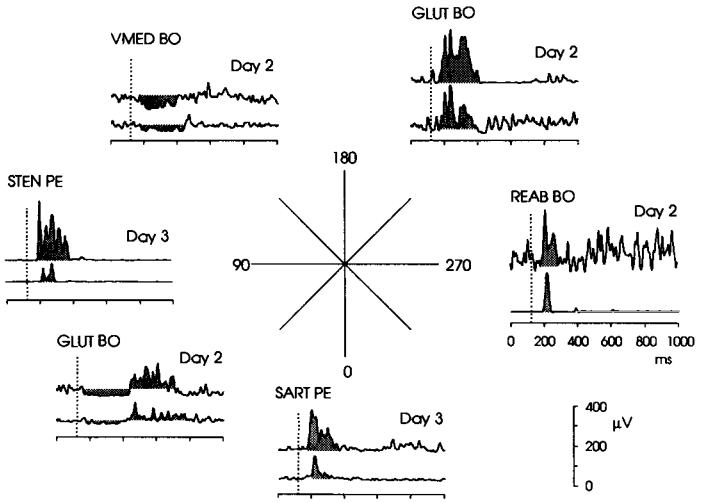

Fig. 4. Averaged EMG activity from various muscles in the left hindlimb or abdomen during response to translation, before (lower traces) and after (upper traces) labyrinthectomy. The shaded areas show the periods of evoked activity that were analyzed. The axis pointing to each pair of traces represents the direction of translation for which the activity was recorded. Gluteus medius at 225° (GLUT), rectus abdominis at 270° (REAB), semitendinosus at 90° (STEN), and sartorius at 0° (SART) all showed significant increases in evoked activity following the lesion. Additionally, vastus medialis at 135° (VMED) and GLUT at 45° exhibited more profound inhibition. Additionally, GLUT showed a larger rebound activation following the inhibition, that probably reflected braking. Abbreviations as in Fig. 2.

EMG activity more or less paralleled the time course of the hypermetria.

Discussion

The effects of bilateral labyrinthectomy on quiet stance and the response to horizontal plane translations of the support surface were remarkably mild. During quiet stance there was a modest shift in the direction of the ground reaction forces to a more lateral orientation, and a change in the tonic activity of some limb and abdominal muscles. Following translation, there was no change in the spatial and temporal pattern of EMG activation or in the strategy used by the animals in terms of the ground reaction forces. The most dramatic effect was a marked hypermetria in evoked response that resolved after 8 – 10 days.

Quiet stance

The lateral shift of the horizontal plane force vectors during quiet stance in the lesioned animals was similar to the directional shift observed in intact cats that were compelled to stand with their forelimbs and hindlimbs closer in the sagittal plane than their preferred stance distance (unpublished observations). When the longitudinal distance between forelimbs and hindlimbs was shortened in the intact cat, by moving the force plates closer together, the force vectors during quiet stance became more laterally oriented. This was somewhat unexpected, since it is the longitudinal extent of the base of support that is being foreshortened. Intact cats also showed a shortening of the quiet stance vectors with shorter stance distance, in contrast to the lesioned animals which showed a transient (8 – 10 days) increase in vector amplitude. In the first week following the lesion, the labyrinthectomized cats assumed a stance on the floor that was broad-based compared to their pre-lesion stance. On the platform, however, the animals were required to stand with their paws at the same separation as prior to the lesion. Thus, it is likely that the lesioned animals adopted a new set-point in their preferred stance distance that was

longer than the control stance, and that this new set-point persisted as long as the animals were tested. If so, then the observed change in force vector orientation could be considered a normal strategy in response to the required foot placement. This needs to be tested by determining the force vector orientation when the lesioned animals are allowed to assume their preferred stance distance on the force plates.

The changes observed in the tonic activity levels of the sampled muscles may be related to the change in orientation of the quiet stance forces under the paws. Assuming that the semiflexed limb was in a similar position before and after lesion, a change in the force vector orientation would have caused the vector to pass closer to some joints and further from others than in the control condition. The resultant change in moment arm would change the muscular force required at each joint to keep the body upright. Thus, if the post-lesion ground reaction force passed more posterior to the knee joint and closer to the hip joint centre, the observed increase in vastus medialis activity and decrease in gluteus medius activity would be expected. To verify this idea, kinematic data of the limb segment positions with respect to the ground reaction force vector before and after lesion are required.

Response to translation

Bilateral labyrinthectomy did not affect the dynamic responses to platform translation in terms of the spatial and temporal patterning of evoked EMG activity, nor did it prevent the use of the force constraint strategy. Thus, vestibular afferent input is not required for the selection or triggering of the appropriate postural response in this task. The role of the vestibular system in the triggering of postural responses to unexpected perturbations is a subject of controversy. Several studies have shown that patients with bilaterally absent vestibular function have delayed and/or smaller amplitude postural responses than controls (Bussel et al., 1980; Allum and Pfaltz, 1985; Fries et al., 1988; Kleiber et al., 1990), suggesting that vestibular inputs are necessary for the control of balance under certain task conditions (e.g., rotation of the support surface, pushing on the trunk). In contrast, studies using other tasks such as support surface translation have demonstrated that vestibular patients have normal postural responses for maintaining balance (Dietz et al., 1988a,b; Horak et al., 1990). It is not clear what features of a balancing task would require the involvement of vestibular over somatosensory afferents in the selection and timing of the appropriate response.

Various authors have speculated that vestibular information is used primarily during slow or low-frequency sway (Begbie, 1967; Nashner, 1971; Mauritz and Dietz, 1980; Schuster and Talbott, 1980; Allum and Pfaltz, 1985; Keshner et al., 1987; Kleiber et al., 1990), and somatosensory information is used primarily during high-velocity perturbations (Berger et al., 1984; Dietz et al., 1988a). Furthermore, the EMG activity evoked by vestibular stimulation in intact subjects is of low amplitude (Dietz et al., 1988b; Shupert et al., 1990). If vestibular inputs are important for the response to slow perturbations, one would expect a deficit in the response of our cats to translation. The translations were rather slow (plateau velocity 15 cm/sec) and the amplitude of the initial linear acceleration recorded at the head was small, averaging 0.3 m/sec^2 (Inglis and Macpherson, 1991). The amplitude of evoked EMG activity was also small, as compared to amplitudes observed during locomotion or paw shake in the cat (Smith et al., 1977, 1985). Nevertheless, loss of vestibular inputs did not change the timing or pattern of evoked activity. Hence, the velocity of the perturbation, or of the induced sway, cannot be the only factor that determines which sensory system will predominate in the postural response.

Similarly, human subjects without vestibular function are able to execute a normal ankle strategy, generating torque about the ankle joints to reduce sway, following a slow (15 cm/sec) translation of the support surface (Horak et al., 1990). It is significant that these patients were unable to respond to the same perturbation using a different type of postural response, the hip strategy (Shupert et al., 1988;

Horak et al., 1990), in which the hip is flexed or extended in order to generate shear forces against the surface. In the hip strategy, the head is actively counterrotated with respect to the hip rotation, whereas in the ankle strategy, the head appears to move passively, and only by a small amount (Nashner et al., 1988).

Perhaps it is the nature of the postural strategy that is selected, rather than the characteristics of the perturbation, that determine whether vestibular information is necessary for the adequate execution of the response and the maintenance of balance. Different strategies can be used for the same perturbation, depending both on perturbation characteristics and prior experience (Horak et al., 1989). Moreover, the amplitude of the evoked activity, and perhaps the selection of the postural strategy, is independent of such variables as amplitude of head acceleration or amount of stretch of the ankle muscles (Dietz et al., 1988a; Gollhofer et al., 1989). Thus, the ability of vestibular absent subjects to maintain balance may depend not on the acceleration of the head that results from the perturbation, but on the nature of the postural strategy that is selected, specifically the component related to active control of the head upon the trunk. Vestibular input may be essential if the postural strategy requires active control of head position relative to the trunk. Indeed, during platform translations cats exhibit very small movements of the head relative to the trunk (unpublished observations). Additionally, the balance problems experienced by vestibular patients during platform rotation may be due to the need for active head stabilization (Keshner et al., 1987), rather than the fact that the induced sway is in the low frequency range.

The most dramatic effect of bilateral labyrinthectomy on the postural responses of the cats was hypermetria during the initial 8 – 10 days following lesion. This was characterized by an initial overshoot in the response followed by braking activity to restore balance. The mechanism of the overshoot is not clear, since there was only a modest increase in the evoked excitation of a subset of the recorded extensor muscles. If may be that other muscles were recruited that do not normally take part in the response in the intact animal. However, there was no change in the pattern of response for each of the muscles that were sampled (i.e., range of perturbation directions for which responses were evoked). A more profound effect was observed on the recruitment of flexors and derecruitment of extensors which can account for the increased amplitude of the active force vectors for some of the directions of perturbation. These observations would be expected with a decrease in vestibulospinal activity and the resulting decrease in tonic inhibition of flexors and facilitation of extensors (Wilson and Yoshida, 1969; Grillner et al., 1970). In addition, there may have been an overall change in the stiffness of the limbs that would change the mechanical characteristics of the response to perturbations (e.g., a decreased stiffness could result in a larger sway).

Loss of vestibular afferents has been reported to result in a transient hypermetria of gaze (Dichgans et al., 1973, 1974) and in a hypermetria of postural response to different velocities of platform translation in human subjects (Horak, 1990). This latter study provides an interesting contrast between human and cat, since the hypermetria was transient in the cat, resolving after 8 – 10 days, but was long-lasting in the human study, being observed in well-compensated patients. Unlike the human subjects, the cats had considerable practice with the perturbations prior to their lesion, and were always given perturbations in blocked trials, so that they could predict the direction and amplitude of each translation. Perhaps the predictive nature of the trials allowed the animals to adapt their responses after a certain period of recovery. If so, then one would expect a return of the hypermetria under conditions in which the perturbation was not predictable. Indeed, even after five months of recovery, hypermetria was occasionally observed in these animals during various behaviors in their home environment.

The underlying cause of the hypermetria is not clear. The decrease in facilitation of extensors due to reduced activity in the direct vestibulospinal pathways should produce an under-response, or

hypometria in the evoked activity. On the other hand, a decreased drive onto cerebellar Purkinje cells due to reduced firing in vestibular afferents may result in a disinhibition of descending pathways of the motor system, resulting in hypermetria. Clearly, there are multiple pathways and multiple systems that are affected by labyrinthectomy, and the results of such a lesion are difficult, if not impossible, to predict from the anatomy alone.

In conclusion, bilateral labyrinthectomy in the cat produces remarkably little effect on both quiet stance and on the response to translation of the support surface in the horizontal plane. The most notable effect was a transient hypermetria in the response to translation. These findings are surprising in light of the profound effects of this lesion on the animal's general motor behavior (Thomson et al., 1991). We conclude that vestibular information is not required for the selection or the triggering of the appropriate postural response to translation.

Acknowledgements

The authors would like to thank Dr. R.H. Schor for performing the labyrinthectomies, and for his thoughtful discussions on this study. We also thank D. Thomson for his valuable assistance. This work was supported by grants to JMM from the MRC of Canada and Queen's University.

References

Allum, J.H.J. and Pfaltz, C.R. (1985) Visual and vestibular contributions to pitch sway stabilization in the ankle muscles of normals and patients with bilateral peripheral vestibular deficits. *Exp. Brain Res.*, 58: 82 – 94.

Begbie, G.H. (1967) Some problems of postural sway. In: A.V.S. de Reuck and J. Knight (Eds.), *Myototic, Kinesthetic and Vestibular Mechanisms,* Little Brown, Boston, MA, pp. 80 – 104.

Berger, W., Dietz, V. and Quintern, J. (1984) Corrective reactions to stumbling in man: neuronal co-ordination of bilateral leg muscle activity during gait. *J. Physiol. (Lond.),* 357: 109 – 126.

Bussel, B., Katz, R., Pierrot-Deseilligny, E., Bergego, C. and Hayat, A. (1980) Vestibular and proprioceptive influences on the postural reactions to a sudden body displacement in man. In: J.E. Desmedt (Ed.), *Spinal and Supraspinal Mechanisms of Voluntary Motor Control and Locomotion,* Karger, Basel, pp. 310 – 322.

Carpenter, M.B., Fabrega, H. and Glinsmann, W. (1959) Physiological deficits occurring with lesions of labyrinth and fastigial nuclei. *J. Neurophysiol.*, 22: 222 – 234.

Dichgans, J., Bizzi, E., Morasso, P. and Tagliasco, V. (1973) Mechanisms underlying recovery of eye-head coordination following bilateral labyrinthectomy in monkeys. *Exp. Brain Res.*, 18: 548 – 562.

Dichgans, J., Bizzi, E., Morasso, P. and Tagliasco, V. (1974) The role of vestibular and neck afferents during eye-head coordination in the monkey. *Brain Res.*, 71: 225 – 232.

Dietz, V., Horstmann, G. and Berger, W. (1988a) Involvement of different receptors in the regulation of human posture. *Neurosci. Lett.*, 94: 82 – 87.

Dietz, V., Horstmann, G.A. and Berger, W. (1988b) Fast head tilt has only a minor effect on quick compensatory reactions during the regulation of stance and gait. *Exp. Brain Res.*, 73: 470 – 476.

Dow, R.S. (1938) The effects of unilateral and bilateral labyrinthectomy in monkey, baboon and chimpanzee. *Am. J. Physiol.*, 121: 392 – 399.

Fries, W., Dieterich, M. and Brandt, T. (1988) Otolithic control of posture: vestibulo-spinal reflexes in a patient with a tullio phenomenon. In: E. Pirodda and O. Pompeiano (Eds.), *Neurophysiology of the Vestibular System,* Karger, Basel, pp. 162 – 165.

Gollhofer, A., Horstmann, G.A., Berger, W. and Dietz, V. (1989) Compensation of translational and rotational perturbations in human posture: stabilization of the centre of gravity. *Neurosci. Lett.*, 105: 73 – 78.

Grillner, S., Hongo, T. and Lund, S. (1970) The vestibulospinal tract. Effects on alpha-motoneurones in the lumbosacral spinal cord in the cat. *Exp. Brain Res.*, 10: 94 – 120.

Grossman, G.E. and Leigh, R.J. (1990) Instability of gaze during locomotion in patients with deficient vestibular function. *Ann. Neurol.*, 27: 528 – 532.

Horak, F.B. (1990) Comparison of cerebellar and vestibular loss on scaling of postural responses. In: T. Brandt, W. Paulus, W. Bles, M. Dieterich, S. Krafczyk and A. Straube (Eds.), *Disorders of Posture and Gait,* Thieme, New York, pp. 370 – 373.

Horak, F.B., Diener, H.C. and Nashner, L.M. (1989) Influence of central set on human postural responses. *J. Neurophysiol.*, 62: 841 – 853.

Horak, F.B., Nashner, L.M. and Diener, H.C. (1990) Postural strategies associated with somatosensory and vestibular loss. *Exp. Brain Res.*, 82: 167 – 177.

Igarashi, M., Watanabe, T. and Maxian, P.M. (1970) Dynamic equilibrium in squirrel monkeys after unilateral and bilateral labyrinthectomy. *Acta Otolaryngol.*, 69: 247 – 253.

Inglis, J.T. and Macpherson, J.M. (1991) Head acceleration following linear translations in the freely-standing cat. *Exp. Brain Res.*, 87: 108 – 112.

Kasai, T. and Zee, D.S. (1978) Eye-head coordination in

labyrinthine-defective human beings. *Brain Res.*, 144: 123 – 141.

Keshner, E.A., Allum, J.H.J. and Pfaltz, C.R. (1987) Postural coactivation and adaptation in the sway stabilizing responses of normals and patients with bilateral vestibular deficit. *Exp. Brain Res.*, 69: 77 – 92.

Kleiber, M., Horstmann, G.A. and Dietz, V. (1990) Body sway stabilization in human posture. *Acta Otolaryngol.*, 110: 168 – 174.

Lacour, M. and Xerri, C. (1981) Vestibular compensation: new perspectives. In: H. Flohr and W. Precht (Eds.), *Lesion-Induced Neuronal Plasticity in Sensorimotor Systems*, Springer, New York, pp. 240 – 253.

Macpherson, J.M. (1988a) Strategies that simplify the control of quadrupedal stance. 1. Forces at the ground. *J. Neurophysiol.*, 60: 204 – 217.

Macpherson, J.M. (1988b) Strategies that simplify the control of quadrupedal stance. 2. Electromyographic activity. *J. Neurophysiol.*, 60: 218 – 231.

Macpherson, J.M., Lywood, D.W. and van Eyken, A. (1987) A system for the analysis of posture and stance in quadrupeds. *J. Neurosci. Methods*, 20: 73 – 82.

Magnus, R. (1926) On the co-operation and interference of reflexes from other sense organs with those of the labyrinths. *The Laryngoscope*, 36: 701 – 712.

Marchand, A. and Amblard, B. (1979) Contrôle postural chez les chats délabyrinthés à la naissance. *Agressologie*, 20: 201 – 202.

Marchand, A.R., Amblard, B. and Cremieux, J. (1988) Visual and vestibular control of locomotion in early and late sensory-deprived cats. In: O. Pomeiano and J.H.J. Allum (Eds.), *Progress in Brain Research, Vol. 76*, Elsevier, Amsterdam, pp. 229 – 238.

Mauritz, K.-H. and Dietz, V. (1980) Characteristics of postural instability induced by ischemic blocking of leg afferents. *Exp. Brain Res.*, 38: 117 – 119.

Money, K.E. and Scott, J.W. (1962) Functions of separate sensory receptors of nonauditory labyrinth of the cat. *Am. J. Physiol.*, 202: 1211 – 1220.

Nashner, L.M. (1971) A model describing vestibular detection of body sway motion. *Acta Otolaryngol.*, 72: 429 – 436.

Nashner, L.M. (1973) Vestibular and reflex control of normal standing. In: R.B. Stein, K.G. Pearson, R.S. Smith and J.B. Redford (Eds.), *Control of Posture and Locomotion*, Plenum, New York, pp. 291 – 308.

Nashner, L.M., Shupert, C.L. and Horak, F.B. (1988) Head-trunk movement coordination in the standing posture. In: O. Pompeiano and J.H.J. Allum (Eds.), *Progress in Brain Research, Vol. 76*, Elsevier, Amsterdam, pp. 243 – 251.

Schuster, D. and Talbott, R.E. (1980) Optimal and adaptive control in canine postural regulation. *Am. J. Physiol.*, 239: R93 – R114.

Shupert, C.L., Black, F.O., Horak, F.B. and Nashner, L.M. (1988) Coordination of the head and body in response to support surface translations in normals and patients with bilaterally reduced vestibular function. In: B. Amblard, A. Berthoz and F. Clarac (Eds.), *Posture and Gait: Development, Adaptation and Modulation*, Elsevier, New York, pp. 281 – 289.

Shupert, C., Horak, F., Dietz, V. and Horstmann, G.A. (1990) Automatic responses to head/neck perturbations. In: T. Brandt, W. Paulus, W. Bles, M. Dieterich, S. Krafczyk and A. Straube (Eds.), *Disorders of Posture and Gait*, Thieme, New York, pp. 177 – 180.

Smith, J.L., Edgerton, V.R., Betts, B. and Collatos, T.C. (1977) EMG of slow and fast ankle extensors of cat during posture, locomotion, and jumping. *J. Neurophysiol.*, 40: 503 – 513.

Smith, J.L., Hoy, M.G., Koshland, G.F., Phillips, D.M. and Zernicke, R.F. (1985) Intralimb coordination of the paw-shake response: a novel mixed synergy. *J. Neurophysiol.*, 54: 1271 – 1281.

Thomson, D.B., Inglis, J.T., Schor, R.H. and Macpherson, J.M. (1991) Bilateral labyrinthectomy in the cat: motor behavior and quiet stance parameters. *Exp. Brain Res.*, 85: 364 – 372.

Wilson, V.J. and Yoshida, M. (1969) Comparison of effects of stimulation of Deiter's nucleus and medial longitudinal fasciculus on neck, forelimb and hindlimb motoneurons. *J. Neurophysiol.*, 32: 743 – 758.

J.H.J. Allum, D.J. Allum-Mecklenburg, F.P. Harris and R. Probst
Progress in Brain Research, Vol. 97

CHAPTER 22

Vestibular control of skeletal geometry in the guinea pig: a problem of good trim?

P.P. Vidal[1], D.H. Wang[2], W. Graf[1] and C. de Waele[1]

[1] *Laboratoire Physiologie Neurosensorielle du C.N.R.S., 75270 Paris Cedex 06, France and* [2] *Department of Physiology and Biophysics, New York University Medical Center, New York 10016, U.S.A.*

Motor control of different segments of the body with multiple degrees of freedom appears to be coordinated by utilizing preferred axes of motor activity. This hypothesis may also be applied to vestibular control of posture. To explore this question we studied the anatomical relationship between the head and the cervical vertebral column by taking radiographs of the head-neck region in unrestrained alert guinea pigs. We determined that biomechanical constraints contribute to the stereotypical skeletal geometry observed in the resting animal and to a functional segmentation of the head-neck movement apparatus. Subsequent lesion studies of vestibular end organs with quantification of the resulting postural syndromes suggest that the functional segmentation of the cervical vertebral column corresponds to a functional partitioning of vestibular afferents. Our findings also indicate that the sensorimotor transformation mechanisms necessary to convert a given head velocity signal into the appropriate neck motor frame are already embedded in the networks provided by second-order vestibular neurons. Good trim of postural control will be the end result of an appropriate internal representation of the objective vertical.

Key words: Postural control; Vestibular system; Gravity vector; Head-neck system

Introduction

Our group has been studying three-dimensional skeletal geometry in various species of vertebrates focusing on the head-neck ensemble. Two major findings resulted from these investigations. First, the resting posture in alert subjects displays common characteristics across species, including humans. That is, the cervical vertebral column is held oriented vertically and the plane of the horizontal semicircular canals is kept tilted upward by 10 – 20° (Fig. 1; Vidal et al., 1986). This head posture brings the utricular macula approximately into the earth horizontal plane (Graf et al., 1992b). Secondly, the ranges of motion of the head-neck articulations are a significant constraint, limiting the number of movement possibilities of the head-neck ensemble (Vidal et al., 1988; see also Graf et al., 1992a). We hypothesize that this reduction in degrees of freedom simplifies the computational load of the CNS during head-neck movements such as gaze shifts, gaze stabilization, feeding behavior, etc. It should be kept in mind, however, that the resting posture may not be a similar and constant phenomenon across higher vertebrates. Inter-species and inter-individual differences regarding the manifestation of this posture are quite noticeable. It is also obvious that many different postures can be adopted when an animal is at rest. Finally, the term "rest" is difficult to define. Our use of this term implies precise quantified behavioral observations for which some invariant geometrical characteristics need to be interpreted.

The existence of a stereotyped resting posture also introduces the question about its stabilization because the described skeletal geometry is not embed-

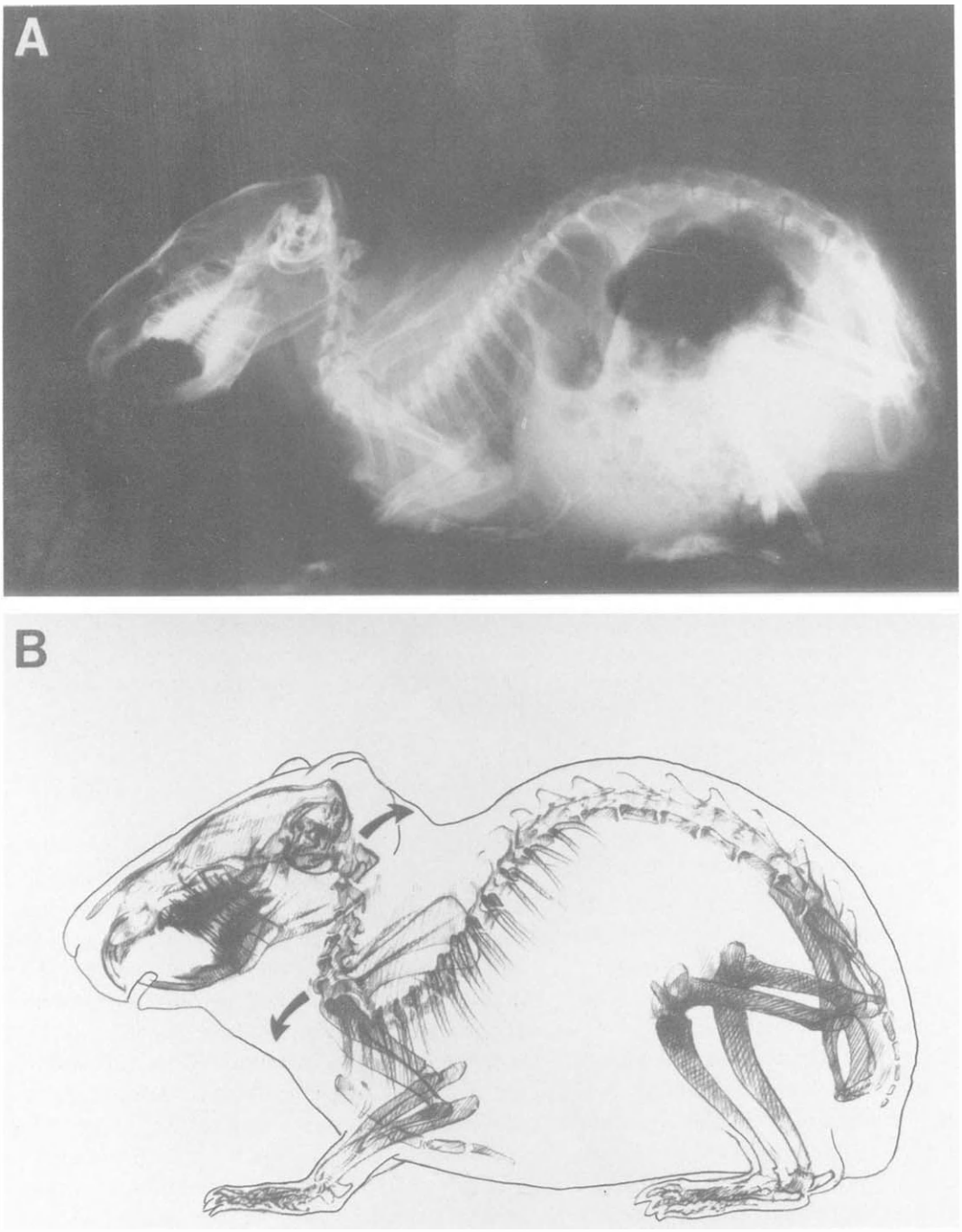

Fig. 1. Lateral X-ray exposure and sagittal plane biomechanics of the head-neck movement system in the guinea pig, as an example of a quadrupedal vertebrate. *A*. Lateral radiograph of the animal at rest. *B*. Artist's rendering of the same exposure. Note vertical orientation of cervical vertebral column. Curved arrows indicate the directions of movement that are possible at the atlanto-occipital articulation and at the cervico-thoracic junction. Since the atlanto-occipital joint is fully flexed in the resting position, only extension movements (raising of the head) are possible at this joint. Similarly, since joints between the vertebrae forming the cervico-thoracic junction are fully extended at rest, only movements in the flexion direction (lowering of the head-neck apparatus) are possible at this junction. Large scale flexion/extension movements within the cervical spine are not possible.

ded in the skeletal structure. Intrinsic biomechanical constraints do not appear to force various animals to adopt a defined resting posture. The postural system is, in theory, overcomplete. Most investigators have introduced concepts such as body schemata or the subjective vertical when trying to explain postural stabilization. Our results point in a slightly different direction. Using a naval analogy, we would like to propose that, in case of resting posture, it is important for higher vertebrates to be in good trim. The subject is envisioned as operating in the gravity field like a boat in water. This comparison illustrates the fact that a particular symmetrical posture in the frontal, sagittal and horizontal planes is implemented and controlled. According to this viewpoint, the vertical and straight ahead directions should be considered more adequately as the perceptual consequence of a seemingly correct symmetrical posture rather than the critical variables to be controlled.

One obvious candidate to control trim is the vestibular system. Despite its name, the vestibular nuclear complex in essence contains a three-dimensional representation of head, trunk, and probably leg positions including movement in space on the basis of a number of sensory inputs: vestibular, visual and proprioceptive information converges at this level. The system is organized bilaterally and good trim may simply arise from the vestibular control of various motoneuron pools influencing the axial musculature on both sides of the body.

Nearly 30 years ago, Cohen, Suzuki and colleagues published a pioneering series of studies (Cohen and Suzuki, 1963; Suzuki and Cohen, 1964; Cohen et al., 1964; Suzuki et al., 1964): they stimulated electrically the surgically isolated three semicircular canal nerves and the utricular nerve. By quantifying the resulting eye rotations, these authors were able to predict numerous characteristics of the vestibulo-ocular network. Subsequent electrophysiological studies following their publications confirmed the interest in their elegant experimental approach (see, e.g., Baker and Berthoz, 1977). One of the main conclusions of their work was that the sensorimotor transformations underlying ocular stabilization were embedded in a hard-wired neuronal network linking each of the vestibular end organs to particular sets of extraoculomotor motoneurons.

A few years ago we decided to utilize the experimental approach of Suzuki and Cohen (1964) in the field of head-neck stabilization. The underlying hypothesis was that by stimulating unilaterally each of the nerves coming from the different vestibular end organs, a new trim of posture should be induced. A new skeletal geometry should be the result of the activation of a hard-wired connectivity linking a given end organ to the respective motoneuron pool that it controls. In theory, this approach would allow us to differentiate which body segments are controlled by the semicircular canals, and which by the otoliths (sacculus and utriculus). Furthermore, it should be possible to determine the reference plane of each of the end organs. Such experiments would also allow the testing of our hypothesis whether the number of possibilities how head-neck posture can be stabilized is limited. For example, according to our interpretation of the biomechanics of the system, head movements in the frontal plane in quadrupedal mammals are performed by a rotation of the thoracic vertebrae, possibly accompanied by a flexion of the legs: when the cervical vertebral column is held upright, none of its vertebrae can bend laterally in the frontal plane. We also hypothesized that the sacculus, because of its macular orientation at the resting position, should be suited best to control the vertical orientation of the neck in the frontal plane. Adding these two ideas together led to the prediction that a unilateral saccular nerve stimulation should produce a contralateral tilt of the head-neck ensemble in the frontal plane via rotation of thoracic vertebrae. Thus, saccular input is thought to be relayed to motoneuron pools controlling axial back muscles.

Our paradigm of alert and unrestrained animals, however, posed some problems regarding posture of the entire animal. Therefore, we decided to utilize selective lesions of the peripheral subdivisions of the vestibular nerve instead of selective stimulation. The idea was to induce the mirror image of skeletal

geometry changes expected during selective stimulation.

The guinea pig was chosen as an experimental animal because the anatomy of its middle ear allows selective surgical approaches. Moreover, this animal is our current model for the study of membrane properties of vestibular neurons in vitro.

Methods

Experimental animals were pigmented guinea pigs (400 – 800 g body weight). During surgery and non-invasive lesioning (centrifugation), the animals were anesthetized with a Rompun (4 mg/kg)/ketamine (100 mg/kg) mixture. Selective lesions were either performed surgically or by centrifugation (for otolith ablations).

Surgical procedures

Selective lesions were performed on the horizontal and anterior ampullary nerves, the utricular and saccular maculae, and the posterior semicircular canal ampulla. Sections of the horizontal and anterior ampullary nerves were performed 2 mm below the ampulla. However, it was impossible to perform separate selective lesions of the utricular and posterior ampullary nerves. In other animals, the otolithic maculae and posterior canal ampullae were both destroyed by a sharp stylus introduced into the oval window and membranous labyrinth in front of the ampulla, respectively. In one serendipitous case, only the saccular macula was destroyed. This case is reported here because it confirms the data obtained with centrifugation (see below). Aspiration of endolymphatic liquid was carefully avoided and any leakage was prevented by applying bone wax. Depending on the question, the selective lesions were isolated or several of them were performed on the same animal. Control operations, i.e. isolated openings of the oval window and the membranous labyrinth near the posterior canal ampulla were undertaken without destruction of the receptors. Subsequently, the openings were resealed.

Centrifugation procedure

Following the method of Wittmaak (1909), anesthetized animals were placed in a centrifuge and spun at approximately 30 $\times$ g for 45 sec. Changing head position with respect to the force vector allowed any combination of unilateral/bilateral saccular or bilateral utricular lesions. Parameters for selective lesions were determined previously (described in detail by de Kleijn and Magnus, 1921a,b; de Burlet and de Haas, 1923; see also Magnus, 1924) and tested in pilot experiments in our laboratory.

Animals were positioned vertically in restraining tubes in the centrifuge. Successful bilateral utricular lesions were obtained when the animal's head was tilted backwards by 120° from a normal earth horizontal position with the back of the head pointing outward. Saccular lesions were achieved with the animal's head in the same position, but with a 90° rotation about a vertical axis compared to the previous position. In that condition, either the left or the right ear pointed outward and thus the force vector acted laterally on the head rendering unilateral saccular ablations. For a bilateral saccular ablation, the animal was rotated by 180° and the procedure repeated. For a complete ablation of all otoliths, the animals had to be centrifuged three times with different head orientations in reference to the force vector. Following centrifugation, the animals briefly required artificial ventilation until they breathed spontaneously.

As soon as the animals had recovered from general anesthesia, they were tested for postural reflexes following the protocol of de Kleijn and Magnus (1921a), as an immediate control for successful otolith ablation.

X-ray radiography

After full recovery from anesthesia (ca. 4 – 7 h post-operatively) X-ray photographs were taken. Exposures were obtained from above with the X-ray tube 60 cm away from the film, and laterally at a distance of 90 cm. After each X-ray session, top views

and frontal photographs were taken. The following parameters were analyzed:

In the normal guinea pig, resting posture is characterized by the animal looking straight ahead. In that condition the two tympanic bullae are superimposed. Horizontal head rotation, occurring by vertical axis head rotation at the atlanto-axial articulation and the underlying cervical vertebrae, can be detected by an anterior/posterior shift of the anterior edges of the two tympanic bullae on profile views (see arrows in Fig. 2*A*).

The lateral tilt of the cervical column in the frontal plane can easily be appreciated on top views by measuring the distance between the atlanto-occipital articulation and an axis passing through the sacrum and the first thoracic vertebra (Th_1) (see long arrow in Fig. 7*B*). Lateral tilt can also be detected in profile view because it induces a superior/inferior shift of the two inferior edges of the two tympanic bullae (see arrows in Fig. 7*A*).

The tilt of the head-neck ensemble in the frontal plane is caused by rotations of thoracic and lumbar vertebrae about their longitudinal axes. This rotation can be detected on top view X-ray photographs allowing determination of the rotation of each thoracic and lumbar vertebra by locating the position of the respective spinous processes (see short arrows in Fig. 7*B*).

The rotation of the cervical column in the sagittal plane takes place at two levels. Upward movement of the head appears at the atlanto-occipital articulation (see arrows in Figs. 1*B* and 3*A*). Downward movement of the head is performed at the cervico-thoracic junction (see arrows in Figs. 1*B* and 8*A*). Both of these rotations can easily be appreciated on profile views. Finally, placement of the limbs can be determined from top view X-rays.

All above described parameters can be measured precisely as described earlier (de Waele et al., 1989). However, our previous preliminary report dealt only with the qualitative description of the postural syndrome following selective lesions.

Histological procedures

After the conclusion of all experiments and controls, the animals were killed with an overdose of pentobarbital. The heads were fixed for several days in standard formaldehyde solution. All skin and muscle tissue was removed and the bone was decalcified in decalcifying solution (American Scientific Products; Rapid Decalcifier Eurobio) for three days. After this procedure, the heads were embedded in paraffin and sections were prepared for light microscopy following standard procedures (see de Waele et al., 1989).

In the centrifugated animals, the receptor cells were typically separated from the supporting cells and the otoconial membrane was disrupted indicating that the otoconia had been sheared off the maculae. Due to the treatment with formaldehyde, the otoconia were dissolved during the fixation process in all preparations (see Graf et al., 1992b).

Selective lesions of the semicircular canal system

Horizontal semicircular canal nerve lesions

The horizontal semicircular canal system is organized in a push-pull fashion. A unilateral lesion should produce a head rotation towards the side of the lesion in the horizontal plane (Fig. 2*B*). The cervical vertebral column is still held vertically in the frontal and in the sagittal plane. Head rotation in the horizontal plane is indicated by the presence of an anterior/posterior shift of the anterior edges of the two tympanic bullae, and by the absence of a superior/inferior shift of the inferior borders. Our previous biomechanical studies suggest that this head displacement occurs by a vertical axis rotation at the atlanto-axial articulation and by small degree rotations of the underlying cervical vertebrae. The direction of the displacement indicates that a given activated horizontal semicircular canal will excite contralateral motoneuron pools in the upper cervical cord. Considering the pulling directions of the neck muscles, in this case motoneurons innervating obliquus capitis, splenius, rectus and complexus muscles presumably will be excited. These muscles act as rotators of the head in the earth horizontal plane.

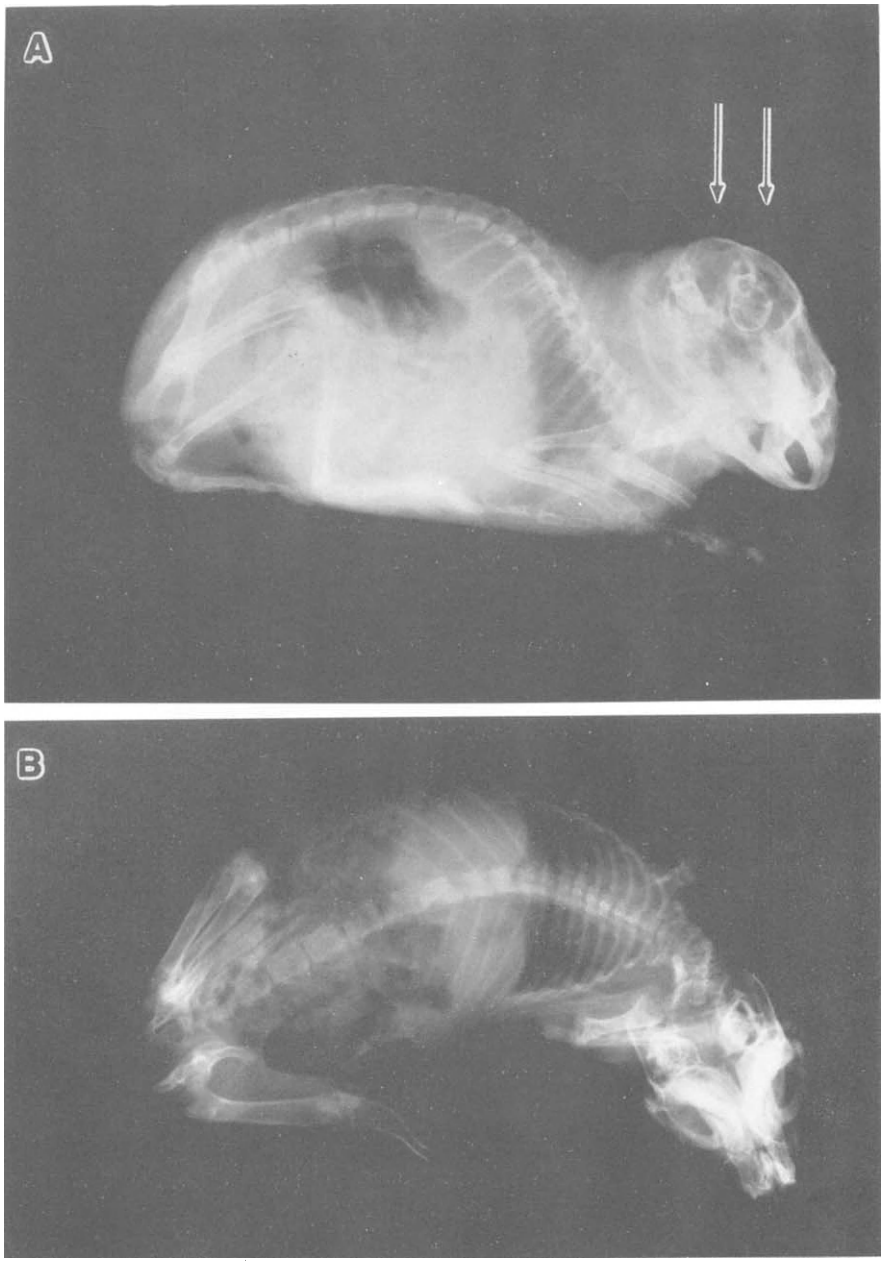

Fig. 2. Lateral (*A*) and top view (*B*) X-ray exposure of a guinea pig with a unilateral horizontal canal lesion. Note head rotation towards the ipsilateral (right) side of the lesion. Arrows indicate anterior/posterior, but no vertical displacement of the tympanic bullae. The top view illustrates the head rotation and bending of the body towards the right (lesioned side).

Posterior semicircular canal ampullae lesions

For a few hours post-operatively, bilateral lesions of the posterior semicircular ampullae induced a bilateral extension of the forelimbs coupled with an upward head movement involving the atlanto-occipital joint. In that situation, input from the two anterior canals dominated the animal's postural adjustments inducing a "correction" of trim oriented

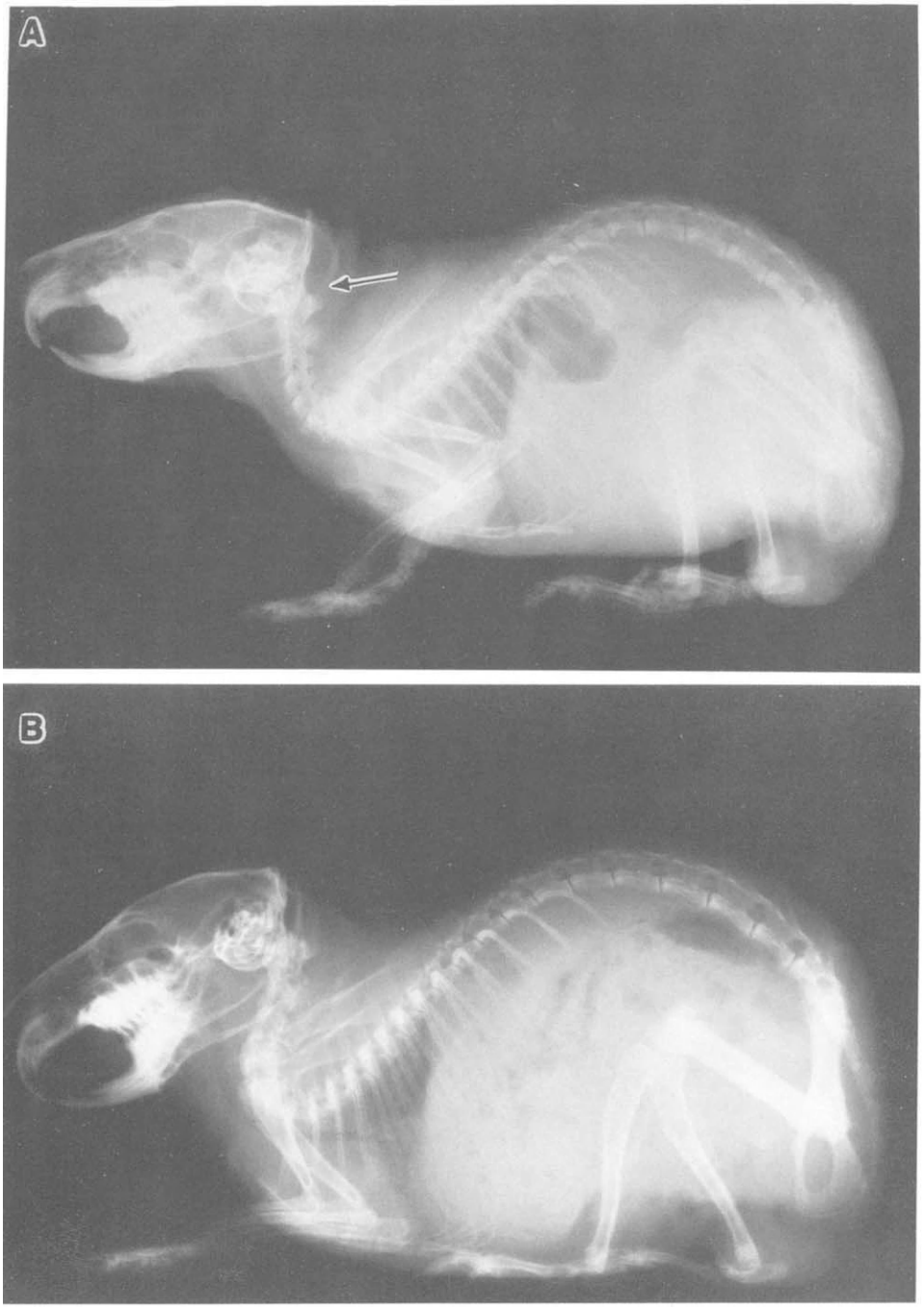

Fig. 3. Lateral X-ray photographs of guinea pigs with bilateral (*A*) and unilateral (*B*) posterior canal lesions. Note slight elevation of the head in *A* occurring at the atlanto-occipital articulation (arrow). Unilateral lesion of the posterior canal does not produce any lesion symptoms.

backward in the sagittal plane. This posture is induced by a perceived forward tilt subsequent to the lesion.

This result was predicted from our biomechanical studies. We hypothesized that from the resting posture, large upward gaze shifts in the sagittal plane have to take place at the atlanto-occipital articulation. Upward gaze shifts involving the entire head-neck ensemble could not occur at the cervico-thoracic junction because there the vertebrae are held near their limits of extension when the animal is at rest. Our results predict that motoneurons controlling the muscles inserting at the lower cervical and upper thoracic vertebrae and originating from the lambdoid ridge of the skull (splenius, complexus and rectus capitis elevators) should be the primary target of excitatory anterior semicircular canal inputs. Unilateral lesion of a posterior semicircular ampulla did not induce any prominent change in the overall head-neck configuration at rest (Fig. 3*B*). The absence of any asymmetry suggests that information coming from an intact posterior semicircular canal is conveyed to motoneurons on both sides of the spinal cord. This observation is in accordance with the projection pattern of the respective second-order vestibular neurons (Shinoda et al., this volume). In addition, convergence from the two anterior semicircular canal afferents could also take place at the interneuronal level in the spinal cord (see Wilson et al., this volume).

Anterior semicircular canal nerve lesions

Bilateral lesions of the two anterior canal nerves remain to be performed because of the surgical complexity of these lesions. However, unilateral lesion did not produce any noticeable change in the skeletal geometry at resting posture (Fig. 4). Thus, we propose that anterior canal afferent information is also distributed bilaterally to the spinal cord. Again, this prediction is partially supported by the branching pattern of inhibitory second-order vestibular neurons to dorsal neck muscles (see Shinoda et al., this volume). No information is available as yet regarding excitatory neurons. We expect these neurons to project to motoneuron pools controlling the muscles that lower the head-neck ensemble at the cervico-thoracic junction. Indeed, lowering of the head in the sagittal plane has to take place at that level by moving the neck. The atlanto-occipital articulation is already maximally flexed at the resting posture adopted by most higher vertebrates, including humans.

Bilateral lesions of all semicircular canals

After initial severe left/right oscillations of the whole body, the animals were reasonably able to control their posture (Fig. 5). Since the semicircular system is essentially suited to respond to a dynamic disturbance, it did not come as a surprise when the combined selective lesions of all six semicircular canals (anterior and horizontal canal nerves, posterior canal ampullae) failed to produce a detectable change in the skeletal geometry of the resting posture (Fig. 5). This observation simply reinforced the idea that the otolithical system controls the overall static configuration of the head-neck ensemble while the semicircular canal system implements the return to the resting posture when it is disturbed. Along that line of thought, a bilateral lesion of the semicircular canal system leads to vast randomly distributed head and neck movements when the posture of the lesioned animals is perturbed. Similar results have been obtained in canal plugged cats (Schor et al., 1984).

Lesions of the otolith system

The otoliths are the main candidates to assure a good trim of the head-neck ensemble at rest position since they sense both linear head acceleration and head orientation with respect to gravity. For the same reason, the system is well suited to provide concurrent information about verticality. The orientation pattern of the sensory hair cell on the utricular and saccular macula allows predictions about the direction of a given corrective response. For example, the saccular and the utricular system should correct trim in the frontal and sagittal planes, respectively. Bilateral lesions of the otolith system did not produce gross disturbances of the skeletal

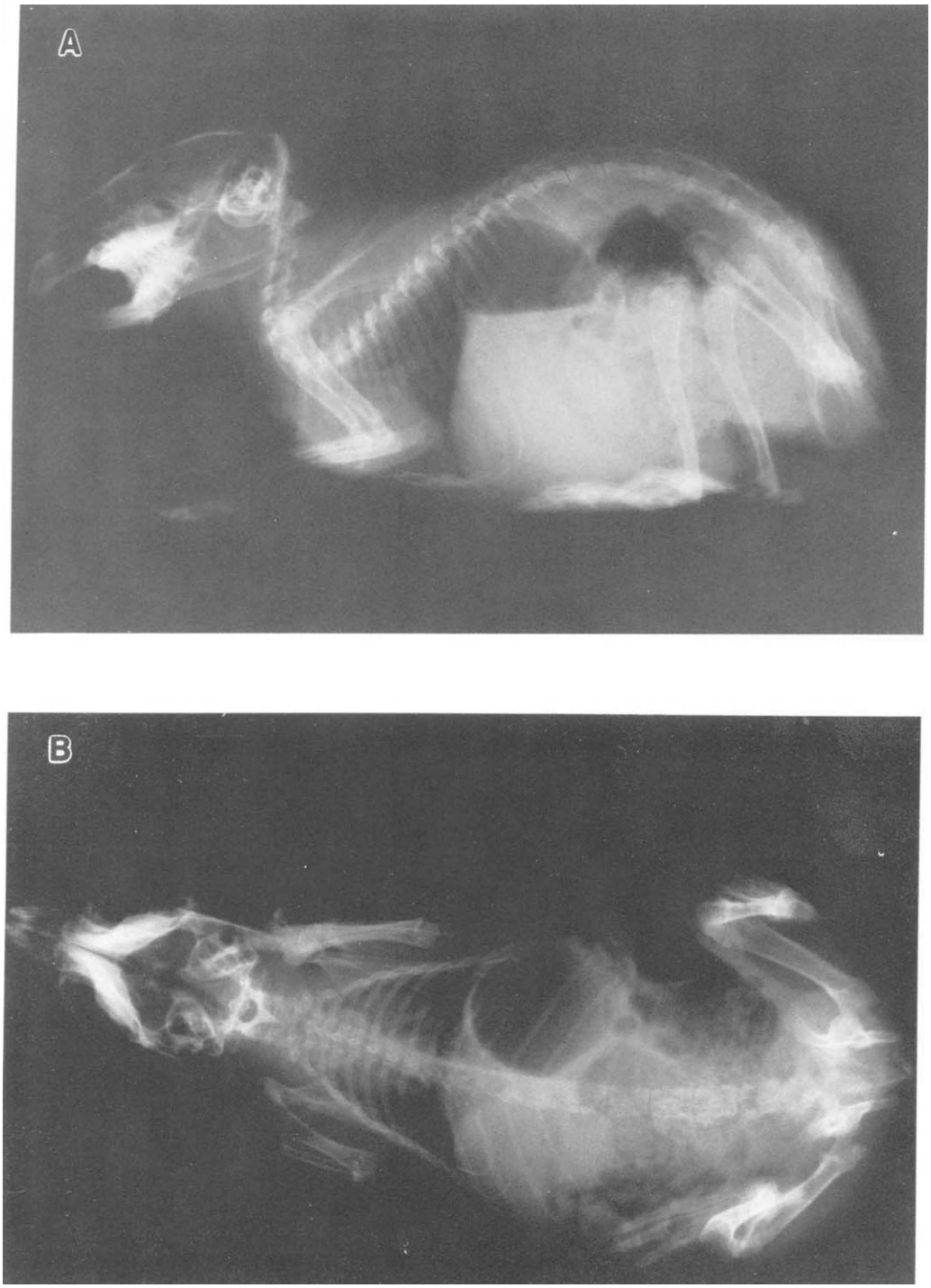

Fig. 4. Lateral (*A*) and top view (*B*) X-ray photographs of a guinea pig with a unilateral anterior canal lesion. There are no noticable lesion symptoms.

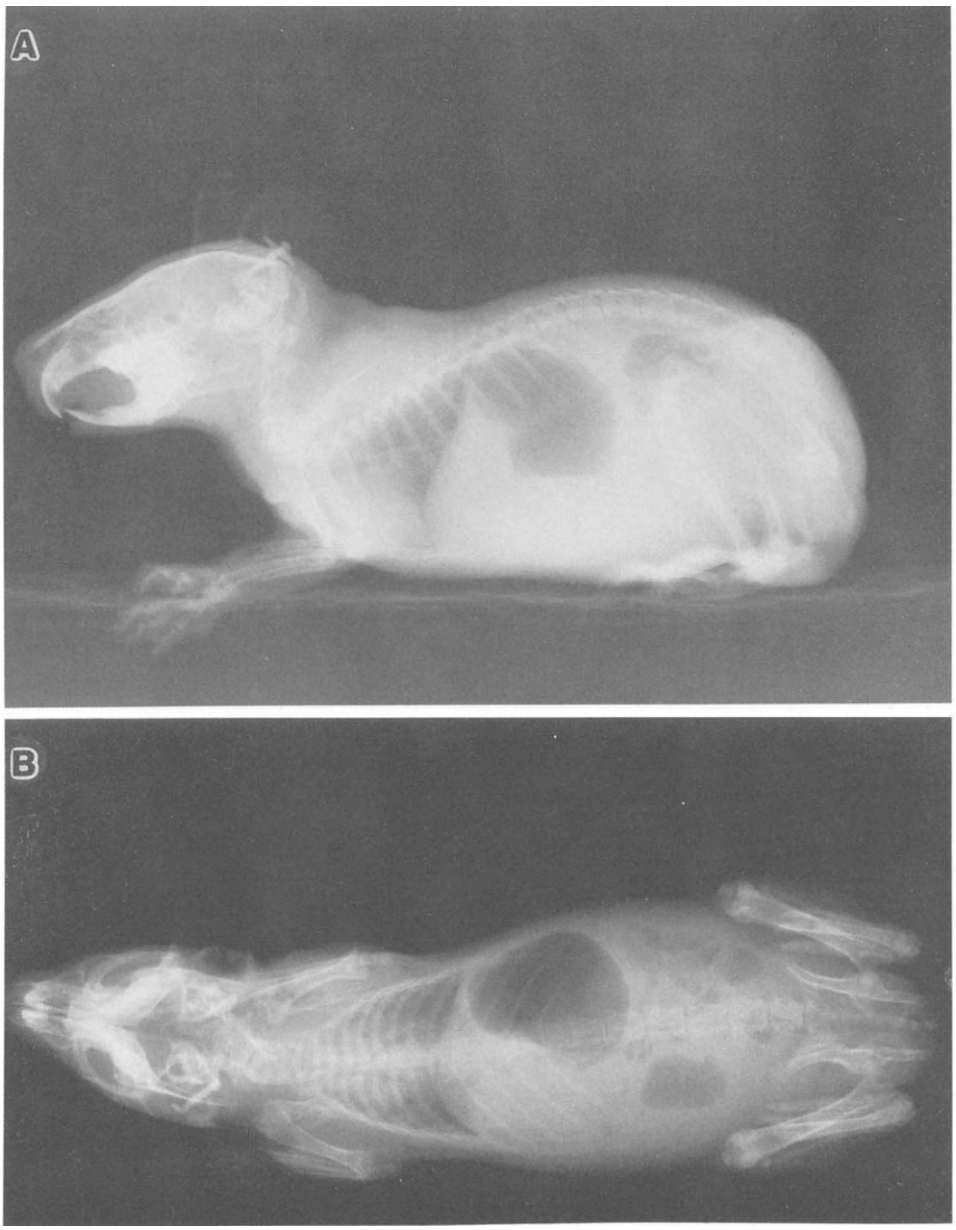

Fig. 5. Lateral (*A*) and top view (*B*) X-ray photographs of a guinea pig with a bilateral complete semicircular canal lesion. After initial symptoms have subsided, the animal is able to control its posture quite satisfactorily.

geometry at resting position when the animal was kept in a lit environment and after initial disorientation had subsided (see Fig. 6). In such a case, visual and proprioceptive information converging at the vestibular nuclear level provided sufficient cues to maintain a reasonably correct static head balance.

Selective surgical lesions of otoliths

Unilateral otholith lesions sparing the semicircular canals induced a side-tilt of the head-neck ensemble towards the side of the lesion (Fig. 7). Top view X-ray photography of the cervical column and the head did not indicate any rotation about the vertical

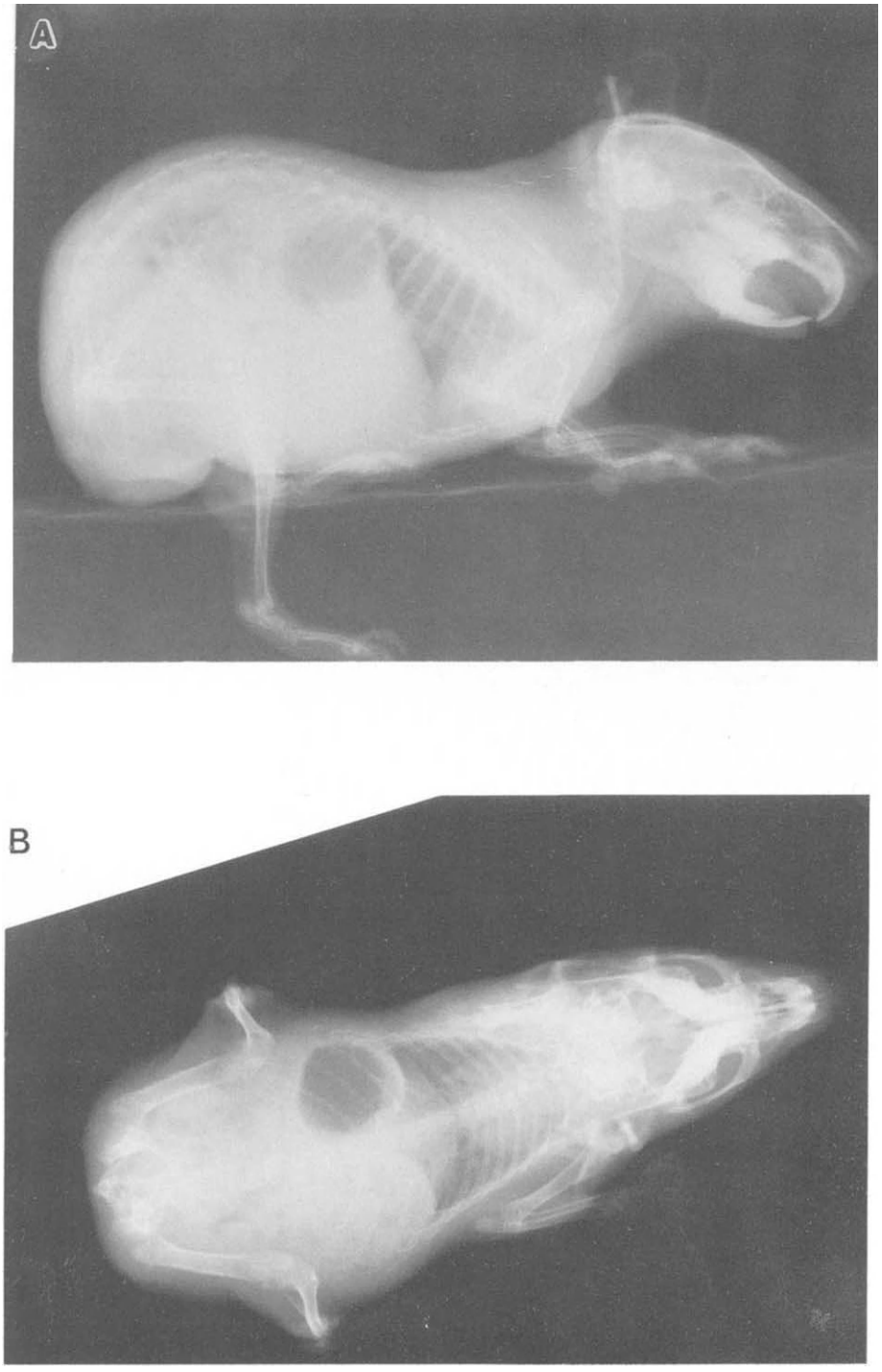

Fig. 6. Lateral (*A*) and top view (*B*) X-ray photographs of a guinea pig with bilateral otolith ablation. After initial disorientation has subsided, the animal has a reasonable postural control in a lit environment.

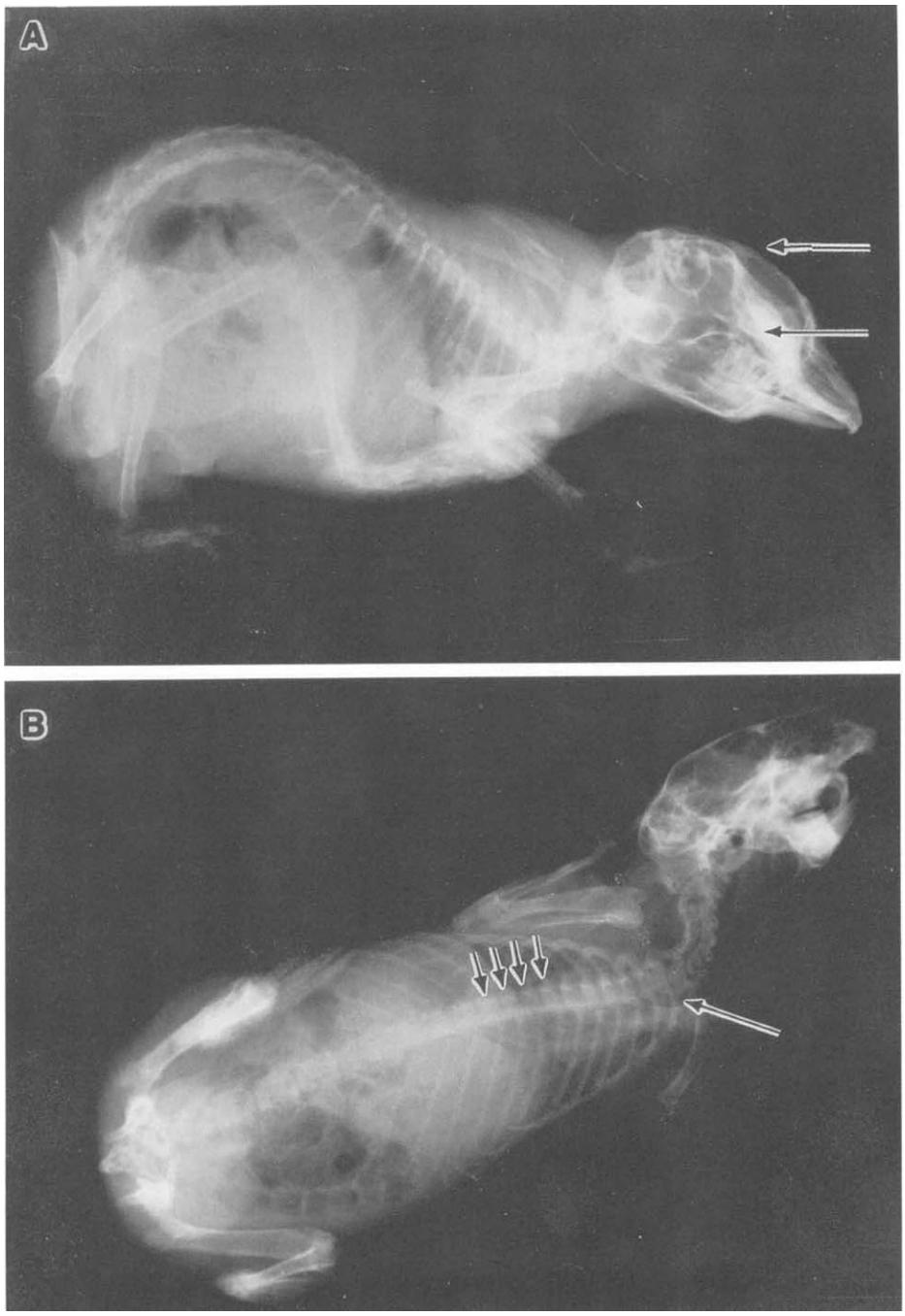

Fig. 7. Lateral (*A*) and top view (*B*) X-ray photographs of a guinea pig with a unilateral otolith ablation. Note side tilt of the entire head-neck ensemble towards the side of the lesion. Arrow in *A* indicate vertical, but not anterior/posterior displacement of the tympanic bullae. Long arrow in *B* indicates the first thoracic vertebra (Th_1). Short arrows indicate progressive rotation of spinous processes of thoracic vertebrae.

axis, i.e., the animal was looking straight ahead (Fig. 7*B*). This is also illustrated on the profile view where the anterior edges of the tympanic are transposed vertically but not in the anterior-posterior direction (Fig. 7*A*; see also de Waele et al., 1989). As proposed earlier, neck rotation in the frontal plane has to occur when the upper thoracic vertebrae rotate about the longitudinal axis. This rotation is illustrated on top view X-ray photographs by a progressive shift in the localization of the spinous crests of the thoracic vertebrae toward the lesioned side (Fig. 7*B*; see also de Waele et al., 1989). Our results suggest that excitatory input from the entire otolith system controls motoneurons of the axial musculature of the back.

In one animal, one utricular macula was left intact. All the same, the postural syndrome was identical, although less severe, to that observed with combined utricular and saccular lesions. This finding suggests that saccular input contributes to the stabilization of the neck in the frontal plane. In any case, surgical lesions of either the utricular or saccular macula proved to be extremely difficult. In an effort to investigate the respective saccular and utricular contribution to head-neck stabilization, an attempt was made to lesion these receptors using centrifugation.

Selective otolith lesions using centrifugation

After bilateral utriculus ablation, X-ray photographs taken immediately after the animals awakened from the anesthesia (typically within 1 h after centrifugation) showed that the head-neck ensemble was lowered in a forward direction in all

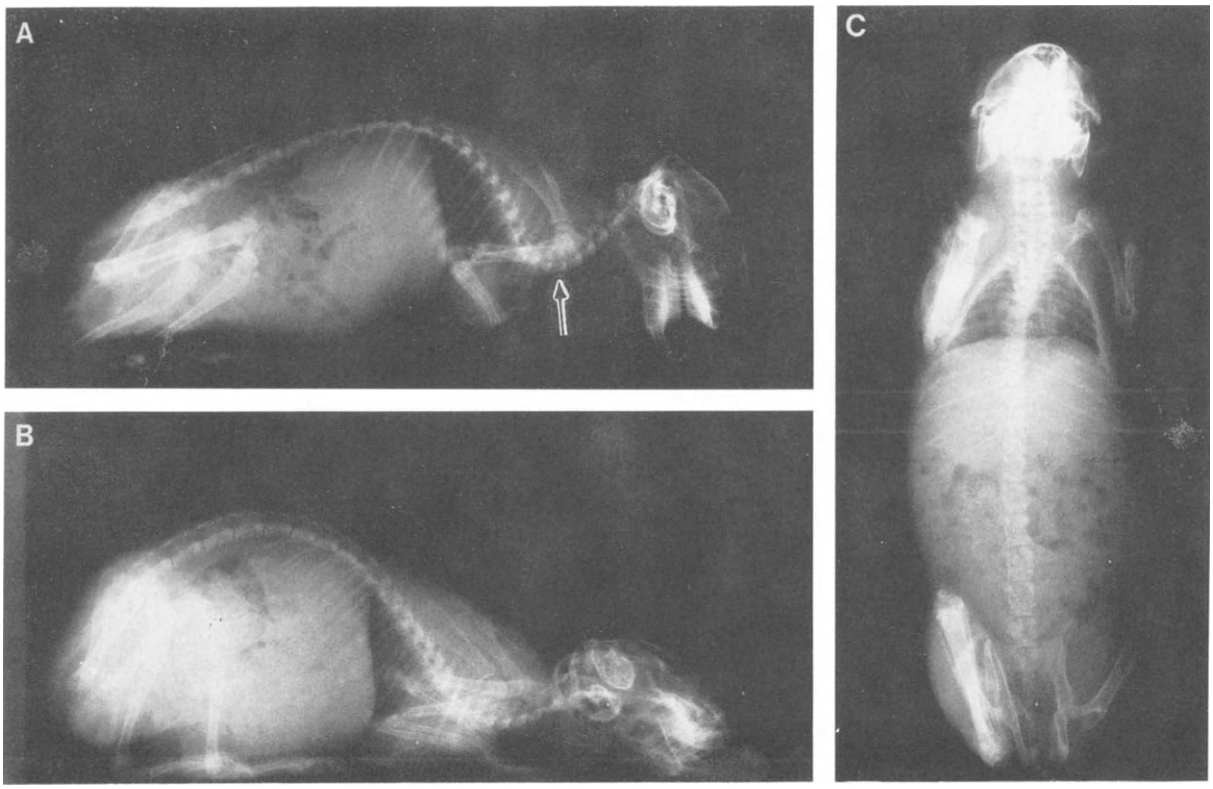

Fig. 8. Lateral (*A,B*) and top view (*C*) X-ray exposure of a guinea pig with bilateral utricular lesion 1 h post-operatively. Note forward tilt of the entire head-neck ensemble (*A*). When the animal is placed in a dark environment, it loses complete control of posture (*B*). The top view (*C*) shows that no left/right asymmetry, i.e., side tilt of the head, is present. Arrow indicates the cervico-thoracic junction.

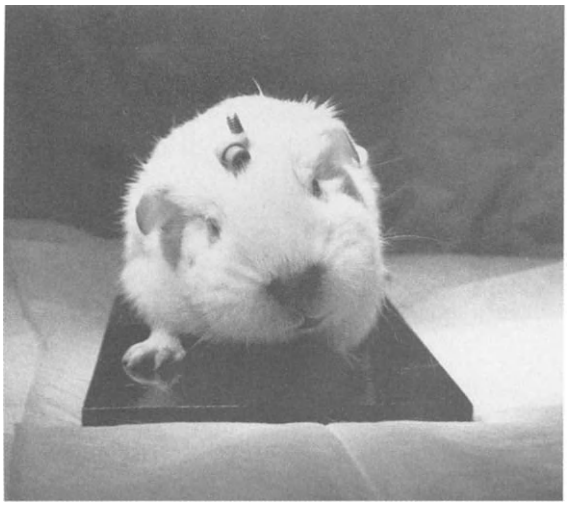

Fig. 9. Portrait photograph of a guinea pig with unilateral sacculus lesion. Note slight head tilt towards the side of the lesion.

animals (Fig. 8*A*). There was no left-right asymmetry (Fig. 8*C*). Lack of vision deprived the animal completely of its spatial orientation. In such case, the head-neck ensemble was not raised from the floor (Fig. 8*B*). At this stage, there were individual differences in the severity of lesion symptoms. After 24 h, a more consistent overall postural composition of the animals emerged, when recovery from the immediate consequences of centrifugation and anesthesia had occurred. In all cases, the cervical spine was held tilted forward. The animals' postures in regard to cervical vertebral column orientation never reached their pre-operative states. Exposure to total darkness exacerbated this symptom, although the animals were now able to hold their heads raised above the floor.

Symptoms following unilateral saccular lesions were side tilts of the entire head-neck ensemble towards the side of the lesion (Fig. 9). In one serendipitous successful unilateral ablation of the sacculus using surgical methods, the same lesion symptoms were produced.

From our observations and those of earlier investigators we thus conclude that the utriculi are mainly responsible not only for maintaining left/right symmetry of head-neck posture but also for fore/aft orientation of the cervical column. The sacculus may play a limited role in left/right orientation of the cervical column.

Concluding remarks

In the course of this study we were able to demonstrate that the guinea pig, like other vertebrates, also adopts a stereotyped resting posture. As a working hypothesis, we presume that this posture restricts the number of degrees of freedom of the head-neck system (Fig. 1) which in turn may relieve the CNS of controlling trajectories of complex multi-articulate segments of the body. We propose that the maintenance of good trim is an elucidating analogy to explain vestibular control of the resting posture. Good trim will be the end result of an internal representation of the objective vertical.

Our behavioral results are in accordance with the projection pattern for monosynaptic contacts of different categories of second-order vestibular neurons relaying the information from the semicircular canals to the spinal cord. This coincidence is unexpected considering the complex network linking each of the semicircular canal ampullae to somatic motoneurons. Our findings suggest that monosynaptic connections are indeed of functional importance. The latter issue is still a matter of debate. Our findings also reinforce the hypothesis that the sensorimotor transformation necessary to convert a given head velocity signal into the appropriate neck motor frame is already embedded in the network provided by second-order vestibular neurons (see also Schaefer et al., 1975; Simpson and Graf, 1985). This is similar to the situation in the vestibulo-oculomotor system (Szentágothai, 1943, 1950).

Finally, we would like to emphasize that second-order vestibular neurons entail a three-dimensional representation of head velocity and position in space with at least three sensory inputs: vestibular, visual, and proprioceptive. Whatever the lesion, motoneurons cannot distinguish whether an excitatory postsynaptic potential is induced by vestibular, visual or proprioceptive afferents. Most probably, there is no pure vestibular signal after the first synapse of the

primary vestibular afferents. This has two implications. In the first case, the term "vestibular control of posture" may be a misleading term, even if the animal is kept in darkness. Secondly, proprioceptive and visual inputs have to be organized in the same frame of reference as the vestibular system (Schaefer et al., 1975). Such a congruence of reference frames has been shown in the visual system (Graf, 1988; Graf et al., 1988) It also has to occur within the proprioceptive system. The latter maybe the reason for an abundance of muscle spindles in the neck muscles.

Acknowledgements

This study was supported by NIH Grant EY04613.

References

Baker, R. and Berthoz, A. (1977) *Control of Gaze by Brain Stem Neurons,* Elsevier, Amsterdam, New York.

de Burlet, H.M. and de Haas, J.H. (1923) Die Stellung der Maculae acusticae im Meerschweinchenschädel. *Z. Anat. Entwicklungsgesch.,* 68: 177 – 197.

de Kleijn, A. and Magnus, R. (1921a) Labyrinthreflexe auf Progressivbewegungen. *Pflüger's Arch.,* 186: 39 – 60.

de Kleijn, A. and Magnus, R. (1921b) Über die Funktion der Otolithen. II. Mitteilung. Isolierte Otolithenausschaltung bei Meerschweinchen. *Pflüger's Arch.,* 186: 61 – 81.

deWaele, C., Graf, W., Josset, P. and Vidal, P.P. (1989) A radiological analysis of the postural syndromes following hemilabyrinthectomy and selective canal and otolith lesions in the guinea pig. *Exp. Brain Res.,* 77: 166 – 176.

Cohen, B. and Suzuki, J.I. (1963) Eye movements induced by ampullary nerve stimulation. *Am. J. Physiol.,* 204: 347 – 351.

Cohen, B., Suzuki, J.I. and Bender, M. (1964) Eye movements from semicircular canal nerve stimulation in the cat. *Ann. Otol. Rhinol. Laryngol.,* 73: 153 – 165.

Graf, W. (1988) Motion detection in physical space and its peripheral and central representation. *Ann. N.Y. Acad. Sci.,* 545: 154 – 169.

Graf, W., Simpson, J.I. and Leonard, C.S. (1988) Spatial organization of visual messages of the rabbit's cerebellar flocculus. II. Complex and simple spike responses of Purkinje cells. *J. Neurophysiol.,* 60: 2091 – 2121.

Graf, W., de Waele, C. and Vidal, P.P. (1992a) Skeletal geometry in vertebrates and its relation to the vestibular endorgans. In: A. Berthoz, W. Graf and P.P. Vidal (Eds.), *The Head-Neck Sensory Motor System,* Oxford University Press, Oxford, New York.

Graf, W., Wang, D.H., de Waele, C. and Vidal, P.P. (1992b) The role of otoliths in maintaining the upright posture of the head-neck system in the guinea pig. In: H. Shimazu and Y. Shinoda (Eds.), *Vestibular and Brain Stem Control of Eye, Head and Body Movements,* Japan Scientific Societies Press, Tokyo, and Karger, Basel.

Magnus, R. (1924) *Körperstellung,* Springer, Berlin.

Schaefer, K.-P., Schott, D. and Meyer, D.L. (1975) On the organization of neuronal circuits involved in the generation of the orienting response (visual grasp reflex). *Fortschr. Zool.,* 23: 199 – 212.

Schor, R., Miller, A. and Tomko, D. (1984) Responses to head tilt in cat central vestibular neurons. I. Direction of maximum sensitivity. *J. Neurophsyiol.,* 51: 136 – 146.

Simpson, J.I. and Graf, W. (1985) The selection of reference frames by nature and its investigators. In: A. Berthoz and G. Melvill-Jones (Eds.), *Reviews of Oculomotor Research, Vol. 1. Adaptive Mechanisms in Gaze Control,* Elsevier, Amsterdam.

Suzuki, J.-I. and Cohen, B. (1964) Head, eye, body and limb movements from semicircular canal nerves. *Exp. Neurol.,* 10: 393 – 405.

Suzuki, J.-I., Cohen, B. and Bender, M.B. (1964) Compensatory eye movements induced by vertical semicircular canal stimulation. *Exp. Neurol.,* 9: 137 – 160.

Szentágothai, J. (1943) Die zentrale Innervation der Augenbewegungen. *Arch. Psychiatr. Nervenkr.,* 116: 721 – 760.

Szentágothai, J. (1950) The elementary vestibulo-ocular reflex arc. *J. Neurophysiol.,* 13: 395 – 407.

Vidal, P.P., Graf, W. and Berthoz, A. (1986) The orientation of the cervical vertebral column in unrestrained awake animals. I. Resting position. *Exp. Brain Res.,* 61: 549 – 559.

Vidal, P.P., de Waele, C., Graf, W. and Berthoz, A. (1988) Skeletal geometry underlying head movements. *Ann. N.Y. Acad. Sci.,* 545: 228 – 238.

Wittmaak, V. (1909) Über Veränderungen im inneren Ohre nach Rotationen. *Verhandl. Otol. Gesellschaft,* 18: 150 – 156.

J.H.J. Allum, D.J. Allum-Mecklenburg, F.P. Harris and R. Probst
Progress in Brain Research, Vol. 97

CHAPTER 23

Geometrical approach to neural net control of movements and posture

A.J. Pellionisz[1] and C.F. Ramos[2]

[1] *NASA Ames Research Center 242-3, Moffett Field, CA 94035-1000, U.S.A. and* [2] *University of California, Biophysics Group, 101 Donner Laboratory, Berkeley, CA 94720, U.S.A.*

In one approach to modeling brain function, sensorimotor integration is described as geometrical mapping among coordinates of non-orthogonal frames that are intrinsic to the system; in such a case sensors represent (covariant) afferents and motor effectors represent (contravariant) motor efferents. The neuronal networks that perform such a function are viewed as general tensor transformations among different expressions and metric tensors determining the geometry of neural functional spaces. Although the non-orthogonality of a coordinate system does not impose a specific geometry on the space, this "Tensor Network Theory of brain function" allows for the possibility that the geometry is non-Euclidean. It is suggested that investigation of the non-Euclidean nature of the geometry is the key to understanding brain function and to interpreting neuronal network function. This paper outlines three contemporary applications of such a theoretical modeling approach. The first is the analysis and interpretation of multi-electrode recordings. The internal geometries of neural networks controlling external behavior of the skeletomuscle system is experimentally determinable using such multi-unit recordings. The second application of this geometrical approach to brain theory is modeling the control of posture and movement. A preliminary simulation study has been conducted with the aim of understanding the control of balance in a standing human. The model appears to unify postural control strategies that have previously been considered to be independent of each other. Third, this paper emphasizes the importance of the geometrical approach for the design and fabrication of neurocomputers that could be used in functional neuromuscular stimulation (FNS) for replacing lost motor control.

Key words: Motor control; Geometry; Sensorimotor; Modeling; Computer simulation; Posture; Neurocomputers; Functional neuromuscular stimulation

Introduction

Experimental neuroscience must be founded in theory. Especially in the field of sensorimotor research, it is an anachronism not to have a solid theoretical foundation.

Today, progress towards a theoretical focus in experimental neuroscience is inevitable due to increasing pressures from computer science, from the so-called "neurocomputer" research. (Anderson and Rosenfeld, 1987; Anderson et al., 1990). Technological breakthroughs in the development of brain-like computers will not be possible, however, without a mathematical theory of brain function (Pellionisz, 1983). Such a theory should emerge from sensorimotor system neuroscience, and particularly from research of the vestibular system and the cerebellum (Pellionisz, 1985, 1988b). From some time now, vestibular and cerebellar research has found mathematical modeling a necessity in order to keep the large body of data coherent. One promising candidate for a mathematical foundation is the multidimensional vectorial, or coordinate system approach which appears to be one of the most common threads in the work of a good number of neuroscientists. In this approach, investigation first

focused on quantitatively establishing nature's coordinate systems (Blanks et al., 1975; Curthoys et al., 1975; Ezure and Graf, 1984; Simpson et al., 1986; Daunicht and Pellionisz, 1987). Then, neural network models were worked out for transformation of such coordinates (Pellionisz, 1984; Simpson and Pellionisz, 1984; Pellionisz and Graf, 1987; Pellionisz and Peterson, 1988; Peterson et al., 1989). Theory provided a basis for the "coordinate system approach" in experimental neuroscience (Pellionisz et al., 1986; Droulez and Berthoz, 1987; Eckmiller and von Malsburg, 1988; Andersen and Zipser, 1988; Berthoz et al., 1988; Bloedel et al., 1988; Georgopoulos et al., 1988; Soechting and Flanders, 1989; Fiala and Lumia, 1991; Werbos and Pellionisz, 1992).

The geometrical approach started to unfold approximately a decade ago (Pellionisz and Llinás, 1980) with the introduction of a geometrically framed hypothesis for neural network modeling of sensorimotor integration. According to the theory, sensorimotor integration involves generalized vector (tensor) transformations between descriptive vectors whose basis sets are non-orthogonal and are related to frames of reference intrinsic to the biological system. Further, tensor theory recognizes the likelihood that the underlying geometry of these spaces may be non-Euclidean in nature. This "tensor theory" of brain function is characterized by two conceptual distinctions over previous theories. First, the theory abandons any notion that the vectors and matrices used in a multi-dimensional approach must be expressed in a Cartesian coordinate system, and instead emphasizes dual (covariant and contravariant) vectorial representations of sensory and motor vectors. Second, the theory does not presume that the underlying space must obey a Euclidean geometry. In fact, the theory emphasizes the likelihood that the geometry is non-Euclidean, and that it is precisely this aspect of the space which holds the key to understanding brain function (Pellionisz, 1991).

Introduction of this geometrical approach to understanding of the function of biological neural networks ran parallel with the ascent of neurocomputing (Hopfield, 1982). It became evident that overall functional performance of the CNS (such as sensorimotor compensation in gaze control and its adaptive cerebellar coordination) must be explained not only in mathematical terms but also in terms of the computational properties of neural networks (Pellionisz and Llinás, 1982). Over the past decade, two schools of thought developed. According to the intrinsic approach, mathematics of brain function inherent in neural nets, such as those of gaze control, must be learnt from the biological substrata (Pellionisz, 1985). Once principles are discerned from nature, their transfer to and utilization in engineering should pose the secondary, less severe problem (Pellionisz, 1983). The other, alternative school of thought maintains (implicitly) that neuroscience is not yet mature enough for revealing nature's mathematical principles, and that mathematical-theoretical tools must be imported to neuroscience from engineering. This "extrinsic" approach was expressed by an emulation of the multidimensional approach in gaze research (Robinson, 1982). He imported mathematics of engineering, that is, he used vectors and matrices in a Cartesian sense implying Euclidean geometry, rather than learning the nature of geometry from Nature and developing the field of intrinsically non-Euclidean neural geometry. Others expressed doubts about the geometrical approach (Arbib and Amari, 1985).

The drive towards "intrinsic" coordinate systems and neural net transformations has led to a neurocomputational learning paradigm of cerebellar neural nets (Pellionisz and Llinás, 1985). This mathematical theory has been experimentally confirmed (Gielen and van Zuylen, 1986; Pellionisz and Peterson, 1988). Presently, this research proceeds not only towards elaborating neural network models of complex gaze reflexes, but also towards using them as blueprints of neurocomputer prototypes (Pellionisz et al., 1990), as well as towards experimentally revealing the non-Euclidean neural geometry (Pellionisz and Bloedel, 1991). Moreover, the initial pioneering approach towards revealing

the geometry of metrical gaze-control function, has been broadened towards neural geometries including non-metrical spaces (fractals) (Pellionisz, 1989).

An alternative to the mathematically based and experimentally proven tensor network theory of gaze reflexes has not been presented by the critiques of the approach. In fact, within a decade, the critique itself turned towards the formerly criticized tensor geometry (Amari, 1991). International recognition of the geometrical approach is also expressed in Germany (Eckmiller, 1990).

Importing concepts into neuroscience from technological neural net studies has not stopped. For instance, the "backpropagation" mathematical algorithm developed in engineering (Werbos, 1974) has been brought into gaze research (Anastasio and Robinson, 1989) just at the time when its inventor looks "beyond backpropagation" (Werbos and Pellionisz, 1992). This trend runs counter to the "intrinsic" approach which aims not only at discerning mathematics of nature but applying it to neural net technology (Pellionisz and Werbos, 1992; Werbos and Pellionisz, 1992).

Theoretical methodology

The geometrical approach to modeling brain function has been described previously (Pellionisz and

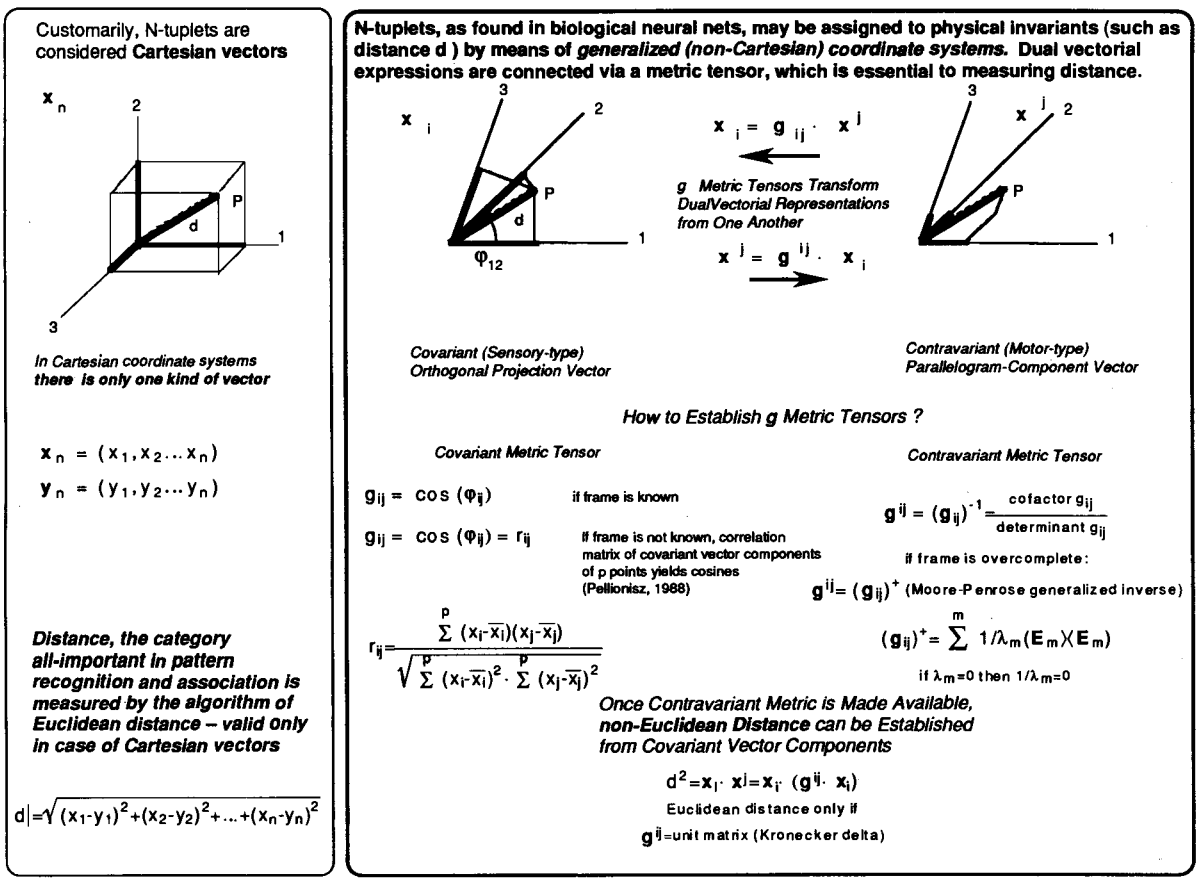

Fig. 1. Fundamental differences of vectors expressed in a Cartesian orthogonal system of coordinates (panel on left) and generalized (co- and contravariant) vectors expressed in non-Cartesian frames (panel on right). Most importantly for Cartesian vectors, distance can be calculated by the Euclidean measure, while for generalized vectors, found in natural neural networks, the establishment of the metric is needed to measure distance.

Llinás, 1985) and its main tenets are shown in Fig. 1. Generally speaking, neural network theory and modeling involves the "metaorganization principle" which allows for the transformation of sensory afferent information into motor efferent activities that generate intentional motor behavior. Both the sensory and the motor signals are expressed as multidimensional vectors, and thus the neuronal network behaves as a tensor, sending the former to the latter.

CNS function can thus be described in terms of the underlying geometries defined by these metric tensors. In this mathematical framework, the sensory afferents would define a covariant vector while the motor efferents would define a contravariant vector. The fundamental mathematical principle involved is that simultaneous knowledge of both the covariant and contravariant vectors, as they span a global moving frame, completely determines the geometry of the space, or manifold, defined by the neuronal network. The significance of discussing CNS function in terms of its underlying geometry is that, although the metric tensor is often written using a local coordinate system, the geometry of the manifold is coordinate system-independent. Thus, while the activity of a neuronal network might be interpreted with respect to the high-dimensional covariant/sensory and contravariant/motor coordinate systems involved, the key to understanding CNS function rather lies in discovering the geometry of the manifold. The emergence of neuronal networks that perform sensorimotor integration results from the interactions between the contravariant/motor execution, generating a physical action in the external world via the musculoskeletal apparatus, and the covariant/sensory proprioception which measures the effect of such motor output. In this transformation of contravariants to covariants by the physical morphology of the motor system, a covariant metric tensor is implicitly present.

However, coordinated motor action employs proprioceptive feedback information in generating appropriate motor behaviors. Hence, a contravariant metric tensor, transforming sensory afferents into motor efferent activities, is also required and provided in a neuronal network in the CNS. This tensor is assembled based on the metaorganization principle in which covariant proprioception is used as a recurrent signal to the motor apparatus, yielding the eigenvectors and eigenvalues of the neuronal network. The stored eigenvectors can serve as a means for the genesis of a metric tensor, while the eigenvalues can serve as a means of comparing the eigenvalues that are implicit in the musculoskeletal apparatus to those of the CNS tensor. The difference between these eigenvalues is then used to modify the metric so that it evolves to perform a more acccurate covariant-contravariant transformation.

Applications of the theory

Functional geometry of Purkinje cell population responses as revealed by neurocomputer analysis of multi-unit recordings

As originally introduced (Pellionisz, 1988c), the so-called multi-unit recording technique provides both an opportunity and a need for a geometrical analysis. Multi-electrode techniques have been pioneered through the past decades (Wise et al., 1970; Freeman, 1975; Pickard, 1979; Pochay et al., 1979; Prohaska et al., 1979; Kuperstein and Whittington, 1981; Reitboeck et al., 1981; Bower and Llinás, 1983; Reitboeck, 1983a; Reitboeck and Werner, 1983; BeMent et al., 1986; Carman et al., 1986; Eichenbaum and Kuperstein, 1986; Gerstein, 1987; Eckhorn and Reitboeck, 1988). While processing multi-electrode data is most commonly a correlation analysis (Kruger, 1982; Gernstein et al., 1983; Reitboeck, 1983b), lately the geometrical approach was taken (Aertsen et al., 1986) proposing an interpretation of neuronal activities of n neurons as a point in the n-dimensional vectorspace in which a Euclidean geometry governs.

As shown in Fig. 2, it was pointed out (Pellionisz, 1988c) that instead of the automatic assumption of a Euclidean metric tensor of neural n spaces (on which calculation of geometrical features, such as distances, would be based) the approach needs to be reversed. Geometrical analysis of multi-unit data cannot start with a well-defined geometry (it is basi-

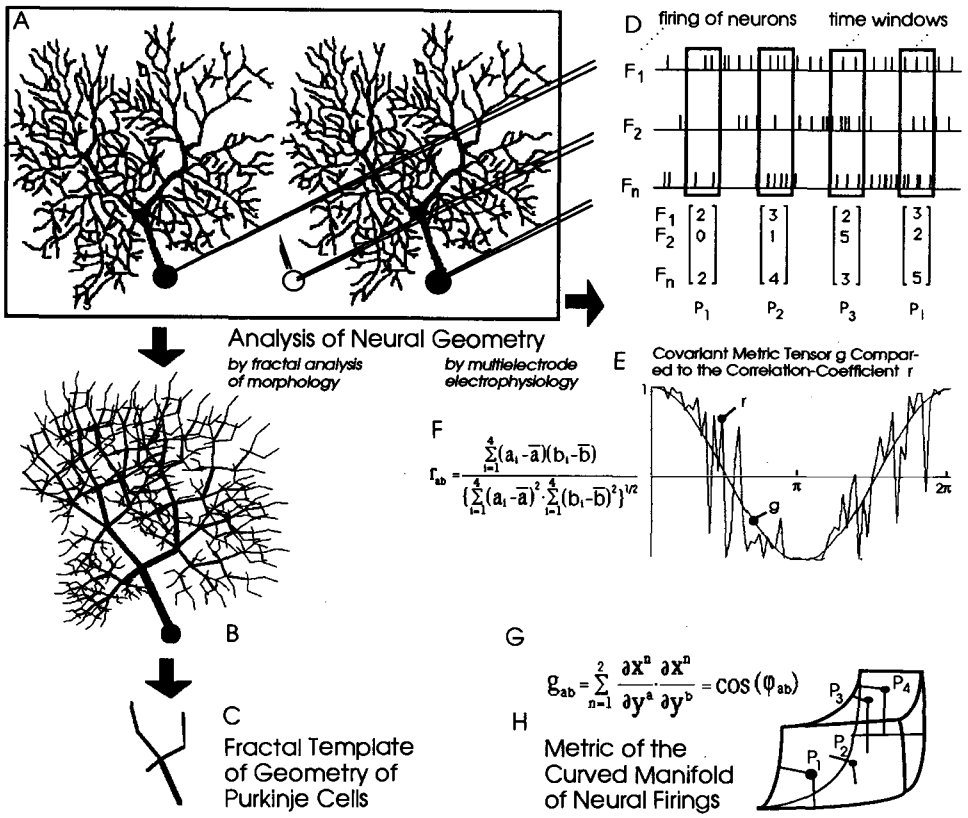

Fig. 2. Two major avenues for the exploration and measurement of non-metrical fractal (*B,C*) and metrical (*D,H*) neural geometries. Panels *A,D – H* show that r, the cross-correlogram of firing frequencies, approximates the g covariant metric tensor, yielding the geometry of the curved functional manifold. Panels *B,C* show that individual neural arbors can be well approximated with a deterministic fractal model, comprising complexity to a template (*C*).

cally unknown). Instead, the multi-electrode analysis method must be the means which results in a geometry, as discerned from experimental data. This appeal was well taken by the community concerned with multi-electrode recording techniques, because it was readily accepted that the assumption of Euclidean geometry is arbitrary; however, for some time, no specific experimental paradigm offered a concrete procedure to define the geometry (measure the metric tensor) of the neural n space.

A cooperative project of AJP and Dr. H. Reitboeck has led to an experimental paradigm by which the geometry (metric tensor) of the neural n space underlying vestibular and cerebellar functional spaces can be quantitatively established. Fig. 3 outlines a skeletomuscular model of the eye-head-neck system coupled with a neural network model of the vestibulocerebellar intrinsic coordinate system transformation (after Pellionisz et al., 1990). As shown in Fig. 3*A*, at two stages of the transformation chain of intrinsic vectors, the experimentally presented physical invariants (such as distances in the angular acceleration space) are represented as covariant, sensory-type vectors. This is physically proven at the first stage, at primary vestibular neurons, as the vestibular semicircular canals take orthogonal projection components of the head acceleration (each in its own plain). Tensor network theory predicts that the cerebellar input (intercepted at the level of cerebellar Purkinje cells) is also a

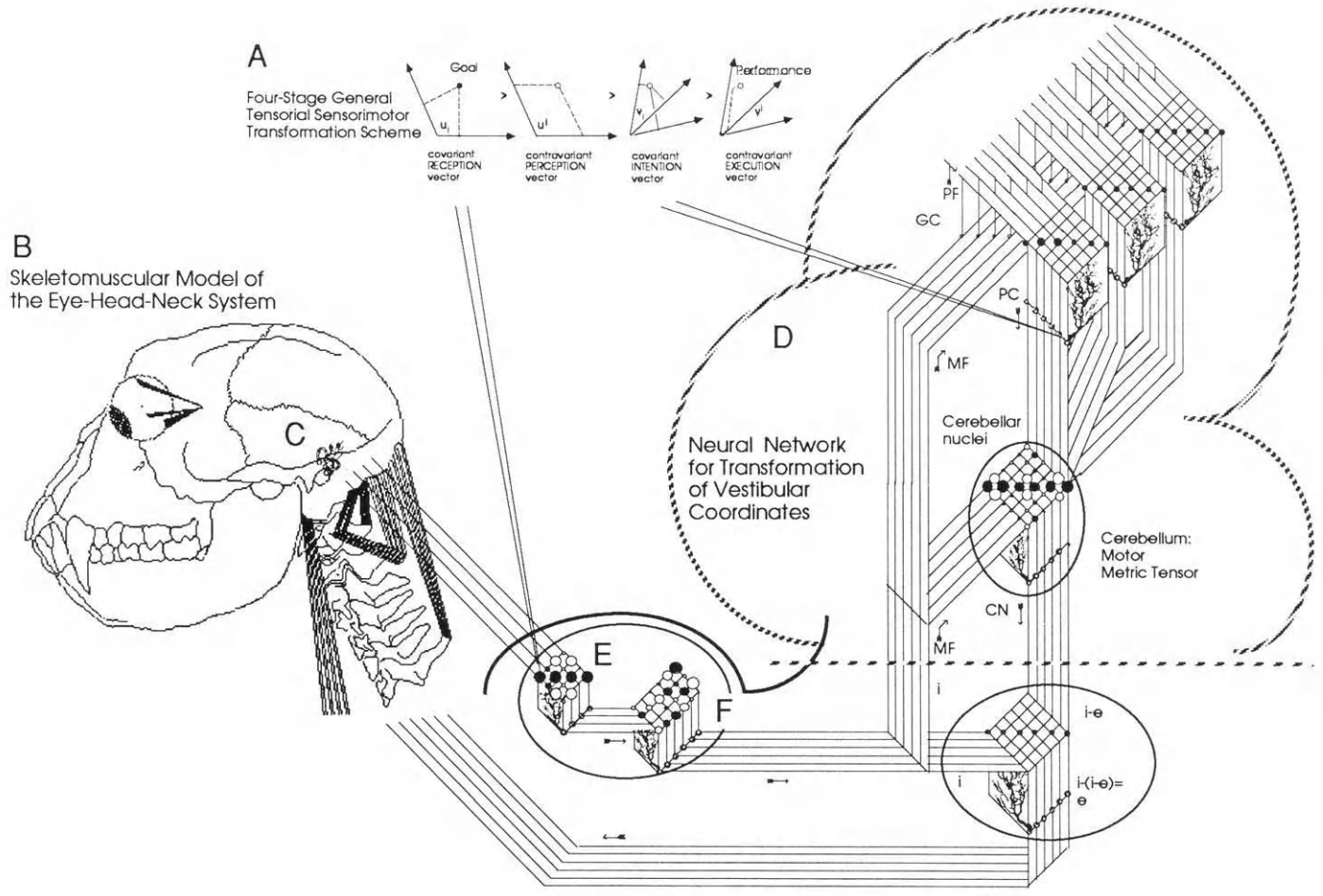

Fig. 3. Proposed theoretical-experimental paradigm to measure, by multi-unit recording technique, the functional vectors intrinsic to natural neuronal network transformations. Neural expression of head acceleration is in the form of covariant vector at the vestibular nuclei (E) and at the cerebellar Purkinje cells (PC). From measurements of covariant expression of physical invariants, the metric tensor of the geometry of the n space can be established as shown.

covariant (sensory-type) intention vector (although it is expressed in the motor frame of reference). Fig. 2*E* shows (for elaboration, see Pellionisz, 1988c) that in case of such covariant vectors the cross-correlogram table of firing frequencies converges to the covariant metric tensor, from which the contravariant metric can be calculated by the Moore-Penrose generalized inverse (Albert, 1972). The proposed procedure of multi-unit data analysis, therefore, yields a specific measure of both metric tensors of the neural n space by which the internal geometrical representation of external physical invariants can be appropriately calculated (Fig. 4).

Fig. 4*D* demonstrates that the direct use of Euclidean distance algorithm on such covariant vectorial expressions would yield a completely erroneous and non-unique "measurement" of such distances. As most sensorimotor coordination events are based on "navigation" of animals in the extrinsic physical space-time manifold, it can be expected that the above type of analysis will reveal how intrinsic metrical geometries (embodied in sensorimotor neural nets) "embed" the external physical space.

The goal of a specific multi-electrode study using experimental data obtained from Bloedel's laboratory (Schwartz et al., 1987) was to determine properties characterizing the population responses of neurons in specific CNS nuclei and to relate those properties to the geometrical tensor theory described above. For this purpose, responses of up to ten simultaneously recorded Purkinje cells were investigated during perturbed and unperturbed locomotion in acutely decerebrated cats. Multi-unit recordings were made to intermittent perturbations

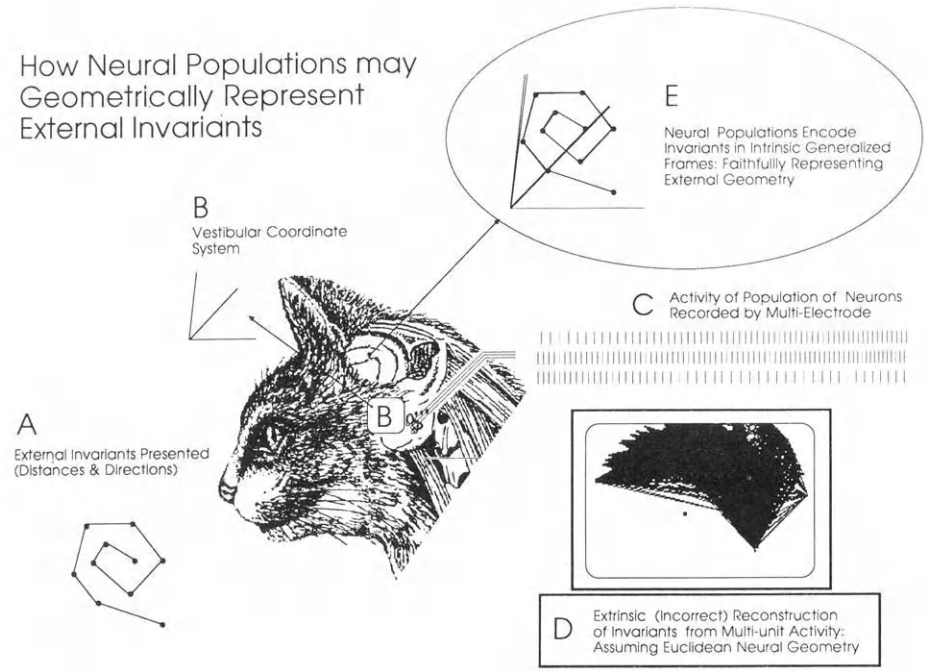

Fig. 4. How does the brain geometrically represent the external world? Schematic diagram of the theoretical-experimental reconstruction of external invariants such as distances and directions (panel *A*) by neural networks of the brain (panel *E*). Panel *B* illustrates a sensory coordinate system intrinsic to neural measurements of external invariants. In the specific case of the vestibular semicircular canal apparatus, such physical invariants are points (distances in the angular acceleration space, which are measured by the non-orthogonal coordinate system of the vestibulum). Panel *C* illustrates a firing frequency response of an array of neurons (detectable from the vestibular nuclei). Given that such an activity vector is covariant, Euclidean measurement and reconstruction of distances is grossly erroneous and non-unique (see "reconstruction of input A" in panel *D*) Using the proposed paradigm for the geometrical analysis of multi-unit recordings, the cross-correlation analysis of firing frequencies yields the metric tensor of the functional space; by this, the external invariant can be faithfully reconstructed (panel *E*).

of the forelimb, and also during the acquisition and performance of a forelimb movement conditioned to avoid an obstacle. The population responses were analyzed based on a method for calculating non-Cartesian axes from the cross-correlogram of the neural activity of n neurons. This procedure also yields the matrix characterizing the covariant matrix tensor (Pellionisz, 1988c). Using a transputer-based neurocomputer (Pellionisz, 1991), the Moore-Penrose generalized inverse (Pellionisz, 1984) was used to derive the contravariant metric tensor characterizing the geometry of the population responses.

The results indicated (Pellionisz and Bloedel, 1991) that the geometry describing the population responses is expressed in non-Cartesian coordinates and that the characteristics of the underlying geometry of the network are comparable to the geometrical characteristics of the locomotor movement. Furthermore, the data revealed that the geometry of the responses is modified when the characteristics of the movement are altered, either by perturbing the swing phase of the ipsilateral forelimb or by changing the treadmill speed. These experimentally found changes in cerebellar Purkinje cell firings provide a possibility of interpreting cerebellar adaptation in terms of alteration of the functional geometry of cerebellar neural network. Initial findings suggest that the derived geometry of the population responses may be the basis for reconstructing physical invariants such as movement direction and distance. If so, this theoretical-experimental method is a candidate for deciphering the neural code internally representing invariants of the external world.

Full-body postural control modeling of a standing human and the unification of "hip versus ankle strategies"

Intentional movements and postural control are phenomena arising from the interaction of three kinds of geometries. The first is the physical geometry of the external world. This "movement space" is endowed with a Euclidean geometry. The second is the geometry of the musculoskeletal apparatus. This can be described in any coordinate system, for example in the same (x, y, z, t) external frame of reference, used to characterize the external world. However, it must be clear that the CNS uses intrinsic coordinate systems for neural control of movements and posture, such as frames composed of the pulling directions of muscles. These are typically overcomplete, non-orthogonal (mathematically, general) coordinate systems. The third, definitely intrinsic geometry is spun in the functional space by firing frequencies of populations of neurons that generate intentional movements and/or postural stability. This third, intrinsic neural geometry may be inherently non-Euclidean and its features can be described by its (e.g., position-dependent) metric tensors.

Therefore, an approach that conceives intentional movements and postural control geometrically leads to questions of: (1) the quantitative representation of coordinate axes intrinsic to skeletomuscular effectors; (2) the mathematical formulation of generalized coordinates and their (tensorial) transformations; and (3) experimental establishment of functional geometries by microelectrode recordings of the neuronal network activities. Graphics-based computer models of various skeletomuscular systems, such as of eye-head-neck apparatus of the monkey (Pellionisz, 1988b; Pellionisz et al., 1990) have shown that sensorimotor function can be mathematically represented as a transformation of generalized coordinates via sensorimotor neural networks (see Fig. 3 and Pellionisz, 1988b).

As a preliminary approach to understanding balance and postural control in standing man, a similar skeletomuscular model was outlined for the full body, a five-link inverted pendulum model in the framework of tensor theory. The model incorporates the following links and muscle groups: head-neck (rectus anticus and splenii capitis), trunk (rectus abdominus and erector spinae), thigh (quadriceps and biceps femoris), shank (tibialis anterior and gastrocnemius), and the foot (tibialis anterior and soleus) (Fig. 5).

As shown in Fig. 5, simulations using the non-Euclidean geometry of a ten-dimensional muscle

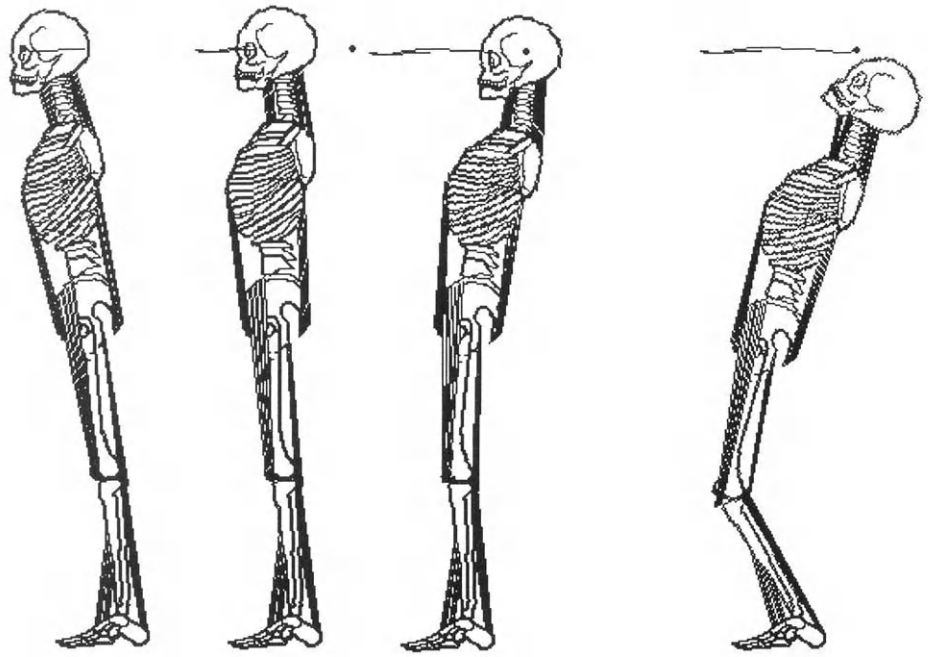

Fig. 5. Postural control model of a standing human, using a 10-muscle full-body skeletomuscular computer model. The postural control strategy is a clear combination of a hip strategy (left three insets), and an ankle strategy (right inset). Figures are taken from video computer simulation.

space conceived posture as being functionally equivalent to "full-body gaze". This can be described as a peering type of motion of the entire upper body (head-trunk). Such an intentional forward gaze might be made, for example, in leaning over to look down a steep cliff. Likewise, an intentional backward gaze might be made, for example, when following the motion of a jet-craft flying towards the observer and then immediately overhead.

The central question considered with this type of "whole-body skeletomuscular computer model" was whether or not postural control strategies for maintaining balance during these types of movement varied in terms of "hip" versus "ankle" strategies (Nashner, 1977). Simulations of the present model imply that the so-called "hip strategies" for postural control are not fundamentally different from the so-called "ankle strategies". Rather, they are simply different manifestations of the same underlying postural control function expressed by the same neural network, governed by a non-Euclidean geometry for the postural muscles involved.

Future projection: neurocomputer implementation of neural control of movements and posture for functional neuromuscular stimulation

The third avenue of research is in the possible biomedical application of the basic neuroscience research that would establish such functional geometries, as exemplified by these first two studies. The application would be in the design and development of neurocomputers for functional neuromuscular stimulation (FNS). Such an optimally designed stimulator would artificially generate natural, coordinated movements of the limbs, while also providing postural control and stability to paralyzed individuals. To date, no bioengineering application of the theory has yet been made, and it is the hope of the authors that interest in this field would be sparked by the ensuing discussion.

The geometrical approach is expected to lead to

design and fabrication of neurocomputers that could be used for replacing lost (biological) control by functional neuromuscular stimulation to generate artificial movement, balance and posture (Pellionisz, 1988a, 1991). Indeed, given the explosive rate of progress of neurocomputer theory and development, it is reasonable to expect that electronic implementation of "geometrical machines" will proceed before the book on neural geometry is completed. Novel generations of neurocomputers are likely to take full advantage both of the functionality that is not attainable by limiting massively parallel array processing to Cartesian vectors (such as the distinction of sensory and motor type expressions), and the flexibility of the architecture designed to accommodate generalized vectorial operations (which fully include the rather specific Cartesian vectorial operations). While such a processor is presently in the development stage (employing INMOS transputers on a Macintosh-II platform), the hardware-software neurocomputer development will co-evolve with those theoretical-experimental advances that provide the basic research background of technological development.

A Functional Neuromuscular Stimulation project that uses neurocomputers fashioned after the functioning biological neural control will complete the circle from learning neural geometry from Nature, to formalize such geometries mathematically, to implement them electronically and, finally, to use "artificial neural networks" for effectively replacing lost movement and posture control. A functional neuromuscular stimulation project of this type by definition integrates skeletomuscular computer modeling, neurocomputer research and development and mathematical (geometrical) theory and modeling of neural network control of movements and posture.

Acknowledgements

This research was supported by Distinguished U.S. Scientist Award, by the Alexander von Humboldt Foundation of Germany (to A.J.P), by the National Research Council of the National Academy of Sciences of the U.S.A. (to A.J.P. and C.R.), by NASA Ames Research Center Director's Discretionary Fund T4967 (to A.J.P. and D.L.T.) and NATO International Research Cooperation Grant 910211 to (to A.J.P. and H.J.R.). The article refers to cooperative studies with Drs. David L. Tomko (NASA Ames Research Center, Vestibular Research Facility), James R. Bloedel (Barrow Neurological Institute, Phoenix, AZ) and H.J. Reitboeck (Marburg University, Germany), whose contributions are gratefully acknowledged.

References

Aertsen, A., Gernstein, G. and Johannesma, P. (1986) From neuron to assembly: neuronal organization and stimulus representation. In: G. Palm (Ed.), *Brain Theory: Proceedings of the First Trieste Meeting on Brain Theory, Oct 1–4, Trieste,* Springer, Berlin, pp. 7–24.

Albert, A. (1972) *Regression and the Moore-Penrose Pseudoinverse,* Academic Press, New York.

Amari, S. (1991) Dualistic geometry of the manifold of higher-order neurons. *Neural Networks,* 4(4): 443–451.

Anastasio, T.J. and Robinson, D.A. (1989) Distributed parallel processing in the vestibulo-oculomotor system. *Neural Comput.,* 1(2): 230–241.

Andersen, R.A. and Zipser, D. (1988) The role of the posterior parietal cortex in coordinate transformations for visual-motor integration. *Can. J. Physiol. Pharmacol.,* 66: 488–501.

Anderson, J. and Rosenfeld, E. (1987) *Neurocomputing: I. Foundations of Research,* MIT Press, Cambridge, MA.

Anderson, J., Pellionisz, A. and Rosenfeld, E. (1990) *Neurocomputing-2: Directions of Research,* MIT Press, Cambridge, MA.

Arbib, M. and Amari, S.I. (1985) Sensorimotor transformations in the brain with a critique of tensor network theory of the cerebellum. *J. Theor. Biol.,* 112: 123–155.

BeMent, S.L., Wise, K.D., Anderson, J., Najali, K. and Drake, K.L. (1986) Solid-state electrodes for multichannel multiplexed intracortical neuronal recording. *IEEE Trans. Biomed. Eng.,* 33: 230–240.

Berthoz, A., Benhamou, M. and Pellionisz, A.J. (1988) Postural positions yielding aligned eigenvectors of coordinate frames intrinsic to vestibular and head-neck muscle systems in human. *Soc. Neurosci. Abstr.,* 14/2: 1235.

Blanks, R., Curthoys, I. and Markham, C. (1975) Planar relationships of the semicircular canals in man. *Acta Otolaryngol.,* 80: 185–196.

Bloedel, J.R., Tillery, S. and Pellionisz, A.J. (1988) Experimental-theoretical analysis of the intrinsic geometry of limb movements. *Soc. Neurosci. Abstr.,* 14/2: 953.

Bower, J. and Llinás, R. (1983) Simultaneous sampling of the responses of multiple, closely adjacent, Purkinje cells responding to climbing fiber activation. *Soc. Neurosci. Abstr.*, 9: 607.

Carman, G.J., Rasnow, B. and Bower, J.M. (1986) Analysis of the dynamics of activity in ensembles of neurons recorded simultaneously in cerebellar cortex. *Soc. Neurosci. Abstr.*, 12: 1417.

Curthoys, I.S., Curthoys, E.J., Blanks, R.M.I. and Markham, C.H. (1975) The orientation of the semicircular canals in the guinea pig. *Acta Otolaryngol.*, 80: 197 – 205.

Daunicht, W. and Pellionisz, A. (1987) Spatial arrangement of the vestibular and the oculomotor system in the rat. *Brain Res.*, 435: 48 – 56.

Droulez, J. and Berthoz, A. (1987) Spatial and temporal transformations in visuomotor coordination. In: R. Eckmiller and C. von Malsburg (Eds.), *Neural Computers*, Springer, Heidelberg, pp. 345 – 359.

Eckhorn, R. and Reitboeck, H.J. (1988) Assessment of Cooperative Firing in Groups of Neurons: Special Concepts for Multiunit Recordings from the Visual System. In: E. Basar (Ed.), *Springer Series of Brain Dynamics 1*, Springer, Berlin, pp. 219 – 227.

Eckmiller, R. (1990) Concerning the emerging role of geometry in neuroinformatics. In: R. Eckmiller, G. Hartman, G. Hauske and C. von Malsburg (Eds.), *Parallel Processing in Neural Systems and Computers*, Elsevier Science Publishers, Amsterdam, pp. 5 – 8.

Eckmiller, R. and von Malsburg, C. (1988) Neural Computers. *Proceedings of the NATO Research Workshop*, Springer, Düsseldorf.

Eichenbaum, H. and Kuperstein, M. (1986) Extracellular neural recording with multichannel microelectrodes. *J. Electrophysiol. Tech.*, 13: 189 – 209.

Ezure, K. and Graf, W. (1984) A quantitative analysis of the spatial organization of the vestibulo-ocular reflexes in lateral- and frontal-eyed animals. II. Neuronal networks underlying vestibulo-oculomotor coordination. *Neuroscience*, 12: 95 – 109.

Fiala, J. and Lumia, R. (1991) *Adaptive Inertia Compensation Using a Cerebellar Model Algorithm*, IJCNN, Singapore, pp. 1 – 8.

Freeman, W. (1975) *Mass Action in the Nervous System*, Academic Press, New York.

Georgopoulos, A.P., Kettner, R.E. and Schwartz, A.B. (1988) Primate motor cortex and free arm movements to visual targets in three-dimensional space. II. Coding the direction by a neuronal population. *J. Neurosci.*, 8: 2928 – 2937.

Gernstein, G.L. (1987) Information flow and state in cortical neural networks: interpreting multi-neuron experiments. In: W. von Seelen, G. Shaw and U.M. Leinhos (Eds.), *Organization of Structure and Function in the Brain*, VCH Verlagsgesellschaft, Weinheim.

Gernstein, G.L., Bloom, M.J., Espinosa, I.E., Evanczuk, S. and Turner, M.R. (1983) Design of a laboratory for multineuron studies. *IEEE Systems, Man Cybern.*, 13: 668 – 676.

Gielen, C.C.A.M. and van Zuylen, E.J. (1986) Coordination of arm muscles during flexion and supination: application of the tensor analysis approach. *Neuroscience*, 17: 527 – 539.

Hopfield, J. (1982) Neuronal networks and physical systems with emergent collective computational abilities. *PNAS*, 79: 2554 – 2558.

Kruger, J. (1982) A 12-fold microelectrode for recording from vertically aligned cortical neurons. *J. Neurosci. Methods*, 6: 347 – 350.

Kuperstein, M. and Whittington, D.A. (1981) A practical 24 channel microelectrode for neural recording in vivo. *IEEE Trans. Biomed. Eng.*, 28: 288 – 293.

Nashner, L.M. (1977) Fixed patterns of rapid postural responses among leg muscles during stance. *Exp. Brain Res.*, 30: 13 – 24.

Pellionisz, A.J. (1983) Brain theory: connecting neurobiology to robotics. Tensor analysis: utilizing intrinsic coordinates to describe, understand and engineer functional geometries to intelligent organisms. *J. Theor. Neurobiol.*, 2: 185 – 211.

Pellionisz, A.J. (1984) Coordination: a vector-matrix description of transformations of overcomplete CNS coordinates and a tensorial solution using the Moore-Penrose generalized inverse. *J. Theor. Biol.*, 110: 353 – 375.

Pellionisz, A.J. (1985) Tensorial aspects of the multidimensional approach to the vestibulo-oculomotor reflex and gaze. In: A. Berthoz and G. Melvill-Jones (Eds.), *Adaptive Mechanisms in Gaze Control*, Elsevier, Amsterdam, pp. 281 – 296.

Pellionisz, A.J. (1988a) Tensor geometry: a language of brains and neurocomputers. Generalized coordinates in neuroscience and robotics. In: R. Eckmiller and C. von Malsburg (Eds.), *Neural Computers*, Springer, Berlin, pp. 381 – 391.

Pellionisz, A.J. (1988b) Tensorial aspects of the multidimensional massively parallel sensorimotor function of neuronal networks. In: O. Pompeiano and J.H.J. Allum (Eds.), *Progress in Brain Research, Vol. 76*, Elsevier, Amsterdam, pp. 341 – 354.

Pellionisz, A.J. (1988c) Vistas from tensor network theory: a horizon from reductionalist neurophilosophy to the geometry of multi-unit recordings. In: R. Cotterill (Ed.), *Computer Simulation in Brain Science*, Cambridge University Press, Cambridge, pp. 44 – 73.

Pellionisz, A.J. (1989) Fractal geometry of Purkinje neurons: relationships among metrical and non-metrical neural geometries. *Soc. Neurosci. Abstr.*, 15: 180.

Pellionisz, A.J. (1991) Discovery of neural geomery by neurobiology and its utilization in neurocomputer theory and development. In: T. Kohonen (Ed.), *International Conference on Artificial Neural Networks, Helsinki*, North Holland, Amsterdam, pp. 485 – 493.

Pellionisz, A.J. and Bloedel, J.R (1991) Functional geometry of Purkinje cell population responses as revealed by neurocomputer analysis of multi-unit recordings. *Soc. Neurosci. Abstr.*, 21: 920.

Pellionisz, A.J. and Graf, W. (1987) Tensor network model of the "three-neuron vestibulo-ocular reflex-arc" in cat. *J. Theor. Neurobiol.,* 5: 127 – 151.

Pellionisz, A.J. and Llinás, R. (1980) Tensorial approach to the geometry of brain function: cerebellar coordination via metric tensor. *Neuroscience,* 5: 1125 – 1136.

Pellionisz, A.J. and Llinás, R. (1982) Space-time representation in the brain. The cerebellum as a predictive space-time metric tensor. *Neuroscience,* 7: 2949 – 2970.

Pellionisz, A.J. and Llinás, R. (1985) Tensor network theory of the metaorganization of functional geometries in the CNS. *Neuroscience,* 16: 245 – 274.

Pellionisz, A.J. and Peterson, B.W. (1988) A tensorial model of neck motor activation. In: B. Peterson and F. Richmond (Eds.), *Control of Head Movement,* Oxford University Press, Oxford, pp. 178 – 186.

Pellionisz, A.J. and Werbos, P.J. (1992) Cerebellar neurocontroller project, for aerospace applications, in a civilian Neurocomputing Initiative in the "Decade of the Brain" *IJCNN,* 3: 379 – 384.

Pellionisz, A.J., Soechting, J., Gielen, C., Simpson, J., Peterson, B. and Georgopoulos, A. (1986) Workshop: multidimensional analyses of sensorimotor systems. *Soc. Neurosci. Abstr.,* 12: 1.

Pellionisz, A.J., Peterson, B.W. and Tomko, D.L. (1990) Vestibular head-eye coordination: a geometrical sensorimotor neurocomputer paradigm. In: R. Eckmiller (Ed.), *Advanced Neurocomputing,* Elsevier, Amsterdam, pp. 126 – 145.

Peterson, B.W., Pellionisz, A.J., Baker, J.A. and Keshner, E.A. (1989) Functional morphology and neural control of neck muscles in mammals. *Am. Zool.,* 29: 139 – 149.

Pickard, R.S. (1979) A review of printed circuit microelectrodes and their production. *J. Neurosci. Methods,* 1: 301 – 319.

Pochay, P., Wise, K.D., Allard, L.F. and Rugledge, L.T. (1979) A multichannel depth probe fabricated using electron beam lithography. *IEEE Biomed. Eng.,* 26: 199 – 206.

Prohaska, O., Pacha, F., Pfundner, P. and Petsche, H. (1979) A 16-fold semimicroelectrode for intracortical recording of field potentials. *Electroenceph. Clin. Neurophysiol.,* 47: 629 – 631.

Reitboeck, H.J. (1983a) Fiber microelectrodes for electrophysiological recordings. *J. Neurosci. Methods,* 8: 249 – 262.

Reitboeck, H.J. (1983b) A multi-electrode matrix for studies of temporal signal correlations within neural assemblies. *Synergetics of the Brain,* Springer, Berlin, pp. 174 – 182.

Reitboeck, H.J. and Werner, G. (1983) Multi-electrode recording system for the study of spatio-temporal activity patterns of neurons in the central nervous system. *Experientia,* 39: 339 – 341.

Reitboeck, H.J., Adamczak, W., Eckhorn, R., Muth, P., Theilmann, R. and Thomas, U. (1981) Multiple single unit recording design and test of a 19 channel micromanipulator and appropriate fiber electrodes. *Neurosci. Lett. (Suppl.),* 7: S148.

Robinson, D.A. (1982) The use of matrices in analyzing the three-dimensional behavior of the vestibulo-ocular reflex. *Biol. Cybern.,* 46: 53 – 66.

Schwartz, A., Ebner, T. and Bloedel, J. (1987) Comparison of responses in dentate and interposed nuclei to perturbations of the locomotor cycle. *Exp. Brain Res.,* 67: 323 – 338.

Simpson, J. and Pellionisz, A. (1984) The vestibulo-ocular reflex in rabbit as interpreted using the Moore-Penrose generalized inverse transformation of intrinsic coordinates. *Soc. Neurosci. Abstr.,* 10: 909.

Simpson, J., Rudinger, D., Reisine, H. and Henn, V. (1986) Geometry of extraocular muscles of the rhesus monkey. *Soc. Neurosci. Abstr.,* 12: 1186.

Soechting, J.F. and Flanders, M. (1989) Errors in pointing are due to approximations in sensorimotor transformations. *J. Neurophysiol.,* 62: 595 – 608.

Werbos (1974) Beyond regression: new tools for prediction and analysis in the behavioral sciences. Ph. D. thesis, Harvard University, Cambridge, MA.

Werbos, P.J. and Pellionisz, A.J. (1992) Neurocontrol and neurobiology: new developments and connections. *IJCNN, IJCNN,* 3: 373 – 378.

Wise, K.D., Angell, J.B. and Starr, A. (1970) An integrated circuit approach to extracellular microelectrodes. *IEEE Biomed. Eng.,* 17: 238 – 246.

J.H.J. Allum, D.J. Allum-Mecklenburg, F.P. Harris and R. Probst
Progress in Brain Research, Vol. 97

Overview and critique of Chapters 24 – 25

R. Klinke

Frankfurt, Germany

The central evaluation of temporal information has concerned scientists over the years. In particular, the use of temporal information for pitch perception has caused major debates, documented, for example, in the Proceedings of the Driebergen Symposium on "Frequency Analysis and Periodicity Detection" (Plomp and Smoorenburg, 1970). In the meantime, it is well established that the fine time structure of an acoustic stimulus is, indeed, analyzed by the brain, at least up to a certain resolution. Results from cochlear implantation have contributed to this view. The papers by Shannon and by Blamey and Dooley treat similar problems and use a similar approach. Their topic is the contribution of temporal information to the analysis of acoustic stimuli.

In implanted patients the electrical stimulus mainly provides temporal information, by evoking action potentials strictly locked to the stimulus. Place information (using stimulation site as a cue) is poor, as the channel separation achievable by present stimulation devices is insufficient (Hartmann et al., 1984; Hartmann and Klinke, 1990). So, it appears that recipients of cochlear implants do receive optimal time information and, apparently, make wide use of it. Thus, it is of consequence to investigate their performance not only for the sake of a possible improvement to prosthetic devices, but also to gain insight into the human central processing of acoustic information.

The present papers use electrical stimulation in patients. They study the time course of masking phenomena prior or subsequent to a masker; gap detection, that is, the detection of a short interruption within a steady stimulus; and the percept of the modulation of an electrical signal.

The terms backward and forward masking stand for stimulus configurations where a probe stimulus is either presented prior to a more intense masker (backward masking) or the probe follows the masker (forward masking) (for a review see, for example, Elliot, 1971). The phenomenon of forward masking within the auditory system was first described by Lüscher and Zwislocki in 1949. Whereas forward masking can easily be looked upon as relief from adaptation, interpretation is less stringent for backward masking (see introduction of Shannon's paper).

The results presented in Shannon's paper are interpreted as demonstrating similarities between normal listeners and implanted patients. However, direct comparison is hampered by the necessity of normalization of the stimulus which is required because intensity functions for loudness in normal listeners differ from those in implanted patients. This also holds for comparisons of neuronal single-cell activity with acoustic and electrical stimulation (Hartmann et al., 1984). Although compensation for these incompatibilities are evidently necessary, the exact quantitative adjustment may be difficult. Also, for a thorough comparison, the paper lacks precise documentation of the configuration of masker and probe stimuli. Similarly, the loudness matching necessary for comparison of gap detection data in normal listeners and patients does contain a certain arbitrariness.

The paper by Blamey and Dooley is complementary to the one by Shannon, as also backward masking is investigated and as short stimulus sequences are used as the masker. The paper shows that forward masking is present immediately after a single-pulse masker. Backward masking, however, requires a multi-stimulus masker to be established. The strength for supra-threshold probe stimulation does, however, depend on the exact timing of the probe stimulus. In case of probe presentations at instances fitting into the 10 msec duty cycle of the masker, the threshold of the probe is high. Thus, central auditory structures establish an expectancy function as described first by Klinke et al. (1968) for vibratory stimuli.

Taken together, these papers provide new insights into central auditory processing.

References

Elliott, L.L. (1971) Backward and forward masking. *Audiology,* 10: 65 – 76.

Hartmann, R. and Klinke, R. (1990) Impulse patterns of auditory nerve fibres to extra- an intracochlear electrical stimulation. *Acta Otolaryngol. (Stockh.) (Suppl.),* 469: 128 – 134.

Hartmann, R., Topp, G. and Klinke, R. (1984) Discharge patterns of primary auditory fibres with electrical stimulation of the cochlea. *Hear. Res.,* 13: 47 – 62.

Klinke, R., Fruhstorfer, H. and Finkenzeller, P. (1968) Evoked responses as a function of external and stored information. *Electroenceph. Clin. Neurophysiol.,* 25: 119 – 122.

Lüscher, E. and Zwislocki, J. (1949) Adaptation of the ear to sound stimuli. *J. Acoust. Soc. Am.,* 21: 135 – 139.

Plomp, R. and Smoorenburg, G.F. (Eds.) (1970) *Frequency Analyses and Periodicity Detection in Hearing,* Sijthoff, Leiden.

J.H.J. Allum, D.J. Allum-Mecklenburg, F.P. Harris and R. Probst
Progress in Brain Research, Vol. 97

CHAPTER 24

Quantitative comparison of electrically and acoustically evoked auditory perception: implications for the location of perceptual mechanisms

Robert V. Shannon

House Ear Institute, Los Angeles, CA 90057, U.S.A.

Electrical stimulation of the human auditory system produces different patterns of spatial and temporal neural activity than those that occur in the normal, acoustically stimulated system. Quantitative comparison of psychophysical performance measured with acoustic and electrical stimulation may allow us to infer the physiological locus of perceptual mechanisms. In this paper we compare psychophysical data on temporal resolution from normal-hearing listeners, cochlear implant listeners, and patients electrically stimulated on the cochlear nucleus. Measures of gap detection, forward masking, and modulation detection will be compared. These comparisons demonstrate that temporal processing is relatively similar across these three groups once the obvious differences in dynamic range are taken into consideration. In addition, preliminary results with speech processors indicate that implant patients can utilize all temporal information in speech. Thus, implant patients have relatively normal temporal resolution and can integrate temporal cues normally for the recognition of complex acoustic patterns such as speech. These results imply that the central auditory systems of implant patients are able to fully utilize the non-natural patterns of temporal neural information produced by electrical stimulation. The differences in the microstructure of the neural pattern (phase locking, stochastic independence of fibers, spatial distribution of activity, etc.) between electrical and acoustic stimulation are apparently not necessary for temporal processing. Thus, the physiological locus of temporal processing mechanisms must be more central in the auditory system than the cochlea and cochlear nucleus.

Key words: Electrical stimulation; Cochlear implants; Psychophysics; Temporal processing

Introduction

It is a natural tendency of sensory physiologists and psychophysicists to attempt to relate as much of perception as possible to characteristics of the sensory end-organ. The sensory end-organ is generally the easiest part of a sensory system to study, and functional descriptions of most sensory end-organs are fairly complete. On the other hand, the complexity of central processing mechanisms precludes simple interpretations of results in terms of discrete central mechanisms.

In the auditory system, the relation between physiological mechanisms and perceptual effects has long been a source of speculation. Models have proposed a link between psychophysical forward masking and the recovery from adaptation (Zwislocki, 1969; Duifhuis, 1973; Shannon, 1986, 1990a), between backward masking and the propagation of the traveling wave as a function of stimulus level (Duifhuis, 1973), between neural firing rate and temporal integration (Zwislocki, 1969), between intensity discrimination and neural firing rates (Delgutte, 1987; Viemeister, 1988), between psychophysical and physiological two-tone suppression (Houtgast, 1972; Shannon, 1975), between distinct peripheral neural sub-populations and intensity coding (Zeng et al., 1991), and between psy-

chophysical critical bands and physiological tuning curves (Greenwood, 1961).

One of the motivating factors in these comparisons is that the physiology of the peripheral auditory system is relatively well characterized. Thus, when a psychophysical phenomenon is measured under similar conditions there is a natural tendency to relate as much of the psychophysical phenomenon to peripheral physiological mechanisms that are understood, rather than to potentially complex and unknown central processing.

The peripheral auditory system is so well characterized that concerted attention is now being given to the secondary mechanisms of auditory processing. Psychophysical attention is now being paid to more complex auditory patterns that produce interference or enhancement of wide-band signals using central mechanisms that cannot be explained by peripheral mechanisms, such as co-modulation masking release (Hall, 1987; Hall and Grose, 1990; Moore, 1992), profile analysis (Green, 1988), modulation masking (Houtgast, 1989) and informational masking (Neff and Callaghan, 1988). Physiological attention is being given to central integration mechanisms and specialized pattern recognition mechanisms in the auditory brain-stem nuclei (Knudsen and Konishi, 1979; Langner, 1983; Langner and Schreiner, 1988; Schreiner and Langner, 1988; Spitzer and Semple, 1991).

We suggest in this paper that, although temporal processing has long been thought to be limited peripherally, new evidence from electrical stimulation indicates that limitations on temporal processing are primarily central. Quantitative psychophysical data on temporal processing are available from normal-hearing listeners, from electrical stimulation of the cochlea, and from electrical stimulation of the cochlear nucleus. We will compare psychophysical performance of these three populations and discuss the implications of the results for the locus of physiological mechanisms for temporal processing.

Methods

Subjects

Twenty-four cochlear implant patients participated in this study. Ten patients had a Richards/Ineraid device, which is a 6-electrode, scala tympani implant with access to the electrodes through a percutaneous pedestal (Eddington et al., 1978). Seven patients had the Cochlear Corporation device, which has 22 electrodes implanted in the scala tympani and the speech processor uses a pulsatile, feature-extraction strategy (Clark et al., 1987). All cochlear implant patients were post-lingually deafened adults.

All seven auditory brain-stem implaint (ABI) patients were deafened as the result of bilateral acoustic tumor removal. Following the tumor removal, an electrode was placed in the lateral recess of the IV ventricle adjacent to the dorsal cochear nucleus. Stimulation of these electrodes produces sound sensation in most patients (Eisenberg et al., 1987; Shannon, 1989b; Shannon and Otto, 1990).

Equipment

For testing of patients with the Richards device and the ABI device we used a PC-clone microcomputer for stimulus generation and data collection. Stimuli were computed digitally and samples were output at a 10 kHz rate through 12-bit digital-to-analog converters (Data Translation DT2801-A). For sinusoidal stimuli, the signal was low-pass filtered at 5 kHz (6 dB/octave filter slope). This analog signal was then passed through an optically isolated, constant-current source (Vurek et al., 1981) to maintain control over stimulus current and for patient safety. The output of the optically isolated current source was connected directly to the patient's percutaneous connector (ITT Cannon). Before each testing session, the equipment was calibrated and electrode impedance was measured to assess electrode integrity.

Stimuli were delivered to the Nucleus device

through a specially designed computer interface capable of controlling the amplitude, pulse duration, and electrode configuration for each pulse in a stimulation sequence (Shannon et al., 1990). For these subjects the stimulus consisted of a 1000 Hz train of 100 μsec/phase biphasic pulses. The charge/pulse was modulated sinusoidally by changing the pulse width, while holding the pulse amplitude constant.

All patients responded on a small hand-held, touch-sensitive tablet (Koala Technologies). They were instructed in the use of a switch that would terminate all connections with the equipment in case of any unpleasant or uncomfortable stimulus.

Procedure

Gap detection, forward masking, and modulation detection data were collected in a two-alternative, forced-choice procedure. One interval contained a standard stimulus while the other contained the target stimulus, which was always a small modification of the standard stimulus. The subject was instructed to indicate which interval contained the target stimulus, either the one with a gap, a short probe tone or a modulated stimulus for gap detection, forward masking, or modulation detection, respectively. The difference between the standard and target stimuli was reduced following three successive correct responses and increased after each incorrect response to converge on the difference that would produce 79.4% correct (Levitt, 1971).

In gap detection, the subject's ability to detect a silent period, or gap, in an otherwise continuous stimulus 400 msec in duration is measured. The gap is reduced in duration to the duration at which the subject can reliably identify the interval with the gap 79.4% of the time.

Forward masking measures the recovery from adaptation following an intense stimulus. A loud stimulus, called a masker, is presented and then turned off. The threshold of a brief signal is measured at various time periods following the offset of the masker. At short time intervals, the signal threshold is elevated indicating the perceptual adaptation produced by the preceding masker. After sufficient time, the signal threshold returns to its unmasked level indicating no residual adaptation from the masker.

Modulation detection measures the patient's ability to detect amplitude variations in an otherwise continuous stimulus. The subject was presented with a 1 sec steady stimulus in one time interval and the same stimulus sinusoidally amplitude-modulated in another time interval. They were instructed to indicate which interval contained the modulated stimulus. The temporal modulation transfer function is the plot of modulation sensitivity as a function of modulation frequency.

Speech recognition was measured on video disk materials (Tyler et al., 1983) with the sound track from the video disk routed through an experimental speech processor (Wygonski et al., 1989). The speech processing strategy implemented was a single-channel version of Wilson et al.'s (1991) continuous interleaved sampler. This processor consists of a high-pass filter to equalize the speech energy, a half-wave rectifier and low-pass filter to extract the speech envelope. This envelope signal was then passed through an amplitude conversion from acoustic to electrical units (Shannon et al., 1992), which was then used to modulate a constant pulse train. Sixteen consonants in a v/C/v context were presented five times each in random order. The subject was shown the set of 16 possible consonants and was instructed to indicate which consonant was heard. Results reported here are from testing in a sound-only condition, i.e., without visual cues.

Results

Fig. 1 compares forward masking data from normal-hearing (from Plomp, 1964), cochlear implant (from Shannon, 1983, 1990b), and ABI listeners (from Shannon and Otto, 1990). The amplitude scale has been normalized to allow direct comparison. Implant listeners have different absolute threshold levels for electrical current depending on the location of the electrode relative to surviving neurons. The dynamic range of sound sensation from electrical stimulation also varies widely across

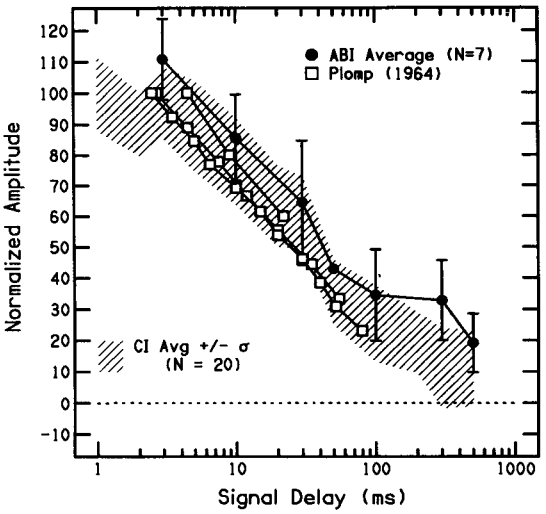

Fig. 1. Forward masked thresholds as a function of signal delay after masker off-set for acoustic, CI and ABI stimulation. Amplitude scales have been normalized in linear μA for electrical stimulation and in dB for acoustic stimulation. CI results from 20 patients are shown as a hatched area. Filled circles represent results from seven ABI patients. Open squares present data from acoustic stimulation from Plomp (1964) for three masker levels.

implant patients, so normalization is necessary to compare data across subjects. Implant data were normalized in linear μAmperes, while acoustic data were normalized in dB (Shannon, 1990b; Zeng and Shannon, 1992). On this normalized amplitude scale, it is apparent that all subjects demonstrate a similar time course of recovery of sensitivity following a stimulus. Immediately following the offset of the masker, signal thresholds are elevated to approximately the level of the masker. The threshold recovers to the unmasked level after 200 – 400 msec.

Fig. 2 compares gap detection data from normal-hearing (from Florentine and Buus, 1984), cochlear implant (from Shannon, 1989a), and ABI listeners (from Shannon and Otto, 1990). All data reported here are consistent with other measures of gap detection in implanted listeners (Dobie and Dillier, 1985; Moore and Glasberg, 1988; Preece and Tyler, 1989). Gap thresholds are presented as a function of the loudness of the stimulus containing the gap. Acoustic data from Florentine and Buus (1984) have been converted to an equivalent loudness scale using loudness scaling data from normal-hearing listeners with the same loudness estimation technique as that used with implant listeners (Shannon, 1983). All subjects required large gaps (20 – 50 msec) for detection when the stimuli were soft, and short gaps (2 – 5 msec) for detection when the stimuli were loud. For intermediate loudness levels acoustic listeners could detect smaller gaps than electrically stimulated listeners. This difference could be at least partly due to incorrect equalization of the loudness levels. Loudness estimates for electrical stimulation have considerable variability. Acoustic data were assigned loudness values using an average loudness function from different subjects than those in whom gap detection was measured. Thus, some of the difference between electrical stimulation and acoustic stimulation may be due to an improper match in the loudness scales.

Fig. 3 compares modulation detection functions for acoustic listeners (from Bacon and Viemeister, 1985), two types of cochlear implants (from Shannon, 1991) and ABI listeners (from Shannon and Otto, 1990). Detection thresholds for modulation

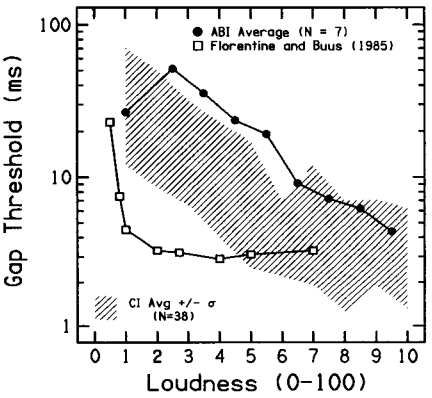

Fig. 2. Gap detection thresholds as a function of stimulus loudness for acoustic, CI and ABI stimulation. Carrier stimulus was a 1000 Hz sinusoid or pulse train for electrical stimulation and white noise for acoustic stimulation. CI results from 38 curves from 20 patients are shown as a hatched area. Filled circles represent results from seven ABI patients. Open squares represent data from acoustic stimulation from Florentine and Buus (1984) translated into loudness using loudness estimation data from Shannon (1983).

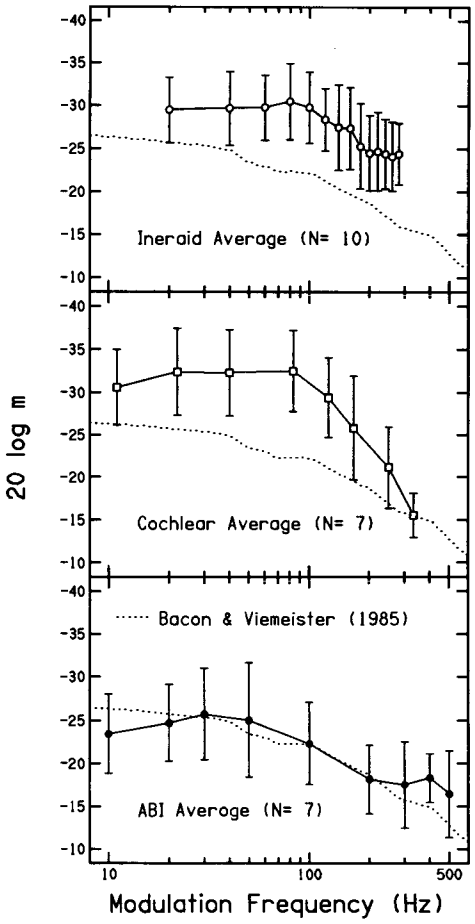

Fig. 3. Modulation detection as a function of modulation frequency for acoustic, CI and ABI stimulation. Carrier stimulus was either a 1000 Hz or 2000 Hz sinusoid or pulse train for electrical stimulation, and white noise for acoustic stimulation. Electrical stimulus levels were chosen to be comfortable-to-loud, i.e., in the range of 5 to 7 on the loudness scale of Fig. 2. Open circles present CI results from ten Ineraid patients. Open squares represent CI results from seven patients with the Cochlear Corp. implant when pulse duration was modulated. Filled circles represent results from seven ABI patients. The dashed line in each panel represents modulation detection data from normal-hearing listeners (Bacon and Viemeister, 1985).

are plotted as a function of modulation frequency. In all cases, the modulation detection functions are low-pass filter functions, with subjects most sensitive to low modulation frequencies. Sensitivity to amplitude modulation decreases with modulation frequency. Average curves for implant listeners are not substantially different from those of acoustic listeners (Shannon and Otto, 1990; Shannon, 1991).

One ABI patient was able to correctly recognize 70% of the 16 consonants in the sound-only condition and 95% correct in the sound-plus-lipreading condition. This level of performance is comparable to that observed by the best single-channel cochlear implant patients and the best performance of acoustic listeners restricted to temporal cues. Van Tasell et al. (1987) restricted normal-hearing listeners to temporal cues by modulating a wide-band noise with the temporal envelope of the speech sound. Without spectral cues, subjects were able to correctly identify 30–40% of consonants in a 16-consonant set. While this level of performance was surprisingly high, subjects could increase their performance to 70% correct after considerable training (Van Tasell, personal communication). Thus, 70% correct identification of consonants is possible using only temporal cues, for normal-hearing listeners or deaf listeners using single-channel implants. Direct electrical stimulation of the cochlear nucleus appears to cause no loss of temporal envelope information.

Discussion

Temporal processing, as represented by forward masking, gap detection and modulation detection, appears to be similar in normal-hearing listeners and in implant listeners electrically stimulated in the cochlea or cochlear nucleus. The patterns of neural activity produced by these three stimulation modes are all quite different. Direct electrical stimulation produces deterministic firing in a wide spatial region while acoustic stimulation produces a "traveling wave" pattern of activation with stochastically independent firing of nerves in any local region. In addition, stimulation of the dorsal cochlear nucleus (DCN) by the ABI electrode probably activates neurons across different tonotopic, morphological and functional regions of the DCN and ventral cochlear nucleus (VCN). Any first-order processing of the neural activity pattern in the cochlea or cochlear nucleus that might normally occur in acoustic stimu-

lation would be bypassed. Yet, in spite of these substantial differences between the spatial and temporal distribution of neural activity produced by the three stimulation modes, perceptual temporal processing is similar. This strongly suggests that the physiological mechanisms responsible for temporal processing are located more centrally than the cochlear nucleus and that these mechanisms are not sensitive to major alterations in the spatial distribution of the neural pattern.

These inferences, based on the quantitative comparison of envelope detection and discrimination, can also be extended to the temporal contribution to the sensation of pitch. It is well documented (Simmons, 1966; Shannon, 1983; Tong et al., 1983; Townshend et al., 1987) that implant listeners and implanted primates (Pfingst and Rush, 1987) can only distinguish temporal rates up to 300 – 500 Hz. Acoustically, Burns and Viemeister (1976, 1981) measured the ability of sinusoidally amplitude-modulated, broad-band stimuli to carry pitch cues. They found that pitch could be conveyed by non-spectral (temporal) cues only for modulation rates below 300 – 500 Hz. Physiologically, phase locking in the inferior colliculus deteriorates sharply for modulation rates above 300 Hz (Merzenich et al., 1973; Harris, 1987; Harris et al., 1990). Thus, temporal rate information in neural responses roughly matches the pitch range produced with electrical stimulation, which produces unnatural spatio-temporal patterns of neural activation. The central auditory system that determines the limits of temporally based pitch sensation must not depend on the fine structure of the peripheral neural pattern.

Where might the physiological mechanism(s) of temporal resolution reside? Langner and Schreiner (Langner, 1983; Langner and Schreiner, 1988; Schreiner and Langner, 1988) demonstrated that the inferior colliculus responds differentially to modulated sounds along the axis orthogonal to its tonotopic axis. They demonstrated that the temporal modulation pattern was converted to a spatial distribution of activity in this central auditory nucleus. This suggests that physiological mechanisms do exist for extracting the envelope information from complex acoustic stimuli. The perceptual data from implant patients suggest that these central mechanisms can extract envelope information from peripheral activity patterns that are unnatural in terms of their spatial distribution and temporal microstructure.

Recent psychophysical evidence has also suggested that temporal envelope information is processed centrally. Houtgast (1989), Bacon and Grantham (1989) and Yost et al. (1989) measured the interference of one envelope modulation frequency on detection of other modulation frequencies. All three studies demonstrated selectivity in the interference to similar modulation frequencies; a masker modulated at one temporal rate produced the most interference at similar rates. Because there is no known peripheral mechanism for segregating two signals based on their temporal patterns, these studies suggest central mechanisms for separating temporal patterns. One possible site is the inferior colliculus and the data of Langner and Schreiner suggest a physiological substrate.

The role of temporal cues in speech recognition has recently received renewed attention (Erber, 1972; Rosen et al., 1981; Grant et al., 1985; Breeuwer and Plomp, 1986; Van Tasell et al., 1987; Balakrishnan et al., 1991; Freyman et al., 1991). These studies suggest that temporal envelope information is particularly important for distinguishing consonants. The present analysis suggests that these cues can normally be perceived by deaf subjects if the proper amplitude transformation is used. Auditory prostheses should be able to provide deaf patients with envelope cues and voicing fundamental frequency, cues which can provide considerable speech discrimination.

Preliminary speech recognition scores indicate that implanted patients can fully utilize temporal cues in discriminating and recognizing consonants (Eddington, 1980; Wilson et al., 1988, 1991; Rosen, 1989; Rosen et al., 1989; Dorman et al., 1990; Shannon et al., 1992). Combined with the psychophysical results, this indicates that electrical stimulation of the cochlea or cochlear nucleus does not disturb temporal envelope information and that patients

with prosthetic devices can utilize these envelope cues normally in speech recognition, once the proper amplitude conversion is made. Thus, any physiological mechanisms that interpret temporal envelope information must lie more centrally in the auditory system, and must not be sensitive to the details of the neural activity pattern that conveys this temporal information.

Acknowledgements

The patience and perseverence of the implant patients is gratefully acknowledged. Supported in part by NIH, the FDA, and HEI.

References

Bacon, S.P. and Grantham, D.W. (1989) Modulation masking: effects of modulation frequency, depth and phase. *J. Acoust. Soc. Am.*, 85: 2575 – 2580.

Bacon, S.P. and Viemeister, N.F. (1985) Temporal modulation transfer functions in normal-hearing and hearing-impaired listeners. *Audiology*, 24: 117 – 134.

Balakrishnan, U., Freyman, R.L., Chuan, C.Y., Nerbonne, G.P. and Shea, K.J. (1991) Effect of consonant-vowel intensity ratio on the intelligibility of spectrally degraded speech. *J. Acoust. Soc. Am.*, 89: S1935.

Breeuwer, M. and Plomp, R. (1986) Speech reading supplemented with auditorily presented speech parameters. *J. Acoust. Soc. Am.*, 79: 481 – 499.

Burns, E.M. and Viemeister, N.F. (1976) Nonspectral pitch. *J. Acoust. Soc. Am.*, 60: 863 – 869.

Burns, E.M. and Viemeister, N.F. (1981) Played-again SAM: further observations on the pitch of amplitude-modulated noise. *J. Acoust. Soc. Am.*, 70: 1655 – 1660.

Clark, G.M. (1987) *The University of Melbourne-Nucleus Multi-electrode Cochlear Implant*, Karger, New York.

Delgutte, B. (1987) Peripheral auditory processing of speech information: implications from a physiological study of intensity discrimination. In: M.E.H. Schouten (Ed.), *Psychophysics of Speech Perception*, Elsevier, Amsterdam, pp. 333 – 353.

Dobie, R.A. and Dillier, N. (1985) Some aspects of temporal coding for single-channel electrical stimulation of the cochlea. *Hear. Res.*, 18: 41 – 55.

Dorman, M.F., Soli, S., Dankowski, K., Smith, L.M., McCandless, G. and Parkin, J. (1990) Acoustic cues for consonant identification by patients who use the Ineraid cochlear implant. *J. Acoust. Soc. Am.*, 88: 2074 – 2079.

Duifhuis, H. (1973) Consequences of peripheral frequency selectivity for nonsimultaneous masking. *J. Acoust. Soc. Am.*, 54: 1471 – 1488.

Eddington, D.K. (1980) Speech discrimination in deaf subjects with cochlear implants. *J. Acoust. Soc. Am.*, 68: 885 – 891.

Eddington, D.K., Dobelle, W.H., Brachman, D.E., Mladevosky, M.G. and Parkin, J.L. (1978) Auditory prosthesis research with multiple channel intracochlear stimulation in man. *Ann. Otol. Rhinol. Laryngol.*, 87 (Suppl. 53): 1 – 39.

Eisenberg, L.S., Maltan, A.A., Portillo, F., Mobley, J.P. and House, W.F. (1987) Electrical stimulation of the auditory brain stem structure in deafened adults. *J. Rehab. Res. Dev.*, 24: 9 – 22.

Erber, N. (1972) Speech envelope cues as an acoustic aid to lipreading for profoundly deaf children. *J. Acoust. Soc. Am.*, 51: 1224 – 1227.

Florentine, M. and Buus, S. (1984) Temporal gap detection in sensorineural and simulated hearing impairment. *J. Speech Hear. Res.*, 27: 449 – 455.

Freyman, R.L., Nerbonne, G.P. and Cote, H.C. (1991) Effect of consonant-vowel ratio modification on amplitude envelope cues for consonant recognition. *J. Speech Hear. Res.*, 34: 415 – 426.

Grant, K.W., Ardell, L., Kuhl, P. and Sparks, D. (1985) The contribution of fundamental frequency, amplitude envelope, and voicing duration cues to speech reading in normal subjects. *J. Acoust. Soc. Am.*, 77: 671 – 677.

Green, D.M. (1988) *Profile Analysis*, Oxford University Press, New York.

Greenwood, D.D. (1961) Critical bandwidth and frequency coordinates on the basilar membrane. *J. Acoust. Soc. Am.*, 33: 1344 – 1356.

Hall, J.W. (1987) Experiments on comodulation masking release. In: W.A. Yost and C.S. Watson (Eds.), *Auditory Processing of Complex Sounds*, Erlbaum, NJ, pp. 57 – 66.

Hall, J.W. and Grose, J.H. (1990) Comodulation masking release and auditory grouping. *J. Acoust. Soc. Am.*, 88: 119 – 125.

Harris, D.M. (1987) Current source density analysis of frequency coding in inferior colliculus. *Hear. Res.*, 26: 257 – 266.

Harris, D.M., Lambert, D. and Shannon, R.V. (1990) Trade-off between spatial and synchrony representations of stimulus frequency of the gerbil IC. In: D.J. Lim (Ed.), *Abstracts of the ARO Midwinter Research Meeting.*

Houtgast, T. (1972) Psychophysical evidence for lateral inhibition in hearing. *J. Acoust. Soc. Am.*, 51: 1885 – 1894.

Houtgast, T. (1989) Frequency selectivity in amplitude-modulation detection. *J. Acoust. Soc. Am.*, 85: 1676 – 1680.

Knudsen, E.I. and Konishi, M. (1979) Mechanisms of sound localization in the barn owl *(Tyto alba)*. *J. Comp. Neurol.*, 133: 13 – 21.

Langner, G. (1983) Evidence for neuronal periodicity detection in the auditory system of the guinea fowl: implications for pitch analysis in the time domain. *Exp. Brain Res.*, 52: 333 – 355.

Langner, G. and Schreiner, C.E. (1988) Periodicity coding in the

inferior colliculus of the cat. I. Neuronal mechanisms. *J. Neurophysiol.*, 60: 1799 – 1822.

Levitt, H. (1971) Transformed up-down methods in psychoacoustics. *J. Acoust. Soc. Am.*, 49: 467 – 477.

Merzenich, M.M., Michelson, R.P., Pettit, C.R., Schindler, R.A. and Reid, M.D. (1973) Neural encoding of sound sensation evoked by electrical stimulation of the acoustic nerve. *Ann. Otol. Rhinol. Laryngol.*, 82: 486 – 504.

Moore, B.C.J. (1993) Comodulation masking release and across-channel masking. In: M.E.H. Schouten (Ed.), *The Auditory Processing of Speech: from Sounds to Words*, Mouton-De Gruyter, Berlin, pp. 167 – 184.

Moore, B.C.J. and Glasberg, B.R. (1988) Gap detection with sinusoids and noise in normal, impaired, and electrically stimulated ears. *J. Acoust. Soc. Am.*, 83: 1093 – 1101.

Neff, D. and Callaghan, B.P. (1988) Effective properties of multicomponent simultaneous maskers under conditions of uncertainty. *J. Acoust. Soc. Am.*, 83: 1833 – 1838.

Pfingst, B.E. and Rush, N.L. (1987) Discrimination of simultaneous frequency and level changes in electrical stimuli. *Ann. Otol. Rhinol. Laryngol.*, 96 (Suppl. 128): 34 – 37.

Plomp, R. (1964) Rate of decay of auditory sensation. *J. Acoust. Soc. Am.*, 36: 277 – 282.

Preece, J.P. and Tyler, R.S. (1989) Temporal-gap detection by cochlear prosthesis users. *J. Speech Hear. Res.*, 32: 849 – 856.

Rosen, S. (1989) Temporal information in speech and its relevance for cochlear implants. In: B. Fraysee and N. Cochard (Eds.), *Cochlear Implant: Acquisitions and Controversies*, Toulouse Implant Conference Proceedings, Toulouse, pp. 3 – 26.

Rosen, S., Fourcin, A.J. and Moore, B.C.J. (1981) Voice pitch as an aid to lipreading. *Nature*, 291: 150 – 152.

Rosen, S., Walliker, J. Brimacombe, J.A. and Edgerton, B.J. (1989) Prosodic and segmental aspects of speech perception with the House/3M single channel implant. *J. Speech Hear. Res.*, 32: 93 – 111.

Schreiner, C.E. and Langner, G. (1988) Periodicity coding in the inferior colliculus of the cat. II. Topographic organization. *J. Neurophysiol.*, 60: 1823 – 1840.

Shannon, R.V. (1975) *Suppression of Forward Masking*, Ph.D. Thesis, University of California, San Diego, CA.

Shannon, R.V. (1983) Multichannel electrical stimulation of the auditory nerve in man: I. Basic psychophysics. *Hear. Res.*, 11: 157 – 189.

Shannon, R.V. (1986) Temporal processing in cochlear implants. In: M.J. Collins, T.J. Glattke and L.A. Harker (Eds.), *Sensorineural Hearing Loss: Mechanisms, Diagnosis, and Treatment*, University of Iowa Press, Iowa City, pp. 349 – 368.

Shannon, R.V. (1989a) Detection of gaps in sinusoids and biphasic pulse trains by patients with cochlear implants. *J. Acoust. Soc. Am.*, 85: 2587 – 2592.

Shannon, R.V. (1989b) Threshold functions for electrical stimulation of the human cochlear nucleus. *Hear. Res.*, 40: 173 – 178.

Shannon, R.V. (1990a) A model of temporal integration and forward masking for electrical stimulation of the auditory nerve. In: J.M. Miller and F.A. Spelman (Eds.), *Models of the Electrically Stimulated Cochlea*, Springer, New York, pp. 187 – 205.

Shannon, R.V. (1990b) Forward masking in patients with cochlear implants. *J. Acoust. Soc. Am.*, 88: 741 – 744.

Shannon, R.V. (1991) Temporal modulation transfer functions in patients with cochlear implants. *J. Acoust. Soc. Am.*, 91: 1974 – 1982.

Shannon, R.V. and Otto, S.R. (1990) Psychophysical measures from electrical stimulation of the human cochlear nucleus. *Hear. Res.*, 47: 159 – 168.

Shannon, R.V., Adams, D.D., Ferrel, R.L., Palumbo, R.L. and Grandgenett, M. (1990) A computer interface for psychophysical and speech research with the nucleus cochlear implant. *J. Acoust. Soc. Am.*, 87: 905 – 907.

Shannon, R.V., Zeng, F-G. and Wygonski, J. (1993) Speech recognition with only temporal cues. In: M.E.H. Schouten (Ed.), *The Auditory Processing of Speech: from Sounds to Words*, Mouton-De Gruyter, Berlin, pp. 263 – 274.

Simmons, F.B. (1966) Electrical stimulation of the auditory nerve in man. *Arch. Otolaryngol.*, 84: 2 – 54.

Spitzer, M.W. and Semple, M.N. (1991) Interaural phase coding in the auditory midbrain: influence of dynamic stimulus features. *Science*, 254: 721 – 722.

Tong, Y.C., Blamey, P.J., Dowell, R.C. and Clark, G.M. (1983) Psychophysical studies evaluating the feasibility of a speech processing strategy for a multiple-channel cochlear implant. *J. Acoust. Soc. Am.*, 74: 73 – 80.

Townshend, B., Cotter, N., van Compernolle, D. and White, R.L. (1987) Pitch perception by cochlear implant subjects. *J. Acoust. Soc. Am.*, 82: 106 – 115.

Tyler, R.S., Preece, J.P. and Lowder, M.W. (1983) *The Iowa Cochlear Implant Test Battery. Laboratory Report*, Department of Otolaryngology, University of Iowa, Iowa City.

Van Tasell, D.J., Soli, S.D., Kirby, V.M. and Widin, G.P. (1987) Speech waveform envelope cues for consonant recognition. *J. Acoust. Soc. Am.*, 82: 1152 – 1161.

Viemeister, N.F. (1988) Psychophysical aspects of auditory intensity coding. In: G.M. Edelman, W.E. Gall and W.M. Cowan (Eds.), *Auditory Function: Neurological Bases of Hearing*, Wiley, New York, pp. 213 – 241.

Vurek, L.S., White, M., Fong, M. and Walsh, S.M. (1981) Optoisolated stimulators used for electrically evoked BSER. *Ann. Otol. Rhinol. Laryngol.*, 90 (Suppl. 82): 21 – 24.

Wilson, B.S., Finley, C.C., Lawson, D.T. and Wolford, R.D. (1988) Speech processors for cochlear prostheses. *Proc. I.E.E.E.*, 76: 1143 – 1154.

Wilson, B.S., Finley, C.C., Lawson, D.T., Wolford, R.D., Eddington, D.K. and Rabinowitz, W.M. (1991) New levels of speech recognition with cochlear implants. *Nature*, 352: 236 – 238.

Wygonski, J., Maltan, A. and Mobley, J.P. (1989) A DSP-based

system for electrical stimulation. *Proc. IEEE Eng. in Med. and Biol. Soc., 11th Annual International Conference,* pp. 1067 – 1068.

Yost, W.A., Sheft, S. and Opie, J. (1989) Modulation interference in detection and discrimination of amplitude modulation. *J. Acoust. Soc. Am.,* 86: 2138 – 2147.

Zeng, F.G. and Shannon, R.V. (1992) Loudness balance between electrical and acoustic stimulation. *Hear. Res.,* 60: 231 – 235.

Zeng, F.G., Turner, C.W. and Relkin, E.M. (1991) Recovery from prior stimulation. II. Contributions to intensity discrimination. *Hear. Res.,* 55: 223 – 230.

Zwislocki, J.J. (1969) Temporal summation of loudness: an analysis. *J. Acoust. Soc. Am.,* 46: 431 – 441.

J.H.J. Allum, D.J. Allum-Mecklenburg, F.P. Harris and R. Probst
Progress in Brain Research, Vol. 97

CHAPTER 25

Pattern recognition and masking in cochlear implant patients

P.J. Blamey and G.J. Dooley

Human Communication Research Centre, Department of Otolaryngology, University of Melbourne, East Melbourne 3002, Australia

Studies of the temporal course of masking using pulsatile electrical stimulation provide a sensitive new technique for the investigation of central pattern recognition. The masked threshold for a single-pulse probe was studied for several different maskers as a function of the time between the probe and the start of the masker. These experiments showed the gradual development of a temporal pattern in the masked thresholds as the number of pulses in the masker was increased. For a 210 msec masker with pulses at 10 msec intervals, both backward and forward masking thresholds showed a well-defined peak at times 10 msec before and after the masker. Probe pulses presented at these times were probably perceived to be part of the masker pattern and therefore were not easily identified as probe pulses. This conclusion was confirmed by using a masker with pulses at 20 msec intervals. Only backward masking was tested, and the results showed a peak approximately 20 msec before the start of the masker, fitting in with the temporal pattern of the masker.

Key words: Masking; Cochlear implant; Pattern recognition

Introduction

The elevation of the threshold of detection of a "probe" stimulus in the presence of another "masker" stimulus is a phenomenon that has been studied extensively to provide insight into the workings of the auditory system (e.g., Moore, 1982). "Backward", "simultaneous" and "forward" masking may occur when the probe precedes, overlaps or follows the masker, respectively. Many aspects of masking have been interpreted in terms of processes occurring at the level of the cochlea or the auditory nerve, although there are obviously some masking effects that require an explanation in terms of more central processing. The most obvious of these is backward masking, where the detection threshold of a probe stimulus is raised by the presence of a masker that follows the probe (e.g., Elliot, 1971). Peripheral effects can be ruled out in this case because the time between the end of the probe and the start of the masker can be made long enough for all traces of the probe to have disappeared from the cochlea and auditory nerve. The central processing involved in backward masking is not well understood.

Masking has also been used to study the auditory sensations produced by cochlear implants (Shannon, 1983; Lim et al., 1989). These researchers were primarily interested in the spread of electric current around the stimulated electrodes, and used forward masking as a measure of this spread. Forward masking was used because its major component is thought to be peripheral and it avoids the problem of physical current summation in the cochlea that might arise in simultaneous masking.

There is, however, another aspect of masking that is particularly relevant to the coding of speech with cochlear implants, and that is the temporal course of masking. The speech signal contains spectral components that change rapidly in amplitude and fre-

quency. Relatively weak spectral components of consonants occur before and after strong vowel components. These vowel and consonant components are represented as electrical stimuli applied to an electrode array in a multiple-channel cochlear implant. Hence, the temporal properties of forward and backward masking are important to the understanding of consonant perception with a cochlear implant. The experiments described here were initiated in order to study temporal effects in masking, with possible applications to speech coding.

Electrical stimulation has a special property that makes these experiments easier to perform and interpret than analogous acoustic experiments. This property is the ability to produce very short electrical stimuli with an excitation pattern in the auditory nerve that is very short in duration (Javel et al., 1987). In the acoustic case, a short stimulus produces a spread of spectral components and the traveling wave in the cochlea extends the duration of neural activity over a longer time than the duration of the stimulus itself. This ability to produce well controlled short stimuli reveals fine details of the masked threshold patterns and allows them to be interpreted unambiguously.

Methods

Several experiments are described below, differing only in the characteristics of the masker. This section describes those aspects of the method that were common to all the experiments.

The electrical stimuli were produced with the University of Melbourne/Cochlear Pty. Ltd. multichannel cochlear prosthesis (Clark et al., 1984) controlled by a personal computer with software written specifically for adjusting the prosthesis. Electrode 10, near the middle of the electrode array was used for all experiments. The electric current flowed between electrode 10 and all other electrodes in the array (common ground stimulation mode). The probe stimulus consisted of a single biphasic pulse applied to the electrode. The current level of the pulse was fixed at the maximum level reliably produced by the implanted receiver/stimulator (approximately 1 mA) and the charge in each phase of the pulse was controlled by varying the duration of each phase in the range of 20 – 200 μsec. There was a fixed gap of 40 μsec between the two phases. As illustrated in Fig. 1, the masker stimuli consisted of one or more biphasic pulses at a fixed charge per phase set to be 6 dB above the threshold for a single (unmasked) pulse. The threshold for a single unmasked electrical pulse was between 65 and 75 μsec.

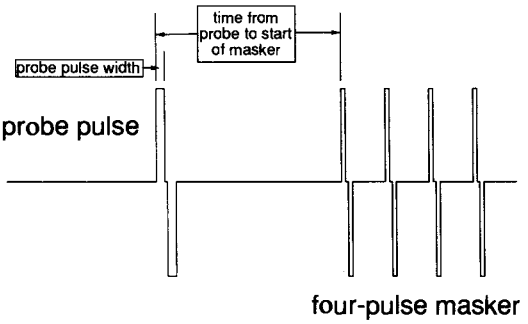

Fig. 1. An example of the electrical current waveforms used, showing the biphasic pulses for the probe and masker. The probe pulse width was varied to find the masked threshold as a function of time between the probe pulse and the start of the masker.

The time between the start of the probe pulse and the start of the masker was varied to study backward, forward and "simultaneous" masking. It should be noted that the probe pulses for the "simultaneous" conditions fell between the masker pulses and did not overlap with them at all so that there was no possibility of electrical current summation in the cochlea. A PEST procedure (Taylor and Creelman, 1967) was used to vary the pulse width of the probe in order to find the threshold. In each trial, four masker stimuli were presented, with 1 sec intervals between them. Only one was accompanied by the probe stimulus and the subject was required to respond with the number of the stimulus containing the probe. Threshold was defined as the pulse width at which 66% of probe stimuli were successfully identified in this four-interval, four-alternative forced-choice procedure. The procedure began with the probe pulse width at 200 μsec and a step size of 40 μsec. The procedure terminated when the pulse width step size had reduced to 5 μsec.

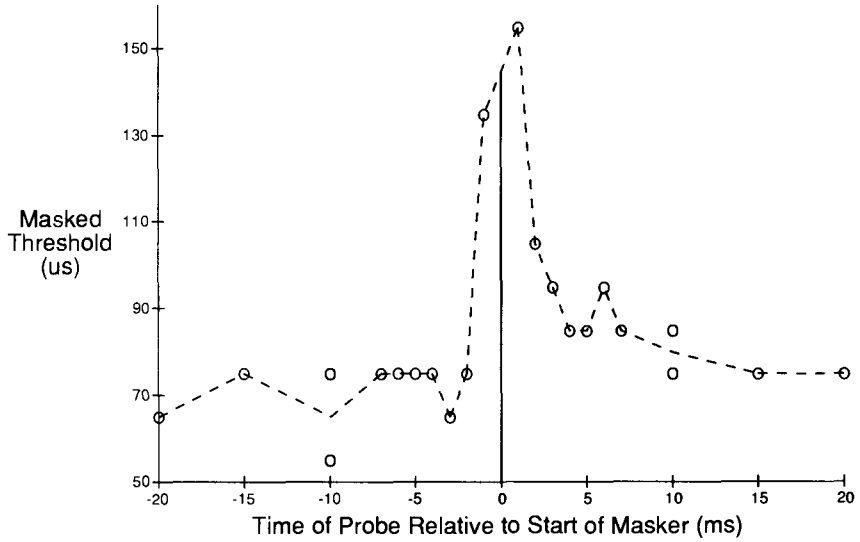

Fig. 2. Masked thresholds for a single-pulse masker. Each circle represents the end-point of a PEST measurement procedure. The vertical line shows the time and pulse width of the masker. The dashed line joins the mean threshold values at different times.

Data for one subject are reported here. This patient (referred to as Patient 67 in previous publications) was a post-linguistically deafened adult who had been using the cochlear implant for two years at the time of these experiments. She was above average in her speech perception results. Data for two other patients have been collected but not analysed in detail. They are consistent with the data reported here.

Experiment 1: single-pulse masker

In this experiment, the masker consisted of a single

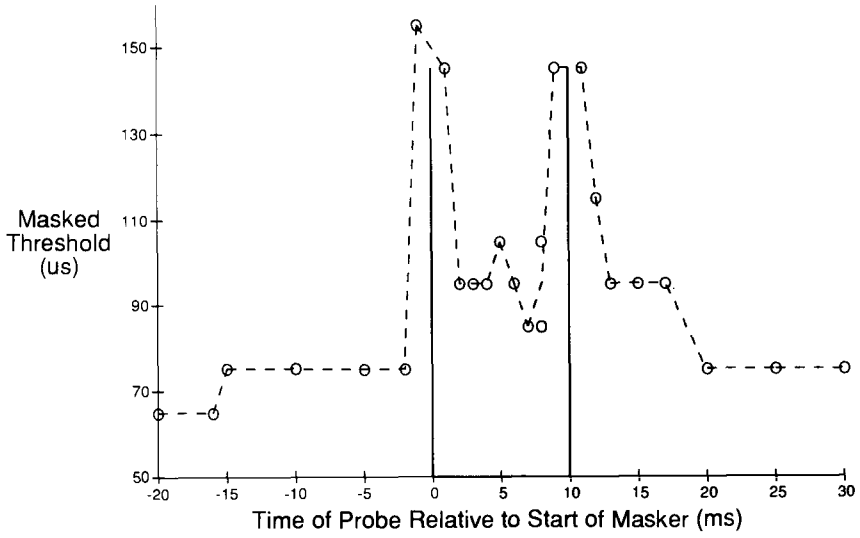

Fig. 3. Masked thresholds for a two-pulse masker.

biphasic electrical pulse with a pulse width of 145 μsec per phase. The threshold of the single-pulse probe stimulus was measured for times before and after the masker. The masked thresholds are shown in Fig. 2. Each circle on the figure corresponds to the end-point of a PEST procedure. The solid line represents the masker pulse. The shape of the threshold curve is reminiscent of the threshold curve during the refractory period of a single neuron but has a duration that is longer than measured refractory times. The forward masking observed is probably peripheral in origin. No backward masking was observed except when the probe occurred 1 msec before the masker.

Experiment 2: two-pulse masker

The masker for this experiment consisted of two biphasic pulses separated by 10 msec, each with a pulse width of 145 μsec per phase. Fig. 3 shows the masked threshold of the probe stimulus as a function of time. The solid lines represent the two masker pulses. The threshold for the probe traced out a curve similar to the addition of two single-pulse masked threshold curves displaced by 10 msec in time. As before, the only backward masking occurred 1 msec before the masker. The "simultaneous" masking between the two masker pulses was no greater than the forward masking produced by the single-pulse masker in experiment 1. Again, the elevation of thresholds observed is probably due to peripheral effects such as the refractory period of the nerves excited by the masker.

Experiment 3: four-pulse masker

In this experiment, the masker was extended to contain four pulses at 10 msec intervals, giving a total duration of 30 msec. The solid lines in Fig. 4 show the timing and pulse width of the masker pulses. The masked thresholds are also shown. The pattern differs from the summation of four displaced single-pulse masking patterns at 10 msec intervals. The forward and simultaneous maskings are higher than would be expected from such a summation, and there appears to be some backward masking although this did not occur in every run of the PEST procedure. This backward masking probably arises

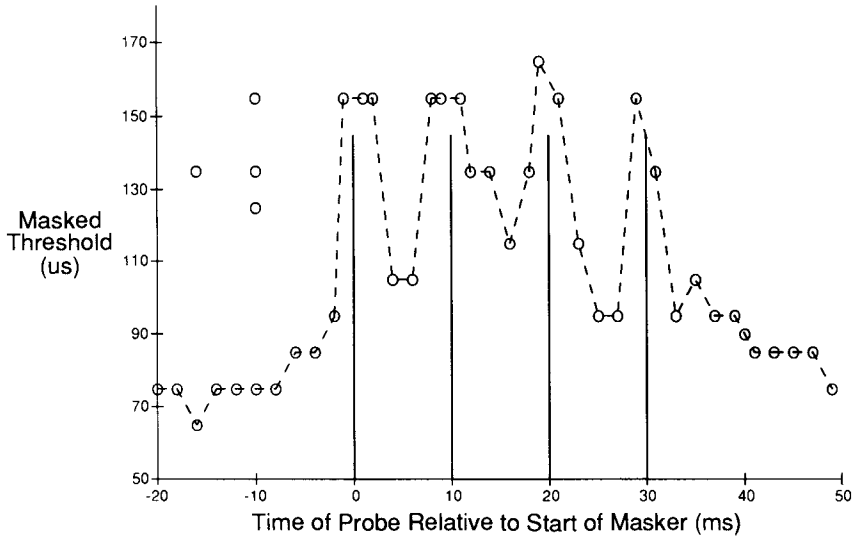

Fig. 4. Masked thresholds for a four-pulse masker. The four thresholds above 120 μsec at times −10 to −16 msec were excluded from the calculations of mean thresholds shown as a dashed line (see pattern recognition discussion in the text).

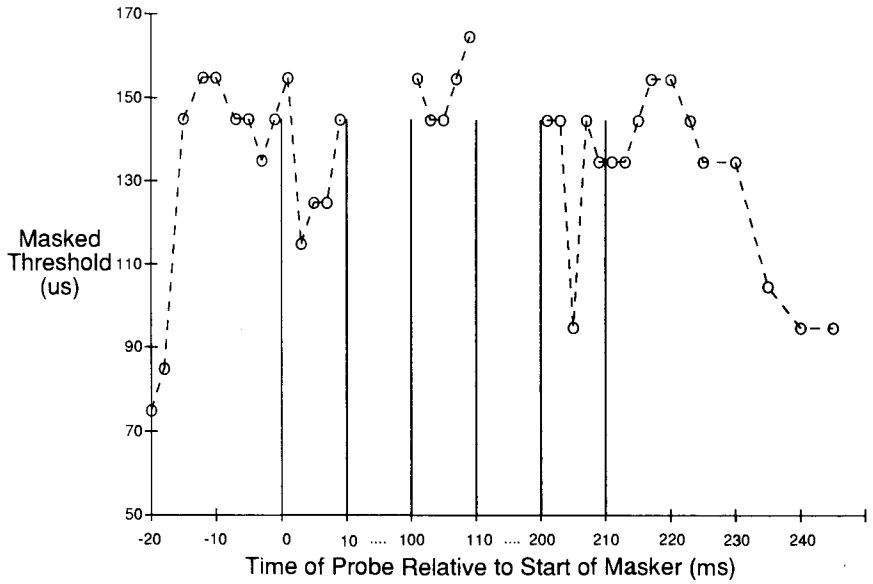

Fig. 5. Masked thresholds for a long (210 msec) masker. Note the breaks in the time scale along the horizontal axis.

from pattern recognition at a central level of processing, but detailed discussion is deferred until after the description of experiment 4.

Experiment 4: long masker (22 pulses)

The long masker was 210 msec in duration, containing 22 biphasic pulses at 10 msec intervals with a pulse width of 145 μsec. This masker was the one most similar to maskers usually used in acoustic masking experiments. The masked thresholds are shown in Fig. 5. Because of the duration of this masker, the probe threshold was not measured for all times during the masker. Instead, measurements were taken at the start and end of the masker, and for the 10 msec period in the middle of the masker. The main features of the masked threshold curve were: (a) strong backward masking extending over times up to 15 msec before the start of the masker with a peak about 10 – 12 msec before the masker; (b) strong forward masking extending for at least 25 msec after the end of the masker with a peak about 10 msec after the masker; and (c) fluctuating thresholds for "simultaneous" masking with peaks corresponding to times close to the masker pulses and dips between them. The dips between the masker pulses at the ends of the stimuli indicated less masking than at the middle of the stimulus.

It is probable that the backward masking arose from a central pattern recognition process described in the next section, and that the simultaneous and forward masking arose from a combination of peripheral and central effects.

Pattern recognition

Although the experiments above have been described in the language usually used for masking, they may also be described as discrimination experiments, where the subject's task was to indicate which one of the four stimuli was different from the other three in each trial of the 4AFC procedure. It should be noted that the probe pulse was presented to the same electrode as the masker pulses and was therefore indistinguishable from them except by the time that it occurred and by its pulse width. The criterion used by the subject to discriminate between the stimuli was not directly under the control of the

experimenter. Examples of criteria that a subject might have used include the following: was there an extra pulse? Was one stimulus louder than the others? Was one stimulus longer than the others? Was the pulse rate consistent throughout the stimulus?

One explanation of the threshold curves for the one- and two-pulse maskers is that the patient could count the individual pulses and the probe pulse was counted whenever it produced a sufficiently large excitation of the auditory nerves.

In the case of the long masker, this explanation is unlikely as there is evidence that a person cannot count more than five events at rates higher than about 10 per second (Garner, 1951). It is also known that the duration difference limen is of the order of 10 – 20% for electrical stimuli that are 200 msec in duration (Blamey et al., 1990). Thus, overall duration is unlikely to be important in discriminating between the stimulus plus probe and the other stimuli. Nor is it likely that the overall loudness of the stimulus would be altered substantially by the addition of an extra pulse of similar intensity to the masker pulses. This would be similar to the loudness judgments required in integration time measures. For acoustic stimulation above threshold (Zwislocki, 1969) and electrical stimulation (Shannon, 1983), integration times are in the range of 50 – 100 msec, much shorter than the long masker used here. The only remaining criteria listed above are concerned with whether the probe pulse fits the pattern of the masker: does it have the same pulse width as the masker pulses, and does it occupy a position in time that is appropriate for a masker pulse? If a probe pulse has pulse width and timing appropriate to the masker pattern, it will be more difficult to recognise than one which is different in pulse width and/or timing. When a probe pulse occurred 10 msec before the masker, or 10 msec after the masker, it matched the masker timing pattern and could be perceived as part of the masker rather than a separate probe pulse unless the pulse width was sufficiently different from the masker pulses.

This explains the peaks that were observed in the masked thresholds 10 msec before and after the long masker. Conversely, probe pulses at times that did not fit the masker pattern were recognised at lower pulse widths, producing dips in the curve.

Next, consider the backward masking results for the four-pulse masker. Fig. 4 shows four points where the masked threshold was elevated above the general level of the other results. These points all occur in the region where the probe pulse occupied a time that approximately fitted the pattern of the masker, and had a pulse width similar to the masker pulses. If the overall duration or intensity of the probe-plus-masker was used to discriminate it from the masker by itself, the psychometric function for a probe 10 msec before the masker would be expected to have a monotonic sigmoid shape. However, if probe pulses with pulse widths close to the masker pulse widths are harder to discriminate than probe pulses with different widths, the psychometric function would be expected to be non-monotonic with a dip in recognition at the masker pulse width. Fig. 6 shows the psychometric function obtained during the PEST procedures for probes occurring 10 msec before the four-pulse masker. Included for comparison are the psychometric functions for times 20 msec before and 4 msec after the first masker pulse. The psychometric function 10 msec before the masker is non-monotonic as expected, while the other functions have the more conventional monotonic sigmoid shape.

Experiment 5: long masker with fewer pulses

A further prediction may be made on the basis of the pattern recognition hypothesis: if the pulse rate of the masker is changed, the peaks in the forward and backward masking threshold curves should be shifted in time to match the pattern of the masker. To test this prediction, an experiment using a long masker (200 msec in duration) with pulses at 20 msec intervals was carried out. Only backward masking was investigated. Through an oversight, the masker pulse width was slightly lower than that used for the maskers in experiments 1 – 4. The result is shown in Fig. 7, together with results for a long masker with pulses at 10 msec intervals and the same pulse width.

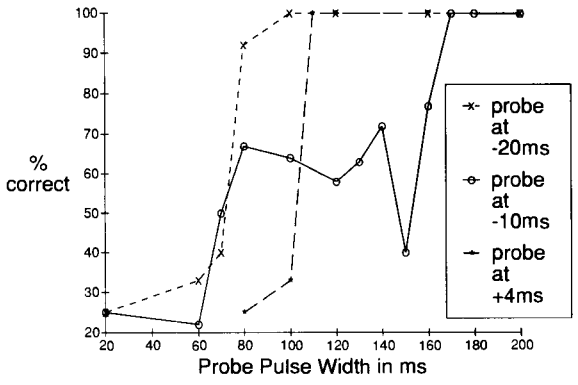

Fig. 6. Psychometric functions obtained from the PEST procedures for the four-pulse masker and probes at −20, −10 and +4 msec relative to the start of the masker.

It is clear that the masker with every second pulse omitted produced more backward masking than the other masker, and that the peak in the masking function moved to an earlier time in accordance with the prediction of the pattern recognition hypothesis.

Conclusion

The results indicate fine temporal detail in the masking patterns produced by pulsatile electrical stimuli. This detail is more easily obtained with electrical stimuli than with acoustic stimuli because of the spectral and temporal spread inherent in short acoustic stimuli. Forward, backward and simultaneous masking occurred for the long stimuli. The backward masking can be explained entirely in terms of a central pattern recognition process. The simultaneous and forward masking had components that were probably peripheral as well as central components. The extent of backward masking was less than the extent of forward masking for long stimuli, and depended on the temporal characteristics (pulse rate) of the masker. The peripheral component of the forward masking extended for at least 25 msec after the masker. Simultaneous masking was stronger near the middle of the masker than near the ends.

The observed masking patterns indicate that the recognition of short acoustic segments such as consonants may be affected by forward or backward masking. This would only be for segments that are not accompanied by simultaneous changes in spectral peaks that would cause stimulation of other electrodes. In terms of the pattern recognition ex-

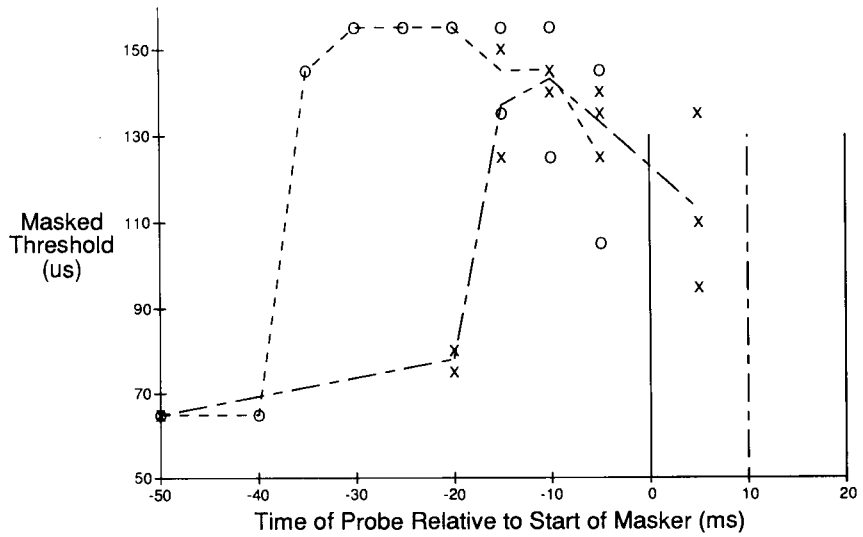

Fig. 7. Backward masked thresholds for long (200 msec) maskers with pulses at 20 msec intervals marked by circles and a dashed line, and at 10 msec intervals marked by crosses and a line with short and long dashes.

planation of masking, a probe on a different electrode from the masker would be discriminated from the masker pattern because of the electrode difference. As a consequence, the amount of central masking would be much less than for a probe on the same electrode as the masker.

The effects observed in these experiments are somewhat different from those normally observed in acoustic masking experiments, but it is likely that pattern recognition effects also play a part with acoustic signals. These effects may have been overlooked in previous experiments because of the longer probe stimuli that are used in acoustic stimulation. In particular, experimenters should be aware of the possibility of different criteria being used by subjects, and the possibility of non-monotonic psychometric functions. These manifestations of the pattern recognition process may cause apparent anomalies in results that would otherwise be difficult to explain.

Acknowledgements

The research reported here was supported by a grant from the Australian Department of Employment, Education and Training to establish the Human Communication Research Centre at the University of Melbourne. The second author also holds a Senior Research Fellowship (Industry) from the Department of Employment, Education and Training.

References

Blamey, P.J., Alcantara, J.I., Cowan, R.S.C., Galvin, K.L., Sarant, J.Z. and Clark, G.M. (1990) Perception of amplitude envelope variations of pulsatile electrotactile stimuli. *J. Acoust. Soc. Am.*, 88: 1765–1772.

Clark, G.M., Tong, Y.C., Patrick, J.F., Seligman, P.M., Crosby, P.A., Kuzma, J.A. and Money, D.K. (1984) A multichannel hearing prosthesis for profound-to-total hearing loss. *J. Med. Eng. Technol.*, 8: 3–8.

Elliot, L.L. (1971) Forward and backward masking. *Audiology*, 10: 65–76.

Garner, W.R. (1951) The accuracy of counting repeated short tones. *J. Exp. Psychol.*, 41: 310–316.

Javel, E., Tong, Y.C., Shepherd, R.K. and Clark, G.M. (1987) Responses of cat auditory nerve fibers to biphasic electrical current pulses. In: G.M. Clark and P.A. Busby (Eds.), *International Cochlear Implant Symposium and Workshop, Melbourne, 1985 – Ann. Otol. Rhinol. Laryngol.*, 96 (Suppl. 128): 26–30.

Lim, H.H., Tong, Y.C. and Clark, G.M. (1989) Forward masking patterns produced by intracochlear electrical stimulation of one and two electrode pairs in the human cochlea. *J. Acoust. Soc. Am.*, 86: 971–980.

Moore, B.C.J. (1982) *An Introduction to the Psychology of Hearing*, 2nd. Edition, Academic Press, New York, London.

Shannon, R.V. (1983) Multi-channel electrical stimulation of the auditory nerve in man. I. Basic psychophysics. *Hear. Res.*, 11: 157–189.

Taylor, M.M. and Creelman, C.D. (1967) PEST: efficient estimates on probability functions. *J. Acoust. Soc. Am.*, 41: 782–787.

Zwislocki, J.J. (1969) Temporal summation of loudness: an analysis. *J. Acoust. Soc. Am.*, 46: 431–441.

J.H.J. Allum, D.J. Allum-Mecklenburg, F.P. Harris and R. Probst
Progress in Brain Research, Vol. 97

Overview and critique of Chapters 26 – 29

E.F. Evans

Keele, U.K.

In the cochlear implant, we have an exciting example of the application of our basic scientific understanding of the hearing mechanism to attempts to enable the profoundly hearing impaired to regain some sort of hearing.

It is a paradoxical fact that while several thousand cochlear implantations have been made, yet the answers to many basic questions concerning the optimal modes of electrical stimulation are still not available. The biological problem is to stimulate, as closely as possible, the normal patterns of activity in the surviving nerve fibres of the cochlear nerve (normally 30000 or so). The obstacles are: the technical problems associated with interfacing stimulation electrodes to the surviving nerve fibres (which means that a relatively very small number of channels of independent stimulation are available); stimulus encoding; and miniaturisation. Therefore, research groups developing cochlear implants have pursued a wide variety of differing stimulation strategies, which attempt to address one or more of these problems. This has inevitably led to a very divergent set of solutions, often based more on technical considerations of convenience than on sound physiological or psychophysical justification. In addition, this reluctance to provide a scientific justification for a particular strategy has been compounded by the MIBTY syndrome ("mine is better than yours"). Furthermore, the fact that each strategy has been tested on different patients, given the very large patient-to-patient variation in performance, has meant that comparisons between strategies have been difficult and frequently impossible.

Fortunately, two main approaches have been emerging from the wide variety of strategies developed. The first is a relatively straightforward analogue transformation of auditory signals (speech and environmental sounds); band-pass filtering into a relatively small number of channels (4 – 6); and the presentation of these signals to a tonotopic array of electrodes within the cochlea. This approach (particularly exemplified by the Ineraid/Symbion device) has the advantages of simplicity (aiding miniaturisation) and a relative resistance to interference by competing sounds. A major problem, however, is interaction between channels ("cross-talk") when simultaneous activation of electrodes occurs. The second approach is quite different, namely a signal processing approach entailing extraction of salient speech features (voice fundamental, lower formants) and their encoding in the rate and position of pulsatile stimulation along a tonotopic electrode array of typically 21 channels (as in the Nucleus device, which currently dominates the commercial market). This strategy has the advantage, because of the need to interleave the pulsatile stimulation, that no more than one channel is electrically stimulated at any one instant, and this is thought to improve spatial localisation of the stimulation, especially when combined with bipolar activation. The disadvantage is that the strategy is optimised for speech and not for environmental sounds, and is extremely susceptible to competing backgrounds (when the speech processing breaks down).

In spite of these radically different approaches,

their performances are remarkably similar in the quiet. However, the former approach shows (as expected) substantial advantages in noise (e.g., Tyler et al., 1989). Both approaches are in the process of lively development.

One of the most exciting developments of the last year or so has been the report by Wilson and collaborators (Wilson et al., 1991) of the advantages afforded to the former analogue strategy of continuous interleaved stimulation (CIS) aimed to deal with its major objection. In this approach, the analogue signals to each channel are sampled as rapidly as possible in turn and each electrode channel stimulated in isolation with the sampled signal. Two of the chapters (28 and 29) deal with this innovation, the first in comparison with the earlier analogue stimulation strategy and the second in comparison with the earlier pulsatile (Nucleus) strategy. These chapters will therefore be reviewed first.

The third chapter (27) addresses primarily an equally important problem in cochlear implants, namely the cosmetic impact of a wearable system on the patient. The fourth (26) is a largely technical summary of the LAURA cochlear implant developed in Antwerp.

The papers are thus considered in logical rather than chronological order.

Chapter 29

This is from the laboratory which developed the CIS strategy in the first place. A major concern for the reviewer is how much the dramatic improvements in speech recognition scores encountered comparing CIS with the former analogue stimulation strategy is in fact due to the interleaved sampling technique and how much is due to other factors such as the increase in the number of channels from 4 to 6, and differences in the degree and nature of the compression applied to the signals (undoubtedly better in the CIS case).

The authors attempt to address these issues by comparing the results obtained with three strategies: compressed analogue (CA) (essentially the original analogue strategy) against interleaved pulse (IP) stimulation and continuous interleaved sampling (CIS), in many cases compared in the same patient.

The results show that CIS stimulation was superior in every way to the other modes of stimulation. In particular, place of articulation and nasality indicated an improvement in spectral representation. Of particular interest is their evidence that the number of channels activated was critical with a substantial improvement as channel number is increased; an improvement in discrimination when the order of stimulating the interleaving of channels was constrained to optimise channel separation; and the resistance of CIS to an adverse signal-to-noise situation.

These findings of course highlight the need for a dissection of the key elements of the CIS strategy. The dependence of results on the number of channels activated highlights the need to determine whether the improvement in CIS is simply due to the extra channels employed (5 – 6) compared with four channels (in the original strategy). The improvement in the behaviour in adverse signal-to-noise conditions again may be related to the improved compression characteristics. It is encouraging therefore that the authors conclude their article by indicating that they will be carrying out a systematic dissection of these factors. Of particular importance should also be the systematic investigation of the upper limit of the amplitude envelope smoothing. On physiological grounds, the fine time structure of cochlear nerve fibre discharges which will be lost if the upper limit is too low, must not be confused with the psychophysical limit of modulation sensitivity.

Chapter 28

This paper summarises preliminary findings in an attempt to compare, in the laboratory, the continuous interleaved sampling (CIS) strategy with the pulsatile encoding strategy employed in the Nucleus 22-channel implant. In this case, the CIS strategy employs between 4 and 22 channels. Inevitably, there is a trade-off between the number of channels interleaved and the maximally achievable rate of stimulation on any one channel. Several CIS schemes were implemented in order to achieve as high stimulation rates as possible on each electrode. These ranged

from (1) a narrow-band spectral analysis, closely similar to the original CIS scheme; through (2) the extraction of a pre-selected number of spectral peaks; to (3) a wide band (octave) filtering strategy. The results showed a systematic and in some cases substantial improvement with the best CIS strategy compared to the patient's own wearable Nucleus devices, and over a simple peak-picking "vocoder" strategy. Interestingly, the narrow-band CIS strategy was superior to the others. The authors conclude that this advantage is produced by better transmission of formant transitions. Also, voicing information was better transmitted by these strategies even though not "explicitly encoded".

The general question, raised by this reviewer, how important it was to map accurately the frequencies of the channels to the place of stimulation within the cochlea was explicitly dealt with by these authors. They interpreted some of their findings in pointing to the importance of accurate mapping.

The authors also raised the obvious question whether, under CIS, the cochlear nerve is responding in a fundamentally different manner with "continuous high excitation states". We have evidence (Morse and Evans, in preparation) that this is not the case. The integration of the sampled signal waveform by the capacitive characteristics of the nerve membrane means that essentially similar nerve responses are obtained between sampled and unsampled stimulation states, providing the mark-space ratio of the sampling is not too great.

Chapter 27

There are two factors determining the clinical success of a cochlear implant. First and obvious, is the gain in intelligibility and awareness of the acoustic world afforded to the patient. Second (and less obvious to researchers!), is the cosmetic appearance of the implant. This second factor weighs surprisingly heavily with patients.

It is this second question which is addressed in the first part of this paper. The authors describe comparisons between a body-worn and an ear level processor, both embodying a wide-band presentation of the original acoustic signal to a single channel electrode in the cochlea.

Interestingly, speech tests revealed a small but significant improvement in performance with the ear level aid compared to the body-worn processor. However, the major preference for the ear level processor was conditioned by factors virtually entirely cosmetic or related to convenience of wearing.

In the second part of the paper, very preliminary results are presented of comparisons (in one patient) between two strategies. The first is a digitally implemented wide-band stimulation strategy to a single electrode, and this is compared with the second: combined stimulation with a wide-band analogue signal to the most apical electrode and multichannel pulsatile stimulation of the remaining few electrodes. In the second case, the pulse rate is determined by the voice pitch, and the electrode site is determined by the frequency of the second formant, both features extracted by signal processing. As expected, the performance of the single channel broad-band but digitally implemented strategy was "approximately equal" to the subject's prior performance with a single channel stimulator. However, a "significant improvement" in vowel recognition was achieved when the additional pulsatile place coding was provided. Unfortunately, no figures are given to substantiate this claim and no indication is given as to whether the expected deterioration of performance occurred in the presence of adverse signal-to-noise conditions.

Chapter 26

Fort the most part this paper is a technical summary of the LAURA cochlear implant developed at the University of Antwerp. It provides little or no physiological or psychophysical rationale for the two digital signal processing strategies outlined. It gives no indication of the number of patients implanted and the merest outline of some of the results obtained.

No data are produced to substantiate a claim concerning the relative advantages of the two main strategies. Cursory information is given on two pa-

tients for whom it is claimed that the second strategy was more effective. Even here, it is not clear whether the patients were tested under a radically modified version of the second strategy. Of the radical modification itself, it is not apparent that it resembles the CIS strategy as is claimed.

References

Wilson, B.S., Finley, C.C., Lawson, D.T., Wolford, R.D., Eddington, D.K. and Rabinowitz, W.N. (1991) Better speech recognition with cochlear implants. *Nature*, 352: 236–238.

Tyler, R.S., Moore, B.C.J. and Kuk, F.K. (1989) Performance of some of the better cochlear implant patients. *J. Speech Hear. Res.*, 32: 887–911.

J.H.J. Allum, D.J. Allum-Mecklenburg, F.P. Harris and R. Probst
Progress in Brain Research, Vol. 97

CHAPTER 26

A digital speech processor and various speech encoding strategies for cochlear implants

S. Peeters, E. Offeciers, J. Kinsbergen, M. van Durme, P. van Enis, P. Dijkmans and I. Bouchataoui

Wilrijk, Belgium

We distinguish two main categories in the speech decoding strategies: those based on feature extraction and those based on time information of the filtered incoming signal. In the first group only those electrode pairs corresponding to the localisation of the four or more, maximum spectral peaks or the formants of the speech signal are stimulated. The second category is essentially based on the timing information that is included in the filter outputs of the filtered speech signal. The Laura implant has the capability to be programmed to the different decodings-strategies. To understand the potential possibilities the main features of the implant are discussed.

Key words: Cochlear implant; Hearing loss; Electrical stimulation; Speech signals

Introduction

The results on cochlear implantation depends on different elements, including the patients, the rehabilitation and the implant system. Important parameters of the implant system are:

- The kind of electrode used. The electrode layout and electrode position affect the interface between the nerve fibres and the implant.
- The way the data transmission information passes through the skin affects the transmission rate of the data to the electrode.
- The design of the speech processor defines its potential to decode speech and acoustic signals.
- The fitting possibilities of the system to the patient influence the way the decoded signals are projected in the perceptual domain.
- And last, but not least, the decoding strategy used. This has been demonstrated by various research workers (see, e.g., Dillier et al., this volume).

The interaction between the above aspects may drastically influence the results derived from cochlear implants. For this reason, we describe the different elements of the Laura cochlear implant, which is the system used and developed in our laboratory at the Antwerp University in collaboration with ABS.

The electrode

The multichannel electrode is a 16-wired, Pt-Ir (90 – 10) electrode. The straight electrode has a little bending at the tip to prevent axial torsion on the electrode during the sliding of the electrode in the scala tympani. Such a torsion would reduce the performance of the electrode because the configuration of the contacts is in a radial position and shifted longitudinally as shown in Fig. 1. For optimum thresholds and selectivity, the bipolar contacts should be directed towards the ganglion cells. The

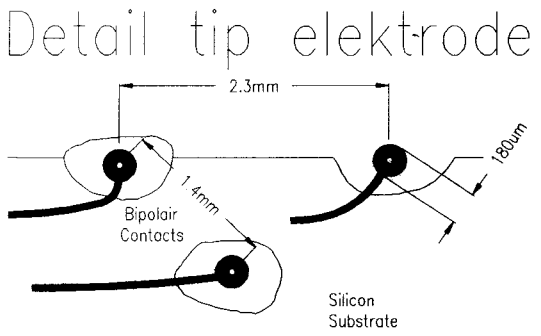

Fig. 1. Position of contacts in the silicon carrier of the multichannel electrode.

contact points at the end of each Pt-Ir wire are located in preformed cups in the silicon carrier of the multichannel electrode. This results in a very smooth surface and improves the insertion of the electrode in the scala tympani.

Interface through the skin

Important is the way information passes through the skin, namely the interface between the electrode and the speech processor. One solution is a percutaneous plug. In this case, the interface does not force any restriction on the communication rate between speech processor and implanted electrode. A second possibility is the use of a transcutaneous RF link across the skin, shown in Fig. 2. In this case, the implanted electronics interpret the incoming information and control the electrode.

Such a RF link necessitates extra power consumption and the necessary compression of information into the RF link. The way the internal circuit treats the incoming signal determines the flexibility and operating speed of the system. Compared with the through-the-skin plug, the implanted electronic system will always have some restrictions. It is important to understand these limitations in the flexibility of the system if one intends to design new decoding strategies. The way information is sent through the skin depends on the internal processor. For this reason, we first describe the main building blocks of the internal chip before discussing the input coding of the chip.

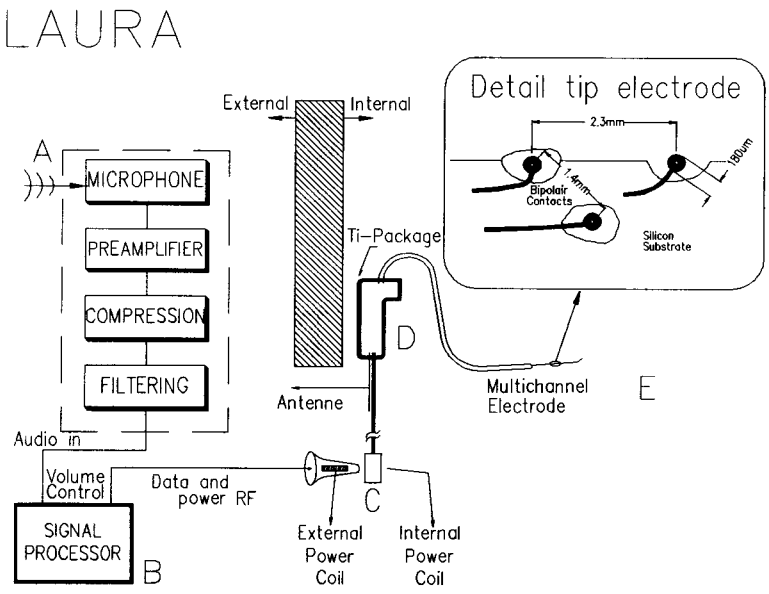

Fig. 2. External unit and internal implant are linked through an RF link.

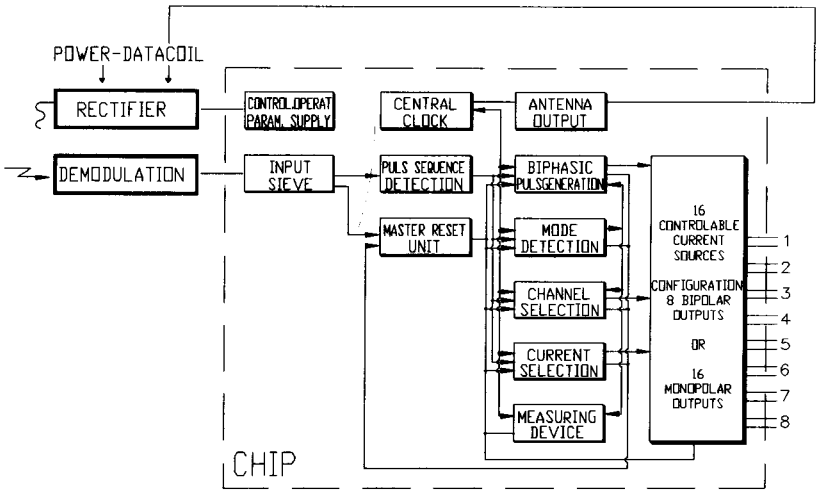

Fig. 3. Block diagram of internal electronic circuitry.

Internal hardware

Fig. 3 shows the block diagram of the internal chip of the Laura prosthesis. There are five main building blocks.

The pulse sequence detector

This circuit unravels the incoming command and controls the different building blocks. The pulse sequence detector is also connected with a Master Reset unit which resets the whole implant if any faults are detected in the input command or if a reset command has been given.

The biphasic pulse generator

A biphasic pulse generator has been implemented in the chip. This generator is pipeline-connected to the Pulse Sequence detector, which means that it can do its job while the detector unit is decoding a new command. This obviously results in a very fast through-put. The pulse duration of this biphasic pulse generator is hardware-adaptable from 10 μsec/phase to 1000 μsec/phase. Hardware-adaptable means that the value is trimmed in the implant itself and can not be changed afterwards. This is done to reach a maximum transfer speed. If some applications need longer or shorter biphasic pulses than the set duration, the user can switch to the programming mode.

The waveform generator

This mode is hardware-controlled by the mode detection unit, the channel detection unit and the current selection unit. The advantage of this programming mode is that the implant is able to program any waveform in a bipolar or monopolar way, simultaneously or sequential in time. However, there is one restriction to this programming mode which is due to the structure of the input command; this will be discussed later.

The measurement unit

The chip also contains a measurement unit which transforms the voltage drops at the tips of the electrode wires into pulse trains with a duration related to these voltage drops. This pulse train is sent back to the outside world and allows the monitoring of the status of the electrode tips. In this way, internal sensors can be connected to the output and their data will be available to the outside processor.

We use this facility to measure the impedance on the contact areas during and after surgery. This could also be helpful in the diagnosis of sudden failures, such as wire breakage.

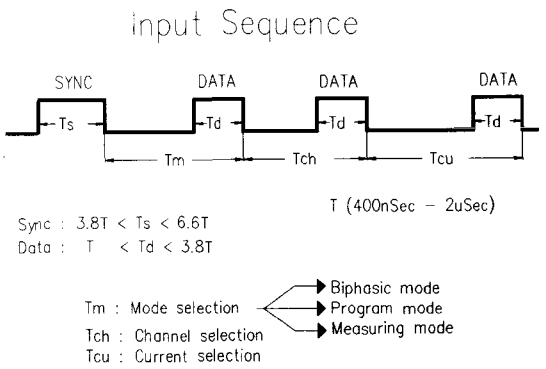

Fig. 4. The command structure is composed of four pulses called the input sequence.

The output stage

The previously described hardware units control the independently controllable current sources of the output stage.

The input sequence controlling the hardware

The composition of the input sequence to control the device gives us the key answer to the limits of the flexibility. The controlling sequence is shown in Fig. 4. This sequence is modulated on the 10 MHz power signal. The information is coded as time intervals between the different pulses of the input signal. This has the enormous advantage that a small shift in time code hardly affects the proper functioning of the internal implant. This would not be the case for pure digital coding where a lost bit means a totally different command.

The first pulse is the synchronization pulse which indicates the start of a new sequence for the hardware. The synchronization pulse is followed by three data pulses which are smaller pulses. The synchronization pulse, as well as the data pulses, should fall between rigorous time intervals. Those boundaries are hardware-trimmed in the implant and can be modified, if necessary. For the implants, the actual synchronization pulse duration must be between 2.5 and 5 μsec, while for the data pulse the limits are programmed to 1 and 2.4 μsec. Interestingly, if the synchronization pulse is out of limit the chip will discard this command. The boundaries of the synchronization pulse width for a second chip can be trimmed to another range so that the system can easily be expanded to a 32 or more channel device. We call this the stack application.

The different modes

The first time interval between the synchronization pulse and the first data pulse is decoded as the working mode of the chip.

The biphasic mode. The first mode is the biphasic mode; if selected, the system will generate a biphasic current pulse between the selected bipolar contacts. There are two possibilities: we called them the biphasic mode + and biphasic mode −. The difference depends on the initial direction of the current flow between the two contact points of the dipole.

The programming mode. The second mode is the programming mode and allows the programming of any waveform. The first example in Fig. 5 represents a sine wave. The minimal time for every step is equal to 50 μsec. The second example shows a simultaneous stimulation with two asymmetrical biphasic pulses. The maximum stimulation frequency is equal to 12.5 kHz if the total pulse width of the biphasic pulse is 80 μsec. If the biphasic pulses are

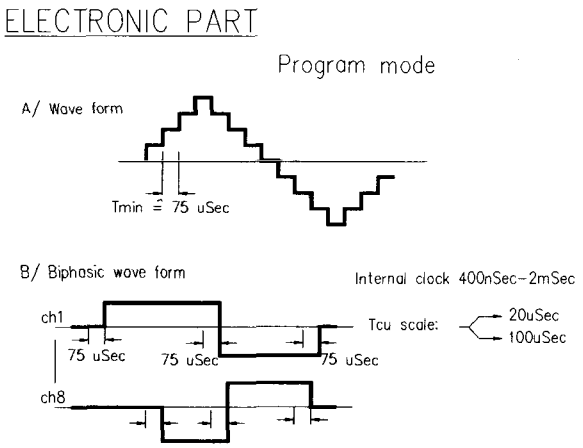

Fig. 5. Examples of different waveforms in the programming mode.

equally distributed among the eight channels, then the stimulation frequency in one channel is equal to 1.5 kHz.

The measurement mode. The measurement mode is essentially the same as the programming mode but in this mode the output voltage drop on the selected electrode is measured and sent back by means of a pulse train modulated on the internal coil.

The selected channel

The time interval between the first and second data pulse is related to the selected electrode to be activated or modified from previous settings.

The output current

The time interval between the second and third data pulses results in three different possibilities. First, if the time is short (less than 4 μsec) the selected electrode becomes floating (high impedance). Second, if the time is fixed between 4 and 7 μsec the selected electrode is connected to the internal interference (low impedance). This allows the programming of certain contact points as an internal reference. Finally, by increasing the time difference, the selected current source is activated. The programmed current value is related to this time difference according to quadratic law (Peeters et al., 1990).

The Laura speech processor

Fig. 6 shows the different components of the Laura 3 speech processor. The design is based on two microprocessors. A 16-bit microprocessor controls the data flow for the different algorithms while the DSP calculates the FFT of digital filters.

The acoustics signal is picked up by the micro-

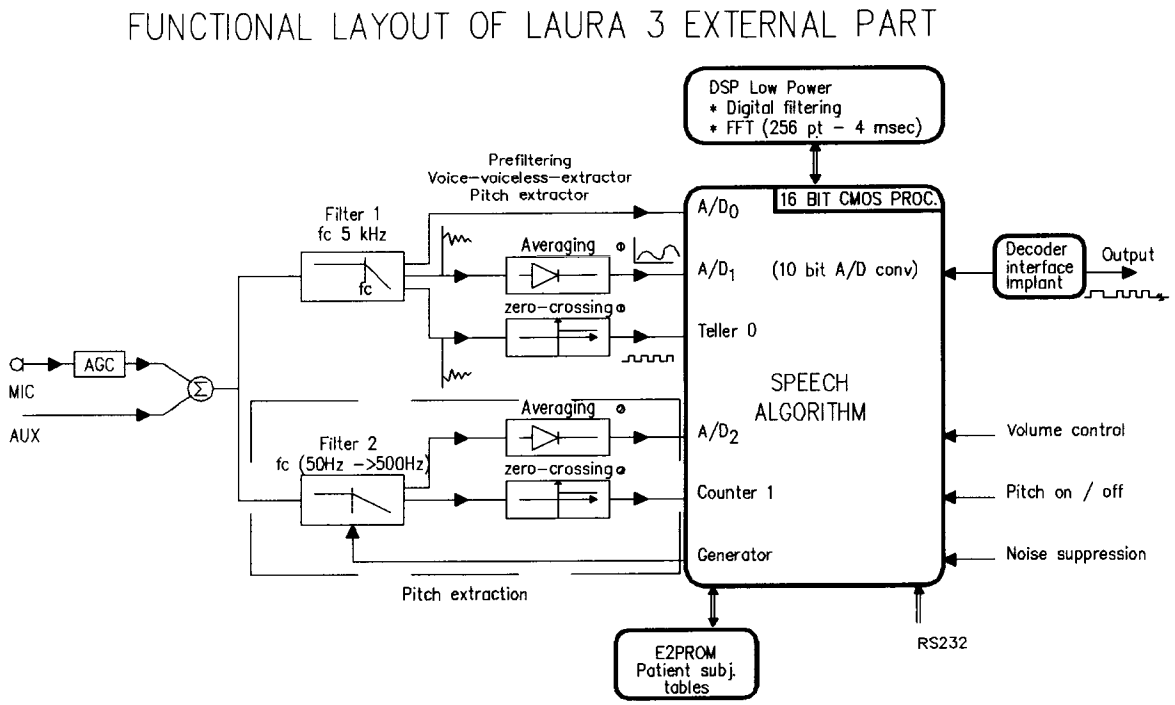

Fig. 6. Laura speech processor.

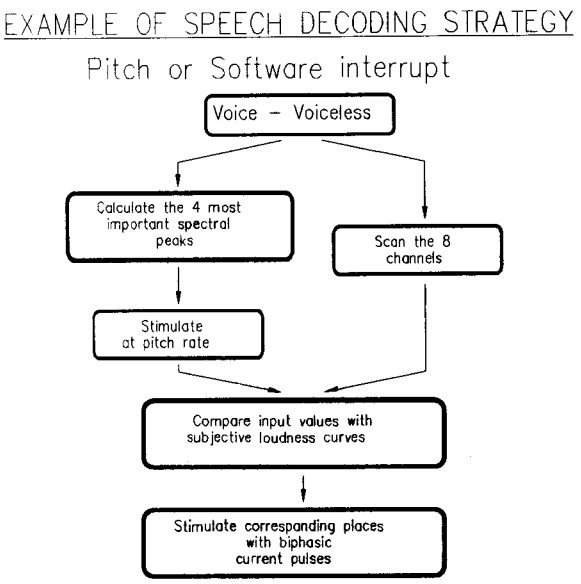

Fig. 7. Flowchart of first decoding strategy.

phone and amplified by means of an AGC control. In this stage, the signal goes through a 6 dB/octave high-pass filter with a cut-off frequency of 1 kHz. The signal is low-pass-filtered at 5 kHz with a slope of 36 dB/octave. The signal goes to a 10-bit A/D convertor which samples the signal at a 10 kHz rate.

Also implemented is a hardware pitch extractor and a voice-voiceless detector. The microprocessor controls the data flow to and from the DSP as well as the output values towards the fast counters which are responsible for generating the input sequence for the implant. This combination of the Laura implant and the dual processor-designed speech processor provides enough freedom for implementing a wide range of processor strategies.

The fitting tables

Two important fitting tables are available to match the stimulation values with the perceptive domain of the patient.

The loudness curves

For each channel the intensity of the input signal is the subjective impression of the patient. Those tables are stored in the EEPROM.

The perceptive channels

Many electrode configurations are possible and each creates, more or less, different pitch and sound sensations. Up to 36 perceptive channels can be defined.

From those 36 perceptive channels, we rank eight or more channels according to the pitch sensation. Those perceptive channels are stored in the pitch table.

The decoding strategies

In our initial trial we compared two decoding strategies. In the first strategy (which we used four years ago) the DSP calculates a 128 point FFT within 2.5 msec for a sliding time window of 10 msec. The DSP combines those 128 points to eight values according to frequency band settings. The microprocessor

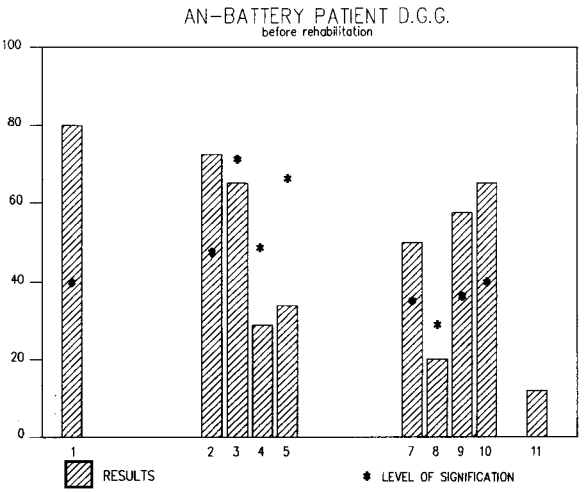

Fig. 8. Results for patient 1. 1, Environmental sounds, 4-choice; 2, number of syllables, 3-choice; 3, sentence accent test, 2-choice; 4, voice-test, 3-choice; 5, speech/noise test, 2-choice; 7, long vowels 4-choice; 8, short vowels, 5-choice; 9, monosyllable test, 4 choice; 10, spondee test, 4 choice; 11, consonant test, open set recognition.

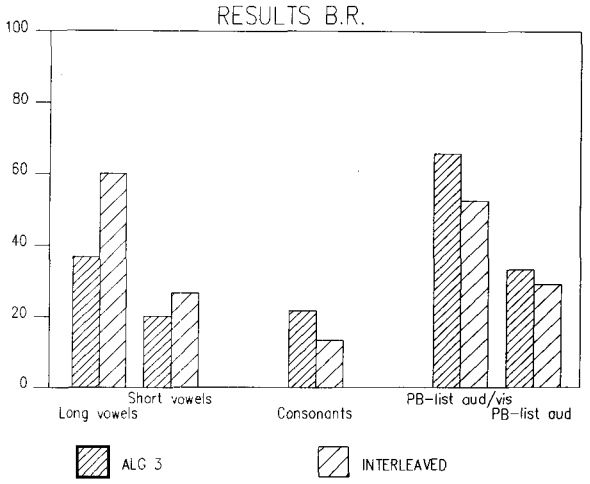

Fig. 9. Results for patient 2.

takes into account the pitch trigger of the external pitch extractor and the voice-voiceless status according to the flowchart of Fig. 7. The second algorithm starts with an eight channel band-pass filtering followed by an envelope detector algorithm. From the eight outputs, the four maximal values were calculated. The corresponding channels are stimulated with these maxima.

Initial results with algorithm two were disappointing. A possible explanation may be the fact that if a certain filter output increases, an abrupt channel switching could be evoked. So we adapted the algorithm. In the adapted version, we started with four filters fixed to four different channels to avoid abrupt switching. This algorithm is nearly similar to the continuous interleaved algorithm of Wilson et al. (1990). The results improved and the two patients claimed a brighter sensation compared with the first algorithm.

Comparative results

Two difficult patients where algorithm 1 was not satisfactory tried algorithm 2; The result in both cases was an improvement.

Results of patients 1 and 2

Patient 1 is 62 years old with four years of deafness due to otosclerosis. At surgery, the cochlea was found to be totally filled with bone growth. After drilling out a semicircular groove only three channels could be inserted. Stimulating the three different channels resulted in three different pitch perceptions. The first algorithm based on pitch was disappointing. We adapted the second algorithm to three channels. The results before rehabilitation are shown in Fig. 8.

Patients 2 is 37 years old and became deaf after a car accident which resulted in bilateral temporal bone fracture two years ago. After the accident he was in coma for ten weeks, and his personality became one of total disinterest. His results were poor with the first algorithm. We tried the second algorithm on four channels. Results before rehabilitation are shown in Fig. 9. He prefers the second algorithm.

Conclusion

The described Laura implant has enormous potential possibilities to adapt the implant to the patient's needs. It is our aim to fully exploit these possibilities.

References

Peeters, S., Offeciers, F.E. and Marquet, J.F.E. (1990) The Laura cochlear prosthesis: technical aspects. *Otorhinolaryngology, Head and Neck Surgery,* Kugler and Ghedini, Amsterdam, pp. 1193-1202.

Wilson, B., Finley, C. and Lawson, D. (1990) A new processing strategy for multichannel cochlear implants. *The Second International Cochlear Implant Symposium,* Iowa University Press, Iowa City, p. 27 (abstract).

J.H.J. Allum, D.J. Allum-Mecklenburg, F.P. Harris and R. Probst
Progress in Brain Research, Vol. 97

CHAPTER 27

New hardware for analog and combined analog and pulsatile sound-encoding strategies

Ingeborg J. Hochmair-Desoyer, Clemens Zierhofer and Erwin S. Hochmair

Institute of Applied Physics and Microelectronics, University of Innsbruck, Innsbruck, Austria

Development for cochlear implants of primarily analog design focusses in two directions. The first direction is miniaturisation. A behind-the-ear (BTE) speech processor has been developed which can replace the body-worn processor for approximately 90% of the users of a MED-EL cochlear implant and works with two 1.4 V hearing aid batteries for between seven and twelve days. Consonant, vowel and sentence testing and patient questioning revealed that the BTE speech processor demonstrates a significant improvement in speech understanding compared to the body-worn processor, and that the patients' device acceptance is superior for the BTE processor. The result of the second direction for our cochlear implant development is the multichannel cochlear implant, CAP, with combined analog and pulsatile stimulation. It aims at complementing the information from the broad-band analog signal by adding spectral information, that is, tonotopic information. This device is capable of simultaneously stimulating one electrode channel with a broad-band analog signal and one of eight electrode channels with a pulsatile signal. The system can also be used for purely analog or for purely pulsatile stimulation. Preliminary results with the first recipient of a CAP cochlear implant system demonstrate that the device works as expected.

Key words: Cochlear implant; Auditory prosthesis; Speech coding; Speech signal processing

Introduction

There are two features of a cochlear implant which would be most welcomed by its users: a further improvement in the speech understanding it can provide and a miniaturised speech processor to be worn at ear's level. Corresponding to these desires, two trends can be observed in cochlear implant development. (1) The first trend aims at accomplishing more complex and more flexible systems preferably for a plurality of different speech-encoding strategies able to deliver more cues for speech understanding. (2) The second trend is the ubiquitous trend towards more miniaturisation resulting in increased comfort for the user.

At present more miniaturisation means specialisation, but as modern microelectronics advances and the technology of implantable packages and of batteries improves, these two trends might merge.

This paper deals with two developments that try to satisfy these two trends; firstly, a miniaturised analog speech processor to fit behind the ear and, secondly, an advanced multichannel cochlear implant for combined analog and pulsatile stimulation. The two developments are both described in this article because they are part of a series of cochlear implants with consistent design and developed to cover the needs of a wide range of different patients.

At present, it appears impossible to design one single cochlear implant that could be considered ideally suited for the existing wide range of CI-candidates encompassing different etiologies, age, degree of deafness and living conditions. An obvious example refers to patients with complete ossification of the cochlea and the difficulty of using long multichannel scala tympani electrodes for these cases.

An improved analog cochlear implant comprising a new behind-the-ear (BTE) speech processor

Methodology and hardware

The best speech recognition via a single-channel cochlear implant can undoubtedly be accomplished using a broad-band analog representation of the speech signal which employs frequency equalisation and an adequate means of amplitude compression as well as correct time constants for attack and release times.

In addition to allowing competitive speech understanding (Tyler et al., 1989), such a system has valuable advantages for the following reasons. (1) No reduction in information content for a speech signal has to be performed when using a broad-band (100 – 600 Hz) analog representation of the speech signal for stimulation. The task of extracting useful speech features is entirely left to the CI-patient. (2) The hardware design for the implant is quite straightforward and does not require a lot of supply power, a fact which, in turn, facilitates the miniaturisation of the external speech processor. (3) The hardware of the implant and of the transcutaneous signal transmission link does not impose any limitations on the stimulation signal because a signal bandwidth of 40 kHz can easily be accomplished.

Information that can be extracted from an analog single-channel implant is time intensity and periodicity information, fundamental frequency, first formant frequency and information on the presence or absence of higher frequencies (Summerfield, 1985). Higher frequency spectral information, especially information on the second formant frequency, usually can not be extracted by the patient's auditory system because in contrast to the time resolution capabilities of CI-patients, the frequency discrimination capabilities of such patients for frequencies above 1 kHz are limited (Dorman et al., 1990).

Since no tonotopic information can be transmitted via only one electrode channel the amount of spectral information which a typical user of an analog single-channel CI can extract is limited. These patients are, thus, very successful in consonant recognition tests and have some room for improvement left with their vowel recognition abilities.

The behind-the-ear speech processor. The development of the new BTE version of the speech processor (Fig. 1) became feasible mainly because of a design-related increase in transmission efficiency and because of improvements in the design of the electrodes.

The BTE speech processor, like the body-worn speech processor it replaces, provides a processed broad-band analog stimulation signal to the stimulation electrode. Like the body-worn speech processor, it uses an automatic gain control circuit. The onset of compression can be adjusted to the background noise level using the sensitivity control. The overall volume control is the second control available to the patient. The frequency response of the BTE processor can be adjusted individually using three small potentiometers. It works on two 1.4 V hearing aid batteries that have to be replaced every 7 – 12 days. Table I lists the differences in electrical characteristics between the body-worn and the BTE-

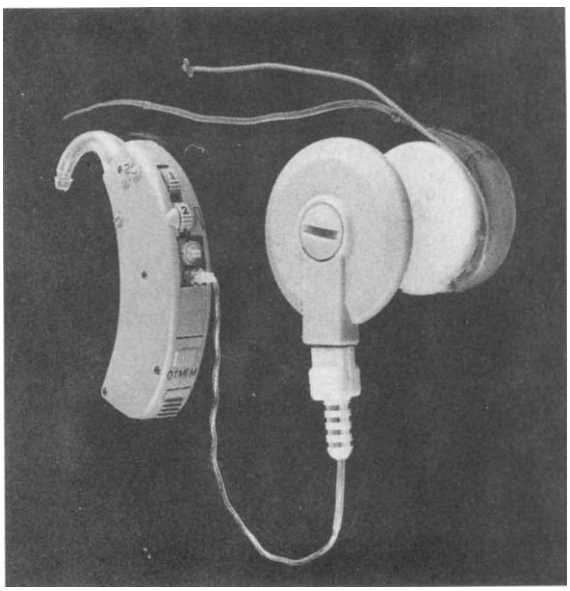

Fig. 1. BTE (behind-the-ear) sound processor and analog cochlear implant with intracochlear two-channel electrode.

processor. Because slight design changes in analog speech processor circuitry could have important influences on speech understanding, comparative speech tests were performed with the two processors.

Comparative results

The first 18 patients who came to Innsbruck to

TABLE I

Technical differences between body-worn processor and BTE processor

	Body-worn processor	BTE processor
AGC	Half wave rectification	Full wave rectification
Compression ratio	6:1	8:1
Release time	45 msec	25 msec
Supply voltage	9 V	2.4 V
Dynamic range	Slight differences in non-linearities and head room	

TABLE II

Demographics

Patient no.	Age	Onset of deafness	Electrode location
1	35	postlingual	IC
2	34	postlingual	IC
3	39	postlingual	IC
4	45	postlingual	EC
5	68	postlingual	IC
6	21	perilingual	EC
7	38	postlingual	IC
8	23	postlingual	IC
9	33	postlingual	IC
10	21	postlingual	IC
11	32	postlingual	IC
12	34	postlingual	EC
13	22	prelingual	IC
14	37	prelingual	EC
15	14	prelingual	EC
16	15	prelingual	EC
17	40	prelingual	IC
18	68	postlingual	EC

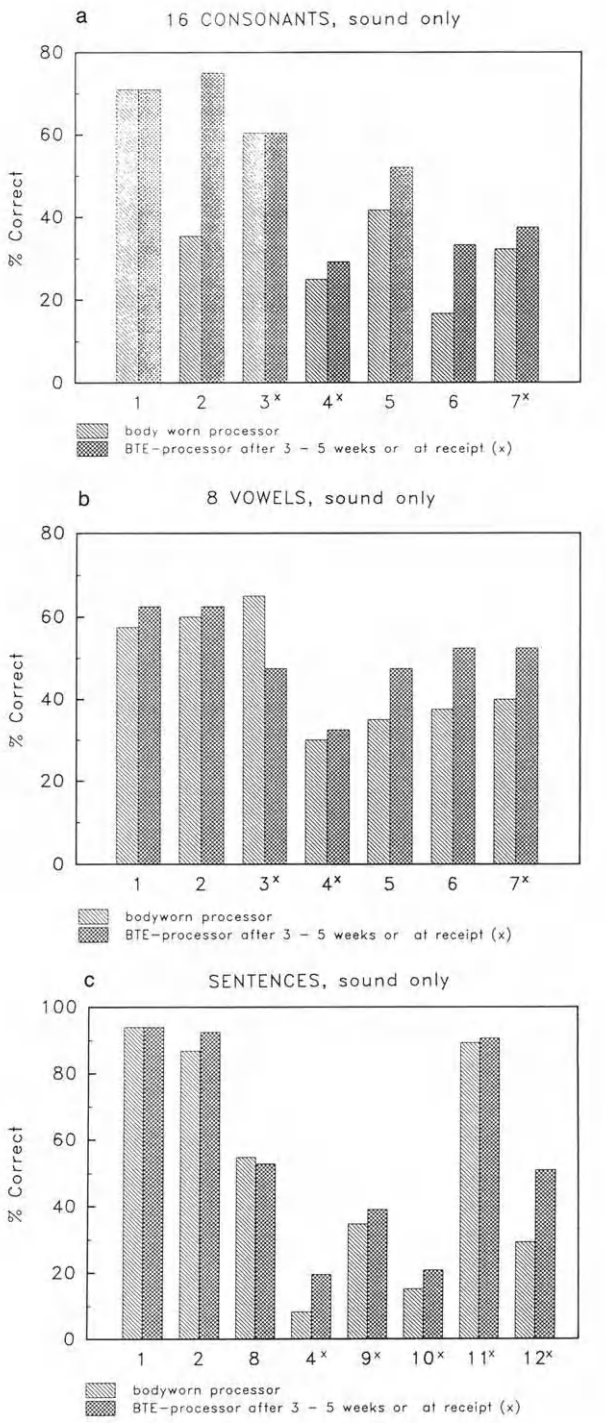

Fig. 2. Results of comparative speech testing performed in the sound-only condition. *a*. Recognition of 16 consonants in an aCa environment. *b*. Recognition of the eight long German vowels in a bVb environment. *c*. Understanding of everyday sentences.

receive a BTE processor participated in comparative speech tests and/or were questioned about the relative merits of the body-worn and the BTE processor. The patients were not selected according to any particular criteria. The aim was to encompass a diversity of cases (Table II). There were 12 postlingually, one perilingually and five prelingually deafened patients between the ages of 14 and 68 in the study. Speech tests were performed in the sound-only condition (Fig. 2). The body-worn processor was always tested on the day of receipt of the BTE processor in order to make sure that the evaluation was performed while the patient was still familiar with the body-worn processor. The BTE processor was evaluated 3 – 5 weeks after its receipt (that is, after getting used to it) or, for patients later in the study (marked by "x" in Fig. 2) the BTE processor was evaluated immediately upon its receipt without allowing the patient to get used to it (that is, at the same time as the body-worn processor was tested).

With the post- and perilingually deafened patients consonant and vowel identification tests using 16 consonants (96 presentations for each processor) and the eight long German vowels (40 presentations for each processor), and sentence tests (six lists of ten sentences each and processor changed after each list) were performed. The postlingually deafened patients 8 – 12 have not been tested for their consonant or vowel recognition. The postlingually deafened patients 3 and 5 were not available for sentence testing; 7 and 18 could not score on the sentence test. For patient 3 still using an epoxy-coated implant, the BTE processor was at its output power limit and already clipping the stimulation signal. The patient later decided to use it with an additional battery doubling its output voltage. The mean value for the BTE processor compared to the body-worn processor was 51.2% vs. 40.4% for the consonant identification test. Fig. 3 details the consonant confusion results for a very successful cochlear implant user (patient no. 1) in whose case the results were very similar for both processors and approached the best consonant recognition possible for a broad band analog stimulation scheme. The vowel identification test resulted in 51.5% vowels correctly identified with the BTE processor versus 46.4% for the body-worn processor (Fig. 2*b*). The respective percentages for the everyday sentences were 58.4% versus 51.5% (Fig. 2*c*).

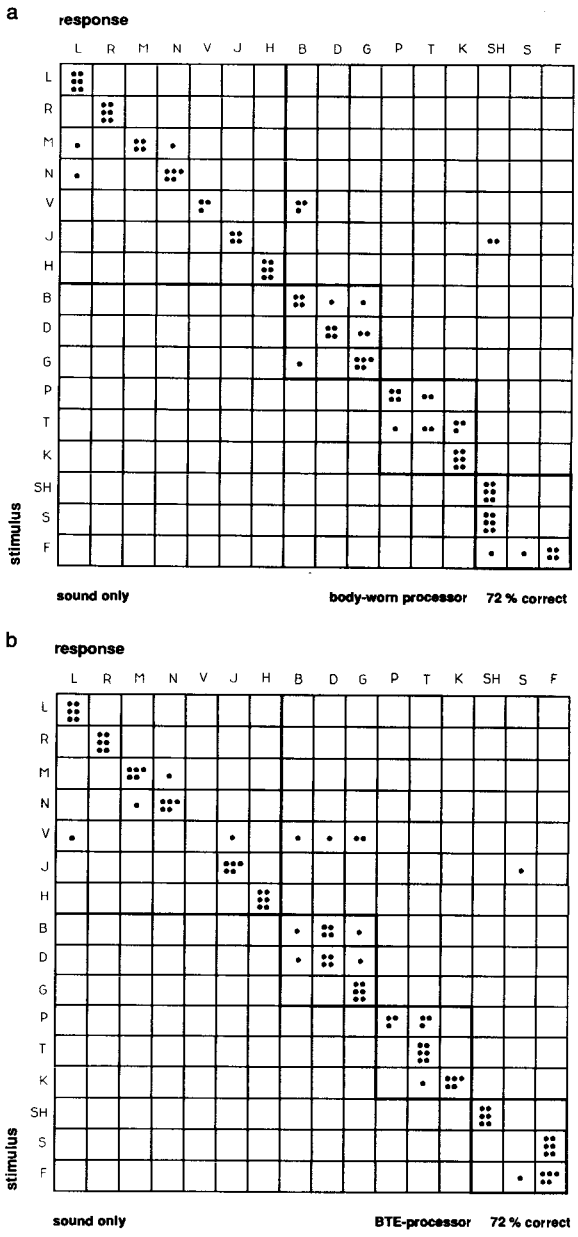

Fig. 3. Consonant confusion data for patient no. 1 via body-worn processor *(a)* and BTE processor *(b)*. Consonants are arranged in subgroups according to manner of articulation.

All three speech tests, thus, revealed an improvement in the respective performance with the BTE processor compared to the body-worn processor which was significant at the 5% level in the *t*-test.

The 18 patients were also questioned about advantages or disadvantages of the new BTE processor. Except for one patient, 68 years of age, who could not get used to handling the small potentiometers of the BTE processor, all patients preferred it over the body-worn processor for the following reasons:

— There is no cable required, that would be an obstacle for certain head movements.

— The body-worn processor is not needed. It no longer tangles around the neck, falls out of the shirt pocket, or, when mounted to the belt, is an obstacle while sitting down or seated. The clothing concerns of what to wear, so the processor can be hidden while still being accessible for volume or sensitivity adjustments, are gone.

— The BTE device without a cable and with no body-worn processor necessary is considered cosmetically more acceptable and less conspicuous.

— The increase in comfort of wearing the BTE processor and the new possibility of wearing it during sports, manual labor, on the beach and during periods alone at home, etc. results in an increase in the duration of daily use.

New sound experience and gains in performance due to increased duration of daily use have been reported by the patients. This will have to be tested objectively.

For the prelingually deafened patients the advantages of the BTE processor were even more apparent in their answers than for the postlingually deafened patients. There are two prelingual and one perilingual non-users among the 18 patients who turned into regular users of the BTE device. Their progress will have to be monitored.

The cochlear implant CAP for combined analog and pulsatile stimulation

Methodology and hardware

The main problem that multisite stimulation causes is channel interaction. Contemporary scala tympani electrodes do not allow the independent simultaneous activation of different subsections of the auditory nerve. With the exception of one device (the Ineraid device), the measure thus taken by all existing multisite stimulation devices is to avoid simultaneous stimulation by restricting the stimulus

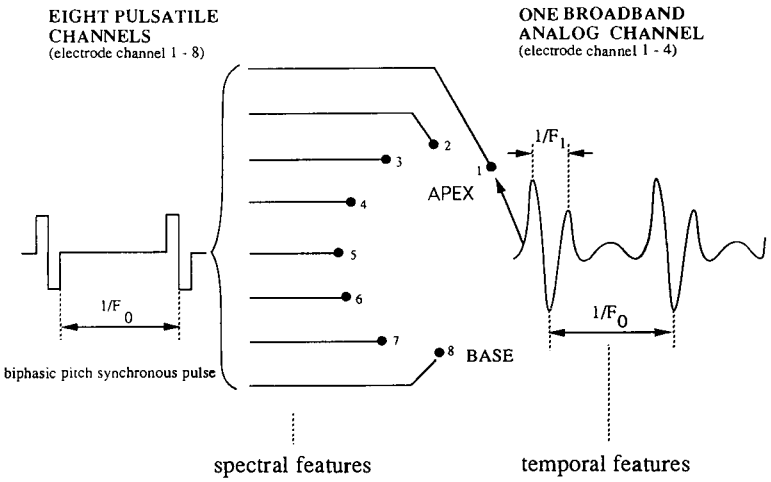

Fig. 4. Schematic for the CAP system designed for eight stimulation sites, two channels at a time, simultaneous analog and pulsatile stimulation. The broad-band analog signal can be delivered to any one of the four most apical electrode channels, the pulsatile signal can be delivered to any one of the eight electrode channels.

presentation to one channel at a time. The stimulation signal can rapidly be switched between electrodes or electrode combinations.

With the CAP system (Fig. 4), two signals can simultaneously be presented to two different electrode channels: the broad-band analog signal and a pulsatile signal which can also be switched rapidly between electrode channels (Hochmair-Desoyer and Hochmair, 1985). For proper timing of the pulses, the information sent via the two channels can be exploited despite the unavoidable overlapping of electrical stimulation fields (von Wallenberg et al., 1990).

The CAP system combines the respective advantages of two strategies: the broad-band analog stimulation and the multisite pulsatile stimulation. A stimulation using the analog signal results in sensations sounding comparatively natural. Noise tolerance is not limited by limitations in feature extraction circuitry and improves considerably with experience. The speech understanding reported is based mainly on the good consonant recognition due to the well preserved fine time structure of the analog stimulation signal. The main advantage of multisite stimulation is, of course, the transmission of spectral information, resulting in good vowel recognition. An adequate combination of these two fairly complementary signals should, therefore, lead to a more redundant set of features transmitted to the auditory system and hence, offer the possibility of more robust speech understanding.

The electrode channel for analog stimulation can be selected among the four most apical electrode channels. In addition to the analog stimulation signal a pulsatile signal whose pulse rate is derived from the pitch frequency, stimulates subsets of the auditory nerve via one of seven additional channels, the particular channel being selected by the frequency of the second formant of the speech signal. (For block circuit diagram of CAP speech processor and implant, see Fig. 5.)

In tests with cochlear implant wearers using our analog device, an adaptive delta modulation (ADM) proved to be suitable for transformation of the analog signal into digital form. A numerical ADM is used in which both step-size adaptation and integration are performed numerically by an arithmetic logic unit (Zierhofer, 1991a). In the digital encoder, the binary information of an analog and pulsatile channel are combined to a synchronous data word format and delivered to the class E transmitter in a serial way (Zierhofer, 1991b).

A serial data transmission of the analog and pulsatile stimulation channel requires the data to be multiplexed. The information to define a stimulation current pulse in terms of pulse amplitude, pulse address and pulse duration differs from the information of the analog channel in two respects: firstly, the stimulation pulse rate lies between 100 and 400 pulses/sec; this results in a comparatively small mean information rate compared to the analog channel with 100 kbit/sec. Secondly, the occurrence of a stimulation pulse has to be controlled externally; so pulse information transmission has to be achieved asynchronously.

Besides the information for the analog channel and the pulse definition information, initializing information has to be transmitted. Initializing information contains, e.g., data defining the current levels of the analog and the pulsatile channel, or data defining the electrode address of the analog channel. An analog information rate of 100 kbit/sec results in a data word rate of 20 kHz, an overall information rate of 200 kbit/sec and a maximum pulse rate of the pulsatile channel of 1.25 kHz. Correct data interpretation can take place only when the bit stream is synchronised; this task is achieved by hierarchically organized synchronisation units involving bit-, data word- and pulsatile word synchronisation.

Output currents are generated by two current sources, which are connected to the stimulation electrodes by multiplexers. The two current sources are completely independent from each other. Therefore, besides the combined analog and pulsatile stimulation, there exists the possibility to stimulate exclusively via the pulsatile or via the analog source. The implant circuitry (Fig. 5) contains two application-specific integrated circuits (ASICs) mounted to a ceramic substrate. The electronic circuit is encap-

sulated in a hermetically sealed ceramic package. Specifications for the CAP system are given in Table III.

Preliminary results

The present status of the CAP development is the following: one postlingually deafened 30-year-old patient has received the CAP-implant so far. Prior to the surgery he had been an experienced successful user of an epoxy-encapsulated Vienna cochlear implant providing broad-band analog stimulation.

Five weeks post-operatively this patient received a take-home sound processor (adjusted to his channel no. 3) which provides him with a broad-band analog representation of the speech signal via the CAP system's digital transcutaneous transmission channel using adaptive delta modulation. (Channel no. 3 was chosen because the patient had a preference for it.) With this patient's and a second patient's help, more data will be collected and the CAP sound processor will be optimized. To date, baseline psychophysical data have been collected and the following has been established:

— The CAP device technically works in a patient as expected.

— The four most apical channels, onto which the analog signal can be switched, show slightly larger than average and consistent dynamic ranges for sinusoidal stimulation (Fig. 6).

— All eight channels show satisfying and similar dynamic ranges for pulsatile stimulation (Fig. 7).

— With just the (digitally transmitted) channel of analog information, performance in sound-only speech tests after six weeks of processor use was 52% for 16 consonants, 45% for eight vowels and 88% for everyday sentences, and, thus, approximately equal to the prior performance.

— A significant improvement in vowel recognition can be achieved when, according to the CAP speech coding strategy, a pulsatile signal is offered in addition to the broad-band analog signal (on either channel 1 or channel 3). This signal's pulse

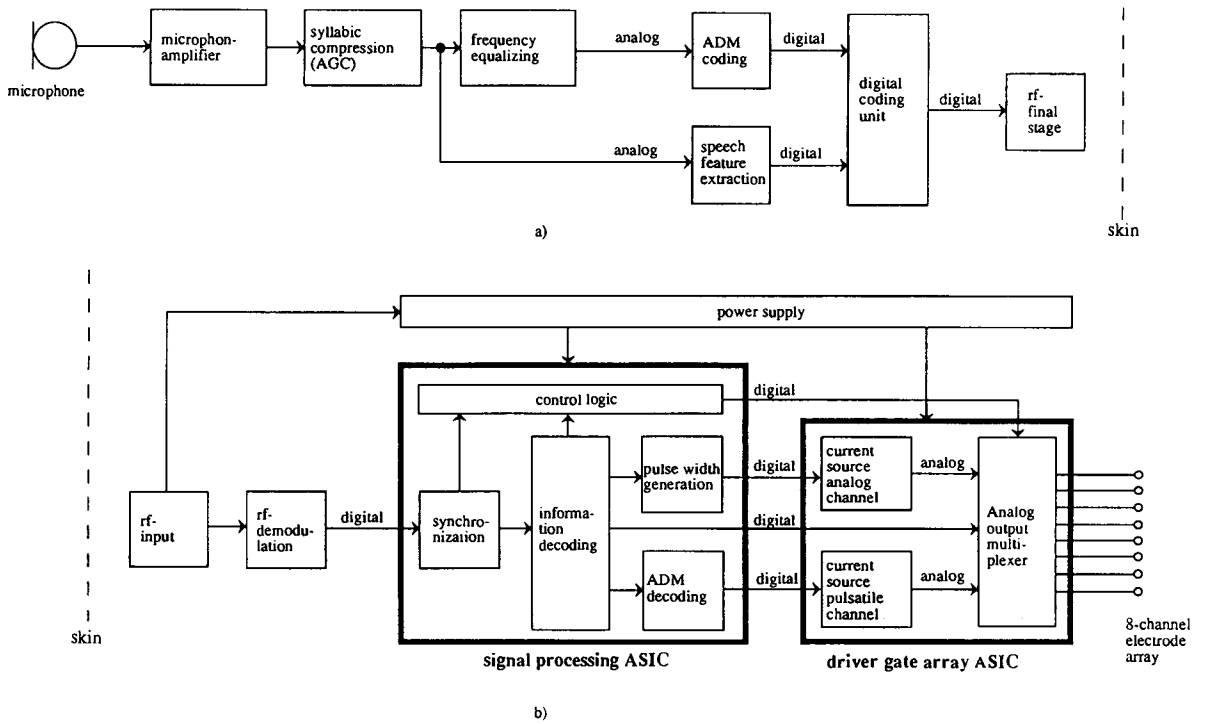

Fig. 5. Block circuit diagram for CAP implant and processor.

rate is determined by the pitch frequency and the electrode address determined by the frequency of the second formant. This result has been achieved with natural vowel stimuli delivered from a hard disk with software-generated pulses.

Conclusions

Two new pieces of cochlear implant hardware have been introduced, a miniaturised behind-the-ear sound processor for the MED-EL broad-band ana-

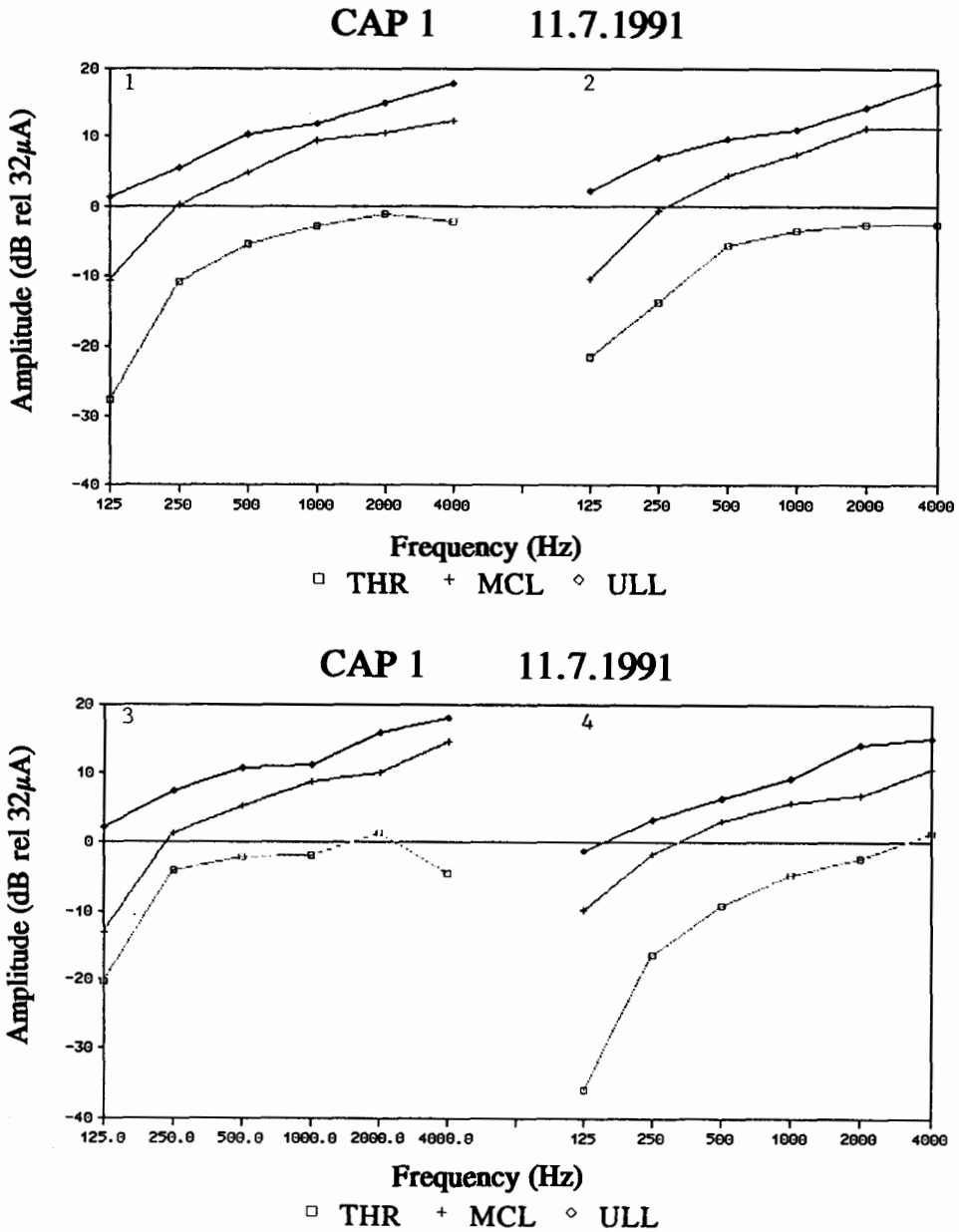

Fig. 6. Threshold (THR), most comfortable loudness (MCL) and uncomfortable loudness level (ULL) for sinusoidal stimulation via the four most apical electrode channels 1 – 4.

TABLE III

CAP system specifications (for combined analog and pulsatile mode)

Analog channel	
Digital signal representation	ADM (adaptive delta modulation)
Sampling rate	100 kHz
Resolution	7 bit linear (including sign)
Minimum current intensity	16 possibilities 1, 2, 3, . . . 16 μA
Overall current intensity range	1 μA – 1 mA (= 60 dB)
Analog channel electrode address	One of the four most apical electrodes (chronically)
Pulsatile channel	
Pulse shape	Symmetrical biphasic pulses (cathodic first)
Resolution	6 bit linear
Minimum current intensity	Four possibilities 2, 4, 8 and 16 μA
Overall current intensity range	2 μA – 1 mA (= 54 dB)
Pulse duration	Eight possibilities, 0.1, 0.2, 0.3, . . . 0.8 msec
Maximum pulsatile stimulation rate	1.25 pulses/sec
Pulsatile channel electrode address	At any given time one of eight electrodes including the analog channel address

log cochlear implant and an 8-channel cochlear implant system (CAP) for combined analog and pulsatile stimulation. The latter complements the information from the broad-band analog signal by adding tonotopic information.

With a group of recipients of the BTE processor it was found that: (1) the speech understanding provided is slightly superior to the one via the body-worn processor; (2) 17 of 18 patients consisting of post-, peri- and prelingually deafened patients prefer the BTE processor over the body-worn processor; and (3) the increased comfort in wearing the device results in an increase in the duration of daily use.

Encouraging results have been achieved with the first recipient of a CAP-system. These results, however, are very preliminary, and it remains to be proven that the improved recognition of simple speech items will lead to the expected improved robust speech understanding.

Because the broad-band analog coding scheme is, at the moment, the only speech coding scheme which lends itself to a miniaturisation of the sound processor, it remains to be seen whether, to the patient, comfort of wearing and inconspicuousness of the device or a somewhat more robust speech understanding are of greater importance.

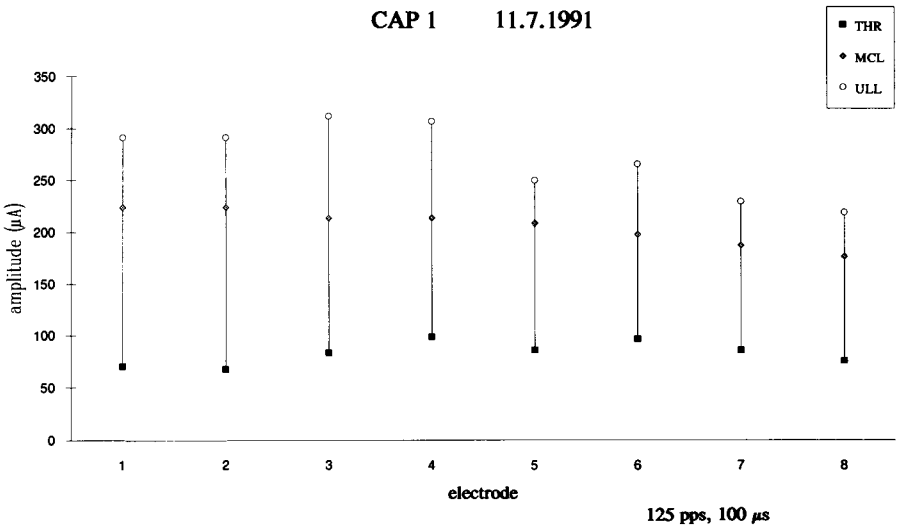

Fig. 7. THR, MCL and ULL values for 125 pulses/sec, 100 μsec per phase biphasic pulses.

Acknowledgements

This work was supported by the Austrian Research Council (Grant no. P8347) and the Austrian Council for Innovation and Technology (Grant no. 323.0033/89). The dynamic range measurements with the first CAP implant patient have been designed and performed by R. Kaufmann. The take-home sound processor has been designed by T. Czylok.

References

Dorman, M.F., Smith, L., McCandless, G., Dunnavant, G., Parkin, J. and Dankowski, K. (1990) Pitch scaling and speech understanding by patients who use the Ineraid cochlear implant. *Ear Hear.*, 11: 310–315.

Hochmair-Desoyer, I.J. and Hochmair, E.S. (1985) *Auditory Stimulation Using CW and Pulsed signals,* US Patent no. 4,593,696.

Summerfield, Q. (1985) Speech-processing alternatives for electrical auditory stimulation. In: R.A. Schindler and M.M. Merzenich (Eds.), *Cochlear Implants,* Raven Press, New York, pp. 195–222.

Tyler, R.S., Moore, B.C.J. and Kuk, F.K. (1989) Open-set word recognition in some of the better cochlear implant patients. *J. Speech Hear. Res.*, 32: 887–911.

von Wallenberg, E.-L., Hochmair, E.S. and Hochmair-Desoyer, I.J. (1990) Initial results with simultaneous analog and pulsatile stimulation of the cochlea. *Acta Oto-Laryngol. (Stockh.) (Suppl.),* 469: 140–149.

Zierhofer, C.M. (1991a) Numerical adaptive delta modulation – a technique for digital signal representation in ASIC applications. *Proceedings of the 6th Mediterranean Electrotechnical Conference – IEEE Catalog no. 91CH2964-5,* pp. 331–334.

Zierhofer, C.M. (1991b) A class E tuned power oscillator for inductive transmission of digital data and power. *Proceedings of the 6th Mediterranean Electrotechnical Conference – IEEE Catalog no. 91CH2964-5,* pp. 789–792.

J.H.J. Allum, D.J. Allum-Mecklenburg, F.P. Harris and R. Probst
Progress in Brain Research, Vol. 97

CHAPTER 28

Speech encoding strategies for multielectrode cochlear implants: a digital signal processor approach

Norbert Dillier, Hans Bögli and Thomas Spillmann

Department of Otorhinolaryngology, University Hospital, Zurich, Institute for Biomedical Engineering, University of Zurich, and Swiss Federal Institute of Technology, Zurich, Switzerland

The following processing strategies have been implemented on an experimental laboratory system of a cochlear implant digital speech processor (CIDSP) for the Nucleus 22-channel cochlear prosthesis. The first approach (PES, Pitch Excited Sampler) is based on the maximum peak channel vocoder concept whereby the time-varying spectral energy of a number of frequency bands is transformed into electrical stimulation parameters for up to 22 electrodes. The pulse rate at any electrode is controlled by the voice pitch of the input speech signal. The second approach (CIS, Continuous Interleaved Sampler) uses a stimulation pulse rate which is independent of the input signal. The algorithm continuously scans all specified frequency bands (typically between four and 22) and samples their energy levels. As only one electrode can be stimulated at any instance of time, the maximally achievable rate of stimulation is limited by the required stimulus pulse widths (determined individually for each subject) and some additional constraints and parameters. A number of variations of the CIS approach have, therefore, been implemented which either maximize the number of quasi-simultaneous stimulation channels or the pulse rate on a reduced number of electrodes. Evaluation experiments with five experienced cochlear implant users showed significantly better performance in consonant identification tests with the new processing strategies than with the subjects' own wearable speech processors; improvements in vowel identification tasks were rarely observed. Modifications of the basic PES- and CIS strategies resulted in large variations of identification scores. Information transmission analysis of confusion matrices revealed a rather complex pattern across conditions and speech features. Optimization and fine-tuning of processing parameters for these coding strategies will require more data both from speech identification and discrimination evaluations and from psychophysical experiments.

Key words: Auditory prosthesis; Digital signal processing; Cochlear implants

Introduction

Today, cochlear implants can partially restore auditory sensations and limited speech recognition for profoundly deaf subjects despite severe technological and electrophysiological constraints imposed by the anatomical and physiological conditions of the human auditory system. Electrical stimulation via implanted electrodes still allows only an extremely limited approximation of normal neural excitation patterns in the auditory nerve. Signal processing for cochlear implants, therefore, is confronted with the problem of a severely restricted transmission channel capacity and the necessity to select and encode a subset of the information contained in complex sound signals.

The search for new signal processing schemes must consider the specific perceptual attributes of various electrical stimulation waveforms and patterns. In order to convey the contents of a particular transmitted message, its primary information elements (e.g., phonetic or acoustic speech features) should be transformed into those physical stimulation parameters which can generate distinctive perceptions for the listener. Practical experience with cochlear implants in the past indicate that some natural relationships (such as growth of loudness and voice pitch variations) should be maintained in

the encoding process.

Speech signals can be considered as sound intensity fluctuations in time and frequency. Due to the large redundancy implicit in speech signals, they can to a great extent be distorted and reduced, and still preserve their essential information content; a property which is most useful for communication systems such as vocoders. The consonant vowel transitions /ba/, /da/ and /ga/, for example, can be synthesized using very few parameters; mostly changes of first, second and third formant frequency (Fig. 1).

One method to decode such speech signals in a cochlear prosthesis is based on the tonotopic mapping of an array of intracochlear electrodes to frequency bands of the signal spectrum. Twenty bandpass filters (BPF) with logarithmically spaced center frequencies spanning the speech bandwidth of approximately 300 – 4000 Hz are indicated on the left of Fig. 1. A complicating constraint for all multielectrode coding schemes is the unnatural tonotopical relationship between the spectral components of the input signal and the place of stimulation along the basilar membrane as illustrated in Fig. 2. Electrodes are typically inserted between 15 and 20 mm into the scala tympani. Thus, the most apical electrode (transmitting the lowest frequency band of up to 300 Hz) will excite nerve fibers at place frequencies of approximately 700 – 1500 Hz (characteristic frequency). Although many CI-users have demonstrated their ability to adapt efficiently to these transposed and distorted frequency mappings, these aspects would certainly warrant additional systematic investigations. The instantaneous energy maxima of the speech spectra, which correspond roughly to the formants (F1, F2, F3 in Fig. 1), are determined and tracked over time. The fundamental voice frequency (about 100 Hz in the example of Fig. 1) triggers the stimulation pulses directed to the appropriate electrodes. Note the interleaved pulse sequence which is selected to avoid simultaneous stimulation of the same area by different electrodes. It is obvious that an encoding strategy based on F1 and F2 only (the strategy implemented in the wearable speech processor, WSP) will never allow a distinction between the synthetic syllable /da/ and /ga/ and also that the discrimination between /ba/ versus /da/ or /ga/ has to rely on only two or three low-amplitude stimulation pulses. It, therefore, seems logical to include information about higher formants in the stimulation patterns and to emphasize formant transitions by applying higher pulse rates.

Several processing strategies have already been designed and evaluated by varying the number of electrodes and the amount of specific speech feature extraction and mapping transformations used (Clark et al., 1990). Recently, Wilson et al. (1991)

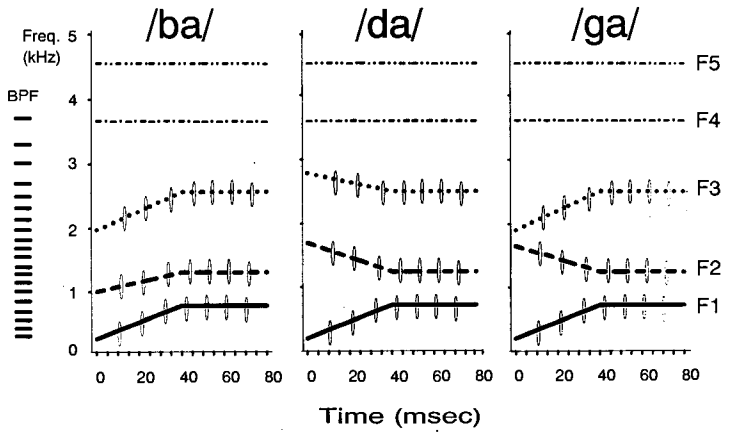

Fig. 1. Speech coding example: synthetic syllables /ba/, /da/, /ga/ (BPF: bandpass filters).

have reported astonishing improvements in speech test performance when they provided their subjects with high-rate interleaved pulsatile stimulation patterns (continuous interleaved sampler, CIS) on six rather than analog broad-band signals on four monopolar electrodes. They attributed this effect partly to the decreased current summation obtained by non-simultaneous stimulation of different electrodes (which might have stimulated the same nerve fibers and, thus, interacted in a non-linear fashion) and partly to a fundamentally different and, perhaps, more natural firing pattern due to an extremely high stimulation rate. Skinner et al. (1991) also found significantly higher scores on word and sentence tests in quiet and noise with a new multipeak speech coding strategy (MPEAK) implemented in the new miniature speech processor (Nucleus-MSP) as compared to the formerly used F0F1F2 of the Nucleus-WSP. Note that the MPEAK strategy does not correspond exactly to the formant extraction scheme denoted in Fig. 1; the presence of high-frequency spectral information (F3 and possibly F4) is signaled on two fixed electrodes within the range assigned to F2. Thus, the MPEAK strategy might generate identical patterns for the two different F3 trajectories of Fig. 1. In contrast, a formant or peak-picking channel vocoder strategy, as described below, would generate different patterns for the three syllables of Fig. 1., albeit with less mapping resolution for F2.

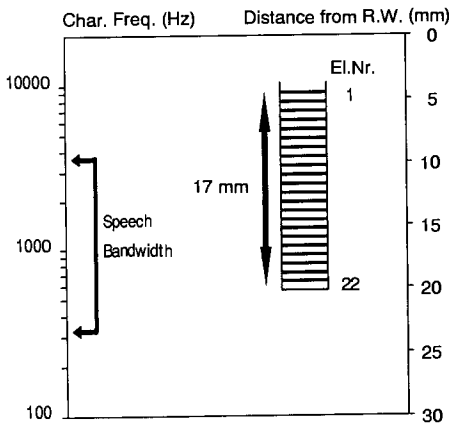

Fig. 2. Electrode positions along the basilar membrane and tonotopic relations (characteristic frequency) according to Greenwood (1990).

The present study was conducted in order to explore new ideas and concepts of multichannel pulsatile speech encoding for users of the Clark/Nucleus cochlear prosthesis. The optimization of signal processing schemes for existing implanted devices must consider a variety of technological and physiological aspects and is largely based on experiments with implanted subjects. With single-chip digital signal processors (DSP's) incorporated in personal computers, different speech coding strategies can be evaluated in relatively short laboratory experiments. In addition to the well known strategies realized with filters, amplifiers and logic circuits, a DSP approach allows the implementation of much more complex algorithms involving speech feature contrast enhancement, adaptive noise reduction and much more. Technological progress will most certainly allow further miniaturization and low-power operation of these processors in the near future.

Materials and methods

As previously described (Dillier et al., 1990), a cochlear implant digital speech processor (CIDSP) for the Nucleus 22-channel cochlear prosthesis was implemented using a single-chip digital signal processor (TMS320C25), Texas Instruments). For laboratory experiments, the CIDSP was incorporated in a general purpose computer (PDP11/73) which provided interactive parameter control, graphical display of input/output, intermediate buffers and off-line speech file processing facilities. For field studies and as a take-home device for patients, a wearable, battery-operated unit has been built. Advantages of a DSP implementation of speech encoding algorithms, as opposed to off-line prepared test lists, are increased flexibility; controlled, reproducible and fast modifications of processing parameters; and use of running speech for training and familiarization.

Speech signals were processed as follows: after analog low-pass filtering at 5 kHz and analog-to-digital-conversion (sampling rate 10 kHz), pre-

emphasis and Hanning windowing (12.8 msec, shifted by 6.4 msec or less per analysis cycle) was applied and the power spectrum calculated via fast Fourier transform (FFT); specified speech features such as formants and voice pitch were extracted and transformed according to the selected encoding strategy; and finally, the stimulus parameters (electrode position, stimulation mode, pulse amplitude and duration) were generated and transmitted via inductive coupling to the implanted receiver. In addition to the generation of stimulus parameters for the cochlear implant, an acoustic signal based on a perceptive model of auditory nerve stimulation was output simultaneously.

Two main processing strategies were implemented on this system. The first approach (PES, Pitch Excited Sampler) was based on the peak-picking channel vocoder concept (Flanagan, 1972) whereby the spectral energies of a number of frequency bands (typically third-octave bandwidths) are transformed into electrical stimulation parameters for up to 22 electrodes. Fig. 3 shows an example of a short-time power spectrum (vowel /a/) and its division into 22 frequency bands. The six largest peaks are marked by filled circles. Note that this coding scheme is not identical to a spectral maxima picker (as used, for example, by McKay et al., 1991) which, in this example, would pick more bands in the F1 – F2 region and disregard the high-frequency peaks. The pulse rate at any electrode is controlled by the voice pitch of the input speech signal. The pitch extractor algorithm calculates the autocorrelation function of a low-pass-filtered segment of the speech signal and searches for a peak within a specified window of time lags. A random pulse rate of about 150 – 250 Hz is used for unvoiced speech portions. Fig. 4 displays schematically the pitch-synchronous sequence of activated electrodes for the spectrum of Fig. 3.

The second approach (CIS, Continuous Interleaved Sampler) used a stimulation pulse rate which is independent of the input signal. The algorithm scans continuously all frequency bands and samples their energy levels as indicated in Fig. 3. As only one electrode can be stimulated at any instance of time, the rate of stimulation is limited mainly by the required stimulus pulse widths (determined individually for each subject) and the time to transmit additional stimulus parameters. As the information about the electrode number, the

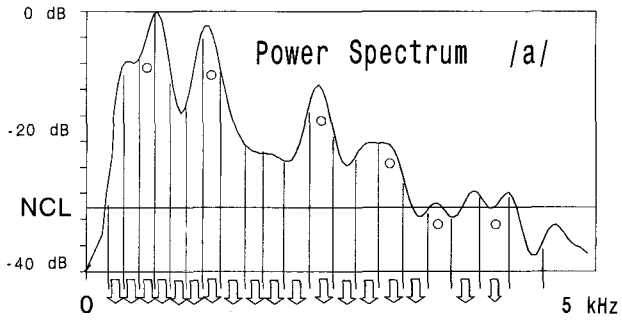

Fig. 3. Short time spectral analysis (128 point Hanning window, FFT, power spectrum) and mapping to *n* frequency bands corresponding to *n* electrode pairs (*n* may typically vary between 16 and 22) for a vowel segment. Frequency bands whose average power exceeds the noise cut level (NCL) are marked by arrows. Spectral peaks (locally maximal band energies relative to the preceding and following bands) are marked by circles.

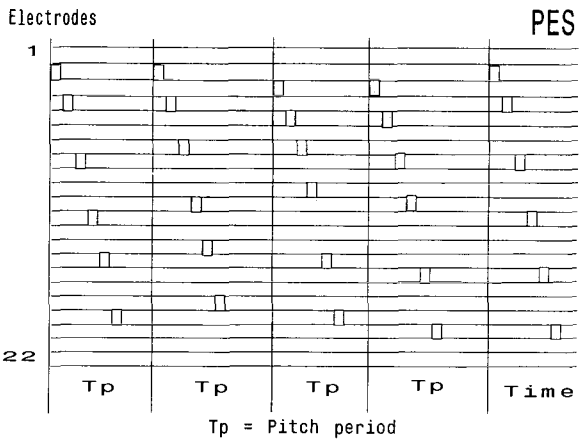

Fig. 4. Two-dimensional electrodogram (active electrodes vs. time) of the PES strategy. Electrodes corresponding to peaks in the short-time spectrum are stimulated pitch synchronously. The signal energy in the corresponding frequency band determines the stimulus amplitude. Five pitch periods are displayed. The third segment corresponds to the power spectrum of Fig. 3 where the six selected peaks are marked by circles. Electrode 22 is mapped to the lowest spectral band, electrode 1 to the highest frequency band.

stimulation mode, the pulse amplitude and width is encoded by high-frequency (2.5 MHz) bursts of different durations, the total transmission time for a specific stimulus depends on all of these parameters. This transmission time can be minimized by choosing the shortest possible pulse width combined with the maximal amplitude. For very short pulse durations, the overhead imposed by the transmission of the fixed stimulus parameters can become rather large. Consider, for example, the stimulation of electrode pair (21, 22) at 50 μsec. The maximally achievable rate varies from about 3600 Hz for high amplitudes to about 2700 Hz for low amplitudes whereas the theoretical limit would be close to 10000 Hz (biphasic pulses with minimal interpulse interval). In cases with higher pulse width requirements (which may be due to poor nerve survival or unfavorable electrode position or other unknown factors), the overhead gets smaller. Thus, typical maximal continuous rates for six electrodes range from 300 to 600 Hz.

In order to achieve maximally high stimulation rates for those portions of the speech input signals which are assumed to be most important for intelligibility, several modifications of the basic CIS strategy were designed. The analysis of the short time spectra was performed either for a large number of narrow frequency bands (approximately third-octave spacing, corresponding directly to the number of available electrodes) or for a small number (typically six) of wide frequency bands (approximately octave spacing) analogous to the approach suggested by Wilson et al. (1991). The mapping of spectral energy within any of these frequency bands to stimulus amplitude at a selected electrode was done according to several rules. The first scheme (CIS-NP) used a pre-selected number of peaks (typically again six) of the narrow-band analysis spectra relying on the same spectral feature extraction as the PES strategy. The second scheme (CIS-NA) was also based on the narrow-band spectral analysis but used all channels whose values exceeded a pre-set noise cut-out level (NCL), as shown in Fig. 5. Two variations of the wide-band analysis scheme were implemented which mapped the spectral energy of each band either to the same pre-selected electrode (fixed tonotopical mapping, CIS-WF) or to those electrodes within the wide bands which corresponded to local peaks (variable tonotopic mapping, CIS-WV). The CIS-WF scheme was supposed to minimize electrode interactions by establishing maximal distances between stimulated electrodes while the CIS-WV would make optimal use of tonotopical frequency selectivity. In both the PES- and the CIS-strategies, a high-frequency pre-emphasis was applied whenever a spectral gravity measure exceeded a pre-set threshold.

Subjects, fitting procedure, speech tests

To date, evaluation experiments have been conducted with seven cochlear implant users. Data of only five of these subjects will be presented in this paper as the remaining two subjects did not participate in all experiments. Table I lists some etiologic and technical information. All subjects were experienced users of their speech processors (time since implantation ranged from five months (KW) to nearly ten years (UT, implantation of single-channel device in 1980) with minimal open speech discrimination in monosyllabic word tests (scores

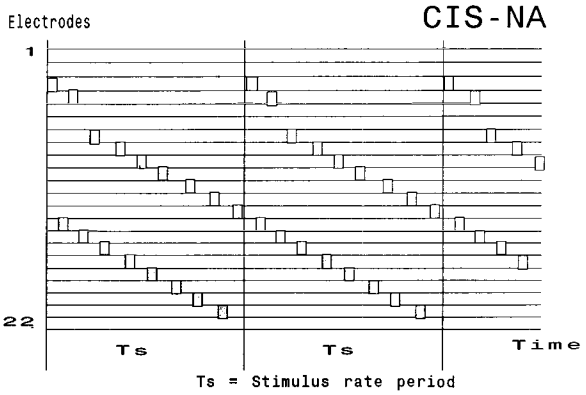

Fig. 5. Electrodogram of the CIS-NA strategy. All electrodes are stimulated sequentially at maximal rate. Spatial distances between sequentially activated electrodes are optimized as indicated in the graph. Values below a pre-set noise cut level (NCL) produce no output pulses. The second segment corresponds to the power spectrum of Fig. 3 where the frequency bands with energy above the NCL are marked by arrows.

TABLE I

Subjects information

Identification (Sex)	UT (f)	TH (m)	HS (m)	KW (m)	SA (f)
Date of birth	6/1941	2/1965	11/1944	3/1947	7/1962
Etiology (duration, years)	Sudden (15)	Trauma (3)	Sudden (14)	Meningitis (28)	Sudden (1)
Implementation date (side)	3/87 (L)	10/89 (R)	11/88 (R)	12/90 (L)	3/89 (L)
Speech processor (strategy)	WSP (F0F1F2)	MSP (F0F1F2)	MSP (MPEAK)	MSP (MPEAK)	MSP (MPEAK)
Electrode pairs	16	20	19	18	20
Stimulation mode	BP	BP + 1	BP	BP	BP
T-level (mean charge/phase, nC)	73	79	38	74	37
C-level (mean charge/phase, nC)	137	157	84	130	62
Pulse width (μsec)	150–204	204	100	204	100

Note: subject UT had pulse widths of 150 μsec on most bipolar electrode pairs except for electrodes 20, 17, 9 and 7 where the pulse width was set to 204 μsec.

from 5 to 25%) and limited use of the telephone. One subject (UT) still used the old wearable speech processor (WSP) which extracts only the first and second formant and stimulates only two electrodes per pitch period. Three subjects used the new miniature speech processor (MSP) with the so-called multipeak strategy whereby in addition to first and second formant information three fixed electrodes may be stimulated to convey information contained in three higher frequency bands. Subject TH used the MSP with the F0F1F2 strategy due to elevated stimulus levels.

The same measurement procedure was used to determine thresholds of hearing (T-levels) and comfortable listening (C-levels) for the CIDSP strategies as when fitting the WSP or MSP. Fig. 6 shows an example of these data for subject HS. Note that the stimulus levels are expressed as charge per phase in

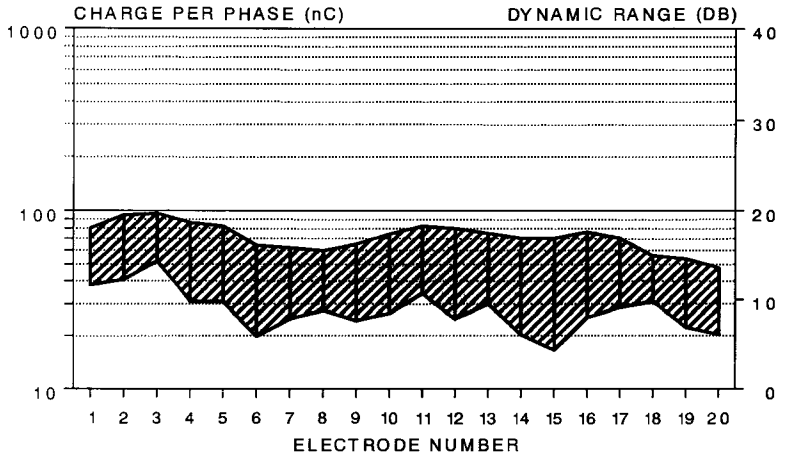

Fig. 6. Thresholds of hearing (T-levels) and comfortable loudness levels (C-levels) for subject HS, electrodes 1 to 20, bipolar stimulation (BP) with 100 μsec pulse width. The charge per phase was calculated as the product of amplitude times pulse width using a calibration table supplied by the electrode manufacturer (Cochlear Pty., Sydney).

nanoCoulomb (nC) instead of fitting software-specific current or stimulus levels. This was done to facilitate comparisons of different stimulus parameters and electrode configurations. As most subjects used fixed amplitudes and varying pulse widths (so-called stimulus levels) with their MSP's, and because the CIDSP algorithms required fixed pulse widths and varying amplitudes, all T- and C-levels were first remeasured prior to speech tests. Overall loudness of processed signals was adjusted by proportional factors (T- and C-modifiers) if necessary, following short listening sessions with ongoing speech and environmental sounds which were played from a tape recorder. T- and C-levels, averaged over all active electrodes, are shown in Table I.

Only minimal exposure to the new processing strategies was possible due to time restrictions. After about 5 – 10 min of listening to ongoing speech, one or two blocks of a 20-items, 2-digit numbers test with feedback of correct or wrong responses were administered. There was no feedback given during the actual test trials. Consonant and vowel identification, as well as multiple-choice, minimal-pair tests (rhyme tests, MAC battery) were performed. All test items were presented by a second computer via a D/A converter, low-pass filter (5 kHz) and attenuator. The subjects' responses were entered via a touch screen terminal (for multiple-choice tests) or keyboard (numbers tests and monosyllable word tests) and recorded automatically by the same computer. Speech signals were either presented via a loudspeaker in a sound-treated room (when patients were tested with their speech processors) or processed by the CIDSP in real time and fed directly to the transmitting coil at the subjects' head. Different speakers were used for the ongoing speech, the numbers tests and the actual speech tests, respectively. Table II shows the 12 consonants presented in /aCa/ context and the phonological and acoustic feature assignment matrices used in the following information transmission analyses (Miller and Nicely, 1955). The second set of features (Envelope, Lowfreq. and Duration) was obtained through an acoustic analysis of the digitized speech tokens used in the experiments and a correlation with the results of a multidimensional scaling analysis of listening experiments which included hearing aid users and cochlear implant users (Dillier and Spillmann, 1988).

Results

Fig. 7 summarizes the results for consonant identification tests for five subjects and six different processing conditions. The percentages of correctly identified tokens have been corrected for chance level. It can be seen that three subjects (UT, TH, SA) scored significantly lower with their own speech

TABLE II

Consonant phoneme features

Phoneme	p	t	k	b	d	g	m	n	l	r	f	s
Voicing	–	–	–	+	+	+	+	+	+	+	–	–
Nasality	–	–	–	–	–	–	+	+	–	–	–	–
Sonorance	–	–	–	+	+	+	+	+	+	+	–	–
Sibilance	–	–	–	–	–	–	–	–	–	–	–	+
Frication	–	–	–	–	–	–	–	–	–	–	+	+
Place	1	2	3	1	2	3	1	2	2	3	2	2
Manner	1	1	1	2	2	2	3	3	4	4	5	5
Envelope	3	3	3	2	2	3	1	1	1	1	2	2
Lowfreq.	+	+	+	–	–	+	–	–	–	+	+	+
Duration	3	3	2	2	3	2	1	1	2	1	3	3

processors than with any of the tested CIDSP strategies. Subject HS performed better with two of the four CIS variations, subject KW did not improve his scores with any of the digital processing strategies as compared to the performance with his MSP (note that KW had been using his speech processor for only five months. He had been deaf for nearly 28 years; all other subjects had lost their hearing less than 14 years before implantation). Most subjects reached more than 10% higher scores with the best CIS strategy compared to the PES coding. Among the four CIS variations, the NA and WF modes turned out to be superior. PES and CIS-NP resulted in about the same performance which could have been predicted by their algorithmic similarity. It is interesting to note that CIS-WV produced mostly lower scores than the similar CIS-WF (subject SA, unfortunately, was not tested with CIS-WV). This points to the importance of the mapping functions between spectral energy and stimulation electrodes. A variable mapping (i.e., a selection of the active electrode based on the local maximum within an octave frequency band) was apparently less effective than a fixed mapping which preserved constant maximal distances between activated electrode pairs. It is also interesting to note that activation of all possible electrodes (CIS-NA) within a stimulation cycle can lead to the same or even better performance as high-rate stimulation of only six electrodes (CIS-WF).

To gain more detailed insight into the performance differences with these processing conditions, an information transmission analysis of the pooled confusion matrices of all five subjects was performed. Fig. 8 shows the percentages of transmitted stimulus information for the phonological feature set of Table II. Again, the overall information transmitted is highest for CIS-NA and CIS-WF and lowest for the patient's own speech processor (WSP for UT and MSP for the other four subjects). Largest differences are seen for the sibilance and frication features (high-frequency a-periodic signals), whereas for sonorant consonants (and for the nasality distinction) the W/MSP seemed to perform as well as the peak-picker strategies (PES, CIS-NP, CIS-WV). It is well known that the phonological features are not orthogonal and may mislead interpretation due to their inherent redundancies. Therefore, a more detailed sequential analysis (Wang and Bilger, 1973) with the same phonological

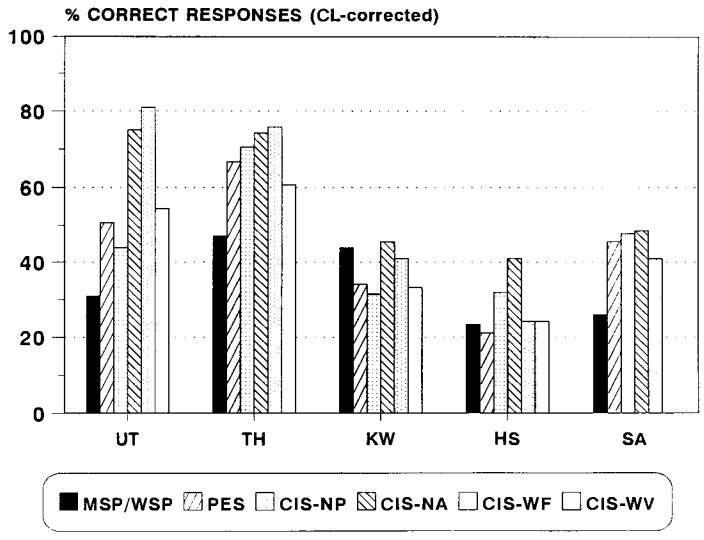

Fig. 7. Percent correct responses for five subjects tested with six different signal processing conditions (12 consonants test /aCa/, 144 trials). Chance level corrected scores: S = (R − CL)/(100 − CL), where R = raw score (%) and CL = chance level (%).

feature set and an additional set of acoustic features was carried out. Table III summarizes the main results of these analyses. The overall percentages are identical to the values displayed in Fig. 8. It can be seen that the phonological feature set (4 – 5 features selected out of seven) explains between 80 and 90% of the stimulus information ("Total" values) whereas the three acoustic features leave between 20

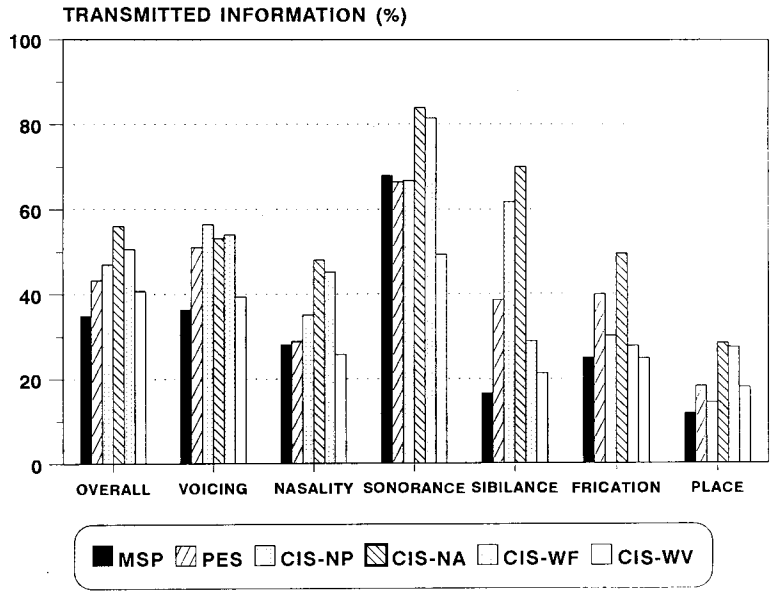

Fig. 8. Information transmission analysis of the consonant identification test data. Confusion matrices of the five subjects were pooled for the six processing conditions.

TABLE III

Sequential information transmission analysis (SINFA) of pooled consonant confusion matrices for five subjects with two different sets of speech features

	W/MSP	PES	CIS-NP	CIS-NA	CIS-WF	CIS-WV
Overall	34.8	45.3	47.0	56.0	50.6	40.7
Voicing	5.2	12.0	13.3	10.8	14.1	13.9
Nasality	3.9				5.9	
Sonorance	49.9	37.6	36.3	38.4	41.3	31.0
Sibilance		8.0	12.7	12.7	5.7	
Frication	7.6	2.3		3.6		8.5
Place	14.9	19.9	18.0	24.2	21.2	23.9
Manner			3.1			
Total	81.5	79.8	83.5	89.6	88.2	77.3
Envelope	57.1	50.5	46.4	50.3	52.6	42.9
Lowfreq.	13.8	16.2	13.1	18.8	14.4	11.7
Duration	6.1	6.9	9.2	8.6	13.3	11.0
Total	77.0	73.5	68.7	77.7	80.3	65.6

and 35% of the stimulus information unexplained. Sonorance information is highest for all conditions, followed by place of articulation and voicing (or sibilance, CIS-NA). As variations of articulatory positions are mainly correlated with changes in second and third formant frequencies, one might conclude that the CIS strategies, in this case, are better encoding information about formant transitions than the other approaches. Note, as well, that voicing information transmission is also improved although the CIS strategies do not explicitly encode the voice pitch as do the speech processor and the PES strategy;

Vowel identification scores, on the other hand, were rarely improved by modifications of the signal processing strategy. Only one of the four subjects (HS) showed significant improvement in total scores, another subject (TH) had markedly deteriorated performance with either PES- and CIS strategies.

Discussion and conclusions

These speech test results should be considered as preliminary. The number of subjects is still very small and data collection for additional subjects is ongoing. It is hoped that other variations of the CIS strategy will lead to even larger improvements in recognition scores for these optimal cases. It should be kept in mind that these data were obtained in the laboratory without specific training and with only minimal exposure to the new processing schemes.

Inspection of the information transmission analysis seems to indicate a strong preference for a non-feature extraction approach such as maximal pulse rates on either all electrodes (narrow-band analysis with wide spatial separation of sequentially stimulated electrodes) or a limited fixed set of electrodes (wide-band analysis with preservation of fine temporal envelope information). The fact that the acoustic feature set used in the sequential analysis could not account for the same amount of stimulus information as the phonological feature set points to the importance of further investigations into the effects of transformation and encoding of speech signals for the specific case of multielectrode cochlear implant configurations (see Soli and Arabie, 1979, for further discussion). These findings need to be confirmed with more subjects. There are still many variables whose influence on the ability of implanted subjects to recognize and discriminate speech information should be explored further. Additional technical solutions may be found in the future which will allow the application of maximally high pulse rates even in subjects with elevated thresholds requiring stimulation with larger pulse widths. Whether the auditory nerve is reacting in a fundamentally different manner at continuously high excitation states and, thus, would generate a more natural auditory percept could be a very interesting basic research question. Psychophysical experiments using stochastic and jittered stimulus patterns (Dobie and Dillier, 1985) have demonstrated the ability of cochlear implant subjects to use pulse rate cues well above 300 Hz. Van den Honert and Stypulkowski (1987) have studied single-fiber response patterns for various pulsatile and analog stimulus waveforms and discussed possible consequences for speech encoding.

It is, however, very encouraging that new signal processing strategies can considerably improve speech discrimination. Consonant identification, apparently, may be enhanced by more detailed temporal information and specific speech feature transformations. Whether these improvements in phoneme discrimination can be transferred to a generally improved word and sentence recognition in quiet and noise environments also remains to be verified. Preferably further optimization of these processing strategies should include more specific data about loudness growth functions for individual electrodes or additional psychophysical measurements.

Although many aspects of speech encoding can be efficiently studied using a laboratory digital signal processor it would be desirable to allow subjects more time for adjustment to a new coding strategy. Several days or weeks of habituation are sometimes required until a new mapping can be fully exploited. Specific interactive training might shorten this

period in the future. Thus, for scientific as well as practical purposes, the miniaturization of wearable DSP's will be of great importance.

Acknowledgements

This work was supported by the Swiss National Research Foundation (grants no. 4018 – 10864 and 4018-10865). Implant surgery was performed by Prof. U. Fisch. Valuable help was also provided by Dr. E. von Wallenberg of Cochlear AG, Basel.

References

Clark, G.M., Tong, Y.T. and Patrick, J.F. (1990) *Cochlear Prostheses,* Churchill Livingstone, Edinburgh, London, Melbourne and New York, 264 pp.

Dillier, N. and Spillmann, T. (1988) Wahrnehmung akustischer Sprachmerkmale mit einkanaligen Cochlea-Implantaten und Hörgeräten. Eine vergleichende Analyse. *HNO,* 36: 335 – 341.

Dillier, N., Senn, C., Schlatter, T., Stöckli, M. and Utzinger, U. (1990) Wearable digital speech processor for cochlear implants using a TMS320C25. *Acta Otolaryngol. (Stockh.) (Suppl.),* 469: 120 – 127.

Dobie, R.A. and Dillier, N. (1985) Some aspects of temporal coding for single-channel electrical stimulation of the cochlea. *Hearing Res.,* 18: 41 – 55.

Flanagan, J.L. (1972) *Speech Analysis, Synthesis and Perception,* Springer, Berlin, 2nd ed., pp. 321 – 405.

Greenwood, D.D. (1990) A cochlear frequency-position function for several species – 29 years later. *J. Acoust. Soc. Am.,* 87: 2592 – 2605.

McKay, C., McDermott, H., Vandali, A. and Clark, G. (1991) Preliminary results with a six spectral maxima sound processor for the University of Melbourne/Nucleus multiple-electrode cochlear implant. *J. Otolaryngol. Soc. Austr., 6:* 354 – 359.

Miller, G.A. and Nicely, P.E. (1955) An analysis of perceptual confusions among some English consonants. *J. Acoust. Soc. Am.,* 27: 338 – 352.

Skinner, M.W., Holden, L.K., Holden, T.A., Dowell, R.C., et al. (1991) Performance of postlingually deaf adults with the wearable speech processor (WSP III) and mini speech processor (MSP) of the Nucleus Multi-Electrode Cochlear Implant. *Ear Hear.,* 12/1: 3 – 22.

Soli, S.D. and Arabie, P. (1979) Auditory versus phonetic accounts of observed confusions between consonant phonemes. *J. Acoust. Soc. Am.,* 66: 46 – 59.

Van den Honert, C. and Stypulkowski, P.H. (1987) Temporal response patterns of single auditory nerve fibers elicited by periodic electrical stimuli. *Hearing Res.,* 29: 207 – 222.

Wang, M.D. and Bilger, R.C. (1973) Consonant confusions in noise: a study of perceptual features. *J. Acoust. Soc. Am.,* 54: 1248 – 1266.

Wilson, B.S., Finley, C.C., Lawson, D.T., Wolford, R.D., Eddington, D.K. and Rabinowitz, W.M. (1991) Better speech recognition with cochlear implants. *Nature,* 352: 236 – 238.

J.H.J. Allum, D.J. Allum-Mecklenburg, F.P. Harris and R. Probst
Progress in Brain Research, Vol. 97

CHAPTER 29

New processing strategies for multichannel cochlear prostheses

D.T. Lawson, B.S. Wilson and C.C. Finley

Neuroscience Program, Research Triangle Institute, Research Triangle Park, Durham, NC 27709, U.S.A.

Various strategies for representing speech information with multichannel cochlear prostheses were compared in tests with implant patients. The strategies included the compressed analog (CA) approach of a standard clinical device, and alternative interleaved pulses (IP) and continuous interleaved sampling (CIS) strategies. CA and IP strategies had been compared in previous studies with a wide range of subjects. The present studies compared all three types in tests with one subject and CA and CIS strategies in tests with six additional subjects. Subjects for the present studies were selected for their excellent performance with the clinical CA processor, and the tests included closed-set identification of consonants and open-set recognition of words and sentences. For every test, every subject obtained his or her highest score, or repeated a score of 100% correct, using a CIS strategy. In the comparisons of all three approaches, IP processor scores were between those obtained with CA and CIS processors. The results are discussed in terms of their implications for processor design.

Key words: Cochlear prosthesis; Speech processing; Speech perception; Hearing; Deafness

Introduction

Cochlear implants have improved the lives of many deaf people. Most patients enjoy remarkable gains in face-to-face communication when the implant is used as an adjunct to lipreading and some are able to understand portions of conversational speech with hearing alone. Full restoration of speech recognition without visual cues, however, has remained elusive. In this paper, we describe a significant step toward that goal, at least for patients who have relatively high levels of performance with a standard clinical device.

Methods

Seven users of the Ineraid implant, selected for their excellent performance with compressed analog (CA) processors, participated as subjects. CA, interleaved pulses (IP) and continuous interleaved sampling (CIS) processors were compared in tests with one of the subjects, and CA and CIS processors were compared in tests with the remaining six. Experience with the clinical CA processors exceeded two years of daily use for each subject. In contrast, experience with IP and CIS processors was limited to no more than a few hours before formal testing.

Processing strategies

The strategies and procedures to evaluate them have been described in detail elsewhere (Wilson et al., 1990, 1991a,b). Briefly, CA processors first restrict or compress the wide dynamic range of input microphone signals to the narrow dynamic range of electrically evoked hearing using an automatic gain control (AGC). The AGC output then is filtered into frequency bands for simultaneous analog stimulation of separate intracochlear electrodes.

IP and CIS processors use non-simultaneous interleaved pulses as stimuli, with amplitudes derived

from the envelopes of bandpass filter outputs. Envelope signals are formed by rectification and low-pass filtering, and the amplitude of each stimulus pulse is determined by a non-linear transformation of the corresponding channel's envelope signal at that time. This transformation compresses each signal into the dynamic range appropriate for that channel.

Differences in IP and CIS processors lie primarily in the timing of stimulation sequences across the electrode array. In IP processors, distinctions between voiced and unvoiced segments of speech are explicitly represented. During voiced segments, stimulation sequences are presented at a rate equal to the estimated fundamental frequency (F0) of the speech sound; while, during unvoiced segments, stimulation sequences are presented either at a fixed, higher rate or at a non-uniform "jittered" rate.

CIS processors, on the other hand, continually present sequences of pulses at fixed rates higher than those used in IP processors, making no distinction between voiced and unvoiced intervals.

As illustrated in Fig. 1, the CA, IP and CIS strategies provide fundamentally different representations of speech signals at the electrode array. The CA strategy presents the greatest amount of temporal information through its use of analog stimuli. However, most implant patients cannot perceive changes in the temporal variations of a stimulus above a "pitch saturation limit" of about 400 Hz (e.g., Shannon, 1983). Also, the simultaneous presentation of stimuli in the CA strategy may produce significant interactions among channels through vector summation of the electric fields from each electrode (e.g., White et al., 1984). Both IP and CIS strategies eliminate such interactions through the use of non-simultaneous stimuli. The relatively high rates of pulsatile stimulation used in CIS strategies allow representation of rapid variations in speech by pulse amplitude.

Tests

The three strategies were evaluated with a variety of speech reception tests. Because each subject had excellent performance with his or her CA processor, results from only the most difficult tests are reported here. These included identification of 16 consonants (/b, d, f, g, dʒ, k, l, m, n, p, s, ʃ, t, δ, v, z/) in an

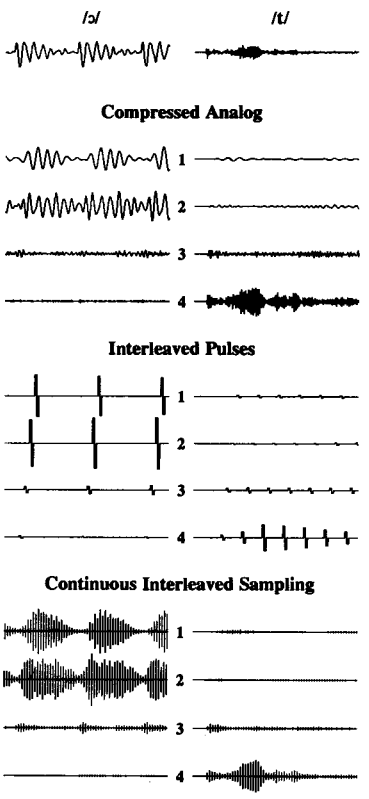

Fig. 1. Waveforms produced by simplified implementations of CA, IP and CIS strategies. The top panel shows pre-emphasized (6 dB/octave attenuation below 1.2 kHz) speech inputs. Inputs corresponding to a voiced speech sound ("aw") and an unvoiced speech sound ("t") are shown in the left and the right columns, respectively. The duration of each trace is 25.4 msec. The remaining panels show stimulus waveforms for the three strategies. The waveforms are numbered by channel, with channel 1 delivering its output to the apical-most electrode. To facilitate comparisons, only four channels of stimulation are illustrated here for each strategy. In general, five or six channels have been used for IP and CIS strategies. The pulse amplitudes for IP and CIS strategies reflect the envelope of the bandpass output for each channel. In actual implementations the range of pulse amplitudes is compressed using a logarithmic or power-law transformation of the envelope signal. Note that the prolonged stimulation in the IP processor for the /t/ burst is a consequence of the long time constant of the low-pass filters in the envelope detectors (25 Hz cut-off versus 400 Hz cut-off for the CIS processor).

/a/-consonant-/a/ context (Tyler et al., 1987) and the open-set tests of the Minimal Auditory Capabilities (MAC) battery (Owens et al., 1985).

In the consonant test, multiple examplars of the /aCa/ tokens were played from laser videodisc recordings of male and female speakers. A single block of trials consisted of five randomized presentations of each consonant for one of the speakers. At least two blocks were administered for each speaker, processor, and subject.

The open-set tests included recognition of 50 one-syllable words from Northwestern University Auditory Test 6 (NU-6), 25 two-syllable words (spondees), 100 key words in the Central Institute for the Deaf (CID) sentences of everyday speech, and the final word in 50 sentences from the Speech Perception in Noise (SPIN) test (here presented without noise). In these tests, single presentations of the words and sentences were played from cassette tape recordings of a male speaker.

All tests were conducted with hearing alone, without feedback as to correct or incorrect responses. Results for the consonant identification test were expressed as percent information transfer for various articulatory and acoustic features (Miller and Nicely, 1955), and results for the open-set tests as the percentage of correct responses.

Processor parameters

Each subject's own clinical device was used for the tests with the CA processor. Selection of parameters for the alternative IP or CIS processors was guided by preliminary tests of consonant identification. The standard four channels of stimulation were used for the clinical CA processors (Eddington, 1980), whereas five or six channels were used for the IP and CIS processors to take advantage of additional implanted electrodes and reduced interactions among channels. The IP processor used 100 μsec/phase pulses, presented in a base-to-apex order for each stimulation sequence (an electrode order of 6-5-4-3-2-1). A constant rate of 278 pulses per second (pps) on each channel was used during unvoiced intervals. The envelope detector for each channel used a 25 Hz low-pass filter. All CIS processors had pulse durations of 102 μsec/phase or less, pulse rates on each channel of 817 pps or higher, and a cut-off frequency for the low-pass filters of 400 Hz or higher. In addition, the order of channels in the stimulation cycle was chosen to maximize the spatial separation between temporally adjacent channels. We found that this "staggered order" (6-3-5-2-4-1) produced significant improvements in some subjects' consonant identification scores.

Results and discussion

CA/IP/CIS comparisons

Results for the comparisons among CA, IP and CIS processors are presented in Fig. 2. The top panel shows information transmission (IT) scores for con-

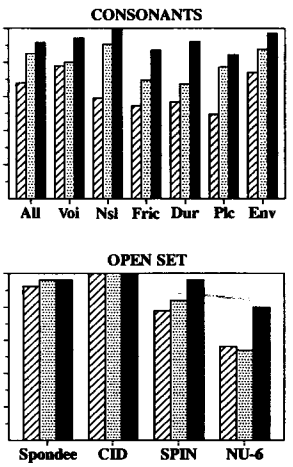

Fig. 2. Comparisons of speech test scores for CA (striped bars), IP (stippled bars), and CIS (solid bars) processors. The top panel shows relative information transfer for articulatory and acoustic features of consonants. The features include overall transmission (All), voicing (Voi), nasality (Nsl), frication (Fric), duration (Dur), place of articulation (Plc) and envelope cues (Env). Full scale corresponds to 100% information transfer. Fifty presentations of each consonant were used in the consonant identification test with the CA processor, and twenty presentations were used in the tests with the IP and CIS processors. The presentations for each processor were equally divided between the male and female speakers. The bottom panel shows scores from the open-set tests of the MAC battery. See text for abbreviations. Full scale corresponds to 100% correct. Data are from tests with Ineraid subject SR2.

sonant features, and the bottom panel shows scores from the open-set tests. The results demonstrate a clear ranking of performances for the three processors. That is, despite four years of daily experience with the CA processor for this subject (SR2), both IP and CIS processors immediately produced superior scores. The particular implementation of the IP strategy used for this subject produced gains over the CA processor for every consonant feature except voicing (where scores are about the same), while the CIS implementation produced gains over both the CA and IP processors for all features. Especially large increases shared by the IP and CIS processors include those for nasality and place of articulation. In addition, substantial increases in the scores for voicing, frication and duration are obtained when the CIS strategy is used instead of the IP strategy.

Because these CIS processor scores approach the 100% ceiling for most consonant features, the increases shown in Fig. 2 may in fact underestimate the relative superiority of that processor. The scores for overall information transmission, voicing, nasality, duration, and envelope cues are 92% or higher with the CIS processor.

The ranking of processors indicated by the consonant results is affirmed in the pattern of scores from the open-set tests. For the tests not at or near the ceiling of 100% correct for all processors, the IP processor scores are equivalent or superior to those of the CA processor, while the CIS processor scores are clearly better than those of the IP processor.

Possible mechanisms underlying the performances of IP and CIS processors include: (a) reduction in channel interactions through the use of nonsimultaneous stimuli; (b) use of five or six channels instead of four; (c) preservation of amplitude cues with channel-by-channel compression; and (d) the shape of the compression function. The observed gains in IT scores for nasality and place of articulation are consistent with possibilities (a) and (b). That is, these features largely reflect the spectral characteristics of consonant sounds above the range of F0 (e.g., above 300–400 Hz; see Miller and Nicely, 1955). An increased salience and resolution of channel cues would be expected to improve the reception of such spectral information.

The observed gains in IT scores for nasality also are consistent with an improved representation of amplitude cues (possibilities (c) and (d) above). Nasals and other sonorant consonants have the highest amplitudes among consonants, including other voiced consonants (e.g., Van Tasell et al., 1987). Perception of such amplitude differences might support discrimination of /l, m, n/ from the other consonants in our set, and therefore produce higher IT scores for nasality.

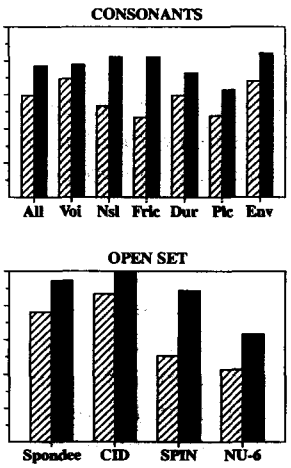

Fig. 3. Comparisons of speech test scores for CA (striped bars) and CIS (solid bars) processors. Feature transmission scores of consonants were derived from the aggregated matrix of stimuli and responses for all seven subjects. A total of 205 presentations of each consonant was used in the tests with the CA processor, and a total of 145 presentations was used in the tests with the CIS processors. Presentations were balanced between the male and female speakers in both cases. The open-set scores are averages across subjects. The scores for the CIS processors are those from each subject's best fitting of that type of processor. For two of the subjects (SR5 and SR8) these processors are somewhat different from the ones used in the consonant tests (Wilson et al., 1990). Schedule limitations did not allow additional consonant tests with the processors finally selected for these two subjects. The CID and NU-6 tests were repeated for five of the subjects (SR3, SR4 and SR6-8), using a different recorded speaker and new lists of words and sentences. Practice or learning effects would be demonstrated by significant differences in the test/retest scores. However, no such differences were found ($P > 0.6$ for paired t comparisons of the CID scores; $P > 0.2$ for the NU-6 scores), and the scores from the first and second tests were averaged.

Finally, the superior IT scores obtained with a CIS processor for the remaining features may be related to an improved representation of temporal events in speech. The relatively high rates of stimulation used in the CIS processor allow representation of envelope variations up to at least 400 Hz. The difference between this limit and the 25 Hz limit of the IP processor may explain, at least in part, the observed increases in IT scores for voicing, frication, duration and envelope cues (see also Van Tasell et al., 1987; Rosen, 1989).

CA/CIS comparisons

Based on the encouraging results with subject SR2, we decided to compare the CA and CIS strategies in tests with six additional subjects. In this way, we could evaluate the generality of the initial results. Each of these additional subjects also had high levels of initial performance with his or her clinical CA processor.

Results from the CA/CIS comparisons are presented in Fig. 3 and Table I. Again, large gains in the scores for the consonant features of overall transmission, nasality, frication and place of articulation are produced with CIS processors (Fig. 3, top panel). In addition, substantial increases are found for consonant duration and envelope cues.

The increases in IT scores for consonants are mirrored in the scores from the open-set tests. As indicated in Table I, every subject scored higher, or repeated a score of 100% correct, using a CIS processor. Also, as indicated in the bottom panel of Fig. 3, remarkable gains in average scores are seen for all tests not subject to ceiling effects. Paired t comparisons show that the increases across subjects are significant for the spondee ($P < 0.05$), SPIN ($P < 0.01$), and NU-6 ($P < 0.002$) tests. The increase in the average score for the CID test is not significant; however, the sentivity of that test may have been severely compromised by ceiling effects.

Additional aspects of CIS performance

In recent studies we have begun systematic investigation of various aspects of CIS performance. These studies include evaluations of CIS performance (a) across numbers of channels, (b) across other manipulations in CIS parameters, and (c) under conditions of noise interference. In addition, we have begun studies with subjects who have relatively poor outcomes with their clinical CA processors.

In this section, we review preliminary studies to evaluate effects of channel number manipulations and of noise interference. Both studies were conducted with subject SR2. Because this subject's high scores had compromised the sensitivity of our consonant and other tests in evaluations of CIS processors with a variety of new parameter sets (i.e., he obtained perfect or nearly perfect scores on the consonant, spondee, CID and SPIN tests, and he obtained scores in the high 80s or low 90s on the NU-6

TABLE I

Individual results from the open-set tests

Subject	Spondee		CID		SPIN		NU-6	
	CA	CIS	CA	CIS	CA	CIS	CA	CIS
SR2	92	96	100	100	78	96	56	80
SR3	52	96	66	98	14	92	34	58
SR4	68	76	93	95	28	70	34	40
SR5	100	100	97	100	94	100	70	80
SR6	72	92	73	99	36	74	30	49
SR7	80	100	99	100	66	98	38	71
SR8	68	100	80	100	36	94	38	66

test), we decided to increase the difficulty of the consonant test by increasing the number of consonants from 16 to 24 (the set of 24 includes /b, d, f, g, dʒ, h, j, k, l, m, n, ŋ, p, r, s, ʃ, t, tʃ, δ, θ, v, w, z, ʒ/). Since this change, however, SR2 has achieved scores of 99% correct with the male speaker using five different implementations of CIS processors. Furthermore, scores for the female speaker have been only somewhat lower (as high as 95% correct).

While the sensitivity of even the 24 consonant test now is inadequate to distinguish among the better implementations of CIS processors for subject SR2, the sensitivity of that test is well suited to studies exploring decrements in performance with reduced numbers of channels or with increasing amounts of noise interference.

Results from the first study are presented in Fig. 4. Here we show the consonant scores for CIS processors with 6, 5, 4, 3 and 2 channels, and for an analogous processor with 1 channel (referred to as a CS processor, since interleaving is not applicable to a single channel). Each *n*-channel processor used the *n* apical-most electrodes and filtered the same total frequency range into *n* bands of equal width on a logarithmic scale. For example, the three-channel processor used apical electrodes 1, 2 and 3. All processors used 33 μsec/phase pulses, presented at the rate of 2525 pps on each channel (delays were interposed between sequential pulses for processors with fewer than six channels to maintain this constant rate). In addition, each processor used 6th-order bandpass filters, full-wave rectifiers, and 400 Hz low-pass filters (1st order). For consistency, a fixed base-to-apex update order was used for all processors; for example, the three channel processor stimulated its electrodes in the sequence 3-2-1.

The results show a strong effect of channel number on consonant identification. Overall percent correct scores decline monotonically, for both the male and female speakers, with reductions in the number of channels. Also, transmission of place information declines precipitously for the male speaker as the number of channels is reduced from 6 to 3, and drops precipitously for the female speaker as the number of channels is reduced from 5 to 4. In all cases the transmission of place information declines monotonically as the number of channels is reduced. In contrast, transmission of envelope information is relatively well maintained when the number of channels is reduced, as is the transmission of voicing, frication and nasality information for the male speaker (indeed, the transmission

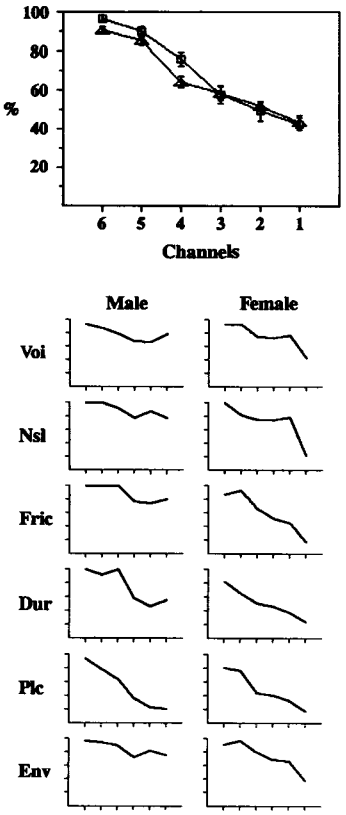

Fig. 4. Percent correct and feature transmission scores for processors using different numbers of channels. Five presentations of each of 24 consonants by the male speaker, and five presentations of each consonant by the female speaker, were used in the tests with each processor. The presentations were arranged in block-randomized order, providing a percent correct score after each set of randomized presentations of all 24 consonants. The square symbols in the top panel show averages of these scores (from five randomized sets) for the male speaker, and the triangles show the averages for the female speaker. Standard errors of the mean are indicated with the vertical bars. The remaining panels show feature transmission scores for the same experimental conditions. Full scale corresponds to 100% information transfer.

of voicing information remains high even for a single channel). Results for the female speaker are somewhat different in that the transmission of voicing and nasality information drops sharply when the number of channels is reduced from 2 to 1, and the transmission of frication information drops rapidly over the range of channel reductions from 5 to 1.

A consistent finding in the data is the dependence of place transmission on the number of stimulation channels. In addition, results from the female speaker suggest that transmission of frication information may depend on number of channels, at least up to five channels, and at least for certain speakers. Further increases in channel number may improve the transmission of place information and other important cues for the correct identification of consonants. As indicated elsewhere (e.g., Tye-Murray and Tyler, 1989; Dorman et al., 1990; Wilson et al., 1990), such identification is highly correlated with open-set recognition of words, sentences and running speech.

Results from the second study, designed to evaluate effects of noise interference, are presented in Fig. 5. Here we show performances of CIS and CA strategies in noise without any special provisions for noise reduction. A six-channel CIS implementation was used with the following parameters: 33 μsec/phase pulses, 2525 pps rate of stimulation on each channel, staggered update order, 12th-order bandpass filters, full-wave rectifiers, and 400 Hz low-pass filters (1st order).

Consonant identification first was measured under quiet conditions, and then progressively greater amounts of multitalker speech babble were added to the primary speech signal. Signal-to-noise ratios (SNRs) included 15, 10, 5 and 0 dB, with 0 dB corresponding to the babble signal amplitude exceeding the maximum consonant waveform amplitude briefly about once per second on average.

While the presence of noise clearly degrades the performance of both processors, relatively high percent correct scores are maintained down to a SNR of 5 dB. The scores for the CIS processor are higher than those for the CA processor at all SNRs. This is especially encouraging inasmuch as the CA processor in the Ineraid device has been identified as the most resistant to the deleterious effects of noise among several tested implant systems (Gantz et al., 1987).

One possible factor underlying the high levels of CIS performance in the presence of interfering speech babble is a good representation of envelope cues. In particular, covariation in envelope information across channels may help maintain high

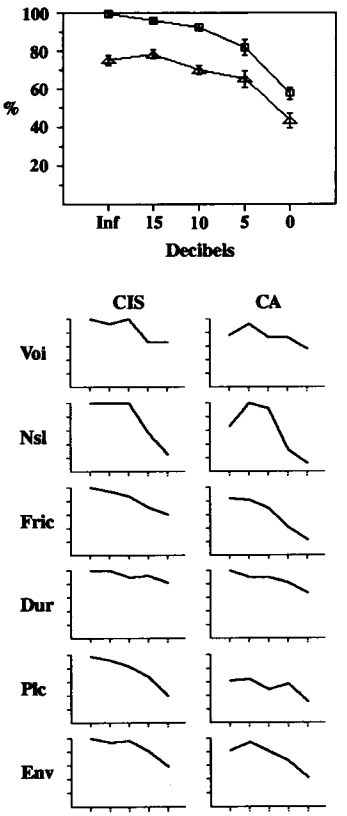

Fig. 5. Percent correct and feature transmission scores for CIS and CA processors as a function of signal-to-noise ratio (SNR). The SNR of "Inf" refers to presentation of the signal without any accompanying noise. Five presentations of each of 24 consonants by the male speaker were used in the consonant identification tests for each processor at each SNR. The square symbols in the top panel show average percent correct scores for the CIS processor, and the triangles show the averages for the CA processor. Standard errors of the mean are indicated with the vertical bars. The remaining panels show feature transmission scores for the same experimental conditions. Full scale corresponds to 100% information transfer.

levels of speech recognition in noise (e.g., Hall et al., 1984; Moore, 1991). Such across-channel information may allow a listener to follow the correlated cues of the primary speech signal, while rejecting the uncorrelated variations produced by the noise.

Another factor that may contribute to the performances found for both the CA and CIS strategies is the fact that neither relies on feature extraction. The accuracy of such extraction can be severely degraded by even modest amounts of noise, as demonstrated in many studies with conventional speech analysis systems (e.g., Rabiner and Shafer, 1978) and in studies with cochlear implant devices (e.g., Gantz et al., 1987).

A key lesson in the present results is that the choice of a basic processing strategy per se can have large effects on performance in noise.

Concluding remarks

The principal results presented in this paper are those from comparisons of CA, IP and CIS strategies. All three strategies were compared in tests with subject SR2, and CA and CIS strategies were compared in tests with subjects SR2-8. All subjects had high levels of initial performance with their clinical CA processors, and all subjects used the Ineraid implant system. The comparison tests included closed-set identification of consonants and open-set recognition of words and sentences.

In all comparisons the CIS processors produced the best scores. Indeed, the sensitivity of several of the open-set tests was limited for these subjects by ceiling effects: five subjects scored 96% or higher on the spondee test using CIS processors; all seven subjects scored 95% or higher on the CID test; and five subjects scored 92% or higher on the SPIN test. In addition, use of CIS processors produced substantial gains in feature transmission scores for consonants, including those for overall transmission, nasality, frication, place of articulation, duration, and envelope cues.

While the present results are most encouraging, we want to emphasize that "the CIS strategy" actually constitutes a rich class of processor implementations with an especially wide range of parametric choices. Future work will focus on systematic evaluation of these choices and on identification of optimal parameters for a wide range of individual patients. In addition, we plan to study subjects using different implant systems, allowing implementations with more than six channels and with electrode couplings other than the monopolar configuration used in the Ineraid device. Results from these studies should help demonstrate the full potential of the CIS approach, and should provide further insight into the mechanisms underlying CIS performance.

Acknowledgements

We thank the subjects of the described studies for their enthusiastic participation. We also are pleased to acknowledge the important scientific contributions of D.K. Eddington, W.M. Rabinowitz, R.D. Wolford and M. Zerbi. This work was supported by NIH projects N01-NS-5-2396 and N01-DC-9-2401, through the Neural Prosthesis Program.

References

Dorman, M.F., Soli, S., Dankowski, K., Smith, L.M., McCandless, G. and Parkin, J. (1990) Acoustic cues for consonant identification by patients who use the Ineraid cochlear implant. *J. Acoust. Soc. Am.*, 88: 2074 – 2079.

Eddington, D.K. (1980) Speech discrimination in deaf subjects with cochlear implants. *J. Acoust. Soc. Am.*, 68: 885 – 891.

Gantz, B.J., McCabe, B.F., Tyler, R.S. and Preece, J.P. (1987) Evaluation of four cochlear implant designs. *Ann. Otol. Rhinol. Laryngol.*, 96 (Suppl. 128): 145 – 147.

Hall, J.W., Haggard, M.P. and Fernandes, M.A. (1984) Detection in noise by spectro-temporal pattern analysis. *J. Acoust. Soc. Am.*, 76: 50 – 56.

Miller, G.A. and Nicely, P.E. (1955) An analysis of perceptual confusions among some English consonants. *J. Acoust. Soc. Am.*, 27: 338 – 352.

Moore, B.C.J. (1991) Comodulation masking release and across-channel masking. In: *Workshop on the Psychophysics of Speech Perception, II, Utrecht, Netherlands, July 1 – 5,* in press.

Owens, E., Kessler, D.K., Raggio, M. and Schubert, E.D. (1985) Analysis and revision of the Minimal Auditory Capabilities (MAC) battery. *Ear Hear.*, 6: 280 – 287.

Rabiner, L.R. and Shafer, R.W. (1978) *Digital Processing of Speech Signals,* Prentice-Hall, Englewood Cliffs, NJ.

Rosen, S. (1989) Temporal information in speech and its relevance for cochlear implants. In: B. Fraysse and N. Cochard (Eds.), *Cochlear Implant: Acquisitions and Controversies,* Impasse La Caussade, Toulouse, pp. 3 – 26.

Shannon, R.V. (1983) Multichannel electrical stimulation of the auditory nerve in man. I. Basic psychophysics. *Hear. Res.,* 11: 157 – 189.

Tye-Murray, N. and Tyler, R.S. (1989) Auditory consonant and word recognition skills of cochlear implant users. *Ear Hear.,* 10: 292 – 298.

Tyler, R.S., Preece, J.P. and Lowder, M.W. (1987) The Iowa audiovisual speech perception laser videodisc. *Laser Videodisc and Laboratory Report,* Department of Otolaryngology, Head and Neck Surgery, University of Iowa Hospital and Clinics, Iowa City, IA.

Van Tasell, D.J., Soli, S.D., Kirby, V.M. and Widen, G.P. (1987) Speech waveform envelope cues for consonant recognition. *J. Acoust. Soc. Am.,* 82: 1152 – 1161.

White, M.W., Merzenich, M.M. and Gardi, J.N. (1984) Multichannel cochlear implants: channel interactions and processor design. *Arch. Otolaryngol.,* 110: 493 – 501.

Wilson, B.S., Lawson, D.T. and Finley, C.C. (1990) Speech processors for auditory prostheses. *Fourth Quarterly Progress Report, NIH project N01-DC-9-2401.*

Wilson, B.S., Finley, C.C., Lawson, D.T., Wolford, R.D., Eddington, D.K. and Rabinowitz, W.M. (1991a) Better speech recognition with cochlear implants. *Nature,* 352: 236 – 238.

Wilson, B.S., Lawson, D.T., Finley, C.C. and Wolford, R.D. (1991b) Coding strategies for multichannel cochlear prostheses. *Am. J. Otol.,* 12 (Suppl. 1): 56 – 61.

J.H.J. Allum, D.J. Allum-Mecklenburg, F.P. Harris and R. Probst
Progress in Brain Research, Vol. 97

Overview and critique of Chapters 30 – 33

M. Hulliger and C.D. Mah

Department of Clinical Neurosciences, University of Calgary, Calgary, Alberta, Canada T2N 4N1

Four papers of this section deal with various aspects of the mechanics and the neural control of posture and gait. Common to all is that they rely, to varying degrees, on mathematical modeling techniques. There is no doubt that the development of rigorous formal models for the description of neural control processes and their interaction with the mechanical constraints of a multi-joint body capable of locomotion and balance is a prerequisite to understanding the integrative features of control and execution of movement. Paradoxically, however, the degree of simplification necessary to make these models manageable appears to be proportional to the complexity of the original system. For example, common to the first two papers is the reduction of the human body to a four- or five-rigid-segment structure consisting of foot, shank, thigh, trunk and neck/head segments, with movements restricted to three or four "joints" (ankle, knee, hip and neck), and with no attempt to model the role of arm or lumbar trunk movements. This is not to belittle the present efforts. Modeling often requires formal definitions, such as the definition of "synergies" as muscle activation sequences, or the identification of "neural effort" with an angle between acceleration vectors. Nevertheless, an appreciation of the many untested assumptions behind such definitions and simplifications serves to remind us, how far there is to go.

A common and significant problem with realistic models of complex biological systems is the fact that many different models can account for the same observations. The implication is that, when models are used to make inferences about certain parameter values, there need not be unique solutions. This is because often not a sufficient number of model parameters can be measured independently and because these parameters must then also be inferred from the observed behavior. When many parameters are fitted on this basis, in order to match model behavior with real system behavior, goodness of fit is no longer evidence of correctness but a foregone conclusion. In constructing models which are falsifiable it is useful to determine the model's sensitivity to variations of individual parameter values. Those parameters, which do not affect the model much, can often be omitted, while those which strongly affect model behavior may suggest critical experiments. As a rule of thumb, a well constructed model should show significant sensitivity to variations in only a limited number of parameters, and parameters with little effect should be lumped or omitted altogether.

Chapter 30

The paper of Allum and Honegger addresses a question of considerable practical importance, namely whether the muscle activation synergies, which can be recorded in normal subjects in response to perturbations of body equilibrium, can be used to design strategies of functional electrical stimulation (FES) of leg muscles in hemiplegic patients, who have lost voluntary control over these muscles, in order to assist maintenance of balance, when the patient walks (with FES support). The motivation for this approach is that it is unrealistic to except that chronic implant and recording tech-

niques will be available in the near future to record the range of sensory feedback signals which the CNS relies on to assess the state of equilibrium and to compute a measure of balance. Further, it would probably be a formidable challenge to mimic the performance of the CNS in this computational task. However, if the sense of balance and its ability to generate orchestrated corrective responses to perturbations of balance still are preserved, this might not even be necessary. The working hypothesis is that corrective responses are based on consistent strategies and muscle synergies, and that these are not altered by part of the motor apparatus being disconnected from central control. It should then be possible to take advantage of the balance computations performed by the CNS and to tap facets of corrective motor strategies by monitoring residual muscle activity in order to restore activation synergies by functional electrical stimulation of centrally paralyzed muscles.

The questions, which arise and which are in part addressed by the authors, are whether corrective response strategies for restoration of balance can be identified in normal subjects; whether the CNS uses a single or a few general strategies or a large number of specific strategies to handle the wide variety of natural perturbations; and whether any of these strategies can be described in terms general enough to permit general FES designs (for references see Allum and Honegger, this volume). The paper gives preliminary answers to these questions. Based on cross-correlation analysis of measured EMG responses and computed joint torques, the conclusion is reached that different strategies can be recognized in responses to different support-surface perturbations (ankle rotation vs. rearward translation). It is left open, whether the different response profiles represent two discrete strategies or whether they are separate manifestations from a continuum of corrective response patterns. Part of the uncertainty is due to the fact that the authors make no attempt to describe their response patterns in more general terms than in pairs of cross-correlations. If, as in the present case, significant numbers of cross-correlation pairs have to be assessed, identification of any underlying general pattern is difficult. For future work, at least two approaches should be explored. First, data reduction for description of general underlying patterns could be attempted, using principal component analysis. Principal components reflecting multiple-muscle synergies would permit description of multi-dimensional data sets with smaller numbers of variables and they would probably permit more general answers regarding the issue of discrete vs. continuous response strategies. Second, it can be argued that for the development of FES strategies explicit description of response strategies would not be required, since adaptive neural network techniques could be used to optimize FES activation patterns, based on recordings of residual muscle activity and a set of performance criteria for maintenance of body equilibrium. Before it is tried, it cannot be judged whether this approach would yield unique solutions. If it did, it would in fact provide answers to some of the above questions, since the strategies learned by neural networks, rather than those employed by the CNS, could then be analyzed to determine whether they are discrete or part of a continuum.

Two concerns about Allum and Honegger's approach and results deserve explicit mention. First, while it is demonstrated convincingly (by comparing normal subjects with patients with vestibular deficits) that vestibular as well as proprioceptive sensory inputs are instrumental for the generation of effective corrective response patterns, and while it is argued that neck muscle responses are likely dominated by cervico-collic and vestibulo-collic reflex components and hence probably little affected by sensory deficits in paralyzed legs, it is less obvious that corrective trunk muscle responses in paraplegics are entirely unaffected by the lack of proprioceptive input from paralyzed legs. This issue could probably be assessed by recording trunk muscle EMG responses to perturbations in hemiplegic patients (with normal vestibular function), when they stand with support of braces, and by comparing them with normal response patterns. Second, while computation of EMG cross-correlograms gives unique solutions, computation of joint torques

from kinematic data does not necessarily do so. The authors were aware of this problem and frankly state that no attempt was made to assess uniqueness of solutions. Therefore it is difficult for the reader to judge the trustworthiness of the computed torque records. These were derived from kinematic measurements, using a simplified four-segment model of the human body, where each joint was characterized by stiffness and viscosity. The parameter values were in turn derived from initial responses to perturbations, before reflex activation or inhibition of the muscles acting across the joint took place. However, both stiffness and viscosity of muscles (and hence of joints) are known to strongly depend on the degree of muscle activation. As above, this problem could be addressed in control experiments, with normal subjects voluntarily co-contracting muscles across the knee and ankle joint, in order to obtain estimates of these parameters at various levels of muscle activity. However, it may finally be pointed out, that the uncertainty regarding the accuracy of joint torque computations should not invalidate one of the main conclusions, i.e., that separate corrective strategies appear to be used in response to different perturbations, since this notion was also supported by the EMG analysis.

Chapter 31

An engineer designing an artificial leg with three joints would probably not equip it with 33 motors (muscles), but nature has done this with the human leg. With each joint having more than a single degree of freedom and with 33 muscles, each potentially under independent central control, it would appear that there should be hundreds of different muscle activation strategies to achieve a given target movement, and that there might be tens of separate strategies to maintain upright posture. However, for kinematics, considering that posture stabilizing leg movements are restricted to three joints, one would intuitively expect that the choice should be much more limited. Kuo and Zajac address this problem using a comprehensive biomechanical model of the human leg. The lay-out of the model is admirably general, as all 33 muscles are represented individually and remarkably realistically (regarding musculoskeletal geometry and functional properties such as maximum force generating capacity). The benefits of this general lay-out are that simplifications are not inherent limitations but tools for exploration. This model is used to compute feasible acceleration sets, i.e., the territory in the three-dimensional joint acceleration space, to which corrective movements are confined by biomechanical constraints. The main conclusion is that for maintenance of upright postural stability in the sagittal plane the choice is remarkably limited. Especially, if perturbations are large, if knee movements are not permitted and if the CNS were to use a minimal "neural effort" approach for muscle activation, there would in fact be a single favored strategy combining hip and ankle movements, rather than relying on single joint movements. For small perturbations a second strategy, restricting movement to the ankle joint, would also be feasible and appears to be used occasionally by experimental subjects, although it is more costly in terms of "neural effort" (defined as a normalized activation signal). The authors suggest that the CNS, when normally favoring the combined hip-and-ankle strategy, in fact relies on a minimization of "neural effort" (or muscle activation) criterion.

In assessing the work and the above conclusions a number of issues arise. First, the benefits and detailed criteria of the notion of minimal "neural effort" remain to be clarified. Minimal neural effort may or may not minimize muscle energy consumption because, for instance, 25% activation of large muscles may consume more energy than 50% activation of small muscles. This difficulty could be avoided by defining neural effort in terms of numbers of motor units activated, rather than in normalized activation percentage, yet, if minimization of muscle (rather than neuronal) energy consumption mattered, scale factors for motor unit size would also have to be added.

Second, it is not obvious, what the benefits of not permitting knee (and also neck) movements for postural compensation should be. The fact is that both knee and neck movements do occur during

postural adjustments (cf. Allum and Honegger, this volume). If these movements were allowed, the uniqueness of a single favored strategy might be less compelling. Also, if knee movements were indeed to be prevented by central control, the joint would probably have to be stiffened by voluntary muscle contraction. High degrees of cocontraction of antagonistic muscles might then be necessary (to maintain minimal joint acceleration), which could easily be at variance with the criterion of minimization of muscle activation.

Third, even if the existence of a single favored strategy stood up, simplicity might be restricted to the final kinematic product, since this might be arrived at through a number of different neuronal strategies (i.e., different central commands, activating different subsets of the 33 muscles available). These could include different degrees of cocontraction (between antagonists) and different degrees of task sharing between synergists. Thus, multiple central activation strategies might still be behind an apparently unique kinematic strategy.

Fourth, the limitation of movements to a very narrow domain in the acceleration space is a remarkable property of a model of such complexity. It is not clear whether this is accounted for by any particular biomechanical constraint, or whether the limitation arises from a combination of constraints. One way of exploring this would be to study various simplified versions of the model in order to determine which of its numerous features are mandatory or immaterial to give rise to such limitation.

Fifth, the present model for the assessment of whole limb postural strategies appears to be at an early stage of development. Initial simplifications of more technical nature would therefore appear acceptable, especially in view of the general lay-out. However, the justification of these simplifications still needs to be established more convincingly, to corroborate the generality of the main conclusions. To name but a few: muscle force production is independent of velocity. While the authors cite preliminary evidence that the effects of omitting force-velocity properties were small, the matter deserves more careful analysis, since fast and slow muscles are bound to differ in this respect. Further, fatique appears not to have been considered, yet it is likely to influence muscle recruitment in postural tasks and should motivate differential treatment of fast and slow muscles. Finally, while the force-length relation has been modeled, short-range stiffness has not. Yet it is very likely that early responses to perturbations of active muscle are strongly influenced by short-range properties, not least since the postural perturbations considered are mostly rather small.

Chapter 32

Winter and colleagues argue convincingly that control strategies for maintenance of balance and principal engagement of various muscle groups are bound to be different for control of gait as opposed to stance. The simplest reason is that during stance the vertical projection of the centre of gravity is kept within the bipedal base of support, while during most phases of a step cycle this is no longer the case. The thrust of their analysis is that ankle muscles, which are significant actors for maintenance of balance during stance, no longer serve this function during gait. Instead, hip muscles assume a dominant role to maintain balance of head and trunk. Moreover, based on head acceleration analysis, the authors conclude, provocatively, that the vestibular system is not involved in this change of strategy.

The analysis rests on inverted pendulum models of the human body. The main conclusions regarding the dominant role of hip muscles for maintenance of balance during gait appear to be borne out by moment of force calculations and are further qualitatively supported by EMG recordings. However, the use of averaged EMG profiles to confirm results obtained with inverse dynamics analysis could have been carried further. One wonders whether it would not be possible to compute estimates of hip moments, based on realistic musculoskeletal geometry, and reasonable assumptions about EMG-force and force-velocity relations, since qualitative interpretation of gait cycle EMG profiles alone is not very discriminative. The present juxtaposition of computed moments and EMG profiles hardly merits the attrib-

ute "integrated EMG/biomechanical model", as suggested in the title.

The case for the putative unimportance of vestibular sensors for the dominant role of hip muscles in maintaining balance during gait is not necessarily convincing. Even if head acceleration is small and were barely perceptible, more effective sub-cortical actions via vestibulo-spinal pathways are by no means ruled out. The apparent absence of appropriate phase advance of head acceleration on hip moments might simply indicate marginally delayed, rather than non-existent, vestibular action. Or else, vestibular signals might be processed (for instance be differentiated, by neuronal networks) to generate the appropriate phase advance. A more convincing argument might be that vestibular action is not needed, because the imbalancing moments at the hip are highly predictable, as they are generated by the locomotor pattern generator. Yet Winter et al.'s emphasis of the high variability of hip moments would go against this. More arguments could be added, yet in the end the most promising approach to resolve this issue might well be to repeat the same analysis in patients with vestibular dysfunction.

Finally, while Winter et al.'s 14 segment model of the human body is much more detailed and realistic than the four and five segment models of the preceding two papers, it would be appealing to see its power tested in predictive applications. In the present study it seems to be merely used as a frame of reference for inverse dynamics analysis and computation of moments. For instance, it would be interesting to see whether the time course of certain types of naturalistic perturbation (such as slip) and of corrective reactions could be predicted accurately. Such extensions would probably involve additional modeling of posture-restoring strategies during gait, which could then be superimposed on the present model, which appears to account adequately for unperturbed gait patterns.

Chapter 33

High level control problems with FES applications are addressed in the papers of Allum and Honegger, and Kuo and Zajac. They are related to the question of what combinations of muscles have to be activated in order to achieve certain kinematic or postural goals. Lower level control problems are associated with the functional properties of muscles themselves and with the technical difficulties of activating them effectively. These aspects are addressed in the paper by Durfee. Particularly important issues are, first, that muscles fatigue and, second, that they appear to operate best when they are activated physiologically, i.e., through a large number of independent and desynchronized channels (motor units). Durfee's approach to the problem of muscle control by FES is particularly informative, because he describes three alternative strategies, each with its benefits and limitations, suggesting that a combination of the three (perhaps also with others) might yield the desirable accumulation of benefits paired with dispersion of their drawbacks.

The first approach is to use a very accurate model of muscle as a reference for a model cancellation controller, which does not rely on kinematic or force feedback from the periphery or the muscle. The main difficulties would appear to lie in the design's inability to handle unforeseen perturbations effectively and in the requirement that the muscle model has to reach very high standards of accuracy. Regarding the latter, the principal shortcoming is the present lack of good models of muscle fatigue. This is not particularly surprising, since the CNS may well not have a comprehensive model of muscle fatigue either, while being able to adjust to it by recourse to sensory feedback.

The second approach is to use a less sophisticated muscle model combined with a more sophisticated adaptive sliding controller and kinematic feedback from the periphery. The advantages are that the system is less vulnerable to model errors, and that fatigue can be taken into account in approximative form, while the need of kinematic feedback obviously limits practical application.

The third approach is to abandon the muscle model altogether and to use a hybrid design based on damped-break orthosis, where movement trajectories are controlled by modulating the mechanical brake. The benefit is that the controller has to deal

with a man-made mechanical rather than a fatiguable biological device; the drawback is the risk of unnecessary muscle activation (and hence fatigue), unless future devices are equipped with sensors detecting excessive contact forces.

Clearly, in their present form none of the three strategies has reached acceptable standards. The main difficulties lie in modeling or monitoring muscle fatigue and the need of feedback signals for the detection of built-in errors or external perturbations. However, it will probably be worth pursuing combinations of the above approaches. In particular there is no compelling reason why in the hybrid system muscles should be treated as if their properties were entirely unknown. Instead, orthotic devices, providing fall-back guidance, could be fitted with kinematic sensors, to supply a non-linear adaptive controller with the kinematic feedback information it requires. Good muscle models would still be useful, but they would not have to be perfect. Empirical fatigue management strategies could then be added, without the need of comprehensive modeling, partly by calibrating individual muscles and patients, and partly by imitating and a priori incorporating the physiological compromise of reducing activation when fatigue unfolds ("muscular wisdom").

J.H.J. Allum, D.J. Allum-Mecklenburg, F.P. Harris and R. Probst
Progress in Brain Research, Vol. 97

CHAPTER 30

Synergies and strategies underlying normal and vestibulary deficient control of balance: implication for neuroprosthetic control

J.H.J. Allum and F. Honegger

Department of ORL, University Hospital, Basel, Switzerland

Future developments of neuroprosthetic control will probably permit locomotion and posture to be maintained without the aid of crutches and will therefore require some form of balance control. Three fundamental questions will arise. First, the question of the location of imbalance-sensing transducers must be assessed. Secondly, the synergy, which is the relative amplitude and timing of muscle activity, and/or the strategy of joint torques required to re-establish a stable posture for different types of balance disturbances must be addressed. Thirdly, the control laws that map either trunk muscle activity or imbalance-sensing transducer outputs into multi-joint postural control of standing by paraplegic individuals must be generated. The most appropriate means of gathering the relevant information applicable to neuroprosthetic control systems is through the detailed analysis of normal and non-normal human models. In order to gain such detailed insights into normal balance control and its dependence on head angular and linear accelerations, the synergy and strategy of balance corrections in normal subjects or patients with vestibular deficits were investigated for two types of support surface perturbation, a dorsiflexion rotation (ROT) and a rearward translation (TRANS). These experimentally induced perturbations to upright stance were adjusted to cause equal amplitudes of ankle dorsiflexion, thus providing additional information about the role of lower leg proprioception on balance control. Synergies defined on the basis of peak cross-correlations of each recorded muscle's EMG to that of the largest muscle response were significantly different for TRANS and ROT. Translation synergies consisted of a sequential coactivation at several levels (soleus and abdominals some 30 msec before hamstrings, and trapezius some 15 msec before paraspinals), whereas the sequential activation of paraspinals and tibialis anterior dominated the balance synergy to ROT. Likewise, response strategies, defined using cross-correlations of joint torques, differed. That for TRANS was organised as a multi-link strategy with neck torques leading those of all other joints by 40 msec or more; hip joint lead ankle torques by 30 msec. That for ROT was organised around hip and ankle torques without a major correlation to neck torques. Vestibulary deficient subjects developed weaker synergies with respect to subjects with normal balance systems under eyes-open conditions and there was no clear synergy with eyes closed. Consequently, hip torques were delayed some 180 msec with respect to ankle torques, and correlations to neck torques were completely out of phase under eyes-closed conditions. Fundamental changes in TRANS synergies and strategies also occurred in vestibulary deficient subjects for eyes-open and eyes-closed conditions. These subjects have difficulty incorporating hip rotation into the multi-link strategy. Our results suggest that vestibular sensors play an integral role in the generation of balance responses. Further, for neuroprosthetic control of balance, artificial activation of leg muscles can be based on the normal balance-correcting activity of trunk and neck muscles, provided that time correlations between natural and artificial activation take into account the rotational and translational aspects of the balance disturbance.

Key words: Balance movements; Vestibular spinal reflex; Stretch reflex; Peripheral vestibular deficit; Electromyographic activity

Introduction

Functional electrical stimulation (FES) is a promising technique that provides standing and slow ambulation by means of nerve-stimulating implants in paraplegic patients. During stimulation, stance stability is almost always achieved with the aid of crutches. Thus, errors in the position of the trunk

Normal

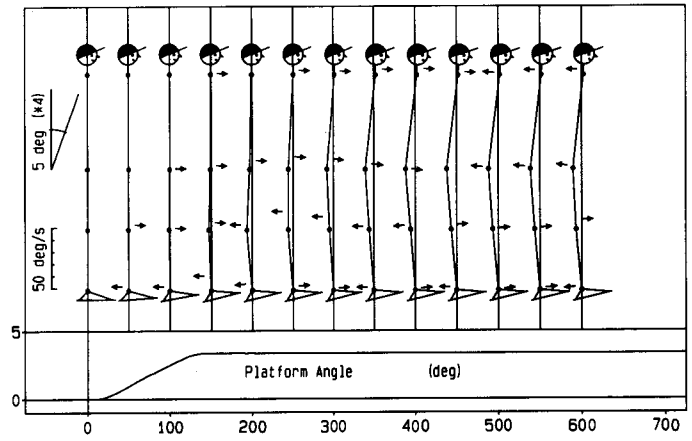

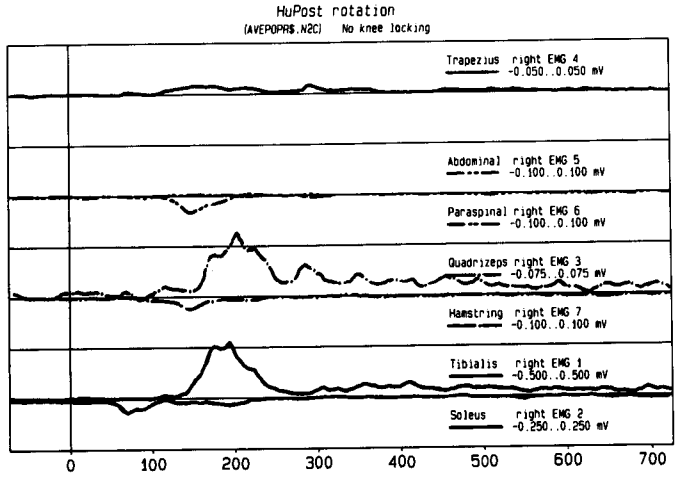

Dorsiflexion Support Surface Rotation

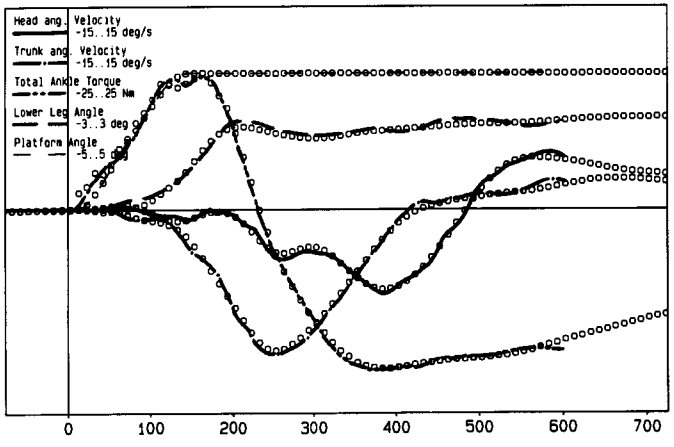

Eyes Closed

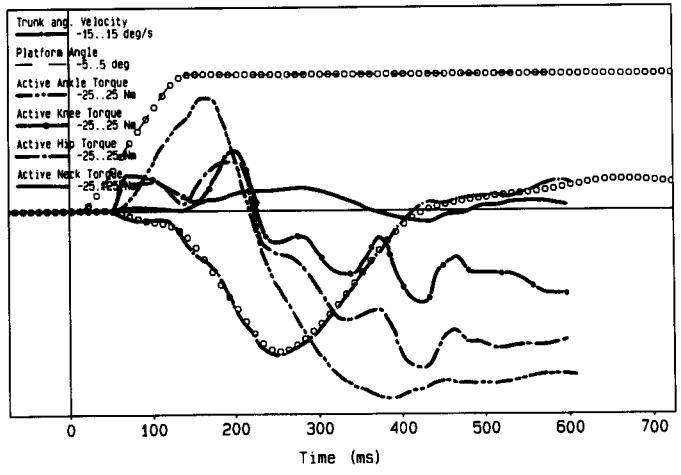

and torques imposed on the legs with respect to those of normal standing and locomotion are not crucial, because it is assumed that unstable postures can be corrected by the arm crutch props. Future developments and the desire to increase acceptance of FES by patients will probably converge towards a point where the need for crutches can be eliminated and near-normal, FES-generated posture and balance can be attained. Two possible means of achieving this goal would be either to integrate the normal activity of the upper body into the FES control of leg muscle stimulation (Graupe, 1989) or to use a robotic external skeleton to provide the necessary joint torques (Popovic et al., 1989). If applied to balance corrections, then the former technique would require knowledge of the activation synergy between trunk and muscle groups, whereas the latter would imply that the strategy of balance-correcting torques applied at different joints be known.

It has been suggested (Berthoz and Pozzo, 1988) that all natural human movements are organised as if the head-trunk unit adopted a stable posture about which the arms and legs move, behaving like the pneumatic pistons of a robot system. In this case, the activity of trunk muscles should be closely related to the activity of normal leg muscles, and torques at the hip and neck should covary with those of the ankle and knee, particularly during balance disturbances. With this suggestion in mind, we explored the activation synergies and torque-controlled movement strategies employed for two types of postural disturbances, a rearward translation (TRANS) and a toe-up rotation (ROT), both with the same amount of dorsiflexion. Our aim was to investigate whether a common strategy would emerge as a result of identical proprioceptive inputs induced at the lower leg (viz. Macpherson et al., 1986); or whether other sensory signals, such as those induced by head movements, would play a more important role in generating balance-correcting synergies and strategies. To this end, we also investigated whether synergies and strategies were altered in subjects with absent vestibular function.

A major issue in current research quantifying postural behaviour concerns the nature of balance corrections. Nashner and colleagues have assigned distinct patterns of responses to normal translations, which they originally termed the ankle and the hip strategy (Horak and Nashner, 1986); and to which they later added the concept of a mixed strategy (Diener et al., 1988). Each strategy was the result of a unique pattern of muscle activation and resultant joint movements. If balance corrections were limited to a few strategies, then the task of interpreting these strategies within a FES system would be reduced in complexity. The evidence in this paper suggests the very opposite, demonstrating

Fig. 1. Average response patterns of a group of seven subjects with normal balance to dorsiflexion rotation of the support surface when tested under eyes-closed conditions. The average surface EMG responses are shown in the upper right panel. With the exception of trapezius, muscles on the ventral surface of the body are plotted positive downwards, and dorsal muscles positive upwards. The deflection amplitude of one vertical gradation is noted next to the muscle name. Average biomechanical responses are shown in the lower left panel. The experimental data are shown as open circles and the model responses by full or interrupted lines. Backward pitching of the lower leg with respect to vertical and trunk and head angular velocity are shown by an upward deflection of the traces. Plantarflexion ankle torque imposed on the support surface is shown by upward trace deflection. Full scale vertical deflection (panel edges) of each trace is noted next to the trace name. Active torques required at each joint to yield the model responses are shown in the lower right panel. Upward deflection of torque traces indicates rearward pitching of body segments proximal to the joint when elements distal to the joint are fixed. The trunk angular velocity (model and experimental data) and platform angle traces are repeated for clarity. Full scale deflections are as indicated. In the upper left panel, the model movements are shown as stick figures at every 50 msec from onset of platform movement. As indicated in the left part of the panel, the angular velocity of each segment is shown as an arrow. The amplitude of the velocity is given by the distance from the lower joint of the segment, the direction is indicated by the direction of the arrow. The velocity scale is shown at the left border of the panel.

strategies that are dependent on the polarity and magnitude of vestibular and/or trunk proprioceptive inputs.

Methods

Balance corrections were induced in subjects standing upright, using either a 4 cm (21cm/sec) rearward translation of the support surface (TRANS) or a 3.4 degree (27 deg/sec) dorsiflexion rotation (ROT). The choice of stimulus parameters yielded ankle dorsiflexion trajectories that were similar over the first 200 msec, but, as Figs. 1 and 2 illustrate, with head angular velocity profiles that were opposite in polarity. The techniques employed in this study to record the biomechanical and electromyographic traces shown in the figures, have been described elsewhere in detail (Allum and Pfaltz, 1985; Keshner et al., 1987; Allum et al., 1989). As in these previous studies, the following measurements were recorded: head angular velocity and acceleration in the pitch plane; head anterior-posterior linear acceleration, trunk angular velocity in the pitch plane; shank pitch angle with respect to vertical; torque about the ankle joint; and support surface rotation and translation. EMG recordings were taken from the tibialis anterior (TA), soleus (SOL), rectus femoris (quadriceps – QUAD), biceps femoris (hamstrings – HAM), lumbar paraspinalis (PARAS), rectus abdominis (ABDOMS), and trapezius (TRAP) muscles.

The balance perturbations consisted of a series of 11 rotations followed by 11 translations. These stimuli were presented first under eyes-open conditions, then were repeated under eyes-closed conditions. Off-line, individual response averages were computed for the first three and last eight of a series of 11 trials. The responses during the last eight trials were the concern of the present study because adaptation effects present in the first three trials were not of interest (viz. Keshner et al., 1987). To facilitate comparisons between populations, across-subject averaging was performed on seven subjects with no history of vestibular abnormalities and on two patients with vestibular deficits.

The biomechanical responses obtained from the subjects were compared with those of a four-segment (shank, thigh, trunk, head) computer model of human posture (see Figs. 1 and 2). Masses and moments of inertia for each segment were equated to those reported by Dempster (1955). The arms were considered to be part of the trunk segment. Movements between segments of the model were constrained by spring and dashpot systems whose initial values for the ankle joint were collated from the available literature (Allum and Mauritz, 1984; Sinkjaer et al., 1988). Combined passive and active visco-elastic resistance at the ankle and other joints was additionally estimated by varying the coefficients of visco-elasticity until a best fit between model and recorded data was obtained for the first 70 msecs of the responses. The 70 msecs limit was based on the time that it takes for stretch reflex responses of ankle muscles to be first observed in ankle torque responses (Allum and Mauritz, 1984). After 70 msecs, it was assumed that visco-elastic elements of the model remained constant, and that additional changes in biomechanical responses from those of the mass-spring-dashpot system were due to active torques applied at each of the segment joints. An iterative approach was used to determine the successful joint-torque combinations that yielded a best fit between model and experimental data between 70 and 600 msec. Normally, the approach taken was first to fit the ankle torque response, then, in 100 – 150 time segments, to adjust knee and hip torques simultaneously until lower leg angle and trunk angular velocity responses were accurately modeled. Readjustment of the ankle torque model was necessary once knee and hip torques were approximately modeled. Finally, the neck and hip torque was varied until both model and experimental data for head and trunk angular velocity were concurrent. Each model torque could consist of a sum of up to eight cosine-bell-on-a-pedestal torques whose onset polarity, rise and fall time and amplitude could be specified by the user. All simulations were performed with Euler-Cauchy integration of the model's equations of motion. The final simulation was rechecked for accuracy with Runge-Kutta-

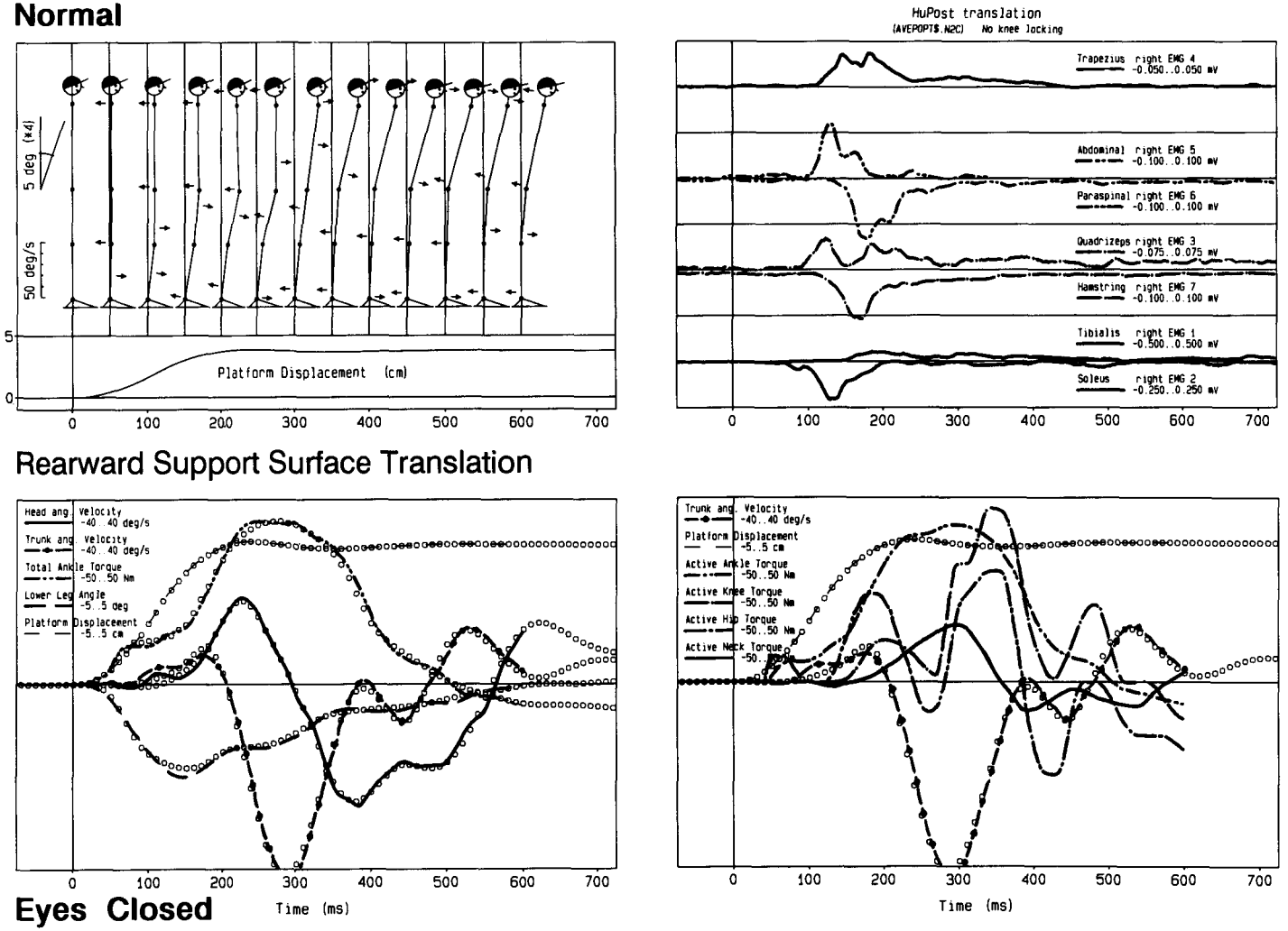

Fig. 2. Average response patterns of a group of seven subjects with normal balance to rearward translation of the support surface when tested under eyes-closed conditions. For details, see legend to Fig. 1. Note the stable position of the head with respect to earth-fixed coordinates in the upper left panel.

Fehlberg integration. No attempt was made to determine the uniqueness of the solution found. Solutions were, however, also well-conditioned because even small 1 Nm variations in knee and hip torque profiles of the best-fit model yielded evident discrepancies between model and real biomechanical data.

Movement strategies were defined on the basis of normalized cross-correlations between the computed active torques. The peak amplitude (with respect to correlation due to the mean torque level between 0 and 600 msec) and latency were used as descriptions of the cross-correlations. Similar normalized cross-correlations were used to define response muscle synergies. However, because 21 possible cross-correlations could be computed from seven muscle responses, analysis was restricted to the eight largest cross-correlations: three associated with the largest muscle response, and five chosen to be common for rotation and translation, thus allowing cross-stimuli comparisons.

Results

At first sight, the response strategies for a toe-upwards (ROT), support surface rotation and rearward translation (TRANS) might appear to be similar because both involve a rotation of the trunk about the hips, as shown by the stick figures in Figs. 1 and 2. The differences in trunk rotation amplitudes with maximum velocities of 10 and 40 deg/sec respectively (see Figs. 1 and 2) could be associated with the differing task requirements. Rotation places the vertical projection of the body's centre of gravity (centre of foot pressure, CFP) more towards the heels and the subject is in danger of falling over backwards. To compensate, the subject must simply bend forward at the hips (see stick figure, upper left, Fig. 1). Rearward translation, however, results in a toe-ward displacement of CFP. This can only be compensated for by rapidly rotating the trunk about the hips, thereby thrusting the hips backwards (see stick figure in Fig. 2), unless a step forward is taken. Thus for ROT and TRANS, the compensating upper body response involves a hip rotation in the same flexion direction. In contrast, it might be argued on the basis of the leg muscle responses in Figs. 1 and 2, that the synergy between the muscle responses could be similar (an ascending, distal followed by proximal, ordering of response onsets), but reversed in polarity (larger responses on the dorsal and ventral surfaces of the leg for ROT and TRANS, respectively) according to differing lower leg stabilization requirements for the two types of disturbances. Consistent with these differing polarities of EMG responses, ankle joint torques occurring 200 msec after stance perturbation onset are also of different polarity as illustrated in Figs. 1 and 2. In order to investigate whether major differences between the strategies and synergies for ROT and TRANS exist and to determine whether, as proposed by Macpherson et al. (1986), a common response synergy underlies balance corrections elicited for ROT and TRANS, cross-correlation plots of joint torques and EMG responses (such as those illustrated in Figs. 3 – 6) were examined in detail.

Normal torque strategies and muscle-response synergies

In Figs. 3 and 4, the characteristic differences between the movement strategies for ROT and TRANS are revealed by the active torque cross-correlations. Major differences between the torque strategies are reflected in the correlation of neck torques to all other joint torques and the oscillatory action of ankle and hip torques. For translation, neck torques were equally well correlated with all other torques. Hip, knee and ankle torques were correlated with each other and had peak values in the range of 0.6 – 0.7. Furthermore, neck torques were found to lead other joint torques by 40 – 60 msec. In contrast, the correlation of neck torque to hip, knee and ankle joint torques was far weaker for rotation (range 0.36 – 0.5), weaker than the correlations of hip, knee and ankle to each other, and was delayed by some 110 msec. The second major difference involves the obvious oscillatory pattern of hip- and knee-joint torques apparent in the lower right part of Fig. 2. This figure depicts the computed active

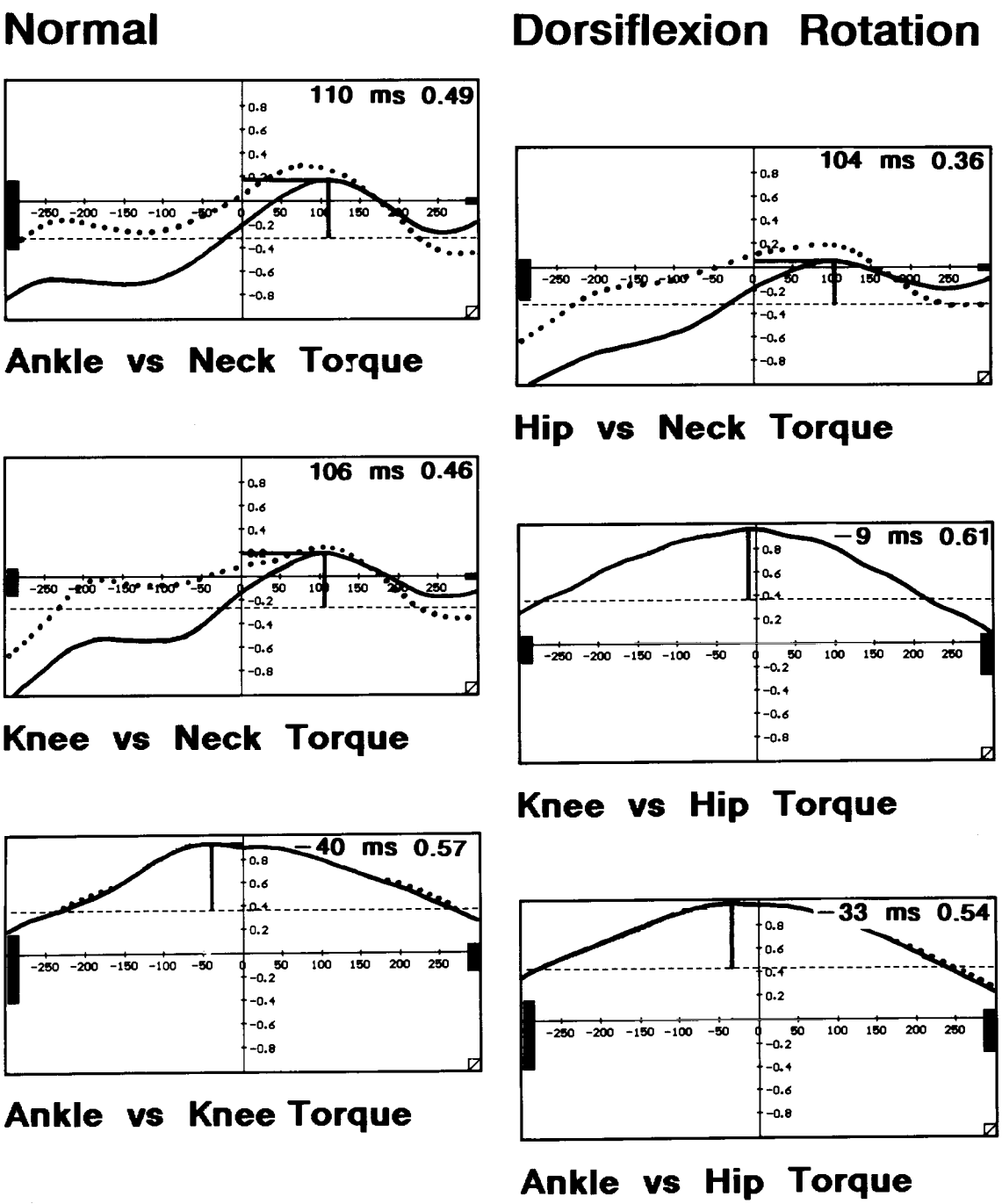

Fig. 3. Average normal movement strategies for dorsiflexion rotation of the support surface. The movement strategy is defined in terms of cross-correlation coefficients between active joint torques whose time histories are shown in Fig. 1 (lower right panel). The full lines are for eyes-closed conditions and the dotted lines (where these differ from the correlations for the eyes-closed condition) are for eyes-open conditions. The time of the peak correlation and its amplitude with respect to correlation of mean torques (dashed horizontal line in each inset) is marked. These values appear in the upper right corner of each inset. The mean positive (backward pitching) and mean negative torque are shown by the thick vertical columns in each inset (full scale 50 Nm).

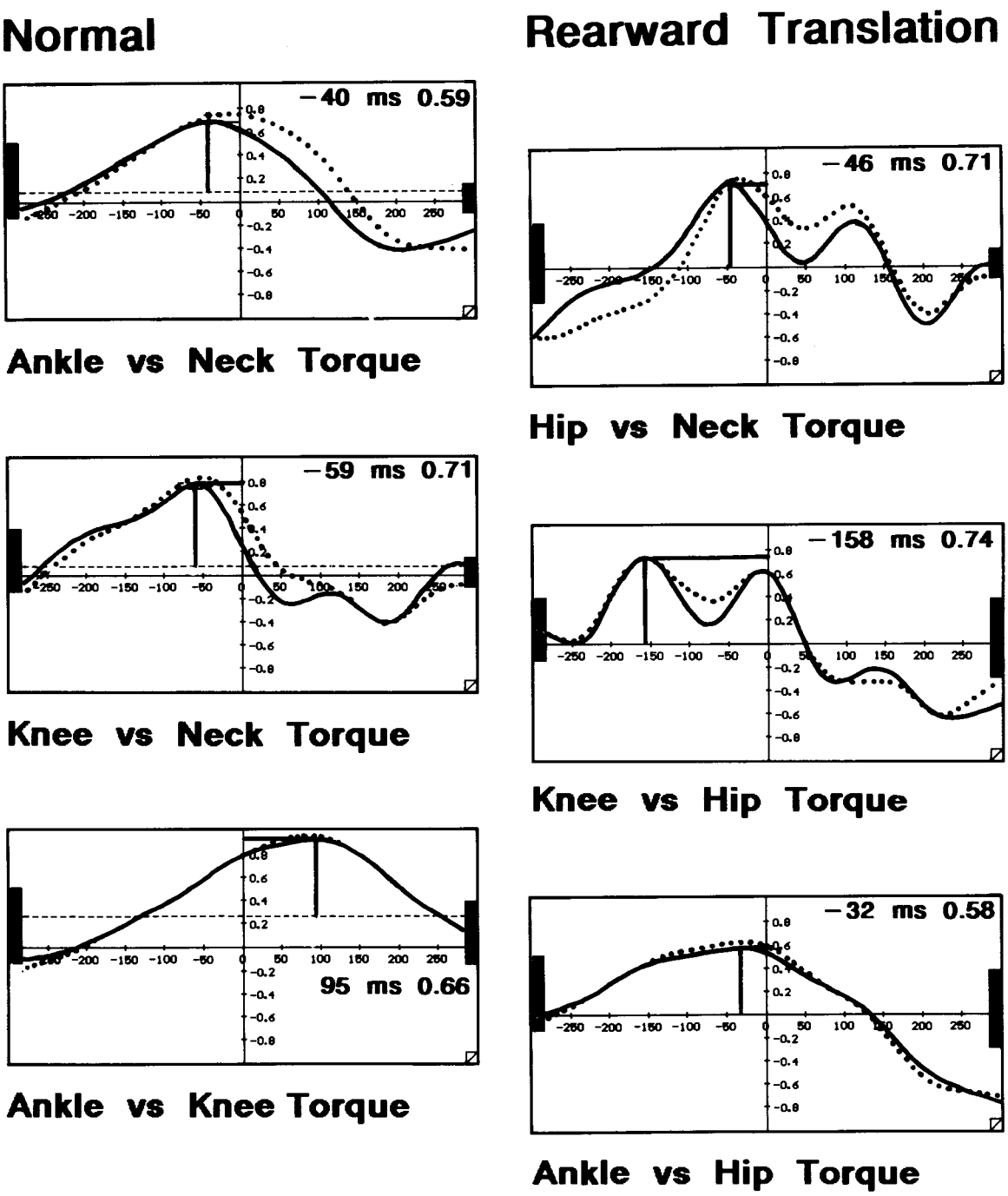

Fig. 4. Average normal movement strategies for rearward translation of the support surface. The movement strategy is defined in terms of the cross-correlation coefficients between the active joint torques whose time histories are shown in Fig. 2 (lower right panel). (For further details, see legend to Fig. 3.)

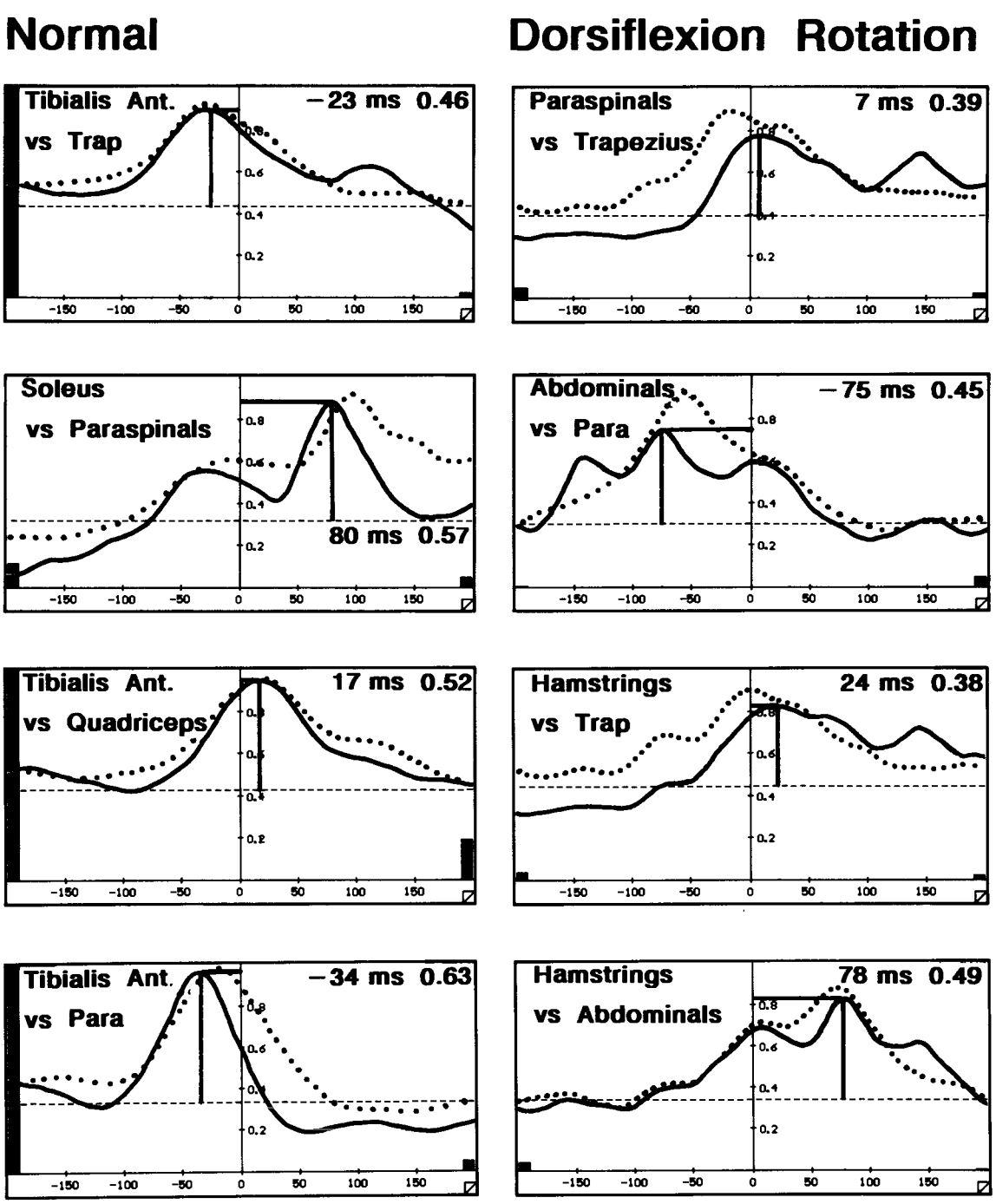

Fig. 5. Average normal movement muscle synergies for dorsiflexion of the support surface. The synergy is defined in terms of cross-correlation coefficients between EMG activity response patterns shown in the upper right panel of Fig. 1. The numerical rotation used is described in the legend to Fig. 3, with the exception of the heavy vertical columns shown at the left and right borders of each inset. These columns represent each muscle's rms activity expressed as a percentage of the maximum response (here tibialis anterior).

joint torques for translation used for the corresponding cross-correlation functions in Fig. 4.

Some common characteristics in the ROT and TRANS strategies exist. One is the remarkable similarity between the ankle-hip cross-correlations, both with peak values of ca. 0.50, at 32 msec, despite differing amplitudes and polarities of joint torques (the vertical columns left and right of each inset in Figs. 3 and 4 indicate rms values of positive and negative torques). Another similarity between the rotation and translation strategies is that the absence of vision (full lines in Figs. 3 and 4; dotted lines, eyes-open correlations) has very little effect on normal movement strategies. A possible similarity between the two strategies is apparent in the ankle-knee correlations. The form of the correlation, with an ill-defined peak for ROT, leads to an apparent difference in timing between ankle and knee torques of ca. 140 msec for rotation and translation, though the general shape of the correlation is identical.

The translation strategy can be viewed as a movement pattern that first generates a stable head platform about which other limbs then rotate, whereas the rotation strategy appears as a stiffening of the posture induced by postural disturbance. By comparing the stick figures in Figs. 1 and 2 at 250 msec (when body limbs move with maximum velocity) and at 500 msec (when limb segments are approaching a stationary position), the basis for terming the translation strategy a multi-link (Allum et al., 1989) rather than an ankle-hip strategy (Diener et al., 1988) can be appreciated. As the cross-correlations in Fig. 4 also indicate, neck and knee torques and hence rotations about the knee and especially about the neck joint comprise an integral, if not fundamental part of the TRANS strategy. In contrast, the rotation strategy, which appears to be constrained to the ankle and hip with little head and knee joint rotation, has been termed a stiffening strategy and might more adequately be termed an ankle-hip strategy (viz. Horak and Nashner, 1986; Horak et al., 1990).

Figs. 5 and 6 show muscle response synergies in the form of cross-correlation functions. These figures provide supporting evidence, in the form of muscle "forces", for differing ROT and TRANS movement strategies. The eight correlations in these figures are an excerpt from 21 possible correlations and were selected on the basis of the largest muscle responses (TA for rotation, SOL for translation) and the most significant correlations. The peaks of the correlations for translations (Fig. 6) duplicate the trend in onset latencies observed by Horak and Nashner (1986), i.e., SOL before HAM before PARAS, as basis for an ascending response synergy. Equally, the correlations confirm the results of Keshner et al. (1988) indicating that an ascending strategy is unlikely because the peak SOL-ABDOM correlation has only a 2 msec and HAM-TRAP a 9 msec delay and thus these muscle pairs appear to be coactivated. Overall, the correlations provide evidence for differing response synergies to rotation and translation and support the evidence already identified for torque strategies.

The correlations in the right columns of Figs. 5 and 6 are for identical muscle pairs. The SOL-PARAS correlation appears in the left column of both figures. All of these correlations show significant shifts of peak latencies between rotation and translation, varying between 30 msec in the case of SOL-PARAS and 123 msec for ABDOM-PARAS. Consistent with the lower neck joint-torque correlations for rotation, all correlations with TRAP were consistently lower for rotation. Interestingly, given the similar torque ankle-hip correlation for rotation and translation, the EMG correlations between the larger muscle response at the ankle and hip (TA-PARAS) and SOL-ABDOM, respectively) were also similar in form.

Effect of a bilateral vestibular deficit on strategies and synergies

Balance corrections attempted under eyes-closed conditions by the two patients with bilateral peripheral vestibular deficits are shown in Figs. 7 and 8 for ROT and TRANS, respectively. A comparison with the normal responses in Figs. 1 and 2 reveals a number of fundamental differences that are most clearly illustrated by the stick figures in the upper left of the figures. When the support surface

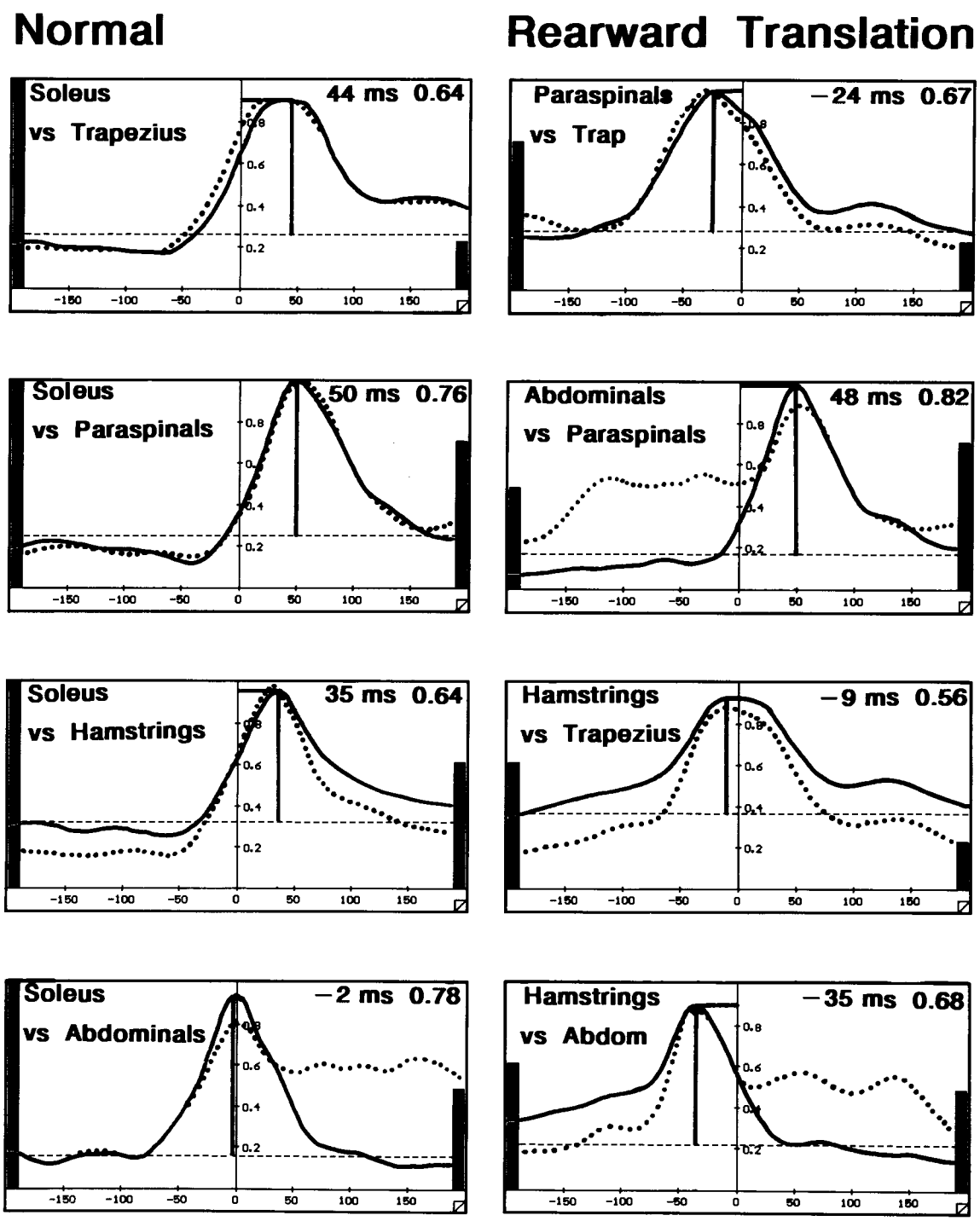

Fig. 6. Average normal movement muscle synergies for rearward translation of the support surface. The synergy is defined in terms of cross-correlation coefficients between EMG activity response patterns shown in the upper right panel of Fig. 2. For further details, see legends to Figs. 3 and 5. The maximum rms response was observed in soleus.

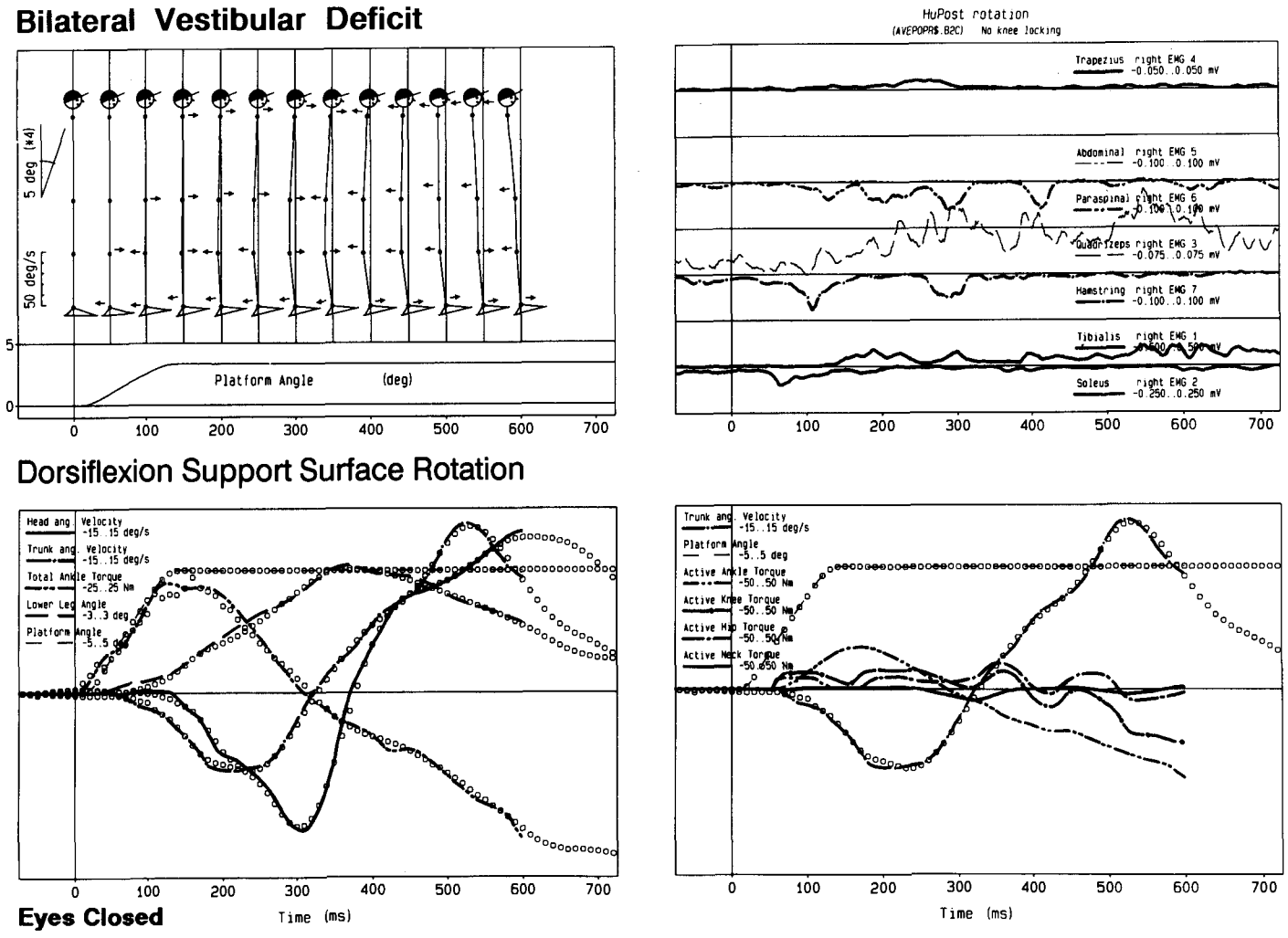

Fig. 7. Average response patterns to dorsiflexion rotation of the support surface of two subjects with absent vestibular function when tested under eyes-closed conditions. For details, see legend to Fig. 1. Note the rearward falling of the stick figure.

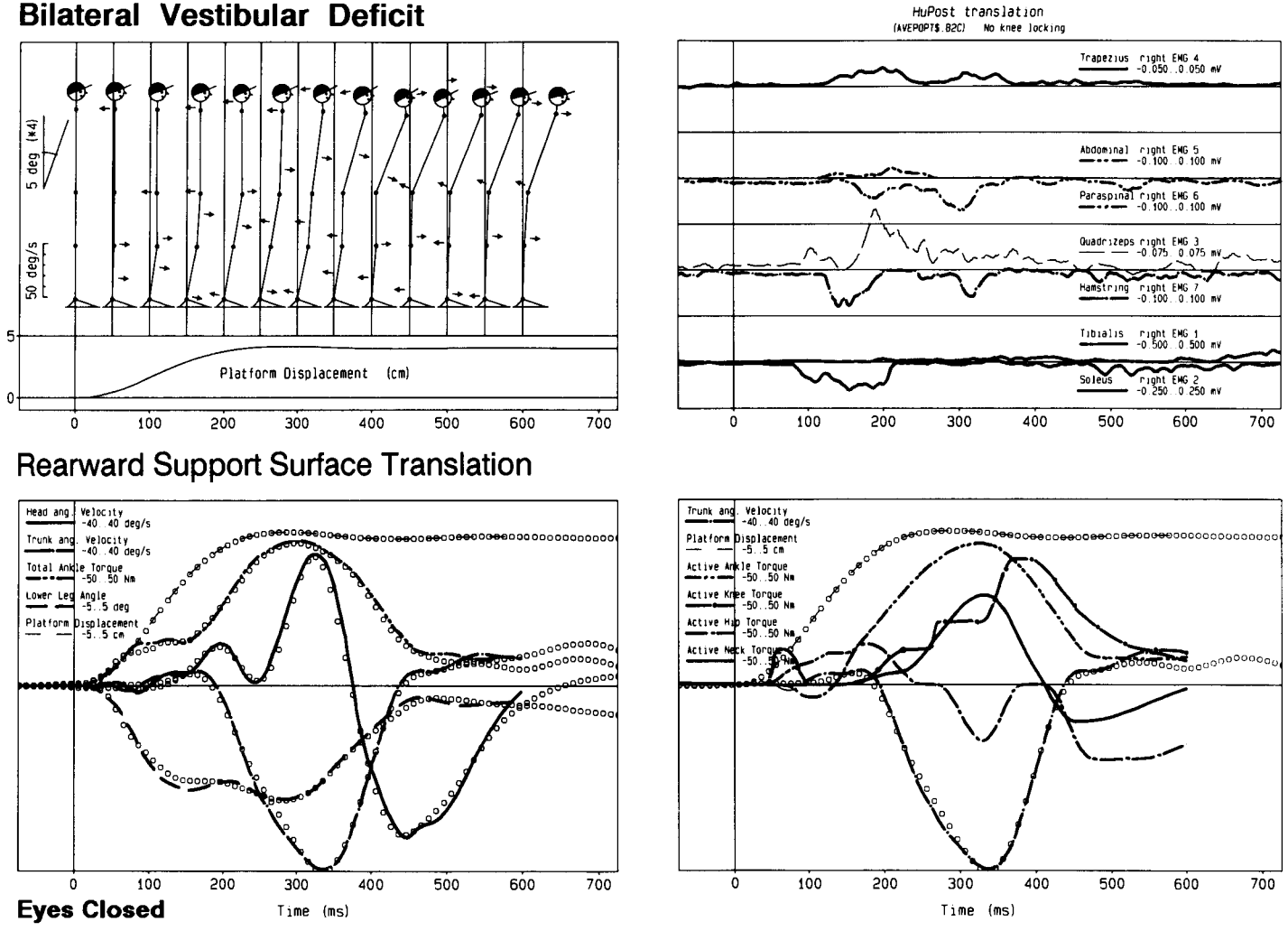

Fig. 8. Average response patterns of two subjects with absent vestibular function to rearward translation of the support surface when tested under eyes-closed conditions. For details, see legend to Fig. 1. Note the increased forward pitching of the trunk at 600 msec and reaward pitching of the head at 350 msec in comparison to normal.

rotates the toes upward, subjects with absent vestibular function cannot bring their stance back to vertical by bending forwards at the hips and activating their TA muscles to rotate the body forward about the ankle joints. In fact, these subjects fall over if they are unsupported. The movement strategy for ROT, which is depicted by active torque cross-correlations in Fig. 9, is very different from the normal response obtained with eyes closed except for ankle-knee correlations. Eyes-open torque cross-correlations are similar to those obtained from subjects with normal balance.

For rearward translation all hip torque cross-correlations are significantly different for patients with vestibular deficits. A cursory inspection of the stick figures in Figs. 2 and 8 would suggest that patients with vestibular loss, even with eyes closed, react normally to a rearward translation by flexing the trunk about the hips and thrusting the hips backwards, as Horak et al. (1990) have suggested. More careful inspection of the computed hip torque traces in Figs. 2 and 8 indicates that it is stabilising hip extension component of the multi-link strategy at 270 msec that is lacking for eyes-closed patient responses. The extended pulse of trunk forward pitching, with respect to the normal response, which peaks at 350 msec for the patients appears to be primarily the result of passive biomechanics. In normal subject, a two-pulse profile of hip extension torque is influencing trunk angular velocity by this time and has the effect of significantly reducing the duration of hip forward flexing angular velocity. Corresponding to this longer duration of hip flexion, hip torques have negative mean levels. Normal mean values of hip torque are approximately zero. Furthermore, hip correlation coefficients, with respect to the knee and ankle torques, are larger in the negative direction than are those of normal subjects indicating that hip torques act in the opposite direction to those of ankle and knee in the patients. These results thus indicate that a deficient hip movement for TRANS involves a lack of righting torque and the end result is that the patient's hip flexes too far forward, as illustrated by the stick figure in Fig. 8. The insufficient hip torques generated by patients with vestibular loss such as hip flexing torque for toe-up rotation and hip extending torque for rearward translation emphasize that the deficient vestibular stimulation causes a major change in the hip torques for ROT and TRANS. Not all joint torque strategies appear to be affected by a vestibular deficit. Those unaffected may well indicate a significant role for proprioceptive inputs in the generation of torque strategies. For example, the correlation between ankle- and knee-joint torques is unaltered following a vestibular loss.

Surprisingly, the neck to ankle torque correlations are influenced differently following a vestibular loss. For ROT, the neck torque is reduced and with it the correlation to ankle torque is drastically changed under eyes-open conditions. The head follows the trunk movement as a passive mass-viscoelastic system. Whereas, for TRANS the ankle-head correlation is unaltered, even with eyes closed. Neck torques, however, are larger than normal and lead to overcompensatory head movements (compare head velocity traces in Figs. 2 and 8). Whether or not this result indicated that an ankle-neck strategy can emerge following vestibular loss, if head movements on the trunk (and thus excitation of collic-vestibulo reflexes) are large enough, remains to be investigated. However this aspect of the multi-link strategy is generated, it still leads to an abnormal head stabilizing reaction.

Discussion

Trunk stability is fundamental to the goal of unassisted gait and stance restoration for paraplegic individuals. Failure to reposition the trunk so that it is either vertical or compensates for the displacement of the body's centre of gravity caused by an inclined support surface will cause either a fall or a stumbling reaction. One way in which trunk movements could be coordinated with those of the lower leg would be to employ trunk muscle activity to generate the appropriate artificial leg muscle stimulation (Graupe, 1989). An alternative approach would be to generate appropriate joint torques with an exoskeletal device once instability had been

Bilateral Vestibular Deficit

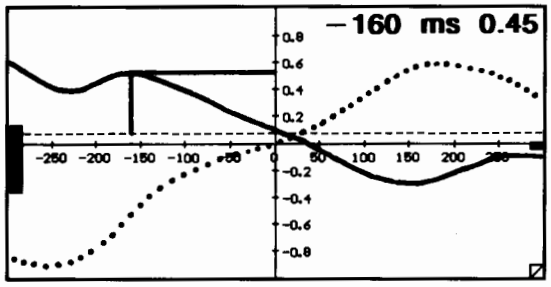

Ankle vs Neck Torque

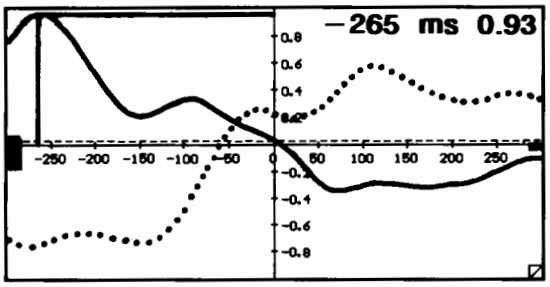

Knee vs Neck Torque

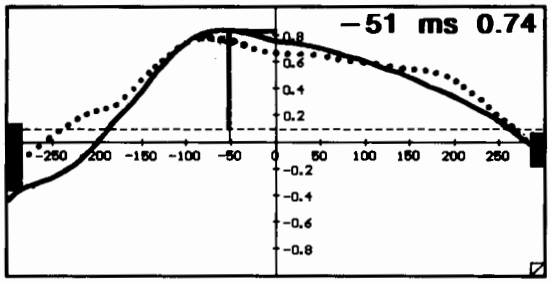

Ankle vs Knee Torque

Dorsiflexion Rotation

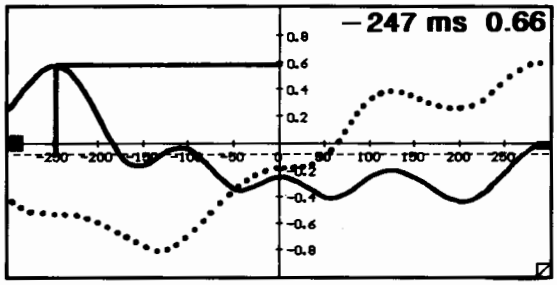

Hip vs Neck Torque

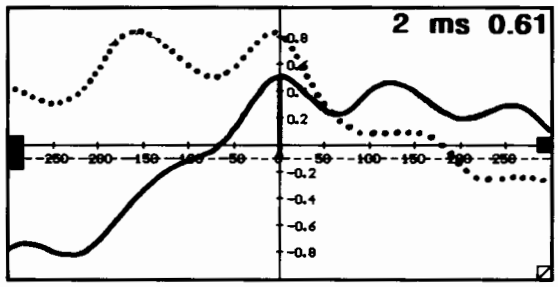

Knee vs Hip Torque

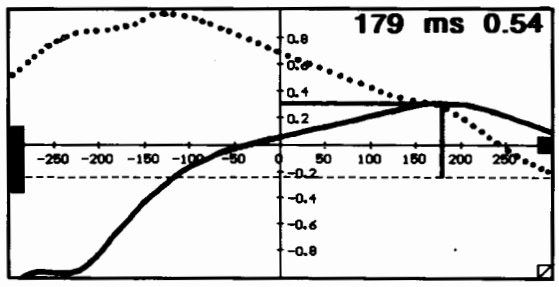

Ankle vs Hip Torque

Fig. 9. Average movement strategies for two subjects with absent vestibular function for dorsiflexion of the support surface. The cross-correlations were computed using the joint torques illustrated in the lower right panel of Fig. 7. For further details, see the legend to Fig. 3. Note the major differences between correlations for the eyes-closed condition (full lines), those for eyes open (dotted lines), and for subjects with normal responses (Fig. 3).

Bilateral Vestibular Deficit

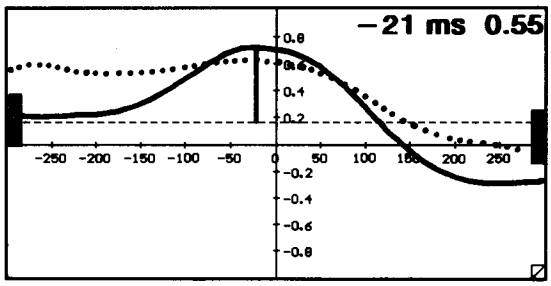

Ankle vs Neck Torque

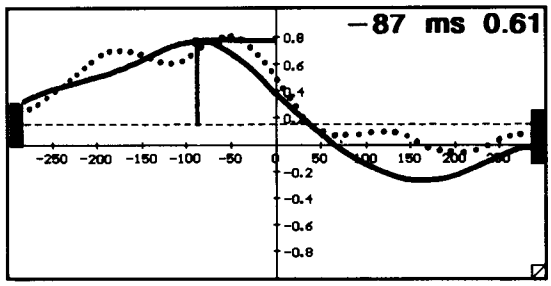

Knee vs Neck Torque

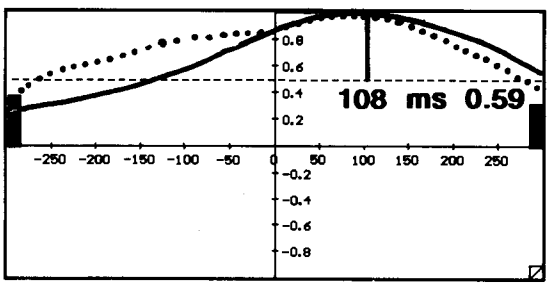

Ankle vs. Knee Torque

Rearward Translation

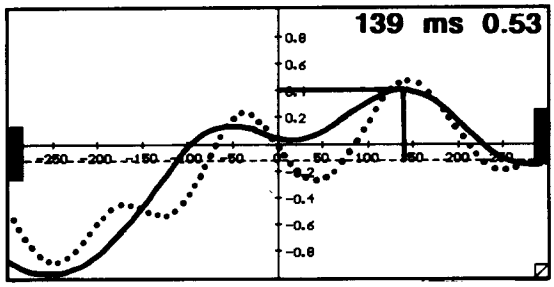

Hip vs Neck Torque

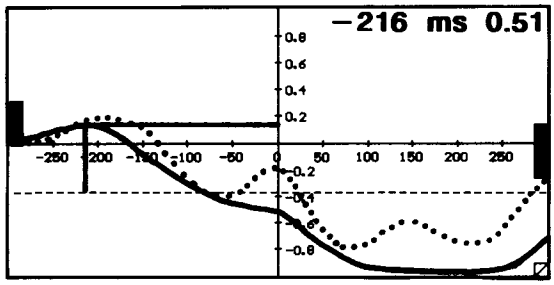

Knee vs Hip Torque

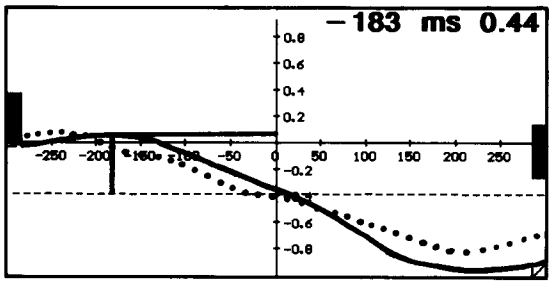

Ankle vs Hip Torque

Fig. 10. Average movement strategies for two subjects with absent vestibular function for rearward translation of the support surface. The cross-correlations were computed using the joint torques depicted in Fig. 8. Further details are given in the legend to Fig. 3. Note the changes in hip-joint-torque cross-correlations with respect to those from subjects with normal balance (Fig. 4).

sensed (Popovic et al., 1989). Yet a third approach could be a combination of the two with trunk muscle activity being employed to generate joint torques. No matter which technique should ultimately be chosen, two major questions must be resolved. First, the position of imbalance sensing transducers and the appropriate algorithm to sense instability must be addressed, and second, the intricate dynamic interrelations between limb segments must be taken into account. Our results comparing normal responses with those of patients with vestibular deficits demonstrate the importance of signals from head-based angular and linear acceleration transducers in generating appropriate muscle synergies and torque strategies. In addition, the major differences in synergies and strategies elicited by disturbances that produce an equal effect on ankle stretch but dissimilar head movements raises the question of how efficiently ankle proprioceptive inputs could generate appropriate balance corrections. The insights into intricate dynamic interreactions between limb segments provided by this study of normal balance control are applicable to functional electrical stimulation (FES).

Two types of balance corrections have been described, each of which is considered appropriate to the change imposed by the postural disturbance. When the support surface is rapidly inclined toes up, torques at the ankle, knee and hip joints rotate the body forward. Conversely, when the surface translates rapidly backwards, the joint torques act in the opposite direction. These two types of responses can be viewed either as opposite poles of a continuum of responses or, as Horak and Nashner (1986) have suggested, two of a limited set of movement strategies. Regardless of the continuous or discrete nature of these righting strategies, only the underlying torque strategy is crucial to FES once the amplitude and polarity of hip torque has been established. Ankle-hip and ankle-knee torque correlations are similar for the two types of disturbance (ROT and TRANS). To determine whether or not the differences in knee-hip torque correlations are important, or whether a common knee-hip correlation could be employed requires practical application to answer.

How then would the amplitude and polarity of hip torque be appropriately generated? Assuming, as we have shown, that the hip torques are highly dependent on vestibular inputs, then the natural destabilising effect of the postural disturbance at the head would lead to a characteristic pattern of trunk muscle activity. For translation, ABDOM responses always lead those of PARAS by 48 msec and for rotation, PARAS lead ABDOMS by 75 msec, if ABDOMS respond at all. Again, how these patterns change under natural circumstances where a mixture of rotation and translation is present is not known. The important considerations are that the trunk muscles lead the response synergies acting as early as SOL for translation and some 30 msec ahead of TA for rotation and that the trunk muscle synergy shows the greatest change between the two types of support surface perturbations when compared to all other muscle cross-correlations. Thus of all synergies, those of trunk muscles seem most suitable for the artificial generation of the correct amplitude and polarity of hip torque, and via hip-knee and hip-ankle torque correlations, those of the knee and ankle.

In proposing this schema for FES torque generation, we are assuming that head stabilization strategies are not altered during stance and gait perturbations in paraplegic individuals such that vestibular signals generating trunk muscle activity are subsequently altered from normal. Head movement strategies in normal individuals always involve a reduction of head movements with respect to earth-fixed coordinates. This may be compared to the movement pattern that occurs when neck torques are absent or are affected by vestibular loss, particularly as shown in Fig. 2. When the trunk of normal subjects moves rapidly, peak head velocities coincide with zero crossings of trunk angular velocities. Such an interaction requires a highly tuned modulation of cervico-collic and vestibulo-collic reflexes as the unstable head velocity profiles in the patients with vestibular loss clearly elucidate. If a lower spinal cord lesion influences cervico-collic reflexes, then changes in head stabilization strategies in paraplegic patients can be expected.

Normal interactions between neck-, hip-, knee- and ankle-joint torques and their underlying muscle synergies are part of an intricate system striving to maintain upright stance. If these normal EMG patterns are to be used to generate FES balance control, then multi-link (TRANS) and hip-ankle (ROT) interactions must be carefully explored for a number of different types of balance perturbation to establish the full range of strategies and synergies prior to clinical use.

Acknowledgements

This work was supported by Grant 3.126.088 from the Swiss National Science Foundation. We thank Mrs. W. Brunetti for typographic assistance.

References

Allum, J.H.J. and Mauritz, K.H. (1984) Compensation for intrinsic muscle stiffness by short latency reflexes in human triceps surae muscles. *J. Neurophysiol.*, 52: 797 – 818.

Allum, J.H.J. and Pfaltz, C.R. (1985) Visual and vestibular contributions to pitch sway stabilization in the ankle muscles of normals and patients with bilateral peripheral deficits. *Exp. Brain Res.*, 58: 82 – 94.

Allum, J.H.J., Honegger, F. and Pfaltz, C.R. (1989) The role of stretch and vestibulo-spinal reflexes in the generation of human equilibriating reactions. In: J.H.J. Allum and M. Hulliger (Eds.). *Afferent Control of Posture and Locomotion – Progress in Brain Research, Vol. 80,* Elsevier, Amsterdam, pp. 399 – 409.

Berthoz, A. and Pozzo, T. (1988) Intermittent head stabilization during postural and locomotory tasks in humans. In: B. Amblard, A. Berthoz and F. Clarac (Eds.), *Development, Adaptation and Modulation of Posture and Gait,* Elsevier, Amsterdam, pp. 189 – 198.

Dempster, W.T. (1955) Space requirements of the seated operator. WADC Tech. Rept. 55 – 159, AD No 87892 Wright Patterson Air Force Base, Ohio.

Diener, H.C., Horak, F.B. and Nashner, L.M. (1988) Influence of stimulus parameters on human postural responses. *J. Neurophysiol.*, 59: 1888 – 1905.

Graupe, D. (1989) EMG pattern analysis for patient-responsive control of FES in paraplegics for walker-supported walking. *IEEE Trans. BME,* 36: 711 – 719.

Horak, F.B. and Nashner, L.M. (1986) Central programming of postural movements: adaptation to altered support surface configurations. *J. Neurophysiol.*, 55: 1369 – 1381.

Horak, F.B., Nashner, L.M. and Diener, H.C. (1990) Postural strategies associated with somatosensory and vestibular loss. *Exp. Brain Res., 82:* 167 – 177.

Keshner, E.A., Allum, J.H.J. and Pfaltz, C.R. (1987) Postural coactivation and adaptation in the sway stabilizing responses of normals and patients with bilateral peripheral vestibular deficit. *Exp. Brain Res.*, 69: 66 – 72.

Keshner, E.A., Woollacott, M.H. and Debu, B. (1988) Neck and trunk responses during postural perturbations in humans. *Exp. Brain Res.*, 71: 455 – 466.

Macpherson, J.M., Rushmer, D.S. and Dunbar, D.C. (1986) Postural responses in the cat to unexpected rotation of the support surface: evidence for a centrally generated synergic organization. *Exp. Brain Res.*, 62: 152 – 160.

Popovic, D., Tomovic, R. and Schwirtlich, L. (1989) Hybrid assistive system - the motor neuroprosthesis. *IEEE Trans. BME,* 36: 729 – 737.

Sinkjaer, T., Toft, E., Andeassen, S. and Hornemann, B.C. (1988) Muscle stiffness in human ankle dorsiflexors: intrinsic and reflex components. *J. Neurophysiol.*, 60: 1110 – 1121.

J.H.J. Allum, D.J. Allum-Mecklenburg, F.P. Harris and R. Probst
Progress in Brain Research, Vol. 97

CHAPTER 31

Human standing posture: multi-joint movement strategies based on biomechanical constraints

Arthur D. Kuo and Felix E. Zajac

Mechanical Engineering Department, Stanford University, Stanford, CA 94305, U.S.A. and Rehabilitation R and D Center (153), Veterans Affairs Medical Center, Palo Alto, CA 94304, U.S.A.

We developed a theoretical framework for studying coordination strategies in standing posture. The framework consists of a musculoskeletal model of the human lower extremity in the sagittal plane and a technique to visualize, geometrically, how constraints internal and external to the body affect movement. The set of all feasible accelerations (i.e., the "feasible acceleration set" or FAS) that muscles can induce at positions near upright were calculated. We found that musculoskeletal mechanics dictate that independent control of joints is relatively difficult to achieve. When muscle activations are constrained so the knees stay straight, to approximate the typical postural response to perturbation, the corresponding subset of the feasible acceleration set greatly favors a combination of ankle and hip movement in the ratio 1 : 3 (called the "hip strategy"). Independent control of these two joints remains difficult to achieve. When near the boundary of instability, the orientation and shape of this subset show that the movement strategy necessary to maintain stability, without taking a step, is quite restricted. Hypothesizing that regulation of center-of-mass position is crucial to maintaining balance, we examined the feasible set of center-of-mass accelerations. When the knees must be kept straight, the acceleration of the center of mass is severely limited vertically, but not horizontally. We also found that the "ankle strategy", involving rotation about the ankles only, requires more muscle activation than the "hip strategy" for a given amount of horizontal acceleration. Our model therefore predicts that the hip strategy is most effective at controlling the center of mass with minimal muscle activation ("neural effort").

Key words: Standing; Posture; Coordination strategies; Dynamics; Motor control

Introduction

Considerable success has been achieved in devising and performing experiments to study sensorimotor control of standing posture. One reason is that motor control output variables (e.g., body segment kinematics, ground reaction force and EMG signals) can be measured with precision. Perhaps more importantly, ingenious methods to manipulate the inputs to this sensorimotor system have been devised and implemented. For example, the surface on which subjects stand can be moved (Nashner, 1976, 1977), and vision can be blocked, using blindfolds, or altered by dynamically moving the visual surround (Nashner et al., 1982; Black et al., 1988). Additional insight into sensorimotor control has been achieved by observing how patients with neurological disorders (e.g., vestibular loss, or dysfunction) react to these controlled disturbances (Allum and Pfaltz, 1985; Allum et al., 1988; Horak et al., 1990).

However, theoretical constructs to analyze experimentally based hypotheses are few, even though theories seem to offer much potential (Nashner and McCollum, 1985; Nashner et al., 1989; Gordon, 1990). The complexity of the biomechanics of the system being controlled is probably what has stymied theoretical investigations. For example, movement about a single joint is complex enough to analyze (Gottlieb et al., 1990), much less the combined properties of many muscles acting in concert

on a multi-segment body (Zajac and Gordon, 1989). Nevertheless, we feel that theoretical studies of posture are a useful adjunct to experimental studies, and perhaps essential to understanding postural control of this complex biomechanical system.

Many experiments in posture have relied on rotating or translating support surfaces to produce perturbations. Researchers have reported consistent strategies in response to such perturbations, and termed these responses "ankle" and "hip strategies" (Nashner and McCollum, 1985; Horak and Nashner, 1986) referring to the joint about which most of the movement occurred. They reported that responses to small disturbances typically entailed the ankle strategy, with a combination of ankle and hip strategies being chosen for shortened support surfaces or faster disturbances (Diener et al., 1988).

Nashner and McCollum (1985) also established a theoretical basis for analyzing posture through examination of the equations of motion for a three-segment model of the human body in the sagittal plane. They established a coordinate system for the body position space using ankle, hip and vertical axes. Since postural movements occur about the ankle and hip (Nashner, 1977), the vertical axis can be disregarded. In the ankle-hip plane, they sketched vectors corresponding to the accelerations produced by respective activation of ankle, thigh and trunk muscles. They suggested that movement strategies are chosen so as to minimize the number of muscles activated, and predicted corresponding acceleration trajectories.

Nashner et al. (1989) explored the constraints imposed by mechanics and sensory thresholds, delineating frequencies and amplitudes for which movements can be detected by sensors (and therefore controlled) and for which the body is capable of producing driving torques. This work was instrumental in delineating the frequencies and amplitude ranges within which postural movements may occur.

While research to date has been successful in quantifying postural behavior, little work has been done to illustrate what causes this behavior to be produced. We believe that postural movement is shaped by the organization of the mechanical characteristics of the human body, as well as the nervous system which controls it. To this end, an analysis of the biomechanics of standing posture will help us understand control strategies underlying postural behavior.

The biomechanics of the musculoskeletal system are complex. Zajac and Gordon (1989) showed that muscle's contribution to acceleration depends not only on the dynamics of the body segments, but also on other characteristics, including the maximum achievable isometric force, moment arm and the length of muscle fibers. Gordon (1990) explored the vectorial contribution of muscles to the acceleration of joints, and proposed computing the bounds on acceleration as a means to visualize and study synergies and constraints on motion.

In this paper, we assemble a musculoskeletal model for the computation of these bounds on acceleration, which we term the "feasible acceleration set" (FAS), and examine the mechanics of the ankle and hip strategies in relation to various constraints. We also explore the hypothesis that acceleration of the body center of mass while minimizing net muscle activation is a central objective in maintaining posture. In so doing, we provide partial explanation of control strategies to counteract perturbations to the upright position.

Analysis

Musculoskeletal model

The model of the lower extremity incorporates the dynamics of both the body and musculotendon actuators (muscle in series with tendon). The body, modeled as a four-segment linkage comprised of the foot, shank, thigh and head-arms-trunk (referred to as the "trunk" hereafter), was assumed to move in the sagittal plane only (Fig. 1). The segment lengths and inertial parameters were prescribed for an "average" adult male (Pandy et al., 1990). The ankle, knee and hip joints were modeled as simple hinge-joints in the sagittal plane. However, a more complex kinematic model was used to characterize the moment arms about the knee (Delp et al., 1990). The path of each musculotendon actuator was de-

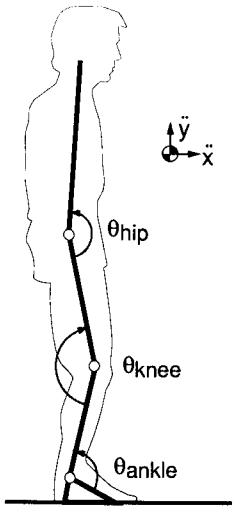

Fig. 1. Four-segment sagittal plane model of the human body. In joint coordinates, angles are defined to be positive in extension, with zero degrees corresponding to the full upright anatomical position. Center of mass movements in x and y directions are defined to be positive in the anterior and upward directions, respectively.

fined by a series of straight lines going through points of origin, insertion, and, if necessary, via points (Hoy, 1990; Delp et al., 1990). This geometric model facilitated the computation of the fiber length of each muscle and its moment arm(s) about the joint(s).

To model each musculotendon actuator, we scaled a generic Hill-type model with four actuator-specific parameters: pennation angle, tendon slack length, peak isometric active force, and optimal muscle-fiber length (Zajac, 1989). Especially pertinent to this study, these parameters determine the maximum force for any given, quasi-static configuration. We grouped 33 lower-extremity musculotendon actuators into 14 muscle groups based on anatomical position (e.g., ankle dorsiflexors, hamstrings, vasti). In summary, the musculotendon model was used to compute the force-generating capabilities of each muscle, the musculoskeletal geometry to compute the moments of the muscle forces about the joints, and the linkage system dynamics to compute the acceleration of the body segments.

We are confident that this type of model is adequate for simulating human movement. A similar musculoskeletal model incorporating additional velocity-dependent terms has been used to produce simulated jumps that reproduce the salient kinetic, kinematic and muscle coordination features observed in humans jumping to their maximum achievable heights (Pandy et al., 1990; Pandy and Zajac, 1991).

Specific to this study of standing posture, we assumed the motion to be quasi-static, i.e., the velocity terms in the dynamical equations, as well as muscle fiber velocities, to be small. In addition, muscle activation dynamics were assumed to be fast (instantaneous) in relation to the movement. Our analysis concerns only selection of acceleration vectors (the set of joint angular accelerations describing movement) at a given instant in time, and neglects muscle activation sequencing. For simplicity, the muscles within each of the 14 muscle groups were assumed to share common activation commands from the nervous system. We also restricted study to configurations in which the feet are flat on the ground, limiting our study to postural movement without taking a step. This constraint reduces the number of degrees of freedom in the model to three.

The feasible acceleration set

The equations of motion determining the joint angular acceleration vector $\ddot{\theta}$ (for ankle, knee, and hip joint angular accelerations) can be written as:

$$\ddot{\theta} = M^{-1}(R \cdot F_0 \cdot F_\ell \cdot a + G) \qquad (1)$$

where a is the vector of normalized muscular activation levels, neglecting whether activation is achieved by frequency modulation or recruitment (Stein, 1974); M is the mass matrix relating torques to angular accelerations; R is the moment arm matrix; G is the vector containing gravity terms; and F_ℓ and F_0 are diagonal matrices characterizing muscle's force-length and peak isometric force characteristics, respectively (Zajac, 1989).

Normalized activation level for each muscle i is confined by the inequality $0 \leq a_i \leq 1$, thus con-

fining feasible activations to an m-cube (for $m = 14$ muscle groups). Eqn. 1 is used to compute the corresponding set of inequalities on the joint angular accelerations $\ddot{\theta}$, transforming the m-cube into a polyhedron in the three-dimensional space defined by ankle, knee and hip axes (Gordon, 1990). The surface of this polyhedron is the outer bound on all possible accelerations, and we denote its entire volume as the theoretically feasible acceleration set (FAS). The FAS represents all possible body accelerations for a given quasi-static configuration.

A FAS can be analyzed to assess "ease in movement" in a specific direction subject to the constraints applicable to that particular FAS. Because any desired acceleration vector from the origin can be viewed in relation to an acceleration vector that is in the same direction but extended to intersect the FAS boundary, the desired acceleration vector can be expressed as a percentage of the maximum feasible acceleration in that direction. If this percentage is low, then this acceleration intensity can be achieved with little muscle activation or "neural effort", so that the "ease of movement" is high.

Equivalently, if maximal neural effort (muscle activation) produces accelerations reaching the boundary of the feasible acceleration set (the surface of the polyhedron), then correspondingly smaller efforts can be used to produce accelerations reaching the boundary of a scaled-down feasible acceleration set. In this sense, accelerating at a specified magnitude in directions for which the FAS boundary is a large distance from the origin requires less muscle activation (less neural effort) than that to accelerate at the same intensity in other directions. Note that the nervous system need not employ such a scaling method for choosing muscle activations; it may in fact choose other patterns for achieving any submaximal acceleration. However, experimental evidence (Diener et al., 1988) has shown that postural responses, including muscle activation, do tend to scale with platform stimulus parameters.

Because activation level is normalized with respect to a muscle's peak isometric force, which in turn is computed from the physiological cross-section area (Pandy et al., 1990), the index of neural effort is equivalent to an index of muscle stress (force divided by cross-section area).

We devised a method for computing and displaying the acceleration bounds describing the FAS polyhedron in ankle-knee-hip acceleration space (the ankle-knee-hip FAS). Mathematically, this involves finding the convex hull of the affine transformation of an m-cube for the m muscle groups. Additional biomechanical constraints are accounted for by displaying the FAS with respect to corresponding half-spaces (described by planes) defined by these constraints. The intersection of these half-spaces shows how these constraints interact to restrict the repertoire of possible movements.

In their analysis, Nashner and McCollum (1985) emphasized that responses to postural disturbances involve ankle and hip, but little knee rotation. The consequence of avoiding knee rotation is to limit the ankle-knee-hip FAS to that region which intersects the plane defined by zero angular acceleration of the knee. This intersection, called the ankle-hip FAS, is bounded by a polygon, because the constraint reduces the three-degree-of-freedom FAS to two degrees-of-freedom. Note that this constraint acts on the controls, limiting the ankle-knee-hip FAS to those combinations of muscles that would keep the knee straight ($\ddot{\theta}_{\text{knee}} = 0$), as opposed to a constraint on the positions, which would be analogous to an external brace on the knee and would require different equations of motion.

We also studied how the constraint of keeping the feet flat on the ground restricts the ankle-hip FAS. This "flat-foot constraint" is actually defined by two constraints, corresponding to accelerations that cause lifting of the heels and of the toes off the ground, respectively. Thus, the feasible accelerations satisfying these two constraints are a subset of the ankle-hip FAS, and are designated the flat-footed ankle-hip FAS.

We also determined the effect of body segment orientation on the ankle-hip FAS. The matrices M, R and F_ρ, as well as the vector G of Eqn. 1, are dependent on body position. Thus, the FAS must also depend on body configuration. This dependence

may dictate different coordination strategies in response to perturbation at different body positions.

Because horizontal center-of-mass position is the final determinant of stable balance and because long-duration upright standing posture seems to demand little effort, we hypothesized that one of the objectives of standing posture is to control the center-of-mass horizontally with minimal neural effort (i.e., muscle activation). Accelerations of the ankle, knee and hip define corresponding accelerations of the center of mass horizontally and vertically. Thus, feasible ankle-knee-hip accelerations define corresponding feasible accelerations of the center-of-mass (i.e., center-of-mass ankle-knee-hip FAS). To examine the hypothesis stated above, we calculated the center-of-mass ankle-knee-hip FAS and the center-of-mass ankle-hip FAS (i.e., knees kept straight). The toe- and heel-off constraints from ankle-hip space were likewise transplanted to the space of vertical and horizontal center-of-mass accelerations.

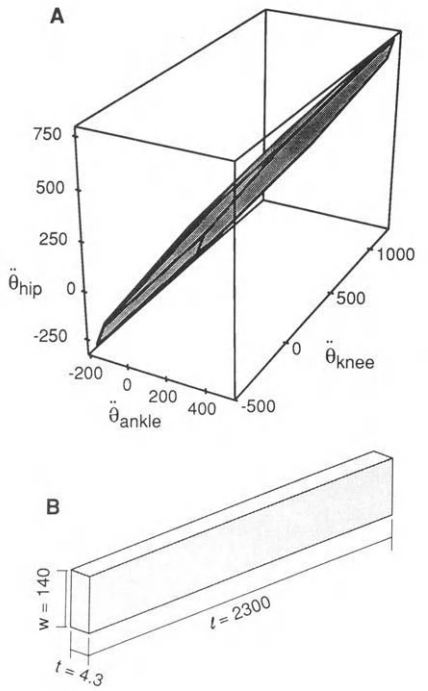

Fig. 2. *A*. Ankle-knee-hip feasible acceleration set (FAS) polyhedron for standing posture in the sagittal plane in a near-upright position. The surface and interior of the ankle-knee-hip FAS define all possible body accelerations from a quasi-static near-upright posture. The surface of the polyhedron represents the maximal achievable accelerations. The solid lines indicate the boundaries of the faces of the polyhedron. *B*. Schematic representation of the ankle-knee-hip FAS, indicating approximate length, width and thickness. Units for *A* and *B* are rad/s^2.

Results

We computed the ankle-knee-hip FAS for a near-upright standing position, with the knees unlocked, and displayed it as a polyhedron with solid lines separating its faces (Fig. 2*A*). The polyhedron is approximately 16 times longer than it is wide, and 33 times wider than it is thick. Its long axis corresponds to a combination of simultaneous ankle, knee and hip angular acceleration in the ratio of 1 : 2.3 : 1.5, with magnitudes of approximately 1500 rad/s^2 in extension and 830 rad/s^2 in flexion. Its width axis corresponds to a combination of simultaneous ankle, knee and hip acceleration in the ratio 1.6 : 1 : −2.7, with magnitudes of approximately 63 rad/s^2 in extension and 75 rad/s^2 in flexion (note that the hip component of the ratio is negative, indicating that when the other joints are accelerating into extension, the hip is accelerating into flexion, and vice versa). Finally, the axis pointing in the thickness direction of the polyhedron corresponds to a combination of simultaneous ankle, knee and hip acceleration in the ratio 2.8 : −1.9 : 1, with magnitudes of approximately 2.2 rad/s^2 in extension, and 2.1 rad/s^2 in flexion.

To examine the effect of keeping the knees straight on the ankle-knee-hip FAS, the polyhedron is intersected with a plane defined by $\ddot{\theta}_{knee} = 0$. This intersection is the set of all achievable accelerations when muscle activations are constrained so as to produce no motion about the knee. This ankle-hip FAS, for the same near-upright posture as in Fig. 2, is a polygon (Fig. 3) and is a single slice of the original volume of the ankle-knee-hip FAS. It also indicates the general shape of the cross-section of the polyhedron in Fig. 2, as the $\ddot{\theta}_{knee} = 0$ plane also cuts through the ankle-knee-hip FAS, though at an

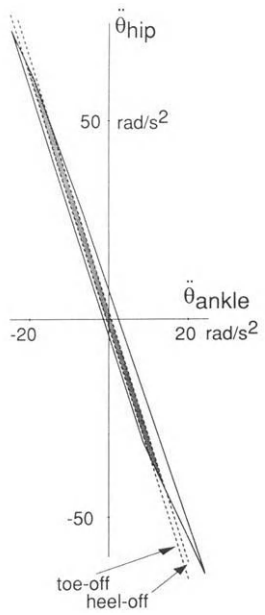

Fig. 3. Ankle-hip FAS for near-upright posture, specifying set of achievable accelerations while keeping the knees straight. This FAS appears in the ankle-hip plane because knee angular acceleration is zero (i.e., the knees are constrained to be straight). Boundaries beyond which the toes or heels lift off the ground are shown as dashed lines. The shaded region (flat-footed ankle-hip FAS) shows the feasible accelerations such that the feet are kept flat on the ground while the knees are kept straight. Accelerations outside this region, but interior to the ankle-hip FAS polygon, are possible but cause either the toes or the heels to lift off the ground. Note that the ankle acceleration scale is expanded.

angle of approximately 52°. The long axis of the polygon corresponds to simultaneous ankle and hip acceleration in the ratio $1 : -3.2$ with magnitudes of approximately 72 rad/s^2 in flexion and 62 rad/s^2 in extension. The constraint for keeping the feet flat on the ground is manifested by two lines, as indicated, beyond which either the toes or the heels lift off the ground. Thus, the region inside both the ankle-hip FAS and within these constraints represents potential acceleration vectors which keep the feet flat on the ground. This flat-footed ankle-hip FAS corresponds to simultaneous ankle and hip acceleration in the ratio $1 : -3.2$, with magnitudes of approximately 67 rad/s^2 in flexion and 43 rad/s^2 in extension.

A change in body position affects the FAS because segmental configuration, segmental orientation with respect to gravity, musculotendon lengths, and moment arms, all of which interact to define the FAS (see Eqn. 1), depend on body position. We found, however, that the ankle-hip FASs are similar in shape and orientation for positions near upright standing (Fig. 4 shows ankle-hip FASs for 12 separate positions. The position boundaries within which the body can maintain stable balance, with the center-of-mass located above the foot between the toes and heels, is shown by the dashed lines).

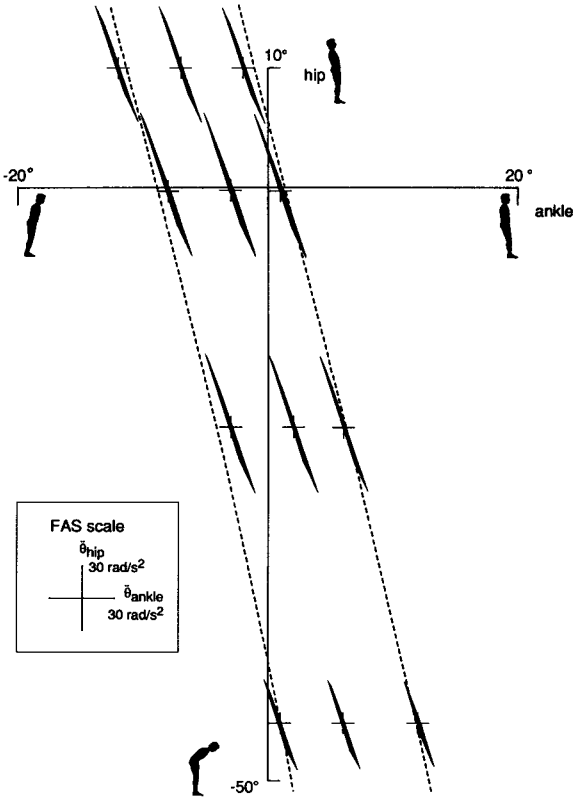

Fig. 4. Ankle-hip FAS plotted for 12 separate body positions (origin indicating body position for each FAS plot is shown by crosshairs). Body position is indicated by ankle angle and hip angle (as defined in Fig. 1). Dashed lines indicate position boundaries beyond which stable balance cannot be achieved. Left line is boundary for falling forward, right line for falling backward. Note that the FASs are similar in size and orientation throughout the body position space. Inset shows scale of axes for FAS plots.

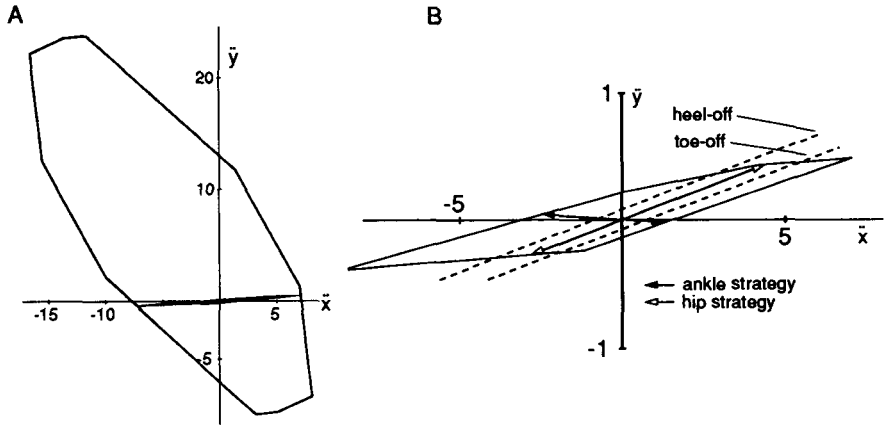

Fig. 5. *A*. Center of mass feasible acceleration set for near-upright position. Darkened region is ankle-hip center of mass FAS (achievable accelerations of center of mass, keeping knees straight). Axes in positive x and y directions denote acceleration forward and upward of the center of mass, respectively (see Fig. 1). *B*. Close-up of darkened region in *A*. Dotted lines show toe-off and heel-off constraints for keeping the foot flat on the ground. Vectors with black arrowheads show effect of ankle strategy. Vectors with white arrowheads indicate effect of possible hip strategy (see Discussion). Note that hip strategy accelerates center of mass in a direction compatible with keeping the feet flat on the ground (i.e., vector is parallel to toe- and heel-off constraint lines). Note that vertical acceleration axis is expanded.

Therefore body position has a relatively small effect on the FAS and conclusions drawn for the near-upright stance studied above can be generalized to the range of typical postural body positions.

When the body is leaning forward (left-most boundary, Fig. 4), the heel- and toe-off constraint lines (as seen in Fig. 3, but not shown in the FAS plots of Fig. 4) both shift to the left. Similarly, when the body is leaning backwards, the constraint lines move to the right. Thus, the feasible accelerations that move the body toward upright posture (i.e., acceleration vectors pointing away from the boundary in Fig. 4), yet keep the feet flat on the ground, become quite restricted. In fact, if the body should be leaning as far forward or backwards as possible (i.e., the body lies on one of the boundaries, Fig. 4), use of a pure ankle strategy will violate one of the constraints, causing either the heels or toes to be lifted off the ground. We also found that the heel- and toe-off constraint lines both move in toward the origin as the support surface shortens (Horak and Nashner, 1986). In fact, with an extremely narrow surface, we predict that balance in the face of a disturbance cannot be maintained using a pure ankle strategy. Therefore, should the body be near the boundary of stable posture, or should the support surface be narrow, both the hips and ankles must accelerate with quite restrictive relative amounts (i.e., ankle to hip acceleration of about $1 : -3.2$).

The center-of-mass ankle-knee-hip FAS (i.e., the set of all feasible accelerations of the center-of-mass derived from moving the ankle, knee and hip) is defined by a two-dimensional polygon because the center-of-mass has only two degrees of freedom, horizontal and vertical, in the sagittal plane (Fig. 5*A*). The center-of-mass ankle-hip FAS (i.e., the center-of-mass FAS when the knees are kept straight) is a small subset of the entire center-of-mass FAS, and is greatly restricted in the vertical direction (darkened region, Fig. 5*A*).

Based on the definition of the ankle strategy as acceleration about the ankles only, and the hip strategy as a combination of ankle extension and hip flexion or vice versa, we constructed acceleration vectors corresponding to these strategies. We found that both ankle and hip strategies are effective at ac-

celerating the center-of-mass horizontally, but that the hip strategy requires less neural effort for a given magnitude of horizontal acceleration (Fig. 5*B*). The toe- and heel-off constraint lines (dashed lines in Fig. 5*B*) are nearly parallel to the long axis of the center-of-mass ankle-hip FAS.

Discussion

The shape of the ankle-knee-hip FAS indicates that certain combinations of joint accelerations require much less neural effort than others (Fig. 2), as indicated by the distance of the FAS boundary from the origin. At near-upright position, the body mass matrix is relatively close to rank 1, meaning that it is difficult to move the joints independently. However, certain combinations of simultaneous ankle, knee and hip acceleration in extension or flexion (see Results), corresponding to movement along the long axis of the polyhedron, require relatively little effort. Movement combinations in the direction of the width or thickness of the polyhedron require much more effort. Thus, the biomechanical relationships of the human body place severe constraints on the relative effectiveness of and neural effort associated with movement in different directions.

The ankle-hip FAS (Fig. 3) shows that keeping the knees straight greatly limits the set of achievable accelerations. It is important to note that keeping the knees fixed is not equivalent to keeping the knee muscles inactivated, as knee torque is still needed to maintain the constraint. Still, independent motion about the ankle and hip joints is constrained by biomechanics such that many acceleration vectors require a great deal of neural effort, or are limited in feasible magnitude. Combinations of ankle and hip extension in the approximate ratio $1 : -3.2$ are easily achievable. However, acceleration about the ankles only or the hip only is relatively more difficult to achieve.

Horak and Nashner (1986) defined the "ankle" and "hip" strategies based on a combination of electromyogram, force plate and kinematic patterns. Because our model does not provide electromyograms or horizontal shear forces, we define similar strategies based purely on observation of joint accelerations, for purposes of comparison. Our own ankle strategy is defined as acceleration about the ankle joint only, keeping the knee and hip fixed, and would correspond to movement along the ankle axis of Fig. 3. Our hip strategy corresponds to acceleration of the ankle and hip in opposite directions, with the hip accelerating about three times more than the ankle, approximately along the toe- and heel-off constraint lines shown for the ankle-hip FAS (Fig. 3). These definitions help to explain our findings in comparison with the work of Horak and Nashner (1986). Such a hip strategy is fairly well-suited to keeping the feet flat on the ground, while requiring less neural effort for a given amount of acceleration, due to the length of the ankle-hip FAS in this direction.

A disturbance tends to accelerate the body away from the upright position, requiring muscles to arrest the motion and bring the body back to erect stance. Faster disturbances require larger acceleration vectors, and because large ankle accelerations are likely to result in toe- or heel-off, the hip strategy is more effective at countering large disturbances and accelerating the center-of-mass toward a more stable position while maintaining the feet flat on the ground.

At the extremes of the stable flat-footed posture (positions near the boundaries shown in Fig. 4), employment of the ankle strategy (i.e., acceleration along the ankle axis toward upright posture) to restore the body to the upright position will easily violate the flat-feet constraint (see Results). The only recourse is to use the hip strategy to bring the body away from the boundaries before using the ankle strategy to restore the nominal position.

Similarly, shortened support surfaces will also require greater reliance on the hip strategy. The toe- and heel-off constraint lines both move closer to the origin with shorter support surfaces, further limiting the efficacy of the ankle strategy.

In our analysis of the center-of-mass FAS (Fig. 5*A*), we found that for motions in which the vertical acceleration of the center-of-mass is limited

($\ddot{y} \approx 0$), the ankle-hip FAS allows for nearly the entire range of horizontal acceleration of the center-of-mass. Thus, preventing knee motion has a more dramatic effect in limiting vertical rather than horizontal acceleration. Despite the limiting effect of the knee constraint on the set of achievable accelerations (see Results), its effect on accelerating the center-of-mass horizontally is negligible.

In accelerating the center-of-mass, the ankle strategy requires more neural effort than the hip strategy, which accelerates the body approximately along the toe- and heel-off constraint lines (Fig. 5*B*). Note also that in comparison to the ankle strategy, the hip strategy can accelerate the center-of-mass horizontally faster and still keep the feet flat on the ground.

A principle favoring acceleration of the center-of-mass while minimizing neural effort to select movement strategies would therefore predict predominant use of the so-called hip strategy, especially when the feet are to remain flat on the ground. Allum et al. (1989) have reported a multi-link strategy similar to our hip strategy in response to relatively fast perturbations. However, Horak and Nashner (1986) have shown that the preferred strategy involves rotation primarily about the ankles in response to relatively slower perturbations, although their experimentally observed ankle strategy may not exclude knee and hip motion entirely, as the theoretical ankle strategy does here. They have also reported use of a hip strategy (similar to the hip strategy defined here) in the case of shortened support surfaces. Since a shortened support surface brings the toe- and heel-off constraint lines closer to the origin (Fig. 3), we would expect greater reliance on the hip strategy.

There are a number of possible reasons for favoring the ankle strategy over the hip strategy in response to slower perturbations. For example, acceleration of the center-of-mass often tends to move the body away from the erect posture, so maintaining balance (i.e., controlling center-of-mass position) is sometimes contrary to the objective of maintaining upright stance. In addition, motion about the hips also causes relatively large movement of the head, and thus may affect vestibular sensors within the skull, which may have implications on sensory feedback to the nervous system.

We can unify the ankle and hip strategies into a single set of criteria for choosing the acceleration vector to restore upright posture, as follows. The speed and position of perturbation specify a minimum response acceleration to keep the body from exceeding the position constraints. The ankle strategy appears to be employed to the extent that the toe- and heel-off constraints allow (as determined by support surface length). If the corresponding center-of-mass acceleration cannot sufficiently counter the perturbation, further acceleration is achieved by moving along the constraint line using a combination of ankle and hip strategies. Mathematically, this can be expressed as a single optimization problem (Kuo and Zajac, 1991).

Our current analysis examines feasible accelerations as determined by body position, neglecting intersegmental velocities. In addition, we do not model the muscle force-velocity relationship (Zajac, 1989). Preliminary investigation has shown that such velocity effects are relatively small, but further work is necessary to quantify their actual contribution. Variations in musculoskeletal model parameters will also cause changes in the FAS. However, we have found the general shape and orientation of the FAS to be relatively insensitive to variations, thus justifying the qualitative results reported here.

Additional work will elucidate the effect of employing ankle and hip strategies on movement and rotation of the head. The effect these strategies have on the sensory input to vestibular sensors may have an impact on which strategies are preferred. Such work may also bring greater understanding to the mechanisms of head rotation during standing.

Finally, we hope that further analysis will provide insight into how to design simple, implantable controllers for stimulating paralyzed muscles to restore upright standing to paraplegics. If control laws can be mapped into the strategies, as defined here,

perhaps a fast feedback algorithm can be designed for multi-joint postural control of paraplegic standing.

Acknowledgements

This work was supported in part by a NSF Pre-Doctoral Fellowship to A.K., NIH Grant NS17662 to F.Z., and the Rehabilitation R and D Service, Department of Veterans Affairs.

References

Allum, J.H.J. and Pfaltz, C.R. (1985) Visual and vestibular contributions to pitch sway stabilization in the ankle muscles of normals and patients with bilateral peripheral deficits. *Exp. Brain Res.*, 58: 82 – 94.

Allum, J.H.J., Keshner, E.A., Honegger, F. and Pfaltz, C.R. (1988) Organization of leg-trunk-head equilibrium movements in normals and patients with peripheral vestibular deficits. In: O. Pompeiano and J.H.J. Allum (Eds.), *Vestibulospinal Control of Posture and Locomotion – Progress in Brain Research, Vol. 76,* Elsevier, Amsterdam, pp. 277 – 290.

Allum, J.H.J., Honegger, F. and Pfaltz, C.R. (1989) The role of stretch and vestibulo-spinal reflexes in the generation of human equilibriating reactions. In: J.H.J. Allum and M. Hulliger (Eds.), *Afferent Control of Posture and Locomotion – Progress in Brain Research, Vol. 80,* Elsevier, Amsterdam, pp. 399 – 409.

Black, F.O., Shupert, C.L., Horak, F.B. and Nashner, L.M. (1988) Abnormal postural control associated with peripheral vestibular disorders. In: O. Pompeiano and J.H.J. Allum (Eds.), *Vestibulospinal Control of Posture and Locomotion – Progress in Brain Research, Vol. 76,* Elsevier, Amsterdam, pp. 263 – 275.

Delp, S.L., Loan, J.P., Hoy, M.G., Zajac, F.E., Topp, E.L. and Rosen, J.M. (1990) An interactive, graphics-based model of the lower extremity to study orthopaedic surgical procedures. *IEEE Trans. Biomed. Eng.*, 37: 757 – 767.

Diener, H.C., Horak, F.B. and Nashner, L.M. (1988) Influence of stimulus parameters on human postural responses. *J. Neurophysiol.*, 59: 1888 – 1905.

Gordon, M.E. (1990) *An Analysis of the Biomechanics and Muscular Synergies of Human Standing,* Ph. D. Thesis, Stanford University, Stanford, CA.

Gottlieb, G.L., Corcos, D.M., Agarwal, G.C. and Latash, M.L. (1990) Principles underlying single-joint movement strategies. In: J.M. Winters and S.L.-Y. Woo (Eds.), *Multiple Muscle Systems,* Springer, New York, pp. 236 – 250.

Horak, F.B. and Nashner, L.M. (1986) Central programming of postural movements: adaptation to altered support-surface configurations. *J. Neurophysiol.*, 55: 1369 – 1381.

Horak, F.B., Nashner, L.M. and Diener, H.C. (1990) Postural strategies associated with somatosensory and vestibular loss. *Exp. Brain Res.*, 82: 167 – 177.

Hoy, M.G., Zajac, F.E. and Gordon, M.E. (1990) A musculoskeletal model of the human lower extremity: the effect of muscle, tendon, and moment arm on the moment-angle relationship of musculotendon actuators at the hip, knee, and ankle. *J. Biomech.*, 23: 157 – 169.

Kuo, A.D. and Zajac, F.E. (1991) Optimization of human standing posture: constraints and objectives. *15th Annual Meeting of the American Society of Biomechanics, Tempe, AZ.*

Nashner, L.M. (1976) Adapting reflexes controlling the human posture. *Exp. Brain Res.*, 26: 59 – 72.

Nashner, L.M. (1977) Fixed patterns of rapid postural responses among the leg muscles during stance. *Exp. Brain Res.*, 30: 13 – 24.

Nashner, L.M. and McCollum, G. (1985) The organization of human postural movements: a formal basis and experimental synthesis. *Behav. Brain Sci.*, 8: 135 – 172.

Nashner, L.M., Black, F.O. and Wall III, C. (1982) Adaptation to altered support surface and visual conditions during stance: patients with vestibular deficits. *J. Neurosci.*, 2: 536 – 544.

Nashner, L.M., Shupert, C.L. and Horak, F.B. (1988) Head-trunk movement coordination in the standing posture. In: O. Pompeiano and J.H.J. Allum (Eds.), *Vestibulospinal Control of Posture and Locomotion – Progress in Brain Research, Vol. 76,* Elsevier, Amsterdam, pp. 243 – 251.

Nashner, L.M., Shupert, C.L., Horak, F.B. and Black, F.O. (1989) Organization of posture controls: an analysis of sensory and mechanical constraints. In: J.H.J. Allum and M. Hulliger (Eds.), *Afferent Control of Posture and Locomotion – Progress in Brain Research, Vol. 80,* Elsevier, Amsterdam, pp. 411 – 418.

Pandy, M.G. and Zajac, F.E. (1991) Optimal muscular coordination strategies for jumping. *J. Biomech.*, 24: 1 – 10.

Pandy, M.G., Zajac, F.E., Sim, E. and Levine, W.S. (1990) An optimal control model for maximum-height human jumping. *J. Biomech.*, 23: 1185 – 1198.

Stein, R.B. (1974) Peripheral control of movement. *Physiol. Rev.*, 54: 215 – 243.

Zajac, F.E. (1989) Muscle and tendon: properties, models, scaling, and application to biomechanics and motor control. In: J.R. Bourne (Ed.), *Critical Reviews in Biomedical Engineering, Vol. 17,* CRC Press, Boca Raton, FL, pp. 359 – 411.

Zajac, F.E. and Gordon, M.E. (1989) Determining muscle's force and action in multi-articular movement. In: K. Pandolf (Ed.), *Exercise and Sport Sciences Reviews, Vol. 17,* Williams and Wilkins, Baltimore, MD, pp. 187 – 230.

J.H.J. Allum, D.J. Allum-Mecklenburg, F.P. Harris and R. Probst
Progress in Brain Research, Vol. 97

CHAPTER 32

An integrated EMG/biomechanical model of upper body balance and posture during human gait

D.A. Winter, C.D. MacKinnon, G.K. Ruder and C. Wieman

Department of Kinesiology, University of Waterloo, Waterloo, Ont., Canada

Full scale biomechanical and EMG analyses of the balance during human gait are required to understand the neural control of locomotion. The purpose of this paper was to develop an inverted pendulum model of upper body balance in both the plane of progression and the frontal plane, and a medial/lateral balance model of the total body. EMG evidence was also recorded to reinforce the conclusions from the moment of force analyses. The kinematics and kinetics for up to ten natural walking trials on each of four subjects and EMG records from walking trials on eleven subjects were investigated. The results support the following conclusions. (1) The hip extensors/flexors have an overpowering role in maintaining dynamic balance of the head, arms and trunk (HAT) in the plane of progression. Because of the lack of suitable neurological and biomechanical delays between the small head acceleration, presumably exciting vestibular afferents, and the hip moment patterns, the vestibular system appears not to be involved as a feedback sensor in the balance control during gait. (2) In the frontal plane, the hip abductors are dominant in countering the large medial-lateral (M/L) imbalance of HAT during single support but are assisted by the medial acceleration of the hip joint. (3) The total body M/L balance is achieved by the M/L placement of the foot with some opposition and some assistance by the M/L acceleration of the subtalar joint. The subtalar invertors/evertors play an insignificant role during single stance. (4) EMG profiles of the pelvic and trunk muscles indicate an active role of these muscles at each spinal level in the stabilization of the more superior segments against inertial and gravitational forces.

Key words: Human gait; EMG; Posture control; Biomechanics

Introduction

Human walking as bipeds provides a particularly challenging balance task to the CNS. This task is very different from the balance task during standing. Studies of balance/posture during quiet or perturbed standing have identified a major stabilization role for the ankle muscles (dorsi-flexors/plantar-flexors, invertors/evertors) as dominant, and this is not surprising when we consider that the task of balance during standing is to keep the body's centre of gravity (C of G) safely within the base of support. However, in gait the ankle muscles are not as important because the balance task is changed (Winter, 1987a). No longer does the CNS attempt to keep the body's C of G within the borders of the foot; rather, during single support, the C of G passes forward along the medial border of the foot (Shimba, 1984; MacKinnon, 1990). Thus, any activity of the ankle muscles cannot avert a fall, their action can merely fine-tune the anterior-posterior (A/P) or medial-lateral (M/L) acceleration of the body's C of G as it moves forward either side of the plane of progression. Fig. 1 demonstrates this precarious trajectory, and only by safe placement of the swing foot do we avert a fall once every step. Thus, only during the two double support periods each comprising 10% of the stride period can restabilization occur, and even during this time the dual support base is not very firm (one foot is ac-

cepting weight on the small area of the heel while the other is pushing off on the forepart of the foot). The second challenging aspect of human gait is that the distribution of body mass is such that 2/3 of the body mass in the head, arms and trunk (HAT) is located 2/3 of body height above the ground. Such an inverted pendulum is inherently unstable when we consider the forward momentum of HAT and trajectory as seen in Fig. 1. A third compounding task for the CNS is the requirement to achieve a safe forward trajectory with minimum toe clearance ($\approx$ 1 cm) and a safe (gentle) foot landing (Winter, 1987b). Finally, during all these challenging control problems the CNS manages to keep the large HAT segment erect (within $\pm$ 1.5°) and head accelerations severely attenuated (Thorstensson et al., 1984; Ruder, 1989). The control of the large inertial load of HAT would require about eight times the moment of force by the ankle muscles compared with the hip muscles. Fortunately, the CNS does not even attempt such control during steady-state walking. In fact, the role of the plantar-flexors during mid-stance is to control the rate of rotation of the leg over the support foot, then during push-off to produce a forceful piston-like upward and forward drive (Winter, 1984). Such action is far from stabilizing to the balance of the HAT.

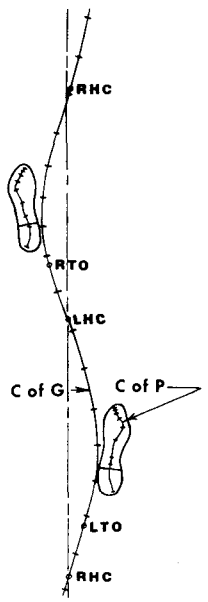

Fig. 1. Centre of gravity (C of G) of the body in steady-state walking is shown to move forward along the medial border of the feet indicating that during single support the body is in an unstable state with the C of G outside the base of support. The control of the medial/lateral component of the C of G trajectory during single support is one phase of the biomechanical analyses.

Research relating to the control of the HAT during gait has been largely limited to the plane of progression and has been largely descriptive. The energetics of HAT has been seen to be energy-conserving by inference from the forward velocity and vertical displacement time histories (Saunders et al., 1953) or by direct calculation of potential and kinetic energies (Ralston and Lukin, 1969; Winter et al., 1976). EMG studies provide activation profiles of hip and low back musculature (Dubo et al., 1976; Knutsson and Richards, 1979; Shiavi, 1985; Winter and Yack, 1987). These reports documented repeatable activity related to the control of the pelvis and the spinal column during stance. Kinematic descriptions of the upper body (Murray, 1967; Waters et al., 1973; Cappozzo et al., 1978; Cappozzo, 1981; Thorstensson et al., 1984) have shown that the trunk varies only a few degrees from the vertical over the gait cycle and that the A/P horizontal accelerations decrease progressively from the pelvis to the thorax and head (Ruder, 1989). M/L displacements of the HAT tend to be more variable (Thorstensson et al., 1984) and M/L accelerations are not attenuated between the pelvis and the head (Cappozzo et al., 1978). Almost all moment-of-force analyses have been confined to the lower limb, with a few reported at the vertebral level (Cappozzo, 1983). The general trend seen in these EMG and moment-of-force profiles shows an extensor hip and spinal pattern during the first half of stance followed by a flexor pattern for the latter half.

With the focus on the hip and more superior muscles as controllers of the HAT multi-segment system a high variability of the hip moments for intra-subject averages across repeat trials and across days has been noted (Winter, 1984). This variability was attributed to a deterministic adaptation during each stride to the dynamic balance control of HAT

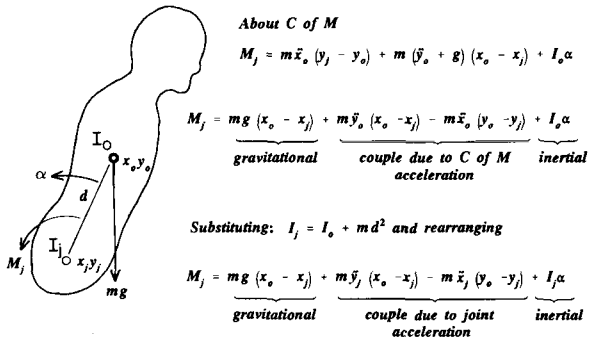

Fig. 2. Inverse dynamics of the inverted pendulum model used in all phases of the analyses presented here. Rearrangement of the terms in the final dynamic equilibrium are to identify the four major components acting about the pivot joint of the inverted pendulum.

(Winter, 1987a). It was also demonstrated that the changes in the hip moment patterns were largely stride-to-stride bias changes that were virtually matched by an opposite change at the knee. The covariance in the hip/knee patterns was almost 90% for repeat trials done days apart and around 65% for strides analysed minutes apart (Winter, 1989). These trade-offs reflected a stride-to-stride change in the A/P direction and were labeled an "index of dynamic balance".

The aim of this paper is to present a biomechanical model of human gait which will attempt to show how balance and posture of HAT is regulated in the A/P and M/L directions. Our results indicate that the hip flexors/extensors dominate control in the A/P direction with some secondary collaboration from the knee muscles and some fine-tuning by the trunk and neck muscles. In the M/L direction our evidence suggests that control is primarily via the position of the foot relative to the plane of progression of the body's C of G. This dominant control is assisted by the hip abductors and lateral muscles of the spine with some very minor tuning by the ankle invertors/evertors.

Theoretical background

Fig. 2 presents a biomechanical model of HAT as an inverted pendulum system which is rotating in any given plane and whose base of support is a joint which undergoes displacements and accelerations. The analysis presented in Fig. 2 transforms the traditional inverse dynamics (equations written about the centre of mass (C of M)) to one written about the base of support:

$$M_j = mg(x_0 - x_j) + m\ddot{y}_j(x_0 - x_j) - m\ddot{x}_j(y_0 - y_i) + I_j\alpha \quad (1)$$

The muscle moment, M_j, is in dynamic equilibrium with three components on the right. The gravitational term will create a load moment if the C of M does not lie directly above the joint centre. The horizontal and vertical accelerations of the joint, $\ddot{x}_j$ and $\ddot{y}_j$, create a couple which may assist or oppose M_j. The sum of the muscle, gravitational and acceleration moments will cause the segment to undergo an angular acceleration, α, with its inertial load being $I_j\alpha$. Although this figure represents the HAT segment rotating about the hip joint in the plane of progression the same equation applies to the frontal plane which has two inverted pendulums; HAT as it undergoes M/L rotation about the hip joint and the total body as it also rotates in the frontal plane about the subtalar joint.

Methods

Full details of the data collection and processing have been presented (Ruder, 1989; McKinnon, 1990) and are now briefly summarized here. Each subject walked along a level walkway over two force platforms while three CCD cameras captured marker coordinate data from one frontal and two sagittal cameras, one located on each side of the walkway. A 14 segment model incorporating two phalangeal, two foot, two leg, two thigh, pelvis, abdomen/thorax, head, upper arms and forearm segments was employed for biomechanical analysis. The L3 – L4 joint was identified and separated the pelvis from the abdomen/thorax segment; the C7 – T1 location defined the neck joint. Inverse dynamics starting with the ground reaction forces yielded the sagittal and frontal moments for the left

and right subtalar, ankle, knee and hip joints. Combining the two hip moments acting on the pelvis enabled an estimate of the L3 – L4 moment. The neck moment was calculated by starting the inverse dynamics solution with the head segment. EMG records were taken using a multichannel biotelemetry system to record the patterns of activity in a number of balance and postural muscles of the thigh, pelvis and trunk: hamstrings, gluteus maximus, erector spinae (L3 – L4), erector spinae (T9) trapezius and splenius capitus. All the spinal muscles were recorded with their electrode sites about 3 cm to the right of the spinous processes. A number of other muscles of the lower limb were also recorded, however, they will not be reported because they have no direct involvement in HAT balance and also because they have been reported elsewhere (cf. Winter and Yack, 1987). Raw EMG was processed as a linear envelope waveform (full-wave rectified, followed by a 3 Hz low-pass filter) designed to produce a waveform that closely followed the muscle tension profile (Winter and Yack, 1987). Stride-to-stride patterns were ensemble averaged to yield an average profile over the stride period. In a similar manner inter-subject ensemble averages were calculated.

Results and discussion

Balance in plane of progression

Kinematic analyses yielded anterior/posterior head, thoracic and pelvic displacements and accelerations. For the repeat trials, the trunk angle varied about 2° over the stride period with a standard deviation of about 2°. The ensemble average of the horizontal and vertical accelerations in the plane of progression revealed the following results: the vertical acceleration was very slightly attenuated from the pelvis to the head indicating very minor shock absorption by the vertebrae. Conversely, the horizontal head acceleration is severely attenuated by more than 75%, thus indicating that the spinal column is acting as a shock absorber in the horizontal direction. The horizontal accelerations experienced by the eye-head fixation system are thus

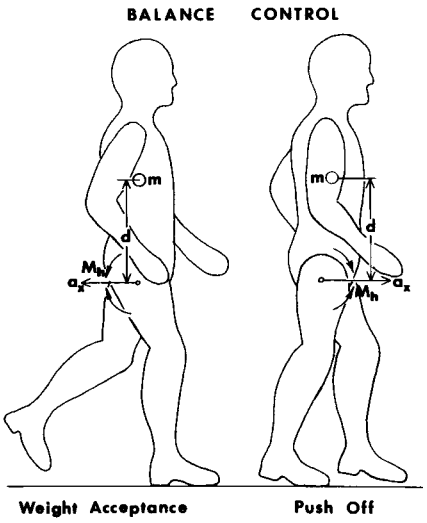

Fig. 3. Weight-acceptance and push-off phases in single support showing the actual directions of hip joint acceleration and hip muscle moments as they act on the inverted pendulum of the head, arms and trunk (HAT).

reduced, thereby simplifying the stabilization task for the vestibulo-ocular reflex. Whether this spinal shock absorption is passive or active remains to be determined; however, EMG evidence to be presented later indicates some active control.

Fig. 3 is presented to show the relationship between the two largest moments in the inverted pendulum model of HAT acting at the hip. The acceleration couple at the hip joint is dominated by the horizontal acceleration vector which is negative during weight acceptance and positive during push-off. The gravitational component is negligible in erect walking. Thus Eqn. 1 reduces to three terms, with the subscript h replacing the general subscript j.

$$M_h = m\ddot{x}_h (y_0 - y_h) + I_h\alpha \qquad (2)$$

These three moments of force are plotted for one subject in Fig. 4. It can be seen that the acceleration couple creates a large moment which tries to unbalance HAT about the support hip joint. We have referred to this couple as an unbalancing moment, M_u and as seen from Fig. 4 the hip moment is almost equal and opposite to M_u. Thus, an almost

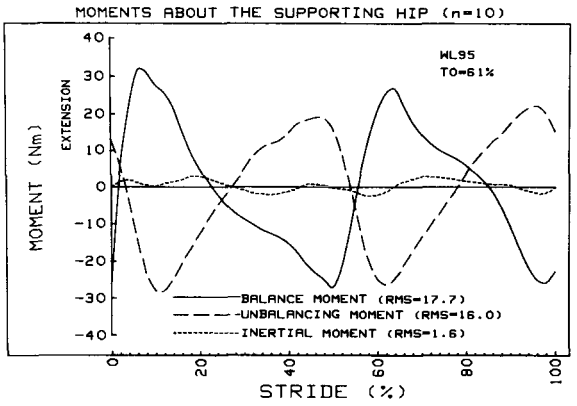

Fig. 4. Plot of unbalancing and balancing moments in the plane of progression for one subject. Curves represent the ensemble average of nine repeat strides shown from HC (0%) to next HC (100%). The hip muscle moment virtually cancels the unbalancing moment due to the hip joint acceleration. See text for discussion of the role of the CNS in achieving the dynamic balance of HAT.

perfect cancellation between M_u and M_h occurs, resulting in a very small $I_h\alpha$. Thus, the resultant α creates the small angular displacement of HAT over the gait cycle. The results from all five subjects that were analysed over about ten repeat walking trials were the same: the active hip moment virtually canceled the unbalancing moment. Such a result emphasizes the dominant and singular role of the hip extensors/flexors during stance: dynamic balance of HAT. From a neurological perspective, it remains to be seen how such an instantaneous control is achieved. The horizontal accelerations seen at the head by the vestibular system are an attenuated version of the unbalancing hip acceleration and thereby have the potential to be used as a control signal. Fig. 4 shows that the balancing hip moment is virtually 180° out of phase with the perturbing acceleration, and the head (vestibular) acceleration though small ($\approx$ 0.05 g) are within consciously recognized thresholds of 0.005 g (Young and Meiry, 1968). It is therefore an open question whether as a potential sensory feedback signal the head acceleration is sufficiently in advance so as to account for neurological latencies and the electromechanical lag in the build-up of hip muscle tension.

Frontal plane balance

In the frontal plane we have two inverted pendulum systems. As shown in Fig. 5*a*, when the body is in single support HAT pivots about the hip joint, and in Fig. 5*b* the total body pivots about the subtalar joint. Because HAT maintains a nearly vertical position (within ± 2°) the total body system can be considered as a first approximation to be a nearly rigid inverted pendulum. Because the C of M of HAT and the total body are always medial of the pivot joint we must consider all acceleration terms in Eqn. 1 including gravitational.

In the global reference system (GRS) the frontal plane moments about the support hip are presented in the upper half of Fig. 6 for one of the eight walk-

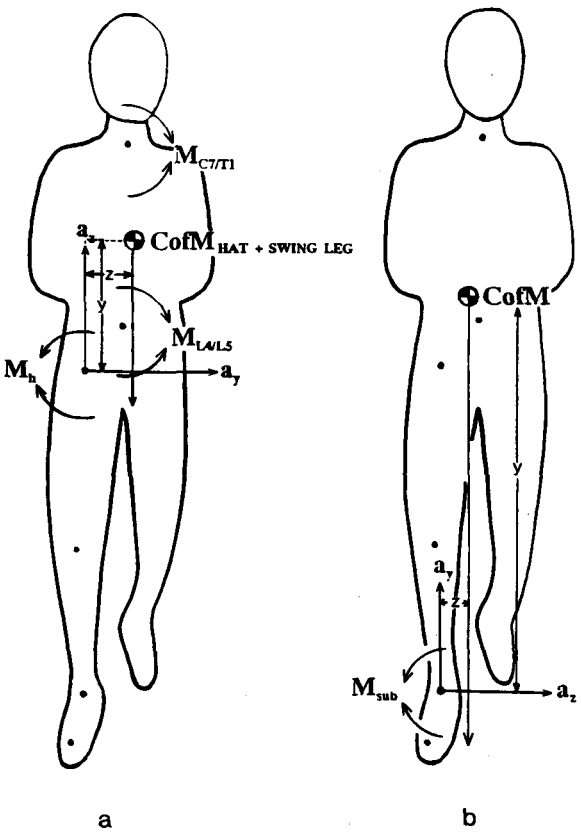

Fig. 5. Frontal plane models of the dynamic balance of (*a*) the HAT segment as it pivots about the hip joint and (*b*) the total body as it pivots about the subtalar joint.

ing trials for one representative subject with low inter-trial variability. The gravitational moment during single support is that calculated about the support hip; during double support a linear weighting is assumed in the transfer between the unloading and weight-accepting hips. A similar transfer was assumed between the right and left hip muscle moments and the acceleration couple. The sum of these three moments are what cause the HAT segment to undergo a M/L angular acceleration; this summation appears in the lower half of this figure (solid line). The angular inertial moment, $I_h\alpha$, appears as a dashed line, and the magnitude of these two curves is quite low, about 10 Nm. The residual difference between these curves is quite small. This small residual is a validation that the inverted pendulum model assumed in the dynamic equilibrium equation during most of weight-bearing was correct. The gravitational load is about 60 Nm during single support and this is countered by the hip abductors

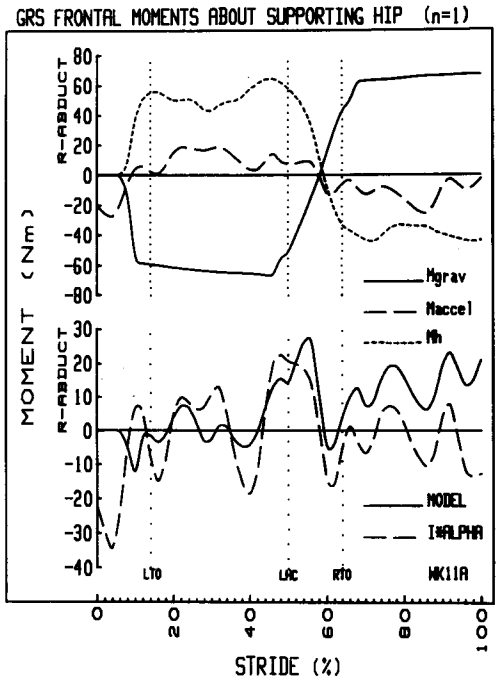

Fig. 6. Dynamic equilibrium moments in the frontal plane acting on the HAT segment as it pivots about the hip joint. See text for detailed discussion.

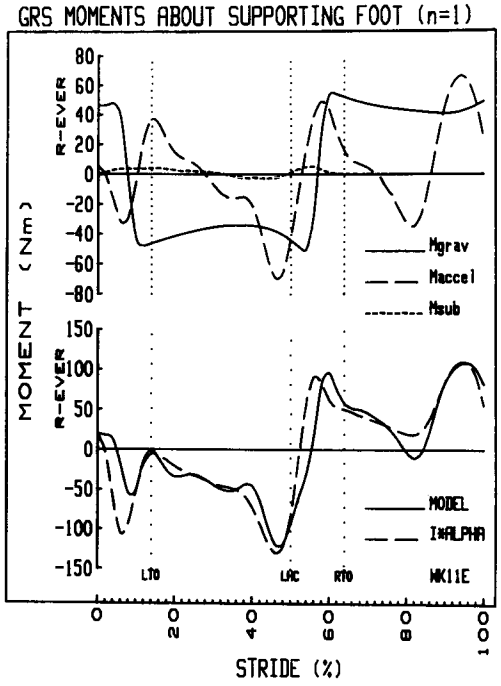

Fig. 7. Dynamic equilibrium moments in the frontal plane acting on the total body as it pivots about the subtalar joint. See text for detailed discussion.

which respond with about 50 Nm, while the hip acceleration (which is medial during single support) also assists with about 10 Nm. These findings support the hypothesis that the CNS can predict the time course of the medial acceleration, accounting for it by reducing the necessary abductor activity.

The inverted pendulum model shown in Fig. 5*b* yielded three moments that acted about the subtalar joint: gravitational, joint acceleration and subtalar muscles (invertor/evertors); these are presented in the upper half of Fig. 7. It is evident that two of the moments dominate. The gravitational moment (solid line) exceeds 40 Nm during single support and is essentially dependent on the distance of the foot placed laterally of the body's C of G. The second major moment is due to the M/L acceleration (long dashed line) of the subtalar joint. The third and almost insignificant contribution is the subtalar moment (short dashed line). As described above the sum of these three moments should equal the inertial

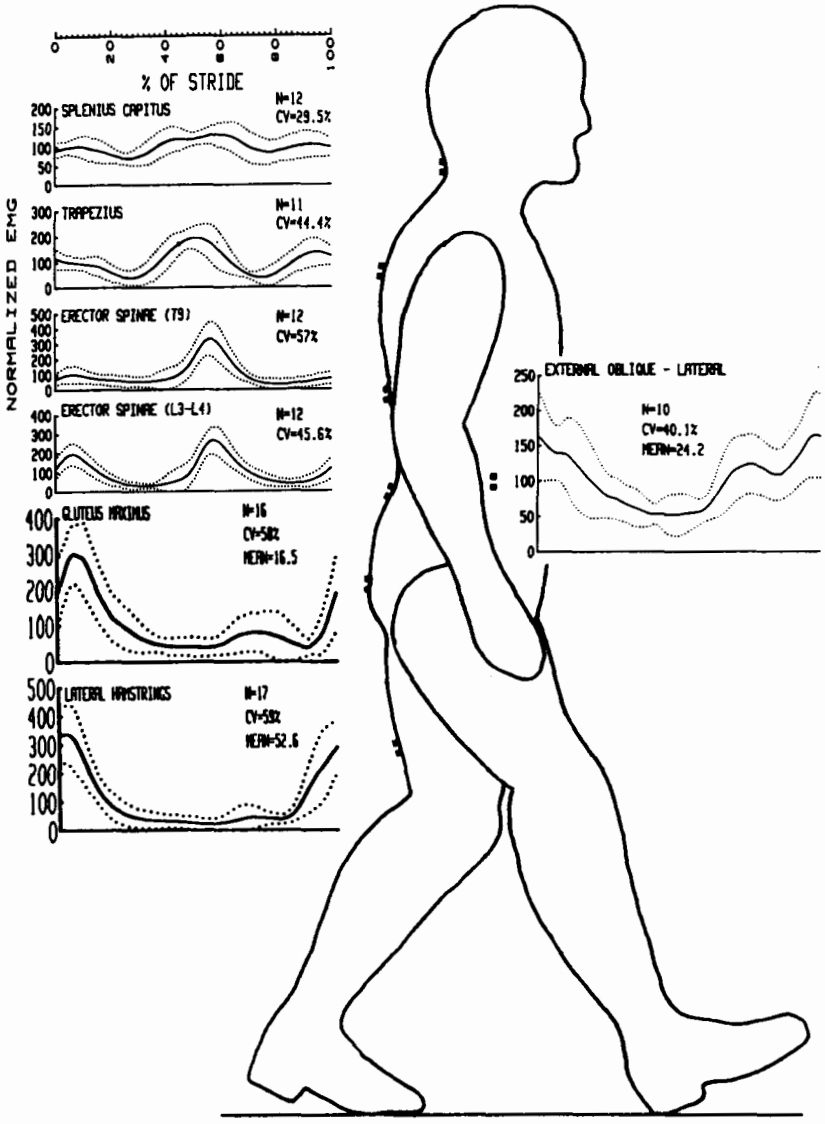

Fig. 8. EMG profiles (ensemble averaged across a number of subjects) of seven muscles of the trunk, pelvis and thigh that are involved with the dynamic balance of HAT during level walking.

moment, $I_s\alpha$; the lower traces of Fig. 7 show a good match of this dynamic equilibrium model (solid line) with the independently calculated $I_s\alpha$.

EMG control of trunk balance

The EMG records of the posterior spinal and pelvic muscles revealed an active control of the multi-link inverted pendulum system. Fig. 8 presents the EMG ensemble average patterns for a number of subjects who walked their natural cadence. Minimally ten strides were averaged for each subject prior to the analysis of the inter-subject averages. As can be seen these profiles show active stabilization of the pelvis and the spinal column. The major activity of the hamstrings (shown laterally) and gluteus maximus was just after HC; this pattern

agrees completely with the first phase of the hip moment seen in Fig. 4: a hip extensor pattern from 5% to 25%. This pattern was repeated one step later when the left hip muscles produce a similar pattern from 55% to 75% of the stride. With these muscles stabilizing the pelvis we now see the action of the spinal extensor muscles stabilizing each section of the trunk. The erector spinae (L3 – L4) had a bimodal pattern of activation, one in phase with the unbalancing moment during each weight acceptance phase. Both bursts of the bimodel pattern were not completely symmetrical in amplitude. Right erector spinae (T9) and trapezius both showed a larger burst during left weight acceptance. Thus, it appears that these trunk muscles have a dual role of anterior/posterior balance and also a transverse plane stabilization of the shoulder girdle (at left weight acceptance the decelerating right arm requires a stable shoulder). The splenius capitus exhibits low background activity plus some modulation of its activity. These posterior neck extensors are required to hold the head erect against the gravitational forces which act considerably anterior to the cervical spine. Superimposed on the background level there is a small cyclic pattern that is in phase with weight acceptance (10% and 60%) when the head is undergoing a small posterior acceleration and therefore requires inertial stabilization.

The only muscles monitored on the lateral side of the trunk were the external obliques. These muscles exhibited a phasic pattern that was not second harmonic (like the erector spinae) but rather a fundamental wave that peaked at HC and reached a minimum at contralateral HC. This phasic pattern correlates with the frontal plane flexion moments (calculated at L4/L5) which prevent excessive lateral flexion towards the support trunk.

The major findings from these EMG patterns is that the posterior spinal musculature appears to be actively involved at each level to stabilize the more superior segments of the trunk against inertial and gravitational forces in both the anterior/posterior, medial/lateral and transverse planes.

References

Cappozzo, A., Figura, F., Leo, T. and Marchetti, M. (1978) Movements and mechanical energy changes of the upper part of the human body during walking. In: E. Assmussen and K. Jorgensen (Eds.), *Biomechanics VI-A*, University Park Press, Baltimore, MD, pp. 272 – 279.

Cappozzo, A. (1981) Analysis of the linear displacement of the head and trunk during walking at different speeds. *J. Biomech.*, 14: 411 – 425.

Cappozzo, A. (1983) The forces and couples in the human trunk during level walking. *J. Biomech.*, 16: 265 – 277.

Dubo, H., Peat, M., Winter, D.A., Quanbury, A.O., Steinke, T. and Grahame, R. (1976) Electromyographic-temporal analysis of normal gait. *Arch. Phys. Med. Rehab.*, 57: 415 – 420.

Knutsson, E. and Richards, C. (1979) Different types of disturbed motor control in gait of hemiparetic patients. *Brain*, 102: 410 – 430.

MacKinnon, D.C. (1990) *Control of Whole Body Balance and Posture in the Frontal Plane during Human Walking*, M.Sc. Thesis, University of Waterloo.

Murray, M.P. (1967) Gait as a total pattern of human movement. *J. Bone Jt. Surg.*, 46-A: 335 – 360.

Ralston, H.J. and Lukin, L. (1969) Energy levels of human body segments during level walking. *Ergonomics*, 12: 39 – 46.

Ruder, G.K. (1989) *Whole Body Balance during Normal and Perturbed Walking in the Sagittal Plane*, M.Sc. Thesis, University of Waterloo.

Saunders, J.B., Inman, V.T. and Eberhart, H.D. (1953) The major determinants in normal and pathological gait. *J. Bone Jt. Surg.*, 35-A: 513 – 558.

Shiavi, R. (1985) Electromyographic patterns in adult locomotion: a comprehensive review. *J. Rehab. Res. Dev.*, 22: 85 – 98.

Shimba, T. (1984) An estimate of the centre of gravity from force platform data. *J. Biomech.*, 17: 53 – 60.

Thorstensson, A., Nilsson, J., Carlson, H. and Zomlefer, M.R. (1984) Trunk movements in human locomotion. *Acta Physiol. Scand.*, 121: 9 – 22.

Waters, R.L., Morris, J.M. and Perry, J. (1973) Translational motion of the head and trunk during normal walking. *J. Biomech.*, 6: 167 – 172.

Winter, D.A. (1984) Kinematic and kinetic patterns in human gait: variability and compensating effects. *Hum. Movement Sci.*, 3: 51 – 76.

Winter, D.A. (1987a) *Biomechanics and Motor Control of Human Gait*, University of Waterloo Press, Waterloo, Ont.

Winter, D.A. (1987b) Balance and posture in human walking. *Eng. Med. Biol.*, 6: 8 – 11.

Winter, D.A. (1989) Coordination of motor tasks in human gait. In: S.A. Wallace (Ed.), *Coordination of Movement*, Elsevier

Science Publishers, New York, pp. 329 – 363.
Winter, D.A. and Yack, H.J. (1987) EMG profiles during normal human walking: stride-to-stride and inter-subject variability. *Electroenceph. Clin. Neurophysiol.*, 67: 402 – 411.
Winter, D.A., Quanbury, A.O. and Reimer, G.D. (1976) Analysis of instantaneous energy of normal gait. *J. Biomech.*, 9: 253 – 257.
Young, L.R. and Meiry, J.L. (1968) A revised dynamic otolith model. *Aerospace Med.*, 39: 606 – 608.

J.H.J. Allum, D.J. Allum-Mecklenburg, F.P. Harris and R. Probst
Progress in Brain Research, Vol. 97

CHAPTER 33

Control of standing and gait using electrical stimulation: influence of muscle model complexity on control strategy

William K. Durfee

Department of Mechanical Engineering, Massachusetts Institute of Technology, Cambridge, MA, U.S.A.

Three approaches to controlling standing and gait in paraplegics through functional electrical stimulation are presented. The approaches differ in their requirements for modeling the muscle actuator. The first approach describes a detailed muscle model and presents methods for rapid experimental parameterization of the model. The second requires a less detailed model and knowledge of model error bounds to design advanced, non-linear controllers which guarantee stability. The third approach needs no muscle model since it controls limb trajectories through combining stimulation with an orthosis containing controllable friction brakes at the joints. Future clinical systems may use one or a combination of these approaches to restore useful function.

Key words: Muscle force; Functional neuromuscular stimulation; Human muscle models

Introduction

Systems which restore function to paralyzed muscle through the application of electrical stimulation have recently been considered as a means for restoring full or partial gait to paraplegic individuals (Kralj et al., 1983; Marsolais and Kobetic, 1983; Cybulski et al., 1984; Peckham, 1987). One of the problems which must be solved before these systems become a clinical reality is how to control the system of stimulated lower limb muscles to generate effective balance and gait. This paper is concerned with the particulars of this applied control problem.

The human body is a multiple-link, unstable inverted pendulum, and remains upright only through CNS motor control programs acting through neuromuscular system actuators. For systems which use functional electrical stimulation (FES) to restore gait, that control must be provided externally. Specifically, the control problem is to provide reliable, static balance while standing and dynamic balance and trajectory tracking while walking. No FES-aided gait system is currently able to provide these functions without auxiliary support such as parallel bars, rolling walkers, crutches or canes.

Because stimulated muscles are non-linear, time-varying actuators, the control problem is difficult. Traditional engineering control approaches are insufficient when applied to the real system. One of the limitations which hinders the design of effective controllers is poor mathematical models of stimulated muscle; however, with more accurate models, better control may be possible. Two strategies can be followed to solve this coupled modeling/control problem. First, one can develop a good model and design a high-performance controller based on the assumption that the model is accurate. Second, one can assume a crude model and design a low-performance controller which is capable of at least guaranteeing system stability in the presence of unmodeled muscle behaviors. Thus the design space is one of balancing model accuracy, control methodology and controller performance.

In designing a neural prosthesis to restore balance

and gait, the engineer can turn to the biological control system for assistance. Most importantly, the CNS stands as an existence proof that the biomechanical system of an upright human can indeed be stabilized and controlled. Thus the problem of the engineer becomes one of emulating at least a certain subset of CNS functions. In approaching this task, much can be learned from the extensive research which has been directed towards understanding natural control of balance and gait since the capabilities of the CNS controller are well known, particularly its ability to adapt to changing environments or to unexpected events such as a stumble.

The challenges in mimicking the CNS controller, however, are daunting. Although it is well understood what the CNS does, the details of how the controller achieves its task remain to be discovered. Further, the actuator channels and sensors available to a neural prosthesis controller are far different than those used by the CNS. With a surface stimulation system, the number of electrodes per leg might range from two to five, while with an implanted system it may reach up to 32 (although many of those channels would be redundant electrodes for fault tolerance). This is still far short of the number of muscles in the trunk and lower limb which the CNS uses for balance control. Even with an appropriate set of muscles to activate artificially, the neural prosthesis controller is at a distinct disadvantage because the means of muscle activation is radically different from that used by the CNS. The CNS has access to each motor unit independently which it uses to recruit muscle fibers in a regular small-to-large size order and also uses it to activate fibers asynchronously generating smooth contractions at a low firing rate for individual fibers. The neural prosthesis, whether using surface or implanted electrode technology, is restricted to a gross signal interface to the muscle. Activation of fibers is synchronous, typically at a fixed firing rate, and unless specialized methodologies are used, recruitment is either in a large-to-small or a random order depending on the electrode and nerve geometry and on the local impedance characteristics of the tissue. Thus, although one can learn from the CNS control, in the short-term it is unlikely that CNS control can be copied at any great level of detail in neural prostheses.

This paper presents work done at MIT in developing controllers fro neural prosthesis systems which restore functional balance and gait to paraplegic individuals. Three approaches to the control problem are reviewed. First, a modified Hill-type model structure has been developed and experiments in isolated, animal model muscle have demonstrated the effectiveness of new model identification methods. Here the strategy was to develop a detailed model of muscle which could be used for the design of traditional engineering control structures such as those which are applied to robotics. Second, work in robust non-linear control structures which require only approximate models is discussed and simulation results presented. Third, a practical approach where stimulation is combined with smart orthotics is presented as a means of achieving precision control of balance and gait without the need for muscle models. Preliminary studies have shown that control of this hybrid system is effective even in the presence of muscle fatigue.

Hill-type model: model selection and identification

Objective

The objective of the muscle modeling work was to select a muscle model structure which could account for most of the dynamics seen when generating force through electrical stimulation, and to develop experimental system identification methods for assigning parameters to the model. Particular attention was paid to parameterization methods which depended on experimental values only and not on values taken from the literature or derived from different muscle systems.

Model

The model is a variant of a Hill-type, lumped-element model (Winters, 1990) and is similar to the model of Crago et al. (1990). As shown in Fig. 1, muscle force is developed as the sum of a passive component containing a parallel spring and dashpot

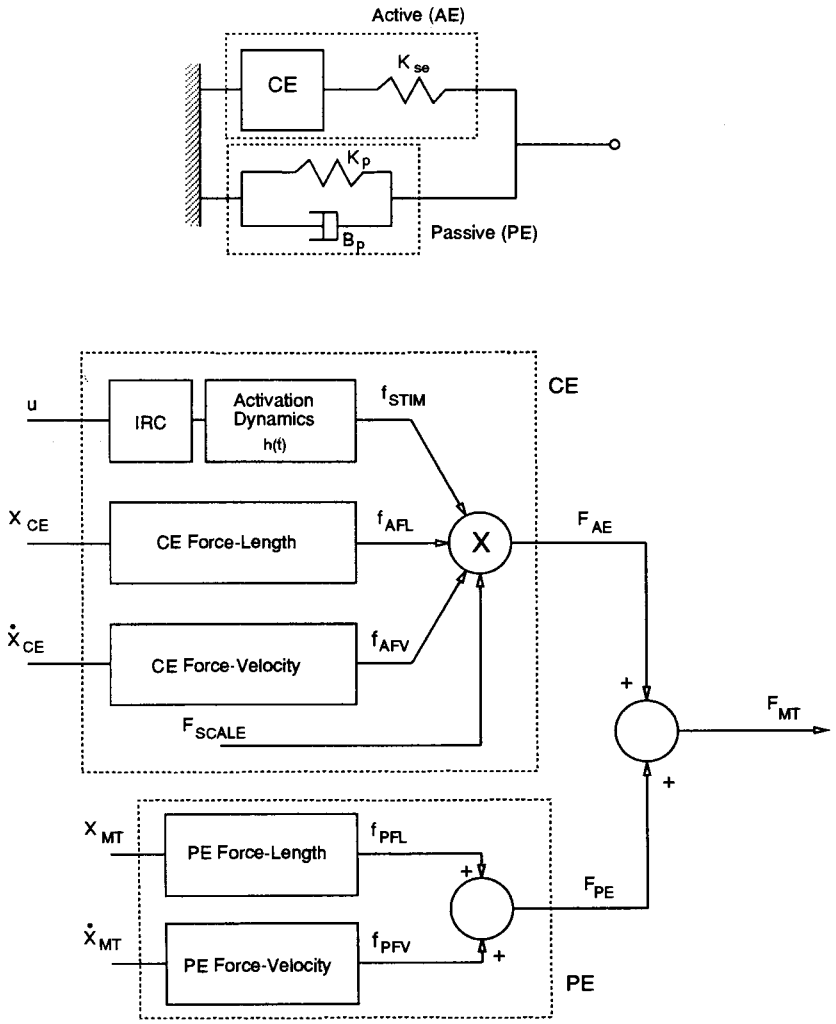

Fig. 1. Detailed model of electrically stimulated muscle. The upper diagram shows a lumped, mechanical model consisting of a parallel active element (AE) and passive element (PE). The AE contains an elastic element (SE) in series with a contractile element (CE). The lower diagram details the model in block diagram form. The PE consists of a parallel spring and damper. The CE force is a multiplicative combination of normalized force-length, force-velocity and force-activation relations and a scaling factor to restore absolute force units. The force-activation properties are developed by a non-linear isometric recruitment curve cascaded with second-order muscle dynamics. In the identification experiments described in the text, the SE is assumed to be infinitely stiff.

and an active component containing an elastic element (SE) in series with the contractile element (CE). The CE contains three multiplicative non-linear terms which describe the force-activation, force-length and force-velocity properties of the muscle. The activation block is formulated as a structure with a static non-linearity representing the isometric recruitment curve preceding a linear dynamic block representing the muscle isometric twitch characteristics.

The model incorporates several key assumptions which although incorrect, are required for tractable parameterization methods. The CE properties are modeled as three independent blocks implying that

the relation in each block is shape-invariant to changes in the other blocks. For example, this means that the shape of the force-velocity curve is assumed not to change with activation level, a property which was proved incorrect by the experimental data of Joyce et al. (1969). The model also assumes that the twitch dynamics do not depend on recruitment level, again incorrect because of the variations in motor unit twitch contraction speeds (McDonagh et al., 1980). Another simplification required to keep the model tractable was to assume that the series elastic component is infinitely stiff. With this assumption, the length and velocity of the CE are the same as the externally measured length and velocity. When the model is parameterized, the properties of the actual SE become embedded in the force-length and force-velocity properties of the CE.

The most glaring model simplification is its time-invariant structure which ignores fatigue completely. Since fatigue is a dominant characteristic of electrically stimulated muscle, future model structures must be time-varying and must include at least a simple model of fatigue. This, however, would greatly complicate the identification procedures.

Identification methods, experiments and results

Parameterizing the muscle model required identification of the passive force-length and force-velocity relations, the active force-length and force-velocity relations, the isometric recruitment curve, and the isometric twitch contraction dynamics. Identification methods were developed and tested experimentally in isolated cat medial gastrocnemius and tibialis anterior muscles (Durfee and MacLean, 1989). Muscles were activated by stimulation through nerve cuff electrodes and through controlled length and velocity inputs provided by a servomotor coupled to the muscle tendon. The estimation experiments used length and activation inputs which are in the normal physiologic range seen by the muscle during standing and gait.

The isometric recruitment curve and twitch dynamics were estimated by the ramp deconvolution method described in Durfee and MacLean (1989). This provides a high-resolution recruitment curve from 2 sec of stimulation data and a rapid, computer-based processing algorithm. The passive and active force-length and force-velocity relations were identified through a least-squares method which assumed that each relation could be modeled as a ten-element, piecewise-linear curve. There were no restrictions placed on the shapes of the force-length or force-velocity relations, although one could, for example, fit the force-velocity relation to a Hill-type hyperbola. The current identification method, however, picked the piecewise linear relations which provided the best fit to the data in a least-squares sense.

Fig. 2 demonstrates the ability of the estimation methods to fit the force output of the muscle when subjected to a fixed level of stimulation and a random length/velocity input. Fig. 3 illustrates that the model is also able to predict the force output of the muscle. Here, the muscle was subjected to random,

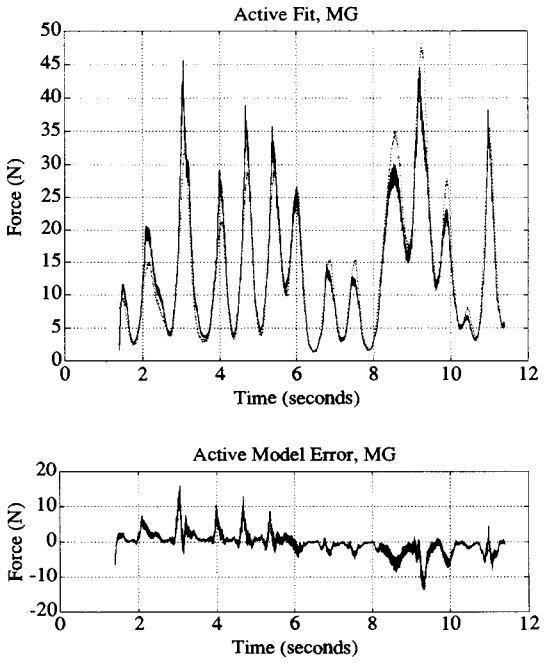

Fig. 2. Model data fitting ability. The muscle was subjected to a random length input at constant stimulation activation and the resulting force (dotted line) compared to the model (solid line). The lower plot displays the error.

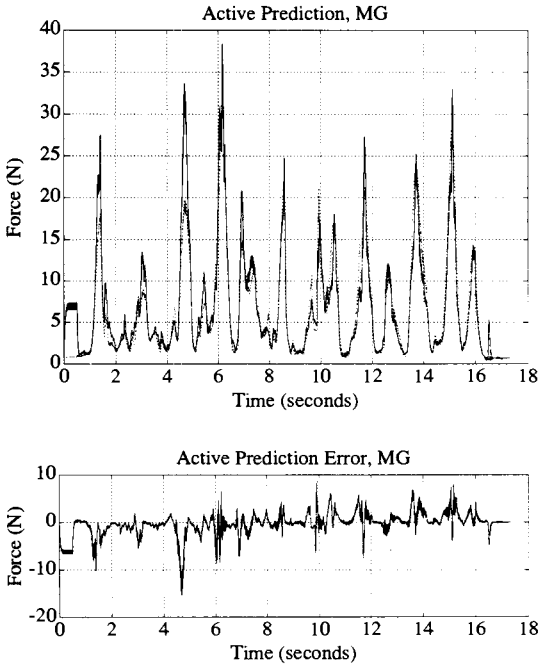

Fig. 3. Model force prediction ability. The muscle was subjected to simultaneous random inputs in length and activation and the output force (dotted line) compared to the force predicted by the model (solid line) when the model was calibrated with a different trajectory input. The lower plot displays the error.

simultaneous stimulus activation and length inputs. The same inputs were applied to the model which had been parameterized in a separate experiment.

Discussion

The experimental results demonstrate that a Hill-type model is capable of predicting the force output of an electrically stimulated muscle with a reasonable degree of accuracy. With this model of the muscle actuator and with a model of skeletal plant (such as that developed by Yamaguchi and Zajac, 1990), one could consider using forms of engineering controllers which have been applied to robotic manipulators but which require accurate models. One possibility is to use feedback linearization methods (Slotine and Li, 1991) which make use of full or partial model cancellation in the controller. Computed torque control (Craig, 1986) is a type of feedback linearization commonly seen in robotics. With accurate models, the advantage of this control approach is its ability to achieve precision tracking which for neural prostheses would imply the capability of generating smooth, natural gait trajectories.

This disadvantage of feedback linearization controllers is that if the model contains significant errors (which it will due to time variations caused by fatigue), performance degrades and stability, even for static balancing, is no longer guaranteed. One could consider incorporating a model of fatigue to ameliorate these model errors. Unfortunately, little is known about the details of how muscle fatigues when subjected to a complex history of stimulation and kinematic inputs, rendering accurate fatigue models beyond our current capabilities. Another possibility would be to measure surface EMG signals along with joint angles. When combined with the muscle model which accounts for the variation in force with length and velocity, this may yield a better estimate of fatigue. Work in detecting EMG in the presence of electrical stimulation, and in processing the signal to reveal underlying muscle state is ongoing in our research group.

One must also be cautious in the application of closed-loop controllers when the muscle fatigues. Without an explicit bound on stimulus activation levels, the controller may struggle to maintain a constant muscle force which may damage the muscle or tendon through overuse. A more appropriate strategy might be to have the system mimic the natural fatigue properties of muscle.

Robust non-linear control: relaxing the model

Overview

A second approach to the control problem is to assume a simpler model for muscle and to use a control strategy which explicitly accounts for model errors at the expense of lower performance. Sliding control and adaptive sliding control are non-linear controller design methodologies developed explicitly for this purpose (Slotine and Li, 1991). We have explored the applicability of these controllers to neural prostheses in simulations of controlling the trajec-

tory of the unloaded, free-swinging shank (Durfee and DiLorenzo, 1990). The specific objective of this work was to determine whether the controllers could maintain their performance in the presence of model uncertainties and time-varying muscle fatigue.

Model and control

Sliding controllers work for systems in canonical form such as those described by the second order dynamics:

$$\ddot{x} = f(\dot{x}, x, t) + b(t)u$$

where f describes the non-linear dynamics, u the control input, and b a possibly time-varying control gain. The controllers are designed for systems where f and b are not known exactly but can be bounded. The free-swinging shank was modeled in this form as a simple pendulum acted on by gravity and by a muscle torque generator at the knee with dynamics described by:

$$\ddot{x} = -\frac{mgL}{J}\sin(x) + \frac{b(t)}{J}u$$

where m is the mass of the pendulum, L its length, J its rotary inertia, x the shank rotation, u the command input developed by the muscle torque generated at the knee, and $b(t)$ a time-varying gain which represents force-length, force-velocity, recruitment and fatigue properties.

The sliding control design process for tracking a desired trajectory x_d (see Slotine, 1984; Asada and Slotine, 1986; Slotine and Li, 1991, for details) then leads to a control law of the form:

$$u = \frac{J}{\hat{b}}[\hat{u} - k\text{sat}(s/\Phi)]$$

which includes the nominal control gain $\hat{b}$ and the nominal control:

$$\hat{u} = \frac{mgl}{J}\sin(x) + \ddot{x}_d - \lambda\dot{\tilde{x}}$$

where λ defines the tracking speed and $\dot{\tilde{x}}$ is the velocity tracking error. The nominal control is augmented by a term which accounts for the uncertainties in the plant and control gain and which guarantees that the controlled system remains stable and converges to the desired dynamics defined by the sliding surface s which is a function of the position and velocity tracking errors. This additional term includes a switching gain defined by:

$$k = (\beta - 1)|\hat{u}| + \beta(F + \eta)$$

where β is the control gain uncertainty, F is the plant uncertainty, and η is a safety factor determined by the designer.

For the simulation experiments of the standard sliding controller, the control gain b was varied sinusoidally by $\pm$ 30% at a 0.5 Hz rate to simulate recruitment curve uncertainties while the mass of the shank m was varied by $\pm$ 20% to simulate plant uncertainties. The muscle control torque u was assumed to be a linear torque actuator with negative saturation at zero to simulate the unidirectional action of the quadriceps and positive saturation to simulate peak recruitment.

An adaptive sliding controller was also designed to track changes in muscle fatigue. For these simulations the plant model was assumed to be known without error, the torque input u was assumed to be a bidirectional, linear actuator with saturation at $\pm$ 10 Nm, and control gain $b(t)$ was taken as an exponentially decaying gain factor with dynamics:

$$b(t) = 0.5 + 0.5e^{-t/\tau}$$

to simulate fatigue where τ is the fatigue time constant which was set to 5 sec in the simulations.

The adaptive design procedure (consult Slotine and Coetsee, 1986, or Slotine and Li, 1991, for details) results in the same control law as the non-adaptive design but with $k = \eta$, the safety factor, since no uncertainties were assumed for the plant or control gain. The control term for gain estimate b followed an adaptation law defined by:

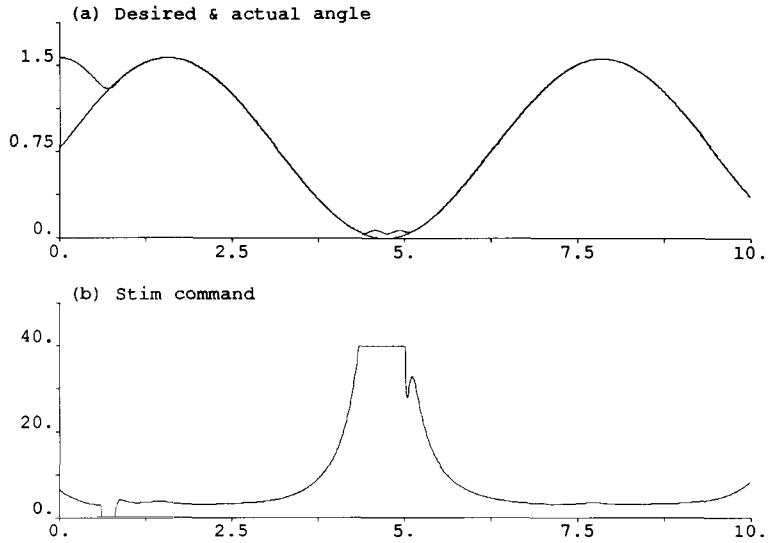

Fig. 4. Simulation results for sliding control of the free-swinging leg during plant and control-gain parameter variations. Desired and actual trajectories in radians (top) and saturated stimulus command output (bottom). The horizontal axis for both plots is time in seconds.

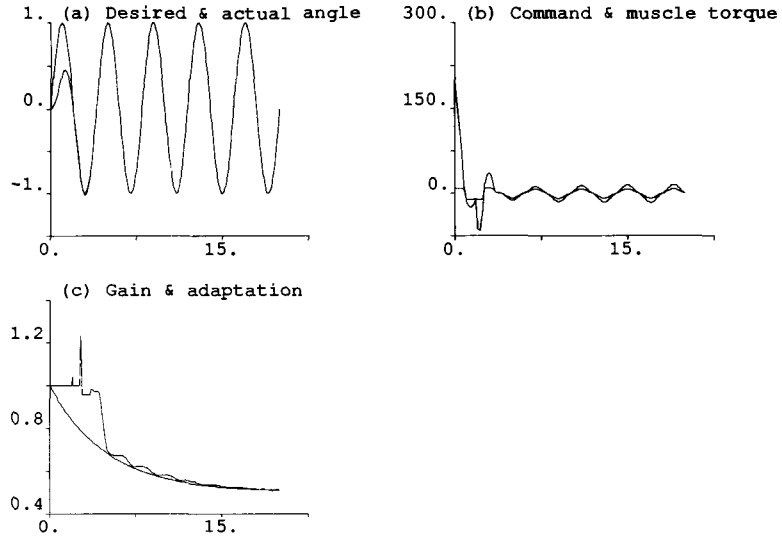

Fig. 5. Simulation results for adaptive sliding control of a simplified muscle undergoing fatigue. (*a*) Desired and actual trajectories. (*b*) Control output showing desired stimulus command and actual, saturated stimulus command. (*c*) Actual and estimated time-varying control gain b. The horizontal axis for all plots is time in seconds.

$$\frac{1}{\hat{b}} = (b_n^2/J)\,[-\hat{u} + \eta \mathrm{sat}(s/\Phi)]s_\Delta$$

with adaptation gain b_n and a term s_Δ to switch the adaptation off when the system was close to the desired trajectory, thus avoiding the problem of adaptation drift found in other adaptive control strategies. The adaptation law was also suspended when the tracking errors were very large to prevent the adaptation from going unstable due to unmodeled plant dynamics such as the muscle saturation.

Simulation experiments

Output from simulations with the standard sliding controller are displayed in Fig. 4 with the top plot showing desired and actual position outputs

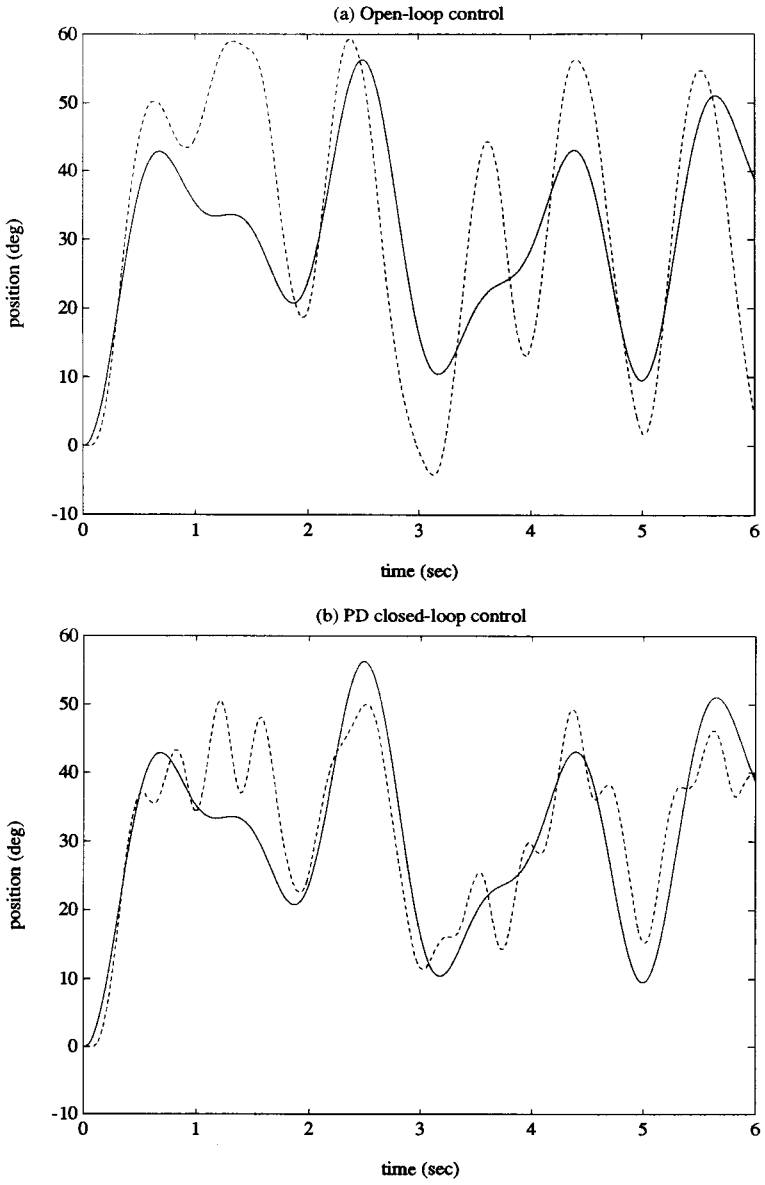

Fig. 6; for legend, see p. 377.

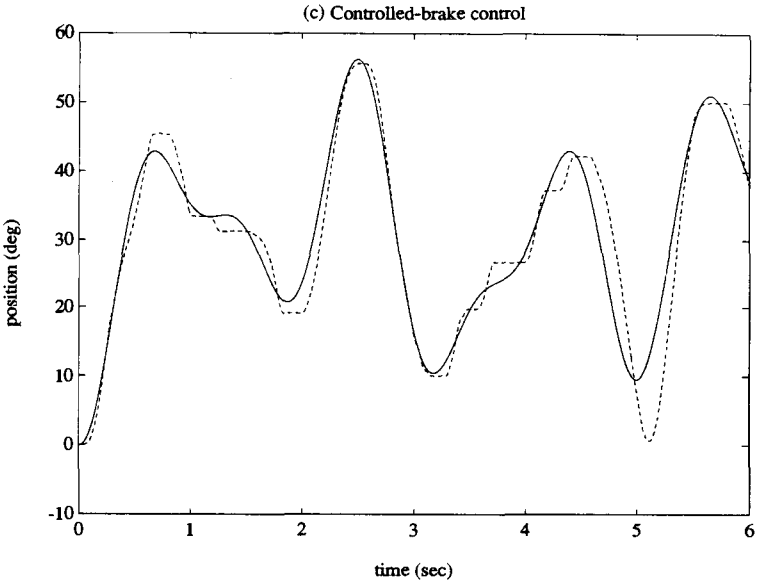

Fig. 6. Measured (dotted line) and desired (solid line) trajectory tracking experiments for controlling the free-swinging leg. (*a*) Open-loop control. (*b*) P-D closed-loop control. (*c*) Controlled-brake control.

while the system tracks a slow, 90° sine path, and the bottom showing the stimulus command to the muscle. After an initial transient, good tracking is achieved despite the sinusoidal mass and control gain variations. Further errors appear near zero degrees (leg fully straight) since saturation limits the maximum torque available from the muscle (bottom plot).

Fig. 5 demonstrates the adaptive sliding controller simulation results with a saturating muscle and decaying control gain to simulate fatigue. Again, after an initial transient, good tracking is achieved. The gain estimate plot shows that the adaptation law is tracking *b(t)* and is turning off when the system is tracking well. The control plot shows that without saturation, the controller would demand excessive muscle torque. A more conventional computed torque controller of the type commonly used in robotics (Craig, 1986) did not do well with this time-varying system and further could go unstable if model errors were added.

Discussion

The simulations demonstrate that systems with simple models can be controlled through an advanced, non-linear control approach which takes modeling errors into account explicitly and which guarantees stability. The implication for control of neural prostheses is that a balance or gait trajectory tracking controller could be designed using simplified muscle models so long as the model errors could be bounded.

The simulations presented are admittedly limited in scope and serve only to demonstrate the potential for non-linear controllers in neural prosthesis applications. Two disadvantages of sliding control are that the system equations must be expressed in canonical form which precludes explicit representation of some of the embedded muscle dynamics, and that full state feedback is required for implementation, which for the simulation system means position and velocity measurements are necessary. Further work to verify the performance of sliding con-

trollers is required in simulations and, more importantly, in experiments.

Hybrid FES: supplementing stimulation with orthotics

Overview

A third approach to the neural prosthesis balance and gait control problem is to transfer the task from one of controlling the stimulated muscle system to one of controlling a combined stimulation/orthosis system. At MIT, we are developing the FES controlled-brake orthosis, a hybrid system which combines muscle stimulation with a smart orthotic brace containing controllable, mechanical friction brakes at the joints. The stimulated muscles are treated as a raw power source and gait trajectories are controlled by modulating the mechanical brake.

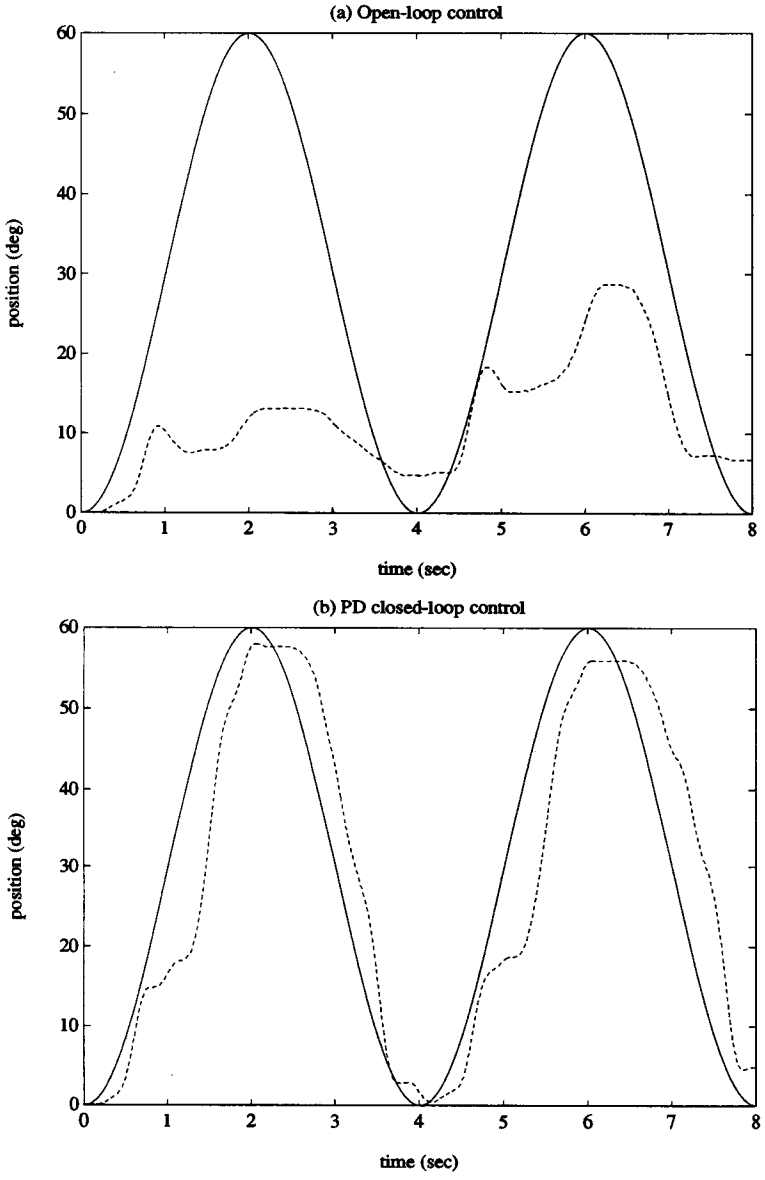

Fig. 7; for legend, see p. 379.

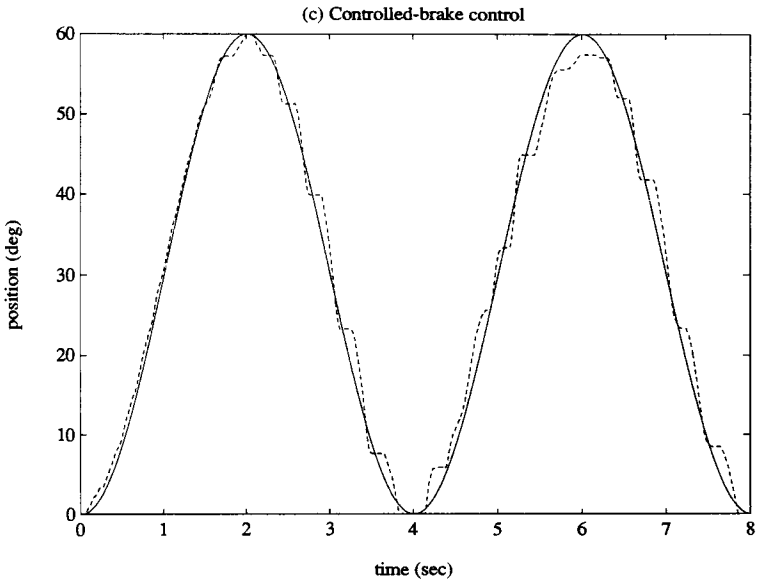

Fig. 7. Similar to Fig. 6 but with fatigued muscles.

The concept is similar to controlling a bicycle while riding downhill where gravity provides the motive force and speed is regulated with the bicycle handbrakes. The advantage of the approach is that no muscle models are required for the control design. A complete description of the concept including a brief review of work by other groups in hybrid FES systems can be found in Durfee and Hausdorff (1990).

Experiments

Experiments were conducted on controlling the position of the unloaded shank of able-bodied subjects using the hybrid controlled-brake orthosis approach. Subjects sat in an apparatus with one leg dangling and strapped on a hinged orthosis whose joint was approximately aligned with the knee. The orthosis was coupled to a magnetic particle brake which could provide controlled damping loads to the knee joint with joint torque, position and velocity being monitored through appropriate transducers. Carbon rubber stimulating electrodes were applied to the skin over the quadriceps and hamstring muscle groups and were activated through a computer-controlled muscle stimulator.

The controller was simple. Muscles were activated reciprocally at either full on or full off with the choice of quadriceps or hamstrings activation depending on the sign of the tracking error. Control stability and tracking accuracy were provided by modulating the brake. The brake was initially off and then activated when the desired position was reached, providing a "wall" to stop the leg motion. The location of this artificial wall moved with the target track and as long as there was sufficient muscle torque to keep the leg pushed against the wall, controlled tracking could be achieved. To soften the impact against the wall and to prevent contact instabilities, the brake damping was ramped up to its maximum value over a small region of tracking trajectory error. The control task was to track sinusoidal and pseudo-random position trajectories with frequencies up to 1.0 Hz. The target track amplitude ranged from zero to 60° where 90° corresponded to the leg in full extension.

Fig. 6 displays results for tracking a random trajectory and compares the controlled-brake strategy with open-loop, feed-forward control and with closed-loop proportional-derivative (PD) control (see Durfee and Hausdorff, 1990, for details).

Fig. 7 demonstrates the performance of the controllers for tracking a 0.25 Hz sine wave but with a fatigued muscle. The open-loop and PD controllers show reduced performance levels because their control gains were calibrated when the muscle was fresh.

Discussion

The experimental results demonstrate the potential for the controlled-brake approach to provide excellent tracking despite wide changes in muscle properties. Further, the design of this controller requires no knowledge of muscle properties other than that they can provide torque. Although having the muscles push against the rigid wall does waste metabolic (but not mechanical) energy, the controller is still able to operate for extended periods so long as the muscles are capable of providing force. Further work is required, however, in developing controllers which take advantage of information from sensors mounted to the orthosis and from a knowledge of muscle properties to minimize muscle metabolic energy.

The primary disadvantage of the controlled-brake approach is the need to design an orthosis which not only will be reliable and functional, but also will meet stringent consumer standards of weight, cosmesis and ease-of-use. An ongoing feasibility study is examining whether the controlled-brake concept extends to controlling standing and gait in ambulating paraplegics and is also exploring preliminary mechanical designs for realistic controlled-brake orthoses.

Conclusions

This paper has presented three approaches for control of standing and gait in neural prosthesis systems where each approach requires a different strategy for muscle model complexity. Since it is generally true that the better the model, the better the control, the first approach calls for a relatively detailed model of stimulated muscle which accounts for non-linear force-length, force-velocity and force-activation properties. Methods for rapidly parameterizing these relations were described. The second approach calls for a less detailed muscle model, but requires that errors between the model and the real system can be given an upper bound. With this information, standard and adaptive forms of non-linear sliding controllers were developed which from simulation results show promise for neural prosthesis applications. The third approach requires no muscle model at all because the control task is shifted to regulating the output of a controlled-brake orthosis. Preliminary experimental studies demonstrated that this hybrid approach may be the most reliable way to control a neural prosthesis gait system, but has the cost of forcing the user to wear a potentially bulky and unwieldy orthosis.

Any practical system must be capable of handling disturbances such as a muscle quick stretch that might be encountered when the leg hits an obstacle. The detailed model is parameterized only for slow, mild kinematic and stimulation inputs so that the controller must interpret the additional input as a pure external disturbance. If a bound can be placed on that disturbance, then the sliding controllers presented in the second approach will maintain their stability. The hybrid orthosis would be able to reject the disturbance if its level were less than the peak holding torque of the controlled brake. All controller designs should, however, take advantage of the spring-like properties of muscle when encountering quick length stretches as the CNS does when developing physiologic motor control programs.

Clinical applications of neural prosthesis systems are still in their infancy (despite having been demonstrated in laboratory systems for many years) and although control is recognized as one of the major problems which must be solved, the proper control strategy remains unclear. It is likely, however, that some combination of the three approaches described here will prove to be useful in future functional systems. For example, information from the muscle modeling studies may be used in designing improved controllers for the hybrid orthosis system. It is also likely that enhanced performance of the controllers can be provided by understanding and incorporating the strategies used by the CNS for control of standing and gait.

Acknowledgements

This work was supported by the Whitaker Foundation, the Whitaker Health Sciences Fund, the W.M. Keck Foundation, and by BRSG 2 S07 RR07047-23 awarded by the Biomedical Research Support Grant Program, Division of Research Resources, National Institutes of Health. Simulations and experiments were performed in the Eric P. and Evelyn E. Newman Laboratory for Biomechanics and Human Rehabilitation at MIT, in the Whitaker College at MIT, and in the West Roxbury Veterans Administration Medical Center, West Roxbury, Massachusetts. Significant contributions were made by MIT graduate students Karen Palmer, Jeffrey Hausdorff, Karon Maclean, Daniel DiLorenzo and Richard Willis.

References

Asada, H. and Slotine, J. (1986) *Robot Analysis and Control,* Wiley-Interscience, New York.

Crago, P., Lemay, M. and Liu, L. (1990) External control of limb movements involving environmental interactions. In: J. Winters and S. Woo (Eds.), *Multiple Muscle Systems,* Springer, Berlin.

Craig, J. (1986) *Introduction to Robotics,* Addison-Wesley, New York.

Cybulski, G., Penn, R. and Jaeger, R. (1984) Lower extremity functional neuromuscular stimulation in cases of spinal cord injury. *Neurosurgery,* 15(1): 132 – 146.

Durfee, W. and DiLorenzo, D. (1990) Linear and nonlinear approaches to control of single joint motion by functional electrical stimulation. In: *Proceedings of the 1990 American Control Conference.*

Durfee, W. and Hausdorff, J. (1990) Regulating knee joint position by combining electrical stimulation with a controllable friction brake. *Ann. Biomed. Eng.,* 18: 575 – 596.

Durfee, W. and MacLean, K. (1989) Methods for estimating isometric recruitment curves of electrically stimulated muscle. *IEEE Trans. Biomed. Eng.,* 36(7): 654 – 667.

Joyce, G., Rack, P. and Westbury, D. (1969) The mechanical properties of cat soleus muscle during controlled lengthening and shortening movements. *J. Physiol. (Lond.),* 204: 461 – 474.

Kralj, A., et al. (1983) Gait restoration in paraplegic patients: a feasibility demonstration using multichannel surface electrode. *J. Rehab. Res. Dev.,* 20(1): 3 – 20.

Marsolais, E. and Kobetic, R. (1983) Functional walking in paralyzed patients by means of electrical stimulation. *Clin. Orthop.,* 175: 30 – 36.

McDonagh, J., et al. (1980) A commentary on muscle unit properties in cat hindlimb muscles. *J. Morphol.,* 166: 217 – 230.

Peckham, P. (1987) Functional electrical stimulation: current status and future prospects of applications to neuromuscular system in spinal cord injury. *Paraplegia,* 25: 279 – 288.

Slotine, J. (1984) Sliding controller design for non-linear systems. *Int. J. Control,* 40(2): 421 – 434.

Slotine, J. and Coetsee, J. (1986) Adaptive sliding controller synthesis for nonlinear systems. *Int. J. Control,* 43(6): 1631 – 1651.

Slotine, J. and Li, W. (1991) *Applied Nonlinear Control,* Prentice Hall, Englewood Cliffs, NJ.

Winters, J. (1990) Hill-based muscle models: a systems engineering perspective. In: J. Winters and S. Woo (Eds.), *Multiple Muscle Systems,* Springer, Berlin.

Yamaguchi, G. and Zajac, F. (1990) Restoring unassisted natural gait to paraplegics via functional neuromuscular stimulation: a computer simulation study. *IEEE Trans. Biomed. Eng.,* 37(9): 886 – 902.

J.H.J. Allum, D.J. Allum-Mecklenburg, F.P. Harris and R. Probst
Progress in Brain Research, Vol. 97

Overview and critique of Chapters 34 – 36

Felix E. Zajac

Rehabilitation Research and Development Center (153), Veterans Affairs Medical Center, Palo Alto, CA 94304, and Biomechanical Engineering Program, Mechanical Engineering Department, Stanford University, Stanford, CA 94305-4021, U.S.A.

This session addressed three problems associated with functional electrical stimulation (FES) systems being developed to restore posture and gait to spinal cord-injured (SCI) persons. Together, all three problems prevent the routine clinical implementation of gait-restoration FES systems. These problems are: (i) how to reduce muscle fatigue in stimulated leg muscles (Boom et al.); (ii) how to conceptually design a real-time controller to coordinate the stimulation of muscles during SCI ambulation (Popovic); and (iii) how to reduce the metabolic energy consumed by SCI patients when they use FES to stand and ambulate (Kralj et al.). (The order in which the papers are discussed is reversed from the order presented.)

Boom et al. studied how the quadriceps muscles of paraplegics develop force and fatigue when excited with two distinct stimulus patterns. Continuous stimulation at maximal and sub-maximal intensities was one pattern. The other was intermittent stimulation (sequence of pulse trains) at maximum intensity. Each 10 min long isometric force trajectory resulting from either stimulus pattern could be described by a simple two-exponential equation (i.e., one exponential is related to the rise in force, and the other to the fall in force to an asymptotic level, which is a consequence of fatigue). The asymptotic force obtainable during continuous stimulation was found to increase with stimulus intensity. However, the rate of fatigue was unaffected by stimulus intensity. During intermittent stimulation, both the rate of fatigue and the asymptotic force (averaged over the total time the muscle is stimulated and unstimulated) were found to be unrelated to duty cycle. Importantly, the rate of fatigue was found to be slower during intermittent stimulation than during continuous stimulation. In fact, the asymptotic force attained during intermittent stimulation (100% stimulus intensity with a duty cycle of 50%) was found to be higher than the force reached during continuous stimulation at 100% intensity.

The development of FES systems depends critically on being able to stimulate paralyzed muscles with patterns that cause the rate of fatigue to be within acceptable limits. Boom et al. show that intermittent rather than continuous stimulation should be the preferred strategy. Indeed, it has been known for over two decades that sequential stimulation of different electrodes, which excite disjoint parts of a muscle (or a set of agonist muscles), is better than synchronous stimulation of the muscle(s). However, the number of available stimulation channels is one factor of many that limits sequential stimulation from being implemented. Perhaps a more important outcome of this study is that a simple equation has been found that describes the force trajectory, including the rate of fatigue. This equation may assist in the design of functional neuromuscular stimulation controllers. However, the constants in the equation are subject-specific. Thus, some kind of identification procedure and/or adap-

tive model-based reference controller will probably have to be included in the overall control design. Ideally, one wants to be able to predict force and fatigue to any stimulus pattern. At the moment, even with the data of Boom et al., such predictions are unachievable. Since the total number of stimulus pulses was fewer with intermittent stimulation, one hypothesis seemingly compatible with their data is that fatigue of electrically stimulated muscle depends on the average stimulus rate. That is, one wonders if the slower rate of fatigue observed during intermittent stimulation is just a consequence of a lower average stimulus rate.

Popovic presents a three-tiered hierarchical control scheme for restoring gait to paraplegics. The control of stimuli to muscles (the bottom tier) and volitional control (the top tier) are not discussed in this paper; however, the control of coordination of the different phases of the gait cycle (the middle tier) is. Finite-state control to coordinate the phases of the gait cycle is proposed because it is compatible with real-time computer control. A finite-state controller operates by processing sensory inputs into a few discrete levels and, by knowing what state it is currently in, assesses whether a change in state is necessary. The discretized outputs of a finite-state controller depend only on the current state of the controller. An example of a finite-state controller for FES-controlled gait is given. This ten finite-state controller processes twelve sensor inputs (foot contact forces, inertial orientation of the thighs, leg segmental velocities) and knowledge of its current state (what phase of the gait cycle it has been in) to determine if it must switch states (i.e., has the gait progressed sufficiently far that the body is entering into the next phase of the gait cycle and thus a switch in actuator control strategy (the bottom tier) is needed?). The six outputs correspond to what action is needed at the six joints (hip, knee and ankle of both legs). For example, the ipsilateral three outputs corresponding to the beginning of the swing phase of the ipsilateral leg are "flex the hip, flex the knee and flex the ankle". Neural networks were used to find how to weight each sensory input and the current state (i.e., to find the state transition matrix). Data from normal human subjects, braced to emulate how paraplegics ambulate with FES, were used to determine the finite-state controller "rules". Data, collected from a paraplegic ambulating with ankle-foot orthoses while six stimulated leg muscle groups and short crutches provided propulsion, were used to teach the neural network. Once taught, it was found that the neural network could control the stimulation pattern and the paraplegic could ambulate. Thus, the feasibility of using a finite-state approach to control FES gait was demonstrated.

Designing a FES controller to restore gait to paraplegics is difficult. Controlling bipedal robots to walk is also challenging. And compared to humans, robots have well-defined segments, joints and actuators. The design and development of a practical FES control system may require a novel approach rather than the "traditional" control engineering approach. Using finite-state control is an attempt at just this. The finite-state controller, one part of a hierarchical control structure, is easily implementable (e.g., the computer-implemented controller could be packaged into a small box). However, the actuator control system (the bottom tier) corresponding to each state (i.e., phase of the gait cycle) also has to be simple to be implementable. It appears that this is possible since the one paraplegic subject referred to in the paper was able to ambulate. However, the trade-offs in gait performance should more sensors, outputs or states be added or deleted needs to be investigated. Also, since paraplegic acceptability of a FES control system depends strongly on the metabolic energy demanded of the paraplegic and his achievable walking speed, this finite-state control system should be thoroughly evaluated by both computer simulations and paraplegic testing. It should also be kept in mind that this, or any other control system, has to assure that the paraplegic will fall with probability approaching zero. It would seem that a finite-state controller could be designed to predict falls and act accordingly (e.g., "fall states" could be defined and the corresponding output control strategies designed to lessen the impact of the fall, or perhaps even prevent a fall).

Kralj et al. briefly review the state-of-the-art in restoring gait to SCI patients with FES systems. It appears, at least in the foreseeable future, that the SCI person will have to use crutches, or a walker, to assist the stimulated leg muscles in providing balance and propulsion. Thus, this means that the crutch/FES-driven gait of a SCI person is fundamentally not bipedal, as it is when able-bodied persons walk, but rather quadrupedal. In fact, paraplegics who ambulate by using the FES system developed by the Ljubljana group employ a quadrupedal crawl gait, similar to the crawling gait of children. This gait is, unfortunately, very energy-consuming, though it is highly stable (i.e., static stability is maintained throughout the cycle because at least three of the four available support structures always contact the ground). Instead, Kralj et al. propose that FES systems be designed and paraplegics rehabilitated so that SCI persons would locomote with two of the other many different quadrupedal gait patterns. These statically unstable gait patterns (cf. the statically stable patterns paraplegics now use) are claimed to be high-speed compatible and energy-efficient.

The metabolic energy cost associated with FES gait systems, where crutches or a walker assist the paraplegic, is currently unacceptably high, and ambulation speed unacceptably slow. However, as Kralj et al. state, for a practical system to be soon available to paraplegics, it is unreasonable to expect passive assistive devices to be eliminated. Their proposed strategy to design the FES system and teach the paraplegic to locomote with a novel quadrupedal gait compatible with high propulsion speed and low metabolic energy expenditure is ingenious. Such a novel approach is highly commendable and the two proposed gait patterns seem reasonable. However, there are serious potential problems. One is that these gait patterns are statically unstable and the probability of falling may increase. As mentioned above, safety is an important issue. Also, the novel gait pattern may be difficult to learn, though success has been demonstrated with one SCI person. Also, will these patterns be so novel as to be unaesthetic? How much feedback control will be required for paraplegics to achieve high speed with these gait patterns? To conclude, Kralj et al.'s proposed strategy for designing a FES system to enable paraplegics to ambulate is conceptually very attractive. Much more work in engineering design, control and laboratory studies is needed to address its feasibility.

J.H.J. Allum, D.J. Allum-Mecklenburg, F.P. Harris and R. Probst
Progress in Brain Research, Vol. 97

CHAPTER 34

FES gait restoration and balance control in spinal cord-injured patients

Alojz R. Kralj[1], Tadej Bajd[1], Marko Munih[1] and Rajko Turk[2]

[1] *Faculty of Electrical and Computer Engineering and* [2] *University Rehabilitation Institute, University of Ljubljana, Ljubljana, Slovenia*

The status of gait restoration in spinal cord-injured patients by means of FES is reviewed and the main aspects are discussed. This introduction highlights the issues of balance control, stimulation sequence synthesis, and control of enhanced gait modes containing unbalancing. The use of statically unstable dynamic weight-transfer phases is important for enhanced gait modes. To show how this phase can be employed the mode of static balance currently used for FES-assisted four-point gait in paraplegic patients is discussed, and how this mode of gait can be converted to a semi-dynamic gait mode is described. The possibilities and consequences of such an approach are briefly discussed.

Key words: Functional electrical stimulation; Paraplegia; Balance control; Gait

Introduction

Since 1979, important advances have been made in locomotion restoration of spinal cord-injured (SCI) patients by means of functional electrical stimulation (FES). The methodology developed for FES-enabled standing-up, standing and sitting has demonstrated that reciprocal bipedal gait restoration in these patients was feasible (Kralj and Grobelnik, 1973; Kralj et al., 1979, 1980; Brindley et al., 1979; Marsolais and Kobetic, 1983; Petrofsky et al., 1983; Holle et al., 1984). Consequently, FES control combined with passive orthotic devices was developed and promising results emerged (Andrews, 1986; Popović et al., 1989; Hirokawa et al., 1990). Here, we briefly describe the state of the art of FES which has enabled locomotion function restoration in SCI patients, and draw attention on balance control, stimulation sequences synthesis and control of enhanced gait modes containing a dynamic weight-transfer phase. The analysis of FES-enabled gait indicates that patients predominantly rely on static stability, hand-controlled balance and generation of propulsion forces. Such a gait is energy-consuming, inefficient, slow and functionally very limited. To enhance functionality and increase speed, FES-stimulated muscles providing propulsion forces must be included in the gait cycle. This would yield efficient energy exchange among the body segments from potential to kinetic energy and vice versa. The latter can be accomplished only if dynamic transfer phases are inserted into the gait cycle. It is important to note that faster link velocities and a more vigorous gait may increase the stress and loading on body segments and joints, provoking, if rectifying measures are not taken, the development of secondary pathologies and possibly long-term destruction of joints (Kralj et al., 1989, 1990a).

FES goals and accomplishments

A commonly accepted long-range goal of a FES system for locomotion restoration in SCI patients is to convert the wheel-chair bound to walkers who will

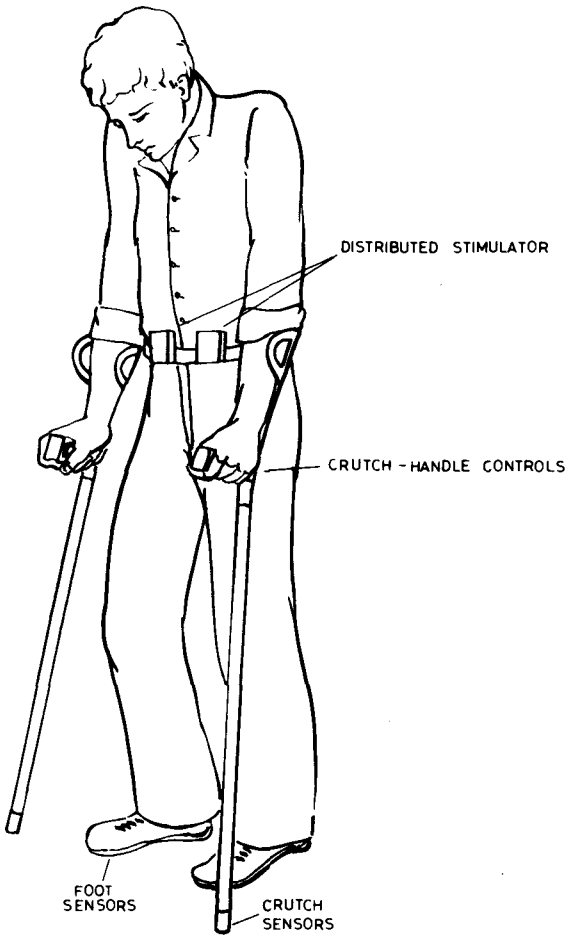

Fig. 1. FES system as proposed for reciprocal gait restoration in SCI patients. It is a distributed modular set-up including external sensors, crutch handle controls and sensory feedback.

occasionally still use the wheel-chair. The FES walking should be capable of negotiating rough terrain, including stairs, and permit work, sports- and entertainment-related activities. For the time being, there are no expectations for achieving active balance in these patients. Therefore, they are dependent on crutches or other balancing and partly supporting aids. Nevertheless, balance aspects are important. Balancing capabilities are not only related to dynamic but also to semi-dynamic gait. Balance control is crucial during standing-up and other transitions (Kralj et al., 1990). Semi-dynamic gait includes a brief tipping unstable-phase.

No matter which stimulation technology is used the current state of sensor development and associated control problems is inadequate for the immediate realization of total body implanted systems. For cosmetic reasons, a distributed modular FES system, such as that depicted in Fig. 1, is most likely to be developed and marketed once the problems of energy consumption and balance mentioned above are solved. For practical reasons chronic users will select implanted systems with an external control unit, while for patients selection, training and functionality testing, surface electrodes systems will be frequently applied. To date, more than hundred SCI patients have been supplied with different FES systems in Ljubljana (Kralj and Bajd, 1989). The types of system used for each injury level are summarized in Fig. 2. Here, two-channel stimulation is provided for standing only, four-channel stimulation for walker or crutch-assisted four-point walking, and six-channel stimulation mostly for research tests and demonstration purposes. About 10% of all admitted SCI patients are candidates for advanced FES rehabilitation (Jaeger et al., 1990). Only 50% of them are utilizing walkers and only 10% crutches. Many of them are using FES systems at their homes. Fig. 3 displays the wheel-chair-attached folding frame for standing and Fig. 4 illustrates patients using FES gait and

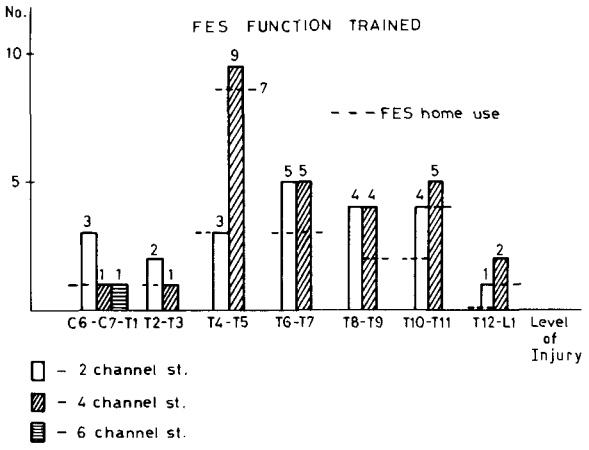

Fig. 2. Patients are grouped according to the type of FES stimulation employed and according to the level of spinal cord lesion.

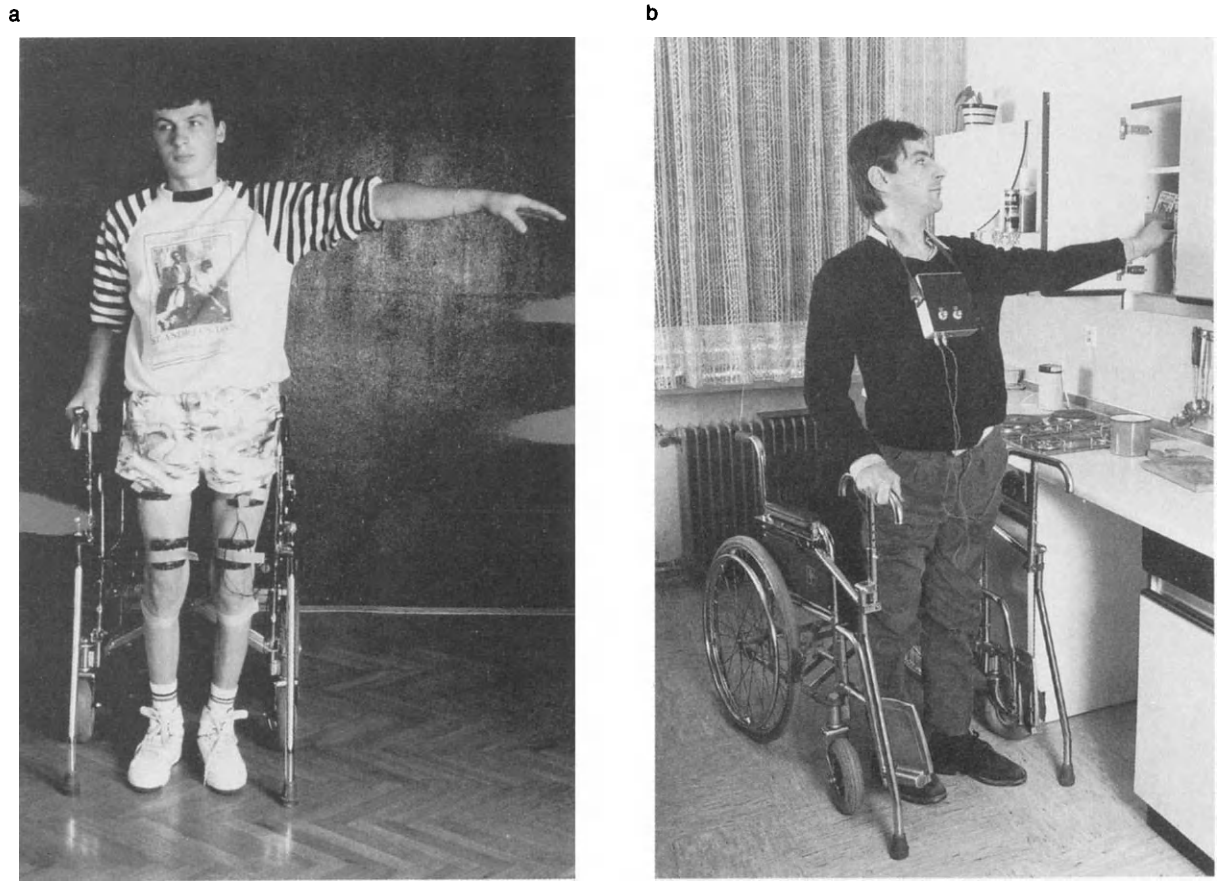

Fig. 3. Wheel-chair attached folding frame for standing. The frame is not interfering with regular wheel-chair functions, but does allow patients to stand-up and select locations for performing some functional tasks (*b*). In (*a*) the patient is demonstrating stability and the ability to use one hand for simpler manipulative tasks with smaller objects. This testing is performed for each hand and is included in regular FES training.

crutches for balance. With FES the time of standing is limited because of fatigue. Typical standing times range from several minutes up to an hour (Kralj and Bajd, 1989). Switching to a new posture, using intermittent FES activation of different muscles, substantially prolongs the standing time (Kralj et al., 1986). The characteristics of our simple FES gait are far from normal gait. In particular, the progression velocity is small, in the range of $0.1-0.4$ m/sec. Only in rare cases can velocities of 0.8 m/sec or higher be achieved (Marsolais and Kobetic, 1987). Because of energy inefficiency and static characteristics of gait the walking distance generally is limited to around 20 m. Several hundred meters can be achieved in some cases. Hybrid systems which rely on mechanical knee locking during standing and restricted ankle joint in plantar flexion submit easier balance. Patients can thus remain standing for nearly unlimited times (Andrews et al., 1989). The gait performance of patients using hybrid systems is improved in several ways compared to simple FES-enabled locomotion. The mechanical support spares FES muscle power and the energy expenditure is reduced. It is our contention that improved FES control could achieve the same improvements. Thus a hybrid system would only be indicated in cases where mechanical bracing is needed because of a partial peripheral lesion. In the present work, we

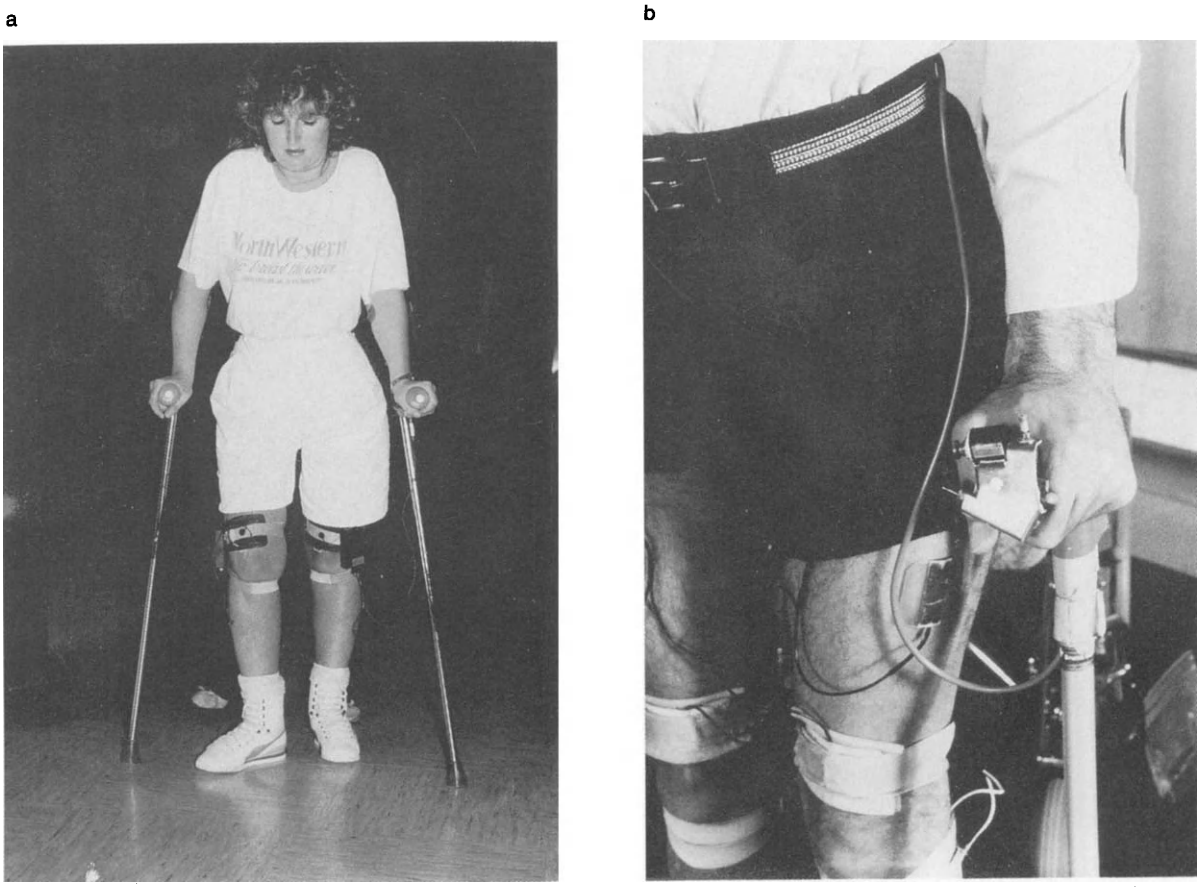

Fig. 4. Patient equipped for four-point walking using FES with crutches for balance assistance (*a*). In this case only a single switch as swing phase trigger is utilized. In (*b*) a more advanced but experimental crutch handle set of controls is displayed.

have focused our attention on these aspects related to the FES gait enhancement and on improved understanding of balancing control during FES-enabled gait.

The measurements of FES-enabled gait in SCI patients show very high energy consumption (Marsolais and Edwards, 1986), and consequently considerable inefficiency. This results in a very low endurance. The inefficiency of the gait is also a consequence of low progression speed. Typical results for our patients utilizing four channels of electrical stimulation are similar to the results obtained by other research groups. Four channels of FES are used as follows: two channels are used to stimulate the left and right quadriceps muscles, thereby providing knee locking during stance and double stance phases. The two remaining channels are utilized to evoke left and right side flexion withdrawal reflexes. The reflex-provoked movement is used for providing a swinging movement. The incorporation of reflex-triggered lower limb flexion into the FES-assisted gait cycle results in very simple hardware, reasonable patient control autonomy, and the lowest possible number of FES stimulation sites. This is the simplest possible FES-enabled gait in completely lesioned SCI patients. This approach is important as it proves that the preserved neural mechanisms of the pathologically organized and dissected spinal cord can be incorporated into the FES gait restoration scheme. Using surface electrodes to simply trigger the reflex has some disadvantages because the electrodes have to be ac-

curately positioned. In addition, habituation of the reflex causes variations in the flexing movements and is dependent on stimulation amplitude, elapsed time and stimulation timing. Our last ten years of FES developments for SCI patients were predominantly concerned with proving feasibility. Recently, the field has entered a stage of development for a chronically usable and marketable system, because FES is recognized as being a potential and promising rehabilitation modality. In spite of the disadvantages, simple gait is possible and numerous patients are using it daily (Kralj and Bajd, 1989). We are seeking to enhance four-channel FES gait using approaches described below.

Enhancement of FES enabled gait

With the four-channel FES system only bilateral m. quadriceps stimulation is used to provide knee joint stability during gait. The hip joint is stabilized by gravitational forces and through the opposing ligamentous locking of the hip joint. The ankle joint is stabilized by horizontal forces applied to the crutches by the hands. To preventing tipping, the patient adjusts the body position using the support forces at its hands. This posture can be simplified by considering the body as an inverted pendulum freely movable only at the ankle joint, neglecting trunk hyperextension movements. In Fig. 5, the supporting area is depicted for quiet standing with the actual locations of the ground force reaction vector (GRV). For quiet standing points 1 – 3 and 6 apply, and when FES of hip extensors/abductors occurred, the GRV was moved to points 4, 5, 7, 8 and 9. Similar relocations of the GRV can be accomplished by the patient himself if he exerts appropriate forces with his hands. If during such standing intermittent bilateral stimulation of the gastrocnemius and soleus muscles is added, the patient can stand up on his toes with a little learning, but he must assist the balance with his hands. Repeating this procedure makes the patient aware of when he should lean forward when standing on his toes. This experiment indicates that the patients is capable, when taught before a mirror, of using his hands to displace his GRV near to the edge of the heels or in front of the toes. SCI patients who sustained a complete lesion at the level of T-10 and upwards to T-4, all learn to adjust their balance during FES gait using either trunk movement or the hands to adjust forces exerted on supporting devices such as walkers or crutches. Their walking starts from a static balanced standing as depicted in Fig. 6, and the static stability is maintained throughout the walking cycle. This kind of static balance is characterized by GRV never leaving the support area during forward progression. The supporting area is rather large in the case of walking with crutches (Fig. 6*a*). During each single phase of walking the patient moves his ground support leg or crutch forward; however, the GRV is moved forward mostly during the four-point stance. After this is achieved, the patient moves the GRV forward in the new area of support by using the hands to push the body weight forward and to prepare the opposite

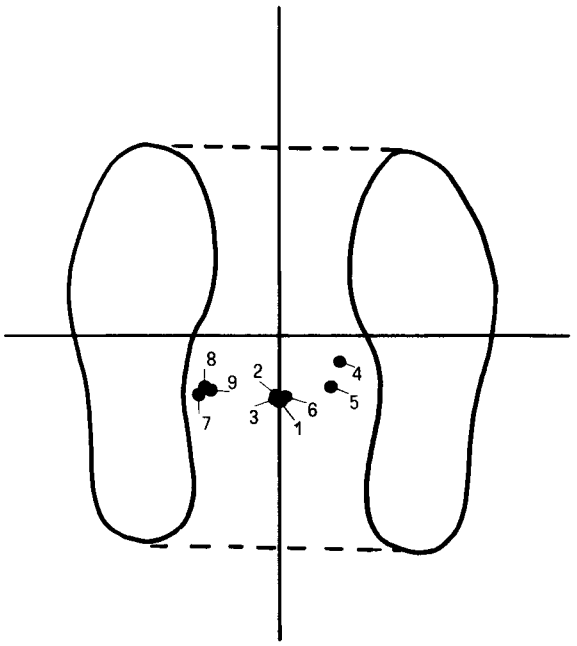

Fig. 5. Bilateral balanced erect standing with FES shown without balancing and support mean forces. Such standing has a support area which is similar to that of normals. During FES standing the patients make exclusive use of the safest central part of the support area.

leg for a step. Sometimes patients have difficulty to move a crutch or a leg. The reason is because they have not unloaded it properly.

Note that during the four-point stance the hands are used to push and move the body forward and thereby displace the GRV to its new location. Therefore we conclude that in such a gait propulsion is generated by the hands and remaining trunk muscle forces during the four-point support. Propulsion can also be generated during three-point contact when both crutches and only one leg are supporting the body. Already here we see that a propulsion force, generated, for instance, by plantar flexors stimulation, may substantially reduce the forces required by the hands and improve forward propulsion. A sequence of supporting area polygons formed by the legs and crutches during four-point gait is depicted in Fig. 7. The figure clearly illustrates the static balancing of the gait. The literature on quadrupedal locomotion (McGhee and Frank, 1968; McGhee and Kukner, 1969) indicates that theoretically 5040 modes of quadruped gait are possible, but only three ensure static stability at all times. Among these three gaits, only one is optimal as it maximizes the degree of static stability. This gait was named crawl gait. Fig. 7 is instructive as it demonstrates that SCI patients employ a crawl gait while walking. They are so afraid of falling that they select the most stable gait. The figure also indicates that – if provisions could be made to improve stability of hip joint, and a regime of different gait training utilizing an improved semi-dynamic stability was given – walking speed and energy consumption could be substantially enhanced. There is, in fact, a vast arsenal of possible gait modes to select from considering a four-point gait. Measurements of the GRV displacement with time using especially equipped force shoes (Kljajić and Krajnik, 1987) confirmed this statement. In patients, the GRV movement range is small and shows total unloading of the leg, well before the GRV reaches a boundary of the area of support (see Figs. 7 and 8). Confirmation of this finding is evident from the narrow vertical force standard deviation in Fig. 8, indicating a rather limited variational and balancing capability. A gait with minimal adaptivity and flexibility

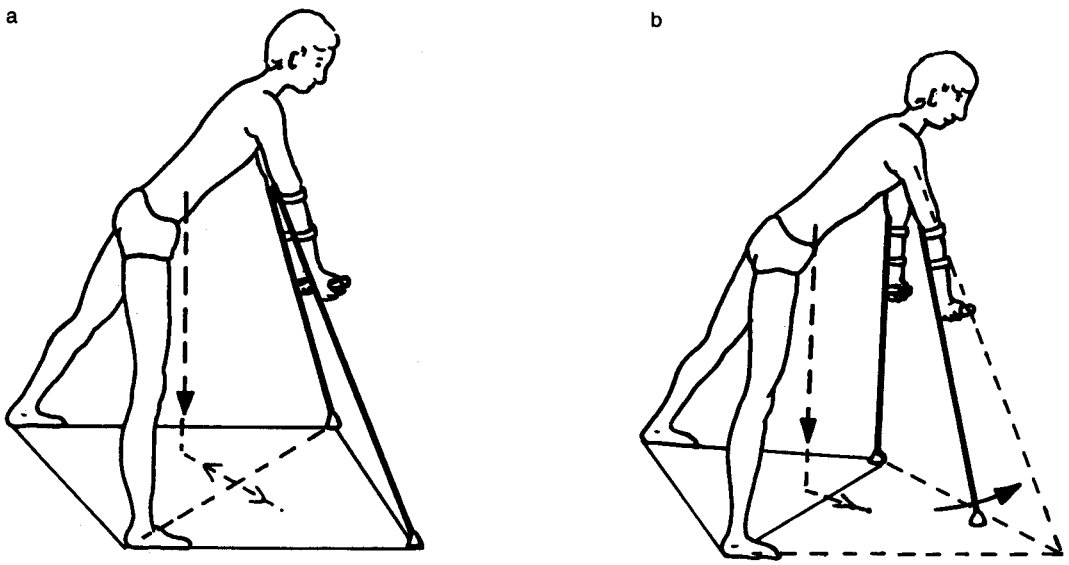

Fig. 6. Support area formed by the four-point standing. The patient is able to move the GRV within the support area using hand forces and trunk leaning to the left or right. After, for example, the crutch is moved forward, the GRV remained within the support area depicted in (*b*); the GRV position changes when the trailing leg is moved forward.

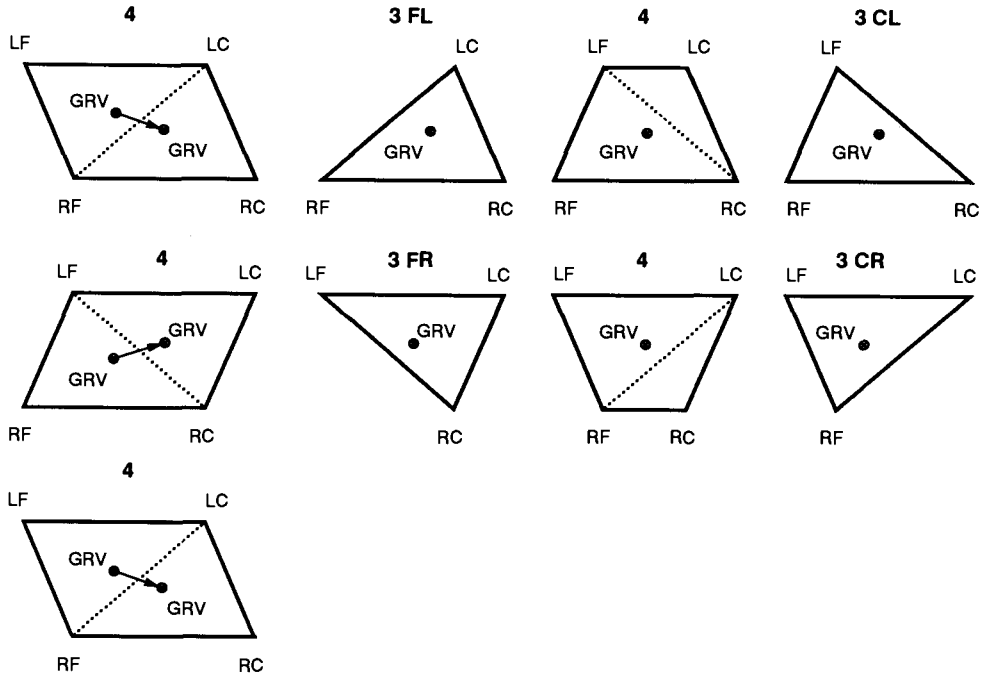

Fig. 7. Graphic presentation of gait sequences and the support areas formed during four-point FES gait. GRV is nearly stationary and relocates forward mostly during the four-point standing phase.

results. If one is interested in converting the statically balanced gait into a dynamically balanced gait, two main requirements have to be ensured: (1) active balance; and (2) for a brief time in the gait cycle the GRV should pass the boundary of an area (Raibert, 1986). Controlled falling is essential because during this time acceleration can take place, and with it potential energy can be converted into kinetic energy. After each brief period of controlled falling restabilization must take place. For this function either the FES muscle power at leg joints, or hand forces with proper crutch placement on trunk movements can be employed. There are several feasible solutions for ensuring effective stabilization by means of active balancing forces. For such gait four (or at least three) supporting points can be selected and therefore, this gait is characterized as quadrupedal. Three- or four-point support is crucial because then numerous gait modes are feasible, which presents a major advantage for SCI patients. Due to lower motor neuron damage some muscles are not available for electrical activation, and therefore the patient may have to be trained to use a different gait pattern. This selection process can only be effective when physical therapists and medical doctors advising the patient have the requisite biomechanical knowledge.

With the above goals in mind we are seeking theoretical evidence that such reciprocal quadrupedal locomotion modes exist. In addition, we are investigating the feasibility of developing a training methodology, considering indications and patients' acceptance (Bajd and Kralj, 1991). In Fig. 7, the assignment, 4, means that all four supporting elements are in contact with ground and accepting load; while 3 FR stresses that three supporting elements are in place but the right foot is unloaded and is in swing phase (Bajd and Kralj, 1991). Using such simple notation the expression for the gait in Fig. 7 can be written as:

$$4 - 3FL - 4 - 3CL - 4 - 3FR - 4 - 3CR - 4. \quad (1)$$

This expression highlights that each state is statically

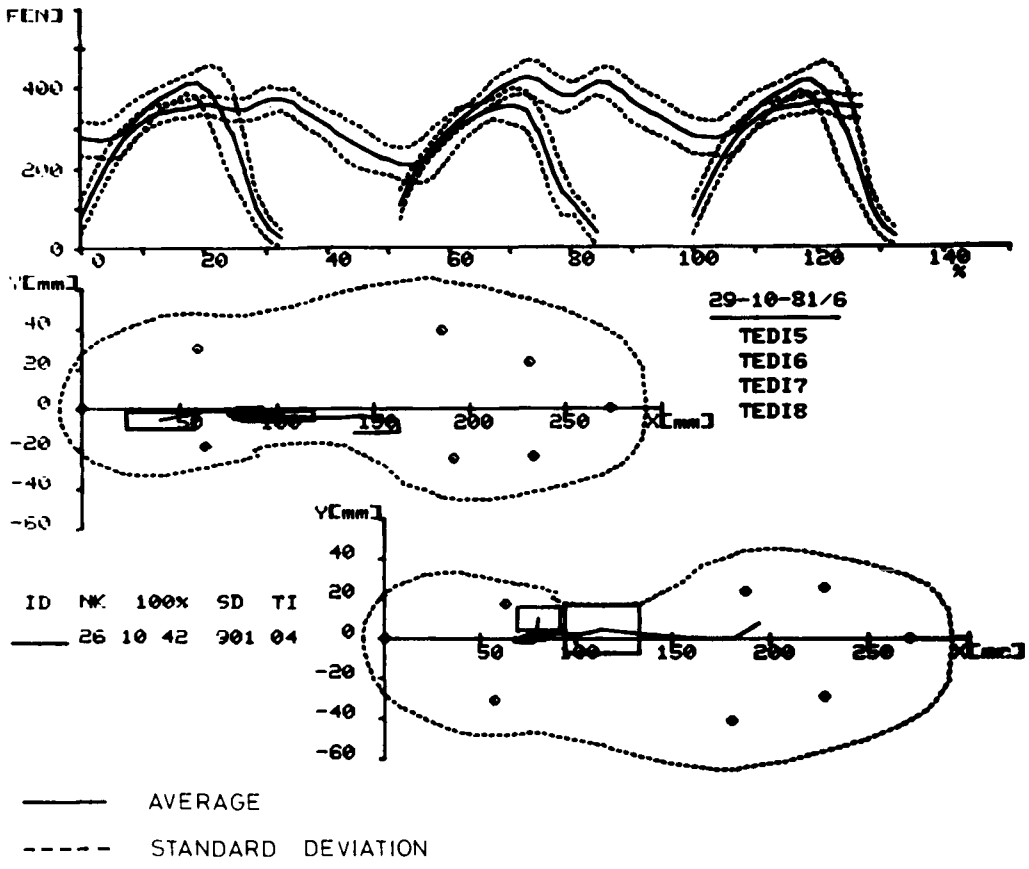

Fig. 8. Vertical component of GRV measured under each foot versus time and spatial movement of the GRV location under each foot. For the vertical component of reaction force the time dependence is displayed with corresponding standard deviation.

stable, and that there are intermittent 4-3-4 transitions. It is also interesting to compare expression (1) with that for swing-through gait in SCI patients. This gait is substantially faster compared to FES gait. Using our notation, expression (2) clearly indicates that in swing-through gait each static stable state is followed by an unstable falling state:

$$4 - 2F - 4 - 2C - 4 \qquad (2)$$

Fast gait modes have to incorporate unstable states for transitions, and restabilization states where stability is ensured and propulsion generated. Expression (2) suggests that we have to modify the four-point gait of expression (1) by reducing the number of states (compare (1) with (2)) and by inserting a dynamically stable tipping phase between restabilization states. The latter state can be a four-point or three-point support state. One logical way to reduce the number of stable states in expression (1) is to combine two stable three-point phases into one unstable two-point support phase. To synthesize such a reciprocal gait pattern either the 2R (2L) or 2CRFL (2CLFR) state can be selected. This reasoning has resulted in two gait patterns: the first we may call an ipsilateral (expression 3), and the second a contralateral reciprocal gait pattern (expression 4):

$$4 - 2R - 4 - 2L - 4 \qquad (3)$$

$$4 - 2CRFL - 4 - 2CLFR - 4 \qquad (4)$$

Because the three-point stance phase is also stati-

cally stable, and can provide adequate stabilization in some less-damaged SCI patients, the four-point phases in expressions (3) and (4) can be substituted with three-point stance phases.

The solution for FES gait described above provides a basic hope that FES gait in SCI patients can be substantially enhanced. It is also important to note that this solution does not preclude restoration of two-legged balance. Rather it provides the patient with an immediate adequate and reasonable stabilization solution with which he can recover balance lost during the dynamically performed unbalancing. This unbalancing is necessary for faster propulsion, increasing progression velocity and more efficient energy exchange. During the static stable states which are inserted between the unstable states the lost balance and potential energy can be restored. Energy can be stored by either increasing the body's potential energy or during the unbalancing phase by accelerating the movement. The latter places increased demands on stabilization. There is a tight association between increased stabilization, actively controlled locking of joints and sensory feedback. Attention to all three aspects of this association may permit the tightly prescribed placement of legs and crutches to be relaxed so that they can be moved more freely to more distant locations, resulting in increased mobility and adaptability. Here, we do not discuss the underlying control issues. The theoretical work by Raibert (1986) provides evidence that even though the dynamics of a segmented and inherently unstable system can be rather complicated, the control rules that use this dynamics can be simple. This leaves the hope that a patient's autonomy will not be reduced with the introduction of the proposed enhanced gait modes. It is also worth pointing out that a series of preprogrammed gait sequences also limits the patient's autonomy, his flexibility and perhaps his functionality. For this reason prestored gait sequences should be avoided.

Conclusions

The restoration of reciprocal bipedal gait in SCI patients using FES is in its current state of development and technology far from being able to restore normal upright balance and stability without depending on supplementary aids such as crutches or walkers. From this point of view, FES-restored gait in SCI patients must be treated as a quadrupedal gait mode. The numerous possibilities already presented in the literature (McGhee and Kukner, 1969) are the most promising for FES explored here. Our findings indicate that SCI patients, while in FES-assisted three-point or four-point stance, are able to balance and maintain upright stability. Our findings also indicate that the current FES-restored gait relies on static stability and can be characterized as quadrupedal crawl gait, which is slow and energy-demanding. Our findings highlight the possibility of including the dynamic transfer phase to change gait from a static to a semi-dynamic mode. The static equilibrium achieved before and after each dynamic transfer ensures sufficient stability. The walking pattern can be considered as simple dynamic gait displaying all the attributes of energy exchange and conversion, and higher progression speed with capabilities of negotiating rough terrain. Further research should focus on the requirements of the unbalancing phase, generation of propulsion by FES muscles, the transfer of energy among segments, the necessary stabilization processes, and training acquired for patients to master the proposed enhanced and dynamic gait.

Acknowledgements

The authors extend their appreciation and acknowledge financial support from the Ministry of Science of Slovenia and from the U.S. Department of Education, National Institute on Disability and Rehabilitation Research, Washington D.C., U.S.A., Grant No H 133G00151.

References

Andrews, B.J. (1986) A short leg hybrid FES orthosis for assisting locomotion in SCI subjects. In: *Proceedings of the Second Vienna International Workshop Functional Electrostimulation, Vienna, Austria,* p. 311.

Andrews, B.J., Barnett, R.W., Phillips, G.F., Kirkwood, C.A.,

Donaldson, N., Rushton, D.N. and Perkins, T.A. (1989) Rule-based control of a hybrid FES orthosis for assisting paraplegic locomotion. *Automedica,* 11: 175 – 199.

Bajd, T. and Kralj, A. (1991) Four-point walking pattterns in paralyzed persons. *Basic Appl. Myol.,* 1: 95 – 100.

Brindley, G.S., Polkey, C.E. and Rushton, D.N. (1979) Electrical splinting of the knee in paraplegia. *Paraplegia,* 16: 428.

Hirokawa, S., Grimm, M., Le, T., Solomonow, M., Baratta, R., Shoji, H. and D'Ambrosia, R. (1990) Energy consumption in paraplegic ambulation using the reciprocating gait orthosis and electric stimulation of the thigh muscles. *Arch. Phys. Med. Rehab.,* 71: 687 – 694.

Holle, J., Frey, M., Gruber, H., Kern, H., Stöhr, H. and Thoma, H. (1984) Functional electrostimulation of paraplegics – experimental investigations and first clinical experience with an implantable stimulation device. *Orthopaedics,* 7: 1145.

Jaeger, R.J., Yarkony, G.M. and Roth, L.L. (1990) Estimating the user population of simple electrical stimulation system for standing. *Paraplegia,* 28: 505 – 511.

Kljajić, M. and Krajnik, J. (1987) The use of ground reaction measuring shoes in gait evaluation. *Clin. Phys. Physiol. Meas.,* 8: 133 – 142.

Kralj, A. and Bajd, T. (1989) *Functional Electrical Stimulation: Standing and Walking after Spinal Cord Injury,* CRC Press, Boca Raton, FL.

Kralj, A. and Grobelnik, S. (1973) Functional electrical stimulation – a new hope for paraplegic patients. *Bull. Prosth. Res.,* 75: 10 – 20.

Kralj, A., Bajd, T., Turk, R. and Benko, H. (1979) Paraplegic patients standing by functional electrical stimulation. In: *Digest 12th Int. Conf. Med. Biol. Eng., Jerusalem, Israel,* p. 59.3.

Kralj, A., Bajd, T. and Turk, R. (1980) Electrical stimulation providing functional use of paraplegic patient muscles. *Med. Prog. Technol.,* 7: 3.

Kralj, A., Bajd, T., Turk, R. and Benko, H. (1986) Posture switching for prolonging functional electrical stimulation standing in paraplegic patients. *Paraplegia,* 24: 221 – 230.

Kralj, A., Bajd, T. and Turk, R. (1989) FES control and secondary pathology development. *Proceedings of the Osaka International Workshop on Functional Neuromuscular Stimulation, Osaka,* pp. 113 – 126.

Kralj, A., Bajd, T. and Munih, M. (1990a) Model based FES control utilizing formal and natural synthesis of muscle activation. *Advances in External Control of Human Extremities, Dubrovnik,* pp. 55 – 66.

Kralj, A., Jaeger, R.J. and Munih, M. (1990b) Analysis of standing-up and sitting-down in humans: definitions and normative data presentation. *J. Biomech.,* 23: 1123 – 1138.

Marsolais, E.B. and Edwards, B.G. (1986) Energy cost of walking and standing with functional neuromuscular stimulation and long leg braces. *Arch. Phys. Med. Rehab.,* 69: 243 – 249.

Marsolais, E.B. and Kobetic, R. (1983) Functional walking in paralyzed patients by means of electrical stimulation. *Clin. Orthop.,* 175: 30.

Marsolais, E.B. and Kobetic, R. (1987) Functional electrical stimulation for walking in paraplegia. *J. Bone Jt. Surg.,* 69A: 728 – 733.

McGhee, R.B. and Frank, A.A. (1968) On the stability of quadruped creeping gaits. *Math. Biosci.,* 3: 331 – 351.

McGhee, R.B. and Kukner, M.G. (1969) On the dynamic stability of legged locomotion system. In: M.M. Gavrilović and A.B. Wilson Jr. (Eds.), *Advances in External Control on Human Extremities,* Yugoslav Committee for Electronics and Automation, Belgrade, pp. 431 – 442.

Petrofsky, J.S., Heaton, H.H. and Phillips, C.A. (1983) Outdoor bicycle for exercise in paraplegics and quadriplegics. *J. Biomed. Eng.,* 5: 292.

Popović, D., Tomović, R. and Schwirtlich, R. (1989) Hybrid assistive system: the motor neuroprosthesis. *IEEE Trans. Biomed. Eng.,* 36: 729 – 737.

Raibert, H. (1986) *Legged Robots that Balance,* MIT Press, Cambridge, MA.

J.H.J. Allum, D.J. Allum-Mecklenburg, F.P. Harris and R. Probst
Progress in Brain Research, Vol. 97

CHAPTER 35

Finite state model of locomotion for functional electrical stimulation systems

Dejan B. Popović

Faculty of Electrical Engineering, University of Belgrade, Belgrade, Yugoslavia, and Division of Neuroscience, University of Alberta, Edmonton, Alberta, Canada

A finite state model of locomotion was developed to simplify a controller design for motor activities of handicapped humans. This paper presents a model developed for real time control of locomotion with functional electrical stimulation (FES) assistive systems. Hierarchical control of locomotion was adopted with three levels: voluntary, coordination and actuator level. This paper deals only with coordination level of control. In our previous studies we demonstrated that a skill-based expert system can be used for coordination level of control in multi-joint FES systems. Basic elements in this skill-based expert system are production rules. Production rules have the form of *If – Then* conditional expressions. A technique of automatic determination of these conditional expressions is presented in this paper. This technique for automatic synthesis of production rules uses fuzzy logic and artificial neural networks (ANN). The special class of fuzzy logic elements used in this research is called preferential neurons. The preferential neurons were used to estimate the relevance of each of the sensory inputs to the recognition of patterns defined as finite states. The combination of preferential neurons forms a preferential neural network. The preferential neural network belongs to a class of ANNs. The preferential neural network determined the set of finite states convenient for a skill-based expert system for different modalities of locomotion.

Key words: Functional neuromuscular stimulation; Human gait; Fuzzy-logic controllers; Neural networks

Introduction

Functional electrical stimulation (FES) can be used for locomotion of paralyzed humans with limited success (Kralj and Bajd, 1989; Popović, 1992). Problems in spinal cord injury (SCI) patients treated with FES arise from: muscle fatigue, reduced joint torques generated through FES compared to volitionally activated torques in healthy subjects, modified reflex activities, spasticity, functional and joint contracture and osteoporosis. Recent FES systems are limited in duration of their use by muscle fatigue.

It is impossible to control redundant muscle groups in the same way that the central nervous system (CNS) does this. A spinal cord injury results in modified reflexes, so numerous unexpected situations may occur, resulting in inappropriate antagonist contractions. In addition, these SCI changes are responsible for the reorganization in tonic and phasic properties of different muscle groups, i.e., spasticity. In some applications it is very difficult to generate functional movements due to these changes. For example, we have not been able to generate functional ambulation in some patients due to so called "functional contracture". A functional contracture relates to lack of performance because one joint movement imposes a movement in its neighboring joint by shortening of two joint muscle-tendon systems. Joint contractures reduce the range of motion, and thus compromise the FES-activated functional movements.

Osteoporosis, normally found in SCI patients, may compromise the use of legs for support and may lead to stress fractures. Speculations that patterned electrical therapy can decrease osteoporosis, have not been verified.

To improve effects of FES systems for locomotion combined use of a mechanical brace and FES for gait restoration was suggested. These systems are known as hybrid assistive systems (HAS) or hybrid orthotic systems (HOS) (Schwirtlich and Popović, 1984; Andrews and Baxendale, 1986; Popović et al., 1989; Solomonow, 1992), but the locomotion was not improved sufficiently to make up for the added complexity of the system. Mechanical braces were applied only as an augmentation of FES systems. This augmentation related mostly to the safety and prevention of pathological events during standing and gait. However, HAS may be expected to fulfil two ambitious goals: (1) extend an inadequate step length by machine intervention; and (2) transform the slow, quasi-static, FES-generated ambulation into a genuine dynamic process (Tomović et al., 1990; Popović et al., 1991).

One of basic limitations for effective rehabilitation of locomotor functions is inadequate external control with man-machine systems. This paper deals only with control issues for FES and HAS systems for locomotion.

To develop a control method it is necessary to generate a model of the system. An engineering approach is to generate a human body model and prescribe desired motion of this skeletal system. Human body models for standing and locomotion studies are multi-segmental rigid body systems with pin and ball joints. The number of joints can be as big as the number of degrees of freedom in an able human body. A multi actuator system has in addition joint torques (motors) or linear actuators (muscles) generating joint torques. This approach is important for a better understanding of the biomechanics of posture and movements, but it is not practical for externally controlled locomotion.

To simplify most of the models one should: (1) limit the number of joints, i.e., degrees of freedom, to number of variables which will be controlled externally; (2) limit the number of control outputs to the number of synergistic muscle groups; and (3) exclude soft tissue, viscosity and elasticity of tendons, ligaments, muscles and bones. These simplifications are often inappropriate for control.

Decomposition of the system into component subsystems is another feasible simplification of the model. Taking into account that an effective assistive system involves man as the decision maker, a hierarchical control structure can be selected with three levels from the top down: (1) voluntary level; (2)

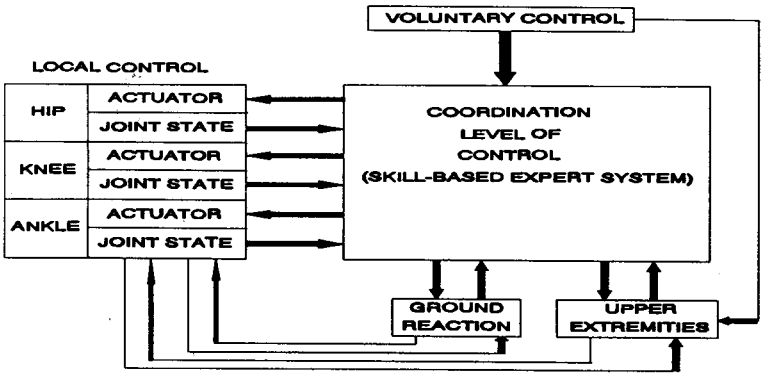

Fig. 1. Hierarchical control scheme for FES system. Coordination level of control is a skill-based expert system. This expert system uses production rules to generate output commands. Production rules have an *If – Then* structure and they are based on joint and actuator finite states. This *If – Then* structure means that if a pattern of joint and actuator states is recognized, then a corresponding mapping (action) to alter or sustain the pattern will be activated. The figure includes only three from six local controllers (three for each leg).

coordination level; and (3) actuator level. This division decomposes the system to several subsystems, but it includes strong coupling between subsystems (Fig. 1).

This paper pertains to the coordination level of control. Namely, once the coordination of the joint motions is successfully solved according to the task requirements, the synthesis of the actuator control may follow the standard state space procedure (Tomović et al., 1987, 1991; Das and McColumn, 1988). However, local control at the actuator level is not simple due to multi-muscle generation of joint torques (co-contractions of agonists and antagonists, double joint muscles, reflex activities) (Chizeck, 1992).

Finite state model of the locomotion

A formal model of locomotion may be derived in several ways (Tomović et al., 1991): (1) recording and analyzing movements and joint trajectories without interfering with the neuromuscular system. Such a modeling procedure is conveniently called the external approach; (2) integrating the computer input into the afferent paths of the motor control system so that the model is driven by natural sensory patterns. This is called the hybrid approach; and (3) integrating both the computer input and output into corresponding paths of the neural network responsible for the motor act. Such modeling is quite close to what may be called computer grafting.

We used the external approach, but model derivation was not the goal in itself. To define a finite state model, the following elements are needed:

$$X(j) = [x(1,j), x(2,j), \ldots, x(k,j)] \text{ (input)}$$

$$Y(j) = [y(1,j), y(2,j), \ldots, y(r,j)] \text{ (output)}$$

$$S = [s(j)], j = 0, 1, \ldots, n \text{ (internal states)}$$

where k is the number of inputs, r the number of outputs, and n the number of finite states. In addition a mapping is needed:

$$s(j) = \delta_j [s(j-1), X(j)] \text{ (state transition function)}$$

As presented in previous mapping (Tomović et al., 1990), a finite state depends on previous state and the present input. δ_j, $\{j = 1, 2, \ldots, n\}$ are mapping functions and they are invariant.

Finite state control was used for FES systems using a similar general approach (Popović, 1992). Hand-crafted *If – Then* expressions were used for simple on-off control of surface FES and HAS systems (Andrews and Baxendale, 1986; Tomović et al., 1990). There were trials to develop automatic design of production rules, but none have been proven to be more effective in comparison with hand-crafted rules.

The goal of this research was to design an automatic procedure for the detection of invariant features of locomotion and to provide information on the role and significance of each of the sensors' monitoring states of joints and actuators. The importance and role of each sensor is of special value. An effective, practical assistive system requires minimal hardware, thus minimal sensory base for reliable performance.

For analysis, we selected a set of sensors to monitor the state of the hip, knee and ankle joint in addition to sensors recording ground force reactions and displacement of segments from the vertical. The state of the joint was monitored using both angular position and angular velocity sensors. We monitored the activity of the main muscle groups responsible for leg movements with surface EMG electrodes. Ground reaction records, angular position of three joints per leg and displacement from the vertical of one segment per side are sufficient information to determine relative position of segments and absolute position in reference to the gravity vector.

This model is meant to simplify control scheme, yet still being effective for standing and limited locomotion of paralyzed humans. The first simplification is to categorize the joint as being in one of four discrete states: free, locked, flexion or extension. A joint state does not refer to an actuator state. It is possible to lock a joint with tetanic contraction of muscles, with co-contraction of several muscle groups, but also with no muscular activity in some positions.

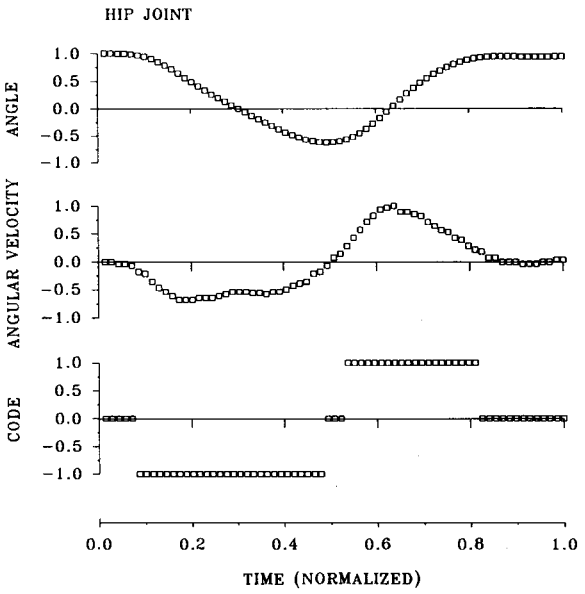

Fig. 2. Normalized hip angular velocity projection to the sagittal plane and corresponding coded values -1, 0 and 1 for level walking. The horizontal axis is normalized to one gait cycle.

A second simplification is the limitation of sensory input to only three states: flexion, extension and no rotation. These states can be described with joint angular velocities as:

$$|\dot{\alpha}| \leq \beta, \text{ no rotation; } \dot{\alpha} > \beta, \text{ extension;}$$
$$\dot{\alpha} < -\beta, \text{ flexion}$$

where β is a arbitrary small number.

This simplification allows real time operation and avoids drifts and noise in sensory inputs, such as joint angular velocities. It can be described as coding technique of normalized signals. If the absolute value of the normalized value was less than the chosen small parameter β the coded value was 0; if the value of the derivative was positive and greater than β the value was 1; and if the value was negative and less than $-\beta$ the coded value was -1, as presented in Fig. 2.

Ground force reactions are monitored in two zones, heel and toe in both legs. Matrix-type distributed sensors are designed to allow easy adaptation of the sensor to the individual shape of the foot. Normalized vertical components of ground reaction forces are presented in Fig. 3. Heel and toe ground reactions are coded. Value 1 is associated with an increase of force, -1 with a decrease of force, 0 to changes smaller then a small parameter β, and 2 when the force is zero. This last code is used to express exclusive disjunction function. (The terms disjunction and exclusive disjunction are explained in the Appendix.)

Sensors monitoring displacement from the

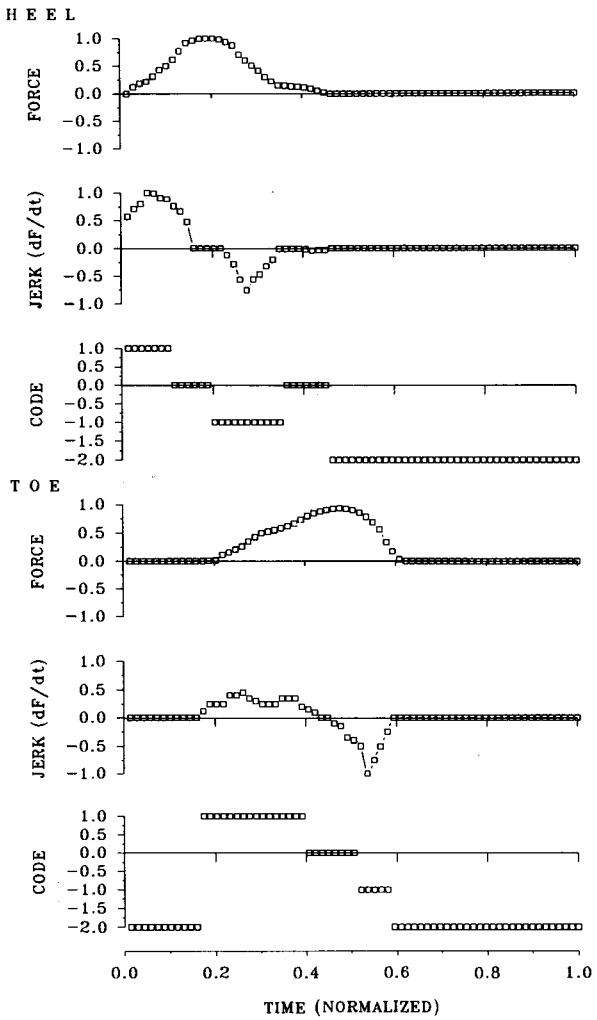

Fig. 3. Normalized heel and toe ground force reactions to maximal force, their derivatives and coded values for ground level walking. Normalized values are total ground forces including both normal and shear forces. Horizontal axis is normalized to one gait cycle.

gravity vector direction of the thigh are elements of the input vector. Due to experimental difficulties in designing a reliable practical sensor (Popović et al., 1991) we monitored the sign and small variations of the angle between the thigh and the gravity vector direction. The coded sensory input and the thigh angle are presented in Fig. 4.

Thus, the sensory system consists of twelve sensors: four force sensors, six angular velocity sensors and two angular sensors.

One side (ipsilateral) coded sensory inputs are shown in Fig. 5. Contralateral side inputs are shifted by 50% of the gait cycle.

We used preferential neural networks (Dujmović, 1991) to identify the relevance of each of sensory inputs for the pattern recognition of state transitions. This relevance of sensory input was used for coding. This technique can be considered as a sensitivity analysis of the system performance to the input variables with neural networks. This sensitivity analysis is of interest because of the high variability of inputs and their unstable influence on the efficacy of the locomotion.

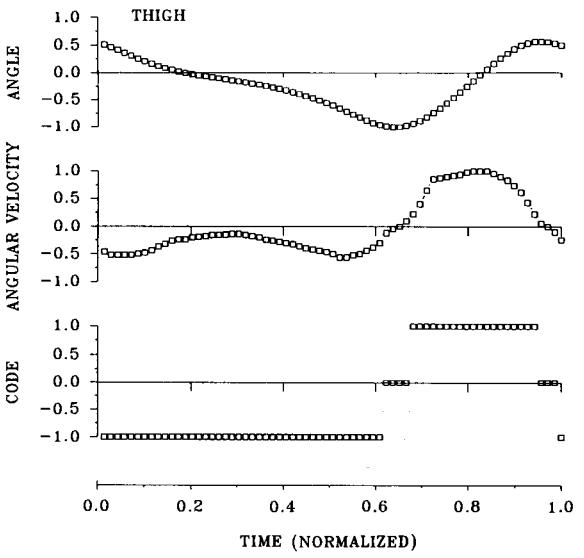

Fig. 4. Normalized displacement (to maximal inclination) of the thigh from the vertical for ground level walking. Coded values are associated with changes of the displacement. Horizontal axis is normalized to one gait cycle.

Preferential neural networks are based on fuzzy logic. The mathematical basis for preferential neurons is the continuous preference logic. Preferential neurons can perform several logic functions: quasi-conjunction (QC), quasi-disjunction (QD) and neutrality. A continuous preferential logic is defined as a mapping of input preferences $x_1, x_2, \ldots, x_n$ into an output preference y_0. In system evaluation some input preferences are required to affect the output preference more or less than other input preferences, and such a variable degree of importance can be easily adjusted using appropriate weights (W_1, $W_2, \ldots, W_n$ ($W_i > 0$, $W_1 + W_2 + \ldots + W_n = 1$)

To describe the meaning of preferences we will use an example. In heel contact (Table I), high preference is obtained for the heel and toe force sensors and the displacement angle from the vertical of the ipsilateral side, as well as the toe force and vertical sensors on the contralateral side. This means that for the heel contact pattern recognition these sensors are important, while other sensors with low preferences are not important. Weight function W_i, being from 0 to 1, is the measure of importance. When $W_i = 1$, preference is maximal and this implies conjunction; when $W_i = 0$, preference is minimal, thus the sensor is not needed (disjunction). For values between 0 and 1 we have quasi-disjunction and quasi-conjunction functions.

The basic elements of preferential neural networks (Dujmović, 1991) can be found in the Appendix.

Preferential neurons were used for sensitivity analysis of all determined gait invariants. This specific procedure was used for analyzing the relevance of the sensory inputs. Sensory relevance for each artificial reflex is expressed with its weight W_i, $i = 1, 12$ (Fig. 6).

The following procedure was used for determination of necessary data for training preferential neurons.

Able-bodied subjects were braced with different types of braces to limit the number of degrees of freedom (Popović, 1990). This was done to produce artificially a situation similar to one when a para-

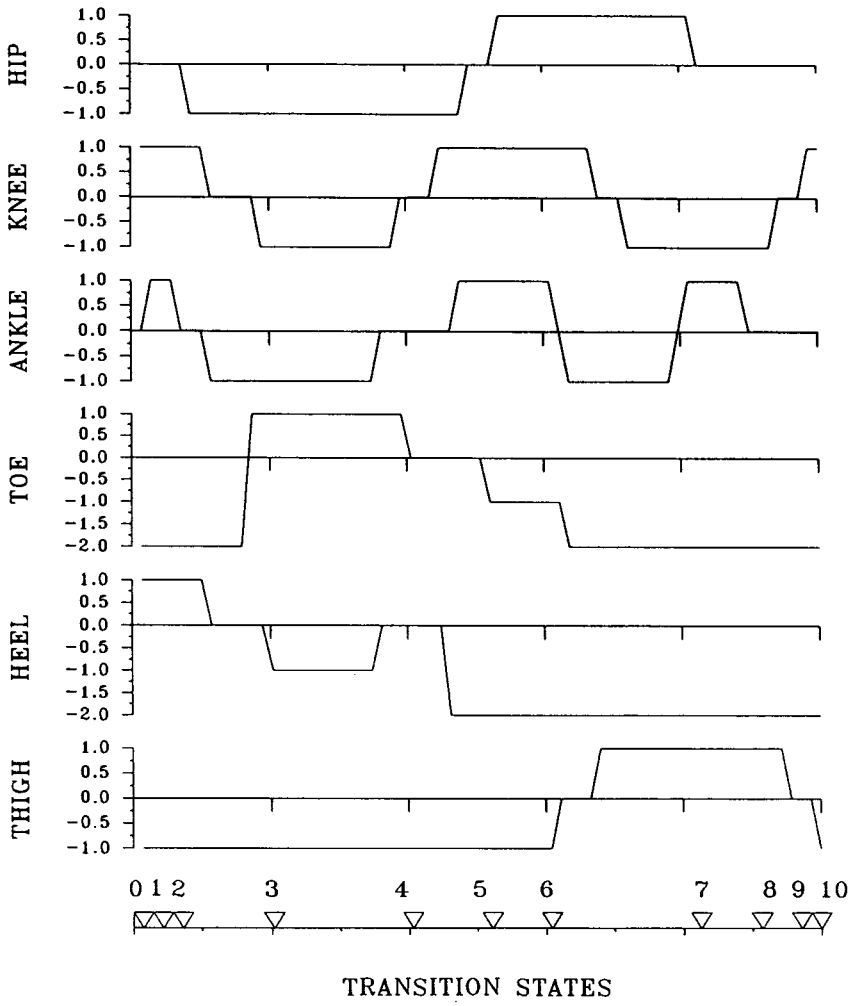

Fig. 5. Ipsilateral coded sensory input for level walking: (*a*) heel force; (*b*) toe force; (*c*) hip angular velocity; (*d*) knee angular velocity; (*e*) ankle angular velocity; and (*f*) thigh angular displacement from the vertical. Time axis is normalized to one gait cycle. Gait cycle is $T = 1.76$ sec, the stride length $l = 83$ cm. Notations $1 - 10$ correspond to state transitions, i.e., artificial reflexes detected with artificial neural network.

lyzed human walks with the FES or HAS systems. Subjects walked on the powered treadmill. The treadmill speed and slope inclination were randomly varied from 0.3 to 1.2 m/sec and from $-5°$ to $5°$ from the ground level. Subjects were trained to adapt to changes of speed and inclination of the slope and they were asked to try to alter their locomotion performance in all possible ways (circumduction, hip hiking etc.), trying to minimize cyclic motions. The type of the brace was selected knowing which externally controlled activities may be expected with a corresponding hybrid assistive system. Muscular activity was monitored with a portable eight channel device (Tepavac et al., 1992a) in quadriceps, hamstrings, gastrocnemius, tibial anterior muscle, gluteus medius en maximus in one side. The Penney and Giles (Tepavac et al., 1992b) system was used to monitor angular changes, and Interlink sensors (Tepavac et al., 1992b) to monitor ground reactions. Each step performance was judged as good or

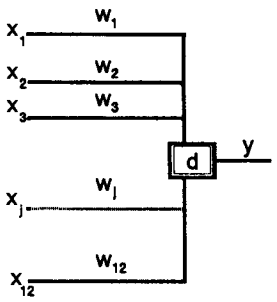

Fig. 6. Generalized conjunction-disjunction preferential neuron. This neuron was used to analyze the sensitivity of the output with variability of the sensory input; x_j are input functions, W_j are weight functions, d is the degree of quasi-disjunction, n is the number of inputs and y is the output. Input and output functions are given and the network provides the weight function as a result of supervised learning. Trained neuron gives the output for any given input, using determined weight functions.

bad. The judgement was made using the energy consumption measured by the uptake of the oxygen as reference. This judgement can be easily replaced with other measures, e.g., ground reaction forces of the upper extremities, heart rhythm etc.

Preferential neurons were trained using conventional unsupervised learning. A number of prescribed inputs were given with corresponding preference value for each input. These preferences were estimated using differences of measured values (forces, angles or angular velocities) to arbitrary selected values. These arbitrary selections were based on the effectiveness of locomotion. The effective gait was assessed using oxygen consumption measurement while the subject walked on the treadmill. A preference of the output was given with each combination of inputs. Each step was initially divided in the following phases: heel contact, flat foot, heel-off, toe-off, initial flexion, terminal flexion and heel contact. Each phase was studied to determine preference of sensors.

To explain these ideas, Table I shows the input range, input preference and output preference for recognition of a particular phase, namely "heel contact". The preference of each recorded sensory output was given as a measure of difference from the mean value for effective locomotion. Many trials of walking were recorded for estimation of preferences. It can be seen that some preferences are as low as 60%, and they still do not affect functional movements. This result was used for the selection of an appropriate sensory set for the real time operation. However, the reproducibility of sensors for ground

TABLE I

Sensory outputs of the ipsilateral and contralateral side; their preference and calculated weights for the heel contact pattern

	F_H/mg	F_T/mg	$d\alpha_H/dt$ (rad/sec)	$d\alpha_K/dt$ (rad/sec)	$d\alpha_A/dt$ (rad/sec)	α_T (rad)
Ipsilateral side	x_1	x_2	x_3	x_4	x_5	x_6
Range of sensory output	0.9 – 1	0.9 – 1	−0.5 to 0.5	−0.3 to 0.3	−0.3 to 0.3	> 0
Preference	0.9 – 1	0.9 – 1	0.6 – 1	0.6 – 1	0.75 – 1	1
Weight (W_i)	0.1	0.1	0.08	0.04	0.01	0.25
Contralateral side	x_7	x_8	x_9	x_{10}	x_{11}	x_{12}
Range of sensory output	0 – 0.25	0.8 – 1.1	> 0	> 0	> 0	< 0
Preference	0.7 – 1	0.8 – 1	0.9 – 1	0.7 – 1	0.9 – 1	1
Weight (W_i)	0.03	0.12	0.01	0.01	0.01	0.14

Preferences and weights are between 0 and 1. Weights W_1 satisfy the condition $W_1 + W_2 + \ldots + W_{12} = 1$. Results demonstrate that displacement of the thigh from the vertical, ipsilateral toe and heel forces and contralateral heel force are relevant for the recognition of the artificial reflex preceding ipsilateral heel contact. This information in conjunction with recognized contralateral support phase and ipsilateral swing phase form a conditional part (*If*) of a production rule. The number of function computations was 663, $d = -10.432$, $W_1 + \ldots + W_{12} = 0.100\text{E} + 0.1$, maximum error was $0.73\text{E} - 0.6$. Total preference was determined to be 0.95. The artificial neuron is presented in Fig. 6.

TABLE II

Gait invariants for the ground level walking determined by the preferential neural network

t/T (%)	0	3	7	21	39	56	60	83	88	93	100
Hip state	L	L	E	E	E	F	F	U	E	U	L
Knee state	U	L	E	L	L	U	F	U	E	E	E
Ankle state	X	X	X	X	X	E	F	F	X	X	X
δ_j	0	1	2	3	4	5	6	7	8	9	10

Abbreviations: L, lock state; U, free or unlocked state; E, extension; F, flexion; X, no action. T is the duration of gait cycle. δ_j are state transitions (switching moments), and they are arbitrary numbered. The state transition 10 is identical to the state 0. The "switching" timing (% of the gait cycle) relates to the gait pattern described in Figs. 2 – 4. Different gait patterns will have different "switching" moments.

reaction and detection of inclination of the thigh to the vertical is very important. This study showed that it is important to have some redundancy in sensors, to secure pattern recognition and execution of functional motions. The weights obtained are measures of relevance for a sensory input to the recognition of the finite state. The results presented in Table I relate to the recognition of the finite state before heel contact. Weights were determined for all other finite states. Weight for the same sensors vary for different finite states; thus, final aggregation requires the combination of preferential neurons to a preferential neural network.

Application of the preferential neural networks with energy consumption as a criterion for the gait quality suggests that for reliable simplified locomotion with a FES system, controlling knee and hip joints with a stable ankle joint, eight sensors provide the minimal sensory information: heel and toe force sensors, knee angular velocity and vertical sensor on the thigh. Simultaneously the increment for the ground force is 15% of body weight, sensivity of angular displacement from the vertical is 5°, and angular velocity decrement is 0.24 rad/sec.

Other bracings, like a knee-ankle-foot orthosis or reciprocal gait orthosis have other preferences and different sensory requirements. The method developed can be applied for any specific configuration of bracing and locomotion pattern.

Generalized conjunction-disjunction logic was used (see Appendix) with several preferential neurons for one joint. Each of preferential neurons is for one set of gait invariants as presented in Table II.

Table II summarizes the most important results of this preferential neural network application. The training of the preferential neural network was as follows. We provided many coded sensory patterns, recognized as finite states, and corresponding preceding finite states, which is called a training set. In our case the training set had 180 facts. These 180 facts were experimentally determined (locomotion of the trained braced able-bodied subject on a motorized treadmill described earlier). The input set appeared to the network as a jumble of unrelated facts, so it would never get a formulation of internal symbology for the overall problem. We used supervised learning. The "teacher" corrected the network's responses to a set of inputs. This correction was marked with preference of the output, knowing that the preference of the output has to be between minimal and maximal input preferences within each learning sequence. This supervised learning causes the network to construct an internal representation that captures the regularities of the data in a distributed and generalized way. This specific type of network is often called an associator or categorizer, because the network tried to associate input connections with a previously defined output category. The preferential neural network used belongs to a multilayered feed-forward system. The trained network

was tested supplying new facts, obtaining predictions for the network and analyzing output variables. An output variable is a number indicating which production rule has to be applied to get a functional moment.

Production rules were integrated using these gait invariants. Production rules have an *If – Then* structure, i.e., when a gait invariant is detected specific action of HAS is activated. The set of rules for level walking is given in Table II. Corresponding switching moments are detected with a sensory system integrated in the HAS. The duration T of the gait cycle (Popović et al., 1991) was estimated from the duration between normal ground force peaks detected with force sensors. Other switching moments are determined with the preferential neural network, and they correspond to different combinations of coded sensory inputs as presented in Fig. 5.

We tested this method in a paraplegic patient. The subject suffered a traumatic complete spinal cord injury at the T_{10} level. The patient used a six channel surface stimulator with hand switches and an ankle-foot orthosis. He was trained to independently walk with under-elbow crutches using the system. We instrumented the assistive system with tacho-generators in both knees and hips, pendulum potentiometers at both thighs and shoe insoles with force sensors to collect data for later automatic control. Recorded data were used to synthesize production rules. These production rules have been integrated into the automatic control and the subject regained a gait similar to the one when he was using hand switches. The system was found to be complex because sensors were positioned on a light brace similar to the self-fitting modular orthosis (Popović, 1990), but we demonstrated the feasibility of the suggested model and designed control.

In this case the inputs were coded information collected using artificial sensors attached to the extremities. We assume that this sensory data base can be expanded to natural sensors, such as muscles and nerves (Popović and Tomović, 1989; Hoffer and Haugland, 1992) in the near future which will complement a fully implantable stimulation system.

Conclusions

In this paper, a methodology has been outlined to derive a finite state model of locomotion using invariant patterns. The main goal of this contribution was to show how this formal modeling can be used for synthesis of the controller for locomotion in paralyzed humans. This formal modeling is proposed to simplify an extremely complex biomechanical system and allow automatic control of standing and locomotion in paralyzed humans.

Compared to other forms of gait descriptions, the finite state model encompasses invariant features of the analog level, identification of relevant sensory patterns, evolution of the locomotion processes in the state space and parametric data. By definition, finite state models of locomotion are meant only for the coordination level. The finite state model presented in this paper relies on an external approach. This approach may be integrated in a hybrid approach and computer grafting as well, thus taking into account incomparably richer information about the nature of motor control.

The use of artificial neural networks is suggested for off-line automatic design of a data base for the artificial reflex control. Preferential neurons, forming a multi-layered feed-forward network, with supervising learning, allow an interactive determination of gait patterns characteristic for each individual case.

Appendix

Preferential continuous logic and preferential neural networks have been developed for evaluation, comparison and selection of complex systems by Dujmović (1991). Basic facts about preferential neural networks necessary to understand the method applied are presented below.

Two fundamental connectives are quasi-conjunction (QC) and quasi-disjunction (QD). Quasi-conjunction implies the coincidence of input preferences; quasi-disjunction implies the replaceability and compensability of input preferences. This

means that a single low preference input in a quasi-conjunction connective will result with low output preference, while the single high input preference will give a high output preference if a QD connective neuron is used. The degree of coincidence of high input preferences is called the *conjunction degree*. The conjunction degree c can be symbolically denoted as follows:

$$x_0 = (W_1x_1 \Delta W_2x_2 \Delta \ldots \Delta W_nx_n)^c \quad 0.5 < c < 1$$

The value c is not an exponent, this is only a convenient way for systematic specification of all parameters affecting the aggregation of input preferences. The symbol Δ is called "and" operator in preferential logic. The conjunction degree c indicates the strength of the quasi-conjunction. Generally for c belonging to [0.5,1] quasi-conjunction satisfies the following conditions:

$$x_1 \wedge x_2 \wedge \ldots \wedge x_n < (W_1x_1 \Delta W_2x_2 \Delta \ldots \Delta W_nx_n)^c < (W_1x_1 + W_2x_2 + \ldots + W_nx_n)$$

The boundary conditions are:

$$(W_1x_1 \Delta W_2x_2 \Delta \ldots \Delta W_nx_n)^{0.5} = W_1x_1 + W_2x_2 + \ldots + W_nx_n$$

$$(W_1x_1 \Delta W_2x_2 \Delta \ldots \Delta W_nx_n)^1 = x_1 \wedge x_2 \wedge \ldots \wedge x_n = \min(x_1, x_2, \ldots, x_n)$$

In a similar way for QD, we have the degree of replaceability d belonging to interval [0.5,1], and following conditions:

$$x_0 = (W_1x_1 \nabla W_2x_2 \nabla \ldots \nabla W_nx_n)^d, \quad 0.5 < d < 1$$

The symbol ∇ is a disjunction operator. The degree of replaceability d demonstrates the strength of the QD. For d between 0.5 and 1 we have:

$$(W_1x_1 + W_2x_2 + \ldots + W_nx_n) < (W_1x_1 \nabla W_2x_2 \nabla \ldots \nabla W_nx_n)^d < x_1 \vee x_2 \vee \ldots \vee x_n$$

The boundary conditions are:

$$(W_1x_1 \nabla W_2x_2 \nabla \ldots \nabla W_nx_n)^{0.5} = W_1x_1 + W_2x_2 + \ldots + W_nx_n$$

$$(W_1x_1 \nabla W_2x_2 \nabla \ldots \nabla W_nx_n) = x_1 \vee x_2 \vee \ldots \vee x_n \max(x_1, x_2, \ldots, x_n)$$

These two functions are integrated, so a generalized conjunction-disjunction function reads:

$$x_0 = L(x; q; W) = (W_1x_1 \Diamond W_2x_2 \Diamond \ldots \Diamond W_nx_n)^q$$

$$x = (x_1, x_2, \ldots, x_n), \; W = (W_1, W_2, \ldots, W_n), \quad 0 \le q \le 1$$

The symbol q is called the degree of compensation. The operator $\Diamond$ is for an *and/or* logic function. A low degree of compensation indicates that a low value of any input preference cannot be easily compensated by high values of other input preferences. Similarly, a high degree of compensation means that a single high input preference can compensate low values of all other input preferences.

One of basic assumptions used in evaluation is that the subsystem and system preferences are between minimum and maximum input preferences:

$$\min(x_1, x_2, \ldots, x_n) \le (W_1x_1 \Diamond W_2x_2 \Diamond \ldots \Diamond W_nx_n)^q \le \max(x_1, x_2, \ldots, x_n)$$

For different values of q generalized conjunction-disjunction operation is reduced to classical conjunction ($q = 0$), QC ($0 < q < 0.5$), neutral function ($q = 0.5$), QD ($0.5 < q < 1$) and classical disjunction ($q = 1$). This is expressed as:

$$(W_1x_1 \Diamond W_2x_2 \Diamond \ldots \Diamond W_nx_n)^q$$

$$= x_1 \wedge x_2 \wedge \ldots \wedge x_n \qquad (q = 0)$$

$$= (W_1x_1 \Delta W_2x_2 \Delta \ldots \Delta W_nx_n)^q \quad (0 < q < 0.5)$$

$$= W_1x_1 + W_2x_2 + \ldots + W_nx_n \quad (q = 0.5)$$

$$= (W_1x_1 \nabla W_2x_2 \nabla \ldots \nabla W_nx_n)^q \quad (0.5 < q < 1)$$

$$= x_1 < x_2 \vee \ldots \vee x_n \quad (q = 1)$$

Acknowledgements

This work was partly supported by the Medical Research Council of Canada, Ottawa, Ontario, the Alberta Heritage Foundation for Medical Research, Edmonton, Alberta and the Research Funds of Serbia, Belgrade, Yugoslavia.

References

Andrews, B. and Baxendale, R. (1986) A hybrid orthosis incorporating artificial reflexes for spinal cord damaged patients. *J. Physiol.*, 380: 19.

Chizeck, H.J. (1992) Adaptive and nonlinear control methods for neuroprostheses. In: R.B. Stein, H.P. Peckham and D.B. Popović (Eds.), *Neural Prostheses: Replacing Motor Function after Disease or Disability*, Oxford University Press, London, pp. 298 – 328.

Das, P. and McColumn, G. (1988) Invariant structure in locomotion. *Neuroscience*, 25: 1023 – 1034.

Dujmović, J. (1991) Preferential neural networks. In: P. Antognetti and V. Milutinović (Eds.), *Neural Networks Concepts, Applications and Implementations, Vol. 2*, Prentice Hall, Inglewood Cliffs, NJ, pp. 109 – 143.

Hoffer, J.A. and Haugland, M.K. (1992) Signals from tactile sensors in glabrous skin: recording, processing and applications for restoring motor functions in paralyzed humans. In: R.B. Stein, H.P. Peckham and D.B. Popović (Eds.), *Neural Prostheses, Replacing Motor Function after Disease or Disability*, Oxford University Press, London, pp. 99 – 128.

Kralj, A. and Bajd, T. (1989) *Functional Electrical Stimulation for Standing and Walking*, CRC Press, Boca Raton, FL.

Popović, D. (1990), Dynamics of the self-fitting modular orthosis. *IEEE Trans. Robotics Automation*, 6: 200 – 208.

Popović, D. (1992) Functional electrical stimulation for lower extremities. In: R.B. Stein, H.P. Peckham and D.B. Popović (Eds.), *Neural Prostheses: Replacing Motor Function after Disease or Disability*, Oxford University Press, London, pp. 233 – 251.

Popović, D. and Tomović, R. (1989) Sensory driven control for gait restoration. In: J. Kawamura, T. Tamaki and K. Akazawa (Eds.), *Proceedings of the International Workshop on FNS, Osaka, Japan*, pp. 79 – 90.

Popović, D., Tomović, R. and Schwirtlich, L. (1989) Hybrid assistive system – neuroprosthesis for motion. *IEEE Trans. Biomed. Eng.*, 37: 729 – 738.

Popović, D., Tomović, R., Tepavac, D. and Schwirtlich, L. (1990) Control aspects of an active A/K prosthesis. *Int. J. Man-Machine Studies*, 35: 751 – 767.

Schwirtlich, L. and Popović, D. (1984) Hybrid assistive systems. In: D. Popović (Ed.), *Advances in External Control of Human Extremities VIII*, Yugoslav Committee for ETAN, Belgrade, pp. 23 – 32.

Solomonow, M. (1992) Biomechanics and physiology of a practical powered walking orthosis for paraplegics. In: R.B. Stein, H.P. Peckham and D.B. Popović (Eds.), *Neural Prostheses: Replacing Motor Function after Disease or Disability*, Oxford University Press, London, pp. 202 – 232.

Tepavac, D., Swenson, J., Stenehjem, J., Sarjanović, I. and Popović, D. (1992a) Microcomputer based portable long-term spasticity recording system. *IEEE Trans. Biomed. Eng.*, 39: 426 – 431.

Tepavac, D., Popović, M., Nikolić, Z. and Popović, D. (1992b) A portable gait assessment system for clinical evaluation of the gait. In: *First International FES Symposium, Sendai, Japan*, pp. 131 – 135.

Tomović, R., Bekey, G. and Carplus, W. (1987) A strategy for the synthesis of grasp with multifingered robot hands. In: *Proceedings of the 1987 IEEE Conference on Robotics and Automation, Vol. 3*, IEEE Press, pp. 85 – 99.

Tomović, R., Popović, D. and Tepavac, D. (1990) Rule based control of sequential hybrid assistive system. In: D. Popović (Ed.), *Advances in External Control of Human Extremities X*, Nauka, Belgrade, pp. 11 – 20.

Tomović, R., Anastasijević, R., Vučo, J. and Tepavac, D. (1991) The study of locomotion by finite state models. *Biol. Cybern.*, 63: 271 – 276.

J.H.J. Allum, D.J. Allum-Mecklenburg, F.P. Harris and R. Probst
Progress in Brain Research, Vol. 97

CHAPTER 36

Fatigue during functional neuromuscular stimulation

Herman B.K. Boom, Arjan J. Mulder and Peter H. Veltink

Biomedical Engineering Division, Faculty of Electrical Engineering, University of Twente, 7500 AE Enschede, The Netherlands

Discontinuous activation of muscle compartments is used to postpone the occurrence of fatigue during both normal activation and artificial stimulation. Periods of force development are interrupted by passive periods during which the muscle can recover. Since it is not known how fatigue parameters depend on intermittent stimulation, we compared fatigue generated by continuous electrical stimulation with fatigue resulting from intermittent stimulation schemes. T5 – T6 paraplegics participated in the experiments. Continuous stimulation generated a torque time course that can be described by a rising and a falling exponential time constant. The falling time constant ranged from 100 to 200 sec in all four patients and did not depend on the amplitude of the stimulation pulses. The torque developed at times greater than 250 sec was asymptotically constant and proportional to the maximal torque developed by each patient. Intermittent stimulation appears to postpone fatigue markedly. The torque time course developed in each on/off cycle again was a double exponential. In intermittent stimulation schemes average torque determines the muscle's performance. Therefore, average torque versus time was calculated from the intermittent stimulation data. These relations also follow a double exponential, accurately providing confident estimates of fatigue parameters. Fatigue caused average muscle torque to decline to a constant level which, for each patient, was uncorrelated with the duty cycle of the stimulation pattern. Between patients these levels varied from 18.3 ± 7.1 to 9.9 ± 4.3 (% of maximal torque ± standard error). These findings result in a model that could be of use in controllers for functional neuromuscular stimulation (FNS) that take into account non-stationarity caused by fatigue.

Key words: Muscle force; Fatigue; Functional neuromuscular stimulation

Introduction

The maintenance of posture has both spatial and temporal demands. One is upright stance, which should be maintained for a minimal time. Due to muscle fatigue, control of posture is a time-dependent problem. One way the organism copes with this lack of stationarity is by feed-back control. Information regarding the decrease of muscle performance is fed back into the peripheral and central nervous system and muscle effort is increased accordingly.

A goal of functional neuromuscular stimulation (FNS) is the restoration of upright posture. Muscle fatigue and the ensuing deterioration of muscle performance conflict with this. During FNS muscle fiber recruitment does not follow strategies physiologically employed to avoid undue fatigue (Blair and Erlanger, 1933; Petrofsky and Phillips, 1981). Physiological strategies include:

- Gradual recruitment according to the size principle, the least fatigueable fibers being activated first.
- Maintenance of an adequate average blood supply to perfuse active muscles. This strategy is mostly effected by switching activity between muscle compartments.
- Switching of activity between motor units of one muscle, individual high threshold motor units being less active at the lower force levels.

Such strategies are difficult to mimic in the FNS situation. In present systems muscles are activated by stimulating nerve endings within the muscle (Kralj et al., 1983). This is often achieved by using

large surface electrodes. The complete muscle is then active. Grading of contraction force is difficult to achieve since the effective recruitment curve, giving the relation between stimulation pulse amplitude or pulse width and muscle force, is steep and unstable as a result of variable geometrical and electrical conditions.

Switching of FNS activity between muscle compartments is feasible (Kralj et al., 1986), and results in delayed fatigue. However, methods for implementing efficient switching of muscle groups are not known. For this reason Mulder et al. (1990) attempted to reduce fatigue simply by rapidly switching between full and no activity of entire muscles involved in standing. They found that grading average muscle force in this way helped to maintain constant muscle performance. The results, however, where variable between patients (Mulder et al., 1992).

As yet it is not clear that FNS activation strategies based on switching of muscle activity, although resulting in delayed muscle fatigue, are appreciably more effective than strategies based on grading continuous stimulation. We therefore decided to investigate systematically the occurrence of muscle fatigue under different intermittent stimulation regimes. In particular, we were interested in whether decreasing muscle activity by reducing the duty cycle of stimulation patterns was a more effective way of avoiding muscle fatigue than by controlling stimulus amplitude. Because FNS schemes are primarily designed to restore motor functions we conducted the experiments on paraplegics.

Methods

Four T5 – T6 level spinal cord-injured patients participated in our study. For a minimum period of two years they were involved in a FNS program aimed at restoring their locomotor function. As part of this program they trained their lower limbs by lifting a weight of 5 kg twice a day for 30 min, by daily FNS standing, and by 30 – 60 min of low-load exercise cycling twice a week. During the fatigue experiments patients lay in a supine position on a bench. The angle between bench and trunk was 45°. Muscle torque was measured as force exerted by the left tibia on a rigid steel bar equipped with a strain gauge bridge. The left quadriceps was stimulated by an adhesive surface cathode and anode (4 × 8 cm, Pals, Axelgaard Manufacturing Corporation Ltd., Fallbrook, CA, U.S.A.). The electrodes were placed over the motor points of rectus femoris/vastus lateralis and vastus medialis, respectively. Torque output and stimulation parameters were controlled by an IBM-AT compatible computer. A high output impedance current stimulator delivered monophasic rectangular pulses with a duration of 300 μsec. The pulse rate was set to 20 Hz, the minimum frequency required for a fused contraction (Jaeger et al., 1989).

For each patient the following experiments were carried out.

(a) Determination of a recruitment curve by measuring a static torque to stimulus amplitude relation. This relation served to assess recovery of the muscle after activation. Over 10 sec a slow ramp-up and ramp-down of stimulus amplitude provided a quick determination of recruitment characteristics.

(b) Stimulation of the leg for 10 min with constant stimulus amplitude, followed by 50 min of rest. Four such epochs were applied corresponding to intensities of 100%, 30%, 10% and 5% of maximal torque as determined for each patient individually (referred to as *continuous stimulation*).

(c) Stimulation of the leg for 10 min epochs during which bursts of stimuli (stimulus on) were interrupted by silent periods (stimulus off). This was referred to as *intermittent stimulation*. On-times (t_{on}) of 0.2 and 0.5 sec, each combined with off-times (t_{off}), of 0.4 and 1.0 sec were used, giving four stimulus timing combinations. Mulder et al. (1990, 1992) found these times to be effective in reducing fatigue effects in controlling knee stabilization of FNS-standing paraplegic patients. Rest periods of 50 min followed the intermittent stimulation epochs. During intermittent stimulation, tetanic torque was defined as the peak torque output occurring in the last 100 msec of each subsequent tetanus.

Parameters of the resulting torque-time relations were estimated by fitting the curves with the formula:

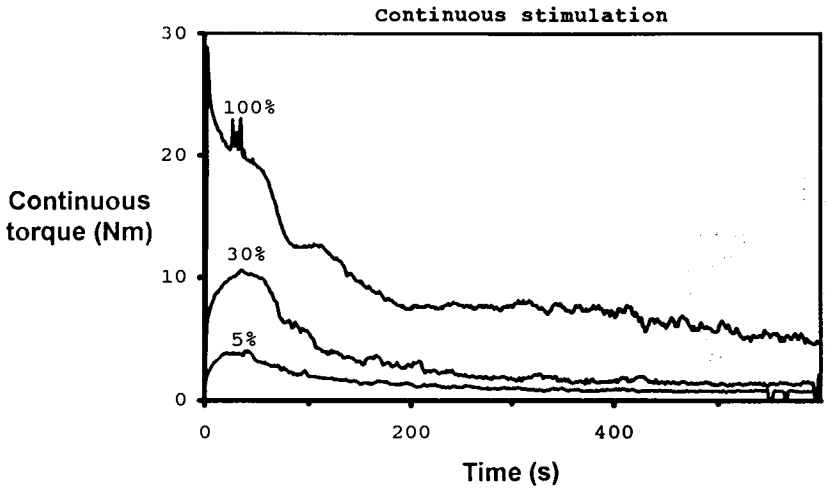

Fig. 1. Time courses of torque developed by patient WS during continuous stimulation at several levels of activation. Peak values are reached within 50 sec. Decline due to fatigue is slower. After 200 sec a steady state level is reached that is lower for lower activation levels.

$$M = (1 - e^{\frac{-t}{\tau_1}}) \{(A - M_0)\, e^{\frac{-t}{\tau_2}} + M_0\} \quad (1)$$

where M is either peak or mean developed torque, t is time and A, M_0, τ_1 and τ_2 are parameters. The model describes a process that first increases to a crest value, then declines to an asymptotic value of M_0 (referred to as *asymptotic torque*). Time constant τ_1 measures force generation, whereas τ_2 describes the fatigue development (fatigue time constant). Starting values for A, M_0, τ_1 and τ_2 were introduced into Eqn. 1 and an approximate value for M was computed. The resulting RMS deviation from the experimental torque values was minimized by computing those increments of the parameters A, M_0, τ_1 and τ_2, which, in a linear first order approxi-

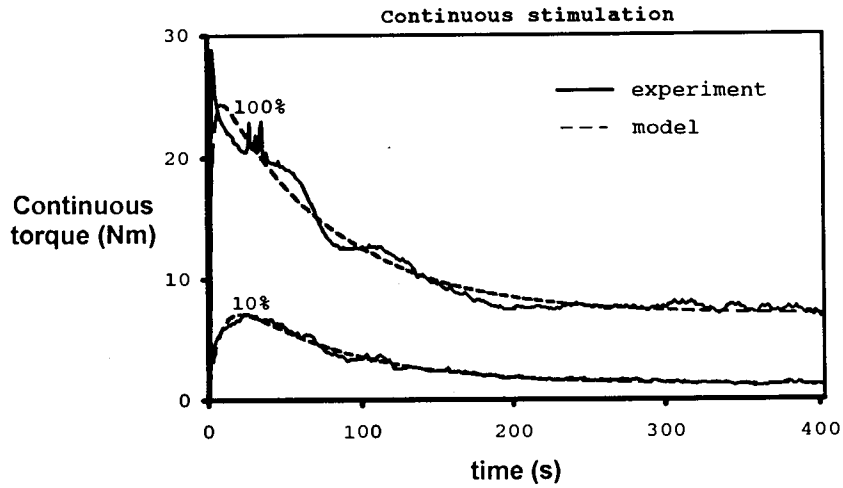

Fig. 2. Comparison of experimentally measured torques and fitted values as described by Eqn. 1. Quadriceps of patient WS were stimulated continuously at full and 10% activation level. Estimated values of τ_2 are used to quantify the speed at which fatigue develops. Values of M_0 are assumed to quantify asymptotically developed torque. Estimation error: 100% activation: 4.5%, 10% activation: 3.2%.

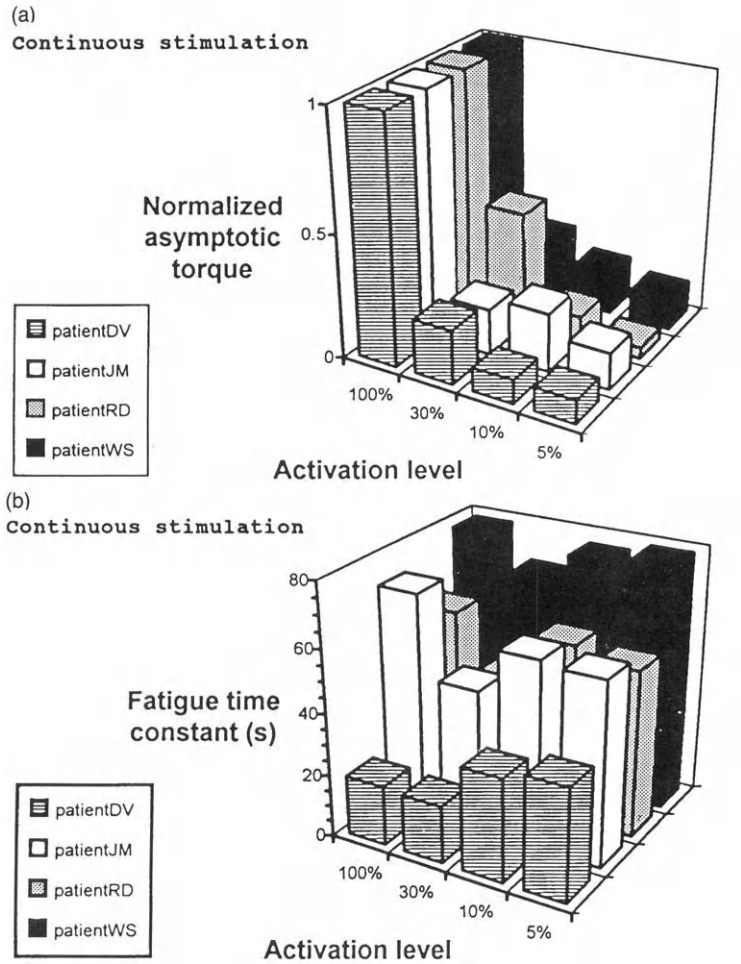

Fig. 3. Normalized asymptotic torque M_0/M_{0max} (*a*) and fatigue time constant τ_2 (*b*), as estimated using Eqn. 1 from continuous stimulation records of all four patients in this study. Asymptotic torque varies strongly with activation level. The pattern for fatigue time constant does not show such a relationship. Note that the activation axis is not linear.

mation would yield the best fit (Margenau and Murphy, 1950). The model presented by Eqn. 1 is nonlinear, thus iteration is required to determine parameter values.

Results

Tetanic torque levels

The recruitment curve measurements yielded individual tetanic force levels of 12, 25, 27 and 45 Nm. From these data we concluded that the four patients' quadriceps clearly had different force generating abilities. This finding will be of interest when responses are compared for continuous and intermittent stimulation.

Responses to continuous stimulation

Fig. 1 illustrates the torque development over time for one patient at three activation levels during continuous stimulation. Torque rises to an early peak, then declines to a steady state level. The figure shows that rise and fall times are approximately equal for the different activation levels. A similar result was obtained in the other three patients. Steady state levels, however, are different, a higher activation yielding a higher steady state torque.

To analyse fatigue characteristics more quantitatively, torque development responses were fitted by Eqn. 1. An example of the fitting procedure is shown in Fig. 2. The RMS error of the fitting proce-

TABLE I

Correlation coefficients for the relation between estimated model parameters and activation level for continuous stimulation protocols

Patient	Fatigue time constant	Asymptotic torque	Relative asymptotic torque
DV	−0.71	1.00	−0.06
JM	0.50	0.92	−0.38
RD	0.30	0.99	0.34
WS	0.12	0.98	0.68

Fatigue time constants do not depend on activation level. Asymptotic torques correlate highly whereas, again, relative asymptotic torques do not correlate any more.

dure relative to the maximum value of activation was low. The quality of the fit is best over the falling part of the curves, from which the asymptotic torque, M_0, can be estimated. Parameter values M_0 and τ_2 estimated for continuous stimulation are shown in Fig. 3.

To compare the results from different patients, torques will be presented as normalized torques which is defined as torque developed normalized with respect to the level of a similar torque that a given patient could achieve at full, continuous activation. Fig. 3*a* supports and generalizes the conclusions from Fig. 1. In all patients, normalized asymptotic torque is related to activation level. Correlation of normalized asymptotic torque with normalized maximal developed torque at the same level of activation is high and significant, even for the small number of data ($n = 4$, $\alpha = 0.01$, Table I).

In contrast, relative asymptotic torque, obtained by dividing asymptotic torque by maximal torque at the same level of activation is unrelated to maximal torque. Consequently, normalized asymptotic torque and normalized maximal torque should exhibit a one-to-one relationship. This is shown in Fig. 4.

Table II summarizes relative asymptotic torque values found in the four patients in our study. The differences are small considering the highly variable maximal torque levels reported above. An ANOVA test revealed no significant differences ($\alpha = 0.05$) between the asymptotic torque levels of the patients.

Whereas asymptotic torques in Fig. 3*a* do depend on the activation level, fatigue time constants as shown in Fig. 3*b* do not. An ANOVA test on the time constant data in Table II confirmed that the mean fatigue time constant differs significantly ($\alpha < 0.005$) between patients. Patients DV and WS are extreme examples of the variation. Their fatigue time constants are below and above the population mean value, respectively. Thus, the fatigue time

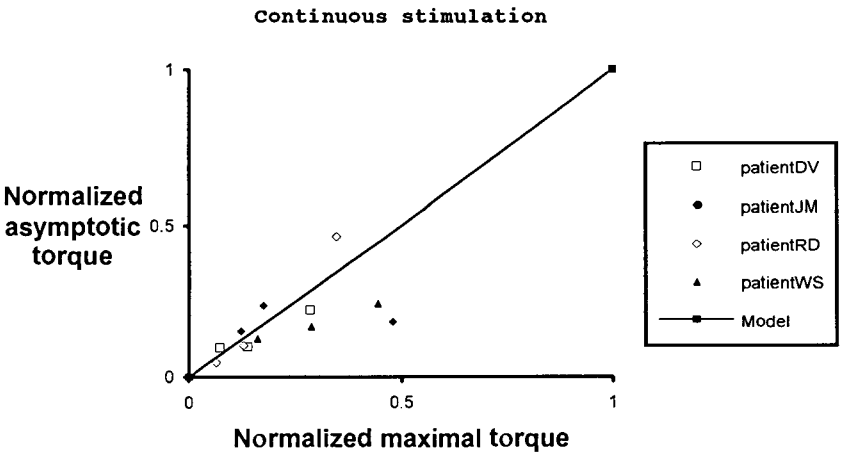

Fig. 4. Relationship between normalized asymptotic torque and normalized maximal torque. Since both values are 1 and 0 at 100% and 0% activation, respectively, the solid line represents the theoretical relation. Experimental values are scattered around this prediction.

TABLE II

Fatigue time constants and relative asymptotic torques for continuous stimulation

Patient	Fatigue time constant (sec)		Relative asymptotic torque (%)	
	Mean	S.D.	Mean	S.D.
DV	27	9	26	7
JM	59	10	16	7
RD	53	8	15	4
WS	75	5	21	6

Fatigue time constants differed between patients (ANOVA test, $\alpha < 0.005$). No significant differences could be detected for mean asymptotic torques (ANOVA, $\alpha > 0.05$).

constant could be one parameter to characterize a particular patient.

Responses to intermittent stimulation

The model of Eqn. 1 also provided an excellent fit for responses to intermittent stimulation, especially in the declining part of the curves. The model fit is more useful in finding asymptotic torque, M_0, in the intermittent than in the continuous case since in the former asymptotic torque is not always reached. Results of the model identification for intermittent stimulation are presented in Fig. 5*a,b*. Decline of torque due to fatigue in the intermittent case is appreciably slower than in the continuous case. This can clearly be seen by comparing Fig. 5*b*, where fa-

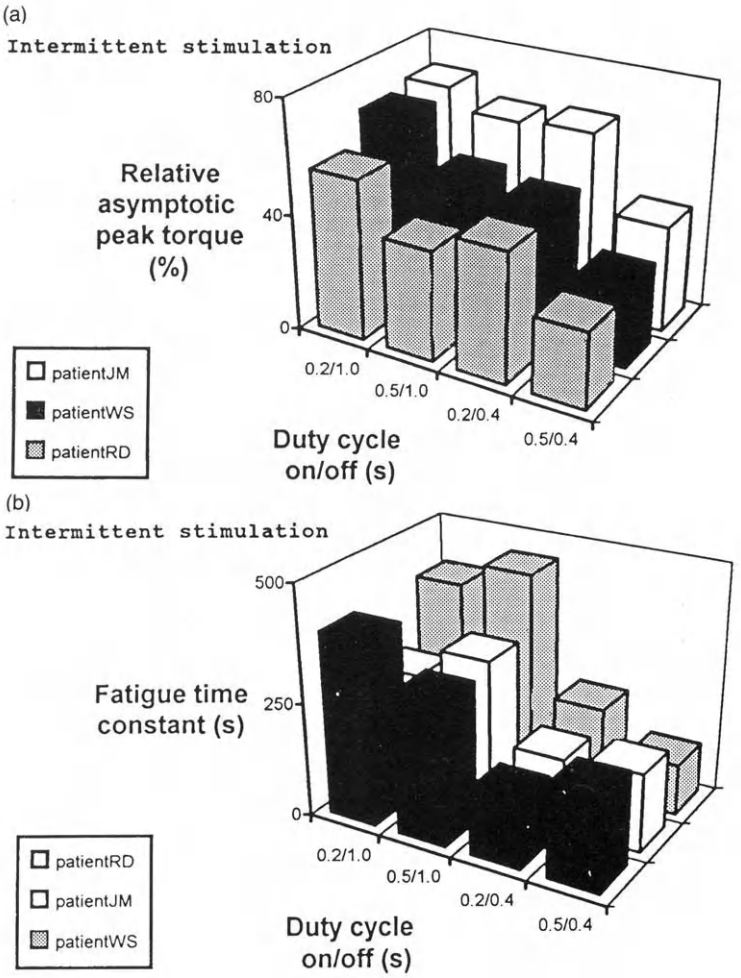

Fig. 5. Relative asymptotic peak torques (*a*) and fatigue time constants (*b*), as estimated during intermittent stimulation. Peak torque decreased slightly with duty cycle. Fatigue time constants are appreciably higher than those shown in Fig. 3*b* for continuous stimulation.

TABLE III

Means and standard deviations of fatigue time constants and relative asymptotic peak torque of each patient estimated for intermittent stimulation experiments

Patient	Fatigue time constant (sec)		Relative asymptotic peak torque (%)	
	Mean	S.D.	Mean	S.D.
JM	231	82	58	15
RD	292	164	41	12
WS	267	112	48	16

Both time constant and asymptotic torques are significantly higher than for continuous stimulation.

tigue time constants are up to 500 sec, to those of Fig. 3*b*. The large time constants are evidently related to the fact that the muscle is only active over a smaller part of a cycle (from 17 to 44%) compared with continuous stimulation (100%). Therefore, less fatigue is developed. Fig. 5*a* shows asymptotic peak torque to increase with decreasing duty cycle, in accordance with this explanation.

Table III summarizes the mean values of estimated peak torque for each patient. Mean fatigue time constants are 4 – 5 times higher than those for continuous stimulation. Asymptotic torque values are also higher, though the differences are less pronounced.

In practice, the effects of intermittent torque development will not be associated directly with peak torque but rather with torque averaged over all on/off cycles. Therefore we recalculated the intermittent stimulation results with the mean torque as the dependent variable. All torque samples during each cycle were added and the sum divided by the number of samples including those with torque zero and a new model fit was made. Fig. 6 shows typical results. The model represented by Eqn. 1 fits the experimental points of the averaged torque-time relation accurately on all parts of the curve. Similar results were obtained for the other patients in the study.

Estimated parameters for mean torque output are summarized in Fig. 7. The fatigue time constant is variable and comparable to that for non-averaged peak torque results. As expected, relative asymptotic averaged torque (thus relative to maximal peak torque at the same activation level) now is appreciably lower, compared with relative asymptotic, non-

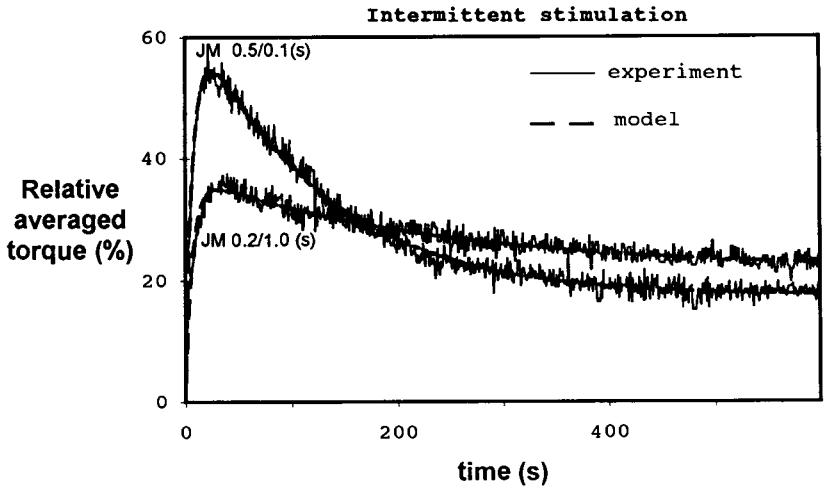

Fig. 6. Comparison of experimentally measured averaged torques and fitted values as described by Eqn. 1 for intermittent stimulation (patient JM). Relative averaged torque was obtained by dividing average torque by the maximal peak torque at the same activation level. Estimated values of τ_2 are used for quantifying the speed of fatigue development. The theoretical curve accurately fits experimental averaged torque. The model is a good predictor of torque development and could be used for FNS controllers.

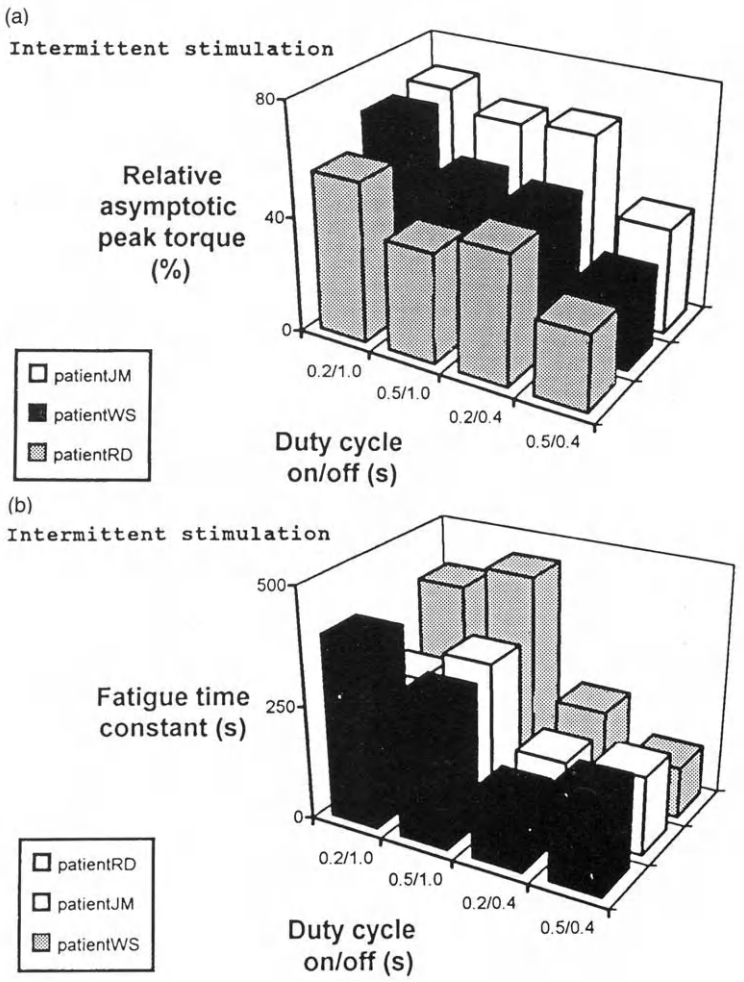

Fig. 7. Relative asymptotic averaged torques (*a*) and fatigue time constants (*b*), as estimated during intermittent stimulation. Relative asymptotic averaged torque was obtained by dividing asymptotic averaged torque by the maximal peak torque at the same activation level. Averaged torques are not correlated with duty cycle. Fatigue times follow a varying pattern.

averaged peak torque data (Fig. 5*a*; Table III). Unexpectedly, it is uncorrelated with duty cycle.

Table IV gives mean values of this uncorrelated asymptotic average torque. These values represent torques achieved by a patient after a longer interval of intermittent stimulation regardless of applied duty cycle. These findings indicate that reducing muscle torque by reducing the duty cycle of intermittent stimulation is more effective in postponing the development of fatigue than reducing torque by decreasing stimulation amplitude. This is illustrated in Fig. 8. The continuous stimulation curves show the reported proportionality between peak amplitude and asymptotic torque. The curve for 30% amplitude activation falls to low values after 200 sec. In contrast, the curve for averaged torque with intermittent stimulation has a maximal value equal to the 30% continuous curve. The torque falls off slowly, approaching the approximately 20% torque level which is characteristic for this patient.

Discussion

That torque levels generated by continuous stimulation fall off after a relatively limited time has been

TABLE IV

Means and standard deviations of fatigue time constants and relative asymptotic averaged torque for intermittent stimulation

Patient	Fatigue time constant (sec)		Relative asymptotic averaged torque (%)	
	Mean	S.D.	Mean	S.D.
JM	189	99	17	5
RD	230	111	18	7
WS	318	219	10	4

a general finding (Kralj et al., 1986; Levy et al., 1990). It has also been observed where muscles were activated by stimulating the femoral nerve (Brindley et al., 1979). Effects of duty cycle on tetanic quadriceps torque have been reported by Kralj et al. (1986) for on/off cycles as long as several seconds.

The relationship between maximal torque and asymptotic, fatigued torque during continuous stimulation is less well documented. It is not clear which mechanism is responsible for the lower asymptotic torque at the lower continuous recruitment levels. At lower torque levels fewer (groups of) motor units will be active. If relative fatigue is not changed, it is clearly linked with such smaller groups rather than with the muscle as a whole. Fatigue during artificial stimulation has been ascribed to local ischemia (Sadamoto et al., 1983; Petrofsky and Hendershot, 1984; Sjögaard et al., 1986). This ischemia is a balanced result of increased metabolic demands on the one side and impaired perfusion on the other. If there is impaired perfusion it must be a local effect. This suggests that local increases of intramuscular pressure occur during incomplete muscle activation.

Other effects act on a local scale as well. The neuromuscular junction has a finite capacity for recruiting neurotransmitter. This could lead to a depletion after prolonged contraction. Furthermore, if artificial stimulation leads to inverse recruitment, where the more easily fatiguible fibers are recruited first, reducing the activation level in continuous stimulation would deactivate the fibers less subject to fatigue leaving those that fatigue easily. Then one would expect fatigue to develop not only to a greater degree but also quicker at low activation levels. Our results do not support this hypothesis.

The model we used to estimate fatigue parameters

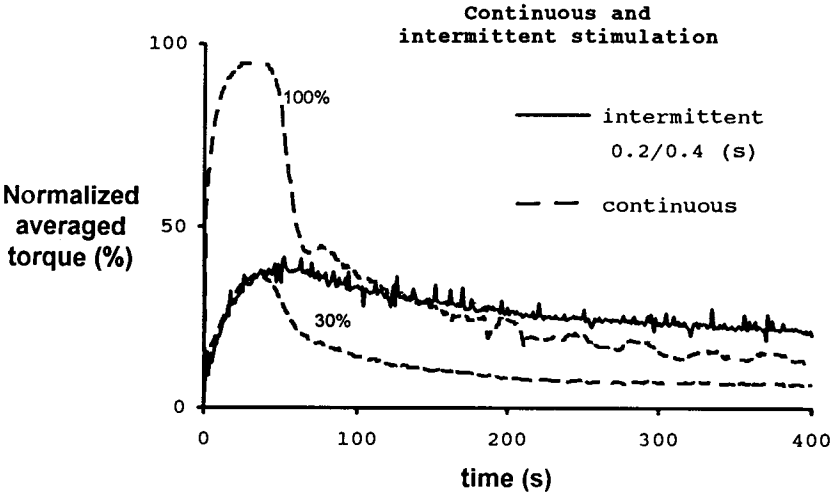

Fig. 8. Comparison of modulating torque by either decreasing continuous activation (broken curve) or by decreasing duty cycle. With intermittent stimulation averaged torque falls off slowly, demonstrating the advantage of this method of torque regulation. Normalized averaged torque was obtained by dividing average torque by the maximal peak torque at the same activation level.

clearly is too crude to be of physiological significance. The model consists of two first order processes starting at the same instant. This is improbable since fatigue cannot be developed before activation has progressed to some degree. Actually, deviations can be seen in the experimental records during the first 10 sec (for example, see Fig. 2).

The identification procedure compensates the overshoot in Fig. 2 by choosing an unrealistically high value for parameter A (especially in the continuous records). This model has not been selected to explain physiological processes, but rather to quantify and, in some cases, to extrapolate parameter values. We feel that the good correspondence of the model with experimental values, especially during the declining phase of the curve will make it useful for designing FNS controllers which compensate for fatigue, on the basis of model parameters.

As far as stable standing of paraplegic patients is concerned, our results indicate that long standing times are achievable only when the external knee load does not exceed approximately 20% of maximal unfatigued torque, in both continuous and intermittent stimulation. For external loads exceeding 20% maximum unfatigued torque standing can be maintained only until all muscle fibers are continuously recruited. This would be achieved by either adaptation of recruitment level or by increasing duty cycle. However, the present study shows that intermittent activation postpones fatigue and thus gives the highest dynamic range of torque output. This suggests that the alternative activation of the separate heads of the quadriceps should be employed instead of using only one pair of electrodes (Pournezam et al., 1988). However, the poor selectivity of muscle activation during transcutaneous stimulation could then be a limiting factor (Hermens et al., 1986).

Acknowledgements

This work was supported by the Dutch Technology Foundation STW, Grant TEL68.0927. The authors wish to thank Dr Eleanor Goodall for reading the manuscript.

References

Blair, E.A. and Erlanger, J. (1933) A comparison of the characteristics of axons through their individual electrical responses. *Am. J. Physiol.*, 106: 524 – 564.

Brindley, G.S., Polkey, C.E. and Rushton, D.N. (1979) Electrical splinting of the knee. *Paraplegia*, 16: 428 – 435.

Hermens, H.J., Mulder, A.J., Tijhaar, W.H., van der Heyden, G. and Zilvold, G. (1986) Research on electrical stimulation with surface electrodes. *Proceedings 2nd Vienna International Workshop on FES*, pp. 321 – 324.

Jaeger, R.J., Yarkony, G.M. and Smith, R.M. (1989) Standing the spinal cord injured patient by electrical stimulation: refinement of a protocol for clinical use. *IEEE Trans. Biomed. Eng.*, 36: 720 – 728.

Kralj, A., Bajd, T., Turk, R., Krajnik, J. and Benko, H. (1983) Gait restoration in paraplegic patients: a feasibility demonstration using multichannel surface electrode FES. *J. Rehab. Res. Dev.*, 20: 3 – 20.

Kralj, A., Bajd, T., Turk, R. and Benko, H. (1986) Posture switching for prolonging functional electrical stimulation standing in paraplegic patients. *Paraplegia*, 24: 221 – 230.

Levy, M., Mizrahi, J. and Susek, Z. (1990) Recruitment, force and fatigue characteristics of quadriceps muscle of paraplegics isometrically activated by surface functional electrical stimulation. *J. Biomed. Eng.*, 3: 150 – 156.

Margenau, H. and Murphy, G.M. (1950) *The Mathematics of Physics and Chemistry*, Van Nostrand, Toronto, pp. 517 – 519.

Mulder, A.J., Boom, H.B.K., Hermens, H.J. and Zilvold, G. (1990) Artificial-reflex stimulation for FES-induced standing with minimum quadriceps force. *Med. Biol. Eng. Comput.*, 28: 483 – 488.

Mulder, A.J., Veltink, P.H., Boom, H.B.K. and Zilvold, G. (1992) Low level finite state control of knee joint in paraplegic standing. *J. Biomed. Eng.*, 14: 3 – 8.

Petrofsky, J.S. and Hendershot, D.M. (1984) The interrelationship between blood pressure, intramuscular pressure and isometric endurance in fast and slow twitch skeletal muscle in the cat. *Eur. J. Appl. Physiol.*, 53: 106 – 111.

Petrofsky, J.S. and Phillips, C.A. (1981) Impact of recruitment order on electrode design for neural prosthetics of skeletal muscle. *Am. J. Phys. Med.*, 60: 243 – 253.

Pournezam, M., Andrews, B.J., Baxendale, R.H., Phillips, G.F. and Paul, J.P. (1988) Reduction of muscle fatigue in man by cyclical stimulation. *J. Biomed. Eng.*, 10: 196 – 200.

Sadamoto, T., Bonde-Petersen, F. and Suzuki, Y. (1983) Skeletal muscle tension, flow, pressure and EMG during sustained isometric contractions in humans. *Eur. J. Appl. Physiol.*, 51: 395 – 408.

Sjögaard, G., Kiens, B., Jorgensen, K. and Saltin, B. (1986) Intramuscular pressure, EMG and blood flow during low-level prolonged static contraction in man. *Acta Physiol. Scand.*, 128: 475 – 484.

Subject Index